

THE JOURNAL OF PHYSICAL CHEMISTRY

(Registered in U. S. Patent Office)

SYMPOSIUM ON ION EXCHANGE, SOUTHEAST REGIONAL MEETING, COLUMBIA, S. C., November 3-5, 1955

R. W. Gable and H. A. Strobel: Non-aqueous Ion Exchange. I. Some Cation Equilibrium Studies in Methanol.....	513
D. R. Asher and D. W. Simpson: Glycerol Purification by Ion Exclusion.....	518
G. E. Myers and G. E. Boyd: A Thermodynamic Calculation of Cation Exchange Selectivities.....	521
O. D. Bonner and Frances L. Livingston: Cation-Exchange Equilibria Involving Some Divalent Ions.....	530
Richard H. Wiley and Samuel F. Reed: Preparation of Variable Capacity Sulfostyrene Cation Exchangers.....	533
* * * * *	
Donald G. Miller: An Analytical Proof that the Extremum of the Thermodynamic Probability is a Maximum.....	536
Yuen Chu Leung and Jürg Waser: The Crystal Structure of Phosphorus Diodide, P ₂ I ₄	539
D. J. C. Yates: The Influence of the Polar Nature of the Adsorbate on Adsorption Expansion.....	543
William E. Haines, R. Vernon Helm, Glenn L. Cook and John S. Ball: Purification and Properties of Ten Organic Sulfur Compounds—Second Series.....	549
Alvin G. Winger, Ruth Ferguson and Robert Kunin: The Electroosmotic Transport of Water across Permselective Membranes.....	556
Louis F. Heckelsberg, Alfred Clark and Grant C. Bailey: Electrical Conductivity and Catalytic Activity of Zinc Oxide.....	559
Adam Chou and Milton Kerker: The Refractive Index of Colloidal Sols.....	562
T. E. Moore, R. W. Goodrich, E. A. Gootman, B. S. Slezak, and Paul C. Yates: Extraction of Inorganic Salts by 2-Octanol. II. Cobalt (II) and Nickel(II) Chlorides and Bromides. Effect of Electrolytes.....	564
J. S. Wagener: Adsorption Measurements at Very Low Pressures.....	567
A. L. Bacarella, Arthur Finch and Ernest Grunwald: Vapor Pressures and Activities in the System Dioxane-Water. Second Virial Coefficients in the Gaseous System Nitrogen-Dioxane-Water.....	573
Ulrich P. Strauss, Norman L. Gershfeld and Evan H. Crook: The Transition from Typical Polyelectrolyte to Polysoap. II. Viscosity Studies of Poly-4-vinylpyridine Derivatives in Aqueous KBr Solutions.....	577
Erwin Sheppard, John Imperante and Irving S. Wright: The Action of Heparin on the Polymerization of Fibrinogen.....	584
James M. Schreyer and L. R. Phillips: The Solubility of Uranium(IV) Orthophosphates in Perchloric Acid Solutions.....	588
C. D. Thurmond and R. A. Logan: The Distribution of Copper between Germanium and Ternary Melts Saturated with Germanium.....	591
L. Elias and H. I. Schiff: A Modified Direct Current Conductance Method for General Application.....	595
A. A. Miller, E. J. Lawton and J. S. Balwit: The Radiation Chemistry of Hydrocarbon Polymers: I. Polyethylene, Polymethylene and Octacosane.....	599
S. Larach, W. H. McCarroll and R. E. Shrader: Luminescence Properties of Zinc-inter-chalcogenides. I. Zinc Sulfo-telluride Phosphors.....	604
J. R. Lacher, Liberty Casali and J. D. Park: Reaction Heats of Organic Halogen Compounds. V. The Vapor Phase Bromination of Tetrafluoroethylene and Trifluorochloroethylene.....	608
Kenzi Tamaru: The Thermal Decomposition of Tin Hydride.....	610
Kenzi Tamaru: Decomposition of Ammonia on Germanium.....	612
D. N. Glew and L. W. Reeves: Purification of Perfluoro- <i>n</i> -heptane and Perfluoromethylcyclohexane.....	615
D. N. Glew and J. H. Hildebrand: The Solubility and Partial Molal Volume of Iodine in Perfluoro- <i>n</i> -heptane.....	616
J. H. Hildebrand and D. N. Glew: The Entropy of Solution of Iodine.....	618
H. Bloom and N. J. Doull: Transport Number Measurements in Pure Fused Salts.....	620
David M. Mason and Stephen P. Vango: Measurement of Optical Absorbance of TiCl ₄ (g) in the Ultraviolet Region.....	622
David A. Yphantis and David F. Waugh: Ultracentrifugal Characterization by Direct Measurement of Activity. I. Theoretical.....	623
David A. Yphantis and David F. Waugh: Ultracentrifugal Characterization by Direct Measurement of Activity. II. Experimental.....	630
William N. Vanderkooi and Thomas De Vries: The Heat Capacity of Gases at Low Pressure Using a Wire-Ribbon Method.....	636
Walter Roth and Walter H. Bauer: The Explosive Oxidation of Diborane.....	639
Leon Lazare, Benson R. Sundheim and Harry P. Gregor: A Model for Cross-linked Polyelectrolytes.....	641
Seymour Newman, William R. Krigbaum and Dewey K. Carpenter: Reversible Association of Cellulose Nitrate in Ethanol.....	648
Lun Hsiao, H. N. Dunning and P. B. Lorenz: Critical Micelle Concentrations of Polyoxyethylated Non-ionic Detergents.....	657
L. J. Tichacek, W. S. Kmek and H. G. Drickamer: Thermal Diffusion in Liquids; The Effect of Non-ideality and Association.....	660
J. T. Kummer: The Catalytic Oxidation of Ethylene to Ethylene Oxide over Single Crystals of Silver.....	666
N. Thorp and R. L. Scott: Fluorocarbon Solutions at Low Temperatures. I. The Liquid Mixtures CF ₄ -CHF ₃ , CF ₂ -CH ₂ , CF ₂ -Kr, CH ₂ -Kr.....	670
Edward P. McLaughlin and Robert L. Scott: Solubilities of Iodine and Anthracene in Hydrofluorocarbons.....	674
Hans Nowotny, Alan W. Searcy and J. E. Orr: Structures of Some Germanides of Formula M ₂ Ge.....	677
Kurt H. Stern: Electrode Potentials in Fused Systems. II. A Study of the AgCl-KCl System.....	679
E. E. Muschlitz, Jr., and T. L. Bailey: Negative Ion Formation in Hydrogen Peroxide and Water Vapor. The Peroxide Ion.....	681
A. K. Wiebe: Elution Time and Resolution in Vapor Chromatography.....	685
W. R. Smith and M. H. Polley: The Oxidation of Graphitized Carbon Black.....	689
F. T. Wall and A. Beresiewicz: Electrolytic Interaction of Nylon with Aqueous Solutions of Hydrochloric Acid.....	692

THE JOURNAL OF PHYSICAL CHEMISTRY

(Registered in U. S. Patent Office)

W. ALBERT NOYES, JR., EDITOR

ALLEN D. BLISS

ASSISTANT EDITORS

ARTHUR C. BOND

EDITORIAL BOARD

R. P. BELL

JOHN D. FERRY

S. C. LIND

R. E. CONNICK

G. D. HALSEY, JR.

H. W. MELVILLE

R. W. DODSON

J. W. KENNEDY

E. A. MOELWYN-HUGHES

PAUL M. DOTY

R. G. W. NORRISH

Published monthly by the American Chemical Society at 20th and Northampton Sts., Easton, Pa.

Entered as second-class matter at the Post Office at Easton, Pennsylvania.

The *Journal of Physical Chemistry* is devoted to the publication of selected symposia in the broad field of physical chemistry and to other contributed papers.

Manuscripts originating in the British Isles, Europe and Africa should be sent to F. C. Tompkins, The Faraday Society, 6 Gray's Inn Square, London W. C. 1, England.

Manuscripts originating elsewhere should be sent to W. Albert Noyes, Jr., Department of Chemistry, University of Rochester, Rochester 20, N. Y.

Correspondence regarding accepted copy, proofs and reprints should be directed to Assistant Editor, Allen D. Bliss, Department of Chemistry, Simmons College, 300 The Fenway, Boston 15, Mass.

Business Office: Alden H. Emery, Executive Secretary, American Chemical Society, 1155 Sixteenth St., N. W., Washington 6, D. C.

Advertising Office: Reinhold Publishing Corporation, 430 Park Avenue, New York 22, N. Y.

Articles must be submitted in duplicate, typed and double spaced. They should have at the beginning a brief Abstract, in no case exceeding 300 words. Original drawings should accompany the manuscript. Lettering at the sides of graphs (black on white or blue) may be pencilled in and will be typeset. Figures and tables should be held to a minimum consistent with adequate presentation of information. Photographs will not be printed on glossy paper except by special arrangement. All footnotes and references to the literature should be numbered consecutively and placed in the manuscript at the proper places. Initials of authors referred to in citations should be given. Nomenclature should conform to that used in *Chemical Abstracts*, mathematical characters marked for italic, Greek letters carefully made or annotated, and subscripts and superscripts clearly shown. Articles should be written as briefly as possible consistent with clarity and should avoid historical background unnecessary for specialists.

Symposium papers should be sent in all cases to Secretaries of Divisions sponsoring the symposium, who will be responsible for their transmittal to the Editor. The Secretary of the Division by agreement with the Editor will specify a time after which symposium papers cannot be accepted. The Editor reserves the right to refuse to publish symposium articles, for valid scientific reasons. Each symposium paper may not exceed four printed pages (about sixteen double spaced typewritten pages) in length except by prior arrangement with the Editor.

Remittances and orders for subscriptions and for single copies, notices of changes of address and new professional connections, and claims for missing numbers should be sent to the American Chemical Society, 1155 Sixteenth St., N. W., Washington 6, D. C. Changes of address for the *Journal of Physical Chemistry* must be received on or before the 30th of the preceding month.

Claims for missing numbers will not be allowed (1) if received more than sixty days from date of issue (because of delivery hazards, no claims can be honored from subscribers in Central Europe, Asia, or Pacific Islands other than Hawaii), (2) if loss was due to failure of notice of change of address to be received before the date specified in the preceding paragraph, or (3) if the reason for the claim is "missing from files."

Subscription Rates (1956): members of American Chemical Society, \$8.00 for 1 year; to non-members, \$16.00 for 1 year. Postage free to countries in the Pan American Union; Canada, \$0.40; all other countries, \$1.20. \$12.50 per volume, foreign postage \$1.20, Canadian postage \$0.40; special rates for A.C.S. members supplied on request. Single copies, current volume, \$1.35; foreign postage, \$0.15; Canadian postage \$0.05. Back issue rates (starting with Vol. 56): \$15.00 per volume, foreign postage \$1.20, Canadian, \$0.40; \$1.50 per issue, foreign postage \$0.15, Canadian postage \$0.05.

The American Chemical Society and the Editors of the *Journal of Physical Chemistry* assume no responsibility for the statements and opinions advanced by contributors to THIS JOURNAL.

The American Chemical Society also publishes *Journal of the American Chemical Society*, *Chemical Abstracts*, *Industrial and Engineering Chemistry*, *Chemical and Engineering News*, *Analytical Chemistry*, *Journal of Agricultural and Food Chemistry* and *Journal of Organic Chemistry*. Rates on request.



(Continued from first page of cover)

D. R. Lewis: The Thermoluminescence of Dolomite and Calcite.....	698
Note: Donald Cohen, E. S. Amis, J. C. Sullivan and J. G. Hazman: Kinetics of the Reaction between Neptunium(IV) and Neptunium(VI) in a Mixed Solvent.....	701
Note: G. C. Bond: The Adsorption of Deuterium by a Platinum Catalyst.....	702
Note: A. Spagnol: The Correction of Stokes' Laws of Friction for Particles of Molecular Size.....	703

THE JOURNAL OF PHYSICAL CHEMISTRY

(Registered in U. S. Patent Office) (© Copyright, 1956, by the American Chemical Society)

VOLUME 60

MAY 14, 1956

NUMBER 5

NON-AQUEOUS ION EXCHANGE. I. SOME CATION EQUILIBRIUM STUDIES IN METHANOL

By R. W. GABLE¹ AND H. A. STROBEL

Contribution from the Department of Chemistry, Duke University, Durham, N. C.

Received October 11, 1955

Equilibrium quotients have been obtained for exchange in the sodium-hydrogen, ammonium-hydrogen and silver-sodium cation systems on Dowex 50 in anhydrous methanol. The ionic strength of the solutions was maintained at 0.1 *m*, and exchange was studied as a function of the resin composition. Alterations in the degree of ion solvation and ion-pair formation are believed to account for the enhanced selectivities in methanol as compared with similar aqueous systems. The sodium-hydrogen exchange was also investigated as a function of water added at a resin fraction of Na⁺-ion of 0.5. The selectivity of the resin for sodium was found to increase rapidly, a maximum being noted at a mole fraction of water in the external solution phase of about 0.25. This is discussed briefly in terms of solvation and the distribution of water between the two phases.

Introduction

The investigations of the fundamental characteristics of ion exchange in aqueous solutions have been numerous and have revealed the broad aspects of the process as well as many interesting details.² In general, these researches have shown that a Donnan type of equilibrium prevails and that both pressure-volume and activity effects must be included for an adequate theoretical interpretation.^{3,4} Perhaps the chief difficulty has been determining activities in the concentrated resin phase where molalities are of the order of 3-10. This problem has not been resolved completely though there have been many worthwhile proposals.⁵⁻⁸

Some confirmation of the influence of variables on the exchange process has been provided by extending the work to non-aqueous solvent-water mixtures. Beginning with the study of Wiegner

and Jenny, the effect of lowered dielectric constants and differences in the solvation of ions in particular have been explored.⁹⁻¹⁴ The swelling and deswelling of exchange resins which accompanies exchange has been shown to be a function of the activity of the ions involved as well as of the character of the solvent.^{13,14}

The present study was undertaken with the thought of obtaining further perspective on equilibrium exchange phenomena from the vantage point of a non-aqueous system. Methanol was selected as providing reasonably high salt solubilities and water-like qualities. Three monovalent cation-exchange systems were studied at a total ionic strength of 0.1 in the external phase and with Dowex 50 cross-linked with 8% divinylbenzene. Water was excluded as completely as possible. In one phase of the study of the sodium-hydrogen system, however, water was deliberately introduced to investigate the influence of competition in the solvation of the ions and the alteration of the dielectric constant.

- (1) American Cyanamid Fellow, 1953-1954.
- (2) Cf. articles on ion exchange in the *Ann. Rev. Phys. Chem.*, Vols. II, III, IV and V, 1951-1954.
- (3) E. Glueckauf, *Proc. Roy. Soc. (London)*, **A214**, 207 (1952).
- (4) G. E. Boyd and B. A. Soldano, *Z. Elektrochem.*, **57**, 162 (1953).
- (5) W. J. Argersinger, W. J. Davidson and O. D. Bonner, *Trans. Kansas Acad. Sci.*, **53**, 404 (1950).
- (6) E. Hogfeldt, E. Ekedahl and L. G. Sillen, *Acta Chem. Scand.*, **4**, 471 (1950).
- (7) J. F. Duncan, *Proc. Roy. Soc. (London)*, **A214**, 344 (1952); *Australian J. Chem.*, **8**, 293 (1955).
- (8) C. W. Davies and G. D. Yeoman, *Trans. Faraday Soc.*, **49**, 975 (1953).

- (9) G. Wiegner and H. Jenny, *Kolloid Z.*, **42**, 268 (1927)
- (10) T. R. E. Kressman and J. A. Kitchener, *J. Chem. Soc.*, 1211 (1949).
- (11) T. Sakaki and H. Kakihana, *Kogaku*, **23**, 471 (1953); *C. A.*, **47**, 10951 (1953).
- (12) B. Sansoni, *Angew. Chem.*, **66**, 330 (1954).
- (13) O. D. Bonner and J. C. Moorefield, *THIS JOURNAL*, **58**, 555 (1954).
- (14) H. P. Gregor, D. Nobel and M. H. Gottlieb, *ibid.*, **59**, 10 (1955).

Experimental

Materials.—Synthetic methanol was purified by reaction with magnesium turnings and iodine. It was distilled slowly in an all-glass system, the central portion of the distillate being collected. The anhydrous solvent was stored and used in a dry box whose atmosphere was maintained by P_2O_5 .

G. Frederick Smith reagent grade sodium perchlorate was recrystallized once from distilled water and dried at 300° . It was stored over P_2O_5 . Ammonium perchlorate was prepared by neutralizing reagent grade perchloric acid with excess ammonia. The salt was recrystallized twice from small amounts of water. Finally, the ammonium perchlorate was dried at 110° and stored over P_2O_5 .

Resins.—Dowex 50, DVB 8, a polystyrenesulfonic acid cation-exchange resin with a nominal divinylbenzene content of 8%, was purchased from the Dow Chemical Company in the form of 50-100 mesh beads. The resin was washed repeatedly with methanol and 1 *N* HCl and finally rinsed free of acid. Deionized water obtained from a monobed resin column was used for this rinsing and all operations involving water mentioned below.

No attempt was made to convert the resin to other cation forms by treatment with methanol solutions. Rather, conversions were made with aqueous solutions by standard column techniques followed by drying as described below. In each case the water rinse was continued until the eluate tested free of conversion reagent.

Drying was accomplished in three stages. The resins were first air dried, then transferred to a P_2O_5 vacuum desiccator. Before use the resins were placed overnight in a system heated to 90° , dried by P_2O_5 , and continuously evacuated by a Hy-vac pump.

Methanolic Solutions.—Methanol solutions of the perchlorate salts were made up by weight in a dry box. When perchloric acid solutions were required, they were prepared by the simple expedient of passing a sodium perchlorate solution of the desired molality through a short column of anhydrous hydrogen resin already wetted with methanol. Only the middle fraction of the eluate was collected; by analysis it was found to be within 2-5% of the starting solution in concentration.

Water Analyses.—Most of the water determinations were made by the Karl Fischer method, using reagent made up with methyl cellosolve.¹⁵ The sensitivity of detection of the end-point allowed volumes to be read to 0.05 ml., which in the usual seven-gram sample of solution was equivalent to about 0.003% water. Thus, for the low water contents involved in most of the systems, the water determinations were only semi-quantitative.

In order to determine the approximate water content of the resins, samples were introduced into about 10 ml. of anhydrous methanol which already had been titrated to the end-point. Fading of the iodine color occurred immediately, and reagent was added while the suspension was stirred until a new end-point which lasted for at least a minute was attained. The validity of the method for resins was checked for a few samples by comparison of titration results with the loss of weight on vacuum drying by the procedure already described. The determinations agreed within 10%.

For the system in which the solvent was varied from pure methanol to water, the water content was too high for the Karl Fischer method. In this case the percentage of water in the solvent was estimated by determining the density, which gave a result accurate to about the nearest percentage of water. The solvent in the resin phase was distilled from blotted beads taken from the equilibrium system. The water content was found by titration.

Equilibration Procedure.—To carry out an equilibrium distribution determination, small amounts of dry, pure resins (usually totalling a gram) and 30 g. of 0.1 *m* methanol solution were introduced into small erlenmeyers. The flasks were then closed with standard-taper caps, sealed tightly with Sealstix and shaken for 24-48 hours at $30.00 \pm 0.05^\circ$. No difficulty was experienced in attaining equilibrium except in the silver-sodium system. As the silver concentration was increased, longer times were found necessary; one set of samples was shaken for two weeks to be certain of equilibrium. For that set the temperature was less well controlled, being $28 \pm 2^\circ$.

Sampling.—The sampling of the equilibrium systems was carried out in a dry box. As the sealed flasks were opened, resin and solution were separated by swirling the suspension into a short 20-mm. Pyrex column closed with a coarse frit. Three samples of the solution were pipetted out and weighed. When the resin had drained well, it was removed from the dry box.

To remove non-exchange electrolyte suction was quickly applied to the resin and alternated with washings by small portions of deionized water. By analysis the amount of salt involved was of the order of 1% of the exchange cations.

Analytical Procedures.—The procedure for the Na-H system will be discussed in detail since it is representative. The essential differences are noted in Table I. One cation designated A and the total cations, A + B, were determined in each phase. The other cation, B, was found by difference.

TABLE I
ANALYSIS OF RESIN PHASE

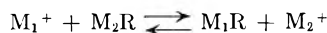
Sys-tem	Eluent soln.	Cation ti-trated	End-point	Titrat
A. Determination of Cation A				
Na-H	NaCl in MeOH-H ₂ O	H ⁺	pH 7	NaOH
NH ₄ -H	NaCl in MeOH-H ₂ O	H ⁺	pH 5.6	NaOH
Ag-Na	NH ₄ NO ₃ in dil. NH ₃ -H ₂ O	Ag ⁺	potentiometric (Ag electrode)	NaI

B. For the total cation content, resin samples from the Na-H and NH₄-H systems after part A were converted to the H-form and the above procedure repeated. In the Ag-Na system, the resin was next converted to the Ag-form and the steps repeated.

In the Na-H system, cation A was hydrogen. One sample of solution was titrated directly with standard NaOH. To determine A + B another sample was passed through a column of H⁺-form resin. After rinsing with water until the eluate was neutral, the total eluate was titrated with base.

For the resin only one sample was needed. The hydrogen content was found by eluting with a methanolic solution containing 10% water and saturated with sodium chloride. These conditions were ideal for displacing the hydrogen ion (cf. Table III). This eluate was titrated for H⁺. The resin was then rinsed thoroughly with water and converted quantitatively to the hydrogen form by 1 *N* HCl, so that A + B could be determined as the hydrogen equivalent. The resin was once more eluted with methanolic sodium chloride, etc.¹⁶

Selectivities.—Conventional equilibrium quotients K_2^1 were calculated for the exchange equilibrium where ion-1 is displacing ion-2



The value of K_2^1 , which may also be termed a selectivity coefficient, has been defined as

$$K_2^1 = \frac{(X_{M_1R})(m_{M_2})}{(X_{M_2R})(m_{M_1})}$$

where the X's indicate the mole fractions of the resin capacity in the two ionic forms, respectively, and the *m*'s identify the respective solution phase molalities of the ions.

Swollen Volumes.—Resin volumes were determined by two techniques. The first, a microscopic method similar to that of Gregor,¹⁴ involved determination of the diameters of individual beads free of imperfections by measurement in three directions. The second, a column method, called for observation of the volumes of a packed column of about 10 g. of the different resin forms in a 50-ml. buret. Care was taken to ensure a complete change of solvent medium by backwashing gently and by going from methanol to water. No correction was made for voids, but the degree of approximation was reduced by using only volume ratios.

(16) A few Na-H resin samples were analyzed by washing with 1 *N* AgNO₃ and titrating the eluate for hydrogen ion using pH 5.4 as the end-point. The resin sample, at that point in the silver form, was rinsed and eluted with barium nitrate solution. Potentiometric analysis of the eluate for silver then gave the total cations in the resin.

(15) E. D. Peters and J. L. Jungnickel, *Anal. Chem.*, **27**, 450 (1955).

Results

Methanol Systems.—In Fig. 1 the equilibrium results for the methanol exchange systems are presented in the form of distribution data. The mole fraction of the cation content comprised by one ion in the solution phase is plotted *versus* its mole fraction in the resin phase. Actual equilibrium quotients are shown in Fig. 2 as a function of resin composition for the Na-H and NH₄-H systems. Smoothed equilibrium quotients for the Ag-Na methanol system are listed in Table II.

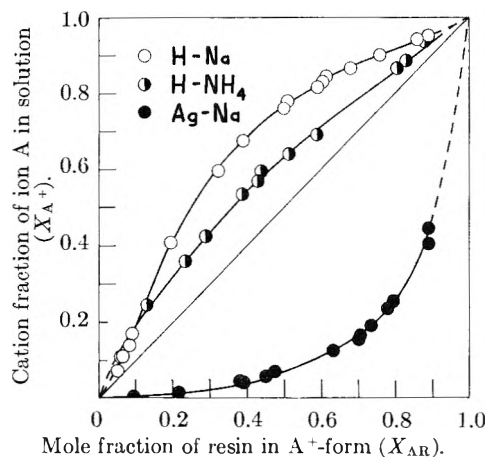


Fig. 1.—Equilibrium distribution of ions between 0.1 *m* perchlorate methanol solutions and Dowex 50, 8% DVB, at 30°. Ion A is either H⁺ or Ag⁺.

The amount of water present was kept sufficiently low so that any variations introduced by altering its amount were within the limits of experimental error. The hydrogen resin proved hardest to dry, and the use of that resin introduced small amounts of water. The solution phase was always analyzed for water content after an equilibration. It is believed that this analysis was a fair measure of the total water content. In the Na-H system, *e.g.*, at 0.05% water in the external solution, there was less than 0.1% water in the resin. The figure 0.1% very definitely is an upper limit imposed by the titration method and size of resin sample used. External solution phase water contents were $\leq 0.03\%$ in the Ag-Na system, $\leq 0.05\%$ in the Na-H and NH₄-H systems. Exceptions were the three points with $X_{HR} > 0.75$ in the Na-H system and those at $X_{HR} = 0.44, 0.80$ and 0.83 in the NH₄-H system. For those points the percentage of water was between 0.1 and 0.2.

TABLE II

X_{NaR}	K_{Na}^{Ag} IN METHANOL AND WATER	
	Methanol ^a $t = 30^\circ$	Water ^b $t = 25^\circ$
0.1	11.2	3.7
.3	11.9	3.0
.5	12.3	2.9
.7	14.1	2.9
.9	17.0	3.0

^a Interpolated values.

The individual equilibrium quotients determined in this study were reproducible to $\pm 3\%$, and the curves as drawn in Figs. 1 and 2 are believed

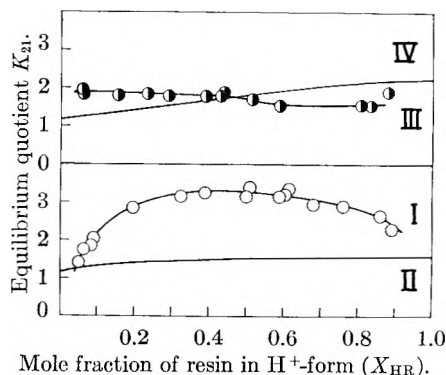


Fig. 2.—Equilibrium quotients for cation exchange in methanol and water: I, K_H^{Na} in methanol; II, K_H^{Na} in water¹⁷; III, $K_H^{NH_4}$ in methanol; IV, $K_H^{NH_4}$ in water.¹⁷

reliable to $\pm 2\%$. The results are least accurate at the ends of the curves where the fraction of the cation analyzed for directly (H⁺ or Ag⁺) is high, for there the amount of the other cation was determined as a small difference between large numbers.

For comparison the smoothed aqueous data of Bonner and co-workers¹⁷ for the same cation systems at 25° with resin of the same specifications and an ionic strength in the external solution of 0.1 *M* are included in Fig. 2 and Table II. Since the effect of temperature on most ion-exchange equilibrium quotients is moderate,¹⁸ these data should be comparable.

The Na-H-MeOH-H₂O System.—The addition of moderate amounts of water produced a striking effect on the Na-H exchange as may be seen in Table III. These experiments were so carried out that the mole fraction of resin capacity in hydrogen form at equilibrium was 0.50 ± 0.03 except where noted otherwise. Agreement with Bonner and Rhett's 25° equilibrium quotient in pure water was obtained.

TABLE III

EXCHANGE DATA IN Na-H-MeOH-H₂O SYSTEM AT $X_{HR} = 0.5$

Mole fraction H ₂ O in external soln. ^a	Equil. quotient ^b	Wt. % H ₂ O in resin soln. / Wt. % H ₂ O in ext. soln.	Meq. H ₂ O in resin / in meq. resin
0.001	3.4		
.005	3.9	>4.5	
.01	4.4	4.5	0.4
.02	5.7	4	0.8
.05	9.6	3	1.5
.10	13.8	2.3	2.8
.25	17.2	1.1	6.4
.50	10.2 ^c	~1	
.75	4.7 ^c		
1.00	1.52 ^c 1.55 ¹⁷		

^a Calculated as mole fraction of total solvent in external phase. ^b Interpolated values. ^c For these equilibrium quotients X_{HR} was about 0.6.

An investigation of the distribution of water between the solution and resin phases also was made. In Table III are listed the distribution coefficients of water between the external solution

(17) O. D. Bonner and V. Rhett, *THIS JOURNAL*, **57**, 254 (1953); O. D. Bonner and W. H. Payne, *ibid.*, **53**, 183 (1954).

(18) J. I. Bregman, *Ann. N. Y. Acad. Sci.*, **57**, 125 (1953).

and resin phases for the range of mixtures over which reliable values were obtained.

Swelling.—A few measurements on the swelling of the resin forms in water and methanol are reported in Table IV. They were obtained by both microscopic and column techniques and are reliable to perhaps $\pm 7\%$.

Discussion

By correlating these equilibrium ion-exchange data in anhydrous methanol with data for aqueous exchanges there is an opportunity further to discuss the role of the solvent in electrolyte solution phenomena. Methanol is water-like in structure and behavior but is a little less polar, having a dipole moment (vac.) of 1.68 debyes compared with the value for water of 1.85.¹⁹ As a result of having larger molecules and a lower density, methanol has a considerably smaller dielectric constant than water. At 30° the values are 31.67 and 76.75, respectively.²⁰ From these properties it can be predicted that (1) the degree of solvation of a given ion in methanol will be somewhat less than in water and that (2) electrostatic interactions between ions should be much greater in methanol. Experimental results generally confirm these ideas.

Some indication of the magnitude of these effects in the present work is available in the swelling results listed in Table IV. It is of interest to compare the relative values of the swollen volumes (which are more reliable than the absolute values), so that the role of the cations can be emphasized. All resins were less swollen in methanol than in water. Only the hydrogen and ammonium forms imbibed appreciable amounts of pure methanol. It is worth noting that the resin phase molalities in the Ag-Na system, based on solvent up-take, were about 50 compared with values of 5-10 observed for other methanol and most aqueous cases.² Similar values for the Ag and Na resins may be deduced from the results of others.^{13,14}

TABLE IV
SWELLING OF RESINS IN METHANOL AND WATER

Resin form	Cation radius (crystallo- graphic)	Ratio $\frac{\text{swollen vol.}}{\text{dry vol.}}$ for resin		
		MeOH	$X_{H_2O} = 0.2^a$	H ₂ O ^b
H	0	1.74	1.96	2.07
Na	0.95	1.12	1.69	1.94
Ag	1.26	1.05	1.23	1.70
NH ₄	1.48	1.43	1.52	1.83
0.5 Na-0.5 H		1.79		
0.5 NH-0.5 H		1.77		
0.5 Ag-0.5 Na		1.0		

^a Obtained only by column technique. Mole fraction of water is for external solution. ^b For resin of same specifications the data of H. P. Gregor, *et al.*, *J. Colloid Sci.*, **6**, 245 (1951), at 25° are 2.19, 1.94, 1.76 and 1.73, respectively.

From the small swelling of the silver and sodium resins, it appears that solvent-ion interaction is particularly small in these and that there may be considerable ion-pair formation between the cations and the resin sulfonate ions. Even in water con-

ductance studies on silver resinate have indicated about one-third association.²¹ In a medium of dielectric constant as low as that of methanol, association would be expected to be very much greater. Gregor¹⁴ has reported on the silver resin sulfonate system in mixed solvents and concluded the resin is more or less completely associated in mixtures of dielectric constant below 50.

The behavior of sodium ions in the resin phase is more difficult to assess. The small crystallographic radius of these ions and the slight solvation of the pure sodium resin in methanol imply that some ion-pairing may be occurring. An additional indication of this is the very marked increase in the swelling of this resin on addition of a small amount of water to the methanol-saturated beads. Since the solvated volumes of the ions in methanol and water must be only a little different,²² the swelling appears better explained by an increase in dissociation and thus in osmotic activity as well as solvation. On the other hand, the high degree of solvent uptake in the mixed sodium-hydrogen resinate suggests caution in attempting to describe the situation of sodium ions in actual exchanges. The matter is considered further in the next section.

A contrast is provided by the ammonium and hydrogen resins, both of which appear dissociated in methanol. The first seems to swell in methanol, not particularly as a result of solvation—even in water the large ammonium ion is considered lightly solvated—but as a result of osmotic activity engendered by the ions. Gregor¹⁴ reached a similar conclusion for this resinate in mixed solvents. For the hydrogen resin solvation and swelling both seem important.

Exchange Systems.—In both the Na-H and Ag-Na exchanges in methanol equilibrium quotients were significantly different from comparable aqueous values. Assuming that the exchange equilibrium is of a Donnan type^{4,23} the resin selectivity is definable in terms (1) of the difference in the partial molal volumes of the exchanging ions in the resin phase and (2) of the ratio of the activities of those ions in the resin phase and the external solution. In exchange, therefore, the resin will prefer the ions with smaller solvodynamic volumes and lower resin activities. This statement presumes that external solution activities may be considered roughly proportional to molalities when the ionic strength is kept constant as in this study.

A qualitative consideration of the Na-H system on the basis of what has already been suggested would predict the observed increase in resin preference for sodium ions in shifting from water to methanol. There is insufficient evidence, however, to separate the effect of the change in solvodynamic volumes from that in activity on shifting from water to methanol. Some preliminary experiments on the NH₄-Na exchange in methanol appear to favor the idea of association. Those results show that sodium is favored in methanol, while in water the opposite is true.¹⁷ Also, Kress-

(19) R. Gurney, "Ionic Processes in Solution," McGraw-Hill Book Co., New York, N. Y., 1953, p. 266.

(20) A. A. Maryott and E. R. Smith, Natl. Bur. Standards (U. S.), Circ. 514 (1951).

(21) E. Heymann and I. J. O'Donnell, *J. Colloid Sci.*, **4**, 405 (1949).

(22) Reference 19, chapter 4.

(23) H. P. Gregor, *J. Am. Chem. Soc.*, **73**, 643 (1951).

man and Kitchener¹⁰ have reported a reversal for the $\text{NH}_4\text{-Na}$ exchange in ethanol-water.

In the Ag-Na system it seems well substantiated that the silver ions are strongly associated, and the strong preference of the resin for silver over sodium as evidenced by the large $K_{\text{Na}}^{\text{Ag}}$ is not surprising. The slow rate of equilibrium attainment in these systems at high silver concentration provides additional evidence of the highly associated state and consequent slow diffusion of the silver ions.

Only in the case of the $\text{NH}_4\text{-H}$ exchange is the shift from water to methanol accomplished with little change in selectivity. This result appears to be in accord with the deductions from the measurements of amounts of swelling of the resin forms.

The $\text{Na-H-MeOH-H}_2\text{O}$ System.—The addition of water produced an effect on the equilibrium point of the Na-H exchange which was dependent in a complex fashion on the concentration of water. Two interrelated distributions are involved in such a system, (1) that of the solvents and (2) that of the ions. These will be discussed separately.

It was found that water was selectively imbibed over the range from zero to at least 40% water by weight in the external solution. At very low water concentrations only upper limits on the water in the resin were determinable by the analytical procedure used, and the distribution is known only to favor water in that region. The correlation between the relative resin solution phase and the milliequivalents of water per milliequivalent of resin capacity shown in Table III is believed significant, though not too much confidence should be placed in the absolute values. Certainly competition for the solvents by the ions present in the resin phase will be a key factor in the water uptake. Since the energetics of solvation favor the interaction of the ions with water rather than methanol,²⁴ a large portion of the first entering water will become "bound" water. In the light of the recent study on water sorption thermodynamics by Glueckauf and Kitt,²⁵ the order of hydration on the addition of water to a dry polystyrene sulfonate will probably be H^+ , RSO_3^- and Na^+ for the ions of interest. As increasing percentages of the different species become hydrated, interaction with additional water molecules should become less favorable. Macroscopically, the result expected would

be a diminishing preference of the resin phase for water. In one milliequivalent of resin in the work being reported there were 1 meq. RSO_3^- , $1/2$ meq. H^+ , and $1/2$ meq. Na^+ . At the point where the ratio of the per cent. water in the resin solution to that in the external solution had fallen to 1.1, it was calculated that there were roughly 3 molecules of water present per ion. It is very likely that some of this amount is not hydration water, but "swelling water"—*i.e.*, water brought in as a result of osmotic activity.

Previous studies on water selectivity in alcohol-water mixtures on the same resin by Bonner and Moorefield¹³ and Gregor, Nobel and Gottlieb¹⁴ have been less detailed but have shown that the silver and ammonium forms have an increasing preference for water in ethanol-water mixtures as the concentration of ethanol is increased. According to the second paper, in methanol-water mixtures the resins show relatively little preference for water, but few data are presented. It is worth noting that the measurements were not extended to methanol concentrations above 60%. In the first paper the hydrogen form was reported as having a very slight preference for ethanol.

The difficulty in interpretation of the behavior of the equilibrium quotient of this system is one of analyzing the importance of different interrelated factors. Sakaki and Kakihana¹¹ have also reported on the Na-H exchange in methanol-water mixtures using Amberlite IR-120 resin, another polystyrene sulfonate type. They reported comparable dependence of K_{H}^{Na} on solvent composition—*i.e.*, the appearance of a maximum in selectivity below $N_{\text{H}_2\text{O}} = 0.35$ but did not give any data for that region. It is not known whether they had any results in anhydrous methanol. On the water side of the maximum they found that the equilibrium quotient could be related satisfactorily to the dielectric constant of the medium and the hydration of the ions using two adjustable parameters.

As the water content drops below $N_{\text{H}_2\text{O}} = 0.35$ this system seems to bear a close resemblance to a chromatographic equilibrium where ions compete for different complexing or solvating agents while being absorbed on a column. At present, without activity and other thermodynamic data, it is felt that it would be unwarranted to attempt a theoretical analysis. In future publications it is planned to incorporate such data.

(24) Ref. 19, Chapter 13.

(25) E. Glueckauf and G. P. Kitt, *Proc. Roy. Soc. (London)*, **A228**, 322 (1955).

GLYCEROL PURIFICATION BY ION EXCLUSION

BY D. R. ASHER AND D. W. SIMPSON

Physical Research Laboratory, The Dow Chemical Company, Midland, Michigan

Received October 22, 1955

Purification of glycerol by ion exclusion has been evaluated on a laboratory scale. Many advantages can be gained using this newer method of solute separation for removing ionic impurities from crude glycerol solutions. By a method of recycle, it is possible to obtain a glycerol product of near feed concentration while reducing the ionic content to a low value. It was found that separations were improved by the use of elevated temperatures and that the optimum feed volume for this method of operation was 30–35% of the bulk resin bed volume. For maximum product concentration the feed should contain 30–35% glycerol. The salt concentration does not greatly affect the separating capacity of the resin, although higher salt concentrations will tend to improve the product concentration. For best results, the copolymer matrix should contain 4 to 12% cross-linking agent. Under these conditions it is possible to obtain a separating capacity greater than 4# of glycerol/ft.³ of resin/hour, with a product concentration of 20% or more. The application of ion exclusion to large scale purification of non-ionic materials is becoming more attractive because of the inherent low cost, simplicity of operation, and ease of unit scale-up.

Introduction

Essentially all of the processes for producing glycerol have a common problem, the removal

of the ionic impurities associated with its production. In the past, purification has been carried out by a series of distillation steps and more recently with the development of high capacity resins ion exchange¹ has been used advantageously. The relatively new process of ion exclusion has been evaluated for separating impurities from the glycerol and appears to be a promising technique.

Ion exclusion can be used to separate any two or more solutes as long as the solutes in question have different resin-liquid distribution ratios. Solute distribution ratios (K_d)² have been determined for a number of solutes from a variety of solute-water-resin systems.³ As previously shown ionic materials usually have relatively small K_d values (0.1 to 0.2) while the K_d values for non-ionized materials range from 0.4 to 2. The difference in distribution ratios for different solutes is the basis of ion exclusion and the degree of separation is related to the magnitude of the difference between the distribution ratios of the solutes in the system. Solute distribution ratios are usually not constant and variations may be found in any given system. For the system of glycerol-sodium chloride-Dowex 50-water, Shurts⁴ has shown (Figs. 1 and 2) how the distribution ratios of glycerol and salt may vary with glycerol concentration, sodium chloride concentration and total concentration. These variations made it difficult to theoretically predict the desired operating conditions without a backlog of laboratory data.

The optimum operating conditions are dependent on the mode of operation and the results that are desired. The authors are attempting to point out a type of operation which will yield a product concentration approaching the feed concentration, thus reducing the evaporator load. To achieve this product concentration, the feed volume should be large enough to produce an overlapping of the two solute concentration waves as they appear in the effluent stream. The effluent stream must be separated into three or four fractions as indicated in Fig. 4. The first fraction (assuming the salt is to be discarded) is sent to waste. The second

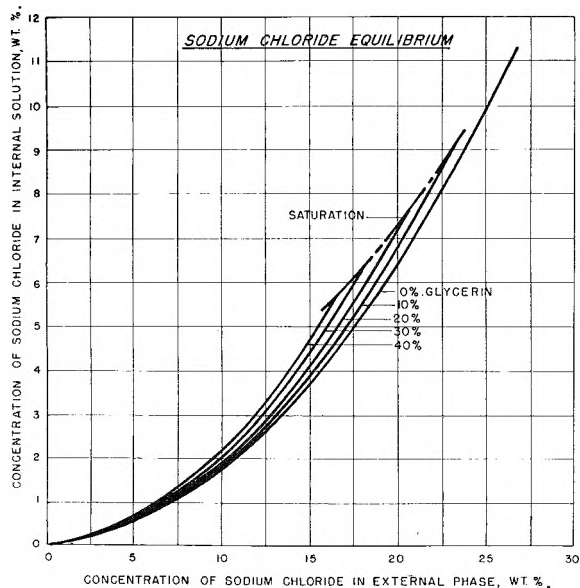


Fig. 1.—Sodium chloride equilibrium.

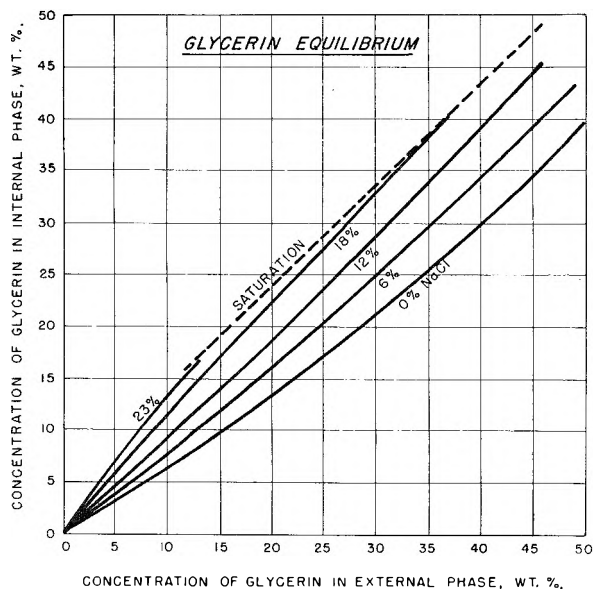


Fig. 2.—Glycerol equilibrium.

(1) G. W. Bushy and D. E. Grosvenor, *J. Am. Oil Chem. Soc.*, **29**, 318 (1952).

(2) $K_d = \frac{\text{concn. of solute in internal liq. phase}}{\text{concn. of solute in external liq. phase}}$

(3) R. M. Wheaton and W. C. Bauman, *Ann. N. Y. Acad. Sci.*, **57**, 159 (1953).

(4) E. L. Shurts, Doctoral Thesis, University of Michigan, 1955.

fraction containing the cross contaminated portion of the effluent is mixed with the feed for the next cycle. The third fraction which is essentially free of salt becomes the glycerol product fraction. Improved product concentration may be maintained by treating the dilute tail wave as a fourth cut. This fourth fraction can be used as a feed diluent or it can be recycled through the resin bed following the feed, or in some systems, it may precede the feed through the bed. How this fourth fraction is handled depends entirely upon the system and the limitations placed upon the operation.

Experimental

The laboratory column (0.6" i.d. \times 72") was jacketed for temperature control. Resin bed temperatures were maintained by circulating water through the jacket from a constant temperature bath. The column was filled to a height of 60" (278 ml.) with the sodium form of Dowex 50 (50-100 mesh) of the desired cross-linkage. The resin bed temperature was allowed to equilibrate with the jacket temperature prior to each run. The feed solutions were prepared from C.P. glycerol (95.6% glycerol) and C.P. sodium chloride. A measured amount of feed solution was layered on the flooded resin bed and allowed to pass through the bed at a controlled rate (0.5 g.p.m./ft.²) by adjusting a valve at the bottom of the column. Deionized water was used to rinse the salt and glycerine from the bed with the resin bed being maintained in a flooded state throughout the run. The effluent was collected in 10-ml. fractions and subsequently analyzed for sodium chloride and glycerol. The sodium chloride concentrations were determined by titrating potentiometrically with silver nitrate. The glycerol concentrations were determined by refractive index and when salt was also present by refractive index difference. Results are graphed on standardized plots; effluent volumes are divided by total resin bed volume (V_e/V_T) and effluent concentrations by feed concentrations for both sodium chloride and glycerol (C_e/C_f). Reducing these data to a common denominator minimizes the differences due to bed dimensions or feed concentrations.

Results

This study was not directed toward any specific crude glycerol source. It was meant to show the feasibility of using ion exclusion in the glycerol purification step and to establish the operating conditions that would yield the best results. The authors also attempted to establish the limiting feed concentrations and feed volumes that might be used in this type of operation. Other variables examined were the operating temperature and type and cross-linkage of the resin.

Temperature.—Since the viscosity of aqueous glycerol solutions increases rapidly with concentration, it was assumed that elevated temperatures would aid in the separation process. The improvement found by using higher temperatures, 80° as controlled by the constant temperature bath (Fig. 4) when compared to those at room temperature 24–26° (Fig. 3), becomes apparent. At room temperature, the trailing edge of the salt wave is not sharp and extends across the heart of the glycerol wave, thus contaminating the desired product fraction. It is noted that the glycerol also trails at the lower temperature. It is believed that this trailing is a viscosity effect. The high temperature runs repeatedly, gave much sharper waves and improved average glycerol concentration of the product fraction.

Feed Volume.—Using the proposed recycle method, the feed volume should be such that the

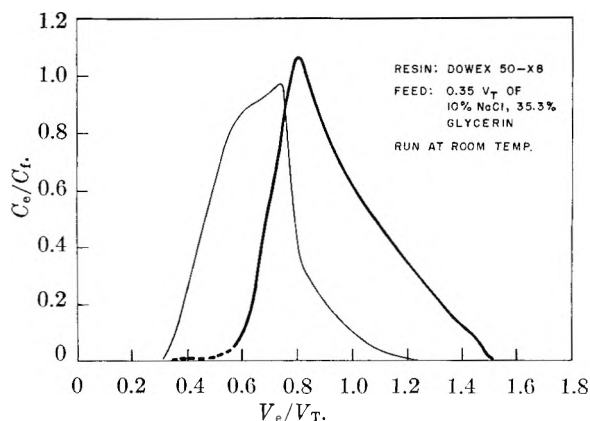


Fig. 3.—Ion exclusion.

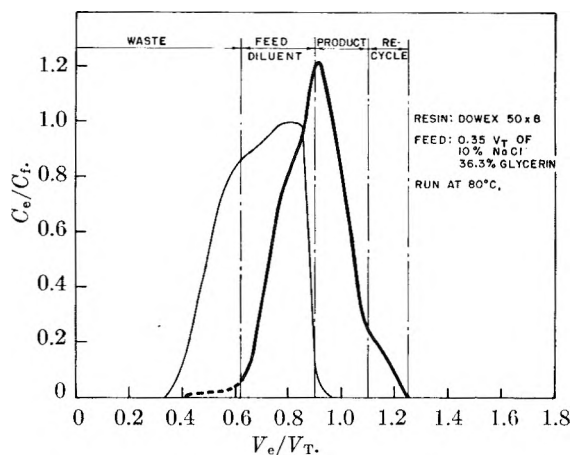


Fig. 4.—Ion exclusion.

solute effluent concentration waves cross at a value approaching the concentration of the solutes in the feed solution as shown in Fig. 4. A smaller feed volume results in a more dilute glycerol effluent wave and, hence, a more dilute product. Figure 5 in which the feed volume was approxi-

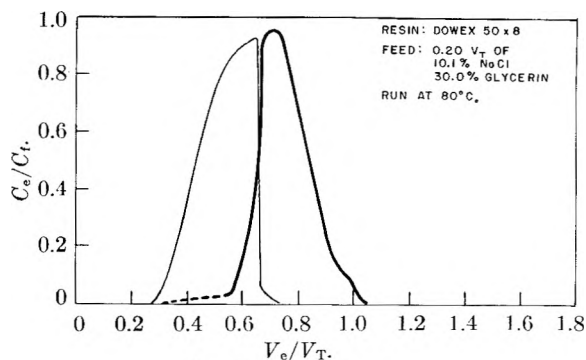


Fig. 5.—Ion exclusion.

mately 20% of resin bed volume indicates a nearly complete separation was obtained. However, the average product concentration can be improved by increasing the feed volume. If the feed volume is too large, the two solutes will plateau at feed concentration for a volume equivalent to the amount by which the column is overfed. Figure 6, in which the feed volume was approximately 50% of resin bed volume, shows the results obtained when the separating capacity of the resin bed

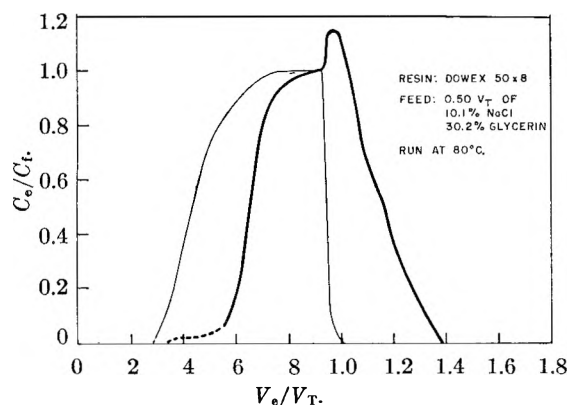


Fig. 6.—Ion exclusion.

(pounds of glycerol/hour/cubic foot of resin) has been exceeded.

Solute Concentrations.—Variations of ionic or non-ionic concentration or total concentration in the feed solutions are reflected in the shape and location of the elution waves. For example, an increase in the salt concentration not only increases the K_d value of the salt (Fig. 1) but also effects an increase in the K_d value of the glycerol (Fig. 2). As shown by Simpson and Bauman⁵ this variation of K_d due to the presence of the salt delays the appearance of the glycerol fraction. As the salt wave disappears, the K_d of the glycerol rapidly decreases to its normal value, thus causing a large amount of glycerol to transfer from the internal to the external phase.

This sudden transfer of glycerol from the internal to external liquid phase causes the glycerol to concentrate at this point to a value greater than its concentration in the feed. If the salt concentration is appreciable (10 to 20%) the glycerol effluent concentration can be made to peak at two or three times its initial concentration in the feed solution as shown in Fig. 7. To realize the full value of this concentrating effect, a recycle method as previously described must be employed. The effect is evident in Figs. 4 and 6, though the maximum concentrating effect cannot be obtained in one pass through the bed.

The shape of the salt wave is dependent upon the initial salt concentration and, to a lesser extent, the glycerol concentration. An increasing salt concentration increases the salt distribution ratio and also dehydrates the resin which dilutes the forward portion of the salt wave. Both of these factors also tend to sharpen the tail of the salt wave. The effects due to the presence of glycerol, even though shifting the distribution coefficient of the salt, appear to be swamped out in actual operation by all the other factors except at exceedingly high glycerol concentrations. At high glycerol concentrations (>30% at room temperature and >40% at 80°), the tail wave of the salt trails across the heart of the glycerol wave. There could be at least three factors causing the salt to trail: (1) Variations in the degree of trailing would suggest that the viscous glycerol solutions may cause an uneven flow pattern within the

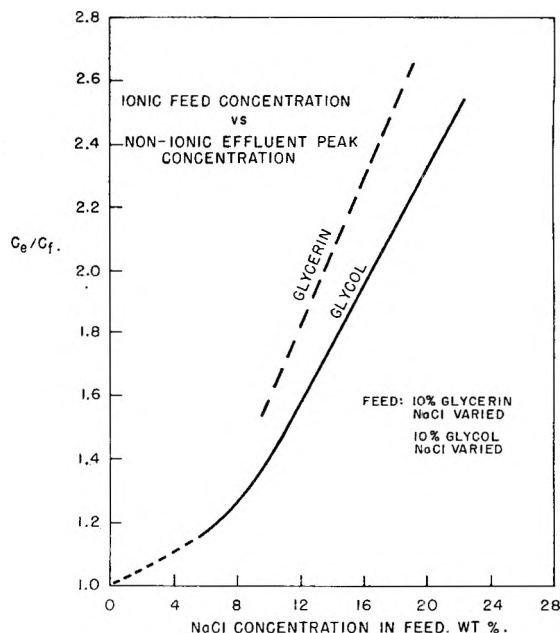


Fig. 7.—Ion exclusion concentrating effect.

column. (2) Viscous solutions decrease the rate of diffusion which result in a greater volume of cross contaminated effluent material. (3) High glycerol concentrations will decrease the activity of both the salt and sulfonic acid groups. A decrease in the activity of the salt would tend to make it less ionic in character, thus contributing to an increase in its distribution ratio. A decrease in activity of the ionic groups ($-\text{SO}_3-\text{Na}^+$) within the resin would decrease the ion exclusion properties of the resin and would also tend to increase the distribution ratio of the salt. The magnitude of the effect due to any single contributing factor has not been determined.

Type and Cross-linkage of Resin.—It should be pointed out that the cross-linkage of the resin can be an important variable in ion exclusion. As previously outlined⁶ 4 to 12% cross-linked resins give the best operating results for most ion exclusion separations. Lower cross-linked (<4%) resins swell and shrink to a greater degree with changing concentrations, especially with ionic materials, thus causing a changing bed volume and a changing pressure drop across the bed which makes the operation more difficult. Also the lower cross-linked resins have fewer exchange sites per unit volume and, hence, a smaller exclusion factor which results in poorer separations. A highly cross-linked (>12%) resin decreases the solute diffusion rate and decreases the resin separating capacity.

Separations have been made using Dowex 50 sodium form and a comparable anion resin, Dowex 1, in the chloride form. The separations are essentially identical. Dowex 50 was used throughout this study on the premise that cost and stability factors would preclude the use of anion resins.

Discussion

In general, any contemplated separation to be made by ion exclusion requires a preliminary in-

(5) D. W. Simpson and W. C. Bauman, *Ind. Eng. Chem.*, **46**, 1958 (1954).

(6) D. W. Simpson and R. M. Wheaton, *Chem. Eng. Prog.*, **50**, 45 (1954).

vestigation since the variables encountered are somewhat specific for any given system. The maximum capacity, recovery and product concentration are functions of the system and the method of operation. For example, the product concentration is dependent upon the concentration of both the ionic and non-ionic concentrations in the feed solution. It is also dependent upon the volume of feed used per cycle. In the case of viscous solutions, such as glycerol, elevated temperatures increase the resultant product concentration.

The ion exclusion technique is applicable to a number of glycerol solutions. It can be used to separate the ionic impurities directly from the spent soap lye solutions (5–10% glycerol and 12–15% salt) or from solutions obtained from the synthetic glycerol (7–8% glycerol and 12–15%

salt) process. These relatively high salt concentrations have a concentrating effect on the glycerol and a product can be obtained approximately equivalent in concentration to that of the feed solution. In this case, the concentrating effect roughly balances out the dilution effect normally associated with ion exclusion. If these glycerol solutions are concentrated to 80–85% to remove the bulk of the salt, the remaining salt (7–8%) can be separated by ion exclusion by diluting this solution to 30–35%. A product cut can be obtained which is equivalent in concentration (20%) to that obtained by ion exchange and at only a small fraction of the cost. Using this 30–35% glycerol feed solution and the proposed recycle method of operation, a separating capacity of 4 lb. of glycerol per cubic foot of resin per hour can be obtained with a glycerol recovery of 98–99%.

A THERMODYNAMIC CALCULATION OF CATION EXCHANGE SELECTIVITIES¹

BY G. E. MYERS AND G. E. BOYD

Contribution from the Chemistry Division, Oak Ridge National Laboratory, Oak Ridge, Tennessee

Received October 22, 1955

A complete and thermodynamically rigorous computation of the selectivity coefficients, D , shown by variously cross-linked sulfonated polystyrene cation exchangers in the exchange of hydrogen, lithium, potassium and cesium ions with sodium ion was carried out using the Gibbs–Donnan equation. Exact evaluations of the osmotic free energies and of the activity coefficient ratios for the exchangers were performed using cross-differentiation relationships which are valid for ternary mixtures. A comparison of experimentally determined D values with those computed showed a general agreement within the errors involved. However, significant discrepancies were found with the more highly cross-linked exchangers. The important conclusion was drawn that cation exchangers prepared by the sulfonation of polystyrene–divinylbenzene copolymers are chemically heterogeneous in that more than one type of ionogenic group may be present in their structure.

It is now appreciated that the equilibrium selectivity shown at constant temperature by polymeric organic ion exchangers is dependent upon the number and nature of the structurally bound ionogenic groups, upon the cross-linking of the polymer, upon the ionic composition of the exchanger, and upon the nature and composition of the external aqueous mixed electrolyte solution. Several reports^{2a–5} have appeared during the past five years wherein differing approaches to the descriptions of ion-exchange equilibria have been presented in the attempt to give a framework for the interpretation of the foregoing facts.

The most general and fruitful of these thermodynamic treatments recognizes that the distribution of ions between an exchanger and an aqueous electrolyte solution differs essentially from the more usual partition of solutes between immiscible phases because of the presence of non-diffusible, ionic functional groups in the exchanger. The partition of the freely diffusible ions found in both

phases accordingly must be governed by a Donnan membrane equilibrium. Cognizance is also taken in this treatment of the dependence of the swelling of ion exchangers on their cross-linking and ionic composition by assuming that the variation of the free energy of the polymeric network with volume resulting from the osmotic penetration of water molecules into the resin serves to define a swelling pressure, P . A straightforward application of thermodynamic methods⁶ then leads to the relation

$$RT \ln K_a = P(z_2\bar{v}_1 - z_1\bar{v}_2) \quad (1)$$

where K_a is the "mass law" activity product ratio for the exchange reaction at equilibrium between like-charged ions, \bar{v}_1 and \bar{v}_2 are the partial molal volumes of the exchanger salts formed with ions 1 and 2, and z_1 and z_2 are the charges carried by these ions, respectively. All the ions in the exchanger are regarded as existing in an aqueous solution, which, for the case in hand, may be regarded as that of resins 1 and 2 in the water of gelation. The standard states for the mixed aqueous resinate and for the external aqueous electrolyte solutions are chosen to be the same, so that $\Delta\mu^0 = 0$. The molal scale of concentrations will be employed, and the reference state is so chosen that the mean ionic activity coefficient approaches unity when the concentration is reduced to zero.

(1) Presented before the Symposium on Ion-Exchange, Southeast Regional Meeting, American Chemical Society, Columbia, S. C., November 3–5, 1955.

(2) (a) H. P. Gregor, *J. Am. Chem. Soc.*, **73**, 642 (1951); (b) W. J. Argersinger, Jr., W. J. Davidson and O. D. Bonner, *Trans. Kansas Acad. Sci.*, **53**, 404 (1950).

(3) E. Hogfeldt, E. Ekedahl and L. Sillén, *Acta Chem. Scand.*, **4**, 828 (1950).

(4) E. Glueckauf, *Proc. Roy. Soc. (London)*, **214**, 207 (1952).

(5) G. E. Boyd and B. A. Soldano, *Z. Elektrochem.*, **57**, 162 (1953).

(6) F. G. Donnan, *Z. physik. Chem.*, **168A**, 369 (1934).

The selectivity coefficient, D , for like, *singly charged* ions may be defined by

$$D \equiv (m_2/m_1)_r / (m_2/m_1)_w \quad (2)$$

where the quantities m_1 and m_2 are the experimentally measured stoichiometric concentrations in the resinous exchanger, r , and external solution, w , respectively. Substitution into eq. 1 gives the basic equation governing ion-exchange selectivity

$$\log D = P(\bar{v}_1 - \bar{v}_2)/2.3RT + \log (\gamma_1/\gamma_2)_r - \frac{2 \log (\gamma_1/\gamma_2)_w}{2} \quad (3)$$

where γ_1 and γ_2 are the mean molal activity coefficients for salts 1 and 2, respectively. The importance of eq. 3 is that it affords the basis for the independent evaluation of D if the three terms of the right-hand member can be estimated. It will be the object of this paper to demonstrate that these estimations can be performed in a thermodynamically rigorous fashion, and to compare the calculated values of D with those obtained from experiments in which the equilibrium partition was measured.

Method for the Evaluation of the Osmotic Free Energy

The first term of the right-hand member of eq. 3 hitherto has not been evaluated, although two differing thermodynamic methods for obtaining the swelling pressure have been described.^{4,5} In the past it has been assumed that the quantity $(\bar{v}_1 - \bar{v}_2)$ may be approximated by the difference $(\bar{v}_1^0 - \bar{v}_2^0)$, between the partial molal volume of ions 1 and 2 at infinite dilution. This undoubtedly incorrect assumption has been justified by the fact that in many instances the magnitude of the first term has been quite small relative to the second term of eq. 3. It will now be shown that it is possible to evaluate $(\bar{v}_1 - \bar{v}_2)$ using measurements of the densities of various salt-forms of ion exchangers as a function of their moisture contents. These measurements serve to define the equivalental volumes, $V_{\text{eq.}}$, of an exchanger which, for the ternary mixture of resinsates 1 and 2 and water, is given by

$$V_{\text{eq.}} = x_w \bar{v}_w + x_1 \bar{v}_1 + x_2 \bar{v}_2 \quad (4)$$

where \bar{v}_w is the partial molal volume of water. The equivalental fractions of water and of resinsates 1 and 2 are defined by: $x_w = n_w/(n_1 + n_2)$ and $x_1 = n_1/(n_1 + n_2) = (1 - x_2)$.

Differentiating

$$dV_{\text{eq.}} = (\bar{v}_1 - \bar{v}_2)dx_1 + \bar{v}_w dx_w \quad (5a)$$

Applying the cross-differentiation identity which holds since $dV_{\text{eq.}}$ is an exact differential gives

$$[\partial(\bar{v}_1 - \bar{v}_2)/\partial x_w]_{x_1} = (\partial \bar{v}_w / \partial x_1)_{x_w} = -(\partial \bar{v}_w / \partial x_2)_{x_w} \quad (5b)$$

The desired partial molal volume difference at a particular x_1 is then found by integration

$$\left[(\bar{v}_1 - \bar{v}_2) = (V_1 - V_2) - \int_0^{x_w} (\partial \bar{v}_w / \partial x_2)_{x_w} dx_w \right]_{x_1} \quad (5c)$$

where V_1 and V_2 are the molar volumes of the pure, moisture-free resinsates 1 and 2, respectively. The evaluation of the integral in eq. 5c may be carried out by: (a) measuring the variation of equivalental volume with moisture content for a

series of given exchanger compositions and then evaluating the partial molal volume of water using the definition that $\bar{v}_w = (\partial V_{\text{eq.}} / \partial x_w)_{x_1}$; (b) deriving the value of the differential quotient, $(\partial \bar{v}_w / \partial x_2)_{x_w}$, from the variation of \bar{v}_w with composition; and finally (c) integrating this quotient with respect to the equivalental moisture, x_w , graphically between the limits x_w corresponding to the moisture content of the cross-linked exchanger and zero.

Method for the Evaluation of the Ionic Interaction Free Energy

The second term of eq. 3 may be regarded as a measure of the total free energy of interaction of resinsates 1 and 2 in the ion exchanger. As yet, it has not been evaluated independently of an experimental measurement of D . However, two empirical attempts have been published^{4,7} wherein moisture absorption measurements on pure resinsates (*i.e.*, weakly cross-linked, homo-ionic exchangers) have been employed to estimate $\ln (\gamma_1/\gamma_2)_r$ after assuming a relation involving two adjustable parameters for the concentration variation of the resinate activity coefficients. The first of these⁴ has succeeded in accounting for the increase in D with exchanger cross-linking but has failed to explain its variation with ionic composition. The second attempt appears to have succeeded in this latter regard, but only by introducing additional empirical constants. In the treatment now to be presented it will be shown that the resinate activity coefficient ratio may be evaluated using experimental moisture absorption determinations by use of a rigorous thermodynamic procedure requiring no empirical constants. This method is based on the important contribution of H. A. C. McKay⁸ to the problem of the evaluation of activity coefficients in ternary systems.

For equilibria with dilute aqueous electrolyte mixtures the exchanger may be regarded as a ternary mixture of resinsates 1 and 2 and water. The variation of the Gibbs free energy with the exchanger composition will then be given by

$$dG = RT \ln a_1 dn_1 + RT \ln a_2 dn_2 + RT \ln a_w dn_w \quad (6)$$

Holding one of the components, say n_2 , constant and using the cross-differentiation identity

$$(\partial \ln a_1 / \partial n_w)_{n_1, n_2} = (\partial \ln a_w / \partial n_1)_{n_2, n_w} \quad (7a)$$

Introducing molalities

$$0.018 \left[\frac{\partial \ln a_1}{\partial (1/m_2)} \right]_{m_1/m_2} = \left[\frac{\partial \ln a_w}{\partial (m_1/m_2)} \right]_{m_2} \quad (7b)$$

Multiplying both sides of eq. 7b by $[\partial(1/m_2)/\partial \ln a_w]$

$$0.018 \left[\frac{\partial \ln a_1}{\partial \ln a_w} \right]_{m_1/m_2} = - \left[\frac{\partial(1/m_2)}{\partial (m_1/m_2)} \right]_{a_w} \quad (7c)$$

Combining eq. 7c with a similar equation for the variation of a_2 , and substituting the definition, $a_i = m_i \gamma_i$, remembering that m_1/m_2 is constant

$$0.018 \left[\frac{\partial \ln (\gamma_1/\gamma_2)}{\partial \ln a_w} \right]_{m_1/m_2} = - \left[\frac{\partial(1/m_2)}{\partial (m_1/m_2)} \right]_{a_w} + \left[\frac{\partial(1/m_1)}{\partial (m_2/m_1)} \right]_{a_w} \quad (7d)$$

(7) B. Soldano, Q. V. Larson and G. E. Myers, *J. Am. Chem. Soc.*, **77**, 1339 (1955).

(8) H. A. C. McKay, *Nature*, **169**, 464 (1952); *Trans. Faraday Soc.*, **49**, 237 (1953).

The total molality of resinate, m , is given by $m = m_1 + m_2$ and, defining the fractions, $x_1 = m_1/m$ and $x_2 = m_2/m$ gives upon substitution and simplification

$$0.018 \left[\frac{\partial \ln (\gamma_1/\gamma_2)}{\partial \ln a_w} \right]_{x_1} = - \left[\frac{\partial (1/m)}{\partial x_2} \right]_{a_w} \equiv -Y \quad (7e)$$

The desired resinate activity coefficient ratio at constant composition, x_1 , is given by eq. 8

$$\log (\gamma_1/\gamma_2)_r - \log (\gamma_1^*/\gamma_2^*)_r = -55.51 \\ \int_0^{\log a_w} Y \, d \log a_w = -55.51 I_R \quad (8)$$

The evaluation of the integral, I_R , in eq. 8 may be accomplished by: (a) measuring the variation in the equivalental moisture (*i.e.*, 1000/ m) of a series of mixed exchangers with composition, x_2 , at various known water activities, a_w ; (b) determining the value of the derivative, Y , from this variation, and then (c) integrating Y at constant x_2 with respect to $\log a_w$ either graphically or analytically between the limits, zero and the value of $\log a_w$ corresponding to the water activity in a given cross-linked ion-exchanger. In the application of the foregoing procedure the difficulty arises that it has not yet been possible to perform moisture absorption measurements on resinate mixtures sufficiently dilute to satisfy the condition that $\log (\gamma_1^*/\gamma_2^*)_r = 0$. Practically, however, this limitation may be overcome by conducting measurements with a very weakly cross-linked exchanger (*i.e.*, 0.5% DVB) for which the swelling pressure (*cf.* eq. 3) is effectively zero. An experimental determination of the selectivity coefficient, D^* , shown by the 0.5% DVB exchanger when in equilibrium with 0.01 N mixed aqueous electrolyte thus serves to fix the value of $\log (\gamma_1^*/\gamma_2^*)_r$ needed in eq. 8.

The evaluation of the third term of eq. 3 depends upon measurements of the activity coefficients for salts in ternary aqueous electrolyte mixtures. Fortunately, accurate values have become available in recent publications for all of the mixtures used in this work.

Experimental

As indicated already, all measurements on equilibrium moisture contents were carried out using a weakly cross-linked polystyrenesulfonic acid cation exchanger made available to us through the Physical Research Laboratory of the Dow Chemical Company, Midland, Michigan. This preparation was treated initially to exclude all defective particles; then it was repeatedly cycled with acid and base and finally washed with ethanol and thoroughly rinsed with high-grade, de-ionized water to ensure the removal of any residual linear polyelectrolyte before conversion to the desired pure and mixed resinate salt forms. Reagent grade hydrochloric acid and alkali metal chlorides were employed. The cesium salt was analyzed for rubidium and potassium by flame photometer methods which indicated a high degree of purity. After conversion to the desired salt forms, the various preparations were analyzed to determine the equivalent fractions, x_1 and x_2 , of cation resinates using the exchange capacity for the resin which was estimated by careful acidimetric titration of the pure hydrogen form. The uncertainty in the exchanger compositions was estimated to be approximately one per cent.

The equilibrium moisture absorptions of the pure and mixed salt-forms of the 0.5% DVB Dowex-50 were measured using the isopiestic equilibration technique previously described⁹ wherein saturated salt solutions are used to maintain accurately known water activities at 25°. Attention was paid to the purity of these salts, and to the minimization of any possible effects resulting from supersatura-

tion. Auxiliary studies were conducted on the various factors affecting the attainment of moisture absorption equilibrium. Six samples of nearly identical weight of the sodium salt of the 0.5% DVB polysulfonate resin were spread in silver dishes, two each of 6.4, 4.9 and 2.6 cm. diameters. All of these samples were then equilibrated in the same isopiestic unit at 25.00°, with the vapor phase of saturated solutions having water vapor pressures of 0.980, 0.902, 0.070, 0.902, 0.62, respectively. The conclusions drawn from the measured moisture contents may be summarized briefly: (a) specific moisture contents could be reproduced with an average deviation of about 0.8%. This deviation appeared to be independent of the dish size, and of the water activity generally, although a somewhat larger deviation was found at very high water activity. (b) Attainment of equilibrium, as judged by the constancy of the specific moisture content to within a few tenths per cent., required four to five days for all dish sizes, and for a variety of changes in water activity. This length of time is of the same order as that reported for ordinary aqueous solutions.⁹ As would be expected, the greater the change in water activity the longer the time for the attainment of equilibrium. Because of the above criterion for equilibrium, considerably longer times were required to pass from $a_w = 0.902$ to $a_w = 0.070$ than in the reverse process. (c) The amounts of resin employed were such that the effect of resin packing (*i.e.*, dish size) could be observed only at highest water activities where the resins were greatly swollen; under such conditions the equilibration appeared to be slightly retarded in the smallest dishes. It is felt, however, that fairly large differences in packing would be required for this kind of an effect to be of practical significance. (d) A comparison of the results from this auxiliary study with general observations on isopiestic work in this Laboratory leads to the conclusion that the major factors governing the attainment of moisture equilibrium are the cross-linking and the salt form of the particular exchanger. Consequently, the conduct of such measurements by a pre-determined schedule is not feasible; rather, the attainment of equilibrium must be judged individually for each material.

Another type of behavior observed in the isopiestic studies, which has also been noted elsewhere recently,¹⁰ was the effect of drying at elevated temperatures. Appreciable increases in the moisture uptake were found after drying the 0.5% DVB exchanger as compared with that observed before drying, suggesting that possibly a structural change such as the breaking of divinylbenzene cross-links may have occurred. All the isopiestic data presented below were obtained on salt forms previously dried to constant weight *in vacuo* at 105°.

The experimental selectivity coefficient values with which a comparison is made below were taken in part from an earlier publication.⁷ In this study selectivity coefficients were also measured for the sodium-hydrogen and potassium-sodium ion exchanges for exchangers cross-linked with 2, 4, 8, 12, 16 and 24% DVB, respectively. The analytical procedures followed used radioactive sodium and potassium and acidimetric titration of hydrogen ion. The aqueous and exchanger phases were analyzed for both ions, and activity and/or material balances were established. In general, it has appeared that D values may be obtained with a precision of 2% or better. Equivalental moisture contents for all the cross-linked exchangers in equilibrium with 0.1 N electrolyte were also taken from earlier work.⁷ However, these data were "smoothed" to adjust certain obviously incorrect values.

Experimental Results and Calculations

Experimentally observed values showing the variation of the equivalental moisture (g. H₂O per equivalent) with water activity are presented in Table I for four systems involving the exchange of hydrogen, lithium, potassium and cesium ions with sodium ion. The data for the sodium-hydrogen system are plotted in Fig. 1 to illustrate

(9) R. A. Robinson and D. A. Sinclair, *J. Am. Chem. Soc.*, **56**, 1830 (1934).

(10) E. Gluckauf and G. P. K. tt, *Proc. Roy. Soc. (London)*, **228A**, 322 (1955).

TABLE I

EQUIVALENTAL MOISTURE ABSORPTION IN VARIOUS ION-EXCHANGE SYSTEMS USING A WEAKLY CROSS-LINKED (NOMINAL 0.5% DVB) POLYSTYRENE SULFONATE CATION EXCHANGER

Equivalent fraction	0.00346	0.00877	0.03395	0.04484	0.07438	$-\log a_w$ 0.09307	0.12332	0.14978	0.20901	0.27687
Sodium-Lithium										
x_{Na}										
0.000	1075	626	261	218	161	139	118	107	85.2	69.9
.203	1025	591	242	201	150	131	116	101	79.9	65.7
.431	992	563	224	187	139	123	104	93.7	74.3	61.3
.806	934	521	203	170	131	114	97.8	88.1	70.7	59.3
1.000	880	476	183	153	122	107	91.8	83.4	67.7	57.3
Sodium-Hydrogen										
x_{Na}										
0.000	1020	600	270	235	190	164	137	125	107	89.0
.271	1001	584	249	211.4	160.6	139.6	117.6	106.8	88.9	75.5
.515	986	566	235	193.2	142.5	123	107	97.4	78.2	65.8
.759	915	518	206	169.6	124.8	110.3	95.9	86.1	68.8	58.0
1.000	880	476	183	153	122	107.4	91.8	83.4	67.7	57.3
Potassium-Sodium										
x_K										
0.000	880	476	183	153	122	107.4	91.8	83.4	67.7	57.3
.237	871	454	171.1	143.6	114.7	101.7	86.5	78.8	64.5	54.6
.406		444	158.6	132.7	106.2	93.2	80.1	73.1	60.0	51.0
.712	829	412	144.1	123.2	99.3	88.2	75.7	69.4	57.4	49.3
1.000	809	391	132.2	116.5	94.5	83.5	71.3	66.4	55.8	48.1
Cesium-Sodium										
x_{Cs}										
0.000	880	476	183	153	122	107.4	91.8	83.4	67.7	57.3
.238	843	442	169	142	111	97.7	84.5	75.6	61.6	51.9
.764	808	409	158	130	98.6	86.8	75.9	68.9	56.7	47.7
.940	784	399	152	126	94.3	82.4	71.9	66.3	54.7	46.8

three types of dependence of $(1/m)$ on the exchanger composition, x_2 . The most frequent type (type I) is that of a linear moisture, composition dependence, as is shown, for example, by the sodium-lithium and the potassium-sodium systems over a wide range in $-\log a_w$. The cesium-sodium

ion exchange system exhibited moisture-composition curves which were convex to the composition axis (type II) almost exclusively. Thus far, it is only in the sodium-hydrogen exchange that this curve has been found concave to x_2 (type III).

The variation of the equivalental moisture with $-\log a_w$ for the sodium-lithium exchange system is shown in Fig. 2. This behavior is typical of that for all the systems in Table I. Moisture values for the sodium equivalent fraction, $x_{Na} = 0.5$ were interpolated from a $(1/m, x_{Na})$ plot similar to Fig. 1.

Several attempts were made to derive the value of the derivative $Y = [\partial(1/m)/\partial x_2]a_w$ from the

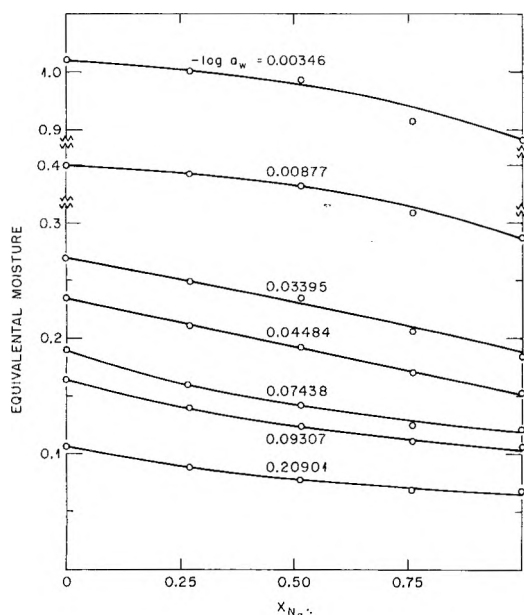


Fig. 1.—Variation of the equivalental moisture of nominal 0.5% DVB polystyrene sulfonate with sodium equivalent fraction in the sodium-hydrogen ion-exchange system.

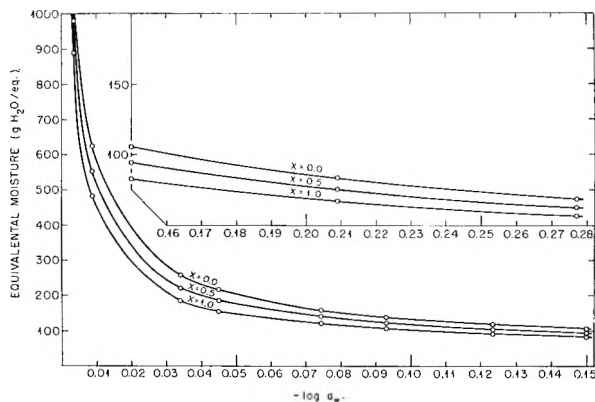


Fig. 2.—Variation of the equivalental moisture of nominal 0.5% DVB polystyrene sulfonate with water activity in the sodium-lithium ion-exchange system.

TABLE II

CONSTANTS FOR THE LEAST SQUARES "BEST FIT" OF THE EXPERIMENTAL DATA TO EQ. 10

-log a _w	Sodium-Lithium		Potassium-Sodium		Sodium-Hydrogen			Cesium-Sodium		
	a	-b	a	-b	a	-b	c	a	-b	c
0.00346	1.071	0.1833	0.883	0.0745	1.021	0.0356	-0.1108	0.877	0.125	0.0333
.00877	0.624	.1409	.476	.0859	0.600	.0238	-.1018	.475	.142	.0678
.03395	.259	.0742	.182	.0517	.270	.0598	-.0273	.182	.0523	.0233
.04484	.216	.0611	.151	.0370	.235	.0868	+.0040	.153	.0454	.0189
.07438	.1585	.0366	.120	.0279	.190	.125	.0559	.122	.0450	.0178
.09307	.138	.0308	.106	.0243	.164	.107	.0491	.107	.0384	.0138
.12332	.119	.0269	.0908	.0206	.137	.0764	.0312	.0914	.0277	.0080
.14978	.106	.0228	.0823	.0172	.125	.0722	.0302	.0830	.0312	.0150
.20901	.0837	.0167	.0668	.0122	.107	.0772	.0373	.0674	.0242	.0120
.27687	.0685	.0119	.0564	.0093	.0894	.0614	.0288

data of Table I. Since $1/m = f(x, y)$ where $y \equiv -\log a_w$, a fit of all of the data to the "best" least squares surface given by the polynomial

$$1/m = f(x, y) = c_0 + c_1x + c_2x^2 + c_3x^3 + c_4xy + c_5xy^2 + c_6x^2y + c_7y + c_8y^2 + c_9y^3 \quad (9)$$

was performed using the Oak Ridge high-speed electronic digital computer. Unfortunately, the values of the constants were such that this equation gave inflections within the range of the experimental data so that reliable $Y(x, y)$ values could not be obtained. A variety of other attempts, all of which proved inadequate, were made.

The procedure finally adopted was to determine the least squares best fits to a polynomial of the type

$$(1/m) = a + bx + cx^2 \quad (10)$$

for each value of $y = -\log a_w$ at which equivalental moistures were determined as a function of exchanger composition. Values for each of the constants in eq. 10 for the four systems examined are summarized in Table II. The required derivatives were computed by differentiation. An illustrative $(-Y, y)$ plot is given in Fig. 3. It may be

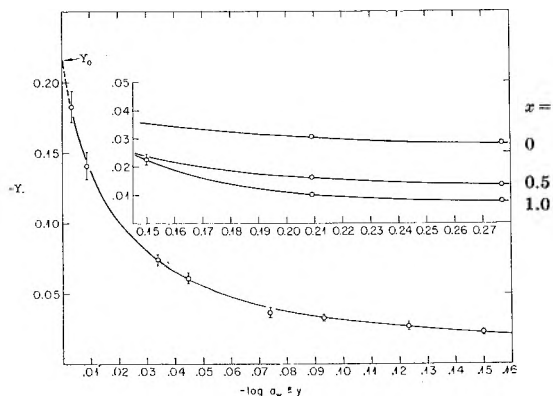


Fig. 3.—Variation of the slope, $-Y$ with $-\log a_w$ for the sodium-lithium ion-exchange system.

noted that all the slopes, Y , found in this study were negative. The integrations of Y with respect to $\log a_w$ required by eq. 8 were performed either analytically or graphically depending on whether or not an empirical function could be found for $Y = f(-\log a_w)$. The smooth extrapolation (cf. Fig. 3) of Y to $-\log a_w = 0$ was based on con-

siderations which showed that a finite value was to be expected.¹¹

The necessary computations for the required partial molal volume difference, $(\bar{v}_1 - \bar{v}_2)$, indicated by eq. 5c were carried out using data available in the literature.¹² Values for the partial molal volume of water, \bar{v}_w , were obtained by a graphical differentiation of plots of the variation of the equivalental volume, $V_{eq.}$, with equivalental moisture, x_w (moles H₂O/equiv.) for various pure salt forms of Dowex-50. The \bar{v}_w so derived are shown plotted against x_w in Fig. 4. Values for the quantity $(\partial\bar{v}_w/\partial x_2)x_w$ were obtained from plots of \bar{v}_w against x_2 and then were plotted against x_w for graphical integration. An example of the latter is given in Fig. 5 for the sodium-lithium ion-exchange equilibrium. The values for $x = 0.5$ appearing in Tables III-VI were estimated by taking the arithmetic average of the values for $x = 0$ and $x = 1.0$, respectively.

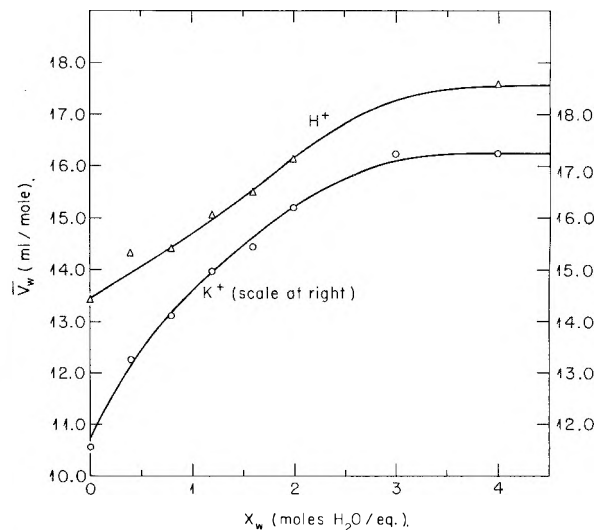


Fig. 4.—Variation of the partial molal volume of water, \bar{v}_w , with the degree of hydration of Dowex-50. (Computations based on data given in ref. 11.)

The Sodium-Lithium Ion-exchange Equilibrium.—Details for the complete computation of $\log D$ using eq. 3 are summarized in Table III. Values of $-\log a_w$ appearing in the fourth column were read from Fig. 2 using the equivalental moistures

(11) The authors are indebted to Professor George Scatchard for the proof of this fact.
 (12) H. P. Gregor, B. R. Sundheim, K. M. Held and M. H. Waxman, *J. Coll. Sci.*, **7**, 511 (1952).

TABLE III

COMPUTATION OF LOG D FOR VARIOUS COMPOSITIONS AND CROSS-LINKAGES IN THE SODIUM-LITHIUM ION-EXCHANGE SYSTEM

$$\log D = P(\bar{v}_{Li} - \bar{v}_{Na})/2.3RT' - 55.51I_R + \log(\gamma_{Li}^*/\gamma_{Na}^*)_r - 2 \log(\gamma_{LiCl}/\gamma_{NaCl})_w$$

% DVB	Sodium equiv. fraction	Equiv. moisture (g. H ₂ O/eq.)	$-\log a_w$	$-55.51I_R$	$\log \frac{(\gamma_{Li}^*)}{(\gamma_{Na}^*)}_r$	P (atm.)	$-\Delta\bar{v}$ (ml.)	$-P\Delta\bar{v}/2.3RT'$	$2 \log \frac{(\gamma_{LiCl})}{(\gamma_{NaCl})}_w$	$\log D$	$D_{calcd.}$	$D_{obsd.}$
	0.0	625	0.0089	0.0922	0.0253	17	13.3	0.0040	0.0060	0.1075	1.28	1.12 ± 0.03
2	0.5	569	.0081	.0853	.0191	15	13.0	.0035	.0076	.0933	1.24	1.10 ± 0.03
	1.0	513	.0078	.0827	.0128	12	12.7	.0027	.0090	.0838	1.21	1.08 ± .02
	0.0	357	.0227	.1837	.0253	45	11.8	.0094	.0060	.1936	1.56	1.40 ± .03
4	0.5	330	.0209	.1733	.0191	38	11.7	.0079	.0078	.1767	1.50	1.44 ± .03
	1.0	303	.0194	.1650	.0128	32	11.5	.0065	.0090	.1623	1.46	1.48 ± .03
	0.0	196	.0542	.3071	.0253	120	11.6	.0246	.0060	.3018	2.00	1.72 ± .03
8	0.5	181.5	.0474	.2860	.0191	108	11.4	.0218	.0080	.2753	1.88	1.80 ± .04
	1.0	172	.0373	.2500	.0128	90	11.2	.0179	.0090	.2359	1.72	1.89 ± .04
	0.0	129.5	.1042	.4183	.0253	245	11.0	.0478	.0060	.3898	2.45	2.15 ± .04
12	0.5	122.5	.0940	.3999	.0191	218	10.95	.0424	.0080	.3686	2.33	2.05 ± .04
	1.0	115.4	.0812	.3743	.0128	190	10.7	.0361	.0090	.3420	2.20	1.95 ± .04
	0.0	119	.1234	.4491	.0253	315	10.7	.0598	.0060	.4086	2.56	2.40 ± .05
16	0.5	109	.1156	.4372	.0191	280	10.6	.0527	.0080	.3956	2.48	2.13 ± .04
	1.0	99	.1056	.4207	.0128	245	10.5	.0457	.0090	.3788	2.39	1.88 ± .04
	0.0	80.5	.2192	.6103	.0253	580	10.2	.1052	.0060	.5244	3.34	3.25 ± .07
24	0.5	76.0	.2038	.5462	.0191	505	10.2	.0913	.0082	.4658	2.92	2.40 ± .05
	1.0	71.4	.1834	.5218	.0128	430	10.1	.0774	.0090	.4482	2.80	1.80 ± .04

of the various cross-linked exchangers listed in column 3. The necessary integrations to determine the quantity $-55.51I_R$ were performed using the empirical equation: $-Y = 1/(5.064 + 268.4y)$

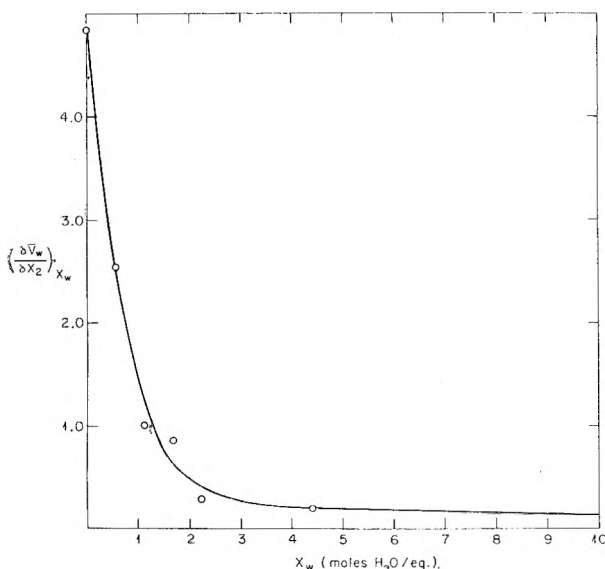


Fig. 5.—Plot for the estimation of $(\bar{v}_{Li} - \bar{v}_{Na})$ by graphical integration using eq. 5c.

derived from a least squares fit to the data shown in Fig. 3. From the values listed in the sixth column, it may be seen that the contribution of the term for the activity coefficients of the lithium and sodium resins in the 0.5% DVB exchanger is relatively quite small. The term containing the activity coefficient ratio for the aqueous mixed electrolyte was evaluated using the data of Robinson and Lim¹³ which were extrapolated down to a concentration of 0.1 molal. The contribution of this term to $\log D$ is also relatively quite small.

(13) R. A. Robinson and C. K. Lim, *Trans. Faraday Soc.*, **49**, 1144 (1953).

The osmotic free energy term, $P(\bar{v}_{Li} - \bar{v}_{Na})/2.3RT'$, is small and varies in its contribution to the calculated selectivity coefficient from about 1% for the 2% DVB exchanger up to 27% for the most highly cross-linked exchanger. The predominant term is clearly that involving the various interactions of the sodium and lithium ions in the exchangers as measured by $\log(\gamma_{Li}/\gamma_{Na})_r = -55.51I_R + \log(\gamma_{Li}^*/\gamma_{Na}^*)_r$. It is the term, $-55.51I_R$, which also contributes the largest uncertainty and hence is responsible in the main for any disagreement between the calculated selectivity coefficients and those observed experimentally. The error in the integral, I_R , arises from two sources: (a) From the errors in the slopes, Y , derived from the variation of the equivalental moistures with resin composition; (b) from errors in $-\log a_w$, the upper limit of the integral, I_R , arising from uncertainties in the equivalental moistures of the cross-linked exchangers and from errors in interpolation from curves such as those in Fig. 2. The least squares procedure employed in deriving the Y values for the sodium-lithium exchange also gave the standard errors in this quantity. These ranged from 5.5 to 11.8% with the average being $7.8 \pm 2.1\%$. The error introduced through the uncertainty in $-\log a_w$ appeared to be approximately 3% or less. The error in the calculated selectivity coefficients therefore is estimated to vary between 8 and 14%. Considering the errors in the observed D values the agreement with the calculated values appears to lie within the limits of the uncertainties involved, except for the 2% DVB exchanger where the experimental values are considered to be incorrect, and for the most highly cross-linked exchangers where, for $x_{Na} > 0.5$, a real discrepancy occurs. The possible significance of this discrepancy will be discussed after the data for the other systems are presented.

The Potassium-Sodium Ion-exchange Equilibrium.—Table IV summarizes the steps in the

TABLE IV

COMPUTATION OF LOG D FOR VARIOUS COMPOSITIONS AND CROSS-LINKAGES IN THE POTASSIUM-SODIUM ION-EXCHANGE SYSTEM
$$\log D = P(\bar{v}_{Na} - \bar{v}_K)/2.3RT - 55.51I_R + \log(\gamma_{Na^*}/\gamma_{K^*})_r - 2 \log(\gamma_{NaCl}/\gamma_{KCl})_w$$

% DVB	Potassium equiv. fraction	Equiv. moisture (g. H ₂ O/eq.)	$-\log a_w$		$\log \left(\frac{\gamma_{Na^*}}{\gamma_{K^*}} \right)_r$	P (atm.)	$-\Delta\bar{v}$ (ml.)	$-P\Delta\bar{v}/2.3RT$	$2 \log \left(\frac{\gamma_{NaCl}}{\gamma_{KCl}} \right)_w$	$\log D$	$D_{\text{calcd.}}$	$D_{\text{obsd.}}$
				$-55.51I_R$								
2	0.0	513	0.0076	0.0410	0.0873	12	6.3	0.0013	0.0077	0.1193	1.31	1.30 ± 0.03
	0.5	507	.0071	.0385	.0671	10	6.3	.0011	.0060	.0985	1.25	1.22 ± .02
	1.0	500	.0055	.0306	.0462	9	6.2	.0010	.0043	.0715	1.18	1.17 ± .02
4	0.0	303	.0176	.0828	.0873	32	5.4	.0031	.0077	.1593	1.44	1.49 ± .03
	0.5	298	.0151	.0731	.0671	28	5.4	.0027	.0060	.1315	1.35	1.38 ± .03
	1.0	294	.0138	.0681	.0462	24	5.3	.0023	.0043	.1077	1.28	1.29 ± .03
8	0.0	172	.0384	.1455	.0873	90	4.7	.0075	.0077	.2176	1.65	1.71 ± .03
	0.5	169.5	.0320	.1287	.0671	77	4.6	.0063	.0060	.1835	1.53	1.54 ± .03
	1.0	167	.0267	.1133	.0462	64	4.6	.0052	.0043	.1500	1.41	1.37 ± .03
12	0.0	115.4	.0782	.2225	.0873	190	4.3	.0145	.0077	.2876	1.94	1.95 ± .04
	0.5	113.5	.0576	.1869	.0671	163	4.3	.0124	.0060	.2356	1.72	1.72 ± .03
	1.0	112	.0465	.1640	.0462	135	4.3	.0103	.0043	.1956	1.57	1.47 ± .03
16	0.0	100	.1064	.2613	.0873	240	4.2	.0179	.0077	.3230	2.10	2.12 ± .04
	0.5	98	.0863	.2343	.0671	205	4.2	.0153	.0060	.2801	1.90	1.82 ± .04
	1.0	95	.0740	.2158	.0462	170	4.2	.0127	.0043	.2450	1.76	1.51 ± .03
24	0.0	71.4	.1955	.3449	.0873	430	4.1	.0313	.0077	.3932	2.47	2.76 ± .06
	0.5	70	.1646	.3205	.0671	368	4.1	.0268	.0060	.3548	2.26	2.06 ± .04
	1.0	69	.1335	.2917	.0462	305	4.1	.0222	.0043	.3114	2.05	1.30 ± .03

calculation of $\log D$ for this system, and it may be seen immediately that an excellent concordance between the observed and calculated selectivity coefficients was found, except for the more highly cross-linked exchangers when $x_K > 0.5$. Again, the quantity $-55.51I_R$ was determined by integrating the empirical equation: $-Y = 1/(9.169 + 339.6y)$ derived from a least squares fit to the data. The "zero point" selectivity, $\log(\gamma_{K^*}/\gamma_{Na^*})_r$ is somewhat more important for this than for the sodium-lithium system, while the osmotic free energy contribution is considerably less so. The activity coefficient ratio for the aqueous solution which was computed using the data of Robinson¹⁴ was found to be quite small as expected. As with the sodium-lithium exchange system, the chief uncertainty in the computed $\log D$ values arises in the evaluation of I_R . The standard errors in the Y values varied between 3.5 and 15.6% with the average being $9.7 \pm 2.9\%$. This error is larger than that for the Na-Li exchange owing to the fact the same relative errors in the equivalental moistures produce a much larger change in Y when the latter is small than otherwise. The plot of the experimentally measured selectivity coefficients (Fig. 6) was interpolated to obtain the values of $x_K = 0.5$ listed in the final column of Table IV. Recent measurements¹⁵ on the potassium-sodium ion-exchange equilibrium with Dowex-50 were found to be in excellent agreement with the data obtained in this work.

The Cesium-Sodium Ion-exchange Equilibrium.

—An outstanding feature of this system (Table V) is the relatively great importance of the term log

(14) R. A. Robinson and C. K. Lim, Contribution No. 18, "Symposium on Electrochemical Constants," National Bureau of Standards Circular 524, 1951.

(15) J. A. Whitcombe, J. T. Banchero and R. R. White, *Chem. Eng. Prog. Symposium Series*, No. 14, 50, 73 (1954).

$(\gamma_{Na^*}/\gamma_{Cs^*})_r$ which, of course, reflects the predominating influence of the cesium-sodium resinate interactions. The interactions of the chlorides of the same cations in aqueous solutions, as meas-

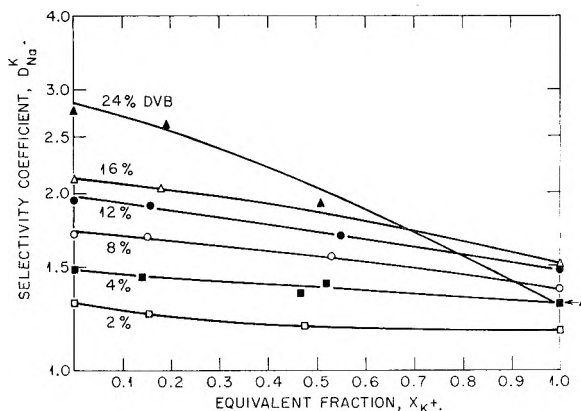


Fig. 6.—Selectivity coefficients at 25° for the potassium-sodium ion-exchange equilibrium with variously cross-linked Dowex-50. (Selectivity coefficients on a logarithmic scale.)

ured by the $\log(\gamma_{NaCl}/\gamma_{CsCl})_w$ values taken from the work of Robinson,¹⁶ while larger than those for any other pair employed in these studies, are relatively unimportant in their contributions to $\log D$. Likewise, the contribution of the osmotic free energy term is small. The evaluation of the quantity $-55.51I_R$ required somewhat more elaborate steps: for $x_{Cs} = 0$ the least squares empirical equation $-Y = 1/(1.696 + 85.54\sqrt{y})$ was integrated. For $x_{Cs} = 0.5$ the equation $-Y = 1/(9.920 + 342.4y)$ was employed, while for $x_{Cs} = 1.0$ the required integration was performed graphically using a polar planimeter. The agreement

(16) R. A. Robinson, *J. Am. Chem. Soc.*, 74, 6035 (1952).

TABLE V

COMPUTATION OF LOG D FOR VARIOUS COMPOSITIONS AND CROSS-LINKAGES IN THE CESIUM-SODIUM ION-EXCHANGE SYSTEM

$$\log D = P(\bar{v}_{\text{Na}} - \bar{v}_{\text{Cs}})/2.3RT - 55.51I_R + \log(\gamma_{\text{Na}^*}/\gamma_{\text{Cs}^*})_r - 2 \log(\gamma_{\text{NaCl}}/\gamma_{\text{CsCl}})_w$$

% DVB	Cesium equiv. fraction	Equiv. moisture (g. H ₂ O/ eq.)	$-\log a_w$	$-55.51I_R$	$\log \left(\frac{\gamma_{\text{Na}^*}}{\gamma_{\text{Cs}^*}} \right)_r$	P (atm.)	$-\Delta\bar{v}$ (ml.)	$-\frac{P\Delta\bar{v}}{2.3RT}$	$2 \log \left(\frac{\gamma_{\text{NaCl}}}{\gamma_{\text{CsCl}}} \right)_w$	$\log D$	$D_{\text{calcd.}}$	$D_{\text{obsd.}}$
2	0.0	513	0.0078	0.0830	0.2097	12	17.5	0.0037	0.0158	0.2732	1.88	1.70 ± 0.03
	0.5	429	.0091	.0443	.1634	10	16.9	.0030	.0126	.1921	1.56	1.49 ± .03
	1.0	345	.0112	.0245	.1070	9	16.6	.0027	.0106	.1182	1.31	1.31 ± .03
4	0.0	303	.0182	.1344	.2097	33	16.4	.0095	.0158	.3188	2.08	1.95 ± .04
	0.5	268	.0190	.0818	.1634	29	16.3	.0084	.0126	.2242	1.68	1.58 ± .03
	1.0	233	.0203	.0331	.1070	24	16.1	.0069	.0106	.1226	1.33	1.27 ± .03
8	0.0	172	.0375	.2022	.2097	92	15.7	.0256	.0158	.3705	2.35	2.45 ± .05
	0.5	158	.0359	.1308	.1634	78	15.7	.0217	.0126	.2599	1.82	1.69 ± .03
	1.0	144	.0357	.0436	.1070	64	15.6	.0177	.0106	.1223	1.33	1.16 ± .02
12	0.0	115.4	.0811	.3166	.2097	190	15.5	.0523	.0158	.4582	2.87	2.95 ± .06
	0.5	107.5	.0693	.1983	.1634	163	15.4	.0446	.0124	.3047	2.02	1.81 ± .04
	1.0	99.5	.0673	.0632	.1070	135	15.4	.0369	.0106	.1227	1.33	1.10 ± .02
16	0.0	99	.1075	.3637	.2097	240	15.4	.0656	.0158	.4920	3.11	3.17 ± .06
	0.5	92.4	.0946	.2351	.1634	205	15.3	.0557	.0122	.3306	2.14	1.86 ± .04
	1.0	85.8	.0862	.0746	.1070	170	15.3	.0462	.0106	.1248	1.33	1.10 ± .02
24	0.0	71.4	.1932	.5019	.2097	440	15.2	.1187	.0158	.5771	3.78	5.89 ± .12
	0.5	65.3	.1790	.3200	.1634	373	15.2	.1006	.0121	.3701	2.35	1.86 ± .04
	1.0	59.2	.1824	.1237	.1070	305	15.1	.0817	.0106	.1384	1.38	1.10 ± .02

TABLE VI

COMPUTATION OF LOG D FOR VARIOUS COMPOSITIONS AND CROSS-LINKAGES IN THE SODIUM-HYDROGEN ION-EXCHANGE SYSTEM

$$\log D = P(\bar{v}_{\text{H}} - \bar{v}_{\text{Na}})/2.3RT - 55.51I_R + \log(\gamma_{\text{H}^*}/\gamma_{\text{Na}^*})_r - 2 \log(\gamma_{\text{HCl}}/\gamma_{\text{NaCl}})_w$$

% DVB	Sodium equiv. fraction	Equiv. moisture (g. H ₂ O/ eq.)	$-\log a_w$	$-55.51I_R$	$\log \left(\frac{\gamma_{\text{H}^*}}{\gamma_{\text{Na}^*}} \right)_r$	P (atm.)	$-\Delta\bar{v}$ (ml.)	$-\frac{P\Delta\bar{v}}{2.3RT}$	$2 \log \left(\frac{\gamma_{\text{HCl}}}{\gamma_{\text{NaCl}}} \right)_w$	$\log D$	$D_{\text{calcd.}}$	$D_{\text{obsd.}}$
2	0.0	943	0.0040	0.0073	0.0020	18	12.7	0.0041	0.0086	-0.0034	0.99	1.02 ± 0.02
	0.5	728	.0051	.0442	.0025	15	13.8	.0037	.0102	+.0328	1.08	1.07 ± .02
	1.0	513	.0074	.1066	.0030	12	13.9	.0030	.0114	.0952	1.25	1.12 ± .03
4	0.0	417	.0171	.0345	.0020	50	13.6	.0121	.0086	.0158	1.04	1.10 ± .03
	0.5	360	.0188	.1329	.0025	41	13.4	.0098	.0102	.1154	1.31	1.28 ± .03
	1.0	303	.0187	.2339	.0030	32	13.1	.0074	.0114	.2181	1.65	1.16 ± .03
8	0.0	219	.0528	.1649	.0020	135	12.5	.0300	.0086	.1283	1.35	1.38 ± .03
	0.5	196	.0430	.2539	.0025	118	12.3	.0258	.0102	.2204	1.66	1.52 ± .03
	1.0	172	.0379	.3780	.0030	90	12.0	.0192	.0114	.3504	2.24	1.20 ± .03
12	0.0	145	.1178	.5527	.0020	290	11.8	.0607	.0086	.4854	3.06	1.95 ± .04
	0.5	130	.0864	.4279	.0025	240	11.6	.0494	.0102	.3708	2.35	1.78 ± .04
	1.0	115.4	.0782	.4911	.0030	190	11.5	.0388	.0114	.4439	2.78	1.13 ± .03
16	0.0	128	.1380	.6365	.0020	365	11.6	.0752	.0086	.5547	3.59	2.23 ± .05
	0.5	114	.1180	.5295	.0025	302	11.5	.0617	.0102	.4601	2.89	1.84 ± .04
	1.0	100	.1013	.5110	.0030	240	11.3	.0481	.0114	.4545	2.85	0.81 ± .02
24	0.0	96	.2580	1.1119	.0020	660	11.3	.1324	.0086	.9729	9.36	6.38 ± .13
	0.5	84	.1858	0.6945	.0025	545	11.2	.1084	.0102	.5784	3.79	2.32 ± .05
	1.0	71.4	.1850	.5785	.0030	430	11.0	.0840	.0114	.4861	3.06	0.69 ± .02

between calculated and experimentally determined D values is within the errors involved in both cases, except for $x_{\text{Cs}} > 0.5$ with the more highly cross-linked preparations. The experimental value for the 24% DVB exchanger at $x_{\text{Cs}} = 0$ is believed to be in serious error.

The Sodium-Hydrogen Ion-exchange Equilibrium.—This system (Table VI) has appeared to be the most complex of all, possibly because of the highly individual behavior of the acid resin, particularly at high concentrations. Quite large selectivities are observed (Fig. 7) for the most highly cross-linked exchangers at $x_{\text{Na}} = 0$, and, strikingly, the dependence of D on the fraction

of sodium ion in the exchanger is so pronounced that a selectivity reversal is sometimes produced. The experimental data presented in Fig. 7 are believed to be reliable; they are in good concordance with measurements recently published¹⁷ wherein selectivity coefficients for differing preparations of polystyrene sulfonate exchangers of nominal 4, 8 and 16% DVB content are reported. It is of interest that the interactions of the sodium and hydrogen resins are slight when they are present in relatively low concentrations as revealed by the small magnitude of the quantity, $\log(\gamma_{\text{H}^*}/\gamma_{\text{Na}^*})_r$. Likewise the contribution of $\log(\gamma_{\text{HCl}}/\gamma_{\text{NaCl}})_w$

γ_{NaCl}^w for the aqueous mixed electrolyte is almost negligible, as is shown in Table VI using the data of Harned.¹⁸ The quantity $-55.51/R$ was evaluated throughout by graphical integrations using a polar planimeter. The dependence of Y on $-\log a_w$ for $x_{\text{Na}} = 0$ showed a maximum, as is a necessary consequence of the change from Type III to Type II equivalental moisture-composition variations observed with this system. The agreement between the observed and computed selectivity coefficients appears satisfactory for the nominal 2, 4, and 8% DVB exchangers at $x_{\text{Na}} \leq 0.5$. However, for $x_{\text{Na}} = 1.0$, and for all higher cross-linkings at all compositions the disagreement is large, and in some cases extreme. In no case is a selectivity inversion predicted.

Discussion

The most general statement that would appear to be justified by Tables III-VI, inclusive, is that eq. 3 affords a suitable basis for understanding the selectivity coefficients for singly charged ions shown by variously cross-linked cation exchangers. However, as was indicated repeatedly above, significant, and sometimes large, deviations between the observed and computed D values were found with exchangers of high nominal DVB contents. Now it is to be stressed that in the application of eq. 3 and its important auxiliaries, eq. 5c and 8, as well as in the use of the equation for estimating the swelling pressures,⁵ it was assumed that only ternary mixtures are being dealt with. All calculations were based on the weakly cross-linked preparation (0.5% DVB) which may be regarded as an almost pure polystyrene sulfonate. The implicit assumption was made that the cross-linked exchangers were chemically identical with the 0.5% DVB exchanger, and that effectively they behaved simply as concentrated versions of the weakly cross-linked preparation. This evident neglect of the divinylbenzene as a component would seem to be justified as a first approximation because of the great similarity it shows with styrene as an element in the polymeric structure of the ion exchanger. If, however, the DVB "bridges" in the co-polymer network are also sulfonated, and, if these sulfonic acid groups differ in their thermodynamic properties from those of the *p*-benzenesulfonic acid groups which make up most of the capacity of the exchanger, then it is no longer appropriate to compare a low DVB with a high DVB preparation, nor can the latter be regarded as a ternary mixture of water and resins 1 and 2. This limitation becomes even more severe if other types of chemical heterogeneities occur such as, for example, those produced by the di-sulfonation of benzene rings, by the sulfonation of the ethylene chains of the network, and/or by the sulfonation of ethylstyrene which also may

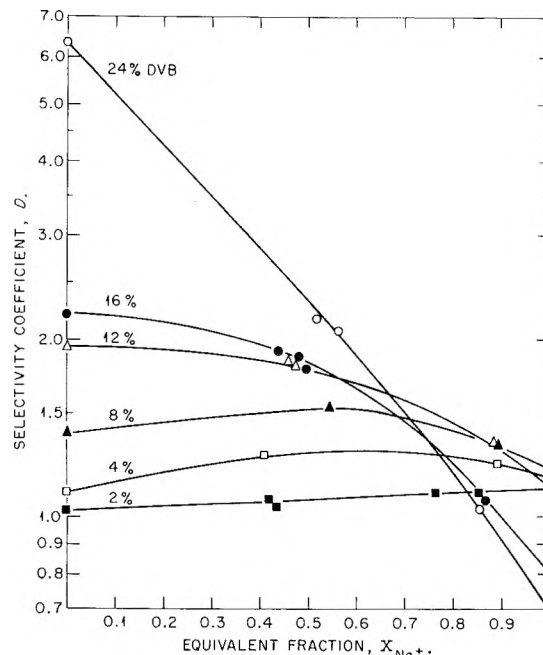


Fig. 7.—Selectivity coefficients at 25° for the sodium-hydrogen ion-exchange equilibrium with variously cross-linked Dowex-50. (Logarithmic scale for selectivity coefficients.)

be present in the structure. In view of the fairly drastic sulfonation procedures usually employed in the preparation of highly cross-linked exchangers it is not improbable that many of the foregoing processes may occur. Accordingly, the discrepancies between the observed and calculated selectivity coefficients reported in this paper for the highly cross-linked preparations are attributed to chemical heterogeneities. The computed D values in the foregoing tables are those for a truly unifunctional ion exchanger with a moisture content the same as that of the actual exchangers for which measurements were made. With unifunctional exchangers, the selectivity coefficients for the cations examined in this research should increase uniformly with cross-linking for all compositions. In addition, the dependence of D on composition will not be pronounced, except possibly for equilibria involving hydrogen ions. The synthesis of truly unifunctional sulfonated polystyrene cation exchangers will be of the greatest interest theoretically.

Acknowledgments.—It is a pleasure to acknowledge the assistance given by Mrs. Hazel Templeton for the numerous, careful isopiestic measurements required in this study, to thank Dr. S. Lindenbaum for his help in the selectivity coefficient determinations, and to express our great appreciation to Dr. J. Z. Hearon for his cooperation in numerous attempts to conduct a complete machine computation of D using the Oak Ridge Analog Computing Engine.

(18) H. S. Harned, *J. Am. Chem. Soc.*, **57**, 1865 (1935).

CATION-EXCHANGE EQUILIBRIA INVOLVING SOME DIVALENT IONS

BY O. D. BONNER AND FRANCES L. LIVINGSTON^{1,2}*Department of Chemistry, University of South Carolina, Columbia, South Carolina**Received October 22, 1965*

Equilibrium studies involving cupric, barium, strontium and calcium ion on Dowex 50 resins of approximately 4, 8 and 16% divinylbenzene content have been made while maintaining a constant ionic strength of approximately 0.1. Selectivity coefficients have been measured at various resin loadings. The characteristic maximum water uptake of the resin in these ionic forms is reported.

A summary of the results of studies of ion-exchange equilibria and maximum water uptake of Dowex 50 resins of 4, 8 and 16% DVB content involving the common univalent cations has been reported previously.³ An extension of this study to polyvalent cations and their inclusion on the same selectivity scale should furnish information on the effect of charge, hydration, ion pair formation, etc., in the ion-exchange process. Experiments of this type are now underway and data on exchanges involving cupric ion and three of the alkaline earth cations are reported herewith.

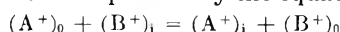
Experimental

The methods of equilibration and separation of aqueous and resin phases for exchanges of univalent ions have been described in detail.⁴ The same experimental procedures were followed in these exchanges also with two exceptions. A longer period of time for equilibration is necessary for exchanges involving polyvalent cations. At least two days was allowed for each of these equilibrations. Also in exchanges involving ions of different valence types such as the cupric-hydrogen and silver-cupric exchanges, the resin phase must be as free as possible of adhering solution before washing with distilled water for subsequent analysis. This precaution is necessary because of the great effect which dilution of a solution containing the two ions in a given concentration ratio will have upon the equilibrium composition of the resin phase. The resin composition must of necessity change in such a manner, upon dilution, so as to offset the change in the ratio $C_{B^+}/C_{M^{2+}}^{1/2}$ (see equation 4 below) and maintain the constancy of the equilibrium constant.

In preparation for analysis the resin phase was first exhaustively eluted with either ammonium chloride or barium nitrate solutions. Aliquots of this effluent and also of the solution phase were then analyzed for both ions being exchanged. The concentration of hydrogen ion in the presence of cupric ion was determined by titration with standard alkali, brom phenol blue serving as an indicator. Cupric ion concentration was determined by the titration of the iodine liberated upon the addition of potassium iodide with standard thiosulfate. Silver ion concentration was determined potentiometrically, standard sodium chloride serving as the titrant or radiometrically using Ag^{110} as a tracer. Calcium, strontium and barium were determined gravimetrically as the oxalate of the former and sulfate of the latter two ions. The precipitation of strontium sulfate was accomplished from a 50% alcoholic solution.

Discussion and Results

In exchanges of univalent ions the exchange reaction has been expressed by the equation



where A^+ and B^+ are the cations involved in the exchange and the subscripts i and 0 represent the

(1) These results were developed under a project sponsored by the United States Atomic Energy Commission.

(2) Part of the work described herein was included in a thesis submitted by Frances Livingston to the University of South Carolina in partial fulfillment of the requirements for the degree of Master of Science.

(3) O. D. Bonner, *This Journal*, **59**, 719 (1955).

(4) O. D. Bonner and V. Rhett, *ibid.*, **57**, 254 (1953).

resin phase and the outside solution, respectively. The thermodynamic equilibrium constant, K , and the selectivity coefficient, k , are related to the concentrations of the ions, C , and their activity coefficients, γ , by the equation

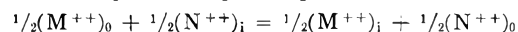
$$K = \frac{C_{(A^+)i} C_{(B^+)0} \gamma_{(A^+)i} \gamma_{(B^+)0}}{C_{(A^+)0} C_{(B^+)i} \gamma_{(B^+)i} \gamma_{(A^+)0}} = k \frac{\gamma_{(A^+)i} \gamma_{(B^+)0}}{\gamma_{(B^+)i} \gamma_{(A^+)0}} \quad (1)$$

For many of the exchange reactions which have been studied the activity coefficient ratio $\gamma_{(B^+)0}/\gamma_{(A^+)0}$ is unknown in mixed aqueous solutions. Dilute aqueous solutions (ionic strength = 0.1) have therefore been used and this ratio has been regarded as unity. This procedure has seemed preferable to applying a partial correction obtained by assuming the values of γ_{A^+} and γ_{B^+} to be the same as in pure solutions. The equilibrium constant may then be calculated from the equation⁵

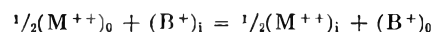
$$\log K = \int_0^1 \log k \, dN \quad (2)$$

where N is the molar fraction of the resin associated with A^+ .

For exchange reactions between two divalent ions or between a divalent and a univalent ion the reactions may similarly be represented as



and



Values of the equilibrium constants for the various exchanges may then be calculated which are directly comparable with those for exchanges between univalent ions, and cations of all valence types may be included in a single selectivity scale. The expressions for the equilibrium constants are

$$K = \frac{C_{(M^{++})i}^{1/2} C_{(N^{++})0}^{1/2} \gamma_{(M^{++})i}^{1/2} \gamma_{(N^{++})0}^{1/2}}{C_{(M^{++})0}^{1/2} C_{(N^{++})i}^{1/2} \gamma_{(M^{++})0}^{1/2} \gamma_{(N^{++})i}^{1/2}} = k \frac{\gamma_{(M^{++})i}^{1/2} \gamma_{(N^{++})0}^{1/2}}{\gamma_{(M^{++})0}^{1/2} \gamma_{(N^{++})i}^{1/2}} \quad (3)$$

and

$$K = \frac{C_{(M^{++})i}^{1/2} C_{(B^+)0} \gamma_{(M^{++})i}^{1/2} \gamma_{(B^+)0}}{C_{(M^{++})0}^{1/2} C_{(B^+)i} \gamma_{(M^{++})0}^{1/2} \gamma_{(B^+)i}} = k \frac{\gamma_{(M^{++})i}^{1/2} \gamma_{(B^+)0}}{\gamma_{(M^{++})0}^{1/2} \gamma_{(B^+)i}} \quad (4)$$

The equilibrium constant for the exchange reaction between two divalent ions may be calculated from equation 2. The constant, K , for the exchange of a divalent ion and an univalent ion may be calculated from the equation⁶

$$\log K = \int_0^1 \log k \, dX$$

(5) O. D. Bonner, W. J. Argersinger and A. W. Davidson, *J. Am. Chem. Soc.*, **74**, 1044 (1952).

(6) W. J. Argersinger, A. W. Davidson and O. D. Bonner, *Trans. Kans. Acad. Sci.*, **53**, 404 (1950).

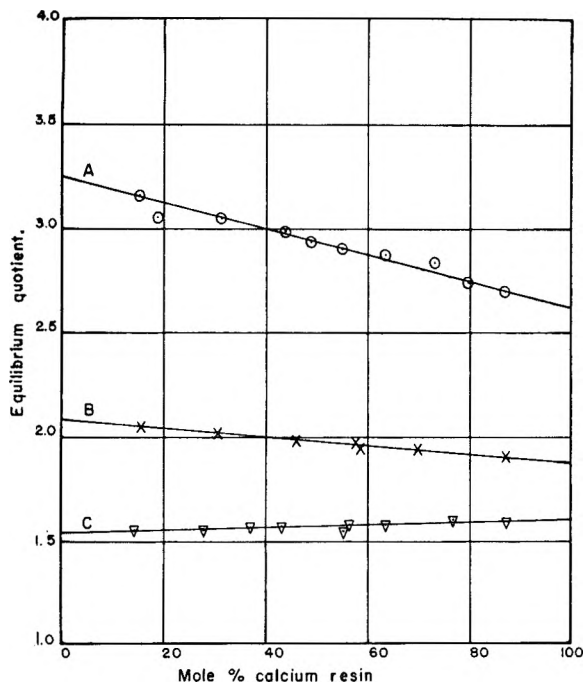


Fig. 1.—Calcium-copper exchange: A, 16% DVB; B, 8% DVB; C, 4% DVB.

$$k = \frac{m_{Cu^{++}}}{m_{Ca^{++}}} \times \frac{N_{CaRes_2}}{N_{CuRes_2}}$$

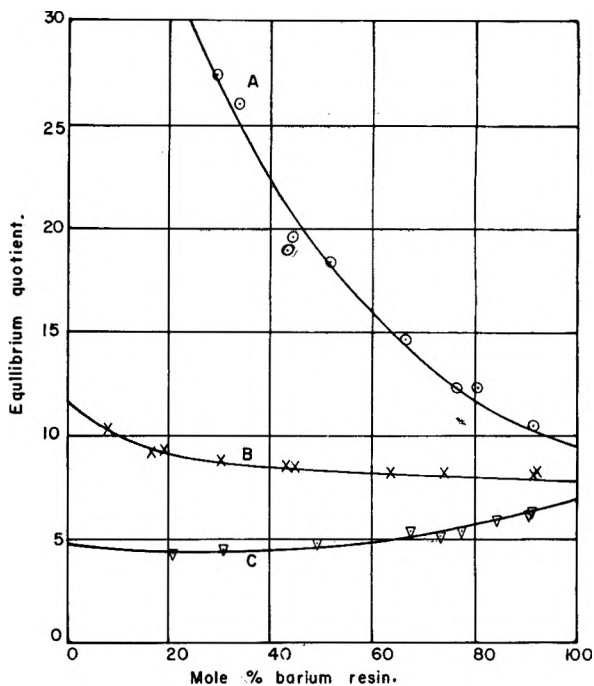


Fig. 3.—Barium-copper exchange: A, 16% DVB; B, 8% DVB; C, 4% DVB.

$$k = \frac{m_{Cu^{++}}}{m_{Ba^{++}}} \times \frac{N_{BaRes_2}}{N_{CuRes_2}}$$

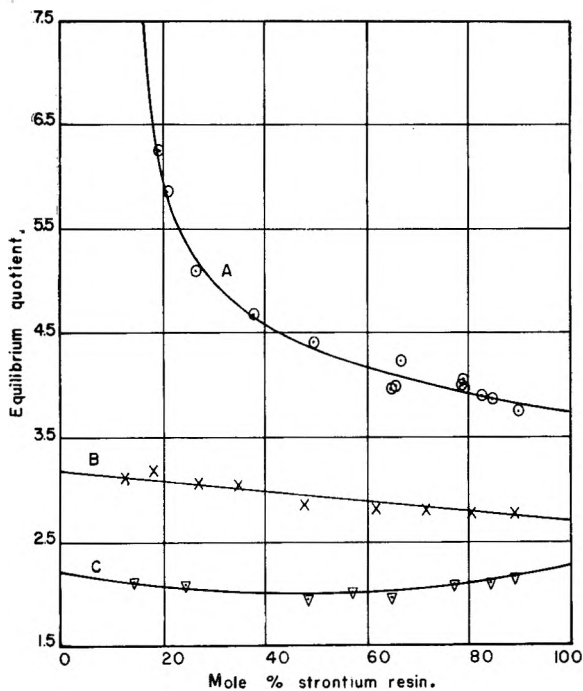


Fig. 2.—Strontium-copper exchange: A, 16% DVB; B, 8% DVB; C, 4% DVB.

$$k = \frac{m_{Cu^{++}}}{m_{Sr^{++}}} \times \frac{N_{SrRes_2}}{N_{CuRes_2}}$$

where X is the equivalent fraction of the resin associated with ion M^{++} (equation 4). The quantity $\gamma_{B+}/\gamma_{M^{++}}$ has a probable value⁷ of about 1.2 ± 0.2 but will vary for each pair of ions studied. This ratio was therefore neglected in the

(7) I. M. Klotz, "Chemical Thermodynamics," Prentice-Hall, Inc., New York, N. Y., 1950, p. 332.

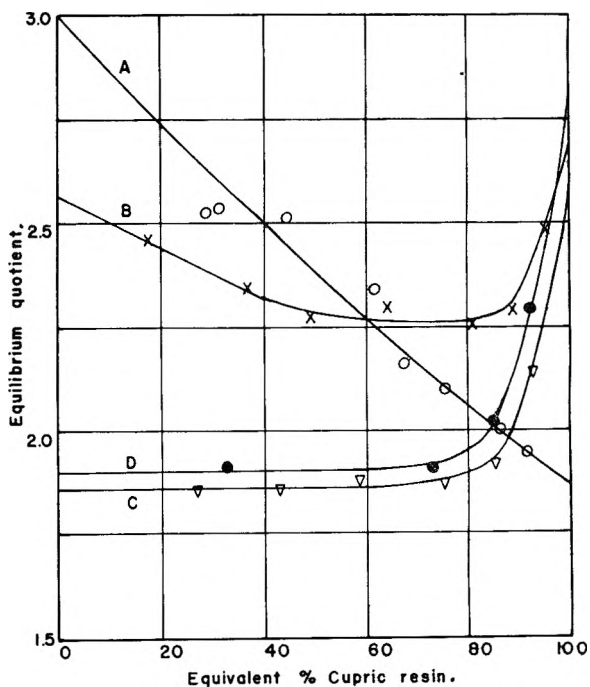


Fig. 4.—Cupric-hydrogen exchange: A, 16% DVB; B, 8% DVB; C, 4% DVB; D, 4% DVB (NO_3^- media).

$$k = \frac{m_{H^{+2}}}{m_{Cu^{++}}} \times \frac{N_{CuRes_2}}{N_{BRes_2}^2}$$

present calculation of K for these exchanges as was done for exchanges involving only univalent ions. The value of K may be corrected for any exchange involving ions for which activity coefficient in mixed aqueous solutions are known.

The experimental data for these exchanges are presented graphically in Figs. 1-5 as a plot of k ,

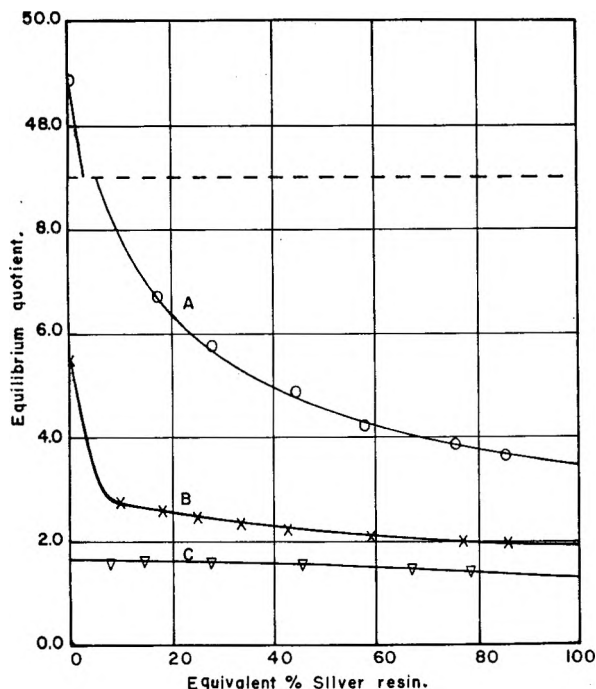


Fig. 5.—Silver-cupric exchange: A, 16% DVB; B, 8% DVB; C, 4% DVB.

$$k = \frac{m_{\text{Cu}^{++}}}{m_{\text{Ag}^+}^2} \times \frac{N_{\text{AgRes}}^2}{N_{\text{CuRes}_2}}$$

the selectivity coefficient as a function of resin composition. The equilibrium constants have been calculated and are given in Table I. The affinity of the resins for the ions studied is $\text{Ba} > \text{Ag} > \text{Sr} > \text{Ca} > \text{Cu} > \text{H}$ for resins of 4 and 8% DVB content and $\text{Ag} > \text{Ba} > \text{Sr} > \text{Ca} > \text{H}$ for the

TABLE I
TABLE OF EQUILIBRIUM CONSTANTS

Exchange system	4% DVB	8% DVB	16% DVB
Ba-Cu	2.24	2.95	4.60
Sr-Cu	1.45	1.72	2.30
Ca-Cu	1.26	1.40	1.71
Ag-Cu(NO ₃ ⁻)	1.52	2.35	5.47
Ag-H(NO ₃ ⁻) ^a	3.08	5.84	13.4
Cu-H(NO ₃ ⁻)	1.99		
Cu-H(Cl ⁻)	1.92	2.38	2.38
Cu-H(calcd.)	2.03	2.49	2.45

Previously reported.

16% DVB resin. These and other divalent ions will be included in the same selectivity scale with the univalent ions when their position is verified by other exchanges between univalent and divalent ions.

The effect of the anion, even in fairly dilute solutions, upon the activity coefficients in the solution phase is apparent in the cupric-hydrogen exchange. An equilibrium constant of 1.92 is obtained for this exchange when cupric chloride and hydrochloric acid solutions are used but the constant is 1.99 when cupric nitrate and nitric acid solutions are used. This effect is to be expected since in solutions of the pure electrolytes the activity coefficient of hydrochloric acid is greater than that of nitric acid while the activity coefficient of cupric nitrate is greater than that of cupric chloride. This effect is of further interest in the triangular comparisons. Upon completion of the silver-cupric exchange a value of the equilibrium constant for the cupric-hydrogen exchange may be calculated since data on the silver-hydrogen exchange are available. It is found that rather satisfactory agreement is obtained for the 4% DVB resin when the nitrates of the various cations are used in all exchanges. The constants for the cupric-hydrogen exchange on 4, 8 and 16% DVB resins using cupric chloride and hydrochloric acid differ, however, from the calculated value by about 5%. Since the discrepancy in the observed and calculated values of K for this exchange on 8 and 16% DVB resins are of similar magnitude, it is believed that the same explanation is applicable.

The maximum water uptake data (Table II) show that the same pattern for divalent ions that was observed for univalent ions. The water uptake is smaller for ions for which the ion-resin affinity is greater. Comparisons of water uptake data for univalent with those of divalent ions does not appear to be profitable at this time.

TABLE II
MAXIMUM WATER UPTAKE OF DOWEX 50 RESINS IN VARIOUS IONIC FORMS (G./MOLE)

Ion	4% DVB	8% DVB	16% DVB
Ba ⁺⁺	333	245	194
Sr ⁺⁺	499	307	227
Ca ⁺⁺	563	319	230
Cu ⁺⁺	643	369	277

SULFOSTYRENES.¹ PREPARATION OF VARIABLE CAPACITY SULFOSTYRENE CATION EXCHANGE POLYMERS FROM STYRENE/ SULFONAMIDOSTYRENE COPOLYMERS

BY RICHARD H. WILEY AND SAMUEL F. REED

Contribution from the Department of Chemistry of the College of Arts and Sciences of the University of Louisville, Louisville Kentucky

Received October 22, 1955

p-Sulfonamidostyrene has been copolymerized with styrene in varying ratios by a modified bulk technique and hydrolyzed with nitrous acid to give a series of variable capacity cation-exchange resins. The nitrous acid hydrolysis has been shown to be substantially complete under conditions (15°) where little, if any, structural change in the polymer can take place. The capacities of twelve hydrolyzed copolymers prepared at 85–136° with varying ratios of monomers are, with one exception, 94–100% of the theoretical value based on the monomer ratios. Swelling and solubility data indicate the copolymers to be cross-linked.

The first studies² on the selectivity coefficients of a series of variable capacity, sulfostyrene-type cation-exchange resins disclosed an unexpected alteration in selectivity coefficients. The coefficients for the sodium-hydrogen exchange decreased as the capacity of the resin was decreased from 5.1 meq./g. to 2.52 meq./g. Furthermore, a complete reversal of selectivity was observed with the resin of lowest capacity. It has been suggested that these effects are attributable to variations in charge densities. These very unusual observations have established the possibility that additional studies on exchange resins varying structurally only in the number of exchange groups on the polymer chain will lead to a distinct advance in our understanding of the fundamental behavior of ion-exchange resins. Such resins have received very little study and are not readily available. It is their preparation that is to be considered in this paper.

The objective in the preparation of an otherwise structurally uniform ion-exchange resin of variable capacity is that of varying the frequency at which a given ionic group occurs along a given polymer chain. This objective can be achieved by either of two different routes. A preformed polymer with suitable exchange groups can be subjected to a reaction which will remove or introduce ionic groups in varying proportions. This procedure has been used² to decrease the capacity of sulfonated polystyrene by the hydrolytic removal of sulfonic acid groups and to decrease the capacity of an acrylic acid polymer by partial esterification.³

The alternative procedure involves the preparation of a series of copolymers of varying composition one of which provides the exchange unit.^{3a} The alternative methods will lead to materials dissimilar in the manner of distribution of the charges on the polymer. In the former the distribution of charges will be determined statistically in terms of the

access of the reagent to the group on the chain being modified. In the other, recognized copolymerization phenomena will determine the distribution of the two monomers, and hence the ionic groups, in the polymer chain. Depending on the particular reaction conditions involved, in the first type, or on the copolymerization characteristics of the two monomers, in the second type, rather extreme variations—all the way from a close bunching at separated intervals to a random distribution with maximum separation of individual units—in the distribution of charges, and hence the charge density, along the polymer chain can be recognized as possible. In the evaluation of an effect which is to be attributed to variations in charge density it is apparent from this that alterations in the manner of preparing the exchanger will possibly alter the type and extent of the variations in selectivity coefficients.

The preparation of a copolymer from two monomers one of which is to serve as a source of ionic groups, while the other does not, requires the development of new modifications in standard polymerization techniques. Those monomers which contain ionic groups—such as sulfostyrene⁴—are not soluble in or miscible with those monomers—such as styrene—which do not contain such groups nor are common solvents for such pairs obvious. This makes the direct copolymerization of such a pair of monomers by any obvious modification of any of the usual copolymerization techniques an unusual event. One obvious way to avoid this impasse is to copolymerize a compatible pair of monomers one of which contains a functional group convertible by some mild reaction, which will not otherwise alter the nature of the polymer chain, to an ionic group. Several possibilities of both types are under study in our laboratories and we wish to describe at this time our results on the preparation of a series of exchange resins of varying capacity prepared by the hydrolysis of a series of styrene-sulfonamidostyrene copolymers.

The basic premise which makes this route rational is that the sulfonamide group can be hydrolyzed to the sulfonic acid group by the action of nitrous acid under very mild conditions.⁵ It was believed,

(1) Presented at the Southeastern Regional Meeting of the American Chemical Society, Columbia, S. C., November 3–5, 1955. Previous paper in this series: Richard H. Wiley, N. R. Smith and C. C. Ketterer, *J. Am. Chem. Soc.*, **76**, 720 (1954).

(2) G. E. Boyd, B. A. Soldano and O. D. Bonner, *THIS JOURNAL*, **58**, 456 (1954).

(3) H. Deuel, K. Hutschenecker and J. Solms, *Z. Elektrochem.*, **57**, 172 (1953).

(3a) Such a procedure has been used for the hydrolysis of copolymers of divinylbenzene with varying amounts of alkyl *p*-styrenesulfonates; I. H. Spinner, J. Ciric and W. F. Graydon, *Can. J. Chem.* **32**, 143 (1954).

(4) R. H. Wiley, N. R. Smith and C. C. Ketterer, *J. Am. Chem. Soc.* **76**, 720 (1954); G. J. Moralli, *Bull. soc. chim. France*, 1044 (1953).

(5) O. Hinsberg, *Ber.*, **27**, 598 (1894).

however, that additional study of this reaction should be made to see if it were applicable to the hydrolysis of polymers and, if so, under what conditions and to what extent hydrolysis could be achieved. A variety of nitrous acid hydrolyses were run on the bulk polymer prepared as previously described⁶ to determine the effect of temperature, mole ratio of nitrous acid to sulfonamide groups and time on the yield of evolved nitrogen. At 50° gas is evolved rapidly but contains brown fumes which undoubtedly result in part from the decomposition of the nitrous acid. After correction for this side reaction on the basis of blank runs, the amount of evolved gas indicated that hydrolysis to the extent of 60 to 75% had taken place. The reaction was then studied at lower temperatures to avoid this decomposition. At 0° no reaction takes place. At 25° hydrolysis was 80–92% complete and at 15° the amount of nitrogen evolved, corrected for a blank, gave reproducible values indicating 96–97% hydrolysis. Other experiments indicated that hydrolysis was more nearly complete using a ratio of 2 moles of acid to 1 mole of sulfonamide than it was with equimolar mixtures and that at least two 24-hour reaction periods, with an additional equal quantity of nitrous acid added prior to the second, were necessary to complete the reaction. The theoretical *vs.* observed exchange capacities, given in Table I, indicate that this procedure gave substantially complete hydrolysis. For only one copolymer was the observed capacity less than 94% of theory. On this basis it was decided to hydrolyze all of the polymers and copolymers to be used in this study by treating each three times with a 2/1 mole ratio of nitrous acid at 15° for 24 hours.

TABLE I

Composition, mol % SAS/S	Temp. of pol., °C.	Wt. loss on vacuum drying/g.	Degree of swelling	Theoretical capacity meq./g.	Total capacity	Titration capacity
100/0	136	0.118	26.2	5.43	5.12, 5.11	5.18
75/25	136	.059	16.6	4.58	4.03, 4.05	3.99
50/50	136	.081	4.8	3.47	3.43, 3.37	3.35
25/75	136	.111	1.3	2.03	1.97, 1.94	1.96
100/0	110	.086	14.1	5.43	4.91, 4.94	5.12
75/25	110	.096	18.3	4.58	4.27, 4.29	4.37
50/50	110	.116	7.4	3.47	3.36, 3.37	3.44
25/75	110	.083	2.0	2.03	1.97, 1.99	2.03
100/0	85	.076	..	5.43	5.15, 5.11	5.18
75/25	85	.166	24.4	4.58	4.22, 4.25	4.43
50/50	85	.098	9.5	3.47	3.47, 3.45	3.44
25/75	85	.113	2.3	2.03	1.95, 1.96	2.03

The polysulfonamidostyrene used in these preliminary hydrolysis experiments was prepared by bulk polymerization from the molten state using no added initiator. The monomer, even though recrystallized carefully several times from benzene and finally from ethanol just before polymerization and even when carefully protected from the atmosphere with a blanket of nitrogen, polymerized without added initiator when melted (m.p. 138–140°).

The problem of preparing polymers and co-

(6) R. H. Wiley and C. C. Ketterer, *J. Am. Chem. Soc.*, **75**, 4519 (1953).

polymers of styrene and *p*-sulfonamidostyrene—which are mutually insoluble—by a process which would give materials suitable for study as variable capacity ion-exchange resins was solved by devising a modified bulk polymerization technique. The two monomers were combined with the minimum sufficient quantity of dimethylformamide to provide a homogeneous molten reaction mixture at the beginning of the polymerization. Dimethylformamide was selected as superior to several other third components tried in preliminary tests. Using 0.5 ml. of dimethylformamide per 1.56 g. of the monomer mixture a series of polymers and copolymers was prepared containing 100, 75, 50 and 25% sulfonamidostyrene at 136 and 110° using 0.01% *t*-butyl peracetate as initiator and at 85° using 0.01% of benzoyl peroxide as initiator. The reaction mixtures were agitated to see that a homogeneous molten state was established during the first few moments at reaction temperature. The cooled solid polymer was pulverized and sized to 40–60 mesh. A vacuum treatment (at 76° and 12 mm.) to constant weight, as a means of removing the *N,N*-dimethylformamide, was customarily given each polymer prior to hydrolysis. One experiment indicated that the formamide was at least partially washed out during hydrolysis to give a product which, on the basis of a slightly lower capacity—4.8 meq./g., may not have been completely freed of inert material. This vacuum treatment gave a weight loss corresponding to the removal of about one-half of the added dimethylformamide. A considerable portion of the solvent also volatilized and condensed onto cooler portions of the flask during the polymerization. The vacuum treated resin was hydrolyzed with dilute aqueous nitrous acid for 72 hours, washed and dried. The swelling characteristics were determined by a previously described displacement method.⁷ The total capacity determinations were made by the method of Topp and Pepper⁸ and the titrations on the resins were run by the method of Kunin and Myers.⁹ Typical data are given in Table II and Fig. 1. The capacity data indicate that the resins have 87–100% of the capacity theoretically possible based on the monomer mixture used.

There are several reasons for believing that these polymers are cross-linked. They are completely insoluble in all solvents tried including aqueous sodium hydroxide and pyridine which are excellent solvents for a high viscosity emulsion polymer prepared from *p*-sulfonamidostyrene. The hydrolysis is almost always incomplete indicating that some of the nitrogen may be left in the polymer as non-hydrolyzable imide linkages. The swelling data also seem to indicate cross-linkage. Because it is of considerable importance to have materials in a known and controlled state of cross-linkage, this problem is receiving further study.

The selectivity coefficient characteristics of these resins are to be studied by Dr. G. E. Boyd.

Acknowledgment.—This research completed under contract AT-(40-1)-229 between the Univer-

(7) H. F. Walton, *This Journal*, **47**, 371 (1943).

(8) N. E. Topp and K. W. Pepper, *J. Chem. Soc.*, 3299 (1949).

(9) R. Kunin and R. J. Myers, "Ion Exchange Resins," John Wiley and Sons, Inc., New York, N. Y., 1950, p. 150.

sity of Louisville and the Atomic Energy Commission. The authors acknowledge this support with appreciation.

Experimental

The *p*-sulfonamidostyrene used in the following experiments was prepared as previously described,² recrystallized several times from benzene, and finally, just prior to use, from ethanol, m.p. 138–139°. The styrene was distilled at reduced pressure just prior to use. The *N,N*-dimethylformamide was carefully fractionated through a helix-packed column with a partial take-off head and that fraction boiling at 152.5–153° separated for use in the polymerizations.

Polymerization of Sulfonamidostyrene with Styrene.—The procedure used in the copolymerization will be illustrated with the details of the preparation of a 75/25 sulfonamidostyrene/styrene copolymer at 110°. Other copolymers were prepared by the same procedure, with the modifications indicated, using different monomer ratios at 85 and 136°. The copolymers prepared at 85° were initiated with 0.1% by weight of benzoyl peroxide.

Five and twenty-four one hundredths g. (0.0286 mole) of *p*-sulfonamido-styrene, 1.0 g. (0.0096 mole) of styrene and 2.0 ml. of *N,N*-dimethylformamide (0.5 ml. per 1.56 g. of monomers) containing 0.624 mg. (0.01% of the monomer weight) of *t*-butyl peracetate were placed in a 125-ml. erlenmeyer flask. The flask was flushed with nitrogen, freed of oxygen by washing with alkaline sodium anthraquinone- β -sulfonate solution, stoppered and placed in an oil-bath held at 110 \pm 1°. During the first 2 to 3 minutes in the oil-bath the flask was revolved to assist in the formation of a clear solution of the ingredients. The solution became viscous within 3.5 minutes. With 75% styrene the mixture was viscous within 15 minutes; with 100% *p*-sulfonamidostyrene within 2 minutes.

At the end of about an hour the mixture was semi-solid. The heating was continued for 20 hours. During this time some liquid condensed on the upper, cooler portions of the flask. The copolymer was obtained as a clear, light-yellow solid which was hard and somewhat brittle. The copolymers containing the most styrene were less brittle. The polymer of sulfonamidostyrene itself prepared by this procedure is a clear, brittle, insoluble, light-yellow solid. For further characterization the solids were pulverized in a mortar and pestle and sized to 40–60 mesh size. The less brittle resins were ground with dry ice. The sized particles were vacuum-dried at 76° and 12–14 mm. to remove the dimethylformamide. A 4.89-g. sample of the 75/25 copolymer lost 0.25 g. in 24 hours; 0.41 g. after 48 hours; 0.43 g. after 72 hours; and 0.46 g. after 120 hours. Samples used in further studies were all vacuum-dried for 72 hours. The loss in weight varied from 5–12%.

Hydrolysis of the Polymers.—Preliminary experiments to determine the conditions required for completion of the nitrous acid hydrolysis were conducted as follows. The polymer was ground and sized with the 40–60 mesh size particles being used in the following experiments. Samples of approximately 0.25 g. (0.00136 mole) of polymer were added to 1 \times 4" test-tubes equipped with a gas outlet tube containing 0.188 g. (0.0027 mole) of sodium nitrite dissolved in 10.0 ml. of distilled water. The mixture was cooled to 0.5° in an ice-water bath and then an excess of hydrochloric acid (3.0 ml.) was added after which the test-tube was sealed with wax and placed in a constant temperature bath at the desired temperature (0–50°). The gas outlet tube was connected to a gas buret and the nitrogen evolved during the next 24 hours collected over water and compared with the calculated theoretical quantity. Blank runs were made to determine the amount of gas formed by decomposition of the nitrous acid.

The series of copolymers and polymers were hydrolyzed according to the following procedure given in detail for the 50/50 (110°) copolymer of *p*-sulfonamidostyrene/styrene. A sample of 3.95 g. of the copolymer (containing 0.014 mole of sulfonamidostyrene) was placed in a 500-ml. erlenmeyer flask, with a cold (0–5°) solution of 1.90 g. (0.028 mole) of sodium nitrite in 100 ml. of water. To this was added 11.5 ml. (0.140 mole) of concd. hydrochloric acid in 100 ml. of water. The mixture was placed in a running water-bath at 15–18° and shaken frequently for 24 hours. In larger runs the mixture was stirred. During the first

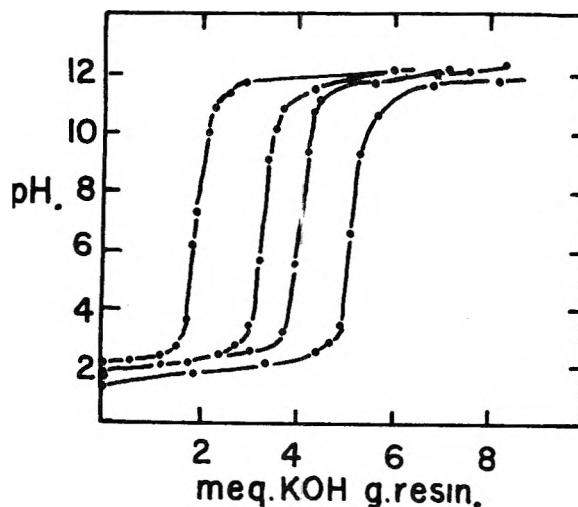


Fig. 1.—Titration characteristics of hydrolyzed sulfonamidostyrene/styrene copolymers polymerized at 85°.

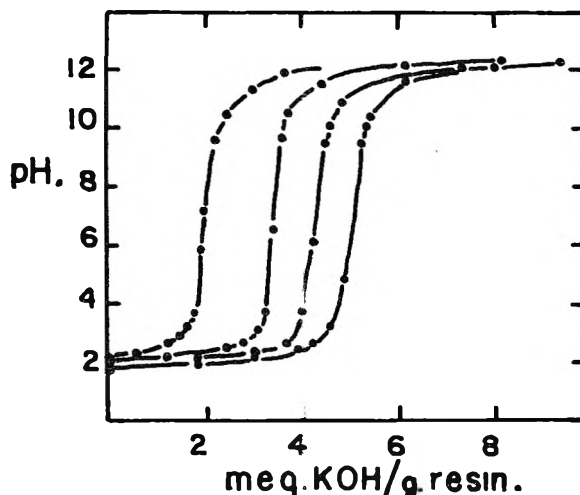


Fig. 2.—Titration characteristics of hydrolyzed sulfonamidostyrene/styrene copolymers polymerized at 110°.

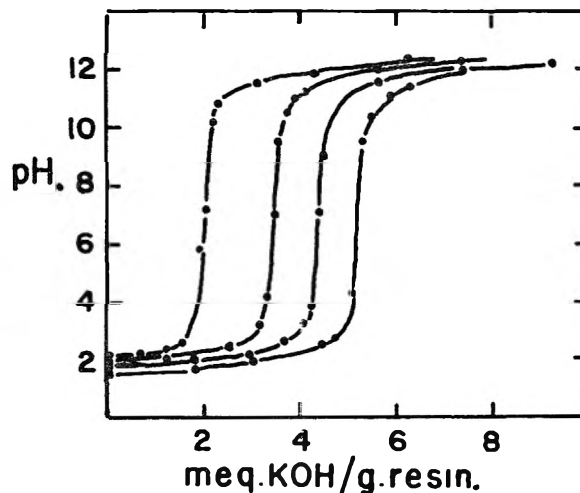


Fig. 3.—Titration characteristics of hydrolyzed sulfonamidostyrene/styrene copolymers polymerized at 136°.

several hours the evolved nitrogen floated the polymer particles. Later they sank to the bottom. The solution was decanted and fresh solutions of nitrite and acid were

added to repeat the process a second and third time. After the third hydrolysis the polymer was placed in a buret and washed at the rate of 1 ml./minute with a minimum of 3 l. of 1 *N* hydrochloric acid to remove the nitrite and then washed with distilled water until free of acid. The polymer was air-dried and vacuum-dried at 55° for a minimum of 18 hours to constant weight prior to titration. Polymer samples containing high percentage of sulfo groups absorbed more water and required longer drying periods.

Swelling Characteristics.—The procedure follows that previously described.⁷ A weighed sample (0.22–0.27 g.) of dried polymer was placed in a graduated cylinder and its apparent volume noted. Two ml. of hexane was added and the volume in excess of 2 ml. was taken as the true volume of the resin. Water was added to displace the hexane and permit swelling. The apparent volume of the swollen resin was noted and corrected by the same factor observed in the ratio of apparent to true value for the unswollen resin. The degree of swelling was taken as the ratio of the corrected volume swollen to the true value unswollen.

Capacity Measurements.—Total capacity determinations⁸ were made by adding 100 ml. of standard (ca. 0.1 *N*) sodium hydroxide to ca. 2.0 g. of dried polymer in its hydrogen form. The flask was stoppered and allowed to stand one week with frequent shaking. Two 10.0-ml. aliquot portions were titrated with standard (ca. 0.1 *N*) hydrochloric acid to the phenolphthalein end-point. Values are given in the table as meq. of base per gram of dry resin in the hydrogen form.

Titration were conducted by the procedure described previously.⁹ The resins were titrated with 0.1 *N* potassium hydroxide using 12 samples of resin of approximately equivalent weight to which was added increments of 1.0 *N* potassium chloride and 0.1 *N* potassium hydroxide in 1.0 *N* potassium chloride to give a total volume of 25 ml. The samples were sealed and allowed to stand for one week with occasional shaking on a machine. The pH of each solution was determined and plotted against meq. of base added per gram of dry resin. A series of such data for the polymers prepared at 110° is given in Fig. 1. The equivalence point is given in Table I in terms of meq. of base per gram of dry resin in the hydrogen form required to neutralize.

AN ANALYTICAL PROOF THAT THE EXTREMUM OF THE THERMODYNAMIC PROBABILITY IS A MAXIMUM¹

BY DONALD G. MILLER²

University of Louisville, Louisville, Kentucky

Received December 20, 1954

An analytical proof is given that the distribution found by extremizing the thermodynamic probability actually is the most probable one. The cases considered are classical statistics, Bose–Einstein and Fermi–Dirac statistics, radiation and Wall's theory of rubber elasticity. In these examples, the proof depends only on the form of W .

Introduction

A standard technique in statistical mechanics is to maximize the thermodynamic probability W of a system and use the most probable distribution so obtained to determine the system's macroscopic properties.³ This procedure is permissible since the number of particles is very large in most systems. In this event it can be shown that the most probable distribution completely dominates all the others.

In general a system is subject to various constraints, such as a constant energy or a constant number of particles. Consequently the location of the maximum of W is most conveniently handled by means of Lagrangian Multipliers.^{4,5} However the Lagrangian Multiplier (LM) method only leads to necessary conditions for an extreme, and it is ordinarily assumed without proof that a maximum is obtained. Although it seems more or less clear that a maximum does result, nevertheless without proof it is conceivable that a minimum or a saddle point could be obtained. It is the purpose of this paper to provide a rigorous analytical proof that the

distribution found actually is the most probable one. The argument will be given for classical statistics; and the Fermi–Dirac and Bose–Einstein statistics, radiation and rubber elasticity will be discussed briefly.⁶

Sufficient Condition for a Maximum.—As noted above, minima inflection points and saddle points will also satisfy the necessary conditions obtained by the LM technique. Therefore it is desirable to have sufficient conditions which will enable one to decide which type of extreme is present. Fortunately these conditions have been worked out, and the following theorem on constrained extremes may be quoted.^{7–9}

Theorem.—Let $F(x_1, \dots, x_n)$ be subject to the m constraints $f^i(x_1, \dots, x_n) = a_i$, $1 \leq i \leq m$, where the a_i are constants. Let $\phi = F - \sum_{i=1}^m \lambda_i f^i$, where λ_i are the Lagrangian Multipliers and are to be treated as constants. Let x_1^0, \dots, x_n^0 be the values of x_1, \dots, x_n at an extreme of ϕ , as found by the usual LM technique. Now form the sequence of determinants

(1) Presented before the Physical and Inorganic Division at the 124th ACS meeting, September, 1953.

(2) Chemistry Department, Brookhaven National Laboratory, Upton, Long Island, New York.

(3) See, for example, Mayer and Mayer, "Statistical Mechanics," John Wiley and Sons, Inc., New York, N. Y., 1940.

(4) Reference 3, appendix VI.

(5) I. S. and E. S. Sokolnikoff, "Higher Mathematics for Engineers and Physicists," McGraw-Hill Book Co., New York, N. Y., 1941, p. 163.

(6) At the time this work was originally carried out, no proofs had ever been published. It has come to the author's attention that L. Page ("Theoretical Physics," 3rd edition, D. Van Nostrand, New York, N. Y., 1952) has independently given a somewhat different one for classical statistics.

(7) C. G. Phipps, *Am. Math. Monthly*, **59**, 230 (1952).

(8) R. P. Gillespie, "Partial Differentiation," Interscience Publishers, Inc., New York, N. Y., 1951.

(9) T. F. Chaundy, "Differential Calculus," Oxford, 1935.

$$\Delta_{k+1}^C = (-1)^{2k+1} \begin{vmatrix} 0 & \epsilon_1 & \dots & \dots & \epsilon_k \\ \epsilon_1 & -\sigma_1^C & 0 & \dots & 0 \\ \cdot & 0 & \cdot & 0 & \cdot \\ \cdot & \cdot & 0 & \cdot & \cdot \\ \epsilon_k & 0 & \dots & 0 & -\sigma_k^C \end{vmatrix} + (-1)^{2k+2\epsilon_{k+1}} \begin{vmatrix} 0 & \epsilon_1 & \dots & \dots & \epsilon_k \\ 1 & -\sigma_1^C & 0 & \dots & 0 \\ \cdot & 0 & \cdot & 0 & \cdot \\ \cdot & \cdot & 0 & \cdot & \cdot \\ 1 & 0 & \dots & 0 & -\sigma_k^C \end{vmatrix} \\ + (-1)^{2k+2\epsilon_{k+1}} \begin{vmatrix} 0 & 1 & \dots & \dots & 1 \\ \epsilon_1 & -\sigma_1^C & \dots & \dots & 0 \\ \cdot & 0 & \cdot & 0 & \cdot \\ \cdot & \cdot & 0 & \cdot & \cdot \\ \epsilon_k & 0 & \dots & 0 & -\sigma_k^C \end{vmatrix} + (-1)^{2k+3\epsilon_{k+1}} \begin{vmatrix} 0 & 1 & \dots & \dots & 1 \\ 1 & -\sigma_1^C & 0 & \dots & 0 \\ \cdot & 0 & \cdot & 0 & \cdot \\ \cdot & \cdot & 0 & \cdot & \cdot \\ 1 & 0 & \dots & 0 & -\sigma_k^C \end{vmatrix} + (-1)^{\sigma_{k+1}^C} \Delta_k^C \quad (11)$$

If the first four determinants of (11) are evaluated by means of the theorem in the appendix and the various terms collected together, it is found that

$$\Delta_{k+1}^C = (-1)^{k+1} [(\epsilon_{k+1} - \epsilon_1)^2 \sigma_2^C \dots \sigma_k^C + (\epsilon_{k+1} - \epsilon_2)^2 \sigma_1^C \sigma_3^C \dots \sigma_k^C + \dots \\ + (\epsilon_{k+1} - \epsilon_k)^2 \sigma_1^C \dots \sigma_{k-1}^C] + (-1)^{\sigma_{k+1}^C} \Delta_k^C \quad (12)$$

By the induction hypothesis Δ_k^C has the sign $(-1)^k$, and since all the terms inside the bracket are positive, Δ_{k+1}^C has the sign $(-1)^{k+1}$. Therefore by the principle of mathematical induction, Δ_t^C has the sign $(-1)^t$ for all t . It has thus been proved that the extreme of $\ln W$ is a true maximum in classical statistics.

It is easy to show by a similar induction argument that the explicit form for Δ_t^C is given by

$$\Delta_t^C = (-1)^t \sum_{j=2}^t \left[\sum_{i=1}^{j-1} (\epsilon_j - \epsilon_i)^2 \prod_{\substack{l=1 \\ l \neq i, j}}^t \sigma_l^C \right] \quad (13)$$

Bose-Einstein Statistics.—All Bose-Einstein quantities will be denoted by a superscript B. In this case, the thermodynamic probability is given by¹⁰

$$W^B = \Pi \frac{(g_i + n_i - 1)!}{(g_i - 1)! n_i!} \quad (14)$$

and the system is again subject to the constraints (3) and (4). Applying Stirling's approximation and carrying out the required differentiations, one obtains equations 6 and

$$\phi_{ii}^B = -\sigma_i^B = -(g_i - 1)/n_i (g_i + n_i - 1) \\ \phi_{jk}^B = 0 \quad (15)$$

The Δ_t^B are clearly of exactly the same form as Δ_t^C except that σ_i^C is replaced by σ_i^B . Hence the final expression for Δ_t^B is just (13) with the same substitution. The sign of Δ_t^B thus depends on the sign of $\Pi \sigma_i^B$. Considerations of the terms of (15) yield the following. The n_i are positive as can be determined from the expression found by the LM method, and the g_i are positive for physical reasons. Moreover the n_i and g_i are ordinarily greater than 1. Consequently the σ_i^B are positive for all i , and as a result Δ_t^B has the sign $(-1)^t$. It has thus been proved that $\ln W$ is maximum for Bose-Einstein statistics also.

Fermi-Dirac Statistics.—All Fermi-Dirac quantities will be denoted by a superscript F. Here the thermodynamic probability is given by¹⁰

$$W^F = \Pi g_i / (g_i - n_i)! n_i! \quad (16)$$

and as before, W^F is subject to the constraints (3) and (4). Again applying Stirling's approximation and carrying out the desired differentiations, equations 6 and

$$\phi_{ii}^F = -\sigma_i^F = -g_i/n_i (g_i - n_i), \phi_{jk}^F = 0 \quad (17)$$

are obtained. The substitution of (6) and (17) in (1) leads to (13) as before, except that σ_i^C is replaced by σ_i^F . It remains to consider the sign of σ_i^F . Clearly g_i and n_i are positive, and in general $g_i > n_i$.¹³ Consequently Δ_t^F has the sign $(-1)^t$, and Fermi-Dirac statistics also leads to a most probable distribution.

Radiation.—In radiation, photons are assumed to obey the Bose-Einstein statistics. However, the number of photons is not conserved so that W^B is subject only to the constraint of constant energy. The evaluation of the Δ_t^R for this case is much easier as the general expression can be written down immediately using the theorem in the appendix. Thus

$$\Delta_t^R = \begin{vmatrix} 0 & \epsilon_1 & \dots & \dots & \epsilon_t \\ \epsilon_1 & -\sigma_1^B & 0 & \dots & 0 \\ \cdot & 0 & \cdot & 0 & \cdot \\ \cdot & \cdot & 0 & \cdot & \cdot \\ \cdot & \cdot & 0 & \cdot & 0 \\ \epsilon_t & 0 & \dots & 0 & -\sigma_t^B \end{vmatrix} \\ = (-1)^t \sum_{i=1}^t \left[\epsilon_i^2 \prod_{\substack{l=1 \\ l \neq i}}^t \sigma_l^B \right] \quad (18)$$

This expression also has the sign $(-1)^t$, and again it has been proved that the maximum is obtained.

Rubber Elasticity.—A less ordinary case comes from Wall's theory of rubber elasticity.¹⁴ Wall

(13) If a case where $g_i = n_i$ arises, its contribution to W is $0! = 1$. Such terms are removed before taking logarithms and differentiating.

(14) F. T. Wall, *J. Chem. Phys.*, **11**, 527 (1943). See this paper for the physical meaning of the symbols. To keep a uniform notation Wall's N_i have been replaced by n_i .

has derived the expression

$$W^E = N! \Pi p_i^{n_i} / \Pi n_i! \tag{19}$$

which is subject to the constraints (3) and

$$l^2 = C \Sigma n_i x_i^2 \tag{20}$$

The form of W^E is analogous to that of classical statistics, and it is easily shown that

$$\Delta_l^E = (-1)^t \sum_{j=2}^t \left[\sum_{i=1}^{j-1} C^2(x_i^2 - x_i'^2) \prod_{\substack{l=1 \\ l \neq i, j}}^t \sigma_l^C \right] \tag{21}$$

Again Δ_l^E has the sign $(-1)^t$, and a most probable distribution is proved to result.

Comment.—In the above examples, it is seen that the squared terms in equations 13, 18 and 21 arise from the constraints. This is due to the

symmetry of Δ_l and the fact that $\phi_{jk} = 0$. Therefore the sign of Δ_l depends only on the sign of the product of diagonal terms. These terms in turn arise solely from the form of W , and consequently the type of extreme is determined solely by the form of W . In our examples, the ϕ_{ii} were all negative. Since each term in the expansion of Δ_l has the product of $t - 2$ of the ϕ_{ii} as a factor, the sign of Δ_l must alternate as t increases. Consequently if the first Δ_l has the proper sign for a maximum, all the others will also.

These observations may be reduced to a simple rule. If $\phi = \ln W - \Sigma \lambda_r C_r$ where λ_r are Lagrangian Multipliers and the C_r are constraining relations, if $\phi_{jk} = 0$, and if ϕ_{ii} are negative for all i , then the extreme of W will be a true maximum.

Appendix

The following theorem is very useful in evaluating the determinants which arose in the previous analysis. It is

$$D = \begin{vmatrix} 0 & a_1 & \dots & \dots & a_k \\ b_1 & x_1 & 0 & \dots & 0 \\ \cdot & 0 & x_2 & \cdot & \cdot \\ \cdot & \cdot & \cdot & \cdot & 0 \\ \cdot & \cdot & 0 & \cdot & \cdot \\ \cdot & \cdot & \cdot & \cdot & \cdot \\ \cdot & \cdot & \cdot & \cdot & 0 \\ b_k & 0 & \dots & \dots & 0 & x_k \end{vmatrix} = - \sum_{i=1}^k a_i b_i \prod_{\substack{j=1 \\ j \neq i}}^k x_j \tag{22}$$

It is very easily proved as follows. First expand the determinant in minors with respect to the first column. Expand each i th of the resulting determinants by its i th row. One obtains

$$D = (-1)a_1 b_1 \begin{vmatrix} x_2 & 0 & \dots & 0 \\ \cdot & \cdot & \cdot & \cdot \\ 0 & \cdot & 0 & \cdot \\ \cdot & \cdot & \cdot & \cdot \\ \cdot & 0 & \cdot & \cdot \\ \cdot & \cdot & \cdot & \cdot \\ 0 & \dots & 0 & x_k \end{vmatrix} + \dots + (-1)^i (-1)^{i-1} a_i b_i \begin{vmatrix} x_1 & 0 & \dots & 0 \\ \cdot & \cdot & \cdot & \cdot \\ 0 & \cdot & 0 & \cdot \\ \cdot & x_{i-1} & \cdot & \cdot \\ \cdot & \cdot & \cdot & \cdot \\ \cdot & 0 & x_{i+1} & \cdot \\ \cdot & \cdot & \cdot & \cdot \\ 0 & \dots & 0 & x_k \end{vmatrix} + \dots + (-1)^k (-1)^{k-1} \begin{vmatrix} x_1 & 0 & \dots & 0 \\ 0 & \cdot & \cdot & \cdot \\ \cdot & \cdot & \cdot & \cdot \\ \cdot & 0 & \cdot & \cdot \\ \cdot & \cdot & \cdot & \cdot \\ 0 & \dots & 0 & x_{k-1} \end{vmatrix} = (-1)[a_1 b_1 x_2 \dots x_k + \dots + a_k b_k x_1 \dots x_{k-1}] = - \sum_{i=1}^k a_i b_i \prod_{\substack{j=1 \\ j \neq i}}^k x_j$$

THE CRYSTAL STRUCTURE OF PHOSPHORUS DIODIDE, P₂I₄

BY YUEN CHU LEUNG AND JÜRIG WASER

Contribution from the Chemistry Department, The Rice Institute, Houston, Texas

Received April 4, 1956

X-Ray examination reveals crystals of P₂I₄ to be triclinic, space group $P\bar{1}$, with one molecule per unit cell. The two P atoms are linked together at a distance of 2.21 Å. with a standard deviation of 0.06 Å. while each P atom is linked to two I-atoms at an average distance of 2.475 Å. with a s.d. of 0.028 Å. The molecular symmetry is 2/m.

Of the two known iodides of phosphorus, PI₃ and P₂I₄, the former has been studied by electron diffraction¹⁻³ while little work has been reported concerning the structure of the latter. The molec-

ular unit in the gas phase is reported to be P₂I₄,⁴ and we found this to hold in the crystalline phase also. The substance thus provides a good object to study the P-P bond under conditions of little or no strain. In addition, the bonding angles of phosphorus, the P-I distances, as well as the molecular symmetry of P₂I₄ are of interest.

(1) A. H. Gregg, G. C. Hampson, G. I. Jenkins, P. L. Jones and L. E. Sutton, *Trans. Faraday Soc.*, **33**, 852 (1937).

(2) O. Hassel and A. Sandbo, *Z. physik. Chem.*, **B41**, 75 (1938).

(3) S. M. Swingle, reported by P. W. Allen and L. E. Sutton, *Acta Cryst.*, **3**, 46 (1950).

(4) L. Troost, *Compt. rend.*, **95**, 293 (1882).

Preparation, Unit Cell and Space Group

Phosphorus diiodide was prepared by mixing stoichiometric amounts of white phosphorus and pure iodine in cold carbon disulfide solutions.⁵ The color of the solution changed from dark brown to transparent orange red when the reaction was completed. Slow evaporation of the solution under a stream of dried carbon dioxide resulted in long lath-like crystals which melted at 122.0° (reported m.p. 124.5°).⁶

The laths were quite thin and were trimmed with a razor-blade in an effort to obtain specimens of a cross-section whose thickness and width were of comparable magnitude. The substance hydrolyzes rapidly when exposed to air, forming several phosphorus oxygen acids, phosphine and hydrogen iodide. The specimens used for diffraction were sealed in thin-walled Lindemann glass capillaries in which they could be kept for months without apparent change.

The unit cell dimensions were determined with a Buerger precession goniometer, film shrinkage being corrected for by calibration with superimposed quartz powder lines. The crystals are triclinic with possible space group symmetry $P\bar{1}$ or $P\bar{1}$. The dimensions and angles are

$$\begin{aligned} a_1 &= 4.56 \text{ \AA.} & \alpha_1 &= 80^\circ 12' \\ a_2 &= 7.06 \text{ \AA.} & \alpha_2 &= 106^\circ 58' \\ a_3 &= 7.40 \text{ \AA.} & \alpha_3 &= 98^\circ 12' \\ a_1:a_2:a_3 &= 0.646:1:1.048 \end{aligned}$$

These data may be compared with the results of an optical investigation⁶ which established the crystals to be triclinic, with axial ratios

$$a_1:a_2:a_3 = 0.636:1:1.037$$

and angles

$$\alpha_1 = 80^\circ 30', \alpha_2 = 106^\circ 25', \alpha_3 = 97^\circ 54'$$

The a_1 axis is oriented parallel to the longest extension of a lath, while a_2 and a_3 lie across the width and thickness. The crystals show cleavage parallel to (010).

No suitable liquid to determine the density of P_2I_4 could be found, as the substance either dissolved or decomposed. However, the small cell size (volume 224 Å.³) makes it very unlikely that there is more than one molecule per unit cell, leading to a calculated density of 4.21 g./cm.³.

Intensity Measurements and Structure Determination.—The intensities of reflections of two zones ($Ok\bar{l}$ and $h0l$) were obtained with Mo $K\alpha$ radiation and a Weissenberg goniometer, the reflections being recorded simultaneously on three films with two interleaved brass foils. The reduction in intensity due to the combination of one sheet each of foil and film had been determined to be 3.60 by comparison of spots on films of different exposure. The relative intensities of the reflections were estimated visually by comparison with an intensity scale which was prepared by recording a prominent reflection on the same film at exposure times successively increased by 20%. Since $(1.20)^7 = 3.60$, the eighth such exposure on one film just matched the first one on a film in front of it, so that an intensity range from 1 to 46.7 = 3.60³ was covered in 21 logarithmic steps on three films. The multiple exposure procedure described at the beginning of the paragraph extends this range by a factor $(3.60)^2$ so that a total range of 1 to 605 is covered. This range was further extended by variation of the exposure times.

The crystal used for the $Ok\bar{l}$ data had the dimensions $N_2a_2 \times N_3a_3 = 0.18 \text{ mm.} \times 0.11 \text{ mm.}$, while the specimen used for $h0l$ measured $N_1a_1 \times N_3a_3 = 0.22 \text{ mm.} \times 0.11 \text{ mm.}$ The large linear absorption coefficient, $\mu = 151 \text{ cm.}^{-1}$, made careful correction

for the absorption factor essential. This was done by the procedure of Evans⁷ in which the absorption factor $\exp(-\mu(t_1 + t_2))$ is numerically integrated over the crystal at various directions of the incident and reflected beams which traverse the respective distances t_1 and t_2 . From a sufficient number of such integrations a graph was constructed showing the absorption factors as functions of the coordinates of the Weissenberg film. The absorption factors varied from 0.092 to 0.220 for the $Ok\bar{l}$ and 0.070 to 0.223 for the $h0l$ reflections. On account of the elaborate absorption corrections no intensities of reflections in other zones were measured. The shortness of the a_1 axis made the zones chosen the most desirable ones in terms of atomic resolution.

The intensity data corrected for absorption were multiplied with the reciprocal values of the Lorentz- and the polarization factors, $K \sin 2\vartheta / (1 + \cos^2 2\vartheta)$, where K is a constant and ϑ is the Bragg angle. This resulted in relative values of the squared magnitudes of the structure factors, *const.* F_{obs}^2 . With these data the projections of the Patterson function⁸ on the (100) and the (010) plane were calculated, using Patterson-Tunell strips.⁹ Both projections showed four major peaks and their equivalents by a center of symmetry. Two of these peaks were about twice as heavy as the other two. This is exactly the situation expected for two pairs of iodine atoms related by a center of symmetry and the positions of the peaks thus yielded preliminary values of the iodine parameters. The peaks corresponding to phosphorus-iodine interactions could not be located with certainty.

Since iodine scatters x -rays much more strongly than does phosphorus, most of the signs of the structure factors are determined by the contribution from the iodine atoms. Accordingly the signs of structure factors calculated by using the preliminary iodine parameters were combined with the corresponding observed values, and Fourier projections along a_1 and a_2 were calculated. The resulting electron density maps yielded parameters for the phosphorus atoms as well as improved iodine parameters. These values were refined by the method of least-squares.¹⁰

Least-squares Refinement.—The least-squares method was chosen for further refinement because it offered a simple way for making allowance for the different degrees of accuracy with which different structure factors were known. Strong reflections were suspected to be seriously affected by extinction, so that without laborious corrections the corresponding intensities are unreliable measures of the structure factors.

Two sets of least-squares cycles were pursued until convergence had been attained. In both sets the $h0l$ and the $Ok\bar{l}$ data were treated separately. The first set included 44 $h0l$ and 69 $Ok\bar{l}$ reflections of intermediate intensity range (see Table I). An ordinary desk calculator was employed and all data used were given the same weight. Scale and

(7) H. T. Evans, *J. Appl. Phys.*, **23**, 663 (1952).

(8) A. L. Patterson, *Phys. Rev.*, **46**, 372 (1934).

(9) A. L. Patterson and G. Tunell, *Am. Mineralogist*, **27**, 655 (1942).

(10) E. W. Hughes, *J. Am. Chem. Soc.*, **63**, 1737 (1941).

(5) F. E. E. Gerstmann and R. N. Traxler, *J. Am. Chem. Soc.*, **49**, 307 (1927).

(6) A. E. Nordenskjöld, *Bihang. Akad. Förh. Stockholm*, **2**, 2 (1874).

TABLE I
OBSERVED AND COMPLETED STRUCTURE FACTORS

Singly (doubly) starred reflections were omitted from the first set (from both sets) of least-squares refinements.

<i>h</i>	<i>k</i>	<i>l</i>	$10F_o$	$10F_c$	<i>h</i>	<i>k</i>	<i>l</i>	$10F_o$	$10F_c$	<i>h</i>	<i>k</i>	<i>l</i>	$10F_o$	$10F_c$	<i>h</i>	<i>k</i>	<i>l</i>	$10F_o$	$10F_c$
0	0	1	98	96-	*3	0	1	346	330	0	2	8-	247	221	*0	5	1-	395	470-
**0	0	2	529	871-	*3	0	2	551	599	**0	2	7-		46-	0	5	0	162	169
*0	0	3	252	239-	3	0	3	195	200-	*0	2	6-	509	618-	**0	5	1		10-
0	0	4	140	127-	**3	0	4		41-	**0	2	5-		52	0	5	2	115	101
*0	0	5	262	270-	3	0	5	108	73-	*0	2	4-	247	266	*0	5	3	374	377
*0	0	6	517	552	3	0	6	133	121-	0	0	3-	134	150	0	5	4	84	66
*0	0	7	338	338	**3	0	7		19-	*0	2	2-	390	505	*0	5	5	584	578-
0	0	8	294	292-	3	0	8	167	162	**0	2	1-	353	506	**0	5	6		16
0	0	9	154	156-	4	0	8-	105	129	**0	2	0	537	1446-	0	5	7	177	168
**0	0	10		11	**4	0	7-		25-	**0	2	1	404	814-	0	6	6-	130	89-
**0	0	11		5	4	0	6-	170	167	**0	2	2	507	946	0	6	5-	282	210-
1	0	10-	205	240	4	0	5-	131	91-	*0	2	3	257	285	0	6	4-	155	134
**1	0	9-		16	*4	0	4-	403	409-	0	2	4	73	62	0	6	3-	121	64
**1	0	8-		1	4	0	3-	103	68	0	2	5	217	223	0	6	2-	123	92
**1	0	7-		71	*4	0	2-	312	324	0	2	6	240	211-	0	6	1-	188	138
*1	0	6-	664	609-	**4	0	1-		62	*0	2	7	528	559-	**0	6	0		26-
1	0	5-	222	215-	4	0	0	92	76-	0	2	8	225	192	*0	6	1	425	491-
**1	0	4-	805	836	4	0	1	118	110	0	2	9	259	243	**0	6	2		9
**1	0	3-	666	707	*4	0	2	326	312-	**0	3	9-		8	*0	6	3	367	362
**1	0	2-	766	745-	*4	0	3	86	76-	0	3	8-	245	182	**0	6	4		24-
1	0	1-	160	138	4	0	4	183	172	**0	3	7-		39	**0	6	5		24
**1	0	0	630	628-	4	0	5	144	126	0	3	6-	161	125	*0	6	6		61
**1	0	1	758	837-	**4	0	6		72-	**0	3	5-		38-	*0	6	7	229	167-
*1	0	2	560	673	5	0	8-	193	202-	*0	3	4-	446	542-	0	6	8	215	212-
**1	0	3	896	1146	**5	0	7-		73-	*0	3	3-	355	483-	0	6	9	231	231
1	0	4	320	306-	5	0	6-	169	171	**0	3	2-	540	1015	0	7	4-	106	81-
*1	0	5	445	439-	**5	0	5-		3	*0	3	1-	275	321	0	7	3-	227	137-
**1	0	6		32	**5	0	4-		59	0	3	0	157	152-	**0	7	2-		15-
1	0	7	214	165-	5	0	3-	84	66	**0	3	1		5	*0	7	1-	341	313
**1	0	8		43	5	0	2-	117	104-	*0	3	2	282	305-	**0	7	0		50-
1	0	9	229	196	5	0	1-	235	239-	**0	3	3	500	804-	**0	7	1		32-
2	0	10-	168	194-	5	0	0	186	160	*0	3	4	381	450	**0	7	2		19-
2	0	9-	299	252-	5	0	1	105	90	*0	3	5	521	681	0	7	3	198	125-
2	0	8-	254	260	**5	0	2		6	0	3	6	197	181-	0	7	4	194	145-
2	0	7-	239	230	**5	0	3		8-	0	3	7	188	148-	0	7	5	273	251
**2	0	6-		1	**5	0	4		-	**0	3	8		17-	0	7	6	185	123
**2	0	5-		18	6	0	5-	134	125-	0	3	9	176	145-	0	7	7	217	182-
**2	0	4-		31-	**6	0	4-		16-	0	4	8-	180	125-	0	8	5-	160	88
**2	0	3-	979	980-	6	0	3-	125	126	**0	4	7-		59-	**0	8	4-		-
2	0	2-	229	209	**6	0	2-		30-	*0	4	6-	364	334	0	8	3-	132	77-
**2	0	1-	945	1082	0	1	10-	245	176	0	4	5-	252	201	**0	8	2-		-
2	0	0	105	118	0	1	9-	177	140-	0	4	4-	254	281-	0	8	1-	119	75-
*2	0	1	399	424-	0	1	8-	168	150-	0	4	3-	84	60-	**0	8	0		-
**2	0	2		8-	**0	1	7-		74-	*0	4	2-	257	263-	0	8	1	222	133
2	0	3	329	369-	0	1	6-	212	173-	*0	4	1-	278	314-	0	8	2	202	135
*2	0	4	312	318-	0	1	5-	148	141	*0	4	0	357	397	0	8	3	252	200-
*2	0	5	513	543	**0	1	4-	582	1054	**0	4	1	502	949	**0	8	4		21-
2	0	6	220	203	**0	1	3-		62-	*0	4	2	388	495-	**0	8	5		18
2	0	7	139	141-	**0	1	2-	465	1382-	*0	4	3	348	366-	0	9	3-	121	43
2	0	8	141	112-	**0	1	1-		29-	**0	4	4		1	**0	9	2-		29
**2	0	9		12	**0	1	0		21	0	4	5	112	96-	0	9	1-	187	98-
**2	0	10		47-	**0	1	1		9-	**0	4	6		33-	**0	9	0		21-
3	0	9-	140	165	**0	1	2	474	866	*0	4	7	406	428	0	9	1	105	56
**3	0	8-		3	**0	1	3	483	807	**0	4	8		37	**0	9	2		1-
3	0	7-	337	328-	**0	1	4	631	1079-	0	4	9	292	266-	**0	9	3		29
3	0	6-	237	225-	*0	1	5	385	425-	0	5	8-	141	114-	0	9	4	143	61
*3	0	5-	515	494	0	1	6	233	214	**0	5	7-		49-	**0	9	5		17-
3	0	4-	139	133	0	1	7	182	120	*0	5	6-		53-	0	9	6	175	153-
3	0	3-	86	60-	*0	1	8	95	66	**0	5	5-		6-	0	10	2	152	92-
3	0	2-	130	135	0	1	9	236	207	0	5	4-	236	199	0	10	3	100	59
*3	0	1-	369	362-	*0	1	10	95	101-	*0	5	3-	343	377					
*3	0	0	513	524-	0	2	9-	139	100	*0	5	2-	308	323-					

temperature factors were readjusted from cycle to cycle from graphs of $\log F_{calc}/F_{obs}$ versus $\sin^2 \theta$, and in the last pair of cycles anisotropic temperature factors were introduced. Convergence was achieved in 4 pairs of cycles. Structure factors computed from the final parameter values of this set of refinements showed good agreement in the weak and intermediate intensity range, but for strong reflections the computed F values were consistently too large, in some cases by more than a factor of two.

In an effort to improve this situation a second

refinement was undertaken, in which only the strongest reflections were excluded. The computations were performed on the high speed digital computer SWAC of the University of California at Los Angeles using the least-squares program of Kenneth N. Trueblood and co-workers¹¹ which includes anisotropic temperature factors for each space-group independent atom. For the $h0l$ refinement 66 of 75 observed reflections were used while the $0kl$ refinement included 100 of 113 re-

(11) R. A. Sparks, R. J. Prosen, F. H. Kruse and K. N. Trueblood, to be published.

TABLE II
PARAMETER VALUES \pm (xyz) AND STANDARD DEVIATIONS

	Least-squares cycles						S. d. in Å.	
	$h0l$	First set $0kl$	Av.	$h0l$	Second set $0kl$	Av.	$h0l$	$0kl$
x_{11}	0.556	0.557	0.008	...
y_{11}	...	0.728	0.730	0.008
z_{11}	.165	.165	0.165	.166	.1645	0.165	.006	.007
x_{12}	.820820008	...
y_{12}805803008
z_{12}	.695	.695	.695	.695	.6945	.695	.007	.007
x_P	.398397028	...
y_P645639029
z_P	.464	.462	.463	.463	.4635	.463	.025	.030

flections. The observational equations were weighted according to a scheme¹² in which the weight is taken proportional to $1/F_{\text{obs}}$ when F_{obs} is larger than four times the smallest observable F and proportional to $F_{\text{obs}}/(4F_{\text{min}})^2$ when F_{obs} is smaller than $4F_{\text{min}}$. Reflections below the observable level were not included in the refinement. Four cycles were run for the $h0l$ data, five for the $0kl$ data.

The values of the structure factors computed from the final parameters of the second refinement set are shown in Table I. The agreement between F_{calc} and F_{obs} is improved over that corresponding to the parameters of the first set of refinements, but mainly on account of the inclusion of more elaborate anisotropic temperature factors. For strong reflections the computed values are in general still larger than the observed values and this to an unusual extent in the $0kl$ zone. This may be due, at least in part, to the presence of rather large extinction.

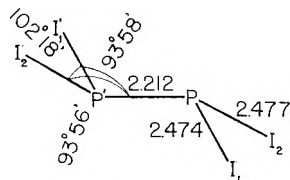


Fig. 1.—Molecular dimensions of P_2I_4 . Non-bonded distances are, in Å., I_1I_2 , 3.856; I_1I_2' , 3.431; I_2I_2' , 3.434.

Table II lists the positional parameters resulting from each set of refinements as well as the standard deviations, in Å., for the atomic coordinates. They were computed from the least-squares residuals and the coefficients of the normal equations. It is noted that there is good agreement between the z parameters which are determined independently by the $h0l$ and $0kl$ refinements. There is also reasonable agreement between the parameters determined in the first set of refinements and those resulting from the second set, except for the y parameters of the P atom.

Table III shows the anisotropic temperature constants in the temperature factors $\exp[-(B_{hh}h^2 + B_{hl}hl + B_{ll}l^2)]$ and $\exp[-(B_{kk}k^2 + B_{kl}kl + B_{ll}l^2)]$. These values may include any effects of the crystal shape which may not have been perfectly corrected for by the absorption factor. The values of the

constants would correspond to atomic root-mean-square displacements varying from 0.15 to 0.28 Å.

TABLE III
ANISOTROPIC TEMPERATURE FACTOR CONSTANTS

	B_{hh}	B_{kk}	$h0l$	B_{ll}	$0kl$	B_{kl}
I_1	0.0575	0.0252	0.0130	0.0112	0.0203	0.0065
I_2	.0559	.0254	.0139	.0138	.0223	.0162
P	.0433	.0149	.0142	.0169	.0188	.0062

Discussion

The length of the P-P bond corresponding to the final parameters is 2.21 Å. with a s.d. of 0.06 Å. while the average of the two P-I bond lengths is 2.475 Å. with an s.d. of 0.028 Å. The values corresponding to the parameters of the first set of refinements are 2.28 and 2.463 Å. Other distances and bonding angles are given in Fig. 1. Within experimental accuracy the molecule possesses the symmetry $C_{2h} - 2/m$. Crystallographically only the inversion center is required, but if one assumes equality of the P-I distances and of the I-P-P bonding angles the molecular symmetry $2/m$ is induced by the center.

The arrangements of the molecules in the crystal are shown in Figs. 2 and 3. The first of these shows two levels of unit cells viewed perpendicularly to the (100) plane (rather than along the a_1 -axis) and contains a record of distances below 4.6 Å. between atoms of different molecules. Figure 3 is a packing drawing perpendicular to the (010) plane.

Since there is only one molecule per unit cell all molecules are parallel to each other. Along the a_1 -axis, the direction of the crystal lath, the molecules lie on top of one another at a distance of 4.56 Å., in such a way that the mirror planes of different molecules merge and rods of monoclinic symmetry are formed. The two pairs of molecules fully drawn out on the left of Fig. 2 provide a top view of this relationship, while Fig. 3 represents an end view of the same pairs. The normal to the plane defined by the iodine atoms of one molecule is at an angle of 22.2° to the axis of the resulting rod-like structure.

The packing of the molecules is summed up by the distance statistics of Table IV and by the right side of Fig. 2. The relationship between neighboring rods is such as to attain efficient packing of the iodine atoms, including a phosphorus-iodine contact. One consequence of this packing is the loss

(12) B. Zaslow, M. Atoji and W. N. Lipscomb, *Acta Cryst.*, **5**, 833 (1952).

of the monoclinic symmetry of the rods, resulting in a triclinic crystal.

TABLE IV
INTERMOLECULAR DISTANCES IN P_2I_4

Distances in Å. to Neighbors

Each distance is followed in parentheses by its frequency of occurrence. The distance between molecules on top of each other, 4.56 Å., was chosen as upper limit. The expected van der Waals contacts, obtained by adding 1.6 Å. to the corresponding covalent bond lengths, are 4.0 Å. for $P \cdots I$ and 4.3 Å. for $I \cdots I$.

Atoms	P	I, same molecule	I, different molecule
P	4.0 (1) 4.56 (2)	4.0 (2)	3.9 (2), 4.0 (1)
I ₁	3.9 (1)	3.9 (1), 4.0 (1)	3.9 (1), 4.1 (2), 4.2 (2) 4.3 (1), 4.56 (2)
I ₂	3.9 (1) 4.0 (1)	3.9 (1), 4.0 (1)	3.9 (1), 4.1 (2), 4.2 (1) 4.3 (1), 4.1 (1), 4.56 (2)

Although, within the accuracy of this determination, P_2I_4 has the symmetry $2/m$ in the crystal, this symmetry may be forced upon it by efficiency of packing within the rods and may not be retained in the vapor phase.

We wish to thank Professor Kenneth N. Tru-blood for his generous help in running the least-squares refinements on SWAC and to Numerical Analysis Research at the University of California at Los Angeles for the use of this high speed digital computer which is supported by the Office of Naval Research and the Office of Ordnance Research.

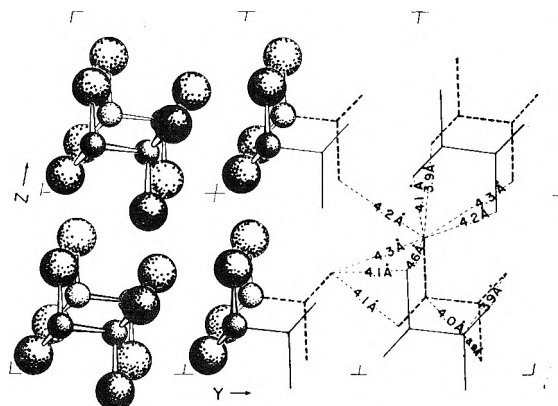


Fig. 2.—Arrangement of molecules in crystal; view perpendicular to the (100) plane.

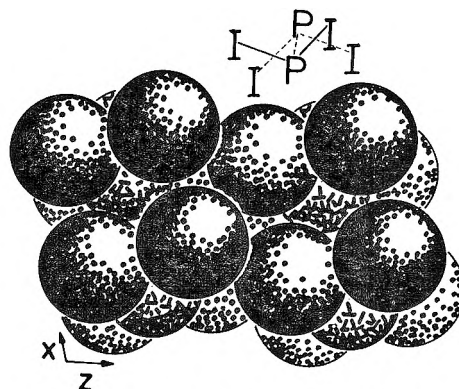


Fig. 3.—Packing drawing of molecules; view perpendicular to the (010) plane.

THE INFLUENCE OF THE POLAR NATURE OF THE ADSORBATE ON ADSORPTION EXPANSION

BY D. J. C. YATES

Ernest Oppenheimer Laboratory, Department of Colloid Science, University of Cambridge

Received June 30, 1955

Following previous work,¹ in which has been reported the design and construction of an interferometer of high sensitivity to measure the small linear expansions resulting from the adsorption of non-polar gases on to porous glass at liquid air temperatures, the range of adsorbates used has been extended to polar materials. With non-polar gases an expansion is always found to occur, irrespective of the volume of gas adsorbed, but with polar gases, in particular carbon monoxide, a contraction is found to precede the expansion in the low coverage region. Further non-polar gases have been investigated, namely, neon and carbon dioxide, and revised results are presented for hydrogen. It is suggested that there may be some correlation between the adsorption expansion of porous glass and the electrical properties of the adsorbates used, and the implications of the initial contraction found with polar molecules are discussed.

Introduction

In an investigation of a theoretical relation which has been derived by the author² between the expansion of a porous solid on the lowering of its surface free energy by the physical adsorption of gases, and the bulk modulus of the solid, only non-polar gases were used as adsorbates.¹

When polar gases were adsorbed, a fundamental change in the character of the expansion process was found to take place. Instead of an expansion over the whole coverage region, a contraction was

found at low coverages, which at higher coverages changed to an expansion. Similar contractions have been observed previously by Haines and McIntosh³ working with charcoal rods, but in their case all of the adsorbates used produced an initial contraction. This paper describes in detail the expansion behavior of porous glass on the physical adsorption of carbon monoxide at liquid air temperatures and measurements with the related gas carbon dioxide. Neon also has been used as an adsorbate, and more accurate data for hydrogen are presented.

(1) D. J. C. Yates, *Proc. Roy. Soc. (London)*, **A224**, 526 (1954).

(2) D. J. C. Yates, *Proc. Phys. Soc.*, **B65**, 80 (1952).

(3) R. S. Haines and R. McIntosh, *J. Chem. Phys.*, **15**, 28 (1947).

Bangham and Razouk⁴ have derived the equation

$$x = -\theta\Delta F' \quad (1)$$

where x is the percentage linear expansion, θ a constant related to the bulk modulus of the solid,¹ and $\Delta F'$ the change in the free surface energy in ergs/cm.². For a mobile film the free surface energy change is related to the two-dimensional pressure π by the equation

$$\pi = -\Delta F' = \gamma_0 - \gamma_1 = \Delta\gamma \quad (2)$$

as a decrease in the surface free energy corresponds to an increase in the two-dimensional pressure. To connect the free energy changes with size changes in the adsorbent, it is necessary to assume that the surface tension lowering ($\Delta\gamma$) is equal to the surface energy lowering. As π is always positive on the assumptions of the Gibbs adsorption equation used in the form⁵

$$\pi = \frac{RT}{M\Sigma} \int \frac{v}{p} dp \quad (3)$$

it is concluded that equation 1 does not hold with polar gases at low coverages and the adsorbent used in this work. In the above equation, R is the gas constant, M the molar volume, v and p the volume and pressure of gas adsorbed at temperature T and Σ the specific surface area.

The mechanism of this contraction is unknown, but it is suggested that it is correlated with the electrical properties of the adsorbates as it is found that non-polar molecules possessing quadrupole moments,^{6,7} such as nitrogen and carbon dioxide, behave in a fashion intermediate between that of polar gases and non-polar gases with zero quadrupole moments (*e.g.*, argon, krypton).

Experimental

Materials.—The porous glass⁸ used in these experiments was the same specimen as used in the previous experiments¹ and was unchanged in size and weight. After the runs reported in the previous paper, the sample was removed from the interferometer for some time for length and weight measurements. The sample was then brought to a reproducible condition by the use of oxygen at 450° as previously described. After re-assembly of the interferometer, the sample was evacuated using the normal technique. An oxygen isotherm was then run at 90°K., and at the monolayer the expansion was 39.6 fringes. The glass was then heated in dry oxygen as usual and then evacuated. Oxygen was then again adsorbed at 90°K., the expansion at unit coverage decreasing to 36.0 fringes. For comparison, the expansion found under the same conditions in the published detailed series of runs was 35.4 fringes.

Carbon monoxide was prepared by the addition of sulfuric acid to sodium formate,⁹ this method having the advantage over the more often used one involving formic acid, that freeing the reagents from dissolved gases before mixing is easier. The gas was purified by passage through traps cooled in liquid air. Carbon dioxide was prepared from sublimation of the commercially available solid, after previously removing inert gases by evacuation while the solid was cooled to 90°K. Any less volatile impurities were removed by passage through traps cooled with a carbon dioxide-acetone mixture. Neon was supplied by the British Oxygen Co. as spectroscopically pure and was not

further purified. Hydrogen was obtained from cylinders and purified as described previously.

Apparatus and Procedure.—A detailed description of the apparatus and procedure has been published.¹ The refractive index correction for the gas in the optical path was calculated from values obtained from the International Critical Tables.¹⁰ The correction for neon was quite large, amounting to some 12% of the total expansion at the highest pressures used at 90°K. For carbon monoxide and dioxide the correction was less than 1% at the maximum. Thermomolecular pressure corrections were not necessary for hydrogen, neon and carbon dioxide, but were made for carbon monoxide by the use of data for nitrogen,^{11,12} as no data could be obtained for carbon monoxide.

When liquid air was used as the refrigerant, the liquid was topped up automatically from a storage dewar, as previously described, but when the carbon dioxide-acetone bath was in use, it was found that sufficient solid carbon dioxide could be added at the end of a day's run to prevent warming up overnight. Mechanical stirring of the acetone was precluded by difficulties due to vibration, and thus a stream of carbon dioxide gas was used.

Results

Although the equation derived by Brunauer, Emmett and Teller¹³ has been criticized on theoretical grounds¹⁴ it has been widely accepted as a practical means of calculating surface areas. An examination has been made of the use of the Huttig¹⁵ equation in deriving areas from the isotherms measured with argon, nitrogen and oxygen, but it was found that only approximately linear plots were obtained and the use of this equation will not be further discussed in this paper. The values of v_m , the monolayer capacity, for carbon monoxide and dioxide have been calculated by the B.E.T. method and are given in Table I, with data for argon, oxygen and nitrogen for comparison. Values for P_0 , the saturation vapor pressure, for carbon monoxide were obtained from the data of Crommelin, Bijleveld and Brown.⁹ For subsequent calculations of the surface free energy lowering, the average value of the specific surface Σ found previously (173.3 m.²/g.) has been used, as the gases argon, oxygen and nitrogen have been the most widely used adsorbates in conjunction with the B.E.T. method.¹⁶

Isosteric heats of adsorption (ΔH) have been calculated, as previously,¹ from large-scale semi-logarithmic isotherms¹⁷ by the Clausius-Clapeyron equation. The values for carbon monoxide as a function of the volume of gas adsorbed are given in Fig. 1, together with values for argon and nitrogen for comparison. The values obtained for hydrogen from the latest isotherms are very similar to those previously published, and are not given in this paper.

The values of the linear expansion (or contraction) in terms of fringe shifts (N) as a function of the volume adsorbed are given in Fig. 2 for the oxides of carbon, and in Fig. 3 for hydrogen and neon. As before, when N is unity the percentage

(10) "International Critical Tables," Vol. 7, McGraw-Hill Book Co., New York, N. Y., 1st Ed.

(11) J. M. Los and R. R. Fergusson, *Trans. Faraday Soc.*, **48**, 730 (1952).

(12) G. L. Kington and J. M. Holmes, *ibid.*, **49**, 425 (1953).

(13) S. Brunauer, P. H. Emmett and E. Teller, *J. Am. Chem. Soc.*, **60**, 309 (1938).

(14) H. M. Cassell, *J. Chem. Phys.*, **12**, 115 (1944).

(15) G. F. Huttig, *Monatsh.*, **78**, 177 (1948).

(16) W. D. Harkins and G. Jura, *J. Chem. Phys.*, **11**, 431 (1943).

(17) T. N. Rhodin, *This Journal*, **57**, 143 (1953).

(4) D. H. Bangham and R. I. Razouk, *Proc. Roy. Soc. (London)*, **A166**, 572 (1938).

(5) G. Jura and W. D. Harkins, *J. Am. Chem. Soc.*, **66**, 1356 (1944).

(6) W. V. Smith and R. Howard, *Phys. Rev.*, **79**, 132 (1950).

(7) R. M. Hill and W. V. Smith, *ibid.*, **82**, 451 (1951).

(8) M. E. Nordberg, *J. Am. Ceram. Soc.*, **27**, 299 (1944).

(9) C. A. Crommelin, W. J. Bijleveld and E. G. Brown, *Commun. K. Onnes Lab. Univ. Leiden*, No. 217b (1931).

TABLE I

SUMMARY OF RESULTS

Gas	Temp. (°K.)	v_m (cm. ³ /g.)	Σ (m. ² /g.)	π at v_m (ergs/cm. ²)	N at v_m (fringes)	$dN/d\pi$	Average $dN/d\pi$
CO	90	44.22	190.0	42.0	39.5	1.247	1.207
	79	45.89	187.2	41.9	41.4	1.167	
CO ₂	195	30.70	140.0	28.9	33.1	1.352	1.352
H ₂	90	2.055	1.828
	79	1.601	
A	90	39.85	162.6	22.8	24.7	1.005	1.012
	79	42.19	165.6	22.6	24.5	1.018	
N ₂	90	41.32	179.9	31.60	31.1	1.130	1.117
	79	42.27	175.0	30.90	32.0	1.105	
O ₂	90	45.45	178.2	27.35	35.2	1.180	1.160
	79	47.19	178.8	26.80	35.2	1.140	

linear change in length of the sample is 5.386×10^{-4} .

The two-dimensional pressure π equivalent to the surface energy lowering ($-\Delta F'$) has been calculated by the method due to Bangham,¹⁸ the procedure being identical with that previously

used. Calculations of π have only been made in the regions of the isotherms for which it is known that capillary condensation has not been taking place, by comparison with isotherms on this

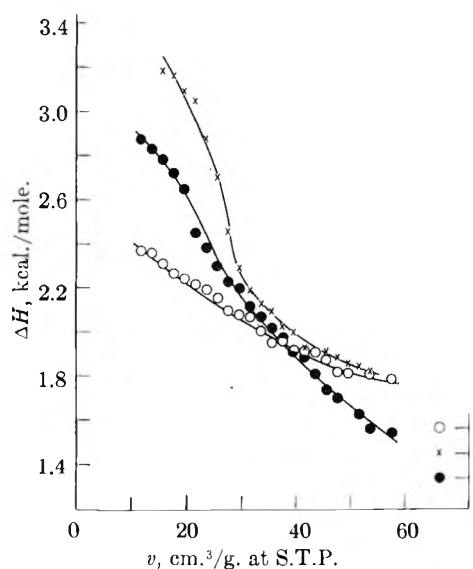


Fig. 1.—The heats of adsorption of argon, carbon monoxide and nitrogen: O, argon; X, carbon monoxide; ●, nitrogen.

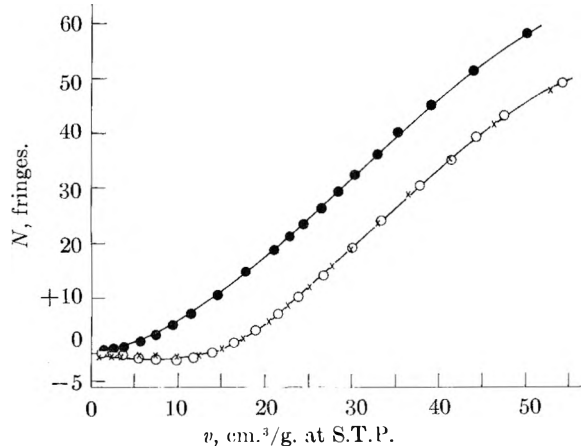


Fig. 2.—The expansion in fringes for carbon monoxide and dioxide: carbon monoxide, O, 90°K.; X, 79°K.; carbon dioxide, ●, 195°K.

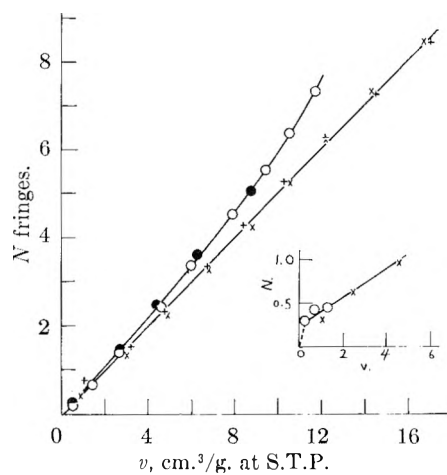


Fig. 3.—The expansion in fringes for hydrogen (large curves) and neon (insert): neon, O, 90°K.; X, 79°K. Hydrogen 90°K., ●, run 41; O, run 42; 79°K., +, run 35; X, run 38.

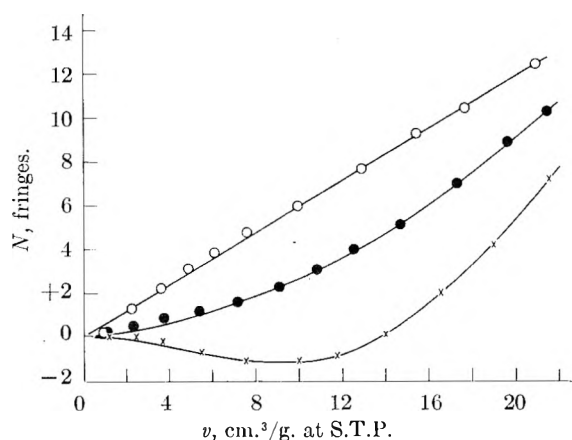


Fig. 4.—Comparative expansion values at 90°K.: O, argon; ●, nitrogen; X, carbon monoxide.

adsorbent published by other workers.¹⁹⁻²¹ In the region of capillary condensation, values of π obtained by the above method have been shown by

(19) P. H. Emmett and T. W. De Witt, *J. Am. Chem. Soc.*, **65**, 1253 (1943).
 (20) P. H. Emmett and M. Cines, *This Journal*, **51**, 1248 (1947).
 (21) R. M. Barrer and J. A. Barrie, *Proc. Roy. Soc. (London)*, **A213**, 250 (1952).

(18) D. H. Bangham, *Trans. Faraday Soc.*, **33**, 805 (1937).

Hill²² to be indeterminate. The π values obtained with carbon monoxide give π - v plots similar to those previously found with nitrogen,¹ and those for carbon dioxide are similar to those for oxygen. Values of π at monolayer coverage are given in Table I for all gases except hydrogen and neon. The values for hydrogen are very similar to the previous values, and values of π have not been calculated for neon as both the expansions and volumes adsorbed are so small.

From relations between N and v given in Figs. 2 and 3, corresponding values of π were obtained from the detailed large scale π - v graphs. The relations obtained between N and π are given in Figs. 5 and 6.

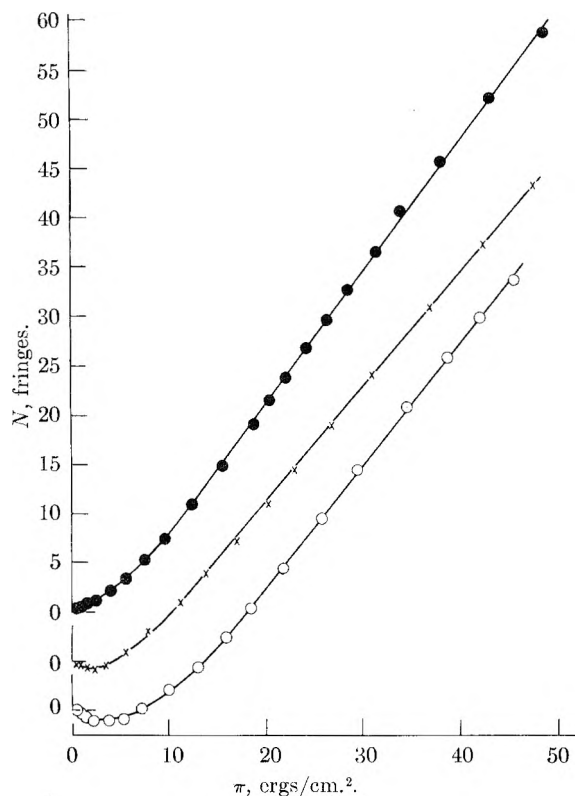


Fig. 5.—The expansion and surface energy lowering for carbon monoxide and dioxide. Carbon monoxide O, 90°K.; ×, 79°K.; carbon dioxide ●, 195°K.

As before, the reversibility of the expansion was determined by pumping the adsorbed gas off the surface under isothermal conditions, and measuring the contraction in fringes with time of pumping. Long times were involved for this process, due to the small pores in the glass, and these times became prohibitively long whenever the pressure of the adsorbed gas was low. Thus it was not found possible to investigate in detail the contraction region found with carbon monoxide. The region where the coverage was about 0.5 was chosen for the reversibility experiment, with an expansion before desorption began of 10.1 fringes. No difficulty was experienced with carbon dioxide due to the much higher equilibrium pressures involved. The results are not given in detail as they are similar to those previously found, but at the maxi-

(22) T. L. Hill, *J. Chem. Phys.*, **17**, 520 (1949).

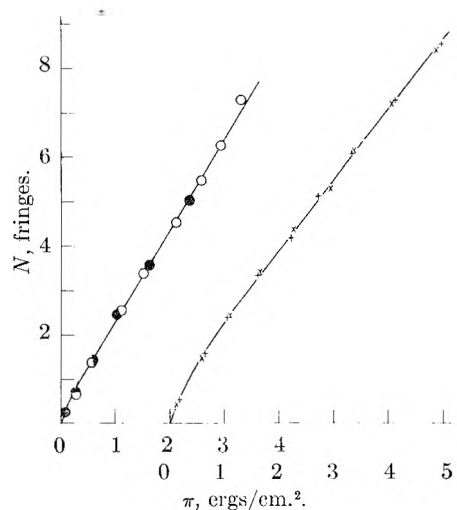


Fig. 6.—The expansion and surface energy lowering for hydrogen at 90°K.: ●, run 41; O, run 42; at 79°K.: +, run 35; ×, run 38.

imum pumping time used, 120 minutes, the carbon monoxide expanded sample, contracted 95% of its initial expansion, and in the run with carbon dioxide the sample contracted 98%.

Discussion

The Specific Surface of the Glass.—It will be seen from Table I that the monolayer capacity, v_m for carbon monoxide, is higher than that found for nitrogen. On the basis of the molecular areas,²³ it is to be expected that the v_m value for these two gases would be very similar.

The v_m value for carbon dioxide, on the other hand, is much smaller than expected, if an area for this molecule (calculated from the liquid density) of 17 Å.² be assumed. To bring the specific surface (Σ) calculated from this v_m value into agreement with the average found for argon, nitrogen and oxygen (173.3 m.²/g.), a cross-sectional area of 21 Å.² has to be assumed. This is in substantial agreement with the data reported by Emmett and Cines²⁰ for carbon dioxide on porous glass; they had to use an area of 20 Å.² to obtain agreement with their nitrogen results.

The above data provide further evidence that on this adsorbent the substrate surface must be exercising a considerable specific effect on the spacing of the adsorbed molecules. This spacing effect has been reported by Beebe, Beckwith and Honig²⁴ using anatase, and more extensively discussed by Walker and Zettlemoyer²⁵ who used magnesium oxide.

Heats of Adsorption.—The values found with carbon monoxide are considerably higher than those for argon, oxygen and nitrogen. This also has been found with the same gases adsorbed on alkali halides²⁶ and on charcoal.²⁷ As previously found,

(23) H. K. Livingston, *J. Colloid Sci.*, **4**, 447 (1949).

(24) R. A. Beebe, J. B. Beckwith and J. M. Honig, *J. Am. Chem. Soc.*, **67**, 1554 (1945).

(25) W. C. Walker and A. C. Zettlemoyer, *THIS JOURNAL*, **57**, 182 (1953).

(26) F. C. Tompkins and D. M. Young, *Trans. Faraday Soc.*, **47**, 77 (1951).

(27) A. van Itterbeck and W. van Dingenen, *Physica*, **4**, 1169 (1937).

anomalously low values of ΔH were obtained in the low coverage region, and these values have not been plotted in Fig. 1. The cause of these low values is unknown, although they have also recently been reported by other workers at low equilibrium pressures.²⁸

Expansion Values on Adsorption.—From Fig. 3 it will be seen that the expansion produced by the adsorption of hydrogen is similar to that produced by argon and krypton. In addition the curves for the two temperatures used do not intersect as they did previously.¹ This change is due to the improved stability of the interferometer and, to show the reproducibility attained, the values from two separate runs at each of the temperatures used are shown on the figure. The expansion values for neon are very small, being only about half those found for argon at the same volumes adsorbed. The cause of this is unknown, but the expansions were so small that no great significance is to be attached to this variation. Until measurements can be made at temperatures below 79°K., it will be difficult to obtain sufficient accuracy, due to the small volumes of neon adsorbed at pressures below atmospheric.

The expansion characteristics of carbon dioxide shown in Fig. 2 will be seen to be similar to those of nitrogen.¹ The gradient of the graph, dN/dv , is substantially constant for the gases argon, krypton, oxygen and hydrogen irrespective of the coverage, but in the case of nitrogen and carbon dioxide dN/dv is very small initially, becoming constant for nitrogen at a coverage of about 0.6, and for carbon dioxide at 0.7. The expansion values for carbon dioxide at any given value of volume adsorbed are larger than for nitrogen, but on a coverage basis the difference is small.

The effect produced by carbon monoxide is quite different from that produced by the other adsorbates used in that a net contraction took place until a coverage of about 0.3 was reached. The actual values from detailed graphs are 0.31 at 90°K., and 0.29 at 79°K. Preliminary results with sulfur dioxide and ammonia also show marked contractions. The comparative length changes at 90°K. for the gases argon, nitrogen and carbon monoxide in the coverage region less than 0.5 are shown in Fig. 4.

The cause of this contraction is uncertain. The contractions found by Bangham and co-workers^{4,29-31} are not considered in this discussion as the surface coverages of the adsorbates they used are uncertain. The work of Amberg and McIntosh,³² who measured the length changes of porous glass due to the adsorption of water, is not discussed here, as they did not present detailed expansion data in the low coverage region. Haines and McIntosh³ found that their charcoal rods contracted prior to expansion when water, butane, dimethyl ether and ethyl chloride were adsorbed,

(28) J. R. Dacey and D. G. Thomas, *Trans. Faraday Soc.*, **50**, 740 (1954).

(29) D. H. Bangham, *Proc. Roy. Soc. (London)*, **A147**, 175 (1934).

(30) D. H. Bangham and N. Fakhoury, *ibid.*, **A130**, 81 (1930).

(31) D. H. Bangham, N. Fakhoury and A. F. Mohamed, *ibid.*, **A147**, 152 (1934).

(32) C. H. Amberg and R. McIntosh, *Canadian J. Chem.*, **30**, 1012 (1952).

the contraction being present at coverages less than a third. In their case contractions were found with all the adsorbates used while in this work only the polar gases produced contractions. Four possible mechanisms have been suggested³ for the contraction: (A) contraction along the length of the rod may have occurred together with a radial expansion; (B) possible solution of the adsorbate in the adsorbent; (C) adsorption in narrow crevices where the range of attractive forces is as great as the crevice diameter; (D) the effects of capillary condensation. While mechanism (A) possibly may be operative in the system used here, it cannot be experimentally determined with the present apparatus. Recent work by Flood and Heyding,³³ using activated carbon rods, has shown that the contraction found with water vapor at low relative humidity takes place both axially and radially to a similar extent. This radial contraction ($\approx 0.03\%$) was measured by winding a fine wire round the rod, and it is thought that this method could not easily be made sensitive enough to measure the very small contractions found with carbon monoxide ($\approx 0.00055\%$) in this work, quite apart from the difficulties due to the low temperatures of adsorption. Whilst it may be possible (B) that solution of the adsorbate in the adsorbent may take place with charcoal and organic vapors, it seems very unlikely with the adsorbate-adsorbent systems used in this work. Adsorption in a narrow crevice with a correspondingly high heat of adsorption as suggested in C may possibly produce a contraction, but due to the fact that the nitrogen molecule has similar size and potential energy parameters to the carbon monoxide molecule, it is to be expected that the same crevices and adsorption sites would be available for both, and thus a contraction should also be found for nitrogen if this mechanism were operative. The final suggestion, D, that capillary condensation is taking place is rather unlikely at the low coverages concerned unless there are much smaller pores in the glass than have been measured by other workers.¹⁹⁻²¹

It is suggested that the anomalous expansion characteristics of some of the adsorbates used are correlated with their electrical properties. Of the gases which behave "normally," argon, krypton and neon have zero dipole moments and have zero permanent electric quadrupole moments. For homonuclear diatomic molecules, the dipole moment is also zero. While it is evident that these molecules may possess quadrupole moments, there is no direct physical method of measuring them. Recent work by Smith and Howard⁶ and Hill and Smith⁷ has shown that values of quadrupole moments can be assessed by the line broadening of microwave spectra. Values for the adsorbates used in this work have been reproduced in Table II. Due to the limitations of the method the values given are not very accurate, but the order of magnitude and important features such as the rather large difference between oxygen and nitrogen are thought to be significant.

On the adsorption of oxygen and hydrogen, it is found that the expansion is a linear function of the

(33) E. A. Flood and R. D. Heyding, *ibid.*, **32**, 660 (1954).

volume adsorbed, within the experimental error. It will be seen from the table that these molecules have relatively small quadrupole moments.

TABLE II
QUADRUPOLE MOMENTS OF THE ADSORBATES

Molecule	Quadrupole moment (Å. ²)	Molecule	Quadrupole moment (Å. ²)
A, Kr, Ne	0.0	CO	0.34
H ₂	<0.10	CO ₂	0.65
O ₂	<0.09	SO ₂	1.60
N ₂	0.27		

For nitrogen and carbon dioxide the quadrupole moments are, respectively, about three and six times those of oxygen and hydrogen and the expansion-adsorption graph has a low gradient at low coverage. The case of nitrogen is particularly interesting as it has been found by many workers^{26,34} to give anomalously high heats of adsorption, compared with argon and oxygen, when adsorbed on to ionic solids. This anomaly is not present for adsorption on to non-ionic solids,³⁵ and Drain³⁶ has suggested that the anomaly can be explained by consideration of the interaction of surface electric fields with the charge distribution of the nitrogen molecule.

The quadrupole moment of carbon monoxide is somewhat larger than that of nitrogen, but in addition the molecule possess a dipole moment of about 0.11 debyes. The other adsorbate which produces a contraction, sulfur dioxide, has a much larger quadrupole moment than carbon monoxide and has a large dipole moment, as ammonia has also. Thus it is suggested that the contractions found with carbon monoxide, sulfur dioxide and ammonia may be correlated with the dipole moments of these molecules and that the relatively low expansion at low coverage found with nitrogen and carbon dioxide may be correlated with the presence of quadrupole moments in these adsorbates. No physical mechanism can be suggested at the present time to produce the observed contractions on the basis of the above correlation.

It is of interest to note that Tykodi³⁷ has recently suggested that there may be some analogy between swelling due to adsorption and that due to electrostriction. Tykodi states that if this analogy is valid the swelling of the solid would be correlated with the electric field in the adsorbed phase, and thus the adsorption properties of the adsorbate would be correlated with its electrical properties.

Relations between Expansion and Surface Free Energy Lowering.—The comparative behavior of the gases used is presented in Figs. 5 and 6. The shape of the $N-\pi$ curve for carbon dioxide is seen to be similar to that found for nitrogen. The low expansion at low coverage for carbon dioxide causes the gradient $dN/d\pi$ to be low at low π values, becoming constant later. When π values greater than about 15 ergs/cm.² are considered,

(34) (a) W. J. C. Orr, *Proc. Roy. Soc.*, **A173**, 349 (1939); (b) G. L. Kington, R. A. Beebe, M. H. Polley and W. R. Smith, *J. Am. Chem. Soc.*, **72**, 1775 (1950).

(35) R. A. Beebe, J. Biscoe, W. R. Smith and C. B. Wendell, *ibid.*, **69**, 95 (1947).

(36) L. E. Drain, *Trans. Faraday Soc.*, **49**, 650 (1953).

(37) R. J. Tykodi, *J. Chem. Phys.*, **22**, 1647 (1954).

constant $dN/d\pi$ values are found for carbon monoxide. In the low coverage region contractions are observed and equation 1 is not valid.

The hydrogen data give a relation between N and π similar to that previously observed with oxygen, argon and krypton. For these gases the shape of the $N-\pi$ plots in the low coverage region is dependent on the $\pi-v$ curves. To show the reproducibility attained with the latest hydrogen runs, expansion values for four independent runs are shown in Fig. 6, the π values being obtained from isotherms averaged from all the runs. The differences between the values given in the figure and those given in Fig. 10 of the previous paper¹ are entirely due to differences in the $N-v$ plots as the $\pi-v$ plots are very similar indeed.

As discussed previously¹ there may be errors in the π values at low coverages, and as there is an anomalous region for carbon monoxide, the gradient $dN/d\pi$ of the linear region of the curves is taken for discussion. The details are given in Table I, and it will be seen that the values for carbon monoxide are slightly larger than those for oxygen, at the same temperatures, while the value for carbon dioxide is considerably greater than either, but smaller than the values for hydrogen. The value for $dN/d\pi$ for hydrogen at 90°K. was previously found to be lower than the value at 79°K., in contrast with the majority of the other gases. The recent values show that the ratio of the gradient at 90°K. to that at 79°K. is similar to that for all the other gases except argon. The average value of the gradient has only changed from 1.781 to 1.828 due to the latest results, and the striking difference between this gas and the group argon, nitrogen and oxygen remains unchanged.

Both in the case of the theory of the expansion advanced by the author² and in that due to Bangham and Maggs,³⁸ it is assumed that equation 1, due to Bangham, holds

$$x = -\theta\Delta F' \quad (1)$$

where x is the percentage linear expansion, $\Delta F'$ the change in surface free energy, and θ a constant. Now $dN/d\pi$ is directly related to $x/\Delta F'$, so that the fact that $dN/d\pi$ varies according to the gas used means that θ must vary also. As far as is known this variation in θ has not previously been reported with such a wide range of adsorbates and, if verified, means that reconsideration will have to be given to the applicability of equation 1. As this large variation in θ is unexplained at the present time, further consideration will not be given in this paper to the relations found previously between θ and the bulk modulus of the solid, using the average value of $dN/d\pi$ for argon.

Apart from consideration of the contractions, the variations in θ may be explained by a change in the value of the bulk modulus with varying adsorbates. It may be possible to measure the bulk modulus under the conditions of use, and thus to determine its constancy.

While the constancy, or otherwise, of the bulk modulus of the adsorbent may be experimentally

(38) D. H. Bangham and F. A. P. Maggs, "Conference on the Ultrafine Structure of Coals and Cokes," British Coal Utilization Research Association Committee, London, 1944, p. 118.

measurable, this is not the case when verification of the correctness of the spreading pressures is considered. The meaning of spreading pressures has been discussed recently by Everett³⁹ and by Pierce and Smith.⁴⁰ Everett considers that although spreading pressures measured on liquids have a perfectly definite meaning, this is not the case for solids where he considers that the physical interpretation of spreading pressures is uncertain. Pierce and Smith consider that for an energetically heterogeneous surface, such as that used in this work, the computation of spreading pressures from isotherms may be misleading. As well as the assumptions involved in the calculation of the surface energy lowering, there is the additional assumption, which has to be made in order to relate the expansion to the elastic constants, that the surface energy lowering is equal to the surface tension lowering. Shuttleworth⁴¹ has emphasized that for solids the absolute value of the surface energy and surface tension may be very different, but he has not considered changes in these quantities. Bingham¹⁸ has shown that in the particular type of physical adsorption in which the adsorbed molecules behave as a two-dimensional gas the surface tension and energy lowering are equal, but he did not consider the case in which molecular mobility takes place by a series of short jumps over the surface during the time of adsorption. For non-uniform surfaces the latter mechanism has been suggested by Tompkins⁴² and de Boer.⁴³

One factor of importance in this work is that it

(39) D. H. Everett, *Trans. Faraday Soc.*, **46**, 942 (1950).

(40) C. Pierce and R. N. Smith, *J. Am. Chem. Soc.*, **75**, 846 (1953).

(41) R. Shuttleworth, *Proc. Phys. Soc.*, **A63**, 444 (1950).

(42) F. C. Tompkins, *Trans. Faraday Soc.*, **46**, 569 (1950).

(43) J. H. de Boer, "The Dynamical Character of Adsorption," Oxford University Press, London, 1953.

shows that adsorbate-adsorbent interaction causes perturbation of the adsorbent.^{44,45} This perturbation has often been assumed negligible in theoretical treatments,^{22,34,46} and in experimental work using the assumption that the thermodynamic properties of the adsorbed gas are those of a one-component system.⁴⁷ If the perturbation of the adsorbent were negligible, it would be expected that no size changes would occur in the adsorbent on adsorption. The fact that size changes do occur, even if small in magnitude, makes the assumption of an inert adsorbent, for physical adsorption, of very doubtful validity.

When adsorption takes place the environment and thus the chemical potential of the surface lattice elements changes; in order to maintain homogeneity in the chemical potential the surroundings of internal lattice elements must change also. These changes result in the swelling of an ionic solid when non-polar gases are adsorbed and in the contraction of the solid when small quantities of certain polar gases are adsorbed, followed by a swelling at higher adsorptions.

The author wishes to thank the Corning Glass Company, of Corning, New York, for the gift of the porous glass used in this work and for information concerning its properties.

Thanks are due to Dr. J. H. Schulman, O.B.E., for helpful discussions and advice. The author wishes to acknowledge the support of the Consolidated Zinc Corporation in the early phases of this work and of the Council of the British Ceramic Research Association in the concluding phases.

(44) M. A. Cook, D. H. Pack and A. G. Oblad, *J. Chem. Phys.*, **19**, 367 (1951).

(45) S. Brunauer, "Structure and Properties of Solid Surfaces," University of Chicago Press, Chicago, 1953, p. 395.

(46) T. L. Hill, *Trans. Faraday Soc.*, **47**, 376 (1951).

(47) L. E. Drain and J. A. Morrison, *ibid.*, **48**, 840 (1952).

PURIFICATION AND PROPERTIES OF TEN ORGANIC SULFUR COMPOUNDS—SECOND SERIES¹

BY WILLIAM E. HAINES, R. VERNON HELM, GLENN L. COOK AND JOHN S. BALL

Bureau of Mines, Petroleum and Oil-Shale Experiment Station, Laramie, Wyoming

Received July 18, 1955

Ten organic sulfur compounds, 2-propanethiol, 1-butanethiol, 2-butanethiol, 2-thiopropane, 2-thiapentane, 3-methyl-2-thiabutane, thiacyclohexane, 2-methylthiophene, 3-methylthiophene and benzo[b]thiophene, were purified to at least 99.9 mole % purity. In addition to the boiling point, freezing point and cryoscopic constant, the following properties were measured at 20, 25 and 30°: density, viscosity, surface tension and refractive index for the *r*, *C*, *D*, *e*, *v*, *F*, and *g* lines. Derived functions, including refractivity intercept, specific dispersion, molecular refraction, parachor and molecular volume, were calculated. Mass, infrared and ultraviolet spectra were determined, permitting some correlation of the effect of sulfur groupings on spectra. The stability of the compounds under storage conditions was investigated.

One of the aims of American Petroleum Institute Research Project 48A, which is cooperatively sponsored by the Bureau of Mines and the API, is to supply fundamental data concerning sulfur compounds that occur in petroleum. High-purity thiols, sulfides, disulfides and thiophenes are pre-

(1) This investigation was performed as part of the work of American Petroleum Institute Research Project 48A on "The Production, Isolation, and Purification of Sulfur Compounds and Measurement of their Properties," which the Bureau of Mines conducts at Bartlesville, Okla., and Laramie, Wyo.

pared so that three groups of physical properties can be determined accurately: (1) common physical properties, including refractive index, density, viscosity, surface tension, melting point, cryoscopic constant and boiling point; (2) reference spectra; and (3) thermodynamic properties. The properties of the first series of ten compounds, including ethanethiol, 2-methyl-2-propanethiol, 1-pentanethiol, 2-thiabutane, 3-thiapentane, thiacyclobutane, thiacyclopentane, 2,3-dithiabutane,

3,4-dithiahexane, and thiophene, were reported previously.² This paper reports the common physical properties and spectra of the second series of ten sulfur compounds. Other investigators recently have reported values for several of these properties.³ The thermodynamic properties of some of these compounds have been reported in separate papers.⁴

A sufficient quantity of each compound is prepared to facilitate the attainment of high purity and to assure an adequate supply for the measurement of properties. A small surplus of each compound usually results and this material is made available to the industry as calibration standards through the API Samples and Data Office at Carnegie Institute of Technology. Because of their use as calibration standards, the storage stabilities of the compounds have been investigated.

The compounds included in the present study, together with their common names and sample numbers, are shown below

Thiols

2-Propanethiol	Isopropyl mercaptan	API-USBM 11-5S
1-Butanethiol	<i>n</i> -Butyl mercaptan	API-USBM 14-5S
2-Butanethiol	<i>sec</i> -Butyl mercaptan	API-USBM 19-5S

Sulfides

2-Thiapropane	Dimethyl sulfide	API-USBM 13-5S
2-Thiapentane	Methyl <i>n</i> -propyl sulfide	API-USBM 18-5S
3-Methyl-2-thiabutane	Methyl <i>iso</i> -propyl sulfide	API-USBM 20-5S

Cyclic sulfide

Thiacyclohexane	Pentamethylene sulfide	API-USBM 17-5S
-----------------	------------------------	----------------

Thiophenes

2-Methylthiophene		API-USBM 16-5S
3-Methylthiophene		API-USBM 12-5S
Benzo[<i>b</i>]thiophene	Thianaphthene	API-USBM 15-5S

Purification.—To meet the needs of the program, approximately 1.5 liters of material with a purity of at least 99.9 mole % was required. The purification procedures used were similar to those described in the previous paper² in which choice of fractions and of methods was guided by freezing point purity measurements. Details of the purification procedures used for individual compounds are de-

scribed below. All distillations were made at atmospheric pressure (585 mm.) unless otherwise noted.

2-Propanethiol.—The raw material consisted of 2.5 l. purchased from Eastman Kodak Company plus 1.5 l. of material that had been recovered from a caustic wash of petroleum naphtha by the Union Oil Company of California. This sample was distilled through a 1-inch by 9-foot column packed with stainless-steel helices (hereinafter designated as column 1). The yield of high-purity (99.98 mole %) material was 1.6 l.

1-Butanethiol.—Approximately 4 l. of material purchased from Eastman Kodak Company was distilled through column 1. The yield of high purity (99.93 mole %) material was 1.5 l.

2-Butanethiol.—Four liters of material, synthesized and given to the Project by California Research Corporation, was distilled through a 1-inch by 8-foot Oldershaw column (column 2). It was impossible to follow the purification by the freezing point method because the compound formed a glass when cooled. A portion of the distillate, estimated to have a purity of 99.9 mole %, was therefore chosen by comparing the mass spectra of the various fractions. A sample of this selected material was submitted to the Thermodynamics Laboratory, Bureau of Mines, Bartlesville, Oklahoma, for determination of purity. The sample failed to crystallize, even under the conditions in the low temperature cryostat, although a sample of less purity (99.7 mole %) had given satisfactory results. Final purity was therefore estimated by mass spectrometry, utilizing the mass spectra of the less pure sample for comparison. The yield of high purity (99.9 mole %) material was 1.5 l.

2-Thiapropane.—Four liters of material purchased from Eastman Kodak Company was dried over anhydrous calcium sulfate and charged to a high temperature Podbielniak heligrid column with a 5-foot packed section (column 3). Approximately 3 l. of pure material (99.99 mole %) was recovered.

2-Thiapentane.—This compound was synthesized by a method based on suggestions of Bordwell and Kern.⁵ Three moles of *n*-propyl bromide was added dropwise to 3 moles of sodium methyl mercaptide prepared by dissolving methanethiol in 10% sodium hydroxide. Stirring was continued for 45 minutes after addition was completed, and the mixture was then refluxed for 2 hours. The product was recovered by steam distillation and washed successively with 5% sodium hydroxide, 5% hydrochloric acid and distilled water. Twenty batches were prepared, with an average yield of 93 mole %. The methanethiol used in this and the succeeding synthesis was donated to the Project by Union Oil Company of California. The crude 2-thiapentane thus prepared (5.6 l.) was dried over anhydrous potassium carbonate and distilled through column 2. The yield of high purity (99.97 mole %) material was 2.0 l.

3-Methyl-2-thiabutane.—This compound was synthesized using isopropyl bromide in place of *n*-propyl bromide in the above procedure. Reflux time was extended to 4 hours. The steam distilled product contained about 15% of unreacted bromide. Correcting for this bromide, the average yield for the 26 3-mole batches was 81% of theoretical. The crude sulfide (7.6 l.) was distilled through a 6-foot Stedman-packed column 1 inch in diameter (column 4). The yield of high-purity (99.99 mole %) material was 3.3 l.

Thiacyclohexane.—This compound was prepared by a method based on the general suggestions of Bordwell and Pitt.⁶ A solution of 486 g. of sodium sulfide (60% fused chips) in 500 ml. of water was refluxed and stirred vigorously while 405 ml. (3 moles) of 1,5-dibromopentane was added. This addition was made dropwise over a period of 2 hours. Stirring and reflux were continued for an additional 4 hours. The product was then steam distilled from the reaction mixture, washed with 5% sodium chloride solution and dried over anhydrous potassium carbonate. The yield of crude thiacyclohexane was 71% of theoretical. Four liters of the crude product was distilled through column 4, yielding 2.0 l. of high purity (99.94 mole %) material.

2-Methylthiophene.—Approximately 3.3 liters of 2-methylthiophene furnished by Socony-Mobil Oil Company was distilled in column 3, yielding 0.8 l. of material with a purity

(5) F. G. Bordwell and R. J. Kern, communication from API Project 48B at Northwestern University.

(6) F. G. Bordwell and B. M. Pitt, communication from API Project 48B at Northwestern University.

(2) W. E. Haines, R. V. Helm, C. W. Bailey and J. S. Ball, *THIS JOURNAL*, **58**, 270 (1954).

(3) D. H. Desty and F. A. Fidler, *Ind. Eng. Chem.*, **43**, 905 (1951); R. L. Denyer, F. A. Fidler and R. A. Lowry, *ibid.*, **41**, 2727 (1949); F. S. Fawcett, *J. Am. Chem. Soc.*, **68**, 1420 (1946); S. Mathias, *ibid.*, **72**, 1897 (1950); D. T. McAllan, T. V. Cullum, R. A. Dean and F. A. Fidler, *ibid.*, **73**, 3327 (1951); S. Sunner, Thesis, University of Lund, Sweden, 1950; A. I. Vogel, *J. Chem. Soc.*, 1820 (1948); P. T. White, D. G. Barnard-Smith and F. A. Fidler, *Ind. Eng. Chem.*, **44**, 1430 (1952).

(4) J. P. McCullough, S. Sunner, H. L. Finke, W. N. Hubbard, M. E. Gross, R. E. Pennington, J. F. Messerly, W. D. Good and Guy Waddington, *J. Am. Chem. Soc.*, **75**, 5075 (1953); H. L. Finke, M. E. Gross, J. F. Messerly and Guy Waddington, *ibid.*, **76**, 854 (1954); J. P. McCullough, H. L. Finke, W. N. Hubbard, W. D. Good, R. E. Pennington, J. F. Messerly and Guy Waddington, *ibid.*, **76**, 2661 (1954); J. P. McCullough, H. L. Finke, D. W. Scott, M. E. Gross, J. F. Messerly, R. E. Pennington and Guy Waddington, *ibid.*, **76**, 4796 (1954).

of 99.8 mole %.⁷ The shoulder fractions from this distillation were combined with 3 l. of additional raw material for distillation in column 1. Fractions from this distillation were combined to yield 2 l. of material with a purity of 99.5 mole %. The latter sample plus the 0.8 l. from the first distillation were combined and distilled through column 2, yielding 1.1 l. of high purity (99.96 mole %) material.

3-Methylthiophene.—Three liters of 3-methylthiophene furnished by Socony-Mobil Oil Company was distilled through column 1, yielding 2 l. of material with a purity of 99.9 mole %. This sample discolored after standing several weeks and later deposited a dark red-brown film on the storage bottles so that a distillation through column 2 and additional purity measurements were made just before bottling *in vacuo*. The yield of high-purity (99.97 mole %) material was 1.4 l.

Benzo[b]thiophene.—Two separate 2-l. batches of material given to the Project by The Texas Company were distilled through column 4 at a pressure of 50 mm. The highest purity fractions from each of these distillations were combined and redistilled in the same column at a pressure of 90 mm, yielding 1.5 l. of high purity (99.97 mole %) material. Because ordinary freezing-point purity measurements gave poor precision, the purity of the final sample was measured by the Thermodynamics Laboratory.

Stability.—Inasmuch as a portion of each of these compounds has been set aside as a calibration standard, the storage stability was of considerable interest. This stability was estimated by an "accelerated" test in the following manner. Samples of the purified compounds were sealed *in vacuo* and exposed to sunlight on the laboratory roof for one year. Control samples were kept in the dark during the same period. Determinations of purity by the freezing point method were made on both the exposed and control samples.

None of the control samples showed any detectable decrease in purity. Five of the samples—2-propanethiol, 1-butanethiol, 2-thiapentane, 3-methyl-2-thiabutane and thiacyclohexane—were unaffected by storage in the sunlight. Two samples having high vapor pressure—2-butanethiol and 2-thiapropene—exploded during the summer months and data on replacements are not yet available.

The two alkyl thiophenes showed different degrees of decomposition after storage in the sunlight. The 2-methylthiophene had a light-straw color and showed a freezing point purity of 99.93 mole %, 0.03 mole % lower than the control sample. The 3-methylthiophene was yellow and had decreased in purity 0.08 mole %.

A marked and interesting decomposition was shown by the benzo[b]thiophene. A 50-ml. sample, sealed *in vacuo*, was found, after 6 months' exposure, to have exploded violently. As the vapor pressure of this solid compound is only 25 mm. at 100°, the explosion cannot be explained on this basis. A 5-ml. breakoff-tip ampoule was exposed for 1 year without incident. The color of this sample had changed from white to red-brown. Because the experience with the first sample suggested that a gas had been formed, the second sample was opened directly into the mass spectrometer to determine what gas, if any, was present. The mass spectrum thus obtained showed large concentrations of hydrogen sulfide and small

(7) As toluene was one of the impurities, invalidation of freezing point purity results would be expected if toluene formed a solid solution with 2-methylthiophene similar to the solid solution formed by benzene and thiophene. Experiments made by adding toluene to the methylthiophene showed no solid solution of these two compounds.

amounts of hydrogen in the gas above the solid sample. Insufficient sample was available for rigorous freezing point purity determination, but a rough measurement showed a decrease in freezing point of 1.8°.

A mass spectrum of the decomposed solid was obtained using an instrument equipped for high mass work. Significant peaks at *m/e* 234 and *m/e* 266, considerably above the parent peak at *m/e* 134, were observed.

An ultraviolet spectrum on the exposed sample differed from that of the control as shown in Fig. 1. The increased long wave length absorption suggests condensation of the molecules.

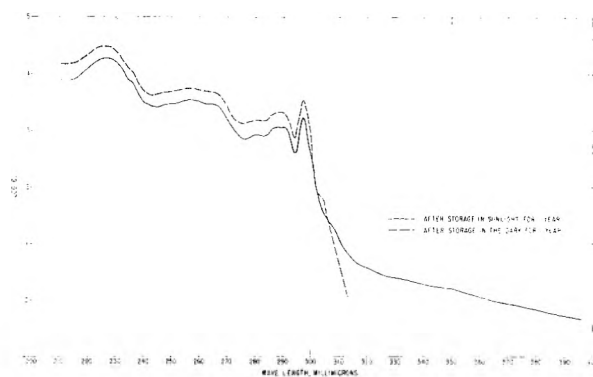
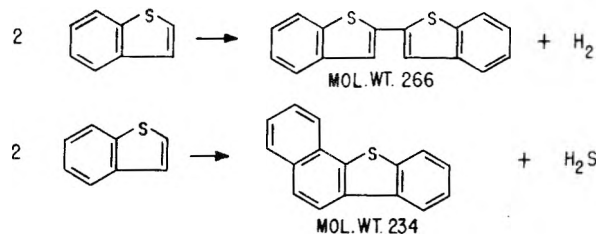


Fig. 1.—Ultraviolet spectra of benzo[b]thiophene.

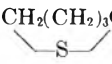
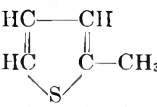
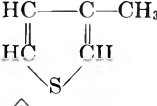
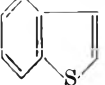
A mechanism that fits the above data is postulated



Physical Properties.—Physical property data for the ten organic sulfur compounds are shown in Tables I and II. Apparatus and procedures used for the first nine compounds were the same as those described in detail in a previous paper.² The following accuracy of each of the measurements was estimated: freezing point, $\pm 0.01^\circ$; boiling point, $\pm 0.1^\circ$; refractive index, ± 0.00006 ; density, ± 0.00005 g./ml.; viscosity, ± 0.001 centipoise; and surface tension, ± 0.1 dyne/cm.

Some modifications in techniques were necessary to determine the physical properties of benzo[b]thiophene. This material has a high dispersion and a melting point above the temperatures at which properties are normally measured. Refractive index was measured with an Abbe refractometer having compensating prisms, and density was determined by means of calibrated pycnometers. Uncertainties for the benzothiophene values reported are: refractive index, ± 0.0001 ; density, ± 0.0001 g./ml.; viscosity, ± 0.003 centipoise; surface tension, ± 0.3 dyne/cm. Estimated accuracies for the freezing point and boiling point are as previously stated.

TABLE I
 REFRACTIVE INDICES OF TEN ORGANIC SULFUR COMPOUNDS

Cpd. no.	Compound	Temp. of measurement, <i>t</i> , °C.	Refractive indices, <i>n</i> _{<i>D</i>} ^{<i>t</i>}						
			Helium r line 6678.1 Å.	Hydrogen C line 6562.8 Å.	Sodium D line 5892.6 Å.	Mercury e line 5460.7 Å.	Helium v line 5015.7 Å.	Hydrogen F line 4861.3 Å.	Mercury g line 4358.3 Å.
1	CH ₃ CHSHCH ₃	20	1.42236	1.42277	1.42554	1.42795	1.43110	1.43248	1.43802
		25	1.41938	1.41978	1.42251	1.42487	1.42802	1.42929	1.43487
		30	1.41613	1.41660	1.41927	1.42163	1.42479	1.42611	1.43156
2	CH ₃ (CH ₂) ₃ SH	20	1.43976	1.44022	1.44298	1.44535	1.44845	1.44982	1.45529
		25	1.43715	1.43758	1.44034	1.44270	1.44582	1.44718	1.45255
		30	1.43433	1.43475	1.43750	1.43982	1.44289	1.44422	1.44962
3	CH ₃ CHSHCH ₂ CH ₃	20	1.43350	1.43399	1.43673	1.43909	1.44219	1.44344	1.44892
		25	1.43081	1.43123	1.43396	1.43632	1.43938	1.44062	1.44607
		30	1.42808	1.42848	1.43114	1.43345	1.43656	1.43786	1.44319
4	CH ₃ SCH ₃	20	1.43198	1.43249	1.43547	1.43798	1.44136	1.44286	1.44883
		25	1.42893	1.42938	1.43231	1.43481	1.43820	1.43957	1.44557
		30	1.42562	1.42607	1.42900	1.43145	1.43485	1.43625	1.44208
5	CH ₃ S(CH ₂) ₂ CH ₃	20	1.44111	1.44158	1.44435	1.44674	1.44993	1.45129	1.45686
		25	1.43841	1.43884	1.44163	1.44400	1.44716	1.44847	1.45402
		30	1.43569	1.43609	1.43888	1.44121	1.44436	1.44567	1.45117
6	CH ₃ SCH(CH ₃) ₂	20	1.43588	1.43631	1.43914	1.44155	1.44475	1.44608	1.45170
		25	1.43308	1.43359	1.43634	1.43871	1.44195	1.44322	1.44879
		30	1.43033	1.43075	1.43354	1.43586	1.43904	1.44031	1.44588
7		20	1.50309	1.50358	1.50684	1.50958	1.51331	1.51484	1.52132
		25	1.50055	1.50107	1.50426	1.50704	1.51068	1.51223	1.51867
		30	1.49801	1.49850	1.50173	1.50447	1.50811	1.50959	1.51604
8		20	1.51502	1.51570	1.52035	1.52440	1.52985	1.53218	1.54212
		25	1.51218	1.51283	1.51744	1.52145	1.52685	1.52918	1.53907
		30	1.50923	1.50988	1.51451	1.51847	1.52384	1.52615	1.53598
9		20	1.51518	1.51585	1.52042	1.52440	1.52984	1.53210	1.54181
		25	1.51241	1.51300	1.51758	1.52153	1.52688	1.52913	1.53885
		30	1.50943	1.51008	1.51455	1.51851	1.52390	1.52612	1.53572
10		35			1.6332				
		40			1.6302				

Derived Functions.—Two types of derived functions have been calculated using the physical property data. Specific dispersion and refractivity intercept, used analytically to distinguish different classes of hydrocarbons, are functions of the non-additive type. The additive or constitutive functions are molecular volume, molecular refraction and parachor. All functions shown in Table III are calculated at 20°. For benzothiophene, properties at 20° were estimated by extrapolation from 35 and 40° properties.

The refractivity intercepts of the sulfur compounds are generally lower than those of the similar hydrocarbons, and consequently sulfur impurities will cause high values in the estimation of cycloparaffins using this function.

Specific dispersion has been used to estimate the aromatic content of oils because of the large difference in the specific dispersion of the paraffin hydrocarbons (about 98) and the aromatics (around 185). Table III shows that the sulfur compounds fall between these values, and thus the presence of sulfur compounds as impurities would cause high values in the estimation of aromatics by specific dispersion.

Molecular refractions, molecular volumes and parachors are shown in Table III. In compliance

with the current practice, the molecular volumes are at 20° rather than at the boiling point, as in the previous paper. Quite satisfactory formulas for calculating these functions for hydrocarbons are available and it would be convenient if an increment for sulfur could simply be added to these equations. However, no such simple relationship was found and insufficient data are as yet available to study the various types of sulfur compounds.

Spectra.—Mass, ultraviolet and infrared spectra were determined on each of the ten compounds and complete spectra are included in the Catalogs of Spectral Data.⁸ Complete discussion of the spectra is beyond the scope of this paper. A few observations, with emphasis on the effect of the sulfur atom, can be made.

Mass Spectra.—The spectra of nine of the compounds were obtained with a Consolidated mass spectrometer, model 21-103 (21-102 modified). The electron current to the collector was automatically maintained at 10.5 microamperes and the temperature of the ion source at 250°. The spectrum of 2-propanethiol was obtained using the procedure described in a previous paper.²

(8) American Petroleum Institute Research Project 44. Carnegie Institute of Technology. Catalog of Mass Spectral Data. Catalog of Ultraviolet Spectral Data. Catalog of Infrared Spectral Data.

TABLE II
 PROPERTIES OF TEN ORGANIC SULFUR COMPOUNDS

Cpd. no.	Compound	Impurity, mole %	F.p. for zero impurity, °C.	Cryoscopic constant A , deg. $^{-1}$	B.p. at 760 mm., °C.	Temp. of measurement, t , °C.	Density at t °C., g./ml.	Viscosity at t °C., centipoises	Surface tension at t °C., dynes per cm.
1	2-Propanethiol (isopropyl mercaptan)	0.02 ± 0.02	-130.54	0.033	52.6	20	0.81431	0.369	22.0
						25	.80864	.352	21.6
						30	.80312	.333	20.8
2	1-Butanethiol (<i>n</i> -butyl mercaptan)	0.04 ± .04	-115.67	.042	98.4	20	.84161	.497	26.1
						25	.83676	.471	25.6
						30	.83197	.445	25.1
3	2-Butanethiol (<i>sec</i> -butyl mercaptan)	0.1 ± .1	-140.14 ^{a,b}	.044 ^b	85.0	20	.82988	.463	24.4
						25	.82480	.438	23.7
						30	.81976	.415	23.1
4	2-Thiapropane (dimethyl sulfide)	0.01 ± .01	-98.27	.027	37.4	20	.84825	.285	24.4
						25	.84230	.275	23.9
						30	.83634	.262	23.1
5	2-Thiapentane (methyl <i>n</i> -propyl sulfide)	0.03 ± .03	-112.97	.044	95.6	20	.84236	.468	25.9
						25	.83741	.444	25.3
						30	.83245	.420	24.7
6	3-Methyl-2-thiabutane (methyl isopropyl sulfide)	0.01 ± .01	-101.51	.036	84.8	20	.82990	.455	24.2
						25	.82486	.430	23.6
						30	.81978	.407	23.1
7	Thiacyclohexane (penta-methylene sulfide)	0.06 ± .06	+ 18.99	.004	141.8	20	.98557	2.440	35.1
						25	.98093	2.196	34.6
						30	.97633	1.985	33.9
8	2-Methylthiophene	0.04 ± .04	-63.38	.025	112.5	20	1.01965	0.703	31.7
						25	1.01422	.660	31.1
						30	1.00891	.620	30.4
9	3-Methylthiophene	0.03 ± .03	-68.94	.031	115.4	20	1.02183	.674	31.8
						25	1.01647	.635	31.0
						30	1.01136	.597	30.4
10	Benzo[b]thiophene (thianaphthene)	0.03 ± .01 ^b	+ 31.34	.0153 ^b	219.9	35	1.1988	2.517	42.6
						40	1.1937	2.423	41.8

^a Triple point. ^b Determined by Thermodynamics Laboratory, Bureau of Mines, Bartlesville, Okla.

 TABLE III
 DERIVED FUNCTIONS

Compound	Refractivity intercept $n_{20D} - \frac{d_{204}}{2}$	Specific dispersion $(n_{20F} - n_{20C})10^4$ $\frac{d_{204}}{d_{204}}$	Mol. refraction $M/d \frac{n_{2D} - 1}{n_{2D} + 2}$	Mol. vol. M/d_{204}	Paraehor $M\gamma^{1/4}/(D - d)$
2-Propanethiol	1.01838	119.2	23.941	93.527	202.8
1-Butanethiol	1.02217	114.1	28.408	107.159	242.2
2-Butanethiol	1.02179	113.9	28.446	108.673	241.7
2-Thiapropane	1.01134	122.3	19.132	73.250	163.1
2-Thiapentane	1.02317	115.3	28.446	107.063	241.6
3-Methyl-2-thiabutane	1.02419	117.7	28.592	108.671	241.1
Thiacyclohexane	1.01405	114.2	30.850	103.692	252.4
2-Methylthiophene	1.01052	161.6	29.284	96.272	228.5
3-Methylthiophene	1.00950	159.0	29.225	96.067	228.2
Benzo[b]thiophene	1.0351	...	39.93	110.53	286.0

Abridged mass spectra of the compounds are presented in Table IV. As with the previously reported compounds, many prominent rearrangement peaks are evident. The ion at m/e 35 (SH_3^+) is a particularly conspicuous rearrangement peak in the spectra of the thiols and sulfides. The sulfides show rearrangement peaks at m/e 48 and m/e 49. The probable configuration for these two ions is CH_3SH^+ and CH_3SH_2^+ . 2-Thiapropane exhibits interesting rearrangement peaks in the C_2 mass range. The peak at m/e 27 (C_2H_3^+) is unexpected as it involves formation of a new carbon-carbon

bond. The magnitude of the m/e 27 peak is comparable with that of many of the peaks resulting from simple splitting of the molecule.

The spectrum of thiacyclohexane contains numerous large rearrangement peaks. The peak at m/e 29 (C_2H_5^+) and that at m/e 43 (C_3H_7^+) are probably formed in a manner similar to like peaks in the spectra of hydrocarbons where the normal molecular formula shows no ethyl or propyl groups. The ion at m/e 67 probably results from the loss of SH_3 from the thiacyclohexane molecule. The base peak for thiacyclohexane occurs at m/e 87. This

TABLE IV
 MASS SPECTRA

Mass no., m/e	Relative intensity									
	2-Propanethiol M.W. = 76	1-Butanethiol M.W. = 90	2-Butanethiol M.W. = 90	2-Thiopropane M.W. = 62	2-Thiapentane M.W. = 90	3-Methyl-2-thiobutane M.W. = 90	Thiacyclohexane M.W. = 102	2-Methylthiophene M.W. = 98	3-Methylthiophene M.W. = 98	Benzo[b]thiophene M.W. = 134
134										100.0
108										4.18
102							97.2			1.61
98							2.28	56.5	53.2	0.46
97							4.63	100.0	100.0	0.19
90		53.5	60.8		46.1	84.5	0.25	0.03	0.08	8.54
89		0.25	0.33		0.54	1.46	4.60			10.5
87		.07	.03		.02		100.0			0.91
76	63.3	.59	.70		.65	4.37	1.56	0.21	0.19	0.79
75	1.49	.24	4.39		9.57	95.1	1.55		.07	2.28
74	0.13	.07	0.54		0.57	0.86	22.7		.03	2.91
71	.53	.62	1.21		1.01	1.20	5.26	4.12	4.63	0.90
69	.85	.62	0.96		0.75	.79	20.1	6.67	6.59	7.88
68	.27	.07	0.19		0.12	.14	71.9	0.66	0.86	0.58
67							44.0		.01	7.88
62	1.23	1.40	3.18	80.5	4.92	0.43	4.83	2.18	.97	4.10
61	39.4	20.6	82.8	30.2	100.0	7.11	66.4	1.80	.90	2.40
60	2.69	2.73	13.1	0.45	0.88	3.00	47.3	0.76	.48	0.49
59	8.41	4.33	11.2	2.87	3.38	14.5	26.6	5.27	1.31	0.33
58	6.10	4.88	10.3	3.27	2.76	6.53	13.6	6.78	4.59	2.64
57	2.86	17.7	90.1	2.73	0.97	1.99	5.00	4.23	3.24	1.89
56	0.40	100.0	14.9	0.64	.15	0.24	14.4	0.33	0.37	0.49
55	0.05	12.3	11.9		.23	0.79	39.5	0.05	0.03	.35
49	1.05	3.25	1.73	4.26	18.7	41.9	2.65	3.04	3.34	.96
48	0.23	6.90	0.57	3.89	39.6	77.6	4.80	0.77	0.89	.15
47	5.47	41.4	15.6	100.0	23.0	50.2	36.1	2.30	2.25	.38
46	1.50	10.4	2.31	41.9	11.7	12.9	67.3	1.55	1.79	.22
45	10.4	17.4	15.5	61.5	24.6	34.8	73.3	22.4	25.5	8.18
43	100.0	12.3	0.52		19.2	83.3	1.68	0.03	0.09	0.55
41	67.9	87.2	100.0		34.4	100.0	69.9	0.41	0.35	0.44
39	29.9	21.4	29.7		18.0	42.1	65.2	14.2	10.3	6.59
35	16.3	9.53	14.3	35.0	14.2	1.75	5.06	0.05	0.05	
34	3.08	3.37	3.18	1.75	0.60	0.69	2.72	.24	.19	0.11
33	5.78	4.09	5.86	1.63	.57	1.06	2.85	.49	.40	.27
32	2.60	1.63	2.09	2.78	.79	1.37	4.48	1.74	1.23	.88
29	0.71	36.8	81.3	0.80	2.90	2.55	19.2	0.16	0.05	.71
27	62.5	56.2	55.4	20.6	34.4	54.3	69.3	8.03	8.15	1.71

is equivalent to the loss of a methyl group from the original molecule and could be considered a rearrangement peak, although the peak may also result from the loss of a methylene group and a hydrogen atom. In the same way as the base peak, the ion at m/e 55 could be considered a rearrangement peak, as it is equivalent to the loss of CH_3S from the molecule. Other rearrangement peaks are m/e 47 (CH_2SH^+ or CH_3S^+), m/e 35 (SH_3^+), and m/e 69. The m/e 69 peak probably results from the loss of SH or S plus H from the molecule.

The aromatic nucleus in the thiophenes is quite stable to electron bombardment, as shown by the absence of large ring-fragment peaks. For example, in the spectrum of benzo[b]thiophene, the largest of these is only 10.5% of the parent. The principal fragment peaks for benzo[b]thiophene result from breaking the five-membered ring to lose SCH forming the complementary peaks at m/e 89 and m/e 45. The peak at m/e 67 probably is due, in large part, to double ionization of the parent molecule.

The base peaks for 2-methylthiophene and 3-methylthiophene occur at m/e 97. From previous

correlations of the mass spectra of thiophenes with molecular structure,⁹ these peaks probably represent the loss of a hydrogen atom from the methyl group.

Ultraviolet Spectra.—The ultraviolet spectra were determined with a Cary ultraviolet spectrophotometer, model 11. To obtain the spectra of the sulfides, purified 2,2,4-trimethylpentane was used as a solvent. Purified cyclohexane was used as a solvent to obtain the spectra of the other compounds. The spectrum of each compound was scanned between 200 and 400 $m\mu$.

A summary of the ultraviolet absorption data is given in Table V, which contains the maxima and minima in the spectrum of each compound. The molar extinction associated with each maximum or minimum also is given.

The spectra of the thiols and sulfides showed only broad bands similar to those reported previously.² In addition to the bands shown in the table, weak shoulders (molar extinctions less than 100) appeared in the spectra of the sulfides. These

(9) I. W. Kinney, Jr., and G. L. Cook, *Anal. Chem.*, **24**, 1391 (1952).

TABLE V
 ULTRAVIOLET ABSORPTION DATA

Compound	$\lambda_{\text{max.}}$ ^a OR $\lambda_{\text{min.}}$	ϵ , l./mole cm.
2-Propanethiol	225-230 (max.)	160
1-Butanethiol	225-230 (max.)	160
2-Butanethiol	225-230 (max.)	135
2-Thiapropane	210-215 (max.)	1000
2-Thiapentane	210-215 (max.)	1000
3-Methyl-2-thia- butane	210-215 (max.)	1000
Thiacyclohexane	210-215 (max.)	1000
2-Methylthiophene	234-235 (max.)	7820
3-Methylthiophene	234-235 (max.)	5600
Benzo[b]thiophene	228 (max.)	34000
	236 (shoulder)	ca. 13100
	244 (min.)	4480
	258 (max.)	5950
	264 (shoulder)	ca. 5200
	277 (min.)	1430
	281 (max.)	1640
	285 (min.)	1530
	289 (max.)	2300
	290 (min.)	2180
	291 (max.)	2300
	295 (min.)	710
	297.5 (max.)	3680

^a Wave length of absorption maximum or minimum in $m\mu$.

shoulders, at 225-235 $m\mu$, appear to be typical of sulfide spectra.¹⁰

The spectrum of each of the methylthiophenes showed only a single broad maximum in the 234-235 $m\mu$ region. The spectrum of benzo[b]thiophene, however, contained fine structure. The spectrum of the latter compound is qualitatively similar to that of typical aromatic and aza-aromatic hydrocarbon systems.¹¹

Infrared Spectra.—The infrared spectra were determined with a Perkin-Elmer spectrometer, model 12C (12B modified). The sample of benzo[b]thiophene was liquefied by adding 1 drop of carbon disulfide to 1.0 g. of sample. The spectrum was then obtained on the liquefied sample. The instrument accessories used with this and each of the nine normally liquid samples were described in a previous paper.²

(10) E. A. Fehnel and M. J. Carmack, *J. Am. Chem. Soc.*, **71**, 84 (1949).

(11) G. M. Badger and R. S. Pearce, *J. Chem. Soc.*, 3072 (1950); G. M. Badger, R. S. Pearce and R. Pettit, *ibid.*, 3199 (1951).

The three thiols exhibit the typical S-H stretching band at 3.9 μ . There are two absorption peaks in the 11-12.2 μ region. At least one of these can be ascribed to the C-S-H bending vibration.⁴

The C-S stretching vibration should appear in the 13.0-15.5 μ region. The thiols and sulfides have medium to strong absorption peaks in or near this region. The thiophenes also have intense peaks in the region but this absorption in the spectra of the methylthiophenes has been assigned to a symmetrical hydrogen bending mode.¹² In the spectrum of benzo[b]thiophene, one of the three strong peaks in this region probably arises from a vibration of the four hydrogens on the ortho-substituted benzene ring.

In thiophenes the vibration of the sulfur atom between the two carbons gives rise to an absorption band near 8.0 μ .¹² This band is strong in the spectra of both 2- and 3-methylthiophene. In the spectrum of benzo[b]thiophene, a band, similar in position and intensity to that found in the spectra of the methylthiophenes, probably arises from the same cause. The band at 21.0-22.0 μ is characteristic of the thiophene nucleus.¹² This band is very weak in the 3-methylthiophene spectrum. The bicyclic compound benzo[b]thiophene also shows the 21.0-22.0 μ band.

The bands due to vibrations of the C-C and C-H linkages appear in the expected positions. The bands near 3.4 μ are assigned to C-H stretching vibrations, those near 7.2 and 13.6 μ to vibrations of the methyl and methylene groups. The thiophenes have a band near 3.2 μ that is analogous to the C-H stretching vibrations of aromatic hydrocarbons. In the spectrum of benzo[b]thiophene, the 5.0-6.0 μ region is typical of the spectrum of an *ortho*-disubstituted benzene.¹³ Additional vibrational assignments have been made for thiacyclohexane, 3-methylthiophene and 2-propanethiol.⁴

Acknowledgments.—This work was done under a cooperative agreement between the Bureau of Mines, United States Department of Interior, and the University of Wyoming. The authors wish to express their thanks to C. W. Bailey for obtaining the infrared and ultraviolet spectra.

(12) H. D. Hartough, "Thiophene and Its Derivatives," Interscience Publishers, Inc., New York, N. Y., 1952, p. 125.

(13) C. W. Young, R. B. Duvall and Norman Wright, *Anal. Chem.*, **23**, 709 (1951).

THE ELECTROÖSMOTIC TRANSPORT OF WATER ACROSS PERMSELECTIVE MEMBRANES

BY ALVIN G. WINGER, RUTH FERGUSON AND ROBERT KUNIN

Rohm & Haas Company, Philadelphia, Pennsylvania

Received July 22, 1955

The electroösmotic transport of water across Amberplex ion exchanger membranes was measured, as a function of internal and external electrolyte concentration, current density and nature of the electrolyte. The results were interpreted by assuming that the net water transport is the difference between the amounts of water transported in opposite directions under the influence of mobile cations and mobile anions. The average number of water molecules transported per ion was calculated for each ion type and correlated with ionic potentials of the unhydrated ions and with intramembrane ionic mobility ratios as measured potentiometrically.

Introduction

Permselective ion exchange membranes¹⁻³ transport water by electroösmosis along with ionic species during electrolysis in aqueous solution. This study was undertaken to obtain experimental data on the magnitude of this electroösmotic transport of water across ion-exchange membranes as a function of the membrane properties and the properties of surrounding solution, since this effect is of considerable practical importance in any electrochemical process involving membranes.^{4,5}

A very simple model was adopted to interpret the experimental data, in which a certain average number of water molecules were assumed to move with each kind of mobile ion in its movement under a potential gradient. For a binary ionic system the model assumed above leads to a simple equation for net water transport

$$\Delta W = \frac{t_c n_c}{Z_c} - \frac{t_a n_a}{Z_a} = t_c \left[\frac{n_c}{Z_c} + \frac{n_a}{Z_a} \right] - \frac{n_a}{Z_a} \quad (1)$$

where ΔW is the net moles of water transferred across the membrane per faraday, t_c and t_a the electrical transport numbers of cation and anion in the membrane, n_c and n_a the average number of water molecules moving with cation and anion, respectively, and Z_c and Z_a the numerical value of the cationic and anionic valence, respectively. ΔW is considered positive when net movement of water is in the direction of the cationic movement.

Experimental

A. Membranes.—The membranes used in this work were Amberplex C-1 and Amberplex A-1 membranes.³ These are heterogeneous membranes composed of sulfonated polystyrene cation-exchange resin and quaternary base anion-exchange resin, respectively, bound into tough pliable sheets by an inert plastic binder. A series of the former type of membranes also were used, with 4, 8.5 and 15% DVB as cross-linking agent. The sections of each type of membrane used in the electrode cells were taken from the same large sheet of membrane and each section was shown to be electrochemically practically identical with the others from that sheet, as judged from membrane potential and conductivity tests. Before use in an electroösmotic measurement, the membranes were placed in the proper ionic form by long equilibration in concentrated solution of the

ion under study, leached with deionized water, and equilibrated in the solution to be used in the electrolysis.

B. Apparatus and Procedure. 1. Single Membrane, Two-chambered Cell, with Pt Electrodes.—A two-chambered, single membrane cell with platinum electrodes was used with hydroxide solutions, where the net result of the electrode reactions would be an electrolysis of water. The half-cells of this apparatus were machined out of Plexiglas and had a capacity of about 150 ml. each. An exact description is given in the literature.⁶ Circular screen platinum electrodes were mounted close to the membrane clamped between the half cells and openings were provided in each half cell for motor driven stirrers and for sampling. The two chambers were filled with two solutions of a certain concentration difference and the electrolyses were run for such a time as required to reverse the concentration difference between the half cells. Since the time average of the concentration gradient across the membrane was thus nearly zero for the entire run, the effects of diffusion and osmosis were minimized. Liquid levels in the two half cells were essentially equal and constant during an electrolysis, eliminating any hydraulic transfer across the membrane. The average concentration of the two solutions remained practically constant due to the equal volumes of solution on both sides of the membrane. At the end of the short, high-current-density (90 amp./ft.² = 0.097 amp./cm.²) runs employed, the volume changes were determined by careful pipetting and the concentration changes by titration of aliquots of acid or base. From these data and the current and time values, electrical transport numbers of the ions and the transport of solvent per faraday were calculated. Calculation of the latter involved correction of volume change data for transport of electrolyte and loss of water by electrolysis and evaporation. Because of the limitation of this method to strong alkali or non-volatile acid solutions, and the difficulty in measuring accurately the volume changes in the system, only preliminary results were sought which would give an indication of the effect of high current density on the apparent ion-solvent interaction and test the validity of equation 1.

2. Two-chambered, Single Membrane Cell with Ag-AgCl Electrodes.—A two-chambered single membrane cell with Ag-AgCl electrodes was used for electrolysis of metal chloride solution, where net result of electrode reaction would be transfer of salt from anolyte to catholyte. The cell was machined from two blocks of Plexiglas with each chamber 3.5 inches in diameter and ⁵/₈ inch deep. A membrane was inserted between the two sections, with a thin rubber gasket on each side and sealed tightly by means of four screws through the outside section. Two holes ³/₈ inch in diameter were drilled diagonally in the top of each section for filling and emptying, and for stirring.

The electrodes were three inch squares of 20 mesh silver screen, the corners of which were turned back about ¹/₂ inch to serve as spacers keeping the electrodes close to the membrane surface. To prevent the electrodes from contacting the membrane, a circle of Saran screen was placed between each electrode and the membrane. The silver chloride cathode was prepared by placing it in the cell in a solution of concentrated HCl (10%) and passing an amount of current sufficient to form a slight excess of AgCl for subsequent electrolyses. After the first electrolysis the electrodes can be reversed for another run.

(1) M. R. J. Wyllie and H. W. Patnode, *THIS JOURNAL*, **54**, 204 (1950).

(2) W. Juda and W. A. McRae, *J. Am. Chem. Soc.*, **72**, 1044 (1950).

(3) A. G. Winger, G. W. Bodamer and R. Kunin, *J. Electrochem. Soc.*, **100**, 178 (1953).

(4) A. G. Winger, G. W. Bodamer, R. Kunin, C. J. Prizer and G. W. Harmon, *Ind. Eng. Chem.*, **47**, 50 (1955).

(5) W. R. Walters, D. W. Weiser and L. J. Marek, *ibid.*, **47**, 61 (1955).

(6) H. C. Bramer and J. Coull, *ibid.*, **47**, 67 (1955).

In order to weigh the contents of each chamber accurately, a vacuum line trap with a special pipet-type side arm for reaching into the chamber was used. Since it was impossible to remove the contents of a chamber completely even with this trap, each chamber was rinsed with the solution to be used in it and emptied with the above trap before pipetting the final solution into a chamber. In this manner error due to residual solution was practically eliminated. The entire trap, side arm included, was weighed before and after filling with the contents of each chamber.

The approximate water transport per faraday of current was obtained from preliminary runs and used to calculate the coulombs necessary to transport about 2 g. of water across the membrane. The initial concentration difference between the two solutions on either side of the membrane was chosen so that passage of the calculated number of coulombs would reverse this difference, minimizing effects of osmosis and diffusion. After rinsing the cell as described above, 75 ml. of the two solutions of known density were pipetted into the chambers, the stirrers inserted, holes stoppered, and the carefully timed electrolysis begun. The ammeter was a Weston Model 280 and a 250-500 ohm variable resistor was connected in series with the cell to smooth out any current fluctuations in the low resistance cell. Constant current was maintained until the voltage drop across the cell terminals reached 1.7 volts, at which time the run was terminated or continued for another time interval at a new, lower current density. When the calculated amount of electricity had been passed through the cell, the chamber contents were emptied into previously weighed traps as described and weighed to the nearest 0.01 g. The initial and final solutions were titrated for chloride ion with standard silver nitrate using dichlorofluorescein with dextrin as indicator. The increase in chloride content (moles per faraday) in the catholyte or the decrease in the anolyte is a direct measure of the electrical transport number of the cation across the membrane, assuming the membrane to be in required ionic state. At very low concentration of external solution some electrical transport is undoubtedly due to H_3O^+ ion from the water, but the error due to this effect was considered negligible for the concentrations used. The changes in weight in catholyte and anolyte, corrected for electrolyte transfer, were generally not numerically equal. Since unavoidable loss by evaporation during the necessarily lengthy runs was shown to be the chief cause of this, the numerical average of the gain and loss in catholyte and anolyte, respectively, was taken to be the most nearly correct measure of the water transport. The individual runs were considered reproducible under identical conditions, to within $\pm 3\%$.

For chloride solutions of nickel and cobalt, a platinum cathode was used and the metal plated out on this electrode. Otherwise the procedure is similar to that described above and appropriately modified calculations give the values for n_c . At the concentrations employed in this work, the cobalt and nickel ions are considered to be in hydrated divalent form, free of complex formation.

Data and Discussion

In Fig. 1 the results of the electrolysis of strong alkali solutions in a two-chambered single membrane cell using Pt electrodes and Amberplex C-1 is given. The cation transport number was varied by changing the average concentration of the two external solutions on either side of the membrane. If equation 1 applies and the magnitude n_c and n_a in the membrane is constant and independent of external solution concentrations, the water transport per faraday should be a linear function of cation transport number t_c . Within the accuracy of the method used in these runs, this seems to be the case, as the plots are essentially linear. Extrapolation of the plots to $t_c = 1$ gives values of n_c for lithium, sodium and potassium of 14.1 ± 1 , 8.6 ± 1 and 7.3 ± 1 , respectively. The extrapolations to $t_c = 0$ are too lengthy for serious consideration but indicate a value of n_{OH^-} approximately equal to 5.

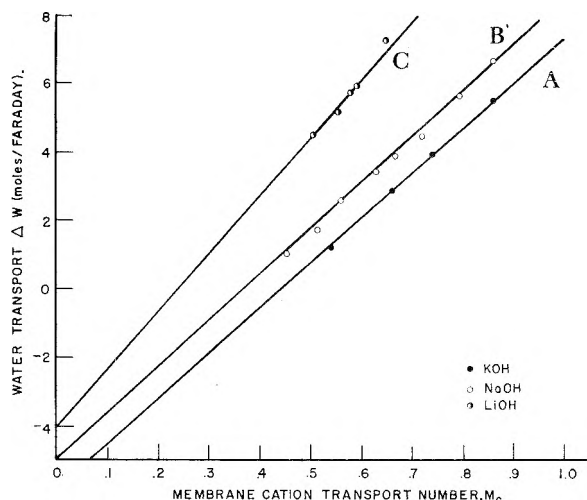


Fig. 1.—Electroosmotic transport of water across cation-exchange membrane in hydroxide solutions: A, KOH; B, NaOH; C, LiOH.

At high concentrations of external solution, the transport numbers of the ions in the membrane approach those in the solution around it⁷ and the net water transport approaches zero. Extrapolation of the plots in Fig. 1, to conditions of zero net water transport, gives the following values for the cationic transport numbers in the membrane $t_c(\text{LiOH}) = 0.24$, $t_c(\text{NaOH}) = 0.38$, and $t_c(\text{KOH}) = 0.45$.



These can be considered the approximate cationic transport numbers in highly concentrated alkali solutions, about 6 molar.

The detailed data for electrolyses of univalent chlorides in the cell with Ag-AgCl electrodes are presented in Table I. The lithium chloride system was studied most extensively, because of its high water transport, to obtain information on the effect of such variables as current density, temperature, external concentration and membrane resin. The results in Table I indicate no definite dependence of water transport on current density or external concentration, in the ranges studied, for alkali cations. The values of n_c for all above cations were calculated from the experimental data using equation 1 and assuming n_a for the chloride ion to be 9. This value was based on electrolyses of quaternary ammonium chloride salts using Amberplex A-1 (anion permselective) membranes. The transport number of the chloride ion in Amberplex C-1 for the runs given in Table I was always 0.1 or less, so that a considerable uncertainty in the n_a value used to calculate n_c for those runs would have little effect on the final value of n_c .

Table II gives the results of water transport measurements on membranes with varying content of the resin cross-linking agent, divinylbenzene. It is apparent that values of n_c are dependent on the ion concentration, C_f , within the resin, and/or on the "pore size" of the membrane resin. However, the n_c value does not vary directly as the water content of the resin or the membrane. As the decrease in degree of cross-linking permits more water to enter the resin, most of the additional

(7) K. Sollner, *J. Electrochem. Soc.*, **97**, 139C (1950).

TABLE I
ELECTROÖSMOTIC TRANSPORT OF WATER ACROSS AMBERPLEX
C-1 MEMBRANES AS DETERMINED FOR CHLORIDE SOLUTIONS
IN CELL WITH Ag-AgCl ELECTRODES

Salt	Average concn., N	Current density (ma./cm. ²)	n_c
NaCl	0.125	1.93	11.2
NaCl	0.225	1.95	11.5
NaCl	1.12	2.25	9.2
KCl	0.235	2.44	6.4
KCl	.235	1.46	7.4
KCl	.991	1.59	7.1
LiCl	.19	2.44	12.9
LiCl	.50	0.49	12.7
LiCl	.50	0.82	13.4
LiCl	.50	1.64	13.9
LiCl	.50	3.29	13.6
LiCl	.50	4.93	13.3
LiCl	1.10	1.80	13.3
LiCl ^a	0.50	1.64	12.7
RbCl	0.20	2.65	7.0
RbCl	1.00	1.64	7.3
CsCl	0.20	1.94	6.8
CsCl	1.08	2.90	6.7
(CH ₃) ₄ NCl	0.145	2.22	20.6
(CH ₃) ₄ NCl	.108	1.39	21.4
(CH ₃) ₄ HCl	.109	1.38	7.7 ^b
 -CH ₃ (CH ₃) ₃ NCl	.232	1.64	30
 -CH ₃ (CH ₃) ₃ NCl	.116	1.64	9.2 ^b
HCl	.24	1.78	5.5
HCl	.50	1.92	5.6
HCl	.61	1.62	2.7
HCl	.74	1.73	3.2
HCl	1.10	1.94	2.9

^a Temperature of run = 1°C. All other runs at room temperature, 24-26°. ^b Amberplex A-1 used for this run, hence value given = n_{Cl^-} .

TABLE II
ELECTROÖSMOTIC WATER TRANSPORT ACROSS HETERO-
GENEOUS SULFONATED POLYSTYRENE MEMBRANES IN 0.5 N
NaCl SOLUTION

Membrane and binder	% DVB of membrane resin	Water content of membrane resin, W_r (g. H ₂ O/meq. fixed groups)	n_c	$\frac{n_c}{n_c(\text{Mem. C})}$	$\frac{W_r}{W_r(\text{Mem. C})}$
A (Geon)	4	0.350	10.5	1.40	2.94
B (Geon)	8.5	.195	9.0	1.20	1.64
C (Geon)	15	.119	7.5	1.00	1.00
D (Polyeth- ylene)	8.5	.195	8.5		

water imbibed is apparently unaffected by mobile counter ions or, presumably, by the fixed ions.⁸ A recent publication⁹ of electroösmotic transport of water across membranes similar to those used here by Japanese workers suggests that the difference in water transport per ion for membranes of differing cross-linking can be explained in terms of "fixed" and "mobile" water molecules,

(8) D. E. Boyd and B. A. Soldano, *Z. Elektrochem.*, **57**, 162 (1953).

(9) Y. Oda and T. Yawataya, *Bull. Chem. Soc. Japan*, **28**, 263 (1955).

despite the conclusion in previous work that the fixed ions in resins are unhydrated.

Bi-ionic potential measurements were made in this Laboratory on Amberplex C-1 membranes by methods described in the literature^{10,11} to obtain the apparent mobility ratios of various ions in the membrane. The linear plots obtained when graphing bi-ionic potentials *versus* mean molal activities agreed closely with the work of Wyllie and Kanaan for the monovalent ion pairs tried. Column 4 of Table III gives the results of the determination of apparent mobility ratios \bar{U}_i/\bar{U}_r in Amberplex C-1 obtained for various cation pairs with lithium ion as reference ion. Column 5 gives the corresponding ratios of the number of water molecules apparently tending to move with each ion in the membrane

$$\frac{n_c(\text{reference ion})}{n_c(\text{ion})}$$

The general agreement between values for $\bar{U}(\text{ion})/\bar{U}(\text{ref. ion})$ and $n_c(\text{ref. ion})/n_c(\text{ion})$ is good and indicates that the mobility of the mobile ions in the membrane is inversely proportional to the magnitude of ion-water interaction for simple cations. If the magnitude of the interaction between polar water molecules and the charged unhydrated ions depends on the electrostatic potential near the ion, as might be expected, the observed direct proportionality between n_c and ionic potential shown in Table III is not surprising. This correlation and the previously cited one suggest that the electroösmotic water transport across membranes of ion exchange resins gives an indication of the relative state of solvation of ions within the ion exchange resins.

TABLE III
CORRELATION OF WATER TRANSPORT PER ION WITH IONIC
POTENTIAL AND WATER TRANSPORT RATIOS WITH IONIC
MOBILITY RATIOS

Ion	n_c	Ionic potential, charge/ radius Å.	$\frac{\bar{U}(\text{ion})}{\bar{U}(\text{ref. ion})}$	$\frac{n_c(\text{ion})}{n_c(\text{ref. ion})}$
Li ⁺	13.5 ± 1	1.3	1.00	1.00
Na ⁺	9.5 ±	1.0	1.40	1.50
K ⁺	7.0 ± 1	0.75	1.83	1.93
Rb ⁺	7.2 ± 0.5	.67	1.78	1.87
Cs ⁺	6.9 ± 0.5	.61	1.82	1.95
Co ⁺⁺	28 ± 2	2.5	1.11	0.97
Ni ⁺⁺	26 ± 2	2.6	1.09	1.04

Ions with the largest "true" hydration numbers, when moving through the micro-pores of the membrane, will tend to transfer momentum to the most unbound water molecules giving highest values of n_c . Recent determinations of "true" ion hydration numbers by Glueckauf¹² show that their values increase in the order Cs-K-Na-Li-Ca-Mg.

Acknowledgment.—The authors wish to acknowledge the assistance of Ruth Cowell and Edward Parkes in the experimental work reported in this paper.

(10) M. R. J. Wyllie, *This Journal*, **58**, 67 (1954).

(11) M. R. J. Wyllie and S. L. Kanaan, *ibid.*, **58**, 73 (1954).

(12) E. Glueckauf, *Trans. Faraday Soc.*, **51**, 1235 (1955).

ELECTRICAL CONDUCTIVITY AND CATALYTIC ACTIVITY OF ZINC OXIDE¹

BY LOUIS F. HECKELSBERG, ALFRED CLARK AND GRANT C. BAILEY

Phillips Petroleum Company, Research Division, Bartlesville, Oklahoma

Received August 15, 1955

Zinc oxides were investigated experimentally both as to electrical conductivity, at 200 to 550°, and as to catalytic activity for hydrogen-deuterium exchange, at -10 to 320°. Lattice defects were produced by heating the various zinc oxides in a selected gas (hydrogen, nitrogen or oxygen) or by incorporating as an impurity the oxide of a metal different from zinc in valence (aluminum, lithium). The results indicate that treatment of the zinc oxides so as to increase the number of lattice defects, increases their electrical conductivity and catalytic activity.

Zinc oxide, which is an n-type semi-conductor, increases in electrical conductivity when the partial pressure of oxygen in contact with it is decreased.² According to the concept of lattice defects in solid semi-conductors,³ the zinc oxide, on losing oxygen atoms, contains excess zinc atoms, which dissociate into zinc ions and quasi-free electrons. Increasing the amount of excess zinc atoms increases the number of quasi-free electrons, thereby increasing the electrical conductivity.

The concentration of lattice defects can be varied as by heating the zinc oxide in a selected gas or by incorporating as an impurity in the zinc oxide the oxide of a metal differing from zinc in valence.⁴ Alumina as an impurity increases the electrical conductivity; lithia decreases it.

Although an investigation of zinc oxide containing alumina or lithia as a catalyst for the hydrogen-deuterium exchange has been reported,⁵ measurements of the electrical conductivity were not included.

In the present work, zinc oxides with different concentrations of lattice defects were investigated both as to electrical conductivity and as to catalytic activity for the hydrogen-deuterium exchange, to see if these two properties could be related.

Experimental

Materials.—Zinc oxide I, of relatively high surface area, was prepared by precipitating and thermally decomposing zinc oxalate,⁶ using zinc nitrate and ammonium oxalate (J. T. Baker labeled C.P.). Its BET surface area was 21 sq. m./g.

Zinc oxide II, of relatively low surface area, was prepared by thermally decomposing zinc nitrate. Zinc oxides II-Al and II-Li were prepared similarly from aqueous solutions of zinc nitrate plus aluminum nitrate and lithium nitrate, respectively. (Their surface areas, by the BET method and by microscopic examination, were in the range 0.01–0.1 sq. m./g.) These three catalysts were heated in flowing dry air at 800° for 60 hours. Zinc oxide II-Al contained, as determined analytically, 0.3 mole % alumina; zinc oxide II-Li contained 0.03 mole % lithia.

The following gases were used: hydrogen, commercial electrolytic, purified by platinized silica gel at 300° and

anhydrous magnesium perchlorate at room temperature; nitrogen (oxygen content found, 6 p.p.m.), Air Reduction Co.'s prepurified, further purified by Drierite, Ascarite and anhydrous magnesium perchlorate; oxygen, USP Linde, purified by Drierite and Ascarite; deuterium, Stuart Oxygen Co.'s 99.5%, purified as was the hydrogen.

Apparatus and Procedure.—The apparatus and procedure for hydrogen-deuterium exchange have been described.⁷ The rate constants were calculated with the assumption that the reaction $H_2 + D_2 \rightleftharpoons 2 HD$ is first order. The conversion was given by the ratio of the hydrogen deuteride concentration in the product, as found by a mass spectrometer, to the equilibrium concentration.

The electrical-conductivity apparatus, which was designed for easy assembling and disassembling, had two vertically aligned shaft-like stainless steel electrodes in a housing of a Pyrex glass tube ending in female taper joints. The contact end of each electrode was a welded-on platinum disk, 12 mm. in diameter. The lower end of the lower electrode was screwed into a rigidly held brass plug fitting the lower end of the housing. The upper end of the upper electrode was attached through a spring-and-screw device to a brass plug fitting the upper end of the housing. A gas inlet and a gas outlet were provided near the upper and lower ends of the housing, respectively. The central part of the apparatus was heated by an electric furnace. The temperature was controlled by a Tagliabue Celestray controller actuated by a thermocouple with its junction outside the housing at a level between the two platinum disks. Another thermocouple, with similarly located junction, measured the temperature.

The apparatus was charged, assembled and used as follows: A paste of zinc oxide particles finer than 120-mesh in water was spread in a layer on the platinum disk of the lower electrode, which was then mounted in the furnace. The housing was lowered into position, and its top was closed with a Pyrex glass plug. A downward flow of about 10 cc./min. of the gas selected for the heat treatment was established. The furnace was heated to the desired heat treatment temperature.

At the end of the heat treatment, the glass plug was replaced by the brass plug with the upper electrode well retracted. The screw was turned to lower the upper electrode into contact with the zinc oxide layer, which had dried to a soft, porous cake. The turning was continued until the brass plug was pushed up, with a perceptible "pop," within the upper end of the housing. The weight of the upper electrode, spring-and-screw device, and brass plug now rested on the zinc oxide layer, exerting a pressure of approximately 300 g./sq. cm. Ten additional turns were made to ensure a contact of good reproducibility. The gas, if hydrogen or oxygen, was now replaced by nitrogen, which removed adsorbed hydrogen or oxygen; and the rate was adjusted to 5 cc./min., which was considered sufficient to prevent leakage of air into the apparatus.

In a typical run the temperature was increased to 560°, and the heating current was switched off. The apparatus cooled at a rate that declined from 9°/min. at first to 1°/min. at 260°. As cooling occurred, the electrical conductivity was measured at 10° intervals, with the initial measurement being made at 550°. The measurement was made by momentary application of a direct current voltage selected in the range of 1.5–135 volts and measuring the resulting current with a microammeter or with a galvanometer. The

(1) Presented in part at the Joint Symposium on Mechanisms of Homogeneous and Heterogeneous Hydrocarbon Reactions at the Kansas City meeting of the American Chemical Society, March 29 to April 1, 1954.

(2) H. H. v. Baumbach and C. Wagner, *Z. physik. Chem.*, **22B**, 199 (1933).

(3) A. H. Wilson, *Proc. Roy. Soc. (London)*, **A133**, 458 (1941); **A134**, 277 (1931).

(4) C. Wagner, *J. Chem. Phys.*, **18**, 62 (1950); E. J. Verwey, P. W. Haaymon, P. C. Roweijne and G. W. Osterhout, *Phillips Research Reports*, **5**, 173 (1950).

(5) E. Molinari and G. Parravano, *J. Am. Chem. Soc.*, **75**, 5233 (1953).

(6) H. S. Taylor and D. V. Sickman, *ibid.*, **54**, 602 (1932).

(7) V. C. F. Holm and R. W. Blue, *Ind. Eng. Chem.*, **43**, 501 (1951).

polarity was reversed after each measurement. At the end of a series of measurements, the apparatus was disassembled, and the thickness of the soft tablet of zinc oxide, which was in the range of 0.5–2.0 mm., was measured with a micrometer caliper. The specific conductivity was calculated by dividing the product of the thickness and the current by the product of the contact area and the applied voltage. A fresh sample of zinc oxide was used for each series of measurements, and at least two series of measurements were made for each set of heat treatment conditions.

Adsorbed Hydrogen.—Adsorbed hydrogen was found to increase the electrical conductivity of zinc oxide enormously; for example, at 100° the electrical conductivity in hydrogen was 10⁸ times as great as in nitrogen or helium. Instances of changes in electrical conductivity because of adsorbed hydrogen have been reported previously.⁸ The amount of hydrogen adsorbed at various temperatures by zinc oxide prepared similarly to zinc oxide I from Merck Reagent Grade chemicals was found by the volumetric method to be as follows; in cc. (STP)/g.: 0°, 0.21; 100°, 0.19; 200°, 0.17; 300°, 0.14; 400°, 0.09; 500°, 0.03. The adsorbed hydrogen multiplied the experimental difficulty of obtaining reproducible measurements of the electrical conductivity so greatly that only a single measurement believed to be reliable could be obtained for a given sample of zinc oxide in hydrogen. Seven such measurements made in the range of 30–100° gave values of –4.8 to –3.0 for the logarithm of the specific conductivity. When plotted against the reciprocal of the absolute temperature these values gave a straight line that indicated an activation energy of 11.3 kcal./mole. In contrast, no difficulty was experienced when measurements were made in helium with another portion of the zinc oxide; in the range of 120–500° the logarithm of the specific conductivity, when similarly plotted, determined a straight line from –10.2 to –5.8, and the activation energy had the much larger value of 18.8 kcal./mole. This observation of increase in activation energy appears to be consistent with the idea that the Fermi level rises with an increase in the number of defects, in this case, adsorbed hydrogen.

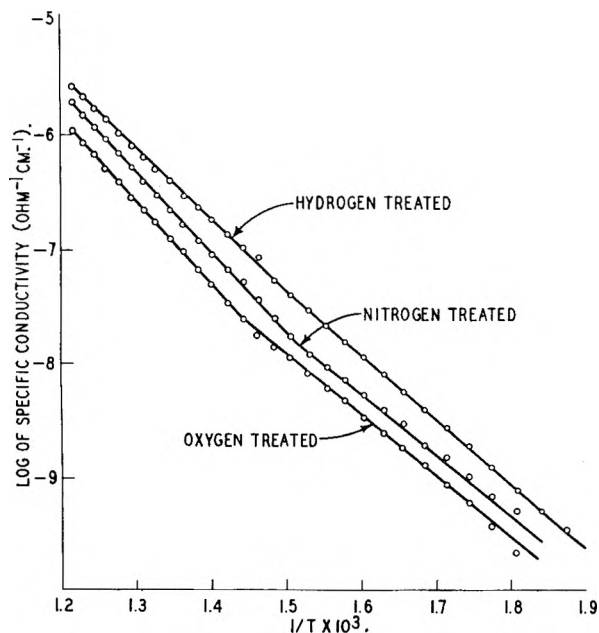


Fig. 1.—Relationship of specific conductivity with temperature for zinc oxide after different heat treatments.

In the major part of the investigation, adsorbed hydrogen was preliminarily removed from the zinc oxide by flushing with nitrogen.

(8) J. S. Anderson and M. C. Morton, *Proc. Roy. Soc. (London)*, **A184**, 83 (1945); P. B. Weisz, C. D. Prater and K. D. Rittenhouse, *J. Chem. Phys.* **21**, 2236 (1953); L. F. Heckelsberg, G. C. Bailey and A. Clark, *J. Am. Chem. Soc.*, **77**, 1373 (1955).

Results and Discussions

Heat-treated Zinc Oxide.—Three portions of zinc oxide I were modified by heating for 16 hours in different flowing gases to obtain relatively high, intermediate, and low concentrations of lattice defects, at the following temperatures: 400° in hydrogen; 500° in nitrogen (4 hours); 500° in oxygen. After the heat treatment, the electrical conductivity of each of these heat-treated zinc oxides was measured at 10° intervals as the zinc oxide cooled in a slow current of nitrogen. The results are given in Fig. 1 in the form of curves for the logarithm of the specific conductivity plotted against the reciprocal of the absolute temperature. (The curves were obtained by the method of least squares from at least two sets of measurements for a given oxide. The plotted points are for only one set of measurements.) The relative positions of the three curves show that the hydrogen-treated zinc oxide, with the highest concentration of lattice defects, had the highest electrical conductivity; the nitrogen-treated zinc oxide, with an intermediate concentration of lattice defects, had an intermediate conductivity; and the oxygen-treated zinc oxide, with the lowest concentration of lattice defects, had the lowest conductivity.

These heat-treated zinc oxides were investigated for catalytic activity for hydrogen–deuterium exchange. The results are given in Fig. 2 in the form

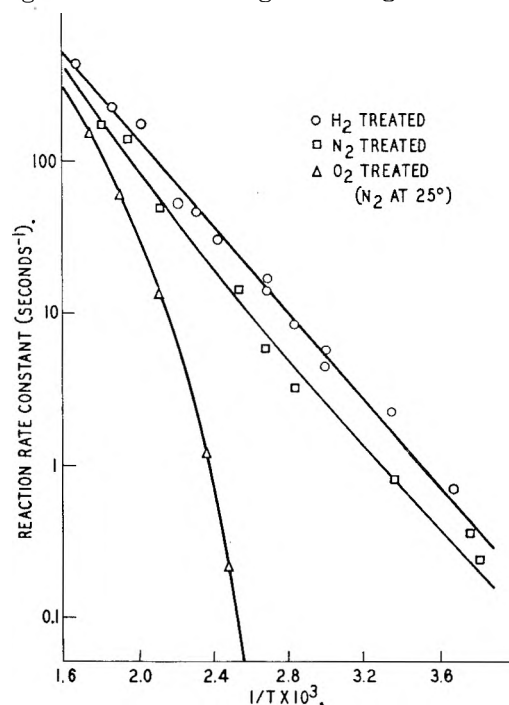


Fig. 2.—Relationship of reaction rate constants with temperature for zinc oxide for different heat treatments.

of curves for the reaction rate constant plotted logarithmically against the reciprocal of the absolute temperature. The three curves are in the same relative order as the corresponding curves of Fig. 1, indicating that the catalytic activity was greater the greater the electrical conductivity or the greater the concentration of lattice defects.

Because of the following circumstance, the curve in Fig. 2 for the oxygen-treated zinc oxide is in fact

for zinc oxide reduced to various undetermined degrees. Since oxygen poisons the hydrogen-deuterium exchange, the oxygen-treated zinc oxide was preliminarily flushed with nitrogen at room temperature for 5 minutes and with the reactant mixture of hydrogen and deuterium at the reaction temperature for 30 seconds, whereupon some reduction occurred. Further reduction occurred during the runs although it was minimized by limiting the runs to 5 minutes each; the second of two successive samples of product collected for analysis always differed from the first by containing more hydrogen deuteride, indicating progressive increase in catalytic activity. A new sample of zinc oxide was used for each run. The curvature of the curve indicates that the extent of reduction increased with increase in reaction temperature.

The energy of activation for the hydrogen-deuterium exchange, calculated from the slope of the curve for the hydrogen-treated zinc oxide in Fig. 2, was 6.5 kcal./mole, in fair agreement with literature values.^{7,9}

Impurity-containing Zinc Oxide.—In Figs. 3 and 4 are given the results for electrical conductivity and for catalytic activity of zinc oxides, II, II-Al and II-Li. The relative positions of the curves in Fig. 3 show, in agreement with the literature, that the electrical conductivity of zinc oxide was increased by alumina and was decreased by lithia. The changes caused by the impurities were relatively much smaller for the oxygen-treated samples than for the hydrogen-treated ones, indicating that relatively fewer stoichiometrically excess metal atoms were present. The fact that part of the curve for the oxygen-treated zinc oxide containing alumina is below the curve for oxygen-treated pure zinc oxide is attributed to experimental difficulties.

Some of the curves in Fig. 3 change slope at about 300–400°. The relatively steep slopes above the inflections indicate an activation energy of the order of 23 kcal./mole. Since this value is about one-half of the energy gap between the valence and the conduction band of zinc oxide, 46 kcal./mole,¹⁰ it appears that the conductivity in this temperature region may be intrinsic conductivity. The less steep slopes below the inflections may be related to the impurity aluminum atoms and/or excess zinc atoms. Similar inflection to a lesser extent may be noted in the curves in Fig. 1.

The slopes of the curves of Fig. 3 decrease in the order of passage from the oxides of low electrical conductivity to oxides of high electrical conductivity, reflecting the fact that the Fermi level moves up with increase in the concentration of electron-donors (aluminum atoms or excess zinc atoms). For lithium, which in comparison with zinc behaves relatively like an electron acceptor, the Fermi level moves down, increasing the slope and the activation energy.

Figure 4 shows that alumina in the zinc oxide increased the catalytic activity for hydrogen-deuterium exchange, and that lithia decreased it. Two batches of hydrogen-treated zinc oxide containing 0.03 mole % lithia showed low catalytic activity; the experimental points were of poor repro-

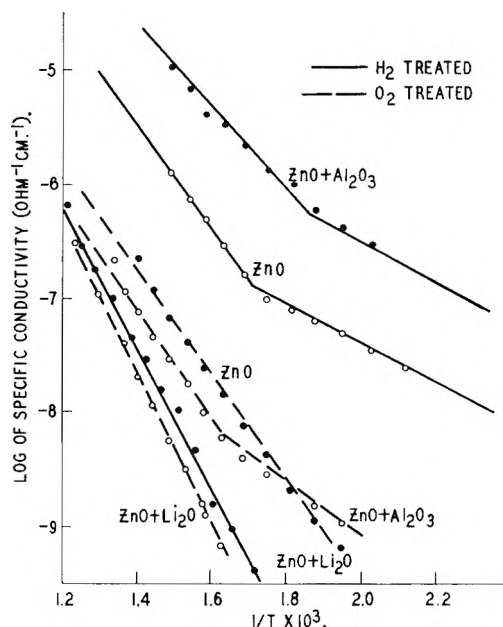


Fig. 3.—Relationship of specific conductivity with temperature for various zinc oxides containing impurities.

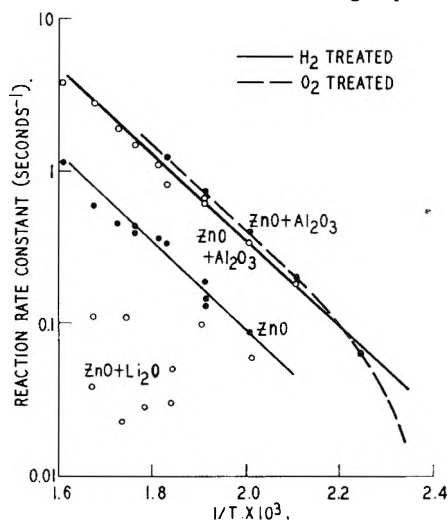


Fig. 4.—Relationship of reaction rate constants with temperature for various zinc oxides containing impurities.

ducibility and did not justify drawing a curve. Two batches of zinc oxide containing 0.3 and 0.8 mole % alumina showed no difference in catalytic activity. The slopes of the curves for the hydrogen-treated zinc oxide II and zinc oxide II-Al gave activation energies of about 12 kcal./mole. These high values in relation to the lower value obtained for zinc oxide I may be related to the movement of the Fermi level downward resulting from fewer defects in the lower surface area oxides. The data for oxygen-treated zinc oxide II-Al, which showed no catalytic activity at 150°, determined a curve similar in general shape to that for oxygen-treated zinc oxide in Fig. 2, reflecting progressive reduction of the zinc oxide. The generally lower catalytic activity shown in Fig. 4, in comparison with Fig. 2, is attributed to the relatively low surface area.

Acknowledgment.—We wish to acknowledge the help of Joan Wirges and Henry Rollmann for mass spectrographic measurements.

(9) E. A. Smith and H. S. Taylor, *J. Am. Chem. Soc.*, **60**, 362 (1938).

(10) C. Kittel, "Introduction to Solid State Physics," John Wiley and Sons, Inc., New York, N. Y., 1953, p. 276.

THE REFRACTIVE INDEX OF COLLOIDAL SOLS¹

BY ADAM CHOU AND MILTON KERKER

*Department of Chemistry, Clarkson College of Technology, Potsdam, N. Y.**Received August 26, 1955*

The refractive index of sulfur hydrosols of various particle sizes has been measured and the intrinsic refractive index computed. The experimental values are in agreement with the requirements of the Zimm-Dandliker theory.

Zimm and Dandliker² have developed a relation between the scattering and refractive index of a colloidal sol which involves the Mie³ scattering functions. This relation is more general than the mixture rules discussed by Heller⁴ since it is not restricted to systems of small particles with a refractive index close to that of the medium. In this paper, we will compare the results of our observations on sulfur hydrosols with the requirements of the Zimm-Dandliker theory.

We have found it convenient to work with

$$n_{sp.} = \frac{n' - n}{n'} = [n]c = \frac{3R(i_1^*)c}{2\alpha^3 D} \quad (1)$$

where

$n_{sp.}$	= specific refractive index
n'	= refractive index of the sol
n	= refractive index of the medium
$[n]$	= intrinsic refractive index
c	= concentration of sol in g./ml.
$R(i_1^*)$	= scattering function
α	= $2\pi r/\lambda$
r	= radius of colloidal particle
λ	= wave length of light in the medium
D	= density of the colloidal particles

The above utilizes the refractive index increment, $n' - n$, rather than the differential refractive index, dn/dc , employed by Zimm and Dandliker.

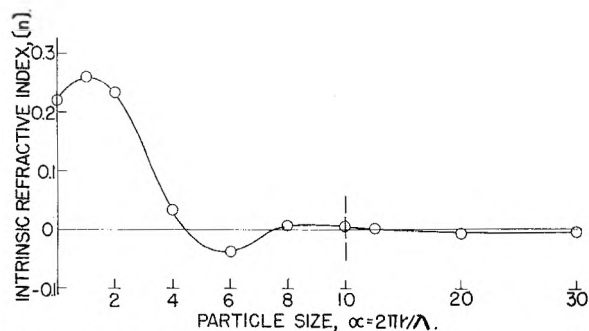


Fig. 1.—Intrinsic refractive index versus α for $m = 1.50$.

The intrinsic refractive index, $[n]$, depends upon the scattering function, $R(i_1^*)$, which in turn is dependent upon the size, shape and refractive index of the colloidal particles. For spherical particles, $R(i_1^*)$ is obtained from the Mie theory. The available Mie theory functions have been reviewed recently.⁵ Using the tables of Gumprecht and

(1) This work has been supported in part by grants from Research Corporation and the Atomic Energy Commission, Contract AT(30-1)-1801.

(2) B. H. Zimm and W. B. Dandliker, *THIS JOURNAL*, **58**, 644 (1954).

(3) G. Mie, *Ann. Physik*, **25**, 377 (1908).

(4) D. Sinclair and V. K. La Mer, *Chem. Revs.*, **44**, 245 (1949).

(5) M. Kerker, *J. Optical Soc. Am.*, in **45**, 1081 (1955).

(6) R. O. Gumprecht and C. M. Sliepcevich, "Tables of Functions of First and Second Partial Derivatives of Legendre Polynomials," Engineering Research Institute, University of Michigan, Ann Arbor, 1951.

Sliepcevich,^{6,7} we have computed $R(i_1^*)$ for refractive index $m = 1.50$ over a wide range of α values. This refractive index is applicable to sulfur hydrosols. These computations and the corresponding intrinsic refractive indexes are presented in Table I. Figure 1 illustrates the variation of the intrinsic refractive index with α .

TABLE I
SCATTERING FUNCTIONS AND INTRINSIC REFRACTIVE INDEX
AS A FUNCTION OF α FOR $m = 1.50$

α	$R(i_1^*)$	$[n] \times 10^4$	α	$R(i_1^*)$	$[n] \times 10^4$
0	...	2206	20	-33.571	-315
1	0.3461	2598	30	-46.716	-128
2	2.4767	2324	40	-47.449	-5.56
4	2.8666	336	50	-143.21	-8.60
6	-11.286	-393	75	-273.20	-4.86
8	3.2061	+47	100	-367.84	-2.76
10	4.8675	37	200	-990.91	-0.93
15	5.4333	12	400	-1646.0	-0.193

If the system is polydisperse, the intrinsic refractive index is given by

$$[n] = \frac{3 \int F(\alpha) R(i_1^*) d\alpha}{2D \int F(\alpha) \alpha^3 d\alpha} \quad (2)$$

where $F(\alpha) d\alpha$ is the fraction of particles with α values between α and $(\alpha + d\alpha)$. When the colloidal particles are sufficiently small so that the Rayleigh law of scattering is applicable

$$[n] = \frac{3(m^2 - 1)}{2D(m^2 + 2)} \quad (3)$$

for polydisperse as well as monodisperse sols. m is the refractive index of the colloidal particles relative to that of the medium.

Use of La Mer Sols.—Zimm and Dandliker have suggested that their theory may be tested with the sulfur hydrosols studied by La Mer and co-workers^{8,9} and it was this suggestion that interested us in this work. These sols, which may be prepared by treating dilute sodium thiosulfate (0.001–0.003 *M*) with dilute hydrochloric acid (0.002–0.006 *M*) are monodisperse and thus offer a method of observing the influence of particle size on the intrinsic refractive index without the complicating effects of polydispersity. Unfortunately, the particle concentration in the La Mer sols is much too low to observe refractive index increments even for those sols consisting of small particles. For sols somewhat more concentrated than those of La Mer (0.02 to 0.04 *M* thiosulfate and 0.06 to 0.12 *M* acid), we did observe a change in refractive index in the

(7) R. O. Gumprecht and C. M. Sliepcevich, "Tables of Light Scattering Functions of Spherical Particles," Engineering Research Institute, University of Michigan, Ann Arbor, 1951.

(8) I. Johnson and V. K. La Mer, *J. Am. Chem. Soc.*, **69**, 1184 (1947).

(9) M. Kerker and V. K. La Mer, *ibid.*, **72**, 3516 (1950).

TABLE II
INTRINSIC REFRACTIVE INDEX FOR SULFUR HYDROSOLS OF VARIOUS PARTICLE SIZES

Particle size	Concn. of S, g./ml.	Concn. of NaCl, g./ml.	$n' - n$	n'	$[n$
I	0.0070	0.00167	0.00235	1.33482	0.25
I	.0065	.00158	.00190	1.33435	.22
I	.0056	.00084	.00180	1.33413	.24
I	.0024	.00045	.00094	1.33321	.29
II	0.00305	0.00080	0.00065	1.33304	0.16
II	.0063	.00568	.00104	1.33415	.12
II	.00061	.00078	.00000	1.33232	.10 ± 0.6
II	.0390	.03100	.00554	1.34173	.11
III	0.00067	0.00012	-0.00009	1.33214	-0.10 ± 0.05
III	.00099	.00009	-.00008	1.33213	-.06 ± .04
III	.00095	.00010	-.00010	1.33209	-.08 ± .04

course of the growth of the sols but were able to relate this to changes in homogeneous salt concentrations rather than to colloidal particles. We assumed that the principal reaction was¹⁰



and that the refractive index of a growing sol was the sum of the refractive indexes of each of the components when separate and at the appropriate concentration. The refractive index at any stage of the reaction was found to be the sum of the values for each of the homogeneous components. Therefore, even for these concentrations, the sulfur content was too low for a determination of the intrinsic refractive index. In order to determine this quantity, it is necessary to work with sols of very high sulfur concentrations and with present techniques this means abandoning monodisperse systems. Fortunately it is possible to obtain some information about the relation between intrinsic refractive index and particle radius even from systems which are not highly monodisperse, provided they have a sufficiently high particle concentration.

Examination of Fig. 1 indicates three regions of particle size convenient for testing. For sols whose particles are less than $\alpha = 2$, the intrinsic refractive index is insensitive to particle radius, only varying from 0.22 to 0.26. The intrinsic refractive index is practically zero for sols with particles greater than $\alpha = 4$. It is only in the intermediate range that the intrinsic refractive index is sensitive to particle radius and, for a polydisperse system, to size distribution. A system with the bulk of its particles in this intermediate range should have an intrinsic refractive index between 0 and 0.22. We have calculated the effect of size distribution on the intrinsic refractive index of a sol with a normal distribution of particle sizes and $\alpha_{av} = 3$. For standard deviations $\sigma = 0, 0.2, 0.5$ and 1.0 the respective values of the intrinsic refractive index were 0.102, 0.098, 0.087 and 0.058.

Preparation of Sols.—We have prepared sols, designated as types I, II and III, whose size distributions correspond to the three ranges described above. Type I sols consist of small particles ($\alpha < 2$) and are prepared by the fractional coagulation technique of Oden.¹¹ They are nearly clear, yellow, quite stable, of high concentration and can be diluted without apparent decomposition.

Type II sols were those for which the bulk of the colloidal material was in the size range $\alpha = 2$ to 6. These were prepared by a modification of Oden's technique. Three volumes of 3 *M* sodium thiosulfate were added dropwise to concentrated sulfuric acid and the resulting solution made 0.25 *M* with respect to NaCl. The sulfur was centrifuged out at 8,000 r.p.m. for half an hour in a Sorvall Type SS-1 centrifuge and the centrifugate was redispersed in warm water and centrifuged again. The supernatant was then fractionated by coagulation with NaCl in the manner described by Oden to form sols which we have referred to as type I. The second centrifugate was then redispersed in warm water and a second series of sols containing particles in the size range for type II was obtained by continual centrifugation and redispersion of the centrifugates. These sols were milky. Electron microscope examination indicated the bulk of the sulfur was in the size range $\alpha = 2$ to 6 although there were always a considerable number of very small particles and sometimes some large ones present.

A seeding technique was used to prepare type III sols, *i.e.*, those with particles greater than $\alpha = 4$. A ten to one ratio of 0.03 *M* sodium thiosulfate and an Oden sol, which provides condensation nuclei, were mixed and the resulting solution was made 0.1 *M* with respect to HCl by addition of the concentrated acid. After standing for half an hour, the solution was centrifuged and the residue redispersed in warm water. These sols were free of the background of small particles which characterized the Oden type sols and they contained a sufficiently high sulfur concentration for an accurate analysis. The size could be controlled by the time between the initial mixing and the centrifuging. We found ten minutes to half an hour provided a convenient range for our purpose.

Experimental

The particle sizes were examined by both electron microscopy and light scattering. The electron microscope samples were prepared by placing a droplet of sol on a water cast collodion film and drying in air. The unprotected sulfur particles could be seen to evaporate in the electron beam of the microscope and just as in the case of sulfur aerosol particles¹² this could be inhibited by sandwiching between two collodion films. In practice we did not find this sandwiching necessary because the evaporated droplets always left a mark on the film which indicated its size. Measurement of the disymmetry of the light scattering at 45 and 135° and the polarization at 90° indicated whether the sols consisted of small particles or not. This technique was used to confirm the type I sols.

In order to calculate the intrinsic refractive index from equation 1, it is necessary to know c , $n' - n$, and n . c was determined by evaporating the sol to dryness, weighing the residue, igniting and weighing the final residue. The final residue was principally sodium chloride and the weight of sulfur was obtained by subtracting it from the weight of the initial residue. This analysis was checked by oxidation of the sol to sulfate with bromine-nitric acid and precipitation of barium sulfate.

The difference in refractive index between the sol and water was measured with a Brice-Phoenix differential re-

(10) E. M. Zaiser and V. K. La Mer, *J. Colloid Sci.*, **3**, 571 (1948).

(11) S. Oden, *Nova Acta Regiae Soc. Sci. Upsalensis*, Ser. IV, **3**, N. 4 (1913).

(12) M. Kerker, A. L. Cox and M. Schoenberg, *J. Colloid Sci.*, **10**, 413 (1955).

fractometer using the 5461 Å. mercury line. From this was subtracted the difference in refractive index between water and sodium chloride solution of concentration equal to that in the sol. This second difference gives $n' - n$. For n , the refractive index of the medium, the value for the above-mentioned sodium chloride solution was used.

Results

The results are presented in Table II. The intrinsic refractive indexes for type I sols range from 0.22 to 0.29. The principal error for this group was in the analysis of the sulfur concentration which we estimate to be within 10%. The results are in agreement with the requirements of the theory for this size range. Oden measured the refractive index of some of his sulfur sols and from his data we have calculated an intrinsic refractive index of 0.25 which would indicate his sols also consisted of small particles.

The results of type II and III sols (Table II) also agree with equation 1. In the latter group and for one sol of the former, the experimental error arises principally in the measurement of the very

small differential refractive index. The estimated errors are given in the tables for these cases. In all the other cases the limiting error is in the sulfur analysis.

A check on the consistency of equation 1 can be obtained from dilution experiments. For a given size distribution, the intrinsic refractive index should be independent of concentration. Table III shows the effect of dilution on three sols. The intrinsic refractive index does remain constant in the course of the dilution which in one case is nearly 30-fold.

TABLE III

EFFECT OF DILUTION ON INTRINSIC REFRACTIVE INDEX

Sol 5		Sol 8		Sol 12	
Concn. of S	[n]	Concn. of S	[n]	Concn. of S	[n]
0.0030	0.16	0.039	0.11	0.0151	0.26
.0024	.15	.029	.10	.0059	.26
.0020	.17	.022	.11	.0023	.26
.0014	.17	.015	.10	.00144	.25
				.00056	.25

EXTRACTION OF INORGANIC SALTS BY 2-OCTANOL. II. COBALT(II) AND NICKEL(II) CHLORIDES AND BROMIDES. EFFECT OF ELECTROLYTES¹

BY T. E. MOORE, R. W. GOODRICH, E. A. GOOTMAN, B. S. SLEZAK AND PAUL C. YATES

Contribution from the Department of Chemistry, Oklahoma A. and M. College, Stillwater, Oklahoma

Received September 1, 1955

An analysis of the distribution coefficients of CoCl_2 and NiCl_2 between 2-octanol and aqueous mixtures with HCl at constant concentration has been made by studying the variations in the non-aqueous and aqueous phase activity coefficients with salt concentration. In approximately 5 molal acid the octanol-rich phase activity coefficient for CoCl_2 remains nearly constant while that for NiCl_2 increases rapidly, thus accounting for the difference in the extractability of the two salts and also their separation by 2-octanol extraction. Study of the effect of different valence-type chlorides upon the distribution coefficient of CoCl_2 showed a marked dependence upon the specific extraction-promoting chloride present. The order of promoting effectiveness is $\text{HCl} > \text{LiCl} > \text{CaCl}_2 > \text{AlCl}_3$ or $(\text{CH}_3)_4\text{NCl}$. This parallels the order of extraction of the promoting electrolytes themselves. As predicted by the Born equation for ion charging, the distribution coefficients of CoBr_2 are greater than those of CoCl_2 at the same concentrations because of the larger anion. The extraction of CoBr_2 from aqueous mixtures with LiBr , CaBr_2 , and AlBr_3 does not depend greatly upon the valence-type of the promoting salt at equivalent concentrations (in contrast with the case of CoCl_2). An explanation for the separation of CoCl_2 from NiCl_2 by 2-octanol extraction is suggested.

The original experiments of Garwin and Hixson² on the separation of CoCl_2 from NiCl_2 based upon the preferential extraction of CoCl_2 by 2-octanol from aqueous mixtures containing HCl or CaCl_2 at high concentrations led to investigation of some of the factors affecting this and related 2-octanol-salt-water partition equilibria. One of the most important of these is the promotion of extraction by electrolytes having a common anion.

The distribution coefficient k_d for a solute is easily shown to be proportional to the ratio of the activity coefficients of the solute in the two phases

$$k_d = K\gamma_1/\gamma_2 \quad (1)$$

where K is the equilibrium constant and γ_1 and γ_2 are the appropriate stoichiometric activity coefficients in the aqueous and non-aqueous phases, respectively. Since the distribution coefficient usually increases with increasing concentration of

both the extracted salt under consideration and the extraction-promoting electrolyte, a study of the variation with concentration of γ_1 relative to γ_2 provides information about the nature and the relative importance of the interactions occurring in the aqueous and non-aqueous phases.

The distribution coefficients of CoCl_2 and NiCl_2 in mixtures with HCl (at constant concentration) were determined by equilibration of the aqueous mixtures with octanol. Ratios of the aqueous phase activities to the non-aqueous phase concentrations (equal to γ_2/K) were then calculated from equation 1. In making the calculations the octanol phase salt concentrations were expressed as moles per 1000 g. of octanol + water, and negligible solubility of the octanol in water was assumed. Activity coefficients of the solutes in the aqueous phases were taken from the data of Moore, *et al.*³

Figure 1 shows the results obtained from equi-

(1) Supported under Contract AT(11-1)-71 No. 1 with the U. S. Atomic Energy Commission.

(2) L. Garwin and A. N. Hixson, *Ind. Eng. Chem.*, **41**, 2298 (1949).

(3) T. E. Moore, E. A. Gootman and P. C. Yates, *J. Am. Chem. Soc.*, **77**, 298 (1955).

brations with mixtures in which the aqueous phase HCl concentrations were 4.84 *m* (CoCl₂ series) and 4.69 *m* (NiCl₂ series). For comparison are also plotted the analogous activity/concentration ratios calculated for CoCl₂ and NiCl₂ extracted by 2-octanol from binary aqueous solutions. The data of Garwin and Hixson⁴ and the activity coefficients listed by Stokes⁵ were used.

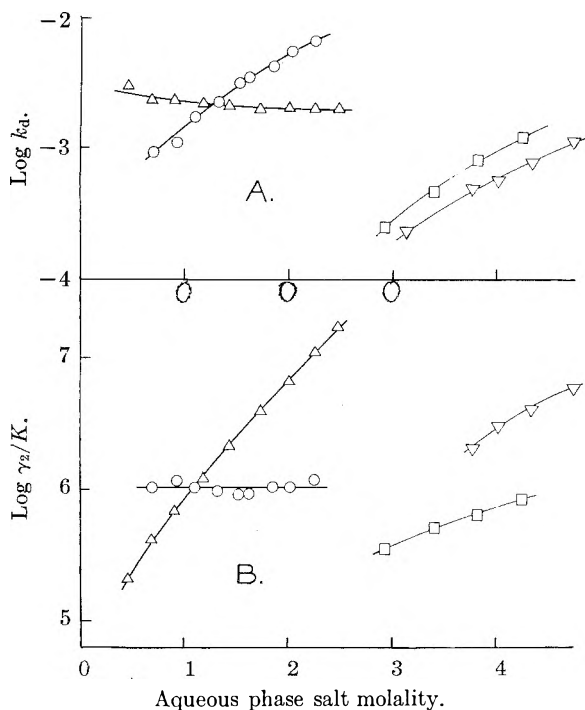


Fig. 1.—A, Distribution coefficients: \circ , CoCl₂ in 4.84 *m* HCl; Δ , NiCl₂ in 4.69 *m* HCl; \square , CoCl₂ alone; ∇ , NiCl₂ alone; B, values of octanol-phase activity/concentration ratios for same solutions.

Since the aqueous phase activity coefficients rapidly increase with salt concentration in every case, reference to Fig. 1 shows that the close conformity of NiCl₂ in mixtures with HCl to the Nernst distribution law can be attributed to the salting-out effect which HCl has upon NiCl₂ in octanol rather than to any ideality of the solute. Similarly, the increase with concentration in values of k_d for CoCl₂ in HCl-promoted extractions can be related to the observed proportionality between its concentration and its activity in octanol. The variation in the activity of CoCl₂ with the first power of its concentration indicates that CoCl₂ is monomeric and undissociated in octanol mixtures of H₂O and HCl, in agreement with the results from a recent spectrophotometric study of CoCl₂ in octanol mixtures with H₂O and LiCl.⁶ It seems likely, therefore, that because of the greater base strength of H₂O as compared to that of octanol, CoCl₂ exists principally in the form of hydrated ions and ion pairs in the non-aqueous phases in the absence of a promoting chloride. The effect of HCl or other extraction-promoting chloride in octanol is then to bring about the

further association of the ions into molecules of CoCl₂ through the mass action of the chloride ions and the competition of the HCl for the water of hydration.

Unfortunately the activity data do not permit a similar analysis to be made of the γ_1/γ_2 ratio as a function of the aqueous phase concentration of the extraction-promoting agent over a wide range of values. However, in the case of CoCl₂ two additional concentrations were studied (6.97 and 8.86 *m* HCl), and in the case of NiCl₂ one other concentration was investigated (6.86 *m* HCl). It was found that increasing the HCl concentration at any salt concentration decreased the values of γ_2 for CoCl₂ and raised them for NiCl₂ while the corresponding values of k_d were increased markedly for CoCl₂ but only slightly for NiCl₂.

If the promoting action were primarily the result of the mass action of the chloride ions, it should be independent of the valence type of the promoting electrolyte at equivalent concentrations. This has been shown to be the case in the perchlorate-promoted extractions of Co(ClO₄)₂ by 2-octanol.⁷ Experiments, therefore, were conducted in which *ca.* 0.1 *m* solutions of CoCl₂ and one of a different group of chlorides, ((CH₃)₄NCl, LiCl, HCl, CaCl₂, AlCl₃) at relatively high concentrations (3–15 *m* Cl⁻) were extracted with octanol. Figure 2 shows that the distribution coefficient of

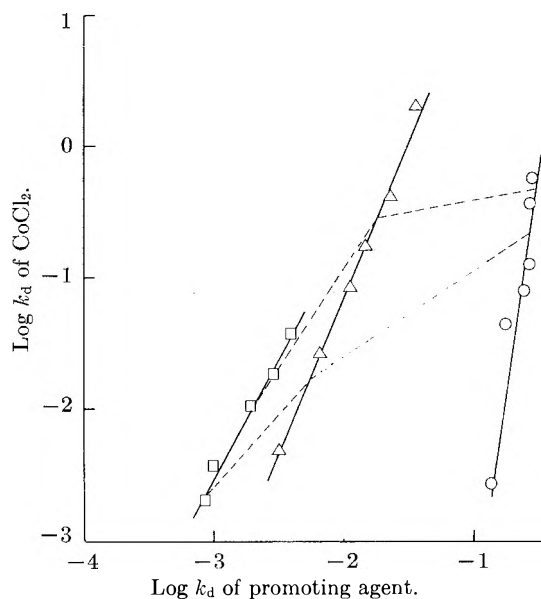


Fig. 2.—Effect of electrolytes on the 2-octanol extraction of 0.1 *m* CoCl₂: \circ , CoCl₂ + HCl; Δ , CoCl₂ + LiCl; \square , CoCl₂ + CaCl₂.

CoCl₂ is strongly dependent upon the nature of the promoting agent present. In this figure the dotted lines connect points of equivalent aqueous phase chloride concentration (upper dotted line 12 *m* and lower line 9 *m* in chloride). Although data are lacking which would permit any reliable estimation of the effect of these electrolytes on the values of γ_1 , the observed correlation between their extractability by octanol and their effectiveness as extraction-promoting electrolytes for CoCl₂ further em-

(4) L. Garwin and A. N. Hixson, *Ind. Eng. Chem.*, **41**, 2303 (1949).
 (5) R. H. Stokes, *Trans. Faraday Soc.*, **44**, 295 (1948).
 (6) W. D. Beaver, L. E. Trevorrow, W. E. Estill, P. C. Yates and T. E. Moore, *J. Am. Chem. Soc.*, **75**, 4556 (1953).

(7) T. E. Moore, R. J. Laran and P. C. Yates, *THIS JOURNAL*, **59**, 90 (1955).

phasizes the importance of non-aqueous phase interactions in the chloride-promoted extraction of this salt.

Theoretical calculation of k_d requires consideration of such a multiplicity of factors that it has not proved feasible, although the distribution coefficient can be partially separated into terms,⁸ one of which involves the electrical work of transfer of the ions from the aqueous phase to the non-aqueous phase. This term can be estimated from the Born equation for the ion-charging process.⁹ Since the work required to transfer an ion from water to a solvent of lower dielectric constant varies inversely with the size of the ion, the extraction of a salt having a given cation and a large anion should be favored over one of similar charge type composed of the same cation but a smaller anion. In Fig. 3 are shown the results of a series of experiments on the distribution of CoBr_2 between H_2O and octanol. In certain of the experiments mixtures of CoBr_2 (2 *m*) with LiBr , CaBr_2 , or AlBr_3 (2–17 *m*) were extracted in order to study the latter bromides as extraction-promoting agents for CoBr_2 . Comparison of the results with those involving CoCl_2 shows that, as predicted by the Born theory, CoBr_2 is more readily extracted than CoCl_2 from solutions of the same concentration. Both the absence of a marked dependence upon the valence type of the promoting bromides, and the higher values of the distribution coefficients for the bromides compared with the chlorides indicate that with increasing anion size in the series CoCl_2 , CoBr_2 , $\text{Co}(\text{ClO}_4)_2$ there is a progressive increase in the importance of electrostatic factors in determining the magnitude of the distribution coefficients.

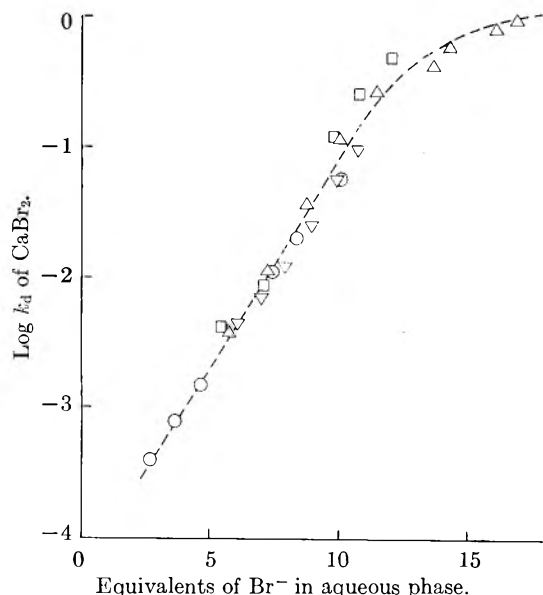


Fig. 3.—Effect of electrolytes on the 2-octanol extraction of CoBr_2 : \circ , CoBr_2 ; \triangle , $\text{CoBr}_2 + \text{LiBr}$; ∇ , $\text{CoBr}_2 + \text{CaBr}_2$; \square , $\text{CoBr}_2 + \text{AlBr}_3$.

The results of this investigation suggest a reasonable explanation for two relationships noted by Garwin and Hixson.² These workers observed

that the degree of extraction of CoCl_2 by 2-octanol could be correlated with the intensity of the blue color of the aqueous solutions and with high values of the activity coefficients of extraction-promoting electrolytes in binary aqueous solutions. Since optical evidence^{3,6} supports the existence of molecular CoCl_2 as the principal source of the blue color in each phase, the optical density of the color indicates the extent of association of the ions into molecules of CoCl_2 . An electrolyte such as HCl which favors the association of Co^{++} and Cl^- in aqueous mixtures would be expected to cause even greater association in the octanol phases, owing to the much lower value of the dielectric constant of octanol compared to that of water. Association of Co^{++} and Cl^- in either phase, however, results in a decrease in the stoichiometric activity coefficient of CoCl_2 so that even though γ_1 and γ_2 are both decreased, the ratio γ_1/γ_2 may be actually increased by the addition of a promoting electrolyte. If the added electrolyte is itself not appreciably extracted, as in the case of $(\text{CH}_3)_4\text{NCl}$, γ_2 will not be decreased relative to γ_1 and the extraction of CoCl_2 will not be promoted even though the aqueous phases are blue.

It has been stated that any reasonable explanation for the high values of the activity coefficients of electrolytes in concentrated solutions must be based upon models of ionic hydration.¹⁰ An electrolyte with ions strongly hydrated (such as HCl) will have high values for its own activity coefficient in binary aqueous solutions and will correspondingly increase the activity coefficients of other electrolytes (such as CoCl_2) in mixtures with it through the removal of "solvent" water by hydration.² Since this results in increase in the values of γ_1 and consequently the ratio γ_1/γ_2 the extraction of CoCl_2 is promoted by the addition of electrolytes having high activity coefficients.

It seems likely that an electrolyte such as HCl may also act to raise the activity coefficient of other solutes in the octanol phase through a similar mechanism, *i.e.*, solvation. This would explain the comparatively high values of γ_2 for both HCl and NiCl_2 in octanol phases containing these solutes. Offsetting a similar increase in γ_2 for CoCl_2 , however, is the greater ionic association, which operates to decrease γ_2 . Thus, the separation factor, defined as the ratio of the distribution coefficient of CoCl_2 to that of NiCl_2 , is increased by HCl .

Experimental

Materials.—All chemicals were C.P. or reagent grades. CoBr_2 was prepared from CoCO_3 and HBr . The octanol was the best grade furnished by the Matheson Coleman and Bell Co. It was found ketone-free, with the boiling point and refractive index as reported for the pure compound.¹¹

Extraction Procedures.—Equilibrations with $\text{HCl-CoCl}_2\text{-H}_2\text{O}$ or $\text{HCl-NiCl}_2\text{-H}_2\text{O}$ mixtures were carried out at $30.00 \pm 0.05^\circ$. Glass-stoppered flasks each containing 30–50 ml. of the aqueous mixtures and an equal volume of octanol were mechanically agitated for 2–8 hours, the aqueous phases separated and discarded, and the octanol phases re-equilibrated with fresh portions of the aqueous mixtures. From 4 to 7 such equilibrations were usually required (as determined by analysis of the non-aqueous phase). After a final

(10) R. H. Stokes and R. A. Robinson, *J. Am. Chem. Soc.*, **70**, 1870 (1948).

(11) G. L. Dorough, H. B. Glass, T. L. Gresham, G. B. Malone and E. B. Reid, *ibid.*, **63**, 3100 (1941).

(8) N. Bjerrum and E. Larsson, *Z. physik. Chem.*, **127**, 358 (1927).

(9) M. Born, *Z. Physik*, **1**, 45 (1920).

12-24 hr. separation period, the octanol phases were removed and analyzed.

In studying the effect of different valence-type metal chlorides on the partition of CoCl_2 between octanol and water, stock solutions 0.1 *m* in CoCl_2 and varying in concentration with respect to the promoting chlorides were prepared and equilibrated once with octanol at 30°. Equal volumes of octanol and the aqueous mixtures were shaken for periods of *ca.* 24 hr. Both phases were analyzed.

Cobalt bromide distribution experiments were carried out in a manner similar to those for CoCl_2 . In the unpromoted-extraction experiments the aqueous phase concentrations of CoBr_2 fell within the range of 1-5 *m* while in the promoted-extraction experiments the initial CoBr_2 concentration was 2 *m* and the promoting bromide concentration ranged from 1 to 15 *m*. Table I gives the exact concentration ranges. Visible attack of the octanol occurred at the highest LiBr and AlBr_3 concentrations, however.

TABLE I
CONCENTRATION RANGES OF EXTRACTION-PROMOTING
ELECTROLYTES

Promoting electrolyte	Aqueous halide, <i>m</i>
HCl	6.4-11.6
LiCl	7.8-14.5
$(\text{CH}_3)_4\text{NCl}$	3.0-7.9
CaCl_2	8.6-14.9
AlCl_3	5.7-6.3

Analytical Methods. A. Aqueous Phases.—The aqueous phases were analyzed by conventional procedures with only slight modifications. Total halide was determined volumetrically with AgNO_3 ; cobalt was determined by electrolysis, gravimetrically as anhydrous CoCl_2 , or by titration of the excess cyanide with AgNO_3 after conversion of the cobalt to pentacyanocobaltate(III) ion; nickel was determined by electrolysis or gravimetrically as bis-(dimethylglyoximo)-nickel. Extraction-promoting electrolytes were determined by difference since they were always present at relatively high concentration.

B. Non-aqueous Phases.—Except in the case of the chloride analyses, the octanol phases were back-extracted with several portions of water and the resulting aqueous solutions analyzed. Chloride analysis was usually done in the octanol solutions by a modified Volhard titration using alcoholic AgNO_3 and aqueous KCNS in the back titration. Cobalt was determined polarographically or by amperometric titration with α -nitroso- β -naphthol.¹² Nickel was determined polarographically after evaporation of the aqueous extracts to dryness and solution of the residues. Extraction-promoting agents were again determined by difference.

Water determinations were made by the Karl Fischer¹³ method employing a dead-stop end-point.

(12) I. M. Kolthoff and J. J. Lingane, "Polarography," Interscience Publishers, Inc., New York, N. Y., 1946.

(13) J. Mitchell, Jr., and D. M. Smith, "Aquometry," Interscience Publishers, Inc., New York, N. Y., 1948.

ADSORPTION MEASUREMENTS AT VERY LOW PRESSURES

By S. WAGENER

Kemet Company, Cleveland, Ohio

Received September 23, 1955

Rates of adsorption are measured by flowing the gas through a capillary to which ionization or Knudsen gages are attached at both ends. From measurements of rates *versus* time, adsorbed quantities as low as 10^{-5} μg . (equal to $1/1000$ of a monolayer per cm^2) can be determined. The factors influencing the sensitivity and accuracy of this method are discussed. The method is used for studying adsorption on thin deposits prepared from a number of metals. Adsorption rates of CO and CO_2 on Ba, Sr and Ni are 5 l./sec. cm^2 , while on Mg, Al and Ag, they are ≤ 5 $\text{cm}^3/\text{sec. cm}^2$. Hydrogen and nitrogen are adsorbed at much smaller rates than the carbon oxides (50 $\text{cm}^3/\text{sec. cm}^2$ for H_2 on Ba). The adsorbed quantities depend on thickness and temperature of the deposits to a considerable extent. The activation energies of the adsorption processes are less than 0.2 kcal./mole for CO and CO_2 on Ba, but 4 kcal./mole for N_2 on Ba. Desorption phenomena are studied by reversing the flow of gas. These show that all adsorption processes investigated with the deposits are chemical. For adsorption of CO on Ba, the pressure of desorbed CO is less than 10^{-7} mm. at temperatures up to 400°.

1. Introduction.—In work on adsorption, rates are mostly referred to qualitatively, by distinguishing between instantaneous or rapid adsorption on one hand and slow adsorption on the other. An accurate measurement of such rates is made difficult by the rapidity at which many adsorption processes take place. Measurements must be undertaken at very low gas pressures, where the time needed for measurement is small compared with that required for covering the adsorbent with a monolayer. A brief calculation shows that the gas pressure has to be of the order of 10^{-6} mm. or lower.

During the last few years, the writer has studied a method for measuring adsorption rates at the low pressures required. The following article will describe this method, its sensitivity, its accuracy, and some of the applications which have been investigated so far.

2. Description of Flow Method.—The method used by the writer is based on Knudsen's laws for the flow of gases at low pressures. Since this method has been described before, in connection with investigation of getter materials,^{1,2}

the description here can be brief. Basically, the experimental arrangement consists of two pressure gages, P and S, which are inter-connected by a capillary (see Fig. 1 in reference 1 or 2). Gage P is also connected to a high vacuum diffusion pump by a short and wide connection tube, while gage S has side arms in which the sorbents to be investigated are located. The gas to be studied is injected *via* a suitable leak valve^{3,4} into gage P where a certain pressure p_p is produced. From here the gas flows through the capillary into the sorbent, establishing a pressure p_s in gage S ($p_s < p_p$). The rate of adsorption G is obtained from these two pressures and from the conductance F of the capillary as

$$G = F \frac{p_p - p_s}{p_s} \quad (1)$$

The rate of adsorption, as defined by this equation, is measured in $\text{cm}^3/\text{sec.}$ or l./sec. and is essentially independent of pressure. This definition was chosen because it has the advantage of providing a constant for any combination of sorbent and gas. If the rate were defined differently, for instance in units liters $\times \mu$ mercury per second, this advantage would be lost.

The gages concerned have to indicate pressures in the range 10^{-6} mm. and lower. Therefore, only ionization gages or Knudsen gages⁵ are suitable.

In order to make it possible to measure adsorption rates

(1) S. Wagener, *Proc. I.E.E.*, **99** [III] 135 (1952).

(2) S. Wagener, *Z. Angew. Physik*, **6**, 433 (1954).

(3) E. F. Babelay and L. A. Smith, *Rev. Sci. Instr.*, **24**, 508 (1953)

(4) J. P. Molnar and C. D. Hartman, *ibid.*, **21**, 394 (1950).

(5) S. Wagener, *Nature*, **173**, 684 (1954).

at pressures of 10^{-6} mm. and lower, the pressure of the residual gas in the vacuum system has to be reduced to a very low level. Therefore, before beginning any measurements, the entire system has to be submitted to a vigorous outgassing treatment consisting of at least one hour's bake at 400 to 500° and of subsequently heating all metal parts to a red heat.

The residual pressures obtained in Gage S, in the writer's experiments, were between 10^{-9} and 10^{-8} mm. The influence of this residual gas on the value of the adsorption rate can be investigated by first measuring the rate in question, then pumping off the gas down to the residual pressure, waiting for a certain period, and finally measuring the rate again at the same pressure as previously. Experiments of this type, undertaken with the system barium-carbon monoxide, showed that the rate measured at a partial pressure of carbon monoxide of 1×10^{-8} mm. did not change noticeably during a waiting period of 1 hour.

3. Sensitivity of Method and Comparison with Other Methods.—The sensitivity of the flow method is given by the smallest rate which can be measured with reasonable accuracy. The accuracy can be obtained by differentiating equation 1 which gives

$$\frac{dG}{G} = \left[\frac{dp_p}{p_p} - \frac{dp_s}{p_s} \right] \times \left(1 + \frac{F}{G} \right) + \frac{dF}{F} \quad (2)$$

The term in square brackets on the right-hand side is determined by variations in the calibration factor of the pressure gages P and S. It can be assumed that this term is equal to 0.05 and also $dF/F = 0.05$. Then, if an accuracy $dG/G = 0.2$ is desired, a sensitivity $G_{\text{sens}} = 1/2 F$ can be obtained.

In the writer's experiments, 2 different conductances, $F = 20$ and $F = 160$ cm.³/sec., were used, the smaller of these two conductances giving a sensitivity of 10 cm.³/sec.

Previous methods for determining rates of adsorption are based on the measurement of gas quantities. The sensitivity of the flow method in terms of quantities is derived from the fact that a rate of 10 cm.³/sec. can be measured within 10 sec. at a pressure of 10^{-7} mm. Therefore, the sensitivity for quantities is $0.01 \times 10 \times 10^{-4} = 10^{-5}$ l. μ which (for carbon monoxide at $T = 300^\circ\text{K}$.) corresponds to 1.5×10^{-5} μg .

For comparison, the microbalance (Gulbransen⁶) has a sensitivity of only 0.25 μg . In a more sensitive method, which was described recently (Becker and Hartman⁷), the adsorbed gas is desorbed by suddenly heating the sorbent to a very high temperature. The quantity of gas sorbed previously is then derived from the pressure rise observed during heating on the assumption that all the sorbed gas is desorbed. This method has the disadvantage that rates can neither be measured continuously nor can they be determined for adsorbents with low or medium melting points which cannot be heated high enough to obtain complete desorption (see Sec. 5.7).

An earlier method by Morrison and Roberts⁸ is based on measurements of the accommodation coefficient of neon which varies with the amount of gas adsorbed. With this method, rates can only be derived by making assumptions on the correla-

tion between accommodation coefficient and quantity of gas adsorbed.

4. Accuracy of Method.—**4.1. Basic Accuracy.**—Basically, the accuracy of the method is given by equation 2. If using again $dp_p/p_p - dp_s/p_s = 0.05$ and $dF/F = 0.05$, we obtain

$$\frac{dG}{G} = 0.1 + 0.05 \frac{F}{G} \quad (3)$$

Accordingly, the conductance F should be small compared with the gettering rate to be measured. An accuracy of 10% can then be expected which can be improved by a more careful calibration of ionization gages and capillary.

4.2. Influence of Dimensions of Side Arms.—The side arms, in which the sorbents are located, have to be kept wide enough in order not to reduce the rate of adsorption while the gas is flowing from gage S to the sorbent. The relation between the observed rate G_{obs} , the true rate G_{tr} and the conductance F_s of the side arm is

$$\frac{1}{G_{\text{obs}}} = \frac{1}{G_{\text{tr}}} + \frac{1}{F_s} \quad (4)$$

or

$$G_{\text{obs}} = \frac{G_{\text{tr}}}{1 + G_{\text{tr}}/F_s} \quad (5)$$

showing that F_s has to be kept large compared with the rate G to be measured.

4.3. Adsorption by Gages and Glass.—Gage S, particularly if this is an ionization gage, will sorb gas at a certain rate, and so will the glass of the parts of the system on the far side of the capillary. This sorption will be included in the observed rate. The sorption of the ionization gage can be kept low by operating it with a small electron current. For instance, by using a current of 1 ma. the sorption rate can be reduced to the order of 1 cm.³/sec.

As for the glass, its influence can be determined by a blank test carried out with no sorbents contained. Such a test is illustrated in Fig. 1 (curve A), showing that the rate of sorption of carbon monoxide on the glass falls to very low values within a few seconds.

4.4. Influence of Impurities in the Gas.—If the gas used for the investigation contains an appreciable percentage of an impurity, this impurity may be adsorbed at a much lower rate than the main part of the gas. In such a case, the impurity gas will establish a smaller pressure gradient across the capillary, and, therefore, its partial pressure will be proportionately much higher on the far side of the capillary than it is on the side near to the pump. This will result in an error in the observed value of the gettering rate.

If this is worked out quantitatively the following equation is obtained between the adsorption rates G_m of the main constituent and G_{imp} of the impurity on one hand and the observed rate G_{obs} on the other.

$$\frac{1}{G_{\text{obs}} + F} = \frac{1}{G_m + F} + \frac{f}{G_{\text{imp}} + F} \quad (6)$$

where f is the mole fraction of the impurity ($f \ll$

(6) E. A. Gulbransen, *Advances in Catalysis*, **V**, 120 (1953).

(7) J. A. Becker and C. D. Hartman, *THIS JOURNAL*, **57**, 153 (1953).

(8) J. L. Morrison and J. K. Roberts, *Proc. Roy. Soc. (London)*, **A173**, 1, 13 (1939).

1).⁹ If $G_{\text{imp}} = 0$ (e.g., inert gas) and $F \ll G_m$, $F \ll G_{\text{obs}}$

$$G_{\text{obs}} = \frac{G_m}{1 + f(G_m/F)} \quad (7)$$

The equations above were checked by using carbon monoxide to which certain percentages of nitrogen and argon were added. The linear correlation between $1/(G_{\text{obs}} + F)$ and f according to (6) was confirmed. When adding 1.7% A, the values measured with barium as an adsorbent were $G_m = 9,000$ and $G_{\text{obs}} = 900$ cm.³/sec. On the other hand, equation (7) with $F = 20$ cm.³/sec. gives $G_{\text{obs}} = 1,040$ cm.³/sec., which shows satisfactory agreement.

If ΔG denotes the percentage error in G to be permitted, then the maximum impurity factor f_{max} which may be allowed can be calculated from equation 9. The result is ($F \ll G_m$ and $F \ll G_{\text{obs}}$)

$$f_{\text{max}} = \frac{(G_{\text{imp}} + F) \times \Delta G/100}{G_m(1 - \Delta G/100)} \quad (8)$$

If $\Delta G = 10\%$, $G = 10,000$ and $G_{\text{imp}} = 0$, $f_{\text{max}} = 0.0002$ which means that in this case the impurity due to rare gases should not exceed 0.02%. If such a purity is not obtainable, the admissible percentage (factor f_{max}) can be raised by increasing the conductance F . A compromise has then to be made in order to find a value of F which is sufficiently high to minimize the error produced by the impurity and which also is sufficiently low to obtain an adequate basic accuracy (see Sec. 4.1). In such cases, a variable conductance which can be matched to the value of the rate to be measured will be useful (Morrison^{10,11}).

5. Applications.—5.1. Experimental Details.—

Most of the adsorbents were metal deposits obtained by evaporation in a high vacuum. Nickel was evaporated from a thin wire wound to a spiral, while lithium, calcium, aluminum and silver deposits were obtained from small lumps or wires placed either on a piece of nickel sheet or into a tungsten spiral. Barium was evaporated from getter wire. All specimens were thoroughly out-gassed previously. The best vacuum conditions were obtained with nickel where the pressure during 15 minutes evaporation varied from 2×10^{-6} to 1×10^{-7} mm.

The metals were deposited on a mica disc which was located in one of the side arms of Gage S and on part of the glass wall of this arm. The density of the deposits was controlled by observing their transparency. Normally, evaporation was ended when the source of the metal vapor, at a temperature of about 1000°, could no longer be seen through the deposit. In this way, an average density of 0.07 mg./cm.² was obtained for barium and of 0.04 mg./cm.² for nickel. The geometric surface area S of the deposits was kept at about 10 cm.².

The gases which were used were of reagent purity, and mass spectrometric analyses were obtained. Carbon monoxide, for instance, contained 0.24%

(9) This is on the assumption that F has the same value for main gas and impurity and that the adsorption processes of the two gases do not interfere with each other.

(10) J. Morrison, *Rev. Sci. Instr.*, **24**, 546 (1953).

(11) J. Morrison and R. B. Zetterstrom, *J. Appl. Phys.*, **26**, 363 (1955).

CO₂, 0.04% H₂, less than 0.1% N₂ and less than 0.005% A.

5.2. Rate versus Quantity Curves.—In order to study the variation of rate as a function of time, gas was injected into Gage P up to a certain pressure and this pressure kept constant subsequently. The types of curve obtained in this manner are illustrated in Fig. 1 for two different cases, sorption of carbon monoxide and hydrogen by barium at room temperature.

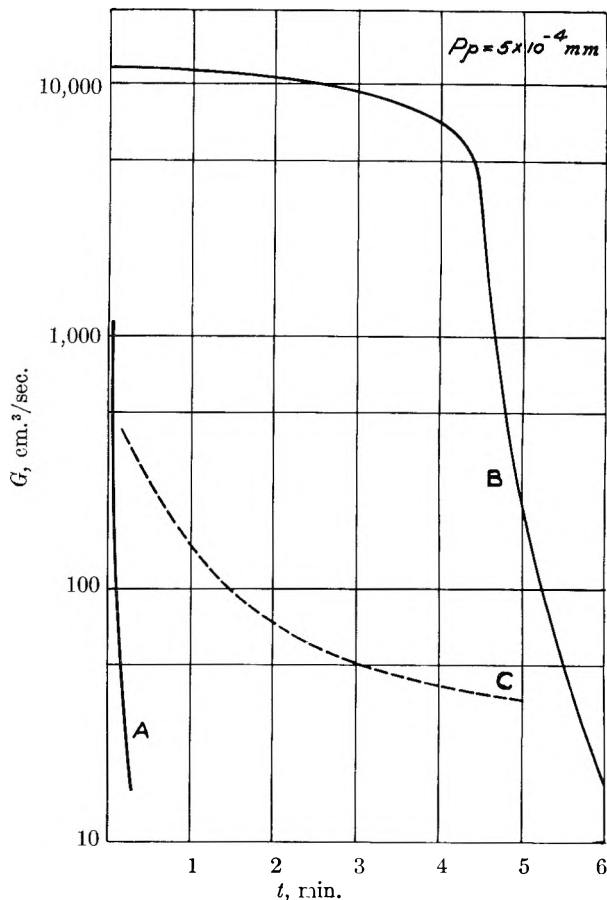


Fig. 1.—Variation of rate of adsorption with time ($F = 20$ cm.³/sec., $T = 315^\circ\text{K}$): A, CO without adsorbent; B, CO on 10 cm.² Ba; C, H₂ on 10 cm.² Ba.

An objection against this method of measurement might be raised because, owing to the fall in rate, the pressure p_s above the sorbent rises continuously during measurement. This objection, however, is not very serious since the rate, as defined in Sec. 2, does not depend on pressure. This independence of pressure is not only evident theoretically, but was established experimentally by a great number of measurements.¹

Apart from this, when measuring with constant pressure in gage P, an advantage is obtained which will be understood from discussing the correlation between "measuring time" and "quantity of gas adsorbed." As derived in an earlier paper,² the latter quantity is given by

$$C = Fp_p \int_0^t \frac{dt}{1 + F/G} \quad (9)$$

(for $p_p = \text{const.}$). Or, if $G \gg F$

$$C \approx Fp_p t \quad (10)$$

Therefore, if the pressure in gage P is kept constant, and if the adsorption rate G is large compared with the conductance F (normally $F = 20 \text{ cm.}^3/\text{sec.}$) the quantity adsorbed is proportional to the adsorption time t . This means that that part of the curves in Fig. 1 which is above the line $G = 100$ illustrates the dependence of adsorption rate on the quantity of gas adsorbed. The proper scale for quantities can be obtained by using equation 10. In this way, the full curves in Fig. 2 were plotted (showing G for unit area). The deviation from the exact curve, derived by employing equation 9 instead of 10 is indicated by the dotted curve.

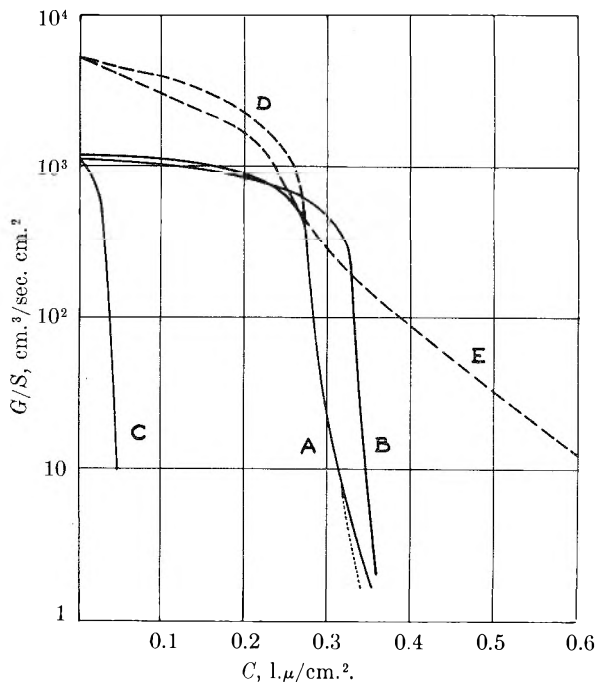


Fig. 2.—Variation of adsorption rate of carbon monoxide with quantity adsorbed ($T = 315^\circ\text{K.}$): A, 0.07 mg./cm.² Ba, $p_p = 5 \times 10^{-4}$, $F = 20 \text{ cm.}^3/\text{sec.}$; B, 0.07 mg./cm.² Ba, $p_p = 2.5 \times 10^{-5}$, $F = 20 \text{ cm.}^3/\text{sec.}$; C, 0.04 mg./cm.² Ni, $p_p = 3 \times 10^{-5} \text{ mm.}$, $F = 20 \text{ cm.}^3/\text{sec.}$; D, 0.07 mg./cm.² Ba, $p_p = 5 \times 10^{-5} \text{ mm.}$, $F = 160 \text{ cm.}^3/\text{sec.}$; E, 0.15 mg./cm.² Ba, $p_p = 5 \times 10^{-5} \text{ mm.}$, $F = 160 \text{ cm.}^3/\text{sec.}$

Of the other metals investigated, nickel was studied more in detail. The general character of the curves for this metal is the same as for barium.

The scale of the abscissa in Fig. 2 can be converted into the number of monolayers of gas which would be formed if the gas were simply piled up on the geometric surface area of the deposits. For instance, for the 100-face of nickel the number of nickel atoms per cm.² is $(2/3.52^2) \times 10^{16} = 1.61 \times 10^{15}$. Assuming that every atom adsorbs one molecule, a monolayer of carbon monoxide per cm.² corresponds to $1.61 \times 10^{15} \times 3.10 \times 10^{-17} = 5.0 \times 10^{-2} \text{ l.}\mu/\text{cm.}^2$,¹² or 0.1 l.µ/cm.² correspond to 2 monolayers. For barium, the number of atoms in one cm.² of a 100-face is $(1/5.02^2) \times 10^{16} = 3.97 \times 10^{14}$. Therefore, a monolayer/cm.² corresponds to $3.97 \times 3.10 \times 10^{-3} = 1.23 \times 10^{-2} \text{ l.}\mu/\text{cm.}^2$, or 0.1 l.µ/cm.² to 8 monolayers in the case of barium.

(12) The factor 3.1×10^{-17} gives the volume in liters of a molecule at 1 µ pressure and $T = 300^\circ\text{K.}$

Referring back to Fig. 2, we see that adsorption of carbon monoxide on barium deposits continues with a very high rate until a quantity corresponding to more than 20 monolayers (with respect to the geometric surface area) is adsorbed. In Section 5.7 it will be shown that carbon monoxide is adsorbed on barium by a process of chemisorption. As the forces producing chemisorption are of a short-range nature, such a process cannot give a great number of monolayers. It must therefore be concluded that the deposits investigated have an extensive internal surface area which contributes to the adsorption. Since most of this internal surface can only be reached by either Knudsen flow or surface diffusion, one of these processes must play an important part in the phenomena observed. (See Section 5.4.)

5.3. Initial Adsorption Rates.—The curves for carbon monoxide in Fig. 2 show an initial rate of slightly above 1 l./sec. cm.² or 10 l./sec. for an area of 10 cm.². This value is so high that it may be easily influenced by impurities in the gas (see Sec. 4.4) and by the flow resistance of the connection to the ionization gage ($F_s = 20 \text{ l./sec.}$, see Sec. 4.2.). In order to eliminate these two influences, the diameter of the capillary between the two ionization gages was increased from 2 to 4 mm., giving a conductance $F = 160 \text{ cm.}^3/\text{sec.}$, and the connection between the capillary and Gage S was relocated in such a way that the gas passed over the adsorbent before it reached the gage. Since the gas flow into the gage is negligible compared with that into the adsorbent, the pressure p_s measured in the gage then indicates the true pressure above the adsorbent, and from this pressure the true rate can be derived.

"Rate versus quantity curves" measured in such a system are shown by the dashed curves in Fig. 2. The value measured for the initial adsorption rate ($5 \pm 0.5 \text{ l./sec. cm.}^2$) may be compared with the rate at which the gas molecules impinge upon 1 cm.² of the geometric area of the adsorbent which is

$$u = 3638\sqrt{T/M} \text{ cm.}^3/\text{sec. cm.}^2 \quad (11)$$

(see, for instance, Dushman,¹³ p. 17), (Table I).

TABLE I
INITIAL ADSORPTION RATES FOR DIFFERENT GASES
ADSORBED BY BARIUM ($T \approx 300^\circ\text{K.}$)

Gas	Max. theoretical rate cm. ³ /sec. cm. ²	Measured rate, cm. ³ /sec. cm. ²	No. of mono- layers adsorbed	Measured rate Theoretical rate
CO	11,900	5000	0.05	0.4
CO ₂	8,800	5000	0.05	.6
O ₂	11,100	300	0.02	.02
H ₂	44,600	50	2	.001
N ₂	11,900	1	0.02	.0003

The fourth column of this table gives the number of monolayers which were adsorbed before and during measurement of the rates listed in column 3. It is seen that the rates in the table correspond to a very early state of adsorption, except for hydrogen where the initial adsorption by gages and glass is much more pronounced and, therefore, more difficult to eliminate.

(13) S. Dushman, "Vacuum Technique," New York, N.Y., 1949, p. 17.

From the values in Table I, the probability of adsorption or sticking probability, indicating the proportion of molecules which are adsorbed after impact, can be derived. If exact values of this probability are to be obtained, the area of the deposit which is exposed to the direct impact of gas molecules must be known. However, it can be assumed that this area, as opposed to the internal surface area, is only slightly larger than the geometric area (not more than 100%), which is confirmed by the observation that the rate values observed for carbon monoxide were not very much affected by sintering of the deposits (heating the barium deposit for 15' at 250° reduced the rate by about 20%).

It follows from this that the ratios quoted in the last column of Table I can be taken as approximate values of the adsorption probability. The probabilities obtained for carbon monoxide and carbon dioxide are of the same order as those found by Becker and Hartman⁷ for adsorption of nitrogen on tungsten.

5.4. Influence of Thickness of Deposit on Capacity.—The total quantity of gas which can be taken up by the adsorbent can only be defined accurately by correlating it to a certain minimum value of the rate. Two such quantities, or capacities, will be defined here: the capacity C_{50} adsorbed until the rate falls to 50 cm.³/sec. cm.², and the capacity C_5 adsorbed until the rate falls to 5 cm.³/sec. cm.².

Consistent capacity values were only obtained if the surface of the glass cylinder was cooled during evaporation; a water bath was found adequate for this.

In Fig. 3 the two capacities C_{50} and C_5 are plotted as a function of the thickness, expressed in mg./cm.² The results agree with those by Beeck, Smith and Wheeler¹⁴ and Rideal and Trapnell¹⁵ in so far as the measured capacities increase with thickness. However, the increase in capacity shows a saturation effect occurring for C_{50} at a smaller thickness than for C_5 . It is thought that this saturation is due to the fact that the adsorbed gas must diffuse into deeper and deeper layers of the adsorbent when its thickness is increased. Owing to this, the rate is more and more limited by diffusion and the tail part of the "rate versus quantity curves" becomes more and more pronounced (see Fig. 2, curves D and E).

Capacity values for some other metals investigated will be seen in Table II. With calcium and lithium, the adsorbed quantities were some-

where in between those for nickel and magnesium. Aluminum gave only a very slow adsorption at a rate of about 0.2 cm.³/sec. cm.², which agrees with observations by Trapnell.¹⁶ No adsorption was observed with silver (observed rate less than 0.1 cm.³/sec. cm.²).

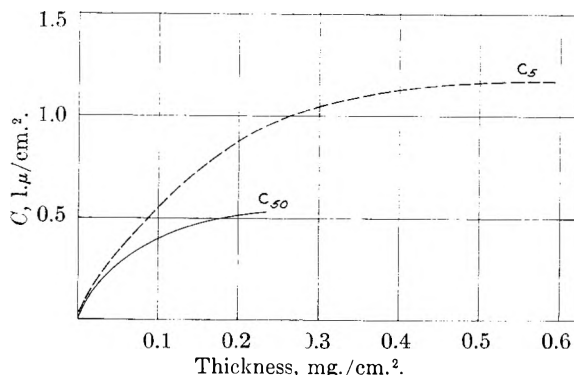


Fig. 3.—Capacity for adsorption of carbon monoxide by barium as a function of the thickness of the deposit ($T = 300^\circ\text{K}.$).

5.5. Influence of Temperature on Capacity.—The influence of temperature was studied by taking a "rate versus quantity curve" first at a low temperature then pumping off and subsequently taking a second curve at a higher temperature. After heating, the initial rate was nearly the same as it was before. It is thought that this is due to diffusion of gas into the deeper layers of the deposit, owing to which the surface is freed from gas, and renewed adsorption can take place. A second possibility would be that the gas, which was adsorbed on the cold adsorbent, is desorbed during heating. However, it will be shown in Sec. 5.7 that this possibility can be excluded.

The increase in capacity due to heating, will be seen from Table III. While the capacity increases slowly up to a temperature of about 400°K., a rapid increase is observed above this value. Evidently, diffusion becomes much more pronounced when this temperature is exceeded.

TABLE III

PERCENTAGE INCREASE ΔC OF ADSORPTION CAPACITY WITH TEMPERATURE OF ADSORBENT (Ba-CO)

Temp., °K.	ΔC_{50}	ΔC_5	Temp., °K.	ΔC_{50}	ΔC_5
78	0	0	475	49	86
200	1.5	7	500	93	127
300	5	16	580	315	365
400	7.5	23			

5.6. Measurement of Activation Energies.—The activation energy of the adsorption process in question can be determined from measurements of the initial rate at different temperatures.^{2,17} During such measurements, variations of rate which are not due to the temperature as such have to be avoided. Such variations may be caused either by the quantity of gas adsorbed during measurement or by changes in the structure of the adsorbent due to heating. The first cause can be eliminated by keeping the pressure above the

TABLE II

QUANTITIES OF CARBON MONOXIDE ADSORBED BY SOME METAL DEPOSITS ($T \approx 300^\circ\text{K}.$)

Metal	Thickness of deposit, mg./cm. ²	C_{50}		C_5		No. of measurements
		l.μ/cm. ²	Mono-layers	l.μ/cm. ²	Mono-layers	
Ba	0.050	0.28	23	0.33	27	5
Sr	.050	.093	5.5	.13	7.5	1
Ni	.036	.041	0.8	.052	1.0	4
Mg00005	0.002	1

(14) O. Beeck, A. Smith and A. Wheeler, *Proc. Roy. Soc. (London)*, **A177**, 62 (1940).

(15) E. K. Rideal and B. M. W. Trapnell, *ibid.*, **A205**, 409 (1951).

(16) B. M. W. Trapnell, *ibid.*, **A218**, 566 (1953).

(17) S. Wagener, *Vacuum*, **III** [1] 11 (1953).

adsorbent at a sufficiently low level, the second one by beginning measurements at the highest temperature and working downward from there.

The activation energies shown in Table IV were measured at $p_s \leq 10^{-7}$ mm. (except the value for N_2 where $p_s \cong 5 \times 10^{-6}$). In the systems Ba-CO and Ba-CO₂, the activation energy is lower than the limit of measurability.

TABLE IV
ACTIVATION ENERGIES OF ADSORPTION PROCESSES

Ad- sorbent	Gas	Temp. range, °K.	Activation energy, kcal./mole	Gages used for measure- ments
Ba	CO	325-500	≤ 0.1	Ionization Knudsen
Ba	CO ₂	325-500	< 0.2	Ionization
Ba	O ₂	225-500	0.09	Ionization Knudsen
Ba	N ₂	320-520	4	Ionization

5.7. Investigations on Desorption.—Let us consider the adsorption of carbon monoxide by barium described by curve B in Fig. 1. This curve can be broken off at any time by suddenly closing the leak valve and pumping off the gas, for instance, at $t = 6$ minutes corresponding to an adsorption rate of about 15 cm.³/sec. After closing the leak, the two pressures p_s and p_p at the ends of the capillary fall as indicated by the dashed and dotted curves in Fig. 4. The fall in pressure p_s above the adsorbent can be compared with the appropriate

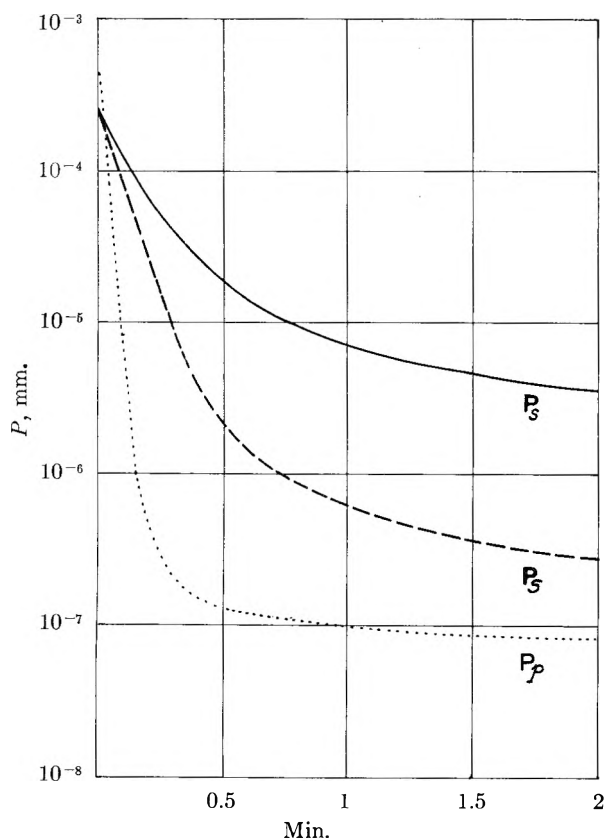


Fig. 4.—Variation of pressures p_p and p_s when pumping off the gas used for adsorption measurements: —, p_s without adsorbent; - - - - - , p_s with 10 cm.³ barium as adsorbent.

fall obtained when no adsorbent is present (full curve). Figure 4 shows that with barium-carbon monoxide the pressure p_s is considerably lower in the presence of the sorbent than it is without it. This clearly indicates that adsorption is going on during the entire pumping-off process, and that there is no desorption.

The procedure described above provides a method for discriminating between physical and chemical adsorption which has the advantage that it can be used for any state of the adsorbent independent of the quantity of gas which was adsorbed previously. Measurements of this type showed that adsorption in the systems barium-carbon monoxide, barium-hydrogen and barium-nitrogen are chemical.

If desorption cannot be obtained at room temperature, the next step evidently is to undertake similar measurements at higher temperatures. Such investigations, which were carried out for the combinations Ba-CO, Ba-CO₂ and Ba-O₂, were described in an earlier article¹⁷ and were repeated since. In the case of Ba-CO for instance, the pressure of the desorbed gas remains smaller than 10^{-7} mm. when the temperature of the barium deposit is raised to 400°.

6. Conclusions.—Carbon monoxide is chemisorbed by deposits made from barium, strontium and nickel at a rate of 5 l./sec. cm.². The activation energy of this adsorption process is smaller than 0.1 kcal./mole, and the equilibrium pressure of desorbed carbon monoxide is less than 10^{-7} mm. at temperatures up to 400°. On the other hand, adsorption of carbon monoxide on magnesium, aluminum and silver is either very slow (< 5 cm.³/sec. cm.²) or non-existent. Carbon dioxide, although not investigated as extensively as carbon monoxide, behaves in a similar way.

The above classification, showing barium on one side and magnesium on the other, indicates that chemisorption is not confined to transition metals. However, the view that chemisorption is due to unfilled or filled d-shells (*e.g.*, Wheeler¹⁸) is supported by these results. Barium and strontium have such an unfilled d-shell (5 d or 4 d resp.) while magnesium has not.

A characteristic feature of the adsorption of carbon oxides is that the high rate is maintained during the greater part of the adsorption process. According to Ehrlich,¹⁹ such a behavior can be explained theoretically. Assuming that chemisorption is preceded by physical adsorption, Ehrlich showed that the adsorption rate will vary very little with adsorbed quantity during the initial stages of adsorption, if the activation energy is small. This is what actually was observed with the carbon oxides.

The fact that the adsorbed quantity increases with the temperature of the deposits indicates that diffusion processes play an important part in the phenomena investigated. Two types of such processes appear to exist: a slow one at temperatures below 400°K. and a faster one at higher tempera-

(18) H. Wheeler in "Structure and Properties of Solid Surfaces," by R. Gomer and C. S. Smith, University of Chicago Press, 1953, p. 439.

(19) G. Ehrlich, *THIS JOURNAL*, **59**, 473 (1955).

tures. It is assumed that the slow process is produced by Knudsen flow which only increases with the square root of the temperature, while the fast one is due to surface migration which will increase with temperature exponentially.

In conclusion, the author wishes to express his appreciation to Dr. J. P. Cels for providing the chemical analyses and to Mr. E. Palsha for his assistance in the experiments, both being with Kemet Company.

VAPOR PRESSURES AND ACTIVITIES IN THE SYSTEM DIOXANE-WATER. SECOND VIRIAL COEFFICIENTS IN THE GASEOUS SYSTEM NITROGEN-DIOXANE-WATER¹

BY A. L. BACARELLA, ARTHUR FINCH AND ERNEST GRUNWALD

Chemistry Department, Florida State University, Tallahassee, Florida

Received September 27, 1955

Vapor pressures and activities in the system dioxane-water were measured by a combination of the static and dynamic method. There are considerable deviations from the ideal laws even in the gas phase. The second virial coefficient for the dioxane-water interaction, -7500 ml. at 25° , is especially large and negative and reflects the tendency of these molecules to form hydrogen-bonded complexes.

Accurate values of the thermodynamic properties of liquid mixtures continue to be of theoretical as well as practical interest. The present note describes some studies in the system dioxane-water. Two experimental methods were used: orthobaric vapor pressures were measured by the static method; and the compositions of the gas mixtures, in equilibrium with the liquids in the presence of nitrogen, were determined at a total pressure of 1 atm. by a dynamic method similar to that described by Washburn and Heuse.²

Experimental

Orthobaric Vapor Pressures.—The static method, using the apparatus described by Dever,³ was employed. Each sample was first outgassed to constant vapor pressure; about 40 experimental points were then obtained in the 25 – 35° range. Pressure equilibrium was approached from both lower and higher temperatures. The composition of the liquids, determined before and after each set of measurements, did not change significantly ($<0.03\%$). For each dioxane-water composition, measurements were made on two liquid samples and the results agreed closely.

Pressure readings were corrected to standard gravity, and temperatures were read to 0.01° on a thermometer recently calibrated by the National Bureau of Standards. The vapor pressures were accurate to at least 0.25% . The vapor pressure of pure water, determined on the apparatus before and after the measurement of the dioxane-water mixtures, was within 0.17% of accepted values⁴ in the experimental range; that of methanol was consistent to 0.1% with other thermodynamic data.³

Gas Phase Compositions.—A known mole number of nitrogen was passed over and equilibrated with liquid samples at a total pressure of 1 atm. The gas mixture was then passed through a cold trap where the vapors were recondensed. From the weight and composition of the condensates and from the mole number of nitrogen, the mole fractions of nitrogen and of the vapor components in the gas phase were computed.

The apparatus of Washburn and Heuse² was modified as follows⁵: the saturators consisted of 50 ml., 14 mm. i.d.

Pyrex tubes connected in pairs by terminal U-tubes. They had central 18/6 ground-glass ball joints, so that sections of several pairs could be connected in series by U-tubes bearing 18/6 socket joints.

More than 20 ml. of liquid in each saturator caused mechanical spray of liquid by the nitrogen. To minimize the danger of spray, the last two saturators in any train were kept dry and were connected to the preceding saturator *via* a U-tube with 3 or 4 helical turns packed with Pyrex helices. For complete saturation of the nitrogen, 6–8 saturators were used.

The vapor traps were conventional cold traps immersed in Dry Ice-acetone and were connected to a Nesbitt absorber containing magnesium perchlorate. The cold traps gave quantitative pick-up of water and dioxane. Since the magnesium perchlorate gave quantitative pick-up of water and better than 90% pick-up of dioxane,⁶ the Nesbitt absorbers both served as a check for the cold traps and safeguarded the traps against back diffusion of vapor from the next series of saturators or from the atmosphere.

A new method for rocking was devised,⁷ which required a smaller motor and facilitated entry and removal of the apparatus from the bath. The angle brass frame (on which the apparatus was mounted) had a longitudinal slot filed into its base which fitted on to a brass knife-edge located on the bottom of the water thermostat. The frame, resting on this knife-edge, was connected *via* an eccentric to a motor and was rocked at 20 cycles per minute, through about 10° from the vertical.

The mounting of saturators and traps on the frame was unexceptional.^{2,5} The saturators were completely immersed in the water thermostat whose temperature was maintained within 0.002° by means of a mercury regulator and $1/8$ H.P. stirrer. Connecting tubes between saturators and cold traps had ball-and-socket joints and were heated, where necessary, to prevent premature condensation of vapor.

In a typical run, two trains (saturators and trap) were connected in series. One contained a reference liquid, the other an unknown liquid. Nitrogen was allowed to flow at the rate of 2 l./hr. until equilibrium was reached (2–4 hr.). The cold traps were tared, and the flow resumed until about 4–10 g. of vapor was condensed in the traps (20–40 hr.). To keep the condensate from clogging the traps, it was sometimes necessary to interrupt the flow and melt the condensate. At the end of a run, the traps were brought to room temperature, weighed (to an accuracy of 1 mg.), and the composition of the condensates immediately determined.

Weight increases of the traps were corrected as follows: (a) For the pressure drop, averaging 0.0003 atm., between

(6) A. L. Bacarella, D. F. Dever and E. Grunwald, *Anal. Chem.*, **27**, 1833 (1955).

(7) We are indebted to Mr. Ralph W. White of the Brookhaven National Laboratory for the design and construction of this apparatus.

(1) Work supported by the Office of Naval Research. Reproduction in whole or in part is permitted for any purpose of the United States Government.

(2) E. W. Washburn and E. O. Heuse, *J. Am. Chem. Soc.*, **37**, 309 (1915).

(3) D. F. Dever, A. Finch and E. Grunwald, *THIS JOURNAL*, **59**, 668 (1955).

(4) F. G. Keyes, *J. Chem. Phys.*, **15**, 611 (1947).

(5) For further details, see A. L. Bacarella, Ph.D. dissertation, Fla. State University, Tallahassee, Fla., 1953.

the two traps. (b) For the loss of vapor and nitrogen while the traps warmed to room temperature. Vapor-loss depends on the warming-up method. The traps may be kept stoppered until room temperature is reached, and then brought to atmospheric pressure; or they may be allowed to warm at atmospheric pressure. By the first method, vapor-loss could amount to as much as 1 mmole for the most volatile vapors. The second method minimizes vapor-loss, since most of the excess nitrogen leaves the trap while the condensate is cold. Loss amounted to considerably less than 0.1 mmole, and could be estimated with sufficient accuracy from previous data for the dioxane-water system.^{8,9} The second method therefore was used; the traps were protected from atmospheric moisture by a drying tube filled with magnesium perchlorate. Vapor loss correction was usually less than 0.1%.

(c) For buoyancy. The ratio of the mass of the unknown vapor condensate to that of the reference condensate, after full correction, is herein termed the *mass ratio*, and is the experimental quantity in the subsequent calculations. The reference liquid was 50.00 wt. % dioxane in all experiments. All mass ratio determinations were made in two or more replications, values of which were within an 0.1% range, except for benzene/50% dioxane and water/50% dioxane, where the standard deviations were 0.12 and 0.33%, respectively. However, with sufficient experiments, the standard deviations of the mean values were brought to 0.05 and 0.10%, respectively.

With the dioxane-water mixtures, the composition of the liquid in the last two saturators was checked in two cases by refractometry at the conclusion of a run and was identical to the initial value.

Composition of most of the vapor condensates of the dioxane-water mixtures was analyzed with a Bausch and Lomb dipping refractometer. Readings were taken at $25.00 \pm 0.005^\circ$, with a mean accuracy (based on samples of known composition) of 0.02%, and maximum error of 0.05%. To ensure their being air- and water-tight, the 6-ml. samples were placed in 10-ml. weighing bottles which fitted into the metal beaker and over the refractometer prism.

The condensates from 50% dioxane were analyzed by interferometry, according to a new method.¹⁰ With carefully prepared standard samples, this method was accurate to ± 0.005 wt. % in the experimental range. The composition of the vapor condensates proved to be reproducible to 0.007%.

Correction was made for the amount of condensate volatilized while the cold traps warmed to room temperature, since the volatilized material is enriched in dioxane. Sufficient accuracy was obtained with existing pressure-composition data^{8,9}; the correction was about 0.02%.

Materials.—Distilled water was redistilled from alkaline potassium permanganate solution and was protected from the atmosphere by a soda lime tube.

Dioxane was purified by the method of Marshall and Grunwald.¹¹ Each batch was titrated for water ($>0.02\%$) by the Karl Fischer method before preparation of the mixed solvents. Freezing curve analysis showed that the mole fraction of total impurity was equal to the Karl Fischer titer for water; refractive index: $n^{25.00D}$ 1.42006; $n^{29.50D}$ 1.41796; m.p. 11.78° .

Benzene was purified by repeated crystallization and distillation. A freezing point curve of the final product showed less than 0.02% impurity.

Results

Vapor Pressures.—Vapor pressures were measured at 25–35°. In this rather narrow range, the data are accurately represented by empirical equations of the form

$$\log p^0 = b - a/T \quad (1)$$

and large scale plots of $\log p^0$ vs. $1/T$ showed no

(8) A. L. Vierck, *Z. anorg. Chem.*, **B261**, 283 (1950).

(9) F. Hovorka, R. A. Schaefer and D. Dreisbach, *J. Am. Chem. Soc.*, **58**, 2264 (1936); **59**, 2753 (1937).

(10) B. J. Berkowitz and E. Grunwald, *Anal. Chem.*, in preparation.

(11) H. P. Marshall and E. Grunwald, *J. Am. Chem. Soc.*, **76**, 2000 (1954)

systematic curvature. Values of the constants a and b for pure dioxane, 50 wt. % dioxane and 70.50 wt. % dioxane are summarized in Table I. The standard error of estimate of p^0 from equation 1 in the range 25 to 35° is calculated¹² to be 0.1%.

TABLE I
CONSTANTS IN VAPOR PRESSURE EQUATIONS^a

Wt. % dioxane	b	a	\bar{L}_1 (kcal.)	\bar{L}_2 (kcal.)	a (predicted)
50.00	8.9123	2,173.4	10.49	8.77	2,105
70.50	8.8032	2,128.5	10.48	8.78	2,141
100.00	8.3159	2,014.8	...	9.22	2,016

^a For p^0 in mm.

On the other hand, our new vapor pressure data differ significantly from previous values.^{9,13} Some relevant comparisons are made in Table III.^{12a}

TABLE II
COMPARISON OF VAPOR PRESSURE DATA, 25.00°

Wt. % dioxane	p^0 (mm.)		
	This work	Ref. 9	Ref. 13
50.00	41.97	41.6	...
70.50	46.18	46.4	...
100.00	36.18	36.9	35.7

The empirical representation of our data by equation 1 is consistent with the heats of vaporization recently measured at 40°. For a 2-component liquid, and assuming ideal laws

$$\frac{d \ln p^0}{d(1/T)} = \frac{-p_1 \bar{L}_1 + p_2 \bar{L}_2}{p^0 R} \quad (2)$$

where \bar{L}_1 and \bar{L}_2 are the partial molal heats of vaporization and p_1 and p_2 the partial pressures of the two components. Since p_1/p^0 and p_2/p^0 are functions of T , the right-hand side of 2 is a function of T even if \bar{L}_1 and \bar{L}_2 are constant, unless $\bar{L}_1 = \bar{L}_2$. Values for \bar{L}_1 and \bar{L}_2 were computed from the data of Stallard and Amis^{14,15} for 50.00 and 70.50 wt. % dioxane and are included in Table I. From the experimental vapor pressures and compositions at 25.00° (Tables I, III), p_1 and p_2 were computed (assuming Dalton's law); from these and equation 2, $p^0 = p_1 + p_2$ was computed at other temperatures up to 35°. On a scale compatible with the accuracy of our data, the resulting plots of $\log p^0$ vs. $1/T$ were absolutely linear. The slopes thus predicted are also given in Table I. Their agreement with the experimental data is satisfactory. The mean deviation is 1.3%, and all deviations are within the combined experimental error of the source data.

Mass Ratios.—The mass ratios of the vapor condensates at 25.00° are summarized in Table III.

(12) H. Margenau and G. M. Murphy, "The Mathematics of Physics and Chemistry," D. Van Nostrand Co., New York, N. Y., 1943, p. 502.

(12a) NOTE ADDED IN PROOF.—The agreement is much better with the vapor pressures reported by A. Niini, *Ann. Acad. Scient. Fennicae*, **A55**, No. 8. At 20.00° the values for 50.00, 70.50 and 100.00 wt. % dioxane are: 31.51; 34.64, 27.51 mm. (Niini); 31.52; 34.89, 27.75 mm. (this work).

(13) W. Herz and S. Lorentz, *Z. physik. Chem.*, **A140**, 406 (1929).

(14) R. D. Stallard and E. S. Amis, *J. Am. Chem. Soc.*, **74**, 1781 (1952).

(15) Their calculations¹⁴ of \bar{L}_1 and \bar{L}_2 are incorrect, since they use the molar composition of the liquid, instead of the gaseous, phase in calculating molar heats of vaporization.

The data were corrected from the barometric pressure during the experiment to exactly 1 atm. using the ideal gas laws. The reference liquid was 50.00 wt. % dioxane. Table III lists also the composition of the vapor condensates.

TABLE III

EXPERIMENTAL MASS RATIOS AND VAPOR CONDENSATE COMPOSITIONS, 25.00°, IN THE PRESENCE OF NITROGEN AT 1 ATM. TOTAL PRESSURE^a

Liquid	Mass ratio	Vapor condensate wt. % dioxane
50.00 wt. % Dioxane	1.0000	83.524
40.00 wt. % Dioxane	0.8449	79.90
60.31 wt. % Dioxane	1.1287	85.86
70.50 wt. % Dioxane	1.2193	87.38
100.00 % Dioxane	1.3937	...
100.00 % Water	0.18339	...
Benzene	3.570	...

^a These data have been fully corrected, as described in the experimental section.

Calculations

General Remarks.—We shall use the symbols x , y and z to denote mole fractions in the liquid phase (x), in the vapor phase under orthobaric conditions (y), and in the vapor phase in the presence of nitrogen at a total pressure of 1 atm. (z). The subscript 1 will refer to water, 2 to dioxane, 3 to nitrogen and 4 to benzene. (Benzene is used as the standard liquid, as will be discussed later.) In computing x_1 and x_2 , the solubility of nitrogen in the liquid phase is neglected; x_3 is less than 0.0005 in pure benzene and pure water at 1 atm.¹⁶ and may be expected to be similarly small in the dioxane-water mixtures. All calculations are based on the slightly imperfect real gas model,¹⁷ which should be sufficiently accurate at the low pressures involved. Thus, for a 3-component gas mixture

$$PV/n = RT + B_m P \quad (3)$$

$$B_m = z_1^2 B_{11} + z_2^2 B_{22} + z_3^2 B_{33} + 2[z_1 z_2 B_{12} + z_1 z_3 B_{13} + z_2 z_3 B_{23}] \quad (4)$$

and the fugacity of, say, component 1

$$f_1 = z_1 P \exp \left\{ \frac{P}{RT} [B_{11}(2z_1 - z_1^2) + 2B_{12}z_2(1 - z_1) + 2B_{13}z_3(1 - z_1) - B_{22}z_2^2 - B_{33}z_3^2 - 2B_{23}z_2z_3] \right\} \quad (5)$$

where n is the total mole number and the B 's are the second virial coefficients.¹⁷⁻²⁰ Accordingly, calculation of fugacity involves knowledge of the mole fractions and of six virial coefficients.

Virial Coefficients.—The following virial coefficients were used for the vapors at 25°. For water, $B_{11} = -1163$ ml.⁴; for dioxane, $B_{22} =$

-1690 ml.²¹; for nitrogen, $B_{33} = -6$ ml.¹⁸; and for benzene, $B_{44} = -1415$ ml.²²

B_{43} may be estimated theoretically with fair accuracy since benzene and nitrogen are both non-polar. Thus, B_{43} is estimated as -150 ml. by the method of Guggenheim,¹⁷ and as -164 ml. by the method of Scatchard and Ticknor.²⁰ The former value has been used in subsequent calculations, but the final results for the dioxane-water system are not sensitive to the difference, as demonstrated in Table V.

B_{13} and B_{23} were measured by means of experimental mass ratios and orthobaric vapor pressures, using benzene as the standard liquid since its orthobaric vapor pressure has been defined within 0.1%,²³ and since the estimation of B_{43} is quite certain. In the presence of nitrogen, the fugacity f_4 is given by

$$f_4 = p_4^0 \exp \{ [B_{44}p_4^0 + v_4(P - p_4^0)]/RT \} \quad (6)$$

$$= z_4 P \exp \left\{ \frac{P}{RT} [B_{44} + (1 - z_4)^2(2B_{13} - B_{44} - B_{33})] \right\} \quad (7)$$

where the total pressure p is 1 atm. and v_4 is the molar volume of liquid benzene. In equation 6 f_4 is corrected from the orthobaric value to 1 atm., and in equation 7 f_4 is expressed by equation 5 specialized for a 2-component mixture. Using the numerical values given in Table V, z_4 is calculated as 0.12772. Thus one mole of nitrogen entrains 11.436 g. of benzene in the dynamic apparatus.

From this information and the mass ratios in Table III, $z_1 = 0.03158$ and $z_2 = 0.04822$ in the presence of nitrogen at 1 atm. From these values and known values of p^0 and v , B_{13} and B_{23} are then calculated analogously, as shown in Table IV. The standard error of B_{13} and B_{23} is about ± 25 ml., plus the error in B_{43} .

TABLE IV
CALCULATION OF B_{13} AND B_{23} , 25.00°

Substance	$\frac{p^0}{(\text{mm.})}$	$\frac{v}{(\text{ml.})}$	B_{13}	
4. Benzene	95.25	89	$(-150)^a$	$(-229)^b$
1. Water	23.752	18	-111	-177
2. Dioxane	36.18	86	-91	-157

^a Estimated by the method of Guggenheim.¹⁷ ^b An arbitrary estimate, serving mostly to show the insensitivity of subsequent calculations to B_{43} .

Calculation of B_{12} .— B_{12} was obtained from vapor pressure-mass ratio-vapor composition data for dioxane-water mixtures by a similar procedure. The working equations are

$$f_1 \text{ (as given by eq. 5)} = f_1^0 \exp \{ \bar{v}_1 [P - p^0]/RT \} \quad (8)$$

where \bar{v}_1 is the partial molar volume in the liquid phase, and f_1^0 is the fugacity under orthobaric conditions. Further,

$$f_1^0 = y_1 p^0 \exp \{ p^0 [B_{11} + y_2^2(2B_{12} - B_{11} - B_{22})]/RT \} \quad (9)$$

(21) This is the average of the following estimates: -1694 ml. (from the empirical equation of Scott, *et al.*, *J. Am. Chem. Soc.*, **72**, 2424 (1950), equation 2), and -1680 ml. (from critical constants¹⁸ and the Berthelot equation).

(22) P. G. Francis, M. L. McGlashan, S. D. Hamann and W. J. McManamy, *J. Chem. Phys.*, **20**, 1341 (1952).

(23) E. R. Smith, *J. Research Natl. Bur. Standards*, **26**, 129 (1941); C. B. Willingham, W. J. Taylor, J. M. Pignoco and F. D. Rossini, *ibid.*, **35**, 219 (1945); J. H. Baxendale, B. W. Enustun and J. Stern, *Trans. Roy. Soc. (London)*, **A248**, 169 (1950); P. W. Allen, D. H. Everett and M. F. Penney, *Proc. Roy. Soc. (London)*, **A212**, 149 (1952).

(16) "International Critical Tables," Vol. III, McGraw-Hill Book Co., New York, N. Y., pp. 256, 262.

(17) E. A. Guggenheim, "Mixtures," Oxford University Press, 1952, Chapter 8.

(18) J. A. Beattie and W. H. Stockmayer, in "Treatise on Physical Chemistry," Vol. 2, H. S. Taylor and S. Glasstone, editors, D. Van Nostrand Co., New York, N. Y., 1951.

(19) Equation 5 is consistent with equation 1 of Scatchard and Ticknor.²⁰

(20) G. Scatchard and L. B. Ticknor, *J. Am. Chem. Soc.*, **74**, 3724 (1952).

Combining equations 8 and 9, f_1° may be eliminated and the resulting expression contains the experimental quantities p^0 , \bar{v}_1 , the z 's and the y 's, and six virial coefficients of which B_{12} is the only unknown. Of the experimental quantities, p^0 is obtained from the data in Table I, \bar{v}_1 from the literature,⁹ and the z 's from the mass ratio and vapor composition data. The y 's are computed from the z 's by means of the equation

$$z_1 y_2 / y_1 z_2 = \exp \{ (\bar{v}_2 - \bar{v}_1 + B_{13} - B_{23})(P - p^0) / RT \} \quad (10)$$

derived as follows. A general expression for $z_1 y_2 / y_1 z_2$ is obtained from equations 5, 8, 9 and their analogs for component 2, and is simplified to the form (10) by making the approximations

$$\exp \{ B_{13} z_1 P / RT \} = \exp \{ B_{13} f_1^0 / RT \}, \quad (i = 1, 2); \text{ and} \\ \exp \{ B_{23} z_2 P / RT \} = \exp \{ B_{23} (P - p^0) / RT \}$$

Except for higher-order terms, $z_1 y_2 / y_1 z_2$ is thus independent of B_{12} and, since it contains only the difference $B_{13} - B_{23}$, is very nearly independent of the initial estimate for B_{43} . This is shown by the data in Table IV where a change of B_{43} from -150 ml. to -228 ml. has no effect on $B_{13} - B_{23}$. The values of $z_1 y_2 / z_2 y_1$ were in the neighborhood of 0.998.

The values of B_{12} calculated from the data for 50.00% and 70.50% dioxane are listed in Table V. The discrepancy between the two values is 4%. For comparison, errors of 0.1% in p^0 , 0.05% in vapor composition, and 0.05% in mass ratio would lead to errors in B_{12} amounting to 10, 13, and 5%, respectively. The close agreement is therefore an indication of the internal consistency of our data.

TABLE V
CALCULATION OF B_{12} (ML.), 25.00°

Data for	Based on $B_{43} =$	
	-150 ml.	-228 ml. ^a
50.00% dioxane	-7596	-7685
70.50% dioxane	-7324	-7438
av.	-7460	-7560

^a Arbitrary estimate, showing the insensitivity of B_{12} to B_{43} .

Activities of the Solvent Components.—Values of f_1 were calculated from equation 5 and of f_2 analogously. The activities a_1 and a_2 (with $a = 1.000$ for each pure liquid component) are listed in Table VI. Allowing errors of 0.25% in the fugacity of pure dioxane, 0.1% of pure water, 0.1% in mass ratio, 0.05% in vapor composition, and 0.25% in the orthobaric vapor pressures of the dioxane-water mixtures, the resulting error in a_1 is 0.5–0.7%, and in a_2 , 0.5%; these are thought to be realistic estimates of the *limits* of error of our data, since changing B_{43} from -150 ml. to -228 ml. changes f_1 and f_2 by only 0.01%. Within these error limits, the values of a_1 and a_2 , in Table VI, are also applicable to orthobaric conditions.

The two values of the derivative, $-d \log a_1 / d \log a_2$, shown in Table VI were obtained by nu-

TABLE VI
ACTIVITY DATA FOR THE SYSTEM DIOXANE-WATER, 25.00°

Wt. % dioxane	z_1	a_1	a_2	$-\frac{d \log a_1}{d \log a_2}$	x_2/x_1
0.00	1.000	1.0000	0.0000
40.00	0.880	0.8947	.4760
50.00	.830	.8614	.5862	0 215	0.205
60.31	.763	.8289	.6778	0 34	0.311
70.50	.672	.7959	.7435
100.00	.000	.0000	1.0000

merical differentiation and should, according to the Gibbs-Duhem equation, be equal to x_2/x_1 . The discrepancies between these two quantities are 5 and 10%. Although this is still compatible with the estimated error in a_1 and a_2 due to the loss in accuracy involved in the measurements of a derivative, the 10% discrepancy is disappointingly near the expected limit of error.

Discussion

The present data further demonstrate that deviations from the ideal gas laws may be very large when one or more of the gaseous components are hydroxylic. The formation of several per cent. of hydrogen-bonded dimer is then possible even at relatively low pressures, resulting in large, negative values of the second virial coefficient. The present value for this coefficient— $B_{12} = -7460$ ml.—in the dioxane-water system may be compared with reported values at 25° of -1163 ml. for water, -1693 ml. for methanol, -2980 ml. for ethanol and -3423 ml. for isopropyl alcohol.^{4,24} Compared to the virial coefficients for the alcohols, our value of B_{12} is not unreasonably negative, especially since a statistical factor of 4 favors the dioxane water complex, due to the 2 H-atoms in water and the 2 O-atoms in dioxane. Compared to the virial coefficient for water, our value is reasonable only if dioxane is a better H-bond acceptor than water. Previous evidence, though not conclusive, points to the contrary. Water is probably somewhat more basic than dioxane,²⁵ and the frequency of the O-D stretching vibration in the infrared spectrum of D₂O in dioxane indicates that the hydrogen bond is of only moderate strength.²⁶ On the other hand, the mixing of liquid dioxane with water is quite exothermic.

Because of the large negative value of B_{12} , assumption of the ideal gas laws results in an error several times larger than the experimental error. For example, using the ideal gas laws, a_1 and a_2 for 50% dioxane are calculated to be 0.877 and 0.595, or 2% larger than the corresponding values in Table VI. Similarly large deviations are to be expected in other partly aqueous systems, such as acetone-water or ethanol-water.

(24) C. B. Kretschmer and R. Wiebe, *J. Am. Chem. Soc.*, **76**, 2579 (1954).

(25) L. P. Hammett and A. J. Deyrup, *ibid.*, **54**, 4239 (1932).

(26) W. Gordy, *J. Chem. Phys.*, **9**, 215 (1941).

THE TRANSITION FROM TYPICAL POLYELECTROLYTE TO POLYSOAP.

II. VISCOSITY STUDIES OF POLY-4-VINYLPYRIDINE DERIVATIVES IN AQUEOUS KBr SOLUTIONS^{1,2}

BY ULRICH P. STRAUSS, NORMAN L. GERSHFELD AND EVAN H. CROOK

Ralph G. Wright Laboratory, School of Chemistry, Rutgers University, New Brunswick, New Jersey

Received October 5, 1955

Five polyvinylpyridine derivatives, prepared by quaternizing 0.0, 6.7, 13.6, 28.5 and 37.9% of the nitrogens of poly-4-vinylpyridine (D.P. = 18,000) with *n*-dodecyl bromide and the remainder with ethyl bromide, were compared by viscosity studies in aqueous solutions containing KBr. While on the addition of KBr the viscosity of ordinary polyelectrolyte solutions always decreases, the viscosity of polysoap solutions in many cases goes through a minimum. The viscosity rise with increasing KBr concentration is especially pronounced in concentrated solutions of the "37.9%" polysoap, where it leads to jelly formation. Results obtained in 0.0226 *m* KBr indicate that the five polymers fall into two distinct classes. The first two show normal values of the intrinsic viscosity and of Huggins' constant, k' , indicating ordinary polyelectrolyte behavior. The last three have intrinsic viscosities between 0.042 and 0.085, and k' -values ranging from 2 to 10. These intrinsic viscosities are an order of magnitude smaller than those estimated for random coils, indicating that the polysoap molecules reach degrees of compactness which ordinary polymers and polyelectrolytes cannot attain in homogeneous solution. The sudden change from polyelectrolyte to polysoap behavior, which occurs over a narrow composition range, suggests the existence of a *critical dodecyl group content* analogous to the *critical micelle concentration* of ordinary soaps. The high k' -values are ascribed to aggregation of polysoap molecules due to "sticky," hydrophobic spots on their surface. The existence of such aggregates has been confirmed by utilizing the slowness of both the aggregation and the disaggregation processes at 25°. The rates of these processes are highly temperature sensitive, indicating a considerable activation energy. Possible explanations for the various unusual features of polysoap behavior are offered.

Introduction

In the first paper of this series the viscosity behavior of aqueous solutions of poly-4-vinyl-N-ethylpyridinium bromide and of four polysoaps, prepared by quaternizing 6.7, 13.6, 28.5 and 37.9% of the nitrogens of poly-4-vinylpyridine with *n*-dodecyl bromide and the remainder with ethyl bromide, was described.³ The results were explained in terms of the molecular dimensions and the interactions of the polysoap molecules; however, it was difficult to resolve these two properties quantitatively since in the absence of added electrolyte the necessary extrapolation of the reduced viscosity to infinite dilution was not feasible. So that the polyelectrolyte or polysoap concentration could be varied at constant ionic strength and the extrapolation accomplished, the same polymers have been studied in aqueous solutions containing excess KBr.

Such studies are of interest for still another reason. While the familiar viscosity lowering effect of simple electrolytes on polyelectrolyte solutions is at least qualitatively understood,^{4,5} their interesting effects on solutions of colloidal electrolytes, where the viscosity often increases to the point of jelly formation with the addition of simple electrolytes, are less clearly comprehended.⁶ Part of the difficulty of interpreting such results with colloidal

electrolytes lies in the fact that the number of soap⁷ molecules in a micelle can change with environmental changes. With polysoaps this difficulty is removed because the basic kinetic unit is not a colloidal aggregate of small molecules, but a macromolecule containing a fixed number of amphipathic groups. Thus by gaining a better understanding of polysoap behavior, we hope to throw light on the behavior of ordinary soaps.

Since the viscosity behavior of polysoaps in electrolyte solutions has not been previously described, we shall first, after a brief experimental section, present a description and tentative interpretation of some observed effects of the addition of KBr to polysoap solutions. This will be followed by a more quantitative comparison of the five polymers in a KBr solution, with special emphasis on deriving the molecular dimensions and intermolecular interactions from the viscosity data. Finally, we shall study the interactions and show that polysoap molecules have a strong tendency to form aggregates.

Experimental

Materials.—The preparation of poly-4-vinyl-N-ethylpyridinium bromide (our sample No. G 254), henceforth denoted by PEB, and of the "6.7%," "13.6%," "28.5%" and "37.9%" polysoaps⁸ (our samples Nos. G339, G147, G146, G145, respectively) has been described in the first paper of this series.³ The degree of polymerization of the poly-4-vinylpyridine (our sample No. G13) from which these five compounds were prepared was estimated there to be 6,000. This estimate was based on the intrinsic viscosity of this polymer in 92.0 weight % ethanol, and on an osmotic pressure molecular weight–intrinsic viscosity relationship which was derived from the data of three samples reported in the literature. Recently a more reliable light scattering molecular weight–intrinsic viscosity relationship has become available,⁹ and with the aid of this relationship we

(7) The term *soap* is used here in its broader sense including colloidal electrolytes in general.

(8) By an "X%" polysoap is meant a compound prepared from poly-4-vinylpyridine by quaternizing X% of the nitrogens with *n*-dodecyl bromide and nearly all of the remaining nitrogens with ethyl bromide. The terms *dodecyl group content* and % C₁₂, used also in this paper, are equivalent to X.

(9) A. Boyes and U. P. Strauss, unpublished results.

(1) This research was supported by a research grant from the Office of Naval Research. Reproduction in whole or in part is permitted for any purpose of the United States Government.

(2) These results are abstracted from two theses, submitted by Norman L. Gershfeld in 1954 and by Evan H. Crook in 1955 to Rutgers University in partial fulfillment of the requirements for the Ph.D. degree and for the B.S. degree with Special Honors in Chemistry, respectively. Presented before the Division of Polymer Chemistry, 129th meeting of the American Chemical Society, Dallas, Texas, April 9, 1956.

(3) U. P. Strauss and N. L. Gershfeld, *THIS JOURNAL*, **58**, 747 (1954).

(4) R. M. Fuoss and U. P. Strauss, *J. Polymer Sci.*, **3**, 602 (1948); *Ann. N. Y. Acad. Sci.*, **51**, 836 (1949).

(5) D. T. F. Pals and J. J. Hermans, *J. Polymer Sci.*, **3**, 897 (1948); *Rec. trav. chim.*, **71**, 433 (1952).

(6) H. L. Booy, in "Colloid Science," Vol. II, H. R. Kruyt, ed., Elsevier Publishing Co., Inc., New York, N. Y., 1949, Chapter 14.

estimate the weight average degree of polymerization of the parent polymer to be 18,000.

Procedure.—The aqueous solutions containing both polysoap and KBr were prepared by weight. The order of dissolution was immaterial provided that the following precautions for obtaining equilibrium were observed. Unless otherwise stated in the text, all solutions were heated at 45° for at least 24 hours and were then allowed to stand at the viscometer bath temperature for at least another 24 hours before the viscosity was measured.¹⁰

Viscosities were measured in a Bingham viscometer¹¹ whose constant (pt)₀ for water at 25° was 7506 g. seconds per square centimeter. The reduced viscosity is η_{sp}/C , where C is the polymer concentration in grams per 100 ml. of solution, and $\eta_{sp} = (\eta - \eta_0)/\eta_0$, η being the viscosity of the polysoap solution, and η_0 being the viscosity of the solvent KBr solution. Unless otherwise stated in the text, viscosities were measured at 25°.

Results and Discussion

Effect of KBr on Viscosity of Polysoap Solutions.—It is now well known that simple electrolytes depress the viscosity of dilute solutions of ordinary polyelectrolytes.^{4,5} A similar effect is observed when KBr is added to a 1.77% solution of

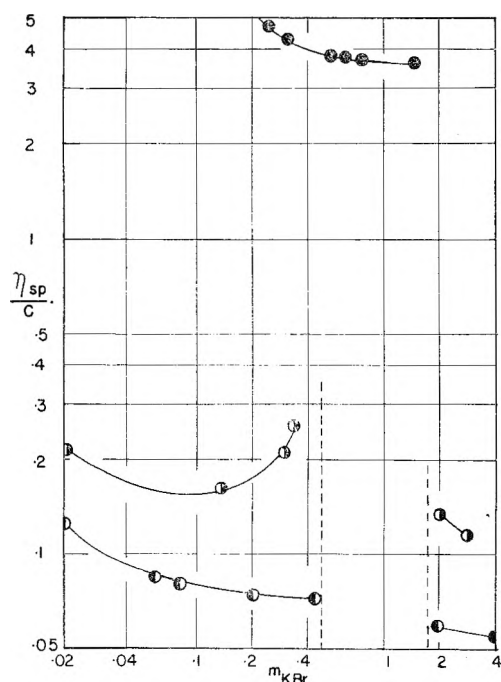


Fig. 1.—Effect of KBr on reduced viscosity of PEB and of “13.6%” polysoap at 25°: ●, 6.00% solution of PEB; ○, 1.77% solution of “13.6%” polysoap; ○, 6.00% solution of “13.6%” polysoap.

(10) The heating to 45° is necessary to break up aggregates of polysoap molecules [U. P. Strauss, S. J. Assony, E. G. Jackson and L. H. Layton, *J. Polymer Sci.*, **9**, 509 (1952)]. As will be shown in the last section of this paper, in some cases a slow partial reversible aggregation takes place when the solutions are cooled to 25° manifesting itself in a slow viscosity increase which levels off completely within 12 hours. By waiting 24 hours, reliably reproducible viscosity values are obtained. Because of this reproducibility, we believe the viscosity values obtained in this manner to represent the true equilibrium states of the solution. In a few instances we have approached equilibrium also from the other direction by diluting a concentrated solution of the “37.9%” polysoap at 25° and following the disaggregation process in the diluted solution by the accompanying viscosity decrease. This process, however, was so slow that the measurements had to be discontinued before the viscosity had completely leveled off. At this stage, the reduced viscosity was in no case more than 25% above the value obtained by the first method.

(11) E. C. Bingham, “Fluidity and Plasticity,” McGraw-Hill Book Co., Inc., New York, N. Y., 1922.

the “13.6%” polysoap, as is illustrated by the bottom curve in Fig. 1. The vertical dotted lines enclose the region in which the “13.6%” polysoap is only partly soluble.¹² It is seen that on both sides of this region the reduced viscosity decreases as the KBr molality increases, reaching values only little more than twice 0.025, the Einstein figure for compact spheres.¹³

A new type of behavior is indicated by the center curve in Fig. 1, which illustrates the effect of KBr on the reduced viscosity of a 6% solution of the same polysoap. While at first the reduced viscosity decreases with increasing KBr molality, it reaches a minimum and increases again near the precipitation region. Beyond this region the reduced viscosity decreases. This behavior is strikingly different from that of a 6% solution of the normal polyelectrolyte, PEB, where with increasing KBr concentration the viscosity decreases uniformly. The lower part of the PEB curve is shown in the top section of Fig. 1. No special effects are observed near the isoelectric point where this polyelectrolyte, which has no dodecyl groups, is completely soluble.¹²

Viscosity minima on the addition of electrolytes have, however, been reported for solutions of ordinary soaps such as sodium and potassium palmitate,^{14–16} and also for dispersions of hydrophobic colloids such as ferric hydroxide.¹⁷

Since the viscosity rise with added KBr occurs only in the more concentrated polysoap solution, it should be ascribed to interactions between polysoap molecules. These interactions will be shown in a later section to involve aggregate formation.

The difference from typical polyelectrolyte behavior and the similarity to ordinary soap behavior is even more striking in the case of the “37.9%” polysoap. The effects of KBr on 6.00% and 1.00% solutions of this polysoap are shown in Fig. 2. As KBr is added at 25° to the 6.00% solution, the reduced viscosity at first decreases slightly then rises increasingly sharply, until at a KBr molality of approximately 0.035 the solution has become a clear thixotropic jelly.¹⁸ With a 1.00% solution a viscosity minimum is also observable, but the rise in the reduced viscosity after the minimum is much less pronounced and no jelly is formed. As the KBr molality is raised above 0.05, the polysoap precipitates as a white curd.

(12) It has previously been shown that in this region poly-4-vinyl-N-alkylpyridinium compounds pass through an isoelectric point due to complex formation with bromide ions. The insolubility region around the isoelectric point becomes wider with increasing hydrophobic group content of the polymers [U. P. Strauss, N. L. Gershfeld and H. Spiera, *J. Am. Chem. Soc.*, **76**, 5909 (1954)].

(13) In order to cover adequately the KBr molality range over more than two decades, the abscissa in Fig. 1 is represented by a logarithmic scale. As a consequence, the reduced viscosity values in the absence of KBr cannot be shown. However, these values can be obtained from Fig. 1 of a previous paper.³ They are approximately 0.3 for each of the bottom and center curves and 30 for the top curve.

(14) F. D. Farrow, *Trans. Chem. Soc. Lond.*, **101**, 347 (1912).

(15) F. Goldschmidt and L. Weissmann, *Z. Elektrochem.*, **18**, 380 (1912).

(16) A. M. King, *J. Soc. Chem. Ind.*, **41**, No. 9, 147 T (1925).

(17) H. W. Woudstra, *Z. chem. Ind. Kolloide*, **8**, 73 (1911).

(18) It is of interest that while such an effect is observed with many ordinary soaps, it could not be obtained with *n*-dodecylpyridinium chloride [W. Philippoff, *Disc. Faraday Soc.*, **11**, 96 (1951)].

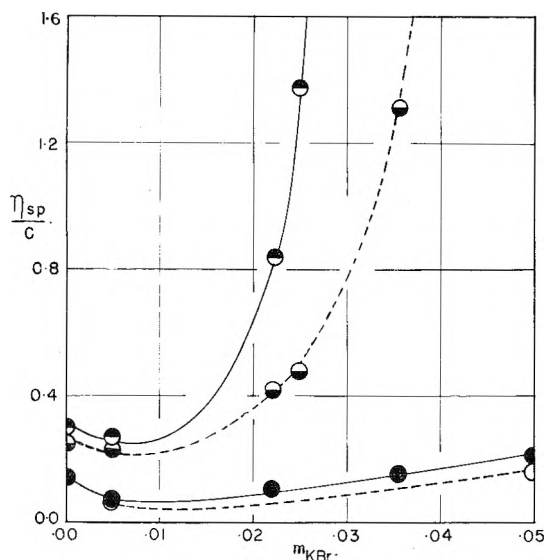


Fig. 2.—Effect of KBr on reduced viscosity of "37.9%" polysoap. 1.00% polysoap solution: ●, 25°; ○, 45°. 6.00% polysoap solution: ◐, 25°; ◑, 45°.

Again the tremendous effect of the polysoap concentration indicates that the viscosity rise is due to interactions between different polysoap molecules. This interpretation is further substantiated by the effect of a temperature increase to 45°. The results at this temperature, which are represented by the dashed curves in Fig. 2, show little deviation from the 25° values where these are relatively small, but exhibit a very strong depression from the 25° values where these are large. Previous observations have shown that the reduced viscosity is quite insensitive to temperature changes when it is controlled mainly by the molecular dimensions of the polysoap molecules, but that it is markedly depressed when it is controlled by interactions between polysoap molecules.^{3,19}

In Fig. 3 an attempt is made to resolve the effects of molecular dimensions and of intermolecular interactions by presenting the "37.9%" polysoap data at 25° as reduced viscosity against concentration plots at various constant KBr molalities. The slopes of the curves which are a measure of the interactions are seen to increase rapidly with increasing KBr content. Because some of these curves are not linear in the lower concentration region, accurate extrapolation to infinite dilution is not attempted. However, it is obvious that the intrinsic viscosity values lie very close together. These results confirm the conclusion that the main effect of KBr on the "37.9%" polysoap molecules is strongly to increase their ability to interact with one another.

Apparently quite a different picture is presented by the "28.5%" polysoap. In Fig. 4 the reduced viscosity against concentration curves are seen to be much less steep than those for the "37.9%" polysoap indicating less interaction. Moreover, since the curves corresponding to the higher KBr molalities are linear they could be extrapolated to obtain intrinsic viscosities which depend only on the configuration of the polysoap molecules. The re-

(19) L. H. Layton and U. P. Strauss, *J. Colloid Sci.*, **9**, 149 (1954).

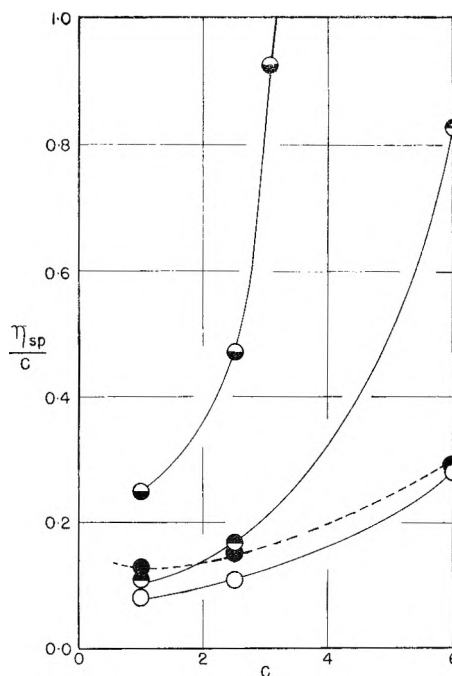


Fig. 3.—Effect of KBr on plot of reduced viscosity against concentration of "37.9%" polysoap at 25°. KBr molality: ●, 0.000; ○, 0.005; ◐, 0.022; ◑, 0.050.

sults show a new and unusual feature. At first the intrinsic viscosity decreases with added KBr, just as it does in the case of ordinary polyelectrolytes. However, the intrinsic viscosity in 0.137 *m* KBr is considerably higher than it is in 0.050 *m* KBr, indicating a minimum in the intrinsic viscosity with added KBr which is not observed with ordinary polyelectrolytes. The intrinsic viscosity decrease may, as usual, be explained in terms of a contraction of the polymer coil caused by a decrease in the electrostatic repulsive forces between different chain segments. Such a decrease in the repulsion with the addition of KBr is to be expected for two reasons: first, the net charge on the polyion is

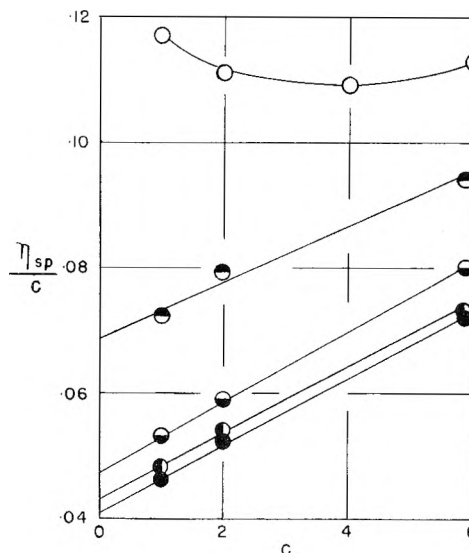


Fig. 4.—Effect of KBr on plot of reduced viscosity against concentration of "28.5%" polysoap at 25°. KBr molality: ○, 0.000; ◐, 0.005; ◑, 0.022; ●, 0.050; ◒, 0.137.

reduced¹²; second, the ionized groups are increasingly shielded by a contracting ionic atmosphere.⁴ The subsequent viscosity increase is more difficult to explain. Perhaps as the already very compact polysoap molecule binds more bromide ions it is somewhat expanded by the volume of these ions. More likely, however, the intrinsic viscosity increase may reflect a change in the shape rather than an isotopic swelling of the compact polysoap molecule. Arguments for the possibility of such shape changes will be presented in the next section. Still another, though in our opinion less likely, possibility is the retention of aggregates even at infinite dilution, as has been observed for some samples of ethyl cellulose in acetone.²⁰ Light scattering studies are planned to clear up this and several other points which cannot be unambiguously explained with the viscosity results alone.

Effect of Dodecyl Group Content on Viscosity in 0.0226 *m* KBr.—We have just seen that the “13.6%,” the “28.5%” and the “37.9%” polysoaps behave quite differently in aqueous KBr solutions. To obtain a more quantitative idea of these differences it was decided to study the viscosimetric behavior of these polysoaps in the same KBr solution. A KBr molality of 0.0226 was chosen as being high enough for the contribution of the weakly ionized polysoaps to the total bromide ion concentration to be negligible and at the same time as being low enough for all the polysoaps to be completely soluble. For comparison the “6.7%” polysoap and the polyelectrolyte, PEB, containing no dodecyl side chains were also included in this study.

The results are shown in Fig. 5. A logarithmic ordinate was used to get all the curves on the same

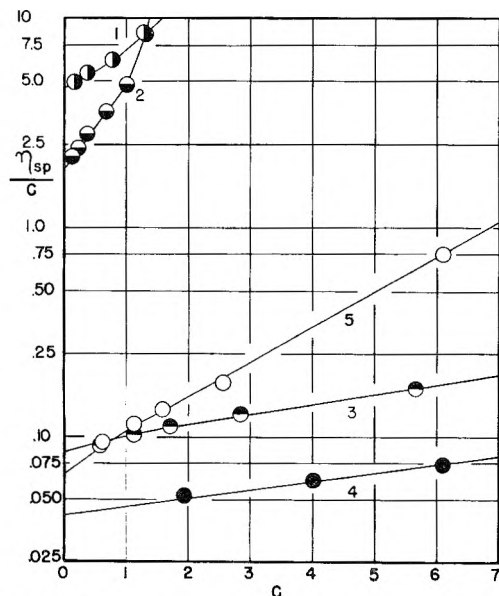


Fig. 5.—Effect of dodecyl group content⁸ on reduced viscosity of polyelectrolytes and polysoaps in 0.0226 *m* KBr at 25°: 1, PEB; 2, “6.7%” polysoap; 3, “13.6%” polysoap; 4, “28.5%” polysoap; 5, “37.9%” polysoap.

graphs. Even so, there is a clearcut separation of the curves into two families. In the upper left hand corner we find curves 1 and 2 corresponding to

(20) H. M. Spurlin, *J. Polymer Sci.*, **3**, 714 (1948).

PEB and the “6.7%” polysoap, respectively; in the bottom half we find curves 3, 4 and 5 corresponding to the “13.6%” the “28.5%” and the “37.9%” polysoaps, respectively.²¹ Curve 2 has a lower intercept but a steeper slope than curve 1 indicating that the effect of replacing 6.7% of the ethyl side chains by dodecyl groups makes the polyelectrolyte molecule more compact and more inclined to interact. However, the largest change in properties comes about when this dodecyl group content is doubled. The intercept of curve 3 is more than an order of magnitude lower than that of curve 2, indicating a higher order of molecular compactness. The smaller slope indicates less interaction. On raising the dodecyl content of the polysoap molecule further, changes of a smaller order occur. It is of interest that both the intercepts and the slopes go through a minimum with increasing dodecyl group content, indicating corresponding changes in molecular dimensions and interactions.

The main features of these results are brought out more clearly in Fig. 6. The shaded circles

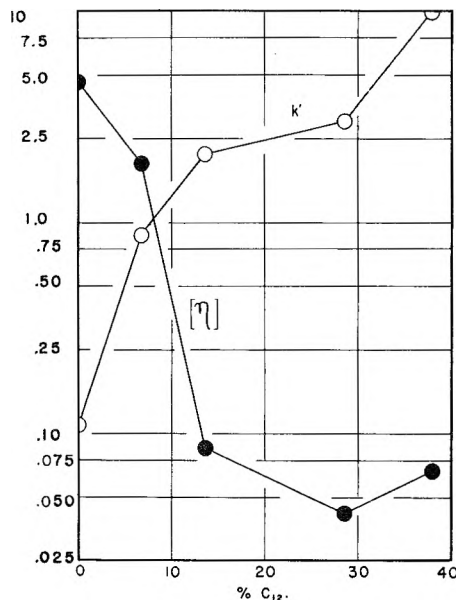


Fig. 6.—Effect of dodecyl group content of polyelectrolytes and polysoaps on the intrinsic viscosity and Huggins' constant in 0.0226 *m* KBr at 25°: ●, η ; ○, k' .

represent the intrinsic viscosity values of the polymers as a function of the dodecyl group content.⁸ It is instructive to consider these intrinsic viscosities in the light of the general principles recently developed by Flory and his co-workers, relating polymer-solvent interactions with molecular configuration and solubility of the polymer chain.^{22,23} One of the most important concepts in this theory is the so-called “ θ -solvent” in which long range interactions between polymer segments vanish and the polymer molecules assume their characteristic random coil configuration, which is determined by

(21) A similar separation into two families of curves was also observed in previous studies with these compounds when pure water was the solvent.³

(22) P. J. Flory and T. G. Fox, Jr., *J. Am. Chem. Soc.*, **73**, 1904 (1951).

(23) P. J. Flory, “Principles of Polymer Chemistry,” Cornell University Press, Ithaca, N. Y., 1953, Chapters 12–14.

the flexibility of the polymer chain and by short range interactions between neighboring segments. In solvents with greater solvent power than the θ -solvent the polymer molecule is more extended. The configuration of the polymer molecule can be characterized by one parameter, the linear expansion coefficient α , which gives the ratio of the root-mean-square end-to-end distance R in the solvent under consideration to that in the θ -solvent, R_0 . The θ -solvent also has the property of being the poorest possible solvent for a polymer of infinite chain length. Therefore, as one goes to solvents poorer in solvent power than the θ -solvent, phase separation sets in, with the higher chain lengths separating out first. As a consequence it should be impossible to find homogeneous polymer solutions in which long chain polymer molecules are appreciably more compact than in a θ -solvent. These principles have in recent years been experimentally verified for a great number of polymers,²⁴ for several conventional polyelectrolytes such as one-third neutralized polyacrylic acid in aqueous NaCl solutions²⁵ and sodium polyphosphate in aqueous NaBr solutions,²⁶ and for so complex a biological polyampholyte as gelatin²⁷ which in some of its molecular aggregation properties²⁸ resembles polysoap behavior.

No solubility studies on ordinary polyelectrolytes derived from poly-4-vinylpyridine have been reported, but a critical examination of the literature reveals no intrinsic viscosity data which would indicate appreciably greater molecular compactness than can be calculated to prevail in a θ -solvent.

Recently molecular dimensions of poly-4-vinylpyridine have been determined by light scattering and viscosity studies.⁹ The results indicated that θ -solvent dimensions are identical with those of polystyrene. At 25°

$$[\eta]_{\theta} = 8.1 \times 10^{-4} M^{1/2} \quad (1)$$

Since our parent polymer has a molecular weight, M , equal to 1.9×10^6 , its θ -solvent intrinsic viscosity, $[\eta]_{\theta}$, equals 1.12. Making use of Flory's relation

$$[\eta]_{\theta} = \Phi \frac{R_0^3}{M} \quad (2)$$

where Φ is a constant²² (whose value is immaterial for our present purposes), and assuming R_0 to be unaffected by quaternization with alkyl halides,²⁹ we can calculate the expected values for $[\eta]_{\theta}$ of the quaternization products by the relation

$$[\eta]_{\theta, Q} = [\eta]_{\theta, P} (M_P/M_Q) \quad (3)$$

where the subscripts P and Q refer to the parent polymer and the quaternization products, respectively. The resulting estimates of $[\eta]_{\theta, Q}$ range from 0.55 for PEB to 0.45 for the "37.9%" polysoap.

(24) T. G. Fox, Jr., and P. J. Flory, *J. Am. Chem. Soc.*, **73**, 1909, 1915 (1951); for further references see ref. 22.

(25) P. J. Flory and J. E. Osterheld, *THIS JOURNAL*, **58**, 653 (1954); it is significant that the above principles hold for this polyelectrolyte despite the strong association forces between the un-ionized -COOH groups.

(26) U. P. Strauss and P. L. Wineman, unpublished results.

(27) E. V. Gouinlock, Jr., P. J. Flory and H. A. Scheraga, *J. Polymer Sci.*, **16**, 383 (1955).

(28) H. Boedtker and P. Doty, *J. Am. Chem. Soc.*, **58**, 968 (1954).

(29) In view of an expected small increase in the steric hindrance between neighboring chain elements, R_0 probably increases slightly as a result of the quaternization. The calculated values for $[\eta]_{\theta}$ of the polysoaps are therefore minimum estimates.

If we now compare the actual intrinsic viscosity values of our polymers in Fig. 6 with these estimates for $[\eta]_{\theta, Q}$ we find that the polymers containing 0.0 and 6.7% dodecyl groups have intrinsic viscosities much higher than $[\eta]_{\theta}$ and therefore may be considered as typical polyelectrolytes. However, the intrinsic viscosities of the "13.6%," the "28.5%" and the "37.9%" polysoaps are an order of magnitude lower than their estimated θ -solvent values. This result shows conclusively that these polysoaps reach degrees of molecular compactness which ordinary high polymers and polyelectrolytes in solution cannot assume without phase separation. Apparently the only other high molecular weight macromolecules for which such small intrinsic viscosities have been observed are the globular proteins³⁰ and some polyvinylpyrrolidone-triiodide complexes.³¹

It is interesting to speculate on the cause for the deviations of polysoap behavior from Flory's general principles. One of the theoretical bases for these principles is the assumption that the interactions between two segments are the same whether they belong to the same or to different polymer molecules. It is quite easy to visualize why this assumption may not apply to polysoaps. Aggregation of the hydrophobic dodecyl groups belonging to the same molecule (which leads to molecular compactness) can occur without extensive aggregation of dodecyl groups belonging to different polysoap molecules (which would lead to phase separation), because hydrophilic pyridinium groups can arrange themselves around the periphery of the individual polysoap molecules and thus shield their dodecyl groups from those of other polysoap molecules. The situation is very similar to the case of ordinary soap molecules which form micellar aggregates containing a finite number of units instead of precipitating out of solution as essentially infinite aggregates. On the basis of these considerations one may predict that other polymers, such as block- and graft-copolymers, containing geometrically well separated lyophilic and lyophobic portions, will also deviate from Flory's principles and behave in many ways like polysoaps.

A feature in Fig. 6 which merits discussion is the sudden drop of the intrinsic viscosity curve as the dodecyl group content increases from 6.7 to 13.6%. It is significant that this steep drop crosses the $[\eta]_{\theta}$ value and coincides with the transition from typical polyelectrolyte to typical polysoap behavior. These properties suggest that if this composition range were covered by more samples, the drop might appear even steeper, and that we may have here a *critical micelle composition* analogous to the *critical micelle concentration* (CMC) observed with ordinary colloidal electrolytes. This conjecture seems quite reasonable, for if the micelle formation in polysoap molecules is to be caused by the same factors as in the case of simple soaps, then it should be the local concentration of the soap molecules attached to a given polymer chain which must be above a critical value. But this local concentration is determined

(30) A. Polson, *Kolloid. Z.*, **88**, 51 (1939).

(31) S. Barkin, H. P. Frank and F. R. Eirich, "Ricerca, International Symposium on Macromolecular Chemistry," September, 1954, in press.

mainly by the density of soap molecules along the polymer chain, *i.e.*, by the dodecyl group content of the polysoap.³² One may further speculate that, analogous to the CMC of ordinary soaps, this critical dodecyl content may depend to some extent on the environment. A polymer whose dodecyl content is in the critical region might then act as a typical polyelectrolyte under one set of conditions and as a typical polysoap under another. Such a change from highly extended polyelectrolyte to highly compact polysoap might be utilized for a more efficient direct conversion of chemical to mechanical energy than has so far been possible with synthetic polyelectrolytes. For this purpose, the polymers would have to be cross-linked, and the change in environment necessary to bring about the contraction or expansion would have to be small. Exploratory research along these lines is in progress.

It is of interest to discuss the structure of the polysoap molecules in somewhat more detail. As has been mentioned, Flory has shown recently that the configuration of ordinary polymer molecules in solution may be completely described by one parameter, namely, the expansion coefficient α , which can be uniquely determined by intrinsic viscosity measurements alone.²² With the compact polysoap molecules there is good reason to believe that both an expansion coefficient and a shape factor may be necessary for a complete description of the molecular configuration. Thus the intrinsic viscosity alone does not suffice for an unambiguous description. The same situation arises in the case of proteins and is adequately discussed in the literature.³³ In the absence of complete information one can still speculate concerning the possible molecular configurations which are consistent with the observed intrinsic viscosity. For instance, let us consider the "28.5%" polysoap whose molecular weight is 4.6×10^6 and whose intrinsic specific volume is assumed to be unity. Its $[\eta]$ of 0.042 in 0.0226 *m* KBr would, in the absence of any swelling by the solvent, be consistent with either the shape of a prolate spheroid of axis ratio $a/b = 3.5$, or with the shape of an oblate spheroid of axis ratio $b/a = 4.3$, where a is the axis of rotation and b is the cross-section.³⁴ In the former case $a = 560 \text{ \AA}$. and $b = 160 \text{ \AA}$. while in the latter $a = 90 \text{ \AA}$. and $b = 400 \text{ \AA}$. If there is swelling by the solvent, the possible axis ratios compatible with the intrinsic viscosity will become smaller. With maximum swelling we would have a sphere with a diameter equal to 290 \AA . It is noteworthy that even the smallest of the possible dimensions is considerably larger than twice 25 \AA ., the estimated length of a stretched methylene-N-dodecylpyridinium group. Thus the usual picture of a soap micelle with all the

polar groups on the outside cannot apply here and we must conclude that a considerable portion of the polymer chain with its attached polar groups winds itself through the interior of the polysoap molecule.

We now turn our attention from the molecular dimensions to the interactions between different polysoap molecules. These interactions which may be measured by the initial slopes of the η_{sp}/C against C plots depend on both the molecular extension of the polymer molecules and on the affinity between polymer and solvent relative to the polymer-polymer and solvent-solvent affinities. It has been shown that these two factors can be resolved by expressing the slope as a product of $[\eta]^2$ and a quantity k' .³⁵ While no completely quantitative theory concerning Huggins' constant k' is available, it is now well established that k' is a measure of relative polymer-solvent affinity. Thus with ordinary polymers³⁶ and polyelectrolytes,³⁷ k' ranges from about 0.1 in very good solvents to 1.0 in very poor ones. The k' -values obtained from viscosity measurements of our polyvinylpyridinium compounds in 0.0226 *m* KBr are shown in Fig. 6 as open circles. It is striking that the two polymers which on the basis of their high intrinsic viscosities have been classified as typical polyelectrolytes have k' -values of conventional magnitude while the three polysoaps have k' -values extending far above the usual range. As will be shown in the next section, these high values of k' are due to a tendency of the polysoap molecules to form aggregates, this tendency becoming more important with increasing dodecyl group content.

Aggregates.—The large values of Huggins' k' and the tendency toward gel formation exhibited by the polysoaps indicate very strong intermolecular interactions. It is our purpose to demonstrate in this section that these interactions are in the nature of aggregate formation.

The picture we have of this phenomenon is as follows. Since the polysoap molecules are so extremely compact, they presumably have a definite surface. While this surface is covered for the most part with hydrophilic pyridinium groups, it may also contain some hydrophobic portions. Such hydrophobic spots on different polysoap molecules would have a strong affinity for each other, causing the polysoap molecules to stick together to form chain-like aggregates. The extent of this aggregation is controlled by several factors: first, by the fraction of the molecular surface which is covered by such hydrophobic spots³⁸; second, by the elec-

(35) M. L. Huggins, *J. Am. Chem. Soc.*, **64**, 2716 (1942).

(36) L. H. Cragg and R. H. Sones, *J. Polymer Sci.*, **9**, 585 (1952).

(37) With polyelectrolytes, k' becomes large at very low ionic strengths, presumably due to electrostatic interactions.⁵ This effect, however, is not present at the high KBr molality employed in our case, and will therefore be ignored in the discussion.

(38) Actually, the number, area and relative position of these spots on the molecular surface all are important. If there is one such spot, only dimers can form; if two, linear aggregates; and if three, branched and cross-linked aggregates. From the observation that for the "28.5%" polysoap, the η_{sp}/C against C curves in Fig. 4 are linear up to at least a 6% concentration, we suspect that this polysoap forms a negligible amount of aggregates greater than dimers. This suspicion is also supported by the fact that the reduced viscosity does not go above 0.1 in KBr solutions. On the other hand the strong curvature of the η_{sp}/C against C curves in Fig. 3 and the jelly formation in the case of the "37.0%" polysoap indicate that this polysoap can form larger aggregates which under extreme conditions cross-link.

(32) It is of interest in this connection that the local concentration of dodecylpyridinium groups inside a hypothetical spherical "10%" polysoap molecule whose $[\eta] = 0.5$ (*i.e.*, the composition and $[\eta]$ corresponding to the approximate mid-point of the sharpest dropping portion of the $[\eta]$ against $\%C_{12}$ curve in Fig. 6) would be about 0.02 molar. This value is of the right order of magnitude for the expected CMC of *n*-dodecylpyridinium bromide in 0.0226 *m* KBr. (The value of the latter CMC in pure water is 0.017 molar [U. P. Strauss and E. G. Jackson, *J. Polymer Sci.*, **6**, 649 (1951)]).

(33) H. A. Scheraga and L. Mandelkern, *J. Am. Chem. Soc.*, **75**, 179 (1953).

(34) J. W. Mehl, J. L. Oneley and R. Simha, *Science*, **92**, 132 (1940).

trical net charge on the polysoap molecules: the higher this charge, the more repulsion and hence the less aggregation; third, by the temperature: the higher the kinetic energy of the polysoap molecules the less they tend to aggregate; moreover, the hydrophobicity of the hydrocarbons and therefore the "stickiness" of the hydrophobic spots decrease with increasing temperature; and fourth, by the average distance of approach between the surfaces of two polysoap molecules: this distance depends on the polysoap concentration and on the effective volume of the polysoap molecules.³⁹ All the unusual interaction effects observed so far with polysoaps can be understood with this picture. Thus, the viscosity maxima occurring with solubilization of benzene or heptanol^{3,40} have been explained in terms of the first of these factors. The observed increase in Huggins' k' with increasing dodecyl content of the polysoaps can likewise be explained in terms of an increase in the hydrophobic fraction in the polysoap molecule surface. The aggregation brought about by the addition of KBr, which caused the concentrated solutions of the "37.9%" polysoap to turn into jellies, can be explained most easily by the second factor: the KBr reduces the electrical charge¹² and with it the repulsion of the polysoap molecules. However, the first factor may play an important role here, too. With increasing ionic strength, the ionic atmospheres around the ionized pyridinium groups contract. In this way, the pyridinium groups cover effectively less of the polysoap molecule surface and the hydrophobic groups correspondingly cover more, thus making the surface more "sticky."

Probably the most convincing argument for the existence of aggregates is based on the observation that the viscosity of a dilute polysoap solution which has been freshly prepared by dilution of a more concentrated solution decreases for a considerable time. The results of four such experiments where portions of an equilibrated 6.09% solution of the "37.9%" polysoap in 0.0226 *m* KBr were diluted with more 0.0226 *m* KBr to yield 2.54, 1.58, 1.12 and 0.61% solutions are shown in Fig. 7. Except for the equilibration of the 6.09% solution, which was carried out as described under Experimental, the temperature was kept constant at 25° during all phases of this experiment. The reduced viscosity of the original 6.09% solution was 0.748. If this relatively high value of the reduced viscosity had been caused by the usual hydrodynamic interactions, the reduced viscosities of the diluted solutions would have reached their equilibrium values immediately after dilution. The fact that such equilibrium values had not yet been attained 12 hours after dilution proves the presence of aggregates in the original 6.09% solution and also indicates that such aggregates have considerable stability.

An attempt also was made to obtain an estimate of the disaggregation rate at 45°. A somewhat different technique was employed, utilizing the

(39) It should be noted that while the reduced viscosity depends on all four of these factors, Huggins' k' has been defined in such a way that it depends on the first three only.

(40) L. H. Layton, E. G. Jackson and U. P. Strauss, *J. Polymer Sci.*, **9**, 295 (1952).

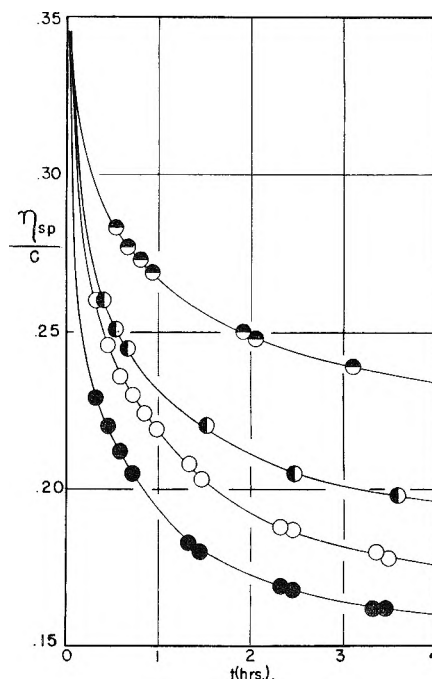


Fig. 7.—Reduced viscosity changes after diluting a 6.09% solution of the "37.9%" polysoap to various polysoap concentrations, C , at 25°. Solvent is 0.0226 *m* KBr. $C =$: ●, 0.61; ○, 1.12; ◐, 1.58; ◑, 2.54. Time is measured starting with dilution process.

temperature dependence of the aggregation state illustrated in Fig. 2. A 6.0% solution of the "37.9%" polysoap in 0.025 *m* KBr was equilibrated in the viscometer at 25°. The reduced viscosity was 1.35. The viscometer containing the solution was then immersed in a 45° bath, and viscosity measurements were begun as soon as the solution had reached temperature equilibrium. The results are shown by the bottom curve in Fig. 8. It is ap-

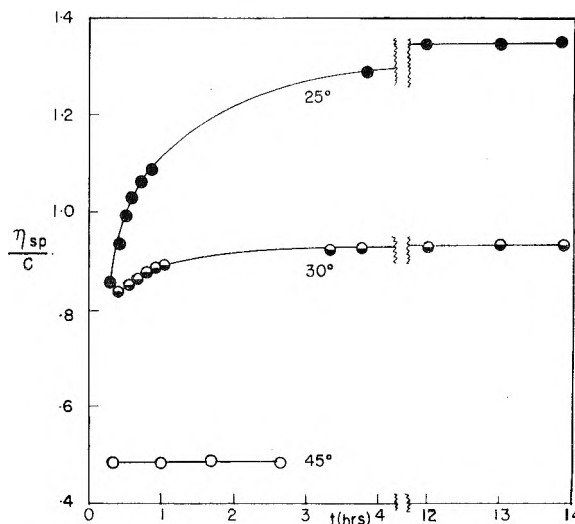


Fig. 8.—Reduced viscosity changes of a 6.00% solution of the "37.9%" polysoap in 0.025 *m* KBr after a temperature change: ○, original temperature = 25°, final temperature = 45°; ●, original temperature = 45°, final temperature = 25°; ◐, original temperature = 45°, final temperature = 30°. Time is measured starting with immersion of viscometer into bath at final temperature. Measurements were started as soon as solution reached final temperature. For further explanation, see text.

parent that the reduced viscosity had reached its equilibrium value of 0.48 before the first measurement could be made. Thus the disaggregation process was completed in less than 15 minutes.⁴¹ This result should be compared with the slow disaggregation obtained in the dilution experiments at 25°. The enormous difference in the disaggregation rates at the two temperatures indicates that the aggregation state is stabilized by a large activation energy.

It is interesting to find out whether the activation energy is also observable for the aggregation process. For this purpose the 6.0% solution of the "37.9%" polysoap in 0.025 *m* KBr which had previously reached equilibrium at 45° was immersed into a bath thermostated at a lower temperature, using essentially the same technique described above for the 45° disaggregation experiment. The results of two such experiments with the lower temperatures at 25 and 30° are illustrated in Fig. 8 by the upper and center curves, respectively. Two features are noteworthy. First, at both temperatures equilibrium was reached not instantaneously, but slowly. Second, equilibrium was reached con-

(41) This statement is not to imply that there is no aggregation at 45°. Figure 2 shows merely that there is less aggregation at 45° than at 25°.

siderably faster at 30° than at 25°. Thus the existence of the activation energy for the aggregation process is confirmed.

The activation energy can be explained in this way: consider two polysoap particles each of which may be either a polysoap molecule or an aggregate of several such molecules. We assume the interaction energy to be zero when the two particles are very far apart. As they approach each other, long range coulomb repulsive forces due to their electrical charges cause the interaction energy to become positive. When the particles are close enough to touch each other, and if conditions are such that their surfaces are sufficiently hydrophobic, the interaction energy decreases again as a result of the short range attractive forces. Thus there will be an energy barrier between the aggregated and the separated states of the two particles.

These considerations should apply equally well to micelles of ordinary colloidal electrolytes. Therefore the increase in viscosity and the gel formation frequently observed on the addition of simple electrolytes to solutions of colloidal electrolytes may also be explainable in terms of a chain-like aggregation of existing micelles, rather than in terms of the more conventionally assumed change in micelle type.

THE ACTION OF HEPARIN ON THE POLYMERIZATION OF FIBRINOGEN¹

BY ERWIN SHEPPARD,² JOHN IMPERANTE AND IRVING S. WRIGHT

Contribution from the Department of Medicine, New York Hospital-Cornell University Medical College, New York, N. Y.

Received October 18, 1955

Light scattering studies have been done to study the effect of heparin on the polymerization of fibrinogen as a function of ionic strength, heparin concentration and pH. It is found that in 0.05 ionic strength phosphate buffer, pH 7.4, heparin blocks the activation and early propagation stages of the fibrinogen polymerization whereas at higher ionic strength levels, gelation occurs and the reaction proceeds to varying degrees of conversion. The inhibitory activity of heparin on the polymerization of fibrinogen *in vitro* is explained on the basis of an electrostatic interaction mechanism.

Introduction

It has been reported in a previous publication³ from this Laboratory that heparin will increase the electrokinetic or zeta potential of the fibrinogen-solid interface in low ionic strength solvents but not in the presence of a high salt concentration. The question next considered was whether or not the increased repulsion associated with the higher zeta potentials^{4,5} could affect the polymerization of fibrinogen. Therefore, the mission of the present investigation was to study the effect of heparin on the conversion of fibrinogen to fibrin *in vitro* and to elucidate its mechanism of action.

(1) This is paper number 7 in the series "Electrostatic Forces Involved in Blood Coagulation." This work was supported in part by the Office of Naval Research, United States Navy, under Contract N6 onr-264, T.O. 10, and by a Grant-in-Aid from the American Heart Association. Reproduction in whole or in part is permitted for any purpose of the United States Government.

(2) Research Fellow of the American Heart Association.

(3) E. Sheppard and I. S. Wright, *Arch. Biochem. Biophys.*, **52**, 426 (1954).

(4) I. Langmuir, *J. Chem. Phys.*, **6**, 893 (1938).

(5) E. J. W. Verwey and J. Th. G. Overbeek, "Theory of the Stability of Lyophobic Colloids," Elsevier Publishing Co., New York, N. Y., 1948.

Light scattering studies were done to follow the kinetics and pathways of the thrombin induced conversion of fibrinogen to fibrin, in the presence of heparin, as a function of ionic strength of solvent, μ , heparin concentration and pH. The results of these studies are herein reported.

Experimental

The apparatus and procedures employed in these investigations have been described previously.⁶ In the current study, dissymmetry measurements were taken at 45 and 135° angles of observation to the incident beam (436 $m\mu$ wave length) at 30- or 60-second intervals until the gel point of the fibrinogen polymerization was reached. The reaction mixture contained 0.2 mg./ml. clottable fibrinogen, 0.02 unit/ml. thrombin, and 0.1 mg./ml. heparin (except where otherwise indicated) in K_2HPO_4 - KH_2PO_4 buffer, pH 7.4, of varying μ .

Bovine fraction I (Armour and Co., Chicago, Ill.), Lot 128-163, containing 44% clottable fibrinogen was fractionated and assayed according to the method of Laki.⁷ Preparation L-3 contained 97% clottable fibrinogen and 1.41 mg. N/ml. and was used for the studies wherein μ and pH were varied. Preparation L-4 containing 96.5% clottable fibrinogen and 1.78 mg. N/ml. was used in the heparin concen-

(6) E. Sheppard, J. Imperante and I. S. Wright, *J. Biol. Chem.*, **212**, 837 (1955).

(7) K. Laki, *Arch. Biochem. Biophys.*, **32**, 317 (1951).

tration studies. The nitrogen content was determined by the Dumas technique. Sodium heparin powder, lot No. 3390, containing 117 U.S.P. units/mg., was obtained from Dr. K. W. Thompson, Organon Inc., Orange, New Jersey. The thrombin (Parke Davis & Co.) contained 19 N.I.H. units/mg.

Results

The Action of Heparin on the Polymerization of Fibrinogen. A. As a Function of μ at pH 7.4.—The polymerization of fibrinogen, catalyzed by thrombin, as followed by light scattering proceeds *via* three stages. There is first the initiation phase during which time (the induction period) the activation of fibrinogen by thrombin predominates and changes in scattering are insignificant since thrombin is splitting off small terminal polypeptides from fibrinogen.⁸ This is followed by the propagation phase in which these altered or activated molecules associate and rapidly grow in size. During this period, particle dissymmetry increases rapidly. Finally gelation occurs and the reaction rate decreases due to intramolecular interaction. Measurements were not taken beyond this point since increases in the intensity of scattered light are negligible.

The effect of heparin on the polymerization of fibrinogen was studied at two stages of the reaction, namely, initiation and early propagation. This was accomplished by adding heparin to the reacting mixture either at zero time (*i.e.*, before thrombin) or at an early stage of the conversion. The ionic strength levels of the phosphate buffer, pH 7.4, were 0.025, 0.05, 0.08, 0.10, 0.15, 0.20 and 0.30. The constant contributions of the added proteins and heparin to the μ of the system could not be taken into account.

During the conversion of fibrinogen to the fibrin gel in the absence of heparin, it was noted that the induction period increased with increasing μ values and maximum dissymmetry coefficient, q , values were obtained at gelation for the system in $\mu = 0.15$. It was also observed that in the μ range of 0.10–0.20, the gel network exhibited a scintillation property when viewed with unpolarized light while the scattering cell was agitated gently.

It was found that the addition of heparin to the system at $t = 0$ or at an intermediate reaction time permanently blocked the polymerization in $\mu = 0.025$ and 0.05 solvents whereas at higher μ levels the reaction rate and pathways of the polymerization were affected but the reaction nonetheless proceeded to the gel point. Figures 1, 2 and 3 illustrate the q vs. t curves for representative studies in $\mu = 0.05$, 0.15 and 0.30 solvents. At $\mu > 0.05$, the increment of the induction period (Δ I.P.) produced by the zero time addition of heparin as compared to the control decreased to a minimum at $\mu = 0.10$ as shown in Table I. It also was noted that although the dissymmetry coefficients for the control and retarded systems reached comparable levels, the intensity of the forward scattered light at 45° was significantly less for the mixtures containing heparin than for the controls.

B. Variation of Heparin Concentration ($\mu = 0.05$, pH 7.4).—The purpose of the next series of experiments was to study the effect of decreasing

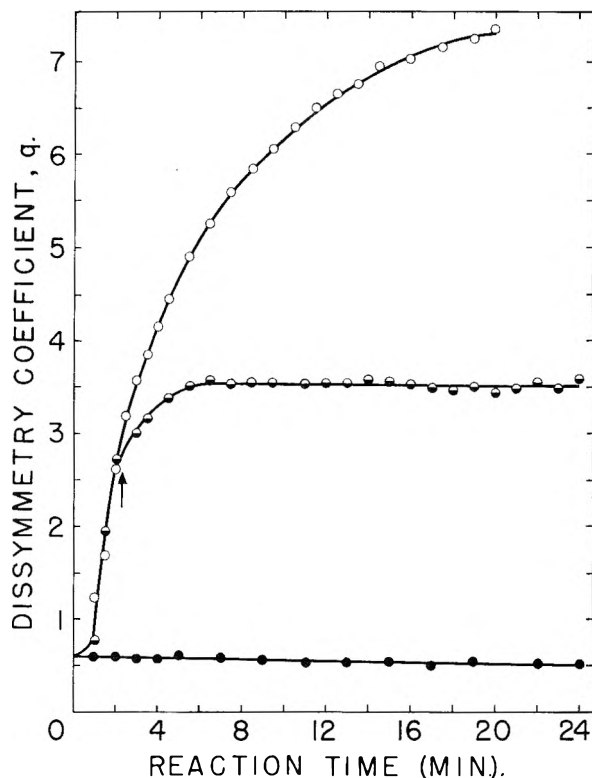


Fig. 1.— q vs. t curves showing the effect of heparin (100 μ g./ml. reaction mixture) on the polymerization of fibrinogen in phosphate buffer, pH 7.4, $\mu = 0.05$: control, O; heparin added at $t = 2.5$ min., \circ ; heparin added at $t = 0$, \bullet .

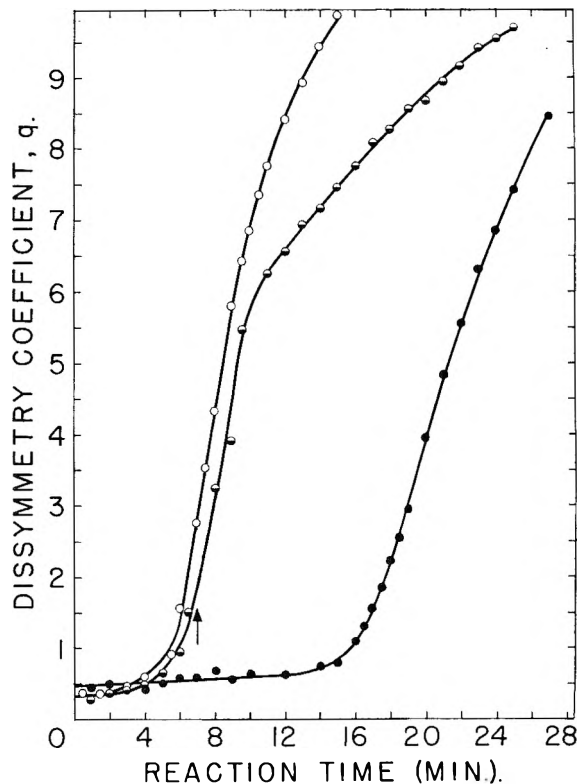


Fig. 2.— q vs. t curves showing the effect of heparin (100 μ g./ml.) on the polymerization of fibrinogen in phosphate buffer, pH 7.4, $\mu = 0.15$: control, O; heparin added at $t = 7$ min., \circ ; heparin added at $t = 0$, \bullet .

amounts of heparin on the fibrinogen polymerization in an ionic strength in which 0.1 mg./ml.

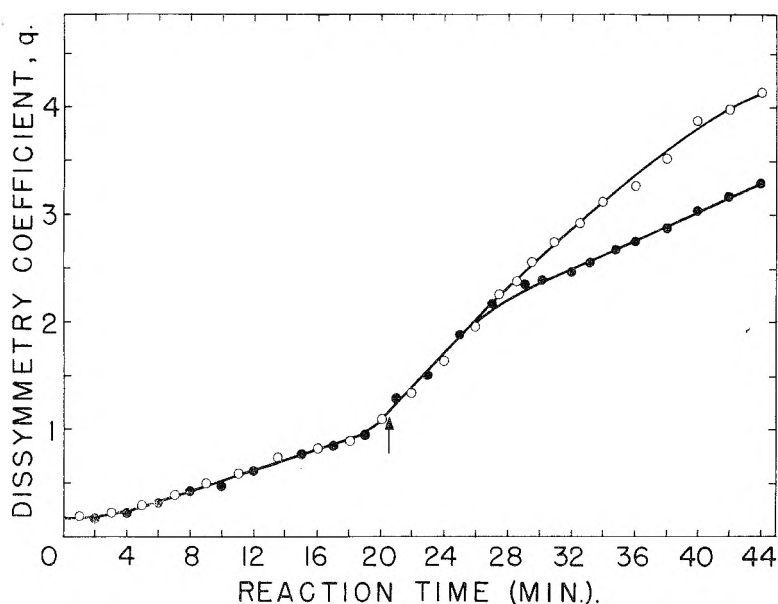


Fig. 3.— q vs. t curves showing the effect of heparin (100 $\mu\text{g./ml.}$) on the polymerization of fibrinogen in phosphate buffer, pH 7.4, $\mu = 0.30$: control, O; heparin added at $t = 20.5$ min., ●.

heparin had blocked the reaction (see Fig. 1). Figure 4 illustrates the results of the experiments in phosphate buffer pH 7.4, $\mu = 0.05$, in which heparin was added to the polymerizing system at $t = 1'45''$. The concentrations of heparin in the reaction mixture were 50, 10 and 2 $\mu\text{g./ml.}$

TABLE I

INDUCTION PERIOD OF THE FIBRINOGEN POLYMERIZATION

μ	Control I.P., min.	Heparin $t = 0$ addn. Δ I.P., min.
0.05	1	No reaction
.08	2	23
.10	2.5	10.5
.15	4	11
.20	7.5	13.5

Fibrinogen preparation L-4 was used in this series. The q vs. t curve for the control was almost identical to that obtained with preparation L-3. After the addition of heparin, it was found that the q values and the intensity of forward scattering continued to increase, slowly for the 50 $\mu\text{g./ml.}$ heparin concentration and more appreciably for the lower concentrations. The gel networks for the retarded systems were smaller and less opaque than the control and readily condensed to form a small compact clot upon agitation. The decrease in the degree of conversion is also evident from the intensity of forward scattering, which, for the 2 $\mu\text{g./ml.}$ heparin concentration, was 50% smaller than the control at $t = 15$ min.

C. Variation of pH, $\mu = 0.05$.—It was also of interest to see if the inhibitory property of heparin (0.1 mg./ml. reacting mixture) in $\mu = 0.05$ would be reduced if the pH of the solvent was lowered. It was found that the dissymmetry coefficient for fibrinogen (L-3) in phosphate buffer had values equal to 2.7 at pH 6.6 and 6.7 at pH 5.9. Presumably the protein at the lower pH was coming out of solution since the pH of the solvent was close

to its isoelectric point of 5.8.⁹ However, when thrombin was added, a coarse fibrin gel formed at both pH levels. The addition of heparin at pH 6.6 and 5.9 to the reaction mixture either at $t = 0$ or shortly after the induction period immediately produced turbid solutions containing suspended particles. Gel formation did not occur at these pH values even though the q values increased in magnitude. Apparently heparin had precipitated fibrinogen from the solutions.

Discussion

The data presented indicate that, *in vitro*, heparin inhibits the polymerization of fibrinogen in phosphate buffer, pH 7.4, $\mu \leq 0.05$, either at the activation or early propagation stages of the reaction. At higher ionic strength levels, the reaction is retarded by heparin. When the ionic strength of the buffer was kept constant at 0.05, decreasing the concentration of heparin in the reaction mixture to levels as low as 2 $\mu\text{g./ml.}$ altered its activity from inhibition to retardation.

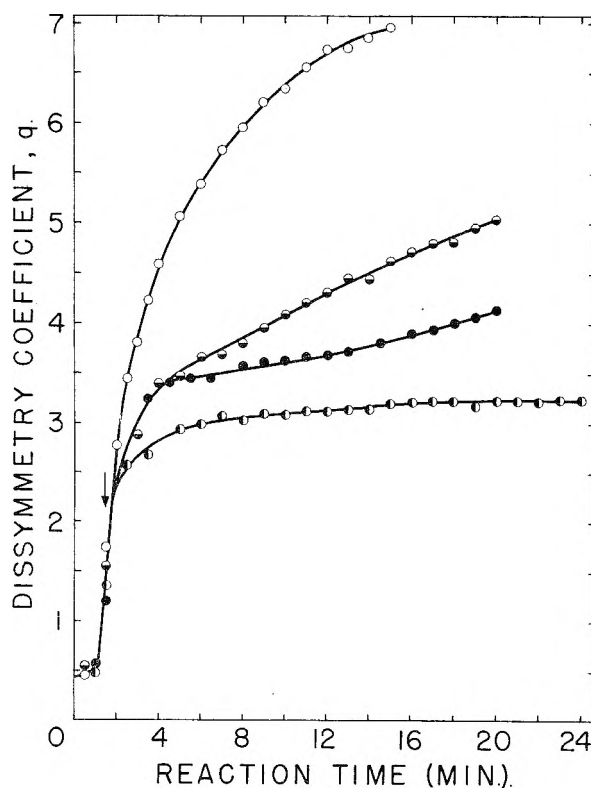


Fig. 4.— q vs. t curves showing the effect of heparin concentration on the polymerization of fibrinogen in phosphate buffer, pH 7.4, $\mu = 0.05$: control, O; heparin added at $t = 1$ min. 45 sec., concn. in mixture, 50 $\mu\text{g./ml.}$, ●, 10 $\mu\text{g./ml.}$, ●, 2 $\mu\text{g./ml.}$, ●.

The dependency of heparin's activity on ionic strength and concentration *in vitro* may be ex-

(9) T. Abe, E. Sheppard and I. S. Wright, *THIS JOURNAL*, **59**, 266 (1955).

plained on the basis of an electrostatic repulsion mechanism due to its polyelectrolyte properties and double layer interaction. Heparin is a sulfated polysaccharide having a repeating disaccharide unit consisting of glucosamine and glucuronic acid with sulfate ester and sulfamic acid linkages.¹⁰ At low ionic strength levels, pH 7.4, the molecular configuration presumably is expanded primarily because of the intramolecular repulsion of the dissociated sulfate groups, since the carboxyl groups are but slightly ionized. Under these conditions (high charge density and large end-to-end distance) heparin was observed to interfere with the activation of fibrinogen by thrombin and with the association of fibrin intermediates. As the ionic strength is increased the heparin molecule can assume more compact configurations; its double layer thickness decreases and as a result its ability to block the fibrinogen conversion is reduced. Nevertheless, heparin at $\mu > 0.05$ affected the degree of conversion. A similar variation in molecular length with μ was observed by Rowen¹¹ for sodium desoxyribonucleate. It was shown by light scattering and flow birefringence that the rod-like charged molecule of sodium desoxyribonucleate was flexible enough to undergo a 36-39% shortening when surrounded by charged ions.

At constant μ , lowering the pH of the reaction mixture reduced the net charge on the colloidal particles. As a consequence, for example, it was noted that the initial fibrinogen solutions at pH 6.6 and 5.9 exhibited larger particle size distributions (higher q values) than at pH 7.4. This tendency toward flocculation is in accord with the previously reported⁹ decrease in the zeta potential for the fibrinogen-solid interface as the pH of the isoelectric point (5.8) was approached. Although there was association of the native fibrinogen at these pH values, thrombin was able to activate the fibrinogen and the reaction proceeded to the gel stage. However, when heparin was added to the mixtures containing the associated fibrinogen, either at $t = 0$ or at an early phase of the reaction, the fibrinogen-heparin complex precipitated. It has been reported¹² that heparin, chondroitin sulfate and hyaluronic acid will precipitate various highly asymmetric plant virus proteins having molecular weights greater than 10^6 at pH values slightly alkaline to their isoelectric points. Conversely, Walton¹³ has shown that at pH 6.8 (μ

of solvent not indicated but > 0.07) heparin and low molecular weight dextran sulfate did not form visible precipitates with fibrinogen whereas high molecular weight dextran sulfates formed loosely bound insoluble complexes. However, below the isoelectric point of fibrinogen, namely, at pH 2.5 and 4.0, heparin and all the dextran sulfates precipitated the fibrinogen. Above the isoelectric point, weak links were formed similar to those involved in the antigen-antibody reaction and below the isoelectric point, salt bonds were formed.

The polymerization of fibrinogen in the absence of heparin is also influenced by the salt concentration. For example, the induction period was prolonged when the ionic strength of the buffer was increased (Table I) at pH 7.4. The fastest rate of q change occurred at $\mu = 0.15$ which is in agreement with the findings of Waugh and Patch¹⁴ who reported a maximum rate constant, k , for the polymerization of fibrinogen at the same ionic strength. It also was noted that the configuration of the associated fibrin molecules at the gel point varied with the ionic strength. This observation has been reported previously by others¹⁵⁻¹⁷ for both human and bovine fibrinogen in terms of fine and coarse textured clots. In our studies, it was found that in the μ range of 0.05 to 0.20, pH 7.4, lateral association of the fibrin molecules predominated at gelation since the q values were comparable to those attained with broad particles.¹⁸ At $\mu > 0.2$, end-to-end orientation predominated at the gel point since the q values approached the theoretical values for long rods. These findings are in concordance with the interpretation of the light scattering studies of Steiner and Laki,¹⁹ and Greene²⁰ who also have reported end-to-end association to exist in high salt concentrations.

It is important to emphasize, however, the difficulty in interpreting high q values in terms of structural configuration for as complex a system as fibrinogen-fibrin. This is due to variations in the distribution of fibrin between the free and cross linked states, the average distance between cross links, and the length to width ratio of fibrils. For these reasons the specific action of heparin was studied at the early stages of the reaction.

(14) D. F. Waugh and M. J. Patch, *THIS JOURNAL*, **57**, 377 (1953).

(15) J. D. Ferry and P. R. Morrison, *J. Am. Chem. Soc.*, **69**, 388 (1947).

(16) S. Shulman and J. D. Ferry, *THIS JOURNAL*, **54**, 66 (1950).

(17) J. T. Edsall and W. F. Lever, *J. Biol. Chem.*, **191**, 735 (1951).

(18) G. Oster, *Chem. Revs.*, **43**, 319 (1948).

(19) R. F. Steiner and K. Laki, *Arch. Biochem. Biophys.*, **34**, 529 (1951).

(20) R. W. Greene, *J. Clin. Invest.*, **31**, 969 (1952).

(10) M. L. Wolfson, R. Montgomery, J. V. Karabinos and P. Rothgeb, *J. Am. Chem. Soc.*, **72**, 5796 (1950).

(11) J. W. Rowen, *Biochem. Biophys. Acta*, **10**, 391 (1953).

(12) S. S. Cohen, *J. Biol. Chem.*, **144**, 353 (1942).

(13) K. W. Walton, *Brit. J. Pharma. Chemo.*, **7**, 370 (1952).

THE SOLUBILITY OF URANIUM(IV) ORTHOPHOSPHATES IN PERCHLORIC ACID SOLUTIONS

BY JAMES M. SCHREYER AND L. R. PHILLIPS

Contribution from Oak Ridge National Laboratory, Union Carbide Nuclear Company, Oak Ridge, Tennessee

Received October 20, 1955

Solubility measurements in the $U(HPO_4)_2 \cdot Cl_2O_7 \cdot H_2O$ system have been made at $25 \pm 0.1^\circ$ in 1.0 to 11.86 *M* perchloric acid. The equilibrium solid phases and their regions of stability have been demonstrated by means of the wet residue method.

I. Introduction

Solubility measurements have been reported in the $UO_2 \cdot P_2O_5 \cdot H_2O$ system at 25° in 1.5 to 15.24 *M* total dissolved phosphate.¹ The existence of $U(HPO_4)_2 \cdot 6H_2O$ and $U(HPO_4)_2 \cdot H_3PO_4 \cdot H_2O$ as the equilibrium solid phases was demonstrated. A procedure for the preparation of $U(HPO_4)_2 \cdot 4H_2O$ was presented.

A proposed investigation of complex ions in solutions of uranium(IV) orthophosphates by spectrophotometric and solubility methods would require the independent variation of the phosphate and uranium(IV) ionic concentrations. In phosphoric acid solutions this variation is limited to high phosphate to uranium ratios. Perchloric acid might serve as a satisfactory solvent if the solubility of uranium(IV) orthophosphate is sufficiently high. Accordingly, solubility measurements were extended to perchloric acid solutions. In the course of this investigation certain interesting phase relations were observed which prompted a more complete study than the initial objectives would have required.

II. Experimental

A. Stability of Uranium(IV) Orthophosphate in Perchloric Acid Solutions.—It was apparent from preliminary experiments that solubility mixtures must be free of oxygen during equilibration to eliminate oxidation of U(IV). The following experiment was conducted to test if the uranium(IV) in equilibrium mixtures would oxidize during the short time needed for filtration and uranium(IV) analysis. A vigorous stream of air was bubbled through 1 *M* perchloric acid solutions containing various concentrations of uranium(IV) at 25° . At various time intervals aliquots were removed for analysis, added directly to ferric chloride solution, 2.5 *M* in H_2SO_4 , and titrated according to the analytical procedure described previously.² The data showed a negligible oxidation of uranium(IV) during one to two hours aeration and it was concluded that it was unnecessary to maintain an oxygen-free atmosphere during filtration and analysis.

B. Preparation of Solids Used in Solubility Determinations. 1. $U(HPO_4)_2 \cdot 4H_2O$.—Samples of this solid were prepared according to the method previously described.¹ Analyses of these preparations were in good agreement with the theoretical composition. The X-ray diffraction patterns of these solids were identical with the pattern for $U(HPO_4)_2 \cdot 4H_2O$ as reported previously.¹

2. $U(H_2PO_4)_2 \cdot (ClO_4)_2 \cdot 6H_2O$.—Samples of this solid were prepared by the following procedure.

An amount of $U(HPO_4)_2 \cdot 4H_2O$ sufficient to give a 5–10% pulp density was added to 200 ml. of approximately 10 *M* perchloric acid solution and shaken for 10 days. The resulting light green solid was filtered almost to dryness on a fritted glass filter. The solid was slurried on the filter with 200 ml. of CCl_4 , filtered and dried by vacuum.

Analyses of two of the preparations gave $U^{+4}/PO_4^{-3}/ClO_4^-/H_2O$ mole ratios of 1/1.95/2.08/5.5 and 1/2.06/2.16/6.3. This method produced $U(H_2PO_4)_2 \cdot (ClO_4)_2 \cdot 6H_2O$

contaminated with excess perchloric acid because of the incomplete removal of free perchloric acid by carbon tetrachloride.³

The wet $U(H_2PO_4)_2 \cdot (ClO_4)_2 \cdot 6H_2O$ residue, without CCl_4 washing, was found to be adequate for use as a starting solid in solubility determinations.

3. $U(HPO_4)_2 \cdot 2H_2O$.—Two samples of this compound were prepared by the following procedure. Dry $U(H_2PO_4)_2 \cdot (ClO_4)_2 \cdot 6H_2O$, prepared by the above procedure, was slurried five times with 500-ml. portions of absolute ethanol, each slurry being shaken for 2 to 3 days before filtration. The final solid was dried on the filter by vacuum. Analyses for these preparations showed $U^{+4}/PO_4^{-3}/H_2O$ mole ratios of 1/1.95/2.13 and 1/1.98/2.17. X-Ray diffraction exposures were made on these preparations, but no patterns were obtained.

4. $U(HPO_4)_2$.—Solid $U(HPO_4)_2$ has not been obtained in a dry state because of its hygroscopic nature. However, during the preparation of $U(HPO_4)_2 \cdot 4H_2O$, anhydrous $U(HPO_4)_2$ is produced from the initial $U(HPO_4)_2 \cdot 6H_2O$ precipitate by washing repeatedly in 1 *M* $HClO_4$. The resultant wet residues, which were shown by Schreinemakers' wet residue method to contain only $U(HPO_4)_2$, were used in solubility determinations. X-Ray diffraction exposures were made on these wet residues but no patterns were obtained.

C. Solubility Studies in Perchloric Acid.—The solubility of uranium(IV) orthophosphate in perchloric acid solutions was studied over the range of 1.0 to 11.86 *M* $HClO_4$ at 25° . All of the solubility determinations were carried out by adding the appropriate solid to an oxygen-free perchloric acid solution of selected concentration, placing the mixture in a round bottom Pyrex flask and shaking in a water-bath at $25 \pm 0.1^\circ$ for periods necessary to attain equilibrium conditions. The attainment of solubility equilibrium was demonstrated by some preliminary studies of the rate of dissolution and by a comparison of solubilities obtained from dissolution and precipitation runs. The solubility apparatus was the same as has been previously reported.¹ The mother liquors were sampled by means of calibrated pipets or pycnometers, depending on the viscosity of the solution. After the determination of the densities of the mother liquors, they were analyzed for uranium, phosphate and perchlorate.¹ In several runs, both U(IV) and ΣU were determined on the same solution to check on possible oxidation during the long shaking times. In other runs either U(IV) or ΣU was determined. All the U(IV) analyses were made immediately after filtration.

A log-log plot of the solubility data is shown in Fig. 1. The coordinates of each point in this figure represent the formal concentrations of uranium and perchlorate in a saturated solution. The solubility curve was found to be composed of four branches, each of which corresponded to a different solid phase. The equilibrium solids with their respective stability ranges are shown in Table I.

The solubility curves of $U(HPO_4)_2$ and $U(HPO_4)_2 \cdot 2H_2O$ appear to intersect at 5.7 *M* $HClO_4$. Such an intersection would indicate a transition between these two solids. However, if the degree of hydration is dependent upon the activity of water in solution the stable solid below 5.7 *M* $HClO_4$ should have a higher degree of hydration than

(3) Acetone could not be used because of removal of perchloric acid from the compound producing $U(HPO_4)_2 \cdot H_2O$. A 10-g. sample when washed with five 500-ml. portions of acetone gave upon analysis a mole ratio of $U^{+4}/PO_4^{-3}/H_2O$ of 1/1.92/1.04. A good X-ray diffraction pattern was obtained which was different from all other uranium(IV) phosphate patterns.

(1) J. M. Schreyer, *J. Am. Chem. Soc.*, **77**, 2972 (1955).

(2) J. M. Schreyer and C. F. Baes, *ibid.*, **76**, 354 (1954).

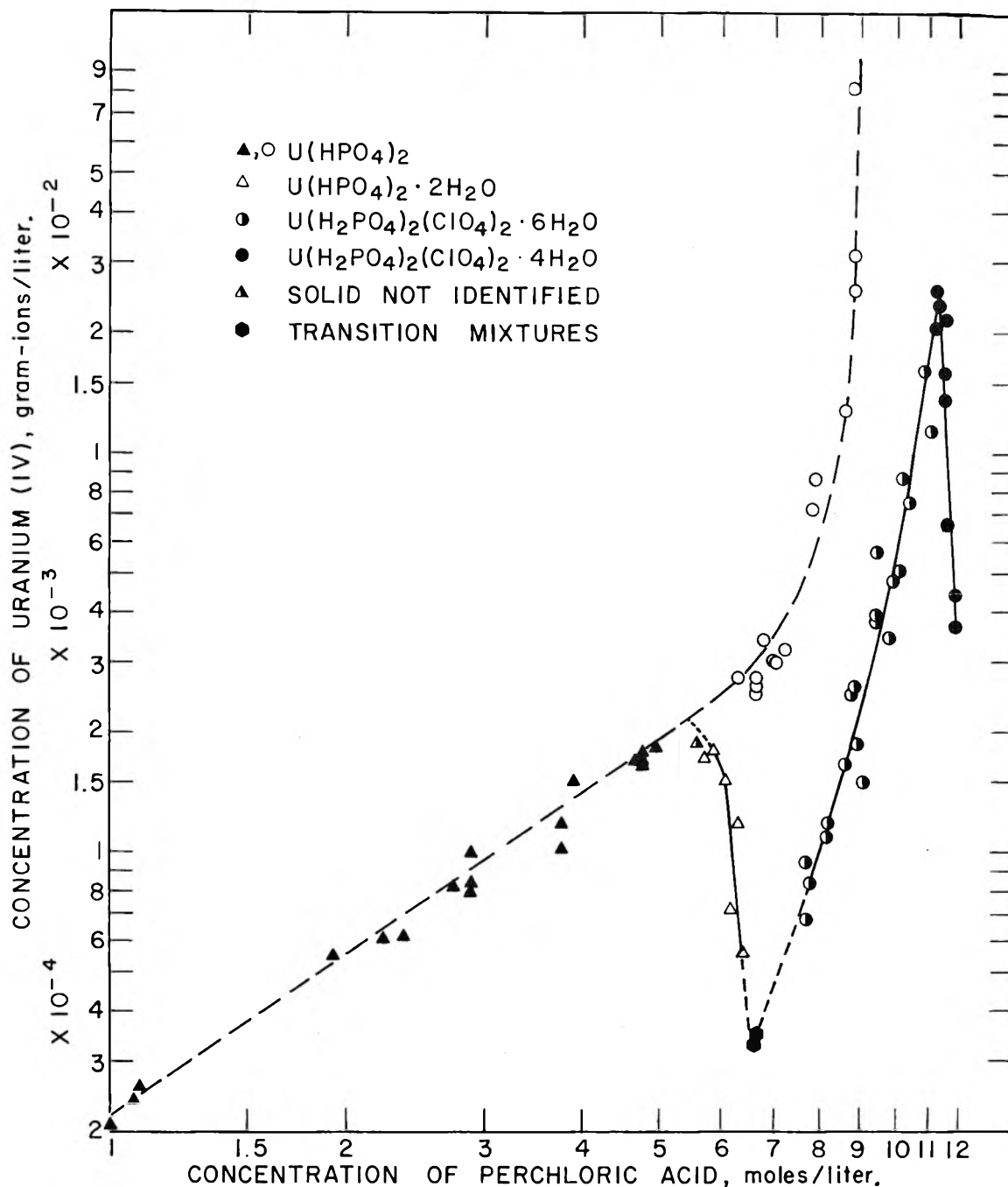


Fig. 1.—Solubility of uranium(IV) orthophosphates in perchloric acid solutions.

$U(HPO_4)_2 \cdot 2H_2O$. Experimental attempts to obtain a stable higher hydrate in this region were unsuccessful. In every instance, whether the starting solid was $U(HPO_4)_2$, $U(HPO_4)_2 \cdot 2H_2O$, $U(HPO_4)_2 \cdot 4H_2O$, or $U(H_2PO_4)_2(ClO_4)_2 \cdot 6H_2O$, the equilibrium solid obtained was $U(HPO_4)_2$, with

no indication of a higher hydrate. Seeding by the addition of the above tetrahydrate to filtered saturated solutions also resulted in the formation of $U(HPO_4)_2$.

When solid $U(HPO_4)_2 \cdot 4H_2O$ was shaken with $HClO_4$ solutions above 5.7 M, in every instance a moderately soluble metastable $U(HPO_4)_2$ solid was formed which later changed to a much less soluble stable solid.

Between 5.7 and 6.6 M $HClO_4$ determinations of the solubility of stable $U(HPO_4)_2 \cdot 2H_2O$ by precipitation became increasingly difficult with increasing acid concentrations because the transformation of metastable $U(HPO_4)_2$ to the dihydrate became progressively slower. In a run at 6.2 M $HClO_4$, solid $U(H_2PO_4)_2(ClO_4)_2 \cdot 6H_2O$ was converted rapidly to the anhydrous salt, but it was found necessary to seed with the dihydrate to accelerate the attainment of the stable equilibrium. Equilibrium was attained in 6.4 M $HClO_4$ solution by the dissolution of solid dihydrate. The gelatinous $U(HPO_4)_2 \cdot 2H_2O$ solid could be detected in

TABLE I

SOLUBILITIES OF URANIUM(IV) PHOSPHATES IN PERCHLORIC ACID SOLUTIONS

Equilibrium solid phase	[$HClO_4$]	[U(IV)]
$U(HPO_4)_2$ (metastable) ^b	1.0 ^a –5.7	0.00021–0.0021
$U(HPO_4)_2$ (metastable)	5.7–8.8 ^a	.0021–0.082
$U(HPO_4)_2 \cdot 2H_2O$ (stable)	5.7–6.6	.0021–0.00034
$U(H_2PO_4)_2(ClO_4)_2 \cdot 6H_2O$ (stable)	6.6–11.24	.00034–0.025
$U(H_2PO_4)_2(ClO_4)_2 \cdot 4H_2O$ (stable)	11.24–11.86 ^a	.025–0.0015

^a Limit of experimental investigation. ^b Stable solid not obtained.

solubility mixtures since it was the only solid in this system which adhered to the walls of the shaking flasks.

All attempts to obtain solubilities at the $U(HPO_4)_2 \cdot 2H_2O - U(H_2PO_4)_2(ClO_4)_2 \cdot 6H_2O$ transition by shaking at 25° were unsuccessful because of the extremely slow transformation from metastable $U(HPO_4)_2$. However, two solubility values for this transition mixture were obtained by shaking slurries of $U(HPO_4)_2$ in $6.6 M HClO_4$ for several days at 45° , followed by equilibration at 25° . These transition mixtures filtered much more slowly than slurries of $U(H_2PO_4)_2(ClO_4)_2 \cdot 6H_2O$ alone, probably because of the presence of appreciable quantities of the gelatinous $U(HPO_4)_2 \cdot 2H_2O$.

From 6.6 to about $7.7 M HClO_4$, no solubilities for $U(H_2PO_4)_2(ClO_4)_2 \cdot 6H_2O$ were obtained by the precipitation method because of the extremely slow transformation from $U(HPO_4)_2$. From 7.7 to $10.5 M HClO_4$ this transformation rate increased rapidly with acidity, permitting the establishment of the solubility curve by both precipitation and dissolution methods.

Solubilities in 10.5 – $11.24 M HClO_4$ were obtained only by the dissolution method. Transformation of the intermediate $U(HPO_4)_2$ into $U(HPO_4)_2(ClO_4)_2 \cdot 6H_2O$ as required by the precipitation method removes $HClO_4$ from solution, which makes the attainment of equilibrium $HClO_4$ concentrations between 10.5 and $11.24 M$ difficult. The addition of a small amount of $U(HPO_4)_2 \cdot 4H_2O$ might be expected to precipitate $U(H_2PO_4)_2(ClO_4)_2 \cdot 6H_2O$ in this region; however, the transformation from the metastable $U(HPO_4)_2$ was found to be excessively slow under these conditions.

When $U(HPO_4)_2 \cdot 4H_2O$ was added to 11.24 – $11.86 M HClO_4$, the metastable $U(HPO_4)_2$ was formed rapidly, giving highly concentrated $U(IV)$ solutions which could not be analyzed because of the immediate precipitation of the much less soluble $U(H_2PO_4)_2(ClO_4)_2 \cdot 4H_2O$. This transformation of $U(HPO_4)_2$ into $U(H_2PO_4)_2(ClO_4)_2 \cdot 4H_2O$ lowers the $HClO_4$ concentration in proportion to the ratio of solid to acid in the initial mixture. In one run enough solid was added in the initial mixture to lower the $HClO_4$ concentration from 11.86 to $11.24 M$. Both $U(H_2PO_4)_2(ClO_4)_2 \cdot 4H_2O$ and $U(H_2PO_4)_2(ClO_4)_2 \cdot 6H_2O$ were visible in the equilibrium mixture. The mother liquor from this transition mixture contained $0.0254 M U(IV)$. Other solubilities for $U(H_2PO_4)_2(ClO_4)_2 \cdot 4H_2O$ were obtained by using smaller amounts of solid in the initial mixtures. The solubility in $11.86 M HClO_4$ was obtained only through the transformation from $U(H_2PO_4)_2(ClO_4)_2 \cdot 6H_2O$, which did not involve the $U(HPO_4)_2$ intermediate stage nor remove $HClO_4$ from solution.

A thorough study was made of the equilibrium solid phases over the entire range of solubilities reported. Filtration of the equilibrium solubility mixtures was continued only to incipient dryness in order to minimize evaporation of the mother liquor in the wet residue. Wet residues from solutions above $11 M HClO_4$ were transferred in a dry box

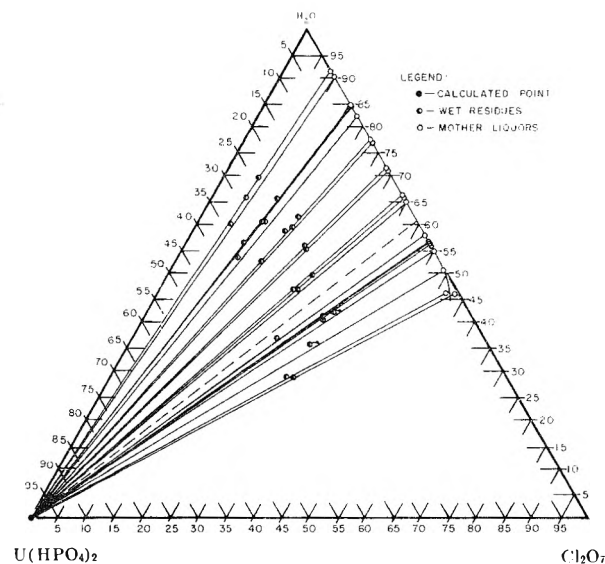


Fig. 2.—A portion of the system $U(HPO_4)_2 - Cl_2O_7 - H_2O$ at 25° : anhydrous $U(HPO_4)_2$ as the solid phase.

from closed filtration apparatus to weighing bottles because of the hygroscopic nature of the solid and the concentrated perchloric acid. The weighed wet residues were analyzed for uranium, phosphate and perchlorate.¹

Since all starting solids and equilibrium solids and solutions were found to contain a $PO_4:U(IV)$ mole ratio of 2 the system can be defined by the three components $U(HPO_4)_2 - Cl_2O_7 - H_2O$. The application of Schreinemaker's wet residue method for the identification of the solids is shown in Figs. 2 and 3, in which portions of the ternary system

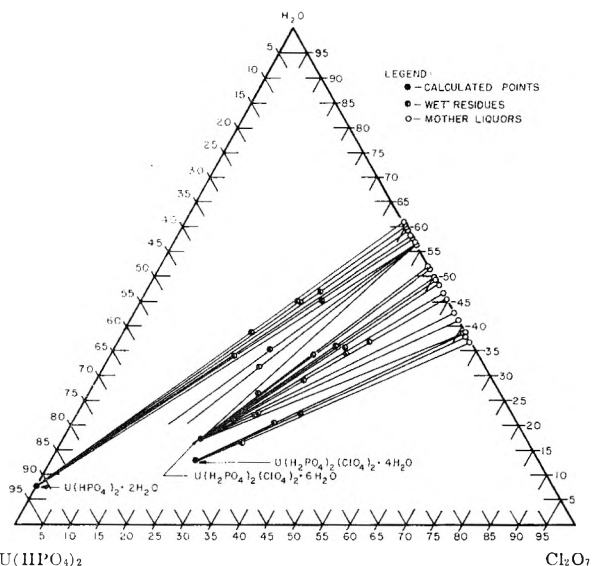


Fig. 3.—A portion of the system $U(HPO_4)_2 - Cl_2O_7 - H_2O$ at 25° : stable equilibrium solid phases above 39.2% Cl_2O_7 .

are presented separately to avoid the overlapping of tie lines of the stable and metastable regions. However, all of the areas of stability of the various equilibrium solids are shown pictorially in Fig. 4.

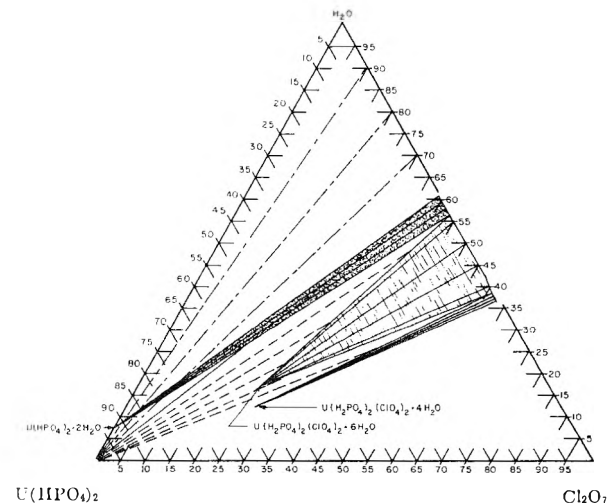


Fig. 4.—The $U(HPO_4)_2 - Cl_2O_7 - H_2O$ system.

Three distinctly different X-ray diffraction patterns were obtained for $U(H_2PO_4)_2(ClO_4)_2 \cdot 6H_2O$, suggesting the existence of three polymorphic forms of this solid. From a limited amount of data it appears that the polymorphic form obtained depends upon the perchloric acid concentration. All of fourteen samples, both slurries and dry solids, obtained from 6.6 to $9.5 M HClO_4$ gave form I, while forms II and III were obtained from more concentrated solutions, as listed in Table II. The conditions for the apparent transformation between forms II and III are not understood.

Chemical analysis and Schreinemaker's wet residue method

TABLE II

POLYMORPHIC FORMS OF $U(H_2PO_4)_2(ClO_4)_2 \cdot 6H_2O$		
Mother liquor [HClO ₄]	Nature of sample	X-Ray diffraction pattern
6.6-9.5	I
9.91	Slurry	II
10.35	Dry solid	II
10.35	Dry solid	III
10.35	Dry solid	III
10.41	Slurry	II
10.41	Wet residue	III
10.61	Dry solid	III
10.84	Slurry	II
10.84	Wet residue	III
11.02	Slurry	III

give only the empirical formulas $UO_2 \cdot P_2O_5 \cdot Cl_2O_7 \cdot 6H_2O$ and $UO_2 \cdot P_2O_5 \cdot Cl_2O_7 \cdot 8H_2O$. Additional information would be necessary before ascribing definitive formulas to these compounds. In the absence of such information the formulas $U(H_2PO_4)_2(ClO_4)_2 \cdot 6H_2O$ and $U(H_2PO_4)_2(ClO_4)_2 \cdot 4H_2O$ have been chosen as being plausible.

III. Conclusions

As a result of solubility studies in 1.0 to 11.86 *M* perchloric acid, four compounds were identified, $U(HPO_4)_2$, $U(H_2PO_4)_2 \cdot 2H_2O$, $U(H_2PO_4)_2(ClO_4)_2 \cdot 6H_2O$ and $U(H_2PO_4)_2(ClO_4)_2 \cdot 4H_2O$. Identification of these solids was made by chemical and X-ray diffraction analyses.

A graph is presented which depicts the solubility of uranium(IV) phosphates over the range of 1.0 to 11.86 *M* perchloric acid at 25°.

Acknowledgments.—Most of the chemical analyses were made by the Analytical Division under the supervision of Dr. M. T. Kelley and Mr. C. D. Susano. The X-ray diffraction analyses were performed by Mr. H. W. Dunn of the Spectroscopy Research Laboratory, Stable Isotopes Research and Production Division.

The authors wish to express their appreciation to Dr. M. A. Bredig and Mr. R. D. Ellison, Chemistry Division for consultations concerning the X-ray diffraction patterns of $U(H_2PO_4)_2(ClO_4)_2 \cdot 6H_2O$.

THE DISTRIBUTION OF COPPER BETWEEN GERMANIUM AND TERNARY MELTS SATURATED WITH GERMANIUM

BY C. D. THURMOND AND R. A. LOGAN

Bell Telephone Laboratories, Inc., Murray Hill, N. J.

Received October 20, 1955

The solubility of copper in solid germanium has been measured as a function of the copper concentration in ternary Ge-Cu-Pb melts saturated with germanium at 700°. Alloys of Ge-Cu-In, Ge-Cu-Sn and Ge-Cu-Au have also been studied but to a more limited extent. The distribution coefficient of copper as a function of melt concentration is explained in terms of the expected interactions deduced from the binary phase diagrams. The measured temperature dependence of the distribution coefficient from dilute ternary alloys has permitted an estimate to be made of the binding energy of copper in the dilute germanium solution.

1. Introduction

The control of impurities in semiconductors is of increasing technological interest. One method which is used to introduce donors or acceptors into semiconductor crystals makes use of a third component. For example, the concentration of copper, an acceptor in germanium, can be controlled in germanium crystals by using molten lead as a carrier.¹

We have measured the distribution of copper between germanium and Ge-Cu-Pb melts saturated with germanium, as a function of the copper concentration in the melts. Alloys of Ge-Cu-In, Ge-Cu-Sn and Ge-Cu-Au have been studied also, but to a more limited extent. An explanation of the observed dependence on concentration of the ratio of copper concentrations in the two phases, is presented.

This ratio, the distribution coefficient of copper, has also been determined as a function of temperature using Ge-Cu-Pb alloys which were dilute enough in copper to be ideal dilute solutions. From these measurements an estimate of the relative partial molar heat content of copper has been made.

2. Experimental

Since copper is an acceptor² which is completely ionized at room temperature in germanium, concentrations as low as 10^{-7} atomic per cent. can be determined readily from simple resistivity measurements. Furthermore, copper diffuses in solid germanium at a remarkably fast rate,³ and consequently crystals of germanium will come to equilibrium with copper in a conveniently short time.

The solid solubility of copper in germanium, χ_s , in the ternary solutions of Ge-Pb-Cu, was determined by heating germanium crystals in contact with Cu-Pb alloys of various compositions. These alloys were made by heating 10 to 15 g. of Pb-Cu mixtures in silica tubes under a helium atmosphere. The tubes were quenched by plunging them into water. Microscopic examination of polished and etched specimens showed uniform distribution of copper through the lead phase.

The copper entering the crystal from the alloy was determined from the change in resistivity of the germanium⁴ which gave a direct determination of χ_s . The corresponding value for χ_l in the alloy was determined by chemical analysis of an initial binary alloy of copper and lead from which the alloys more dilute in copper were made by dilution with lead.

The germanium crystals used in these experiments were cut to the dimensions 0.3 in. × 0.3 in. × 0.050 in. and were of intrinsic resistivity at room temperature. At Dry Ice temperature, the samples were n-type and resistivity meas-

(2) C. S. Fuller and J. D. Struthers, *Phys. Rev.*, **87**, 527 (1952).

(3) L. Esaki, *ibid.*, **89**, 1026 (1953); C. S. Fuller, J. D. Struthers, J. A. Ditzemberger and K. B. Wolfstirn, *ibid.*, **93**, 1182 (1954).

(4) M. B. Prince, *ibid.*, **92**, 681 (1953).

(1) R. A. Logan and M. Schwartz, *J. Appl. Phys.*, **26**, 1287 (1955).

urements at this temperature indicate $N_D - N_A \cong 10^{13}$ atoms/cc.

The germanium samples were specially cleaned⁵ to remove any surface contamination of copper and heated on a chemically cleaned molybdenum boat in a conventional nichrome tube furnace under a hydrogen atmosphere. The samples were placed four in a row on the molybdenum boat; the first and fourth were used as controls to determine the resistivity change produced by the heat treatment, and the inner two were covered with wafers of the Pb-Cu alloy under investigation. This wafer was of dimensions 0.3 in. \times 0.3 in. \times 0.020 in. The wetting of the germanium by the alloy during the heat cycle was good, so that one side of the test crystals was nearly covered with alloy. The heating cycle brought the samples to 700° in about 3 minutes. This temperature was maintained for 30 minutes and lowered to room temperature in about 3 minutes.

Resistivity was measured with the conventional four-point probe.⁶ Prior to each measurement, the alloy was dissolved in hot etch (4 parts $\text{HC}_2\text{H}_3\text{O}_2$, 4 parts H_2O_2 , 10 parts H_2O), and the surfaces were lapped to remove any regrowth material. Uncontrolled thermal conversion, inferred from resistivity measurements on the control wafers, did not exceed about 10^{13} acceptors per cc.

Using experimental conditions similar to those employed here, Fuller, *et al.*,³ have measured D , the diffusion coefficient of copper at 700° and found $D = (2.8 \pm 0.3) \times 10^{-5}$ cm.²/sec. This indicates⁷ that the average concentration of copper in the wafer (as determined by the four-point probe resistivity measurement) will be very nearly equal to equilibrium concentration. To check this, an alloy of 0.368 wt. % Cu in Pb was used for two heating times, 15 and 30 minutes at 700°. In the 30-minute cycle 1.8×10^{16} Cu atoms per cc. were added to the germanium wafer, whereas in the 15-minute cycle, 1.5×10^{15} Cu atoms per cc. were added. The uncertainty of the measured concentration is about equal to this change in concentration so that within the precision of these experiments, equilibrium is established in the 30-minute cycle. This cycle was used in all experiments reported here in which Pb-Cu alloys were used at 700°.

To determine the solid solubility of pure copper in germanium at 700°, samples similar to those described above were copper plated and heated in a sealed quartz tube at 700° for 19 hours. Resistivity measurements similar to those already described were made on these samples. The value obtained is in agreement with other measurements.³

The distribution coefficient of copper in germanium from ternary melts containing indium, tin or gold was determined by the same methods used for the Pb-Cu alloys.

The temperature dependence of the copper distribution coefficient was measured over the temperature range 625 to 700°. The Pb-Cu alloy containing 0.368 wt. % copper was used in each case. Using Esaki's⁸ values for the diffusion coefficient of copper in germanium, heating times were chosen to give an average copper concentration in the crystals greater than 90% of saturation.⁷

The concentration of copper in the ternary melts saturated with germanium was obtained from the composition of the original binary alloy and from the assumption that the solubility of germanium in lead was not changed by the addition of copper. The solubility of germanium in lead is 0.046, 0.035, 0.026 and 0.020 atomic fractions at 700, 675, 650 and 625°, respectively.⁸

3. Results

The solid solubility of copper in germanium is plotted in Fig. 1 as a function of copper concentration in the various ternary melts, all at 700°. In addition, a plot has been made of the distribution coefficient k , which is given by the ratio of the atom fraction of copper in the solid solution to that in the melt (χ_s/χ_l).

In Fig. 2, the logarithm of the limiting value of

(5) R. A. Logan, *Phys. Rev.*, **91**, 757 (1953).

(6) L. B. Valdes, *Proc. I. R. E.*, **42**, 420 (1954).

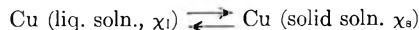
(7) W. Jost, "Diffusion," Academic Press, Inc., New York, N. Y., 1952, p. 37.

(8) C. D. Thurmond, F. X. Hassion and M. Kowalchik, to be published.

the copper distribution coefficient, k° , is plotted as a function of the reciprocal of the absolute temperature. A plot of the estimated limiting value of the copper activity coefficient f° in solid germanium as a function of $1/T$ has been included in Fig. 2.

4. Discussion and Conclusions

4.1. The Distribution Coefficient and the Activity Coefficient.—The distribution coefficient as a function of composition at constant temperature can be discussed conveniently in terms of activity coefficients. For the equilibrium



the equilibrium constant K , which is independent of composition, can be written

$$K = \frac{\chi_s f_s}{\chi_l f_l} \quad (1)$$

where f_s and f_l are the activity coefficients of copper in the solid and liquid solutions, respectively. When the concentration of the third component, say lead, is zero, χ_l will be the concentration of copper in the germanium saturated binary melt and will have the particular value χ_l^* at T , say 700°. Similarly, χ_s will have the particular value χ_s^* , and the liquid and solid phase copper activity coefficients will have the particular values, f_l^* and f_s^* . Consequently

$$\frac{\chi_s f_s}{\chi_l f_l} = \frac{\chi_s^* f_s^*}{\chi_l^* f_l^*} \quad (2)$$

and using the definition of the distribution coefficient, Equation 2 may be written as

$$k = \frac{f_s^* f_l}{f_s f_l^*} k^* \quad (3)$$

Since the solid solubility of copper in germanium is always less than 10^{-6} atom fraction² these solid solutions are most probably ideal dilute solutions; that is, f_s is not a function of composition. This assumption leads to a simplification of (3), namely

$$k = \frac{f_l}{f_l^*} k^* \quad (4)$$

As the concentration of copper is varied from the binary solution value⁹ ($\chi_l^* = 0.575$) to zero, f_l will vary from f_l^* to f_l° , a particular value characteristic of copper in very dilute solutions containing lead as the major component and saturated with germanium. Thus, k will vary from k^* to k° . From Fig. 1 it can be seen that when the concentration of copper in lead-germanium melts is less than about 0.2%, $k = k^\circ$. This means that melts containing copper at concentrations less than about 0.2% can be considered as ideal dilute solutions.

4.2. k as a Function of Concentration.—It is possible to predict qualitatively the change in k in the Ge-Cu-Pb system since certain information is available about the activity coefficients f_s^* and f_l° . In particular, f_l° can be expected to have a value nearly the same as the value in a Pb-Cu binary alloy saturated with copper at 700°. Since the

(9) R. Schwartz and G. Elstner, *Z. anorg. allgem. Chem.*, **217**, 289 (1934); H. Maucher, "Forschungsarbeiten über Metallkunde und Röntgen Metallographie," Folge 20 (1936); C. D. Thurmond, F. X. Hassion and M. Kowalchik, to be published.

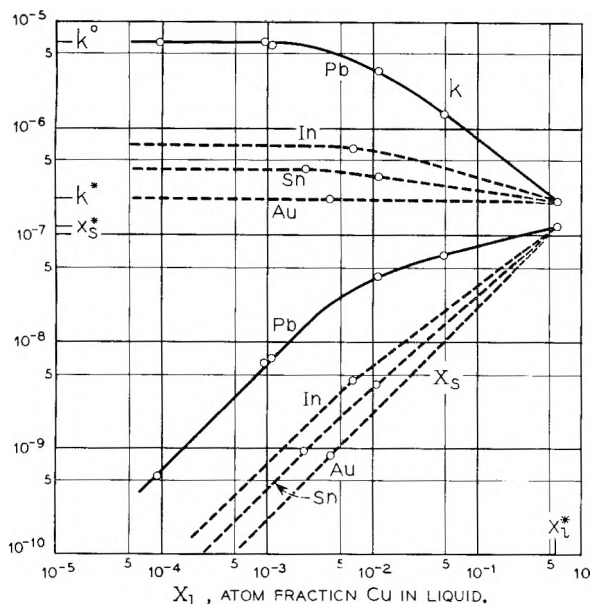


Fig. 1.—The distribution coefficient, k , and the atom fraction of copper in solid germanium, x_s , as functions of the atom fraction of copper in the Ge-Cu-Pb ternary melts saturated with germanium at 700°.

solubility of copper in lead at this temperature, x_1^\dagger , is only 0.056 atom fraction,¹⁰ the activity coefficient of copper, f_1^\dagger probably would not increase very much upon dilution with lead. Since the solubility of germanium in lead is only 0.046 atom fraction,⁴ the activity coefficient of copper in dilute lead solutions probably would not change much upon saturation with germanium. Consequently, it can be estimated that $f_1^\circ \cong f_1^\dagger$, that is, the activity coefficient of copper in germanium saturated lead melts containing small amounts of copper will be approximately the same as the activity coefficient of copper in lead melts saturated with copper.

Since the solid solubility of lead in solid copper is very small,¹¹ the chemical potential of copper in lead melts saturated with copper will be that of pure copper. Taking pure solid copper as the reference state, the activity coefficient f_1^\dagger will be given by

$$f_1^\dagger = \frac{1}{x_1^\dagger} = 18 \quad (5)$$

Information about f_1^* can be obtained from the fact that the chemical potential of copper in the germanium saturated binary melt must be less than that of pure solid copper. Then, $f_1^* x_1^*$ must be less than 1, or

$$f_1^* < \frac{1}{x_1^*} = 1.7 \quad (6)$$

It is concluded that the ratio f_1°/f_1^* would be expected to be greater than 10. Consequently, from equation 4, the conclusion is reached that the ratio k°/k^* should be greater than 10. From Fig. 1 it can be seen that this ratio is equal to 29 for the Ge-Cu-Pb system. Thus, the increase in

(10) O. J. Kleppa and J. A. Weil, *J. Am. Chem. Soc.*, **73**, 4848 (1951).

(11) P. A. Beck, "Metals Handbook," 1948 Ed., Am. Soc. Metals.

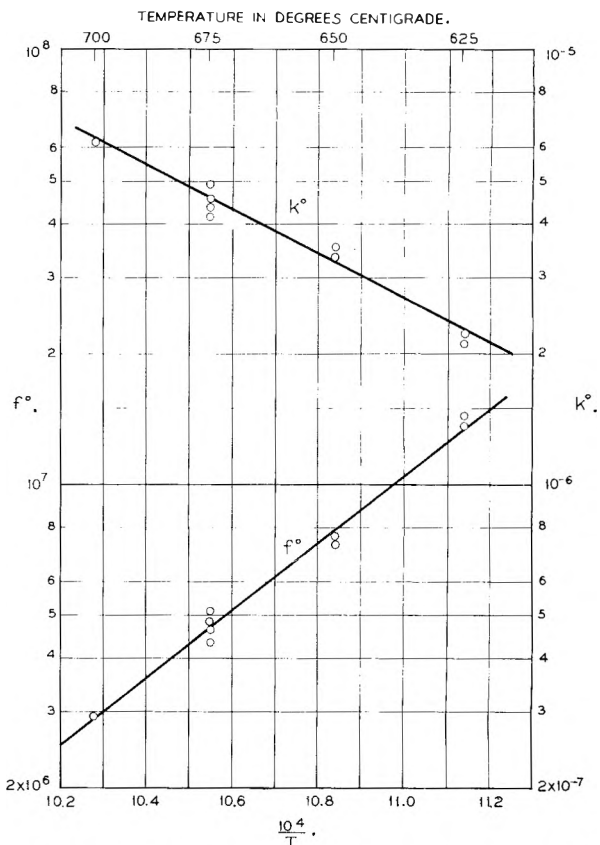


Fig. 2.—The dilute solution distribution coefficient and activity coefficient of copper as functions of the reciprocal of the absolute temperature.

the copper distribution coefficient as lead is added to germanium saturated Ge-Cu melts is a consequence of the fact that lead and copper do not mix well. That is, the activity coefficient of copper in the melt is raised by the addition of lead as would be expected from the properties of lead and copper exhibited by their binary phase diagrams.

The shape of the distribution coefficient curve shown in Fig. 1 for the lead melts suggests, however, that interactions occurring in the ternary system are not quite as simple as suggested by the assumptions made so far. Thus, from Fig. 1 it is seen that the distribution coefficient of copper changes from about 1.5×10^{-6} to 6.2×10^{-6} as the copper concentration in germanium saturated lead melts varies from about 5 atom per cent. to less than 0.2 atom per cent. From equation 4, it follows that this variation gives the change in copper activity coefficient along the solubility isotherm. That is, f_1 , the copper activity coefficient, decreases by 75% as the copper concentration is increased from 0.2 to 5%. This is a larger change than would be expected if the Ge-Cu-Pb melts had the thermodynamic properties of strictly regular solutions.¹² On the basis of the strictly regular solution model where the binary solution parameters are evaluated from the solubility of germanium in lead and copper and from the solubility of copper in lead, it would be concluded that the activity coefficient of copper would

(12) J. L. Meijering, *Phillips Res. Rep.*, **5**, 333 (1951); **6**, 183 (1951).

decrease only about 30% upon increasing the copper concentration to 5 atom per cent.

The rapid decrease in the copper distribution coefficient along the solubility isotherm is evidence that copper and germanium interact rather strongly. The Pb-Cu system shows rather large positive deviations from ideal solution behavior while from the change in k along the solubility isotherm, it is concluded that Ge and Cu interact as if there were large negative deviations from ideal solution behavior. This suggests that the estimate of $f_1^\circ = f_1^\dagger$ may not be very good since the strong Ge-Cu interactions may make $f_1^\circ < f_1^\dagger$. If an attempt is made to account for the distribution coefficient curve of Fig. 1 using the strictly regular solution approximation and adjusting the Ge-Cu parameter to give the rapid decrease of the activity coefficient in the dilute solution region, the conclusion is reached that f_1° may be as small as $f_1^\dagger/2$.

It was shown previously (equation 6) that the activity coefficient of copper in the Ge-Cu melts saturated with germanium at 700° must be less than 1.7. Since the distribution coefficient of copper increased by a factor of 29 as lead was added, and since f_1° is most likely somewhat less than 18 (equation 5) a better estimate of f_1^* is possible. From equation 4 it is concluded that

$$f_1^* = \frac{k^*}{\bar{k}^\circ} f_1^\circ < 0.62 \quad (7)$$

4.3 The Dependence of k on the Third Component.—The distribution coefficient curves of Fig. 1 are in the order of $k_{\text{Pb}}^\circ > k_{\text{In}}^\circ > k_{\text{Sn}}^\circ > k_{\text{Au}}^\circ$. From equation 4 it follows that the activity coefficients of copper are in the same order: $f_{\text{Ab}}^\circ > f_{\text{In}}^\circ > f_{\text{Sn}}^\circ > f_{\text{Au}}^\circ$.

The fact that the distribution coefficients in the indium, tin and gold melts are less than in the lead melts follows directly from the properties of these systems inferred from the binary phase diagrams. Thus, the liquid phase immiscibility of the Cu-Pb system, absent in the Cu-In, Cu-Sn, Cu-Au systems¹³ is evidence that the activity coefficient of copper in these latter melts is less than in the lead melts at the same copper concentrations. Furthermore, the binary phase diagrams of germanium with lead,¹⁴ indium,¹⁵ tin¹⁶ and gold¹⁷ are all of the simple eutectic type in which the solubility of germanium is smallest in the lead melts. Since the activity coefficient of copper was found to decrease along the Ge-Cu-Pb solubility isotherm it cannot be expected that the copper activity coefficients in germanium saturated indium, tin or gold melts could be raised to values higher than in lead melts.

4.4. k° as a Function of Temperature.—The temperature dependence of k° can be used to estimate the binding energy of copper atoms in the

dilute germanium solid solution. By choosing pure solid copper as the reference state for both liquid and solid phases, the equilibrium constant of equation 1 will be 1. Then, for solutions dilute in copper we may write

$$k^\circ = f_1^\circ / f_s^\circ \quad (8)$$

The temperature dependence of an activity coefficient is related to the relative partial molar heat content by

$$\frac{\partial \ln f}{\partial(1/T)} = \frac{\Delta \bar{H}}{R} \quad (9)$$

which permits the temperature dependence of the distribution coefficient to be written as

$$\frac{\partial \ln k^\circ}{\partial(1/T)} = \frac{\overline{\Delta H}_1 - \Delta \bar{H}_s}{R} \quad (10)$$

In this expression, $\overline{\Delta H}_1$ is the relative partial molar heat content of copper in the ideal dilute melt referred to pure solid copper, while $\Delta \bar{H}_s$ is the relative partial molar heat content of copper in the dilute solid solution referred to pure solid copper. From the temperature dependence of k° (Fig. 2), $\overline{\Delta H}_1 - \Delta \bar{H}_s = -23.4$ kcal.

It is possible to estimate $\overline{\Delta H}_1$ from the work of Kleppa and Weil.¹⁰ They found that the logarithm of the solubility of copper in molten lead was a linear function of the reciprocal of the absolute temperature below 500°. Since the solid solubility of lead in copper is very low, the slope of this line gives the relative partial molar heat content of copper in melts which are ideal solutions of copper, referred to pure solid copper. This relative partial molar heat content should be a good approximation to the heat content in the 600 to 700° range and with the solubility of germanium in ternary melts dilute in copper being quite small,⁸ it can be expected that it will be a good approximation to $\overline{\Delta H}_1$ for these ternary melts.

From the measurements of Weil and Kleppa¹⁰ we obtain $\overline{\Delta H}_1 = 9.8$ kcal., and therefore $\Delta \bar{H}_s = 33$ kcal.

It is possible to estimate $\Delta \bar{H}_s$ by a somewhat different method, still using the measurements of Kleppa and Weil. In section 4.2 it was assumed that $f_1^\circ = f_1^\dagger = 1/\chi_1^\dagger$ at 700°. If this assumption is made at temperatures between 625 and 700°, and used in equation 8, we obtain for the activity coefficient of copper in the germanium solid solution

$$f_s^\circ \cong \frac{1}{\chi_1^\dagger k^\circ} \quad (11)$$

The value of f_s° evaluated in this manner has been plotted as a function of $1/T$ in Fig. 2 along with k° . The slope of this line gives $\Delta \bar{H}_s = 35$ kcal. (equation 10).

An earlier estimate of 45 kcal. for $\overline{\Delta H}_s$ has been reported.¹⁸ This was obtained from the temperature dependence of k^* , the copper distribution coefficient in the Ge-Cu system over the temperature range 700 to 937°, using the assumption that the molten phase was an ideal solution. It is

(18) C. D. Thurmond and J. D. Struthers, *THIS JOURNAL*, **57**, 834 (1953).

(13) C. J. Smithells, "Metal Reference Book," Interscience Publishers, Inc., New York, N. Y., 1949.

(14) R. T. Briggs and W. S. Benedict, *THIS JOURNAL*, **34**, 173 (1930).

(15) H. Stohr and W. Klemm, *Z. anorg. allgem. Chem.*, **244**, 205 (1940).

(16) H. Stohr and W. Klemm, *ibid.*, **241**, 305 (1939).

(17) R. I. Jaffee, E. M. Smith and B. W. Gosser, *Trans. AIME*, **161**, 366 (1945).

apparent from the studies reported here on the ternary system Ge-Cu-Pb, that the Ge-Cu melts are not ideal but exhibit negative departures from ideality. That is, equation 7 gives an upper limit to the activity coefficient f_i^* referred to pure solid copper. If referred to pure supercooled liquid copper, the reference state used for the ideal solutions just mentioned, the upper limit to the activity coefficient would even be smaller, namely, 0.4 rather than 0.62.

4.5. The Binding Energy of Copper in Germanium Solid Solutions.—The binding energy of copper can be defined as the difference in molar heat content between copper in the ideal vapor

state and in the dilute solid solution, *i.e.*, $H_g - \bar{H}_s$. Since $\Delta\bar{H}_s = \bar{H}_s - H_s^*$ and the heat of sublimation of copper is $H_g - H_s^*$, the binding energy can be obtained. From Brewer's¹⁹ compilation we obtain 81 kcal. for the heat of sublimation of copper around 700°, which gives a value of 47 kcal. for the binding energy.

5. Acknowledgments.—We wish to thank F. Trumbore for helpful discussions and M. Kowalchik for experimental assistance.

(19) Leo Brewer, "Chemistry and Metallurgy of Miscellaneous Materials: Thermodynamics," National Nuclear Energy Series IV-19B. Ed. L. L. Quill, paper 3, 1st Ed., McGraw-Hill Book Co., New York, N. Y., 1950.

A MODIFIED DIRECT CURRENT CONDUCTANCE METHOD FOR GENERAL APPLICATION

BY L. ELIAS AND H. I. SCHIFF

Department of Chemistry, McGill University, Montreal, Canada

Received October 21, 1955

The relatively simple direct current method developed by Gunning and Gordon for measuring electrolytic conductance has been modified to extend its application to electrolytes for which reversible electrodes are unavailable. Silver-silver halide electrodes were immersed in a suitable halide solution and contact made with the cell solution through liquid junctions. Differences in liquid junction potentials were small and remained constant during the measurements. No contamination of the cell solution by diffusion was observed over a period of at least two hours. The conductance was independent of the current passed through the main body of the cell over the same range as reported by Gunning and Gordon. The method has been applied to several electrolytes in aqueous, methanol and nitromethane solutions, with a precision of ± 0.01 conductance unit.

I. Introduction

The direct current conductance method, as developed by Gordon and his associates, has been applied to aqueous¹ and methanol² solutions with an accuracy comparable to that obtained with the most refined alternating current techniques. The inherent simplicity of the method and its freedom from most of the difficulties encountered in high precision a.c. work recommend its use wherever practicable.

Briefly, the method consists of passing a known current through the solution and measuring the potential difference between two probe electrodes; the conductance is then calculated from Ohm's law. Since no current is passed through the probe electrodes other than the small momentary one before potentiometer balance is obtained, reproducible readings are assured if the probes are reversible with respect to the solution. This, however, limits the method to solutions for which reversible electrodes can be found, which is a rather serious restriction, particularly for non-aqueous solutions. Thus, for example, silver halides were found to be soluble in nitromethane solutions of alkyl ammonium halides.

It is the purpose of this paper to describe a modification of the Gordon conductivity cell which removes this restriction.³

(1) H. E. Gunning and A. R. Gordon, *J. Chem. Phys.*, **10**, 126 (1942); G. C. Benson and A. R. Gordon, *ibid.*, **13**, 470 (1945); R. E. Jervis, D. R. Muir, J. P. Butler and A. R. Gordon, *J. Am. Chem. Soc.*, **75**, 2855 (1953).

(2) J. P. Butler, H. I. Schiff and A. R. Gordon, *J. Chem. Phys.*, **19**, 752 (1951).

(3) D. J. G. Ives and S. Swaroopa (*Trans. Faraday Soc.*, **49**, 367 (1953)) have attempted to extend the applicability of the d.c. method

II. Experimental

Method.—Although the probe electrodes must be reversible with respect to the solution with which they are in contact, this solution need not be the one whose conductance is being measured. In this modification a liquid junction is formed between the cell solution and a suitable halide solution in which each reversible silver-silver halide electrode is immersed. The cell is identical with that described by Gunning and Gordon,¹ and is shown diagrammatically in Fig. 1. The liquid junctions were effected by means of the probe chambers represented in the lower portion of the figure. Type A chambers were used when the probe solution was less dense, and type B when the probe solution was more dense than the cell solution.

Type A chamber was made of 12 mm. Pyrex tubing which was tapered to a 4 mm. opening at its lower end. The 19/38 standard taper inner joint fitted the outer joint of the probe side arm of the cell, and the 12/30 outer joint matched the inner member of the probe electrode. The probe chamber was blocked at the lower end and filled with halide solution to a level just below the rubber bulb. The probe electrode was inserted in the chamber and the 12/30 ground joint wetted with the solution to ensure an air-tight seal. The lower end of the chamber was unblocked and the rubber bulb was depressed to expel about 2 cm.³ of solution. An equal volume of cell solution was drawn up, by releasing the bulb while the tip of the chamber was immersed in a sample of the cell solution. The position of the boundary is shown as a dotted line in Fig. 1.

Type B chamber was made of 13 mm. Pyrex tubing; the by the use of quinhydrone electrodes in potassium hydrogen phthalate stabilizer. However, the precision reported was an order of magnitude lower than that achieved with the Gordon cell. We have constructed a cell similar to the one they describe and found that the long probe path seriously decreased the sensitivity of the measurements.

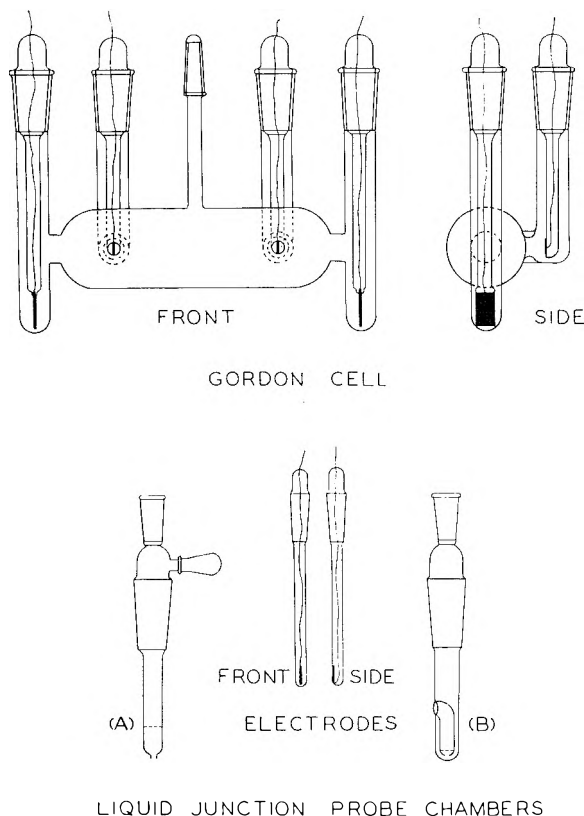


Fig. 1.—Above, the original Gordon cell and probes; below, the liquid junction probe chambers and probe electrodes.

inner tube was 8 mm. in diameter and 3 cm. long. To form the boundary in this chamber, cell solution was first run into the side opening while the top of the chamber was blocked, so that only the inner tube was filled. A clean rubber finger cot was pressed against the side opening while the probe solution was run into the chamber from the top; the boundary formed just above the tip of the inner tube. Finally the probe electrode was inserted and the finger cot removed. Contamination of the cell solution by mechanical mixing was successfully avoided by this procedure.

The filled probe chambers were wiped clean on the outside with filter paper and placed in the probe side arms of the cell. All ground glass joints were aligned by etch marks on the inner and outer members although this did not seem to be at all critical. Rotation of the probes by as much as 90° had no effect on the measured potential differences.

Apparatus and Materials.—The electrical measurements were made in the manner described by Gunning and Gordon¹; the "constant current" circuit was modified slightly to accommodate a 6SJ7 rather than a 1B4P pentode. The probe electrodes were made of thin platinum strips 1 mm. wide and 6 mm. long sealed into Nonex glass in such a manner that no edges were exposed; they were silver plated and anodized in an appropriate halide solution after the method of Brown.⁴ The main, current-carrying electrodes were made of heavily silver-plated platinum. Cell constants were determined using the Jones and Bradshaw 0.01 demal standard.⁵

The oil-bath was regulated to better than 0.005° and set at 25.000° with a mercury-in-glass thermometer which was periodically calibrated by the Thermometry Division of the National Research Council at Ottawa.

Water of specific conductance 0.7×10^{-6} ohm⁻¹ cm.⁻¹ was used in preparing the aqueous solutions. These solutions were degassed by application of water-aspirator vacuum for three minutes and returned to normal pressure with purified air. All solutions were prepared gravimetrically, final weighings being made after the degassing procedure.

All solutions and solvents were transferred by pressure of purified nitrogen.

Methanol was distilled from magnesium turnings; the distillate was found to contain less than 0.006 weight per cent. water by Karl Fischer titration. The nitromethane had a specific conductance of 1×10^{-8} ohm⁻¹ cm.⁻¹; details of the purification of this solvent and the preparation of the quaternary ammonium halides will be given in a future paper.

Reagent grade potassium chloride, twice recrystallized from conductivity water, was fused under a purified, dry nitrogen stream for the preparation of the aqueous solutions, and heated at 600° in a nitrogen atmosphere for the preparation of the methanol solutions. Sodium nitrate was precipitated from a concentrated aqueous solution by the addition of methanol and dried *in vacuo* at 150° for 12 hours. No attempt was made to obtain this salt in ultra-pure form since it was not required for absolute conductance measurements.

III. Results

The most sensitive criterion for a satisfactory probe arrangement is that the calculated resistance must be independent of the current that is passed through the solution. This condition will not be satisfied if the probes perturb the potential gradient in the main body of the cell. Table I shows a typical set of readings for a 0.002 *N* aqueous NaNO₃ solution, with Ag,AgBr probe electrodes in a 0.002 *N* methanol solution of KBr in type A probe chambers. E_s is the potential drop across a 1000 ohm standard resistor in series with the cell. E_c is the potential difference between the probes, taken with the current flowing first in one direction (+), and then in the other (-). The ratio E_c/E_s (and consequently the calculated conductance) is invariant within the limits of error of the measurements (0.01%) for at least a fivefold change in current.

TABLE I
DEPENDENCE OF MEASURED RESISTANCE ON CURRENT

E_s , v.	E_c , v.	E_c/E_s
1.12492	+0.78711	0.69913
	- .78583	
0.69068	+ .48352	.69914
	- .48225	
0.55036	+ .38545	.69917
	- .38414	
0.23990	+ .16837	.6991 ₁
	- .16706	
0.20632	+ .14491	.6992 ₀
	- .14361	

Static bias 0.00066 v.

Effect of Concentration of Probe Solutions.—The probe electrodes were made narrow to minimize the effect of "shorting out" the solution across the probe surface. With the liquid junction arrangement there should be no danger of any "shorting" effect arising from the probe solution if it has a lower specific conductance than the cell solution. To test the stringency of this requirement the resistance of a 0.001 *N* nitromethane solution of Me₄NCl was measured with a series of aqueous KCl solutions in type A probe chambers. Table II shows that an error of not more than 0.01% is introduced when the concentration (or in this case, the specific conductance) is as much as 100 times that of the cell solution. On the other hand, the probe solution cannot be made too dilute without seriously decreasing the sensitivity of the measure-

(4) A. S. Brown, *J. Am. Chem. Soc.*, **56**, 646 (1934).

(5) G. Jones and B. B. Bradshaw, *ibid.*, **55**, 1780 (1933).

ments as well as altering the effective cell factor. The general practice has been to use a probe solution having a specific conductance comparable with that of the cell solution.

TABLE II
DEPENDENCE OF MEASURED RESISTANCE ON
CONCENTRATION OF PROBE SOLUTION

Concn. of probe soln., <i>N</i>	Measured resistance of cell soln., ohm
0.001	1643.2 ₄
0.01	1643.2 ₀
0.1	1643.1 ₃

The Effect of the Liquid Junction Potentials.—There is no completely satisfactory method of estimating the magnitude of liquid junction potentials, particularly if both solvent and solute differ in the two solutions. However, since the method involves the measurement of the potential difference between a pair of electrodes, only the difference between the two liquid junction potentials is of importance. This difference will, of course, be in addition to the usual bias potentials between the two silver-silver halide probe electrodes. It will be seen from Table I that the difference between any pair of E_c readings is independent of the current and is equal to twice the "static bias" measured with no current flowing through the cell. The "bias" was never found to be more than a few millivolts, and, what is more important, did not change with time during the course of the measurements. It therefore appears that any difference in liquid junction potentials can be eliminated along with the usual electrode bias by averaging pairs of E_c readings.

The Effect of Diffusion.—Although diffusion did not seem to affect the difference in liquid junction potentials, there remained the possibility that diffusion of the probe solution might contaminate the cell solution. Consequently the resistance of an aqueous 0.002 *N* NaNO₃ solution was measured over a period of time, with 0.002 *N* KCl in methanol in the type A probe chambers. Table III shows the readings obtained at 15-minute intervals after the cell had been in the oil-bath for one hour. Similar results were obtained with both types of probe chambers for at least two hours after the junction had been formed. As long as there is an appreciable density difference between probe and cell solutions there appears to be ample time to make the measurements without danger of contamination.

TABLE III
TEST FOR CONTAMINATION BY PROBE SOLUTION

Time, min.	Resistance, ohms
0	459.53
15	459.53
30	459.50
45	459.51

Accuracy and Precision of the Method.—The accuracy of the method was tested by measuring the conductance of aqueous KCl solutions. Figure 2 shows the sensitive Shedlovsky Λ'_0 plot of the

results; the radii of the circles correspond to 0.01 conductance units. The open circles were obtained with Ag,AgCl probe electrodes and methanolic KCl in type A probe chambers; the filled circles were obtained with Ag,AgBr probe electrodes and methanolic Me₄NBr in the same probe chambers. The solid curve is drawn from the Onsager-Shedlovsky equation $\Lambda' = \Lambda' + BC + DC \log C$ using the values of the constants given by Benson and Gordon.¹

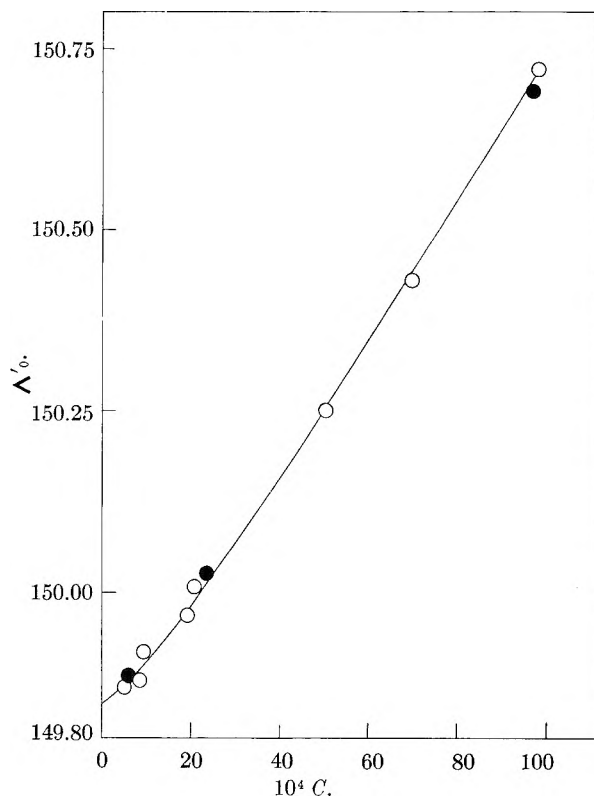


Fig. 2.—Shedlovsky plot for KCl in water at 25°.

The solvent conductance was measured with the unmodified Gordon cell using Ag,AgBr electrodes. Although a few experiments indicated that the solvent conductance could also be measured with the required accuracy using a liquid junction arrangement there appeared to be no advantage in doing so. The solvent conductance measured with a small alternating current cell always seemed to give values which were about 3% too high.

The liquid junction method was also compared with the original method of Gordon by measuring identical methanol solutions of KCl by both techniques; aqueous KCl was used in type (B) probe chambers. Table IV shows the agreement obtained. These results also illustrate the absence

TABLE IV
COMPARISON OF THE LIQUID JUNCTION AND GORDON
METHODS

Concn. of KCl in MeOH, <i>N</i>	Measured resistance, ohms L-j. probes	Gordon cell
0.01	446.85	446.83
.005	765.38	765.35
.002	1775.1 ₅	1775.1 ₉
.0005	6187.2	6186.9

of diffusion of probe solution into cell solution, since conductances of methanol solutions are very sensitive to traces of water.

Figure 3 illustrates the precision obtainable when the liquid-junction method is applied to solutions for which suitable reversible electrodes cannot be found. The curve is a Shedlovsky plot for aqueous NaNO_3 solutions measured with methanol solutions of KBr in type A probe chambers. The solutions were made by dilution of different stock solutions, and were measured in random order. It should be emphasized that since no attempt was made to obtain this salt in a high state of purity these results are not intended to represent accurate conductance data, but merely to serve as an example of the precision possible with this method.

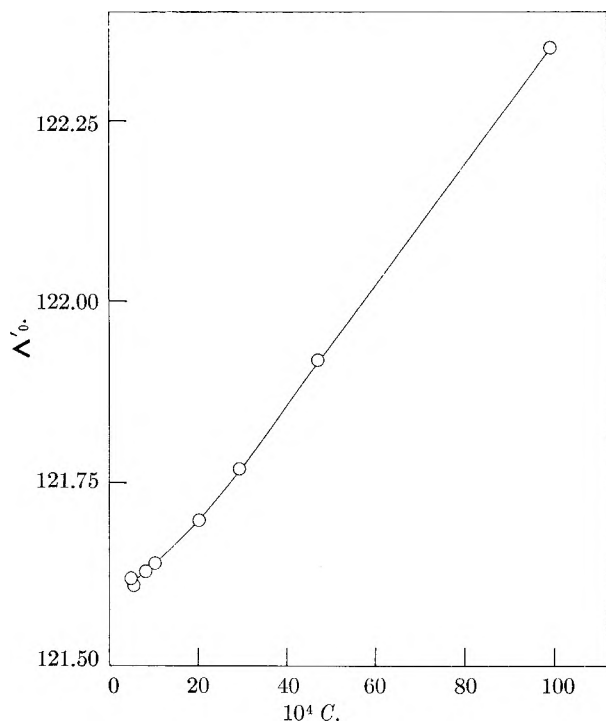


Fig. 3.—Shedlovsky plot for NaNO_3 in water at 25° .

Figure 4 shows a Shedlovsky plot of Bu_4NBr in nitromethane measured with aqueous Bu_4NBr in

type A probe chambers. Details of these measurements along with those of other nitromethane solutions will be published shortly.

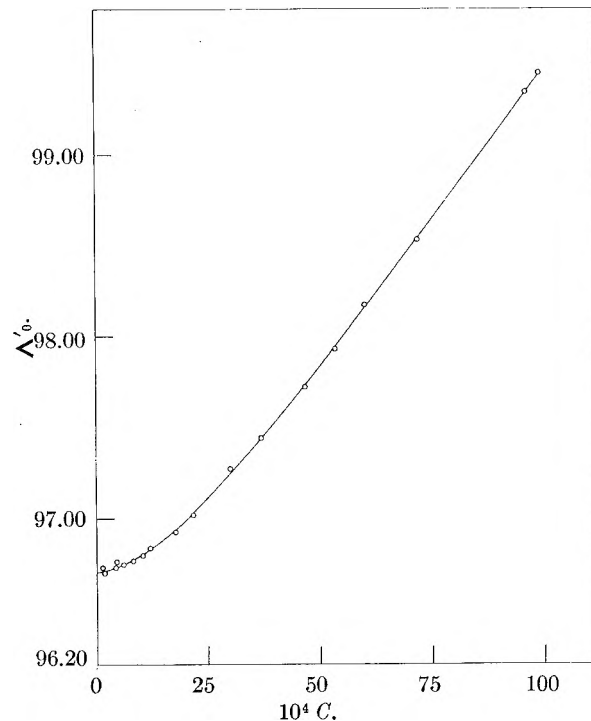


Fig. 4.—Shedlovsky plot for Bu_4NBr in nitromethane at 25° .

Some 200 measurements made during the past two years have convinced us that the liquid junction method is capable of yielding data of similar accuracy to that obtained with the original Gordon method for concentrations as low as $2 \times 10^{-4} N$.⁶ This modification should render the relatively simple direct-current method applicable to any electrolyte.

Acknowledgment.—The authors wish to thank the National Research Council of Canada for a grant-in-aid of this research and for the award of a studentship to L.E.

(6) It should be possible to extend the range to even higher dilution by the use of larger probe chambers.

THE RADIATION CHEMISTRY OF HYDROCARBON POLYMERS: POLYETHYLENE, POLYMETHYLENE AND OCTACOSANE¹

By A. A. MILLER, E. J. LAWTON AND J. S. BALWIT

Contribution from the General Electric Research Laboratory, Schenectady, N. Y.

Received October 21, 1955

Polymethylene, polyethylene and octacosane were irradiated with high-energy (800 kv.) electrons and crosslinking, changes in unsaturation, and gas evolution were measured. The only type of unsaturation formed is *trans*-vinylene and this is produced in approximately equal yields in all three hydrocarbons. About 40% of the hydrogen evolved comes from this reaction, the remainder arising from crosslinking. Volatile hydrocarbons result from C-C scissions near the chain-ends and also at the short branches in polyethylene. The results indicate that in the unbranched hydrocarbons, polymethylene and octacosane, permanent C-C scissions do not occur at random throughout the hydrocarbon chain. In polyethylene the evidence is not as clear but the tentative conclusion is that some main-chain cleavage leading to methyl end-groups may occur. Radiation yields (*G* values) for crosslinking, vinylenic unsaturation, and gas evolution, and a general mechanism for crosslinking of these hydrocarbon structures are presented.

Introduction

In the past few years there has been an increasing amount of research on the effects of high-energy, ionizing radiation in organic polymers. Most of the reported work, however, has been concerned with changes in physical properties due to crosslinking or degradation²⁻⁴ and detailed studies of the chemical changes have been limited. Dole, Keeling and Rose have measured gas evolution and changes in unsaturation in pile-irradiated polyethylene⁵ and Lawton, Zemaný and Balwit have reported similar measurements for electron-irradiated polyethylene.⁶

Earlier studies of the radiation chemistry of pure, low molecular weight organic compounds, particularly hydrocarbons in the gas phase^{7,8} and in the liquid phase,⁹⁻¹² have provided the basis for a general interpretation of radiation effects in gaseous and liquid hydrocarbons.^{13,14} However, although the primary processes may be similar, it is expected that the over-all chemical changes which are observed in solid, high molecular weight hydrocarbons should be greatly modified by such factors as the "cage-effect"¹³ and molecular chain length.

This paper discusses the radiation chemistry of polyethylene, polymethylene and octacosane with respect to changes in molecular weight, changes in unsaturation and gas evolution. These hydrocarbons all have a basic methylene structure, the chain length of which differs widely for the three materials. Also, the polyethylene molecule con-

tains some unsaturation and occasional short branches averaging four carbon atoms.¹⁵

Experimental

The octacosane (Eastman Kodak Co.) was treated with fuming sulfuric acid to remove traces of unsaturated and branched hydrocarbons. Following dilution the molten hydrocarbon was shaken with ten separate portions of hot, distilled water. The oil was vacuum-dried at 80° and re-crystallized from petroleum ether using methanol as the precipitant. The dried, crystalline product showed no discoloration when tested with fuming sulfuric acid. Its melting point was 60° (lit. value 60-62°¹⁶). A one-gram sample of polymethylene was obtained from L. A. Wall of the National Bureau of Standards, who had used similar material in a study of thermal degradation.¹⁷ The polymer had an intrinsic viscosity of 20 deciliters g.⁻¹ when measured in xylene at 120° corresponding to a molecular weight of over 10⁶. Bakelite DYNH polyethylene, of viscosity average molecular weight 20,000, was used in this work.

All irradiations were done with 800 kv. (peak) electrons from a G.E. resonant-transformer cathode ray unit.¹⁸ The thickness of the irradiated samples was never more than 40 mils (0.1 g. cm.⁻²), well below the maximum penetration of the electron beam, which is about 125 mils (0.32 g. cm.⁻²), so that the dose was constant throughout the thickness. The irradiations were always done in a nitrogen atmosphere. In cases where very high doses were given, the samples were irradiated on a water-cooled aluminum block or the dose given in small increments to prevent excessive temperature rise. The sample temperature during irradiation was usually in the range 25-50°. The dosimetry is based on a calibration of the beam current of the cathode ray unit against the ionization current in a specially constructed air ionization chamber at a fixed distance from the window of the cathode ray tube. All samples were irradiated in this same position. The total dose was determined by the exposure time at a constant beam current. The irradiation dose is expressed in terms of roentgens from the ionization chamber measurements according to the definition 1 R. = 84 ergs g.⁻¹ of air. For convenience, the unit 1 MR. (Mega-roentgen) = 10⁶ R. is used. All radiation yields (*G* values) that are derived in this paper are based on the assumption that the roentgen equivalent in these solid hydrocarbons is also 84 ergs g.⁻¹.

In the measurements of gas evolution the procedure described in a previous paper⁶ was followed except that a special irradiation chamber with a thin stainless steel window was used. In all cases the samples were thoroughly out-gassed at 50-80° before and after irradiation and before pressure measurements were made. The total gas evolved was analyzed with a mass spectrometer.

(1) Presented before the Polymer Division (Symposium on Polymer Irradiation) at the Cincinnati Meeting of the American Chemical Society, April 5, 1955.

(2) O. Sisman and C. D. Bopp, ORNL-928 (1951); C. D. Bopp and O. Sisman, ORNL-1373 (1953).

(3) A. Charlesby, *Nucleonics*, **12**, 18 (1954).

(4) E. J. Lawton, J. S. Balwit and A. M. Bueche, *Ind. Eng. Chem.*, **46**, 1703 (1954).

(5) M. Dole, C. D. Keeling and D. G. Rose, *J. Am. Chem. Soc.*, **76**, 4304 (1954).

(6) E. J. Lawton, P. D. Zemaný and J. S. Balwit, *ibid.*, **76**, 3437 (1954).

(7) S. C. Lind and D. C. Bardwell, *ibid.*, **48**, 1575, 2335 (1926).

(8) R. E. Honig and C. W. Shepard, *THIS JOURNAL*, **50**, 119 (1946).

(9) C. S. Schoepfle and C. H. Fellows, *Ind. Eng. Chem.*, **23**, 1396 (1931).

(10) J. P. Manion and M. Burton, *THIS JOURNAL*, **56**, 560 (1952).

(11) L. H. Gevantman and R. R. Williams, Jr., *ibid.*, **56**, 568 (1952).

(12) P. F. Forsyth, E. N. Weber and R. H. Schuler, *J. Chem. Phys.*, **22**, 66 (1954).

(13) See M. Burton, *THIS JOURNAL*, **51**, 611 (1947).

(14) See J. L. Magee, *Ann. Rev. Nuc. Sci.*, **3**, 171 (1953).

(15) F. M. Rugg, J. J. Smith and L. H. Wartman, *J. Poly. Sci.*, **11**, 1 (1953).

(16) G. Egloff, "Physical Constants of Hydrocarbons," Vol. 5, Reinhold Publ. Corp., New York, N. Y., 1953, p. 258.

(17) L. A. Wall, S. L. Madorsky, D. W. Brown, S. Straus and H. Simha, *J. Am. Chem. Soc.*, **76**, 3430 (1954).

(18) E. J. Lawton, W. D. Bellamy, R. E. Hungate, *et al.*, *Tappi*, **34**, 113A (1951); and J. A. Knowlton, G. R. Mahn and J. W. Ranftl, *Nucleonics*, **11**, 64 (1953).

Unsaturation was measured by infrared absorption on a Model 21 Perkin-Elmer instrument (NaCl prism) on 3 mil films of polyethylene and polymethylene and as 16% solutions in CCl_4 for octacosane. The following absorption bands were used: *trans*-vinylene ($-\text{CH}=\text{CH}-$) at 10.35 μ , vinyl ($-\text{CH}=\text{CH}_2$) at 11.0 μ , and vinylidene ($>\text{C}=\text{CH}_2$) at 11.25 μ . From the absorbance the concentration of unsaturated groups was calculated using the relation: weight fraction = $A/(K_{0.1}dl)$ where A is the absorbance, d is the density of the sample, and l is the thickness in units of 0.1 mm. For *trans*-vinylene at 10.35 μ , Andersen and Seyfried's specific absorption coefficient was used, $K_{0.1} = 35.6$.¹⁹

In some cases the total unsaturation also was measured by bromine addition with a correction for substitution.²⁰ In this method 1-gram samples, made up of 10 mil sheets in the case of polyethylene, were dissolved or swollen in hot CCl_4 under nitrogen. After cooling to room temperature, 10 ml. of 0.1 *N* $\text{Br}_2\text{-CCl}_4$ reagent was added and the solutions stored in the dark for 0.5 to 4 hours. One ml. of saturated, aqueous KI solution and 25 ml. of water were added with shaking to absorb the HBr from the gas phase. The liberated iodine was titrated with standard 0.1 *N* sodium thiosulfate (V_A). Excess solid KBrO_3 was added and the iodine titrated with additional thiosulfate (V_S). A blank determination on 10 ml. of the $\text{Br}_2\text{-CCl}_4$ reagent was made (V_B). The number of moles of double bonds in the sample is given by $(V_B - V_A - 2V_S)N/2000$ where N is the normality of the thiosulfate.

Results

Polyethylene Crosslinking Efficiency.—Estimates of crosslinking in polyethylene by swelling and tensile measurements already have been reported from this Laboratory.⁴ For DYNH polyethylene the crosslinking efficiency was found to be 1.1 to 1.5 crosslinks per "ion-pair" (32.5 e.v.), giving G (c.l.) = 3.4–4.6.

Gas Evolution.—Earlier work⁶ on polyethylene of 19,000 molecular weight showed that at a dose of 16 MR. about 85% of the gas evolved is hydrogen, the remainder being condensable (in liquid nitrogen) hydrocarbons, predominantly $\text{C}_2\text{-C}_5$. Also, the ratio of saturates to unsaturates in the condensable fraction was found to be about 0.4. In the present work we confirmed the value for the hydrogen/condensable ratio, obtaining about 85% hydrogen from DYNH polyethylene. Both Charlesby's and Dole's groups using pile irradiation found 96–98% H_2 and only 2–4% hydrocarbons. This difference may be due to the nature of the ionizing radiation or, possibly, to incomplete outgassing of the irradiated polymer in the Charlesby and Dole measurements.

The radiation yields, based on the results in the previous paper,⁶ are $G(\text{H}_2) = 5.7$ and $G(\text{condensables}) = 1.0$.

Unsaturation.—Rugg and co-workers showed from infrared studies that the total unsaturation of DYNH polyethylene is comprised of 60% vinylidene, and about 20% each of vinyl and *trans*-vinylene.¹⁵ We have found that upon irradiation the initial vinylidene and vinyl decrease and disappear at about 15 and 50 MR., respectively, and only *trans*-vinylene unsaturation is produced by irradiation. This is in qualitative agreement with the results of Dole's group.

The change in total unsaturation in DYNH polyethylene at 50 MR. was measured by bromine addition with the results shown in Table I.

(19) J. A. Andersen and W. D. Seyfried, *Anal. Chem.*, **20**, 998 (1948).

(20) See F. R. Mayo, *J. Am. Chem. Soc.*, **75**, 6135 (1953).

TABLE I
BROMINATION OF DYNH POLYETHYLENE

Bromination time, hr.	Bromine added, (moles/g.) $\times 10^4$	
	Unirradiated	Irradiated (50 MR.)
1	0.54 (0) ^a	1.06 (1.35)
2	.51 (0)	1.08 (1.52)
4	.54 (0)	1.08 (1.83)

^a Values in parentheses are for bromine substituted in (moles/g.) $\times 10^4$.

Since this method measures total unsaturation, the formation of *trans*-vinylene must be estimated indirectly. The total initial unsaturation is 0.54×10^{-4} mole/g. agreeing satisfactorily with Rugg's value of 0.38×10^{-4} mole/g. Since vinyl and vinylidene constituting 80% of the initial unsaturation disappear, $0.54 \times 10^{-4} (0.20) = 0.11 \times 10^{-4}$ mole/g., which is the initial *trans*-vinylene, remains. The total unsaturation at 50 MR. is 1.08×10^{-4} mole/g., all *trans*-vinylene. Therefore, the *trans*-vinylene produced by a 50 MR. dose is $(1.08 - 0.11) \times 10^{-4} = 0.97 \times 10^{-4}$ mole/g. This corresponds to $G(-\text{CH}=\text{CH}-) = 2.2$. In relation to the results of Dole's group the bromination measurement described above indicates that considerable substitution may occur in irradiated polyethylene so that the total bromine absorption without a correction for substitution may lead to erroneously high values for unsaturation. This may explain Dole's high value for the fraction of hydrogen arising from unsaturation (70–80%). We obtain only 40% since $G(-\text{CH}=\text{CH}-)/G(\text{H}_2) \approx 0.4$.

The quantitative measurement of *trans*-vinylene unsaturation by infrared absorption (10.35 μ) is complicated by the uncertainty in the state (crystallinity) factor.¹⁵ It was reported earlier⁶ that the increase in 10.35 μ absorbance for a 3 mil film irradiated at 50 MR. is 0.059. Using Andersen and Seyfried's specific absorption coefficient of $K_{0.1} = 35.6$ we obtain 1.0×10^{-4} mole/g. ($G = 2.4$) for a state factor of unity. However, if a state factor of 0.5 is used (see Fig. 1) a value of only 0.5×10^{-4} mole/g. ($G = 1.2$) results. Because of the uncertainty in the state factor we believe that the value derived from bromination ($G = 2.2$) is the more reliable one.

Polymethylene.—A sufficient quantity of polymethylene was not available for an extensive investigation of this polymer. However, a detailed study of the irradiation of a similar structure (an unbranched, highly crystalline ethylene polymer) will be reported in a separate paper by Lawton and co-workers.

The irradiation of polymethylene results in crosslinking but, on the basis of minimum dose for insolubility in hot toluene and the estimated initial molecular weight, at a lower efficiency than for polyethylene. The mass spectrometric analysis of the gas evolved after an irradiation dose of about 100 MR. gave 99.9% hydrogen and only about 0.1% ethane and butane. The quantity of hydrogen evolved corresponds to a yield of $G(\text{H}_2) = 5.4$.

Infrared analyses of 3 mil films of polymethylene showed no unsaturation (10.35, 11.0 and 11.25 μ) in the unirradiated polymer and the formation

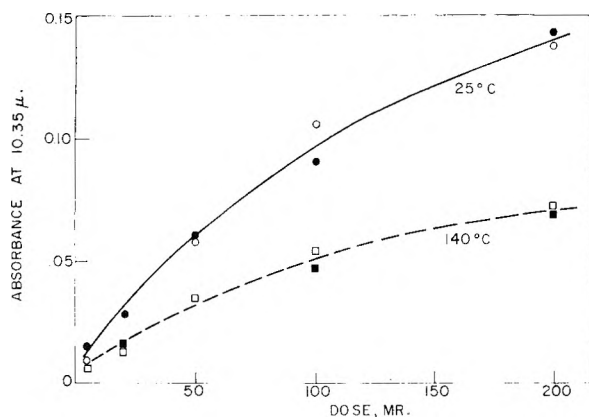


Fig. 1.—*trans*-Vinylene absorbance (10.35μ) in irradiated polyethylene (O, □) and polymethylene (●, ■).

only of *trans*-vinylene (10.35μ) with irradiation up to a dose of 200 MR. A comparison of the absorbance at 10.35μ for 3 mil films of polyethylene and polymethylene measured at room temperature and at 140° , above the crystal melting temperature, is shown in Fig. 1. The absorbances at each dose are almost identical for the two polymers indicating that the formation of *trans*-vinylene is independent of the branching in polyethylene. The 50% decrease in absorbance measured at 140° suggests that the solid \rightarrow melt state factor is about 0.5. However, the effect of temperature alone on the 10.35μ absorbance is not known.

Octacosane: Molecular Weight Change.—The results of duplicate cryoscopic molecular weight measurements (cyclohexane solvent) for octacosane are shown in Fig. 2, in which the reciprocal number average molecular weight is plotted as a function of irradiation dose. The theoretical value for pure octacosane (M.W. = 394) is $1000/\bar{M}_n = 2.54$, somewhat lower than the measured values. However, to be consistent, the experimental value was used for the unirradiated material. The decrease in number of molecules/g./R. is given by the product of the slope in Fig. 2 ($2.7 \times 10^{-12}/R.$) and 6×10^{23} or 1.6×10^{12} molecules/g./R. and this must equal the number of crosslinks since each crosslink decreases by one the number of molecules. (It should be noted that the samples on which the cryoscopic measurements were made were not outgassed to remove the low molecular weight hydrocarbons formed in the irradiation; see next section. It was estimated, however, that the \bar{M}_n values of these samples would be changed by only 2% depending on whether the volatile products remain in the samples or are completely removed by outgassing prior to the cryoscopic measurement.) The value for crosslinks obtained above leads to 33 e.v. per crosslink or $G(c.l.) = 3.1$. Charlesby has reported a value of 32 e.v. per crosslink for saturated, unbranched hydrocarbons, including octacosane, based on infusibility measurements and with pile radiations.^{21,22}

Gas Evolution.—A 0.112-g. sample of octacosane irradiated to a dose of 64.6 MR. gave an average rate of hydrogen evolution of $45.3 \mu/\text{MR.}$ and a rate of $41.2 \mu/\text{MR.}$ at the end of the irradiation. Of

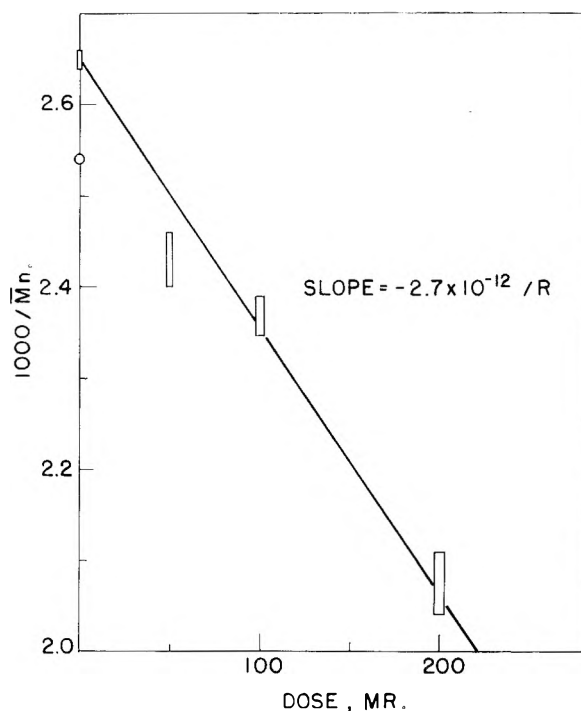


Fig. 2.—Change in reciprocal molecular weight of octacosane by irradiation (O = calculated value for pure octacosane).

the total gas evolved 2938μ , 2660μ (91%) was hydrogen (non-condensable in liquid nitrogen) and 278μ (9%) was condensable. The amount of evolved gas, calculated from the calibrated volume of the gas-measuring system and averaged up to a dose of 64.6 MR. was 2.52×10^{12} molecules/g./R. These data lead to $G(\text{H}_2) = 4.3$ and $G(\text{condensables}) = 0.5$.

A mass spectrometric analysis of the evolved gas gave 91.0 mole % H_2 and 7.2 mole % $\text{C}_n\text{H}_{2n+2}$ hydrocarbons distributed as follows: 0.5% CH_4 , 2.1% C_2H_6 , 1.3% C_4H_{10} , 0.9% C_5H_{12} , 1.1% C_6H_{14} , 0.7% C_7H_{16} and 0.6% C_8H_{18} . The number average molecular weight ($\bar{M}_n = \sum n_i M_i / \sum n_i$) of the volatile hydrocarbon fraction was $\bar{M}_n = 62$ which is close to the value for butane (58).

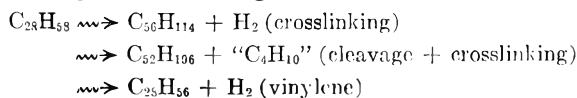
Unsaturation.—Samples of octacosane irradiated up to a dose of 200 MR. were examined as 16% solutions in carbon tetrachloride by infrared absorption. The only change that could be detected was the appearance of absorption at 10.35μ (*trans*-vinylene). For a sample irradiated at 50 MR. the 10.35μ absorbance was 0.058 for a 0.358 mm. thickness of a 16% solution in CCl_4 , which with Andersen and Seyfried's value of $K_{0.1} = 35.6$,²⁰ gives a concentration of 0.81×10^{-4} mole/g. *trans*-vinylene formed. The bromination method on two 2-g. samples, also irradiated at 50 MR., gave 0.89×10^{-4} and 0.80×10^{-4} mole/g. for bromination times of 30 and 60 minutes, respectively. The average value, 0.85×10^{-4} mole/g., is in satisfactory agreement with the infrared estimate and gives $G(-\text{CH}=\text{CH}-) = 1.9$. It is significant that the infrared measurement, made in CCl_4 solution where the uncertainty of the state factor is absent, is not appreciably lower than the total unsaturation measured by bromination. This must mean that *cis*-vinylene, which is not

(21) A. Charlesby, *Proc. Roy. Soc. (London)*, **A222**, 60 (1954).

(22) A. Charlesby, *Radiation Research*, **2**, 97 (1955).

readily observed by infrared absorption, is not formed in the irradiation of these hydrocarbon structures.

Material Balance.—In the irradiation of octacosane, unsaturation (vinylene) is produced only in the solid product and butane was shown to be the average volatile hydrocarbon fragment. The results on octacosane may be associated with the following *over-all* changes



Since each crosslink and each vinylenic group which is formed gives a molecule of H_2 and each molecule of "butane" must result in the crosslinking of the residues, the sum of the crosslinks and vinylenic double bonds formed should equal the number of molecules of H_2 and "C₄H₁₀." The material balance actually obtained, based on the individually measured G values at 50 MR. listed earlier is $\Sigma G(\text{c.l.} + \text{C}=\text{C}) = 5.0$ against $\Sigma G(\text{H}_2 + \text{"C}_4\text{H}_{10}\text{"}) = 4.8$. This satisfactory material balance serves to verify the quantitative estimates of the individual G values in the irradiation of octacosane.

Discussion

Scission of C—C Bonds.—One of the basic questions in the crosslinking of polymers by ionizing radiation is the degree of scission occurring simultaneously in the main-chain. By comparing theoretical and experimental sol-dose relationships Charlesby concluded that in long chain paraffins, including polyethylene, the ratio of main-chain scissions to crosslinks is about 0.3 and he suggested, further, that this ratio is relatively independent of physical state and of molecular chain length over the extreme range from gaseous methane to solid polyethylene.²¹ Baskett and Miller²³ by further irradiation of the extracted gel fraction of lightly crosslinked polyethylene derived a scission/crosslink ratio of about 0.2. Dole, Keeling and Rose⁶ concluded that in polyethylene C—C scissions at the branches occurred much more frequently than in the main chain but they did not make a quantitative estimate of the amount of main-chain C—C scission.

On the basis of the results in the present paper we suggest that in the irradiation of long-chain paraffins of the unbranched, polymethylene-type, permanent random scission of the main chain does not occur to the extent indicated by Charlesby. We base our conclusion on (1) the results of gas evolution and (2) the absence of end-groups which might be expected by main-chain C—C scission.

A comparison of gas evolution in the irradiation of the three hydrocarbon structures studied in the present work is shown in Table II.

Polymethylene with an extremely low chain-end/ CH_2 ratio gives almost pure H_2 in the evolved gas. Octacosane, which is also of unbranched structure but with many more chain-ends (*i.e.*, lower molecular weight), gives a much higher hydrocarbon/ H_2 ratio in the evolved gas. This must mean that permanent C—C scissions giving volatile hydrocarbons occurs only at the chain-ends. This

TABLE II

GAS EVOLUTION IN CROSSLINKING HYDROCARBON POLYMERS	Octa-	Poly-	Poly-
	cosane	methylene	ethylene
Mol. wt.	394	$>10^6$	9,100 ^a
Chain-ends/ $-\text{CH}_2-$	0.07	$<10^{-5}$	$\sim 0.013^b$
H_2 evolved, mole %	91	>99	87
Hydrocarbons, mole %	9	<1	13
Hydrocarbons/ H_2	0.099	<0.01	0.15

^a Bakelite DYNH polyethylene: $\bar{M}_n = 9,100$; 1.3 short branches per 100 C atoms.¹⁵ ^b Including short branches ($-\text{C}_4\text{H}_9$) as chain-ends.

conclusion is valid also for polyethylene if the short ($-\text{C}_4\text{H}_9$) branches are considered as chain-ends. The higher hydrocarbon/ H_2 ratio in polyethylene over octacosane in spite of the much lower number of ends and branches suggests that C—C scission at a branch occurs more readily than in an unbranched C—C bonds of octacosane. (On the basis of the data in Table II cleavage of the branches in polyethylene occurs about 8 times as frequently as the chain-ends in octacosane.) This preferential cleavage is not unreasonable considering the lower C—C bond dissociation energy at a branched carbon atom. The conclusion is that in the irradiation of long-chain paraffins the formation of volatile hydrocarbons is not evidence for *random* C—C scissions throughout the main chain.

It is significant that even in the gas phase, where primary recombination due to a "cage-effect" should be absent, long-chain paraffin molecules under electron impact appear to undergo a preferential C—C cleavage at the chain ends rather than at random throughout the molecule. Figure 3 shows the mass spectrum of octacosane indicating only peaks formed by simple C—C cleavage. The predominant peaks are at C_3H_7^+ and C_4H_9^+ with the higher $\text{C}_n\text{H}^{+}_{2n+1}$ peaks decreasing rapidly in intensity. In a correlation of mass spectra Magat and Viallard have shown that this type of cleavage is general for normal, long-chain paraffins.²⁴ Apparently, this preferred cleavage near the chain ends, particularly at the third and fourth C—C bonds, under electron impact is an inherent characteristic of unbranched paraffin molecules.

The evidence from infrared analysis also suggests that permanent random C—C scission in the main chain does not occur. In the unbranched hydrocarbons, polymethylene and octacosane, permanent scissions should lead to methyl and/or vinyl end-groups by the following processes: (1) $-\text{CH}_2\text{CH}_2\cdot \rightarrow -\text{CH}=\text{CH}_2 + \text{CH}_3\text{CH}_2\cdot$ (disproportionation); (2) $-\dot{\text{C}}\text{H}-\text{CH}_2\text{CH}_2- \rightarrow -\text{CH}=\text{CH}_2 + \cdot\text{CH}_2-$ (β -cleavage following H-expulsion); (3) $-\text{CH}_2\cdot \rightarrow -\text{CH}_3 + \cdot\text{CH}_2-$ (saturation by H-atoms; this is extremely improbable since it requires radical-H atom combination before primary recombination of the polymer radicals occurs; furthermore, the H-atoms probably react by H-abstraction—see next section on mechanism).

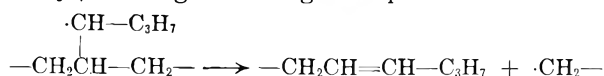
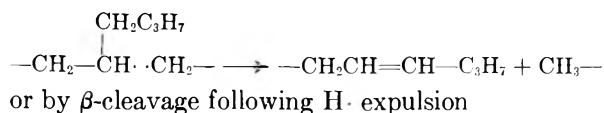
As was stated earlier, infrared analysis showed that vinyl unsaturation (11.0μ) is entirely absent in octacosane and polymethylene irradiated to as

(23) A. C. Baskett and C. W. Miller, *Nature*, **174**, 364 (1954).

(24) M. Magat and R. Viallard, *J. chim. phys.*, **48**, 1 (1951).

high a dose as 200 MR. Furthermore, no increase or change in absorbance due to methyl groups (7.25μ) was found in polymethylene or octacosane, respectively, upon irradiation to 200 MR. It should be emphasized that at these high doses if permanent C-C scissions occurred to the extent indicated by Charlesby, the concentration of vinyl or changes in concentration of methyl should be high enough to be observed readily by infrared absorption at 11.0 and 7.25μ . It must be concluded, therefore, that at least in the unbranched paraffin structures the ratio of permanent, random C-C scission to crosslinks is essentially zero. C-C scissions that do occur are restricted to the ends of the molecules.

In the case of the branched polyethylene, again only *trans*-vinylene unsaturation is produced by irradiation. If it is assumed that this may result from main-chain cleavage near a branch²⁵ either by disproportionation then the formation



of *trans*-vinylene would be dependent on branching. However, it was shown earlier (Fig. 1) that the *trans*-vinylene formed in unbranched polymethylene is quantitatively identical with that formed in branched polyethylene. Therefore, in polyethylene this type of unsaturation must be formed by the same mechanism as in polymethylene and octacosane, that is, by loss of hydrogen atoms from adjacent methylene groups (see next section on mechanism) rather than by the cleavage reactions depicted above.

The infrared evidence with respect to changes in methyl concentration in irradiated polyethylene is not so well-defined. Table III lists the changes in absorbance for $-\text{CH}_3$, and $-\text{CH}_2-$ for 3 mil films of polyethylene (solid).

TABLE III

INFRARED ABSORBANCES FOR METHYL AND METHYLENE IN IRRADIATED POLYETHYLENE

Dose, MR	CH_3- (7.25μ)	$-\text{CH}_2-$ (7.30μ)	$-\text{CH}_2-$ (7.39μ)
0	0.317	0.295	0.200
100	.342	.323	.235
250	.386	.362	.273
500	.445	.415	.322

The data in Table III show a linear and *parallel* increase in the 7.25 , 7.30 and 7.39μ absorbances. Similar measurements on irradiated polymethylene also showed an apparent increase in methylene absorption (7.30 and 7.39μ) at the same rate as in polyethylene. As indicated by Rugg and his co-workers this behavior indicates an environmental (crystallinity) effect on the general absorbance in the 7.25 – 7.39μ region.¹⁵ A further complication, however, arose when the absorbances of the molten

(25) See W. G. Oakes and R. B. Richards, *J. Chem. Soc.*, 2920 (1949) for types of unsaturation formed in the *thermal* degradation of polyethylene.

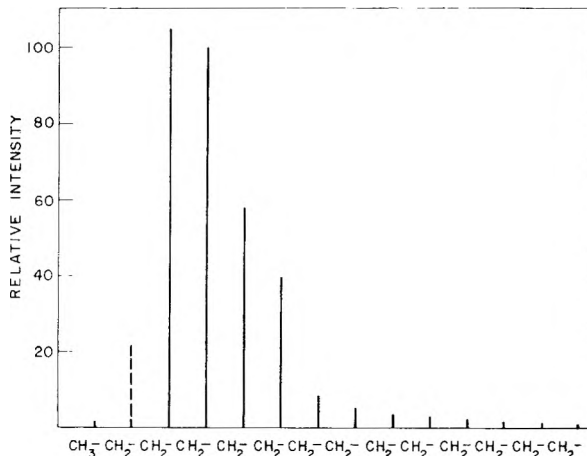


Fig. 3.—Mass spectral cleavage pattern of octacosane, $\text{CH}_3(\text{CH}_2)_{26}\text{CH}_3$ (from A.P.I. #886; 70 volts).

films were measured at 140° . The methylene (7.30 and 7.39μ) absorbances were raised in both polymethylene and polyethylene while the methyl (7.25μ) absorbance in polyethylene remained essentially unchanged. This behavior of the infrared absorption makes our quantitative estimate of changes in $-\text{CH}_3$ in polyethylene with irradiation appear quite uncertain.

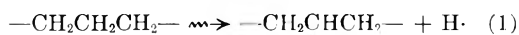
If the increase in 7.25μ absorbance is a real measure of the increase in methyl groups, we have at 100 MR., $\Delta A_{7.25} = 0.025$ (Table III). In terms of Bryant and Voter's specific absorption coefficient,²⁶ $\Delta K' = 3.6$ which, on the basis of their calibration (Fig. 3, their paper), gives $\Delta \text{CH}_3/100$ carbon atoms/100 MR. = 0.32. This corresponds to $G(\Delta \text{CH}_3) = 2.6$. Since main-chain cleavage by disproportionation was ruled out earlier, we must assume that each such scission must give two methyl groups so that for main-chain scission $G = 1.3$. This neglects the possibility of some increase in methyl resulting from cleavages of the short branches giving low molecular weight hydrocarbons which may be partially retained in the sample. The ratio of scissions to crosslinks on the basis of this analysis is $1.3/3.4$ – $4.6 = 0.3$ – 0.4 . Although this is in apparent agreement with Charlesby's ratio of 0.3 it should be repeated that our estimate involves a serious uncertainty regarding the interpretation of the infrared absorbance for methyl at 7.25μ . Furthermore, as was indicated earlier, a cleavage process by which no unsaturation but only methyl end-groups are formed appears to us not to be a very probable one from a kinetic standpoint.

Mechanism of Crosslinking.—Dole, Keeling and Rose⁶ observed the rapid disappearance of vinylidene unsaturation in the pile irradiation of polyethylene and associated this directly with crosslinking. They suggested that the chemically active sites, presumably polymer free radicals formed by the loss of a hydrogen atom, migrate to a vinylidene double bond where crosslinking occurs. We have observed also that the vinylidene initially present disappears before a dose of 10–15 MR. is reached. However, both crosslinks and *trans*-vinylene unsaturation continue to be produced upon continued

(26) W. M. D. Bryant and R. C. Voter, *J. Am. Chem. Soc.*, **75**, 6113 (1953).

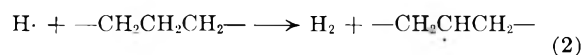
irradiation long after the vinylidene groups have reacted. It seems likely, however, that the initial vinyl and vinylidene do contribute to crosslinking in the early stage of irradiation as is evidenced by the work of Charlesby²² who showed that in long chain hydrocarbons the energy requirement per crosslink drops from 32 e.v. in saturated, unbranched paraffins to 19 e.v. where terminal (*i.e.*, vinyl) unsaturation is present. The rapid disappearance of vinylidene which, as Dole suggests, does appear to be quite specific, might be explained by transfer of energy (not necessarily free radical migration) toward the vinylidene group or by a high reactivity of this group toward free radical attack. Finally, the general observation that normal, saturated paraffins (*e.g.*, octacosane and polymethylene) crosslink indicates that initial unsaturation is not a prerequisite for crosslinking.

For the crosslinking of polymethylene-type hydrocarbons we suggest the following general mechanism:



The primary processes in this reaction are not specified but may involve any or all of the processes usually suggested for radiation-induced reactions.^{13,14}

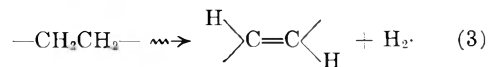
The hydrogen atom formed in (1) may abstract a similar atom on an adjacent or nearby chain leaving two polymer radicals in a favorable position to combine (crosslink). Reaction (2) is exothermic



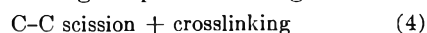
to the extent of 8–9 kcal./mole.²⁷ An analogous reaction in the *gas* phase: $\text{H}\cdot + \text{CH}_3\text{CH}_2\text{CH}_3 \rightarrow \text{H}_2 + \text{CH}_3\text{CHCH}_3$ was shown to have an activation energy of about 8 kcal./mole with a steric factor of

(27) T. L. Cottrell, "Strengths of Chemical Bonds," Academic Press, Inc., New York, N. Y., 1954, p. 187.

about 0.1.²⁸ In radiation chemistry (2) might be especially favored if in reaction (1) the H· atom is expelled with excess kinetic energy (*i.e.*, a "hot" atom).



trans-Vinylene is formed independently of the crosslinking reaction. This reaction may be a molecular process in which adjacent hydrogens are expelled in a single primary event. Indirect evidence for this type of process is the formation of C_2H_4^+ as the principal peak in the mass spectrum of ethane.²⁹ It is of interest to mention that on the basis of a model of the "zig-zag" backbone in the normal paraffin structure the formation of *trans*-vinylene requires only a slight rotation, while the formation of *cis*-vinylene would require almost a 180° rotation, that is, a much more severe distortion of the original paraffin configuration.



It was shown that in octacosane C–C scission occurs near the chain ends giving a large and a small radical, the latter eventually forming a saturated, volatile hydrocarbon molecule and the former remaining to crosslink with another large radical. Similarly, in polyethylene C–C scission at the short branches followed by hydrogen abstraction by the small radical would leave two polymer radicals to crosslink. Scission of the short branches in polyethylene, therefore, must also contribute to crosslinking.

Acknowledgment.—We wish to express our appreciation to R. S. McDonald and C. A. Hirt for measurements and interpretations of infrared spectra and to Miss J. E. Doolittle for the mass spectrometric analyses.

(28) E. W. R. Steacie, "Atomic and Free Radical Reactions," Vol. II, Reinhold Publ. Corp., New York, N. Y., 1954, p. 496.

(29) A.P.I. Mass Spectrum #2.

LUMINESCENCE PROPERTIES OF ZINC-INTER-CHALCOGENIDES. I. ZINC SULFO-TELLURIDE PHOSPHORS

By S. LARACH, W. H. MCCARROLL AND R. E. SHRADER

Radio Corporation of America, RCA Laboratories, Princeton, N. J.

Received October 24, 1966

Luminescence characteristics of phosphors of the zinc sulfo-telluride system have been investigated. These materials included (1) unactivated and unfluxed phosphors, (2) unactivated phosphors, prepared with NaCl flux, (3) phosphors with Ag activator and with NaCl flux, (4) phosphors with Cu activator and with NaCl flux, (5) phosphors with Mn activator, with and without NaCl flux. X-Ray studies show the solubility limit of ZnTe in ZnS to be approximately eight mole %. With increasing proportion of ZnTe, the peak wave length of emission from Zn(S:Te) phosphors generally occurs at longer wave lengths. Phosphors prepared with Mn activator exhibit two emission bands. One band, attributed to the centers responsible for the emission from Zn(S:Te):NaCl, is modified by the presence of Mn; the second band is due to the emission from Mn centers, perturbed by chloride.

Introduction

The luminescence properties of the zinc sulfo-selenide system have been investigated extensively,¹ but practically no work has been reported on other zinc inter-chalcogenide phosphors, such as zinc

sulfo-telluride, zinc seleno-telluride and zinc sulfo-seleno-telluride.

The present work deals with the luminescence characteristics of phosphors of the zinc sulfo-telluride system. Six phosphors were prepared for each experimental composition of host material: (1) unactivated and unfluxed, (2) unactivated, but

(1) H. W. Levensz, "An Introduction to Luminescence of Solids," John Wiley and Sons, New York, N. Y., 1950.

prepared with 2% by weight of NaCl, (3) Ag(0.01), with NaCl(2), (4) Cu(0.01), with NaCl(2), (5) Mn(0.5), with NaCl(2), (6) Mn(0.5), with no flux. Lattice constants were determined for the phases present at each composition.²

Experimental Procedures

Materials. Zinc Sulfide.—The precipitated zinc sulfide used was obtained from Radio Corporation of America, Lancaster, Pa., as LM-476, and contained no spectrographically detectable impurities. X-Ray analysis showed this material to be composed of about 95% cubic ZnS, and about 5% hexagonal ZnS.

Zinc Telluride.—Pure ZnTe was not obtainable from outside vendors, and was therefore prepared in the laboratory as follows.³

Thirty grams of tellurium (ASARCO, special high-purity grade) is added, in several small portions, to 60 g. of molten zinc (spectrographically pure) at 800°, in a hydrogen atmosphere. The temperature is then raised to 1300°, and held there for 15 minutes, to boil away unreacted zinc or tellurium, even though some ZnTe was lost through decomposition. After cooling, the ZnTe is ground, and sifted through a 100-mesh screen.

X-Ray analysis showed the material to be ZnTe, with small amounts of elemental Te present as a separate phase. X-Ray patterns of the fired materials showed that no phase of tellurium remained. Spectrographic analyses⁴ showed that no detectable impurities were introduced by the synthesis procedure.

Preparation of Phosphors.—The materials described above were used in preparing the host crystals. Appropriate amounts of ZnS and ZnTe to give the desired composition, were weighed out and ball-milled for 3 hours. The activators, as the nitrates, were added as solutions in triple-distilled water, and the slurries were dried. The samples were then re-ground, and transferred to silica boats. Crystallization was carried out at 900° in a temperature-controlled, Globar-type, Vycor tube furnace. Purified nitrogen was used as a crystallization atmosphere, and the samples were cooled in purified nitrogen. Incomplete flushing of the firing tube with nitrogen leads to a phase of ZnO being formed in amounts to 7%. Tests showed that ZnO, present in these amounts, did not affect the luminescence properties of the materials. More complete flushing of the firing tube with nitrogen eliminated this complication.

Measurements. Luminescence Characteristics.—Spectral distribution curves, and peak emission intensities were obtained with a recording spectroradiometer designed by one of the authors (RES).

Cathodoluminescence characteristics were obtained using a demountable-type cathode ray tube, with raster operation at 10 kv., and a current density of 5 μ a./cm.². The photoluminescence characteristics were obtained, using a mercury lamp, with filters, as a source of 3650 Å. excitation. All curves of spectral distribution are corrected for the characteristics of the instrument.

Results

Intersolubility of ZnS and ZnTe.—X-Ray analyses show that ZnTe is soluble in ZnS to the extent of 8–10 mole %, and that the cubic ZnS is soluble in ZnTe up to about 5 mole %. The limited solubility is not unexpected, in view of the difference in the ionic radii of sulfide telluride atoms ($r_s = 1.84$ Å., $r_{Te} = 2.21$ Å.). Table I presents a summary of the X-ray data obtained for the Zn(S:Te) system.⁵

Luminescence Characteristics.—The luminescence characteristics are discussed in detail below, and are summarized in Table II.

1. **Zn(S:Te), Unactivated, Unfluxed.**—The effect of ZnTe incorporation on the spectral dis-

(2) X-Ray analyses by Dr. J. A. Amick and Mr. P. L. Read.

(3) Method proposed by Dr. S. M. Thomsen.

(4) Spectrographic analyses by Dr. M. C. Gardels.

(5) All proportions of ZnTe in Zn(S:Te) phosphors are given as mole % ZnTe prior to crystallization.

TABLE I
SUMMARY OF X-RAY ANALYSES OF Zn(S:Te) PHOSPHORS

Phosphor	Phases, No.	Ratio amts. phases 1:2 (approx.)	a_{01}	a_{02}
ZnS	1	...	5.406	...
0.99ZnS:0.01ZnTe	1	...	5.408	...
.98ZnS:.02ZnTe	1	...	5.408	...
.96ZnS:.04ZnTe	1	...	5.409	...
.94ZnS:.06ZnTe	1	...	5.411	...
.92ZnS:.08ZnTe	1	...	5.417	...
.90ZnS:.10ZnTe	2	95:5	5.427	6.05
.15ZnS:.85ZnTe	2	20:80	5.44	6.05
.10ZnS:.90ZnTe	2	1:99	5.41	6.045
ZnTe	1	6.102

TABLE II
COMPARISON OF SOME ZINC INTERCHALCOGENIDE PHOSPHORS

Com-position	Acti-vator	NaCl	λ_{PK}^{CR} , Å.	ϵ_{PK}^{CR} , Å.	λ_{PK}^{UV} , Å.	ϵ_{PK}^{UV} , Å.
ZnS	inert	...	inert	...
...	...	yes	4700	50	4700	42
0.9ZnS:0.1ZnSe	Ag	yes	4500	110	4520	94
...	Cu	yes	5325	108	5350	95
...	5400	7	5450	5
...	...	yes	5450	41	5400	79
...	Ag	yes	4550	76	4800	73
...	Cu	yes	4650	32	4900	50
...	5450	44	5450	74
0.9ZnS:0.1ZnTe	5200	15	5250	11
...	...	yes	5190	16	5350	10
...	~6000	10
...	Ag	yes	5100	16	5350	10
...	Cu	yes	4600	10
...	5400	21	5400	42

tribution of emission is shown in Fig. 1; and on the peak wave length and peak emission intensity in Fig. 2, curves A and E. It is seen that there is a shift in peak wave length to longer wave lengths with increasing ZnTe proportion from 2 to 8%, after which the peak wave length remains constant at 5200 Å.

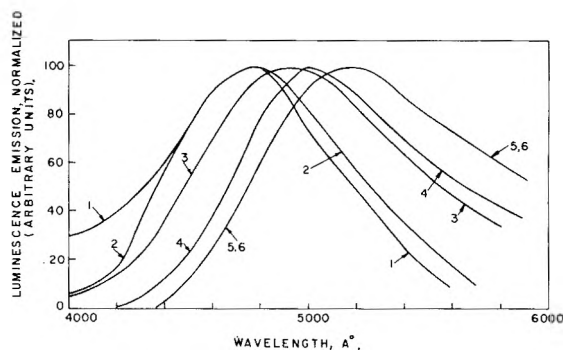


Fig. 1.—Spectral distribution curves of the emission from zinc sulfo-telluride phosphors, unactivated and unfluxed (CR excitation): (1) 0.99ZnS:0.01ZnTe; (2) 0.98ZnS:0.02ZnTe; (3) 0.96ZnS:0.04ZnTe; (4) 0.94ZnS:0.06ZnTe; (5) 0.92ZnS:0.08ZnTe; (6) 0.90ZnS:0.10ZnTe.

Peak emission intensity as a function of ZnTe proportion, under cathode ray or 3650 Å. ultraviolet excitation, is shown in Fig. 2E. The emission intensity scale is normalized to the peak emission intensity, ϵ_{PK} , from rhbdl. $-Zn_2SiO_4:Mn$ being taken as 100 for CR excitation, and to $\epsilon_{PK} = 100$ for hex.-ZnS:Ag:Cu(P2) for ultraviolet excitation. There is an increase in ϵ_{PK}^{CR} with increasing

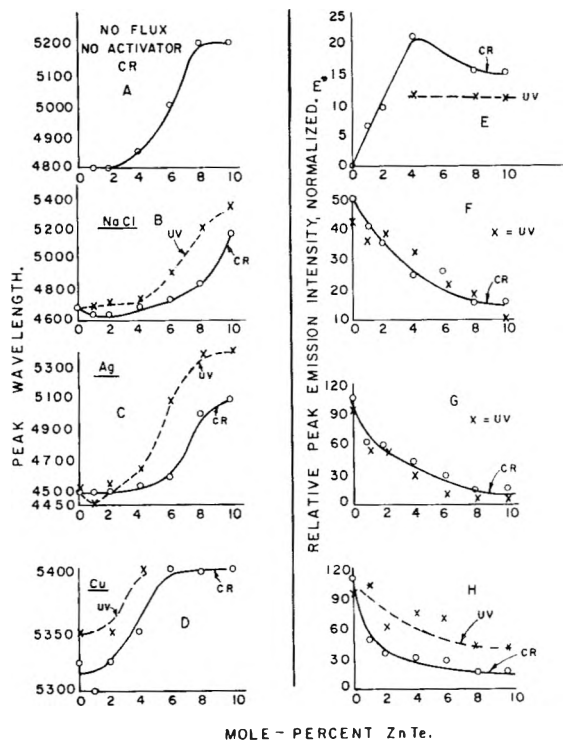


Fig. 2.—A-D: peak wave length of emission as a function of zinc telluride proportion (prior to crystallization), ultra-violet or CR excitation, as indicated: (A) Zn(S:Te), unactivated, unfluxed; (B) Zn(S:Te), unactivated, NaCl flux; (C) Zn(S:Te):Ag(0.01), NaCl; (D) Zn(S:Te):Cu(0.01), NaCl. E-H: peak emission intensity as a function of zinc telluride proportion (prior to crystallization), ultra-violet or CR excitation as indicated: E, F, G, H correspond to materials of A, B, C, D. For CR excitation, intensities are normalized to that of rhbdl.-Zn₂SiO₄:Mn = 100, for ultra-violet excitation, intensities are normalized to that of hex.-ZnS:Ag:Cu (P2) = 100.

proportion of ZnTe to about 4 mole % ZnTe, the maximum ϵ_{PK}^{CR} being 21% that of Zn₂SiO₄:Mn. For excitation with 3650 Å. ultra-violet, no decrease in ϵ_{PK} is indicated to 10 mole % ZnTe.

2. Zn(S:Te), Unactivated, but with NaCl Flux.

—Spectral distribution curves of the emission from Zn(S:Te):NaCl phosphors are shown in Fig. 3; and the peak emission intensities are given in Fig. 2F, and λ_{PK} in Fig. 2B.

The inclusion of NaCl during synthesis has several effects: (1) whereas the *unfluxed* phosphors with up to 2 mole % ZnTe have λ_{PK}^{CR} at 4800 Å., the corresponding *fluxed* materials have λ_{PK}^{CR} at about 4650 Å.; (2) with incorporation of small amounts of ZnTe (up to 2%), there is a decrease in λ_{PK}^{CR} from 4700 Å. for ZnS:NaCl to 4650 Å. for 0.98ZnS:0.02ZnTe:NaCl, after which there is an increase in λ_{PK}^{CR} to 5190 Å. for 0.90ZnS:0.10ZnTe:NaCl; (3) the fluxed materials do not show a levelling-off of λ_{PK} at 8% ZnTe, as do the unfluxed phosphors; (4) fluxed materials with 6–10 mole % ZnTe show a secondary emission band, with λ_{PK} at about 6000 Å., for ultra-violet excitation. Peak emission intensities decrease with increasing proportion of ZnTe, the levelling-off point occurring at about 8 mole % ZnTe.

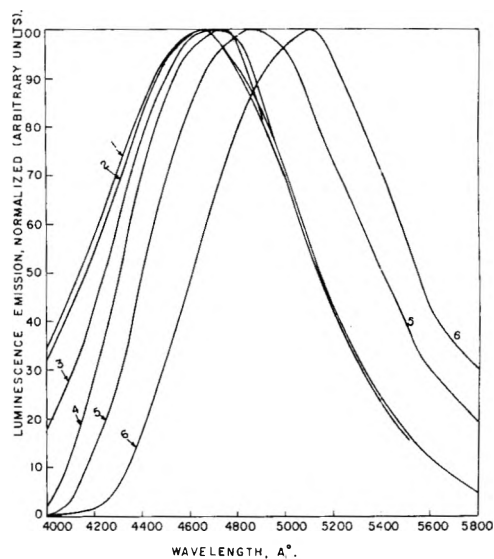


Fig. 3.—Spectral distribution curves of the emission from zinc sulfo-telluride phosphors, unactivated, 2% NaCl (CR excitation): (1) 0.99ZnS:0.01ZnTe; (2) 0.98ZnS:0.02ZnTe; (3) 0.96ZnS:0.04ZnTe; (4) 0.94ZnS:0.06ZnTe; (5) 0.92ZnS:0.08ZnTe; (6) 0.90ZnS:0.10ZnTe.

3. Zn(S:Te):Ag(0.01) (NaCl).—Spectral distribution curves of several of these phosphors, under CR and ultra-violet excitation, are shown in Fig. 4. Variation of λ_{PK} with ZnTe proportion is shown in Fig. 2C, and ϵ_{PK}^{CR} values in Fig. 2G.

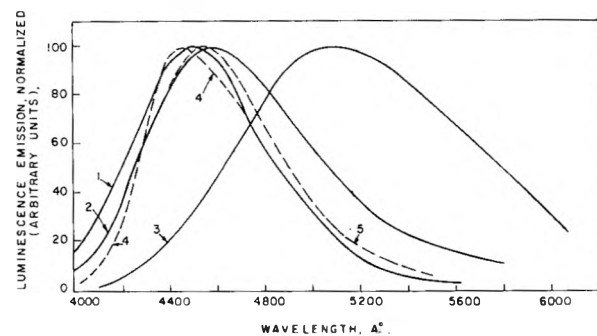


Fig. 4.—Spectral distribution curves of the emission from Zn(S:Te):Ag(0.01), NaCl(2) phosphors; 1, 2, 3, are CR excited; 4, 5 are ultra-violet (3650 Å.) excited: (1) 0.98ZnS:0.02ZnTe:Ag; (2) 0.94ZnS:0.06ZnTe:Ag; (3) 0.90ZnS:0.10ZnTe:Ag; (4) 0.99ZnS:0.01ZnTe:Ag; (5) 0.98ZnS:0.02ZnTe:Ag.

Examining the effect of Ag, in detail, the following may be seen: (1) with the addition of Ag, the peak wave length is shifted toward shorter wave lengths, a well-known effect in ZnS:Ag phosphors¹; (2) with proportions of ZnTe greater than about 4 mole %, a shift in λ_{PK} to longer wave lengths takes place, with an indication that levelling-off is occurring at about 10 mole % ZnTe; (3) the secondary (6000 Å.) band, present in phosphors without Ag, is absent in the corresponding phosphors containing Ag; (4) the decrease of ϵ_{PK} for materials with Ag is very similar to that of materials without Ag, but with NaCl flux.

4. Zn(S:Te):Cu(0.10), (NaCl).—Spectral distribution curves of the copper-activated materials are shown in Fig. 5 for CR excitation, and in Fig. 6 for ultra-violet excitation. With CR excitation, for

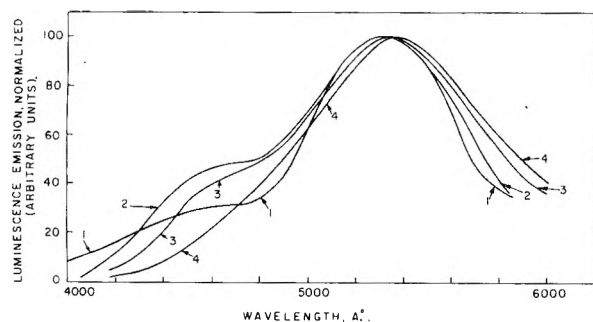


Fig. 5.—Spectral distribution curves of the emission from Zn(S:Te):Cu(0.01), NaCl(2) phosphors (CR excitation): (1) 0.98ZnS:0.02ZnTe:Cu; (2) 0.96ZnS:0.04ZnTe:Cu; (3) 0.94ZnS:0.06ZnTe:Cu; (4) 0.90ZnS:0.10ZnTe:Cu.

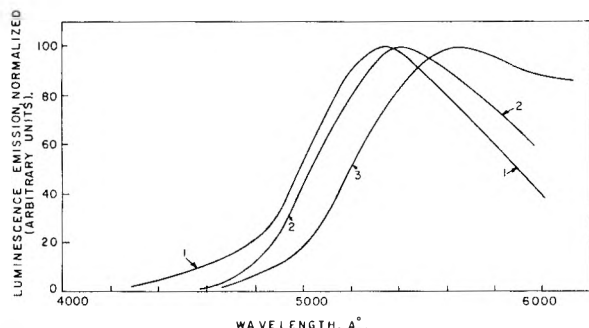


Fig. 6.—Spectral distribution curves of the emission from Zn(S:Te):Cu(0.01), NaCl(2) phosphors (ultraviolet (3650 Å.) excitation): (1) 0.98ZnS:0.02ZnTe:Cu; (2) 0.94ZnS:0.06ZnTe:Cu; (3) 0.90ZnS:0.10ZnTe:Cu.

ZnTe proportions up to about 10 mole %, the spectral distribution consists of at least two bands, (a) the blue (4600 Å.) band of Zn(S:Te), NaCl, and (b) a green (Cu) band. The change of peak wave length of the Cu band as a function of ZnTe proportion is shown in Fig. 2D, and peak emission intensities, in Fig. 2H. Under ultraviolet excitation, the blue band is not evident.

5. Zn(S:Te):Mn and Zn(S:Te):Mn, (NaCl).

—The phosphors prepared with Mn activator, 0.5% by weight, exhibited two emission bands, under CR excitation, designated as band I whose peak wave length was at 4800 Å. and band II, with peak wave length at 5950 Å., both for ZnS:Mn, (NaCl). For the phosphor without NaCl, band I appeared only with 4 mole %, or greater, of ZnTe, whereas band II was present throughout the range of compositions.

The effect of telluride on the peak wave lengths of band I, for phosphors prepared with NaCl and without NaCl is shown in Figs. 7A and 7B. Band I can be related to the intrinsic emission from unactivated Zn(S:Te), NaCl, but a comparison of the data in Fig. 7 with that of Figs. 2A and 2B shows that Mn affects the band I shift in peak wave length with increasing ZnTe proportion. This is shown in Table III.

The emission from centers associated with the Mn activator, band II, is greatly affected by the presence or absence of NaCl flux. This is shown in Figs. 7C and 7D. For materials prepared with NaCl, there is a shift in the peak wave length of band II to longer wave lengths with increasing proportion of ZnTe, to about 4 mole %. Phosphors

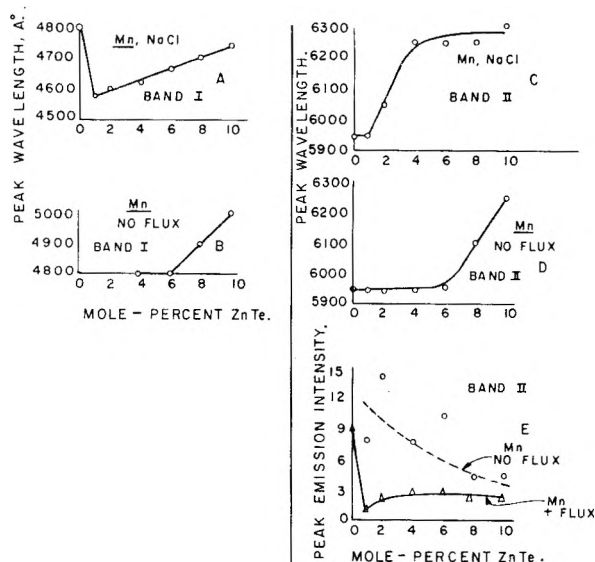


Fig. 7.—A—D: peak wave length of emission as a function of zinc telluride proportion (prior to crystallization), CR excitation: (A) Zn(S:Te):Mn(0.5), NaCl(2), band I; (B) Zn(S:Te):Mn(0.5), unfluxed, band I; (C) Zn(S:Te):Mn(0.5), NaCl(2), band II; (D) Zn(S:Te):Mn(0.5), unfluxed, band II.

Fig. 7E.—Peak emission intensity of Zn(S:Te):Mn(0.5) phosphors, unfluxed and with NaCl(2), as a function of ZnTe proportion, normalized as described in Fig. 2.

prepared without NaCl show no effect with increasing telluride up to about 6 mole %.

A comparison of peak emission intensities, under CR excitation, for phosphors prepared with and without NaCl, is shown in Fig. 7E. The Zn(S:Te):Mn phosphors prepared without flux show higher emission intensities, as has been previously reported for ZnS:Mn phosphors¹ under CR excitation.

TABLE III

EFFECT OF MN ON PEAK WAVE LENGTH OF BAND I EMISSION FROM Zn(S:Te) PHOSPHORS, IN Å.

Mole % ZnTe	NaCl		Without NaCl	
	Unactivated	Mn	Unactivated	Mn
1	4650	4580	4800	...
2	4640	4600	4800	...
4	4700	4620	4850	4800
6	4740	4670	5000	4800
8	4850	4700	5200	4900
10	5180	4740	5200	5000

Discussion

Zinc sulfide, unactivated and unfluxed, crystallized at 900°, shows practically no luminescence emission. With the addition of 1 mole % zinc telluride, luminescence is obtained.⁶ The peak wave length of emission is a function of the proportion of telluride, and occurs at shorter wave lengths than for phosphors prepared with corresponding proportions of zinc selenide. The cathodo-luminescence peak emission intensity increases with increasing ZnTe to about 4 mole % ZnTe. The fact that there is not a double emission band apparent in this system, and that an emission intensity de-

(6) The possibility of activation of ZnS by zinc from decomposition of ZnTe is ruled out, since crystallizing ZnS in Zn vapor (without halide) does not render the material luminescent.

pendence on telluride proportion exists, would indicate that (SZn₄) groups, perturbed by telluride, are the centers. The shift of the peak wave length to longer wave lengths with increasing amounts of ZnTe is in accord with previous experience that substitution with ions of larger ionic radius (Te⁼ for S⁼) results in luminescence emission whose peak wave length is at longer wave lengths.

The phenomenological effect of halide fluxes on the luminescence of zinc sulfide phosphors has been discussed by Rothschild.⁷ With further advances in the work on fluxes for phosphors, Smith⁸ suggested that the chloride is incorporated into the crystal, forming crystal defects, and Kröger and Hellingman⁹ have reported finding incorporated chloride in sulfide phosphors. The crystal perturbations due to incorporated chloride, as evidenced by magnetic studies, have been described by Larach and Turkevich.¹⁰

The nature of curves ABEF (Fig. 2) suggests that the emitting center created by addition of telluride to the ZnS lattice is not essentially equivalent to

the effective center created by the presence of Cl in the ZnS lattice or the Zn(S:Te) lattice. The nearly-identical emission of 98ZnS:2ZnTe and ZnS(Cl) is probably coincidental. The effect of increasing telluride concentration in the lattice or the ZnS(Cl) emission can be accounted for by assuming that the Zn(S:Te) efficiency is increasing (due to increasing number of centers), while the centers related to the presence of Cl are being "poisoned" by the lattice distortion created by the telluride concentration. The exact nature of the Zn(S:Te) center is entirely conjectural. The efficiency plot with telluride suggests that paired defects may constitute the nucleus of the elemental crystal volume giving rise to the emission.¹⁰ Parallel situations exist when Ag and Cu are present to give rise to their characteristic emission.

The Zn(S:Se) systems has no limited solubility, leading one to argue that low concentrations of Se in ZnS do not cause "poisoning" perturbations. Confirmation is offered by the observation that no marked loss of efficiency is experienced with phosphors containing selenide in small amounts.¹¹

(7) S. Rothschild, *Trans. Faraday Soc.*, **42**, 635 (1946).

(8) A. L. Smith, *J. Electrochem. Soc.*, **96**, 75 (1949).

(9) F. A. Kröger and J. E. Hellingman, *ibid.*, **95**, 68 (1949).

(10) S. Larach and J. Turkevich, *Phys. Rev.*, **98**, 1015 (1955).

(11) "Preparation and Characteristics of Solid Luminescent Materials," edited by G. R. Fonda and F. Seitz, John Wiley and Sons, Inc., New York, N. Y., 1948, p. 238.

REACTION HEATS OF ORGANIC HALOGEN COMPOUNDS. V. THE VAPOR PHASE BROMINATION OF TETRAFLUOROETHYLENE AND TRIFLUOROCHLOROETHYLENE¹

BY J. R. LACHER, LIBERTY CASALI AND J. D. PARK

Contribution of the University of Colorado, Boulder, Colorado

Received October 27, 1956

A calorimeter has been constructed in which one can study vapor phase reactions at about 103°. It has been used to measure the heat of formation of hydrogen bromide from its gaseous elements and also to measure the heat of addition of bromine vapor to tetrafluoro- and trifluorochloroethylene.

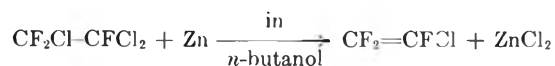
In the previous paper,² a calorimeter was described that uses a condensing vapor as a source of constant temperature. When diphenyl ether is employed, an operating temperature of 248° is produced. Under these conditions, some simple alkyl chlorides could be hydrogenated. A "low temperature" calorimeter also has been constructed that utilizes condensing toluene vapor as its constant temperature environment. The present paper describes its operation and presents data on the vapor phase bromination of tetrafluoroethylene and trifluorochloroethylene.

Materials and Experimental Methods.—Except for minor changes, the "low temperature" calorimeter is identical to the one previously described. Instead of a platinum resistance thermometer, thermistors were employed to sense any temperature change of the condensing toluene. They formed one arm of a conventional Wheatstone bridge. Any unbalance of the bridge was used to modify the pressure on the boiling toluene so as to maintain the temperature constant to 0.001° during an experiment.

The calorimeter catalyst chamber was immersed in a

quart dewar flask containing *n*-butyl ether. The reaction heat was transferred to the ether, and the latter could be cooled by bubbling dry nitrogen through it. In order to measure the temperature differential between the *n*-butyl ether in the dewar and the surrounding temperature bath, a twenty-four junction copper-constantan thermel was used. One end of the thermel was located in a well made of telescopic iron tubing extending about midway in to the *n*-butyl ether, whereas the other end was suspended in a brass well in the condensing vapor bath. The procedure used in making an experiment was identical to that previously described.

The trifluorochloroethylene was prepared by the following dechlorination reaction³



The CF₂=CFCl obtained was then purified on a 100-plate Podbielniak Hypercal column. The starting material was a gift from the du Pont Company. Part of the tetrafluoroethylene used in this work was supplied by the du Pont Company, and the remainder was prepared by the following three reactions⁴:

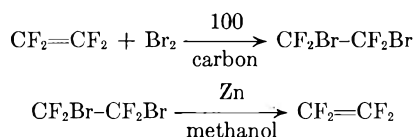


(1) This research was supported by the Atomic Energy Commission, Contract No. AT(11-1)-168.

(2) J. R. Lacher, E. Emery, E. Bohmfalk and J. D. Park, *This Journal*, **60**, 492 (1956).

(3) M. L. Sarrah, Ph.D. Thesis, University of Colorado, 1948.

(4) J. D. Park, *et al.*, *J. Ind. Eng. Chem.*, **39**, 354 (1947).



The crude tetrafluoroethylene obtained by the pyrolysis of difluorochloromethane was brominated to give the dibromide. The dibromide was then distilled on the Podbielniak column. Whenever needed, it was dehalogenated to tetrafluoroethylene and the product condensed into a liquid nitrogen trap. It was then purified by trap to trap distillation and stored in a bomb containing several ml. of "Terpene B" inhibitor to prevent polymerization. The inhibitor was removed from the gas stream as it was metered to the calorimeter by a method previously described.⁵

Reagent bromine (Mallinckrodt) was used without further purification. It was carried to the calorimeter in a stream of nitrogen. The nitrogen gas was dried over phosphorus pentoxide and then bubbled through bromine at 0°. The gas could be sent either to the calorimeter or to an absorption tower to determine the flow rate of bromine. The bromine was absorbed in 3 *N* potassium iodide solution. The liberated iodine was titrated with standard sodium thiosulfate in the usual way.

Experimental Results.—In order to determine whether or not the calorimeter was working properly, it was decided to measure the heat of formation of hydrogen bromide from its gaseous elements. Electrolytic hydrogen of 99.8% purity from the Mathieson Company was used. The oxygen present was removed by methods previously described.² A hydrogenation catalyst consisting of palladium on asbestos brought about a complete reaction of the bromine which was the limiting reactant. Of the eight runs made, four were carried out without experimental difficulties, and the results are given in Table I. The difference between our measured ΔH and the enthalpy change, ΔH° , for the reaction when the reactants and products are in their standard states as hypothetical ideal gases is small in comparison to our

TABLE I
VAPOR PHASE HEAT OF FORMATION OF HYDROGEN BROMIDE
AT 103°

H ₂ flow, moles/min. × 10 ⁴	HBr formation, moles/min. × 10 ⁴	Energy rate, cal./min.	−Δ <i>H</i> , cal./mole, of HBr
10.0	5.318	6.689	12,580
10.4	5.146	6.350	12,340
10.5	4.991	6.204	12,430
10.5	4.679	5.863	12,530

Av. −Δ*H* = 12,473

Twice the standard dev. of the mean⁶ = ±0.85%

experimental errors and is neglected. No direct calorimetric determination of the heat of formation of hydrogen bromide from its gaseous elements has been reported in the literature. However, values of −12.33 at 300°K. and of −12.41 kcal./mole at 400° are given by the Bureau of Standards.⁷ The interpolated value of −12.39 kcal./mole at 375°K. is in satisfactory agreement with the present average of −12.47 kcal./mole. Using heat capacity data our value for the heat of formation becomes −12,377 ± 130 cal./mole at 298.16°K.

(5) J. R. Lacher, J. D. Park, *et al.*, *J. Am. Chem. Soc.*, **71**, 1330 (1949).

(6) F. D. Rossini, *Chem. Revs.*, **18**, 233 (1936).

(7) "Selected Values of Chemical Thermodynamic Properties," Series III, National Bureau of Standards.

The Bromination of Tetrafluoroethylene.—Two catalysts were used in the determination of the vapor phase heat of bromination of tetrafluoroethylene. Antimony bromide on activated charcoal was prepared by mixing finely powdered antimony with charcoal, and the mixture was then placed in a catalyst chamber. Bromine gas entrained in a stream of nitrogen was then passed over it at about 150°. During pilot plant studies, it was found that this catalyst would bring about the quantitative addition of bromine to CF₂=CF₂, CF₂=CFCl and CF₂=CH₂ at 103°. In the case of CF₂—CF=CF—CF₂, the conversion was very

low owing, possibly, to an unfavorable equilibrium. A second catalyst consisting of ferric bromide on activated charcoal was prepared in a similar way. In making a run, an excess of tetrafluoroethylene over bromine was used, and the rate of formation of the dibromide was taken equal to the rate bromine was led into the calorimeter. The experimental results are given in Table II; all runs are

TABLE II
VAPOR PHASE HEAT OF BROMINATION OF
TETRAFLUOROETHYLENE AT 103°

Olefin flow, moles/min. × 10 ⁴	Br ₂ flow, moles/min. × 10 ⁴	Energy rate, cal./min.	−Δ <i>H</i> , cal./mole, of CF ₂ Br—CF ₂ Br
12.9	3.164	11.572	36,570
12.1	2.581	10.020	38,820
9.7	2.803	10.288	36,700
11.4	2.581	10.729	41,570
13.4	2.545	10.260	40,310
11.7	2.454	9.3664	38,170

Av. −Δ*H* = 38,586

Twice the av. dev. of the mean = ±4.2%

9.3	4.446	17.386	39,100
9.3	4.305	16.945	39,360
12.7	4.285	16.761	39,120
8.7	2.855	10.481	36,710
9.7	2.822	10.454	37,040
11.9	4.222	16.644	39,420
3.5	2.843	10.545	37,090
11.5	2.823	10.994	38,940
13.2	5.850	22.213	37,970
12.8	6.130	23.755	38,750

Av. −Δ*H* = 38,350

Twice the av. dev. of the mean = ±1.7%

included except one in which a plugged frit stopped the experiment. The first six runs were made using the antimony bromide catalyst and in every case there was a slight trace of bromine in the exit gases. Also the scattering in the resulting ΔH values was greater than desired. They give an average of −38,586 cal./mole. The apparatus was then dismantled and a ferric bromide catalyst installed in the reaction chamber. With this catalyst the reaction was quantitative. During the remainder of the runs, a special effort was made to vary the ratio of the olefin to bromine flow. The experimental values seem to be independent of these variations. The values for ΔH are more consistent in the second series of runs owing,

TABLE III
VAPOR PHASE HEAT OF BROMINATION OF
TRIFLUOROCHLOROETHYLENE AT 103°

Olefin flow, moles/min. $\times 10^4$	Br ₂ flow, moles/min. $\times 10^4$	Energy rate, cal./min.	$-\Delta H$, cal./mole, of CF ₂ Br-CFClBr
14.5	4.665	14.439	30,950
11.9	4.318	13.294	30,790
10.3	4.512	13.815	30,620
10.1	5.149	16.704	32,440
11.5	5.158	16.160	31,330
12.7	5.074	16.013	31,560
9.4	4.416	13.788	31,220
10.1	4.439	13.902	31,320
10.1	4.103	13.015	31,720
9.3	5.120	16.128	31,500
Av. $-\Delta H = 31,345$			
Twice the av. dev. of the mean = $\pm 1.1\%$			
10.2	4.916	16.056	32,660
9.6	4.928	16.120	32,710
10.1	5.124	16.064	31,350
9.8	4.518	14.657	32,440
9.8	5.213	16.362	31,390
8.7	2.844	9.0233	31,730
Av. $-\Delta H = 32,047$			
Twice the av. dev. of the mean = $\pm 1.6\%$			

perhaps, to a better experimental technique. Their average value is $-38,350$ cal./mole. This is in essential agreement with the first average and shows that the measured heat of reaction is independent of the catalyst used. The average over all sixteen experiments is $-38,478$ cal./mole.

The Bromination of Trifluorochloroethylene.—The bromination of trifluorochloroethylene was carried out by the same procedures as with tetrafluoroethylene. The results are given in Table III. The first ten runs were made using antimony tribromide as a catalyst and the last six with ferric bromide. The average of the sixteen runs gives a heat of reaction of $-31,608$ cal./mole. The runs made with both tetrafluoro- and trifluorochloroethylene show a greater variation in ΔH values than were obtained in the measurements of the heat of formation of gaseous hydrogen bromide. It is believed that this is due to the relatively large amount of products adsorbed on the carbon catalyst. A slight variation of the flow rates will upset the adsorption equilibrium, making it difficult to obtain a steady state. Very little adsorption will take place with the palladium on asbestos catalyst, and a steady state readily is obtained.

THE THERMAL DECOMPOSITION OF TIN HYDRIDE

By KENZI TAMARU

Frick Chemical Laboratory, Princeton University, Princeton, N. J.

Received October 29, 1955

The kinetics of decomposition of tin hydride have been studied by a static method. The decomposition is a first-order reaction in respect to tin hydride, being independent of hydrogen pressure, and the activation energy of the reaction is 9.1 kcal./mole between 100 and 35° . The hydrogen-deuterium exchange reaction did not proceed at a measurable rate on tin film at 60° , where tin hydride decomposed fairly fast. Similarly, when tin deuteride was decomposed in the presence of hydrogen, no hydrogen deuteride could be detected in the reaction product. On the contrary, when mixtures of tin hydride and tin deuteride were decomposed together, hydrogen deuteride was produced. The effect of oxygen on the decomposition was studied. It was found that a small amount of oxygen can stop the decomposition, forming an oxide film on the tin surface. The rate-determining step of the over-all reaction has been discussed briefly.

As has been shown in previous papers,¹⁻⁴ the decomposition of arsine on arsenic surface is a first-order reaction in respect to arsine and the germane decomposition on germanium surface is zero order, while stibine decomposes on antimony surface as a fractional order, between first and zero order. In all these cases hydrogen does not affect the reaction rate. It was suggested that the rate-determining step of the arsine decomposition is the chemisorption of arsine, while that of germane decomposition is the desorption of chemisorbed hydrogen from the germanium surface. In the latter case it was shown⁵ that the germanium surface is virtually covered by the chemisorbed hydrogen atoms during the reaction.

These reaction systems of the hydride decompositions are ideally suitable to study because of the simplicity of the reactions and the fact that clean

elemental surfaces are continuously maintained through fresh deposition of the elements. The decomposition of another hydride, tin hydride, SnH₄, has been studied.

Experimental

The decomposition of tin hydride was studied by a static method. Since hydrogen is the only gaseous constituent resulting from the decomposition, the rate of the reaction was followed by observing the total pressure of the system, which, on completion of the decomposition, was twice the initial pressure.

Preparation of Tin Hydride.—Tin hydride was prepared by adding chemically pure anhydrous stannic chloride liquid to a solution of lithium aluminum hydride in ethylene glycol dimethyl ether in a dry nitrogen atmosphere. The solution of lithium aluminum hydride was cooled with liquid nitrogen as the stannic chloride was added. After the chloride addition the liquid nitrogen was removed to allow the solution to warm up gradually to room temperature. The tin hydride thus prepared was condensed in a liquid nitrogen trap and was purified by distilling several times between solid carbon dioxide and liquid nitrogen. For the preparation of tin deuteride, lithium aluminum deuteride was used instead of hydride.⁶

(6) Anhydrous stannic chloride was obtained from General Chemical Division, Allied Chemical and Dye Corporation, New York, and lithium aluminum hydride and deuteride from Metal Hydrides, Inc., Mass.

(1) K. Tamaru, *THIS JOURNAL*, **59**, 777 (1955).

(2) K. Tamaru, *ibid.*, **59**, 1084 (1955).

(3) K. Tamaru, M. Boudart and H. Taylor, *ibid.*, **59**, 801 (1955).

(4) P. J. Fensham, K. Tamaru, M. Boudart and H. Taylor, *ibid.*, **59**, 806 (1955).

(5) K. Tamaru, in preparation for *J. Phys. Chem.*

Apparatus and Procedure.—A cylindrical Pyrex glass vessel, which had been carefully cleaned, was used for the reaction vessel. The inside diameter of the vessel was 2.7 cm. and its volume was 68 cc. The temperature of the reaction vessel was controlled satisfactorily using vapor baths of water, benzene, carbon tetrachloride and acetone and also using a thermoregulated water-bath. The reaction vessel was attached to a mercury manometer by means of capillary tubing and during the reaction its pressure was followed by the manometer with a cathetometer, keeping the volume constant. Between the reaction vessel and the manometer, a solid carbon dioxide trap was used to prevent the entry of vapor of mercury, grease or other impurities.

Before the reactant was introduced into the reaction vessel a vacuum of less than 10^{-5} mm. was obtained by means of two mercury diffusion pumps backed up by a Cenco High-Vac oil pump.

Experimental Results

Decomposition of Tin Hydride on Glass Surface.

—When 12 cm. of tin hydride was introduced into a glass reaction vessel at 100° , the pressure did not change for the first 15 minutes, then started to increase autocatalytically, producing hydrogen and a silvery tin film on the glass. From the second run in the reaction vessel with tin film the decomposition rate was reproducible without any induction period, which shows that tin hydride decomposition on a glass surface is much slower than that on a tin surface and also that the decomposition in the reaction vessel with a tin surface is positively a heterogeneous reaction and its homogeneous reaction can be ignored.

Decomposition of Tin Hydride on Tin Surface.

—Tin hydride was decomposed at 76.8° at various initial pressures. As shown in Fig. 1, where the logarithm of tin hydride pressure is plotted against time, a straight line is obtained, showing that the decomposition of tin hydride is a first-order reaction in respect to tin hydride pressure. From the slopes of the straight lines in Fig. 1, the rate constants of the reaction are obtained. These are 0.081, 0.081, 0.077 and 0.078 min.^{-1} in order of decreasing initial pressures. This shows that the rate constants of the reaction are independent of the initial pressure of tin hydride and that the partial pressure of hydrogen does not affect the reaction rate.

The kinetics of the decomposition were studied at various temperatures between 100 and 35° and a result of 35.0° is shown in Fig. 2 as an example. Here also the reaction was first order in respect to tin hydride, being independent of the partial pressure of hydrogen. The reaction rates at various temperatures are shown in Fig. 3, which obeys the Arrhenius equation, from which an apparent activation energy of 9.1 kcal./mole is obtained.

The decomposition rate of tin deuteride was measured at 60° , which is shown in Fig. 3 with double circles. The ratio of the decomposition rates of tin hydride and deuteride is, therefore, 1.7:1 at 60° .

Hydrogen-Deuterium Exchange Reaction on Tin Surface.

—2.0 cm. of hydrogen and 3.1 cm. of deuterium were introduced into the reaction vessel with a clean tin surface. These gases were obtained from cylinders, being purified separately by passing through Pd-asbestos at 300° , $\text{Mg}(\text{ClO}_4)_2$, a liquid nitrogen trap and then a Pd thimble at 300° . The reaction vessel was kept at

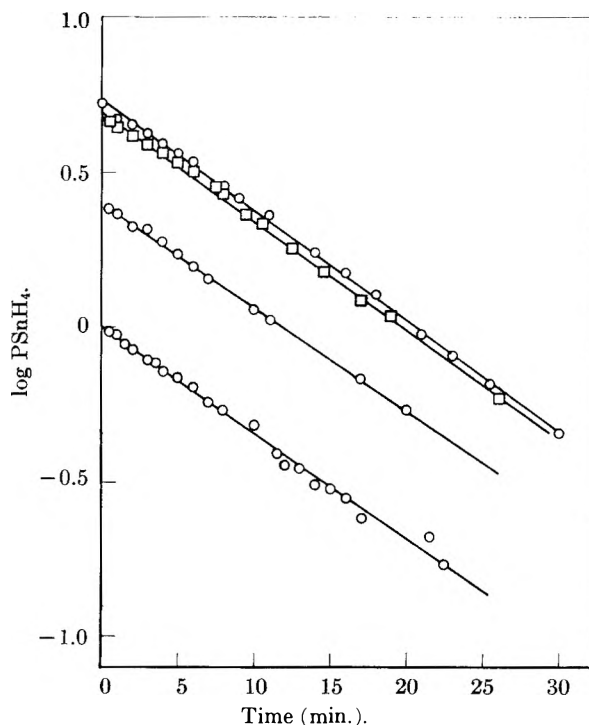


Fig. 1.—Decomposition of SnH_4 on Sn surface at 76.8° .

60° for an hour and was kept standing at room temperature overnight. The gas was then analyzed by means of a mass spectrometer. No hydrogen deuteride formation was indicated by the analysis.

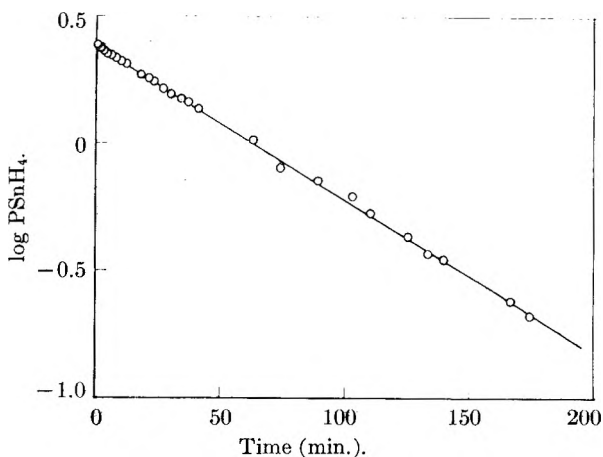


Fig. 2.— SnH_4 decomposition on Sn surface at 35.0° .

8.2 cm. of tin deuteride was decomposed with 8.6 cm. of hydrogen on a tin surface at 60° for 6 hours and the decomposition product was analyzed. Practically no hydrogen deuteride was found in the reaction product. In this case the tin surface was always being renewed by the deposition of fresh tin during the decomposition and no exchange reaction between hydrogen and deuterium took place on the fresh tin surface.

On the other hand, when a gas mixture of 1.2 cm. of tin hydride and 3.8 cm. of tin deuteride was decomposed at 60° , hydrogen deuteride was detected in the reaction product. The amount of the hydrogen deuteride seemed to be less than that

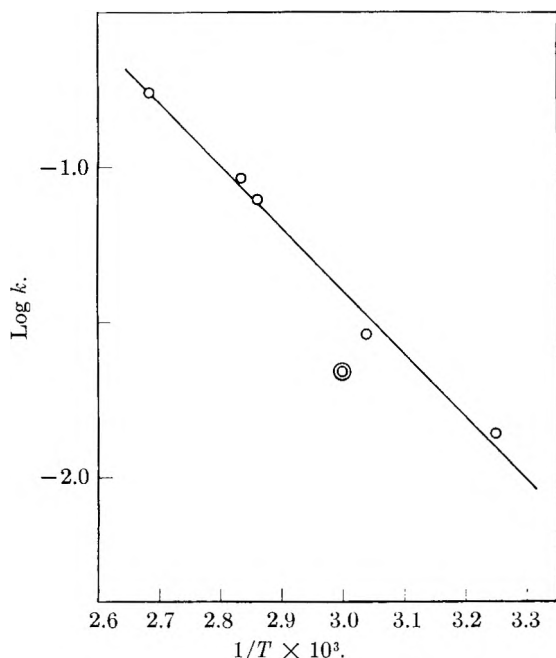


Fig. 3.—Dependence of rate constant upon temperature.

at equilibrium in the system $\text{H}_2 + \text{D}_2 = 2\text{HD}$ at the given temperature.

Trapnell⁷ showed that hydrogen is not chemisorbed on an evaporated tin surface and this is indicated also in this experiment. As will be discussed in detail in a later paper, the rate-determining step of the decomposition of tin hydride can be

(7) B. M. W. Trapnell, *Proc. Roy. Soc. (London)*, **A218**, 566 (1953).

considered as the chemisorption step of tin hydride on a tin surface.

Effect of Oxygen on the Decomposition of Tin Hydride.—When 0.4 cm. of oxygen was put in the reaction vessel before the tin hydride was introduced, no decomposition was observed in 200 minutes at 60°, which means that a small amount of oxygen can stop the decomposition of tin hydride. After evacuating the reaction vessel for an hour, pure tin hydride was introduced into the reaction vessel again, and showed almost the same behavior as the decomposition on a glass surface; that is, the tin hydride decomposed after an induction period. This effect of oxygen can be explained by the non-catalytic action of tin oxide film on the tin surface. It is interesting to note that³ in the case of germane decomposition oxygen continued to accelerate the decomposition, presumably coming up to the surface of the depositing germanium.

Acknowledgment.—The assistance of Mr. B. W. Steiner in the mass spectrometric analyses is gratefully acknowledged.

This work was carried out on a post-doctoral fellowship kindly provided to Princeton University by the Shell Fellowship Committee of the Shell Companies Foundation, Inc., New York City. We wish to express our appreciation of this support. The work in question is also a part of a program of research supported by the Office of Naval Research N6onr-27018 on Solid State Properties and Catalytic Activity. Acknowledgment is made also to this research project for facilities used and for consultation with workers in the project, and to Dean Hugh Taylor for advice and assistance.

DECOMPOSITION OF AMMONIA ON GERMANIUM

BY KENZI TAMARU

Frick Chemical Laboratory, Princeton University, Princeton, N. J.

Received October 29, 1955

The decomposition of ammonia on germanium has been studied by a static method at 278°. It was found that when ammonia was introduced to a germanium surface, hydrogen came off with only a small amount of nitrogen. This occurred rapidly at first, then more slowly tending to a saturation value which was independent of ammonia pressure. The number of ammonia molecules adsorbed was found to be almost exactly half of the number of germanium atoms on the surface. Taking the adsorption of hydrogen on germanium into account, it was shown that the number of hydrogen molecules from the chemisorbed ammonia corresponds to approximately half of the number of the ammonia molecules adsorbed. It is suggested that chemisorbed ammonia covers all the germanium surface fairly rapidly, dissociating to $\text{NH}_2(\text{a})$ and $\text{H}(\text{a})$, and a part of the latter desorbs to form hydrogen molecules in the gas phase. In other words, $\text{NH}_2(\text{a})$ is adsorbed on every other site on the germanium surface and hydrogen atoms occupy some of the remaining sites in equilibrium with hydrogen gas in the gas phase.

Since the work of Brattain and Bardeen¹ on the effect of various gases and vapors on the electrical properties of germanium, many papers have been published on the adsorption of gases on a germanium surface. It was shown by Law and Francois² that nitrogen is not chemisorbed on germanium at temperatures of 20° or higher, and the heat of physical adsorption of nitrogen on germanium³ at 138°K. is 2.4 kcal./mole at a coverage of 10^{-2} .

(1) W. H. Brattain and J. Bardeen, *Bell System Tech. J.*, **32**, 1 (1953).

(2) J. T. Law and E. E. Francois, *Ann. N. Y. Acad. Sci.*, **58**, Art. 6, 925 (1954).

(3) J. T. Law, *This Journal*, **59**, 543 (1955).

As to the adsorption of hydrogen on germanium, it has been shown in a previous paper⁴ that hydrogen can be chemisorbed on germanium at higher temperature and the heat of adsorption is 23.5 kcal./mole at a coverage of 0.05. The activation energy of desorption of chemisorbed hydrogen,^{4,5} which corresponds to that of germane decomposition, is 41.2 kcal./mole at the coverage of unity, while that of chemisorption at $\theta = 0$ is 14.6 kcal./mole at about 250°. These results indicate that for nitrogen the adsorption is purely physical and might be expected to have but little effect on

(4) K. Tamaru, in preparation for *J. Phys. Chem.*

(5) K. Tamaru, M. Boudart and H. Taylor, *ibid.*, **59**, 801 (1955).

the electrical properties of the semi-conductor, while in the case of hydrogen at higher temperatures the properties of germanium can be affected by the adsorption.

The author studied the decomposition of a series of hydrides⁴⁻⁹ and found, for instance, that arsine decomposes fairly rapidly on antimony surfaces at 278°, decomposes more slowly on arsenic surfaces, and more slowly still on germanium surfaces. As an example of another hydride decomposition, the decomposition of ammonia on germanium has been studied.

Experimental

The decomposition of ammonia on germanium surface was studied by static method. The germanium film in the reaction vessel was prepared by the decomposition of germane on clean glass wool in the same way as in a previous paper.⁴ For every experiment the germanium surface was renewed by the deposition of fresh germanium with evacuation to remove all the hydrogen at reaction temperature. Ammonia was obtained from a cylinder, and distilled several times using solid carbon dioxide and liquid nitrogen. The apparatus for the experiment was almost the same as that used for germane decomposition in a previous paper⁶ and a trap of solid carbon dioxide between the reaction vessel and the manometer was used to prevent the entry of vapor of mercury, grease or other impurities. After evacuation to less than 10^{-5} mm. by means of two mercury diffusion pumps backed up by a Cenco High-Vac oil pump, ammonia was introduced into the reaction vessel. The pressure was measured with a cathetometer and during the reaction the reaction vessel was kept at constant temperature using a vapor bath of acenaphthene.

Experimental Results and Discussion

During the course of the reaction, the trap was from time to time cooled to liquid nitrogen temperatures in order to condense the ambient ammonia and to permit measurement of the pressure of uncondensed gas. These pressures are recorded as a function of time in Fig. 1. It was confirmed by special test that this process of condensing ammonia in the trap did not affect the reaction rate. Figure 1 shows that the decomposition of ammonia was initially rapid at 278°, the rate progressively decreasing and approaching, finally, an apparently constant value for the pressure of uncondensed gas. The rate was also independent of the initial ammonia pressure in the experimental pressure range of 0.62 to 2.93 cm. The crosses in Fig. 1 show the results of an experiment without renewal of the germanium surface but with three hours of evacuation at 278° after the preceding run. The original activity of a clean film is not restored by this treatment.

When constant pressure of uncondensed gas was reached, both the reaction vessel and the trap were cooled down to liquid nitrogen temperatures and the total amount of uncondensed gas at that temperature was determined. As an average of four experiments at 278° the volume of uncondensed gas was 0.136 cc. (STP). Mass spectrometric analyses of the gas showed that it consisted of about 20 parts of hydrogen and one part of nitrogen for experiments at both 278 and 444°. This

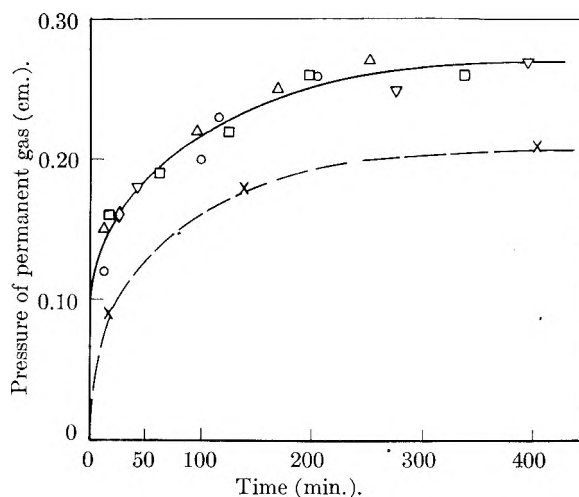


Fig. 1.—Initial pressure (cm.): O, 0.62; □, 1.10; ▽, 2.46; △, 2.93; ×, 2.89 (without renewal of Ge surface).

estimate is based on comparisons with a sample of known composition.

This uncondensed gas can be assigned to two sources (a) the product of NH_3 decomposition in amount

$$0.136 \times (1 + 3)/21 = 0.026 \text{ cc. (STP)}$$

and (b) molecular hydrogen in amount

$$\begin{aligned} 0.136 - 0.026 &= 0.110 \text{ cc. (STP)} \\ &= 0.30 \times 10^{19} \text{ hydrogen molecules} \end{aligned}$$

If the nitrogen and its associated hydrogen came from decomposition of NH_2 radicals (see below) the number of hydrogen molecules in (b) would be somewhat larger, actually $0.136 - 0.019 = 0.117$ cc. (STP) or 0.32×10^{19} hydrogen molecules.

After this determination, the liquid nitrogen around the reaction vessel was replaced by solid carbon dioxide coolant, the liquid nitrogen was removed from the trap and the reaction system was evacuated for one hour. Then the trap was cooled in liquid nitrogen and the reaction vessel was heated to 278°. An appreciable amount of gas condensed in the trap, presumably ammonia desorbed from the germanium surface.

The volume of ammonia adsorbed on germanium or decomposed on the surface at any time during the experiment can be calculated from the volume of ammonia introduced and that in the gas phase. It amounted to 0.349 cc. (STP). This amount of adsorbed ammonia was found to be constant within the experimental error from the first measurement throughout the total reaction time. If we subtract the amount of ammonia which was present as nitrogen and hydrogen in the gas phase, since $2\text{NH}_3 = \text{N}_2 + 3\text{H}_2$, we obtain

$$0.136 \times 2/21 = 0.013 \text{ cc. (STP)}$$

and, by difference

$$\begin{aligned} 0.349 - 0.013 &= 0.336 \text{ cc. (STP)} \\ &= 0.90 \times 10^{19} \text{ ammonia molecules adsorbed} \end{aligned}$$

Next, the surface area of the germanium film was measured by the BET method using the adsorption of *n*-butane at -78° . The area found was $2.2 \times 10^4 \text{ cm}^2$. If we assume, respectively, that the

(6) K. Tamaru, *THIS JOURNAL*, **59**, 777 (1955).

(7) K. Tamaru, *ibid.*, **59**, 1084 (1955).

(8) P. J. Fensham, K. Tamaru, M. Boudart and H. Taylor, *ibid.*, **59**, 806 (1955).

(9) K. Tamaru, *ibid.*, **60**, 610 (1956).

(110) or the (111) crystal face is exposed, the area observed corresponds to

(110) face: 2.0×10^{19}

(111) face: 1.6×10^{19} germanium atoms on the surface

The hydrogen in the gas phase at the end of an experiment was $0.136 \times 20/21 = 0.130$ cc. (STP). Since the volume of the reaction system at 278° corresponded to 25.9 cc. at 0° the final hydrogen partial pressure in the gas phase was 0.38 cm. From earlier experiments on the chemisorption of hydrogen on such germanium films,⁵ and assuming that the presence of chemisorbed ammonia does not affect the extent of coverage of germanium sites by hydrogen, we deduce that the coverage $\theta = 0.26$ of the hydrogen sites at the final state of the system.

If now it is postulated that the chemisorption of ammonia gas on germanium surfaces yields dissociated adsorbed fragments, NH_2 (a) and H (a), and that a part of the latter desorbs to form hydrogen molecules uninfluenced by the adjacent adsorbed NH_2 radicals, we can estimate the number of adsorbed hydrogen atoms in terms of an average number of germanium atoms in the total surface = 1.8×10^{19} . With these postulates the number of adsorbed hydrogen atoms becomes

$$1.8 \times 10^{19} \times 1/2 \times 0.26 = 0.23 \times 10^{19}$$

or 0.12×10^{19} hydrogen molecules

If we add this amount of hydrogen to the molecular hydrogen in the uncondensed gas recorded in (b) above we obtain

$$(0.30 + 0.12) \times 10^{19} = 0.42 \times 10^{19} \text{ hydrogen molecules}$$

$$= 0.84 \times 10^{19} \text{ hydrogen atoms}$$

If we accept the alternative source of nitrogen in the uncondensed gas the corresponding datum is

$$(0.32 + 0.12) \times 10^{19} = 0.44 \times 10^{19} \text{ hydrogen molecules}$$

$$= 0.88 \times 10^{19} \text{ hydrogen atoms}$$

Summarizing the conclusions from these computations we find

Mean no. of Ge sites in surface: 1.8×10^{19}
 No. of ammonia molecules adsorbed: 0.9×10^{19}
 No. of hydrogen atoms adsorbed or
 desorbed as molecules: $(0.84 - 0.88) \times 10^{19}$

These data constitute strong presumptive evidence for the assumed dissociative chemisorption of ammonia to NH_2 (a) and H(a) on adjacent sites, each alternate site being occupied by NH_2 (a) and H(a), of which latter only $\theta = 0.26$, however, are occupied at the termination of the experiment.

Evacuation of the system at 278° after a reaction yields, as was shown, some ammonia. This may arise in part by the recombination of NH_2 (a)

and H(a) or, alternatively, it may result from inter-action of two NH_2 (a) radicals



There is no obvious test for these alternatives. The number of adsorbed ammonia molecules remains constant throughout the total experiment from the first pressure measurement made. This suggests that the dissociative chemisorption on germanium at 278° is fast enough to cover the whole surface within the first 10 minutes of an experiment. The build-up in pressure of uncondensed gas is then due to hydrogen desorption from a surface completely covered initially with the adsorption fragments. This suggests the reason why the uncondensed gas pressure builds up at a rate independent of the prevailing ammonia pressure. The rate of desorption is in this case slower than in the simple germanium hydride experiments.⁴ In the present case the desorption is from next nearest sites as contrasted with nearest sites in the hydride case.

In the decomposition of germane and now in the dissociative adsorption and decomposition of ammonia the germanium surface behaves as though it is markedly homogeneous in its properties.

Wahba and Kemball¹⁰ studied the heat of adsorption of ammonia on nickel, tungsten and iron evaporated films. They assumed that metal which can adsorb hydrogen as atoms can adsorb ammonia as amino radicals and hydrogen atoms provided that the strength of the metal-nitrogen bond is not substantially less than the strength of the metal-hydrogen bond. A comparison of their results for ammonia and hydrogen on nickel would seem to confirm this hypothesis. In the case of germanium this seems also to be the case from the comparison of the strength of the adsorption of hydrogen and the amino radical on germanium.

Acknowledgment.—The assistance of Mr. B. W. Steiner in the mass spectrometric analyses is gratefully acknowledged.

This work was carried out on a post-doctoral fellowship kindly provided to Princeton University by the Shell Fellowship Committee of the Shell Companies Foundation, Inc., New York City. We wish to express our appreciation of this support. The work in question is also a part of a program of research supported by the Office of Naval Research N6onr-27018 on Solid State Properties and Catalytic Activity. Acknowledgment is made also to this research project for facilities used and for consultation with workers in the project, and to Dean Hugh Taylor for advice and assistance.

(10) M. Wahba and C. Kemball, *Trans. Faraday Soc.*, **49**, 1351 (1953).

PURIFICATION OF PERFLUORO-*n*-HEPTANE AND PERFLUOROMETHYLCYCLOHEXANE

BY D. N. GLEW¹ AND L. W. REEVES

Department of Chemistry and Chemical Engineering, University of California, Berkeley, California

Received November 1, 1955

Ultraviolet absorption reveals the presence in these substances of impurities not removed by fractional distillation. A method of purification is described whereby the optical density of both was reduced to 0.2 at 200 $m\mu$. Their densities at 25° are: *n*-C₇F₁₆ 1.72006; cyclo-C₆F₁₁CF₃ 1.78777, both higher than any previously reported. Their boiling points are 82.34 and 76.14°, respectively, and their vapor pressures are reproduced by the respective equations: $\log p = -1824/T + 8.0166$ and $\log p = -1740.7/T + 7.8645$.

Commercial samples of *n*-heptane, *n*-C₇F₁₆ and *n*-methylcyclohexane, cyclo-C₆F₁₁CF₃, show considerable absorption in the ultraviolet between 200 and 240 $m\mu$. The impurities responsible are not removed by fractional distillation. This is illustrated by the curves in Fig. 1. We have therefore resorted to more drastic treatment, designed to oxidize and remove hydrocarbons. Figure 1a, left, shows the absorption of the untreated C₇H₁₆ obtained with Beckman spectrophotometer; curves (b) and (c) were obtained after refluxing with alkaline potassium permanganate and acid chromium trioxide, respectively, steam distilling, separating and drying. Refluxing with ceric sulfate gave no improvement over (a). Curve (d) was obtained after refluxing 24 hours with saturated acid permanganate, neutralizing, steam distilling, drying with P₂O₅, and passing once through dry silica gel. A second passage through fresh, dry gel yielded curve (e). All specimens were measured against an air blank.

Figure 1 shows also spectrograms for C₇H₁₁CF₃ obtained with a Cary recording spectrophotometer: (a) for the original liquid, (b) after fractionation with a 15-plate column at a reflux ratio of 20:1, (c) after refluxing with acid permanganate, and (d) after further treatment by passing through a column of silica gel. The absorption in curves (a) and (b) in the region 250–270 $m\mu$ agrees with that of fluorobenzene.

The substances thus treated had densities, vapor pressures and boiling points as follows

Density, 25°	C ₇ F ₁₆ 1.72006		C ₆ F ₁₁ CF ₃ 1.78777	
	<i>t</i> , °C.	<i>p</i> _{mm} .	<i>t</i> , °C.	<i>p</i> _{mm} .
Vapor pressures	20.02	61.5	-0.73	30.0
	24.93	78.7	15.16	66.2
	29.99	100.2	25.00	105.3
	34.99	125.7	30.16	133.5
	39.88	158.8	34.85	163.5
	44.99	192.9	40.55	207.0
	49.99	237.4		
Boiling points	82.02	751.9	75.7	750.2
	82.34	760.0	76.14	760.0
$\log p_{mm}$	$-1824/T + 8.0166$		$-1740.7/T + 7.8645$	

Oliver and Grisard² purified *n*-heptane by fractional crystallization followed by passage through a 56-foot column of silica gel. Their product boiled at 82.50 ± 0.05°, only 0.16° higher than ours.

(1) Department of Chemistry, University of Natal, Durban, South Africa.

(2) G. D. Oliver and J. W. Grisard, *J. Am. Chem. Soc.*, **73**, 1688 (1951).

Our vapor pressures are approximately 2.5 mm. higher than theirs in the range 20 to 50°. For our purpose it was most important to remove traces of hydrofluorocarbons; isomers could make little difference.

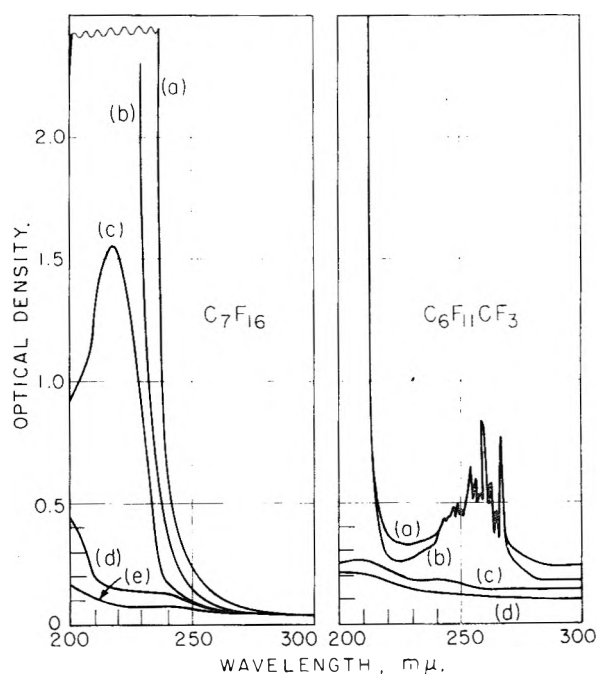


Fig. 1.

Our density for C₇F₁₆ is larger than the value reported by Oliver, Blumkin and Cunningham,³ 1.71802, which seems to mean a more complete removal of hydrocarbons. Grafstein⁴ has described an effective method of purification by treatment with KOH at 135° that yielded a product of optical density in the ultraviolet close to ours.

The original report on C₆F₁₁CF₃ by Fowler, Hamilton, Kasper, Weker, Burford and Anderson⁵ gives its boiling point as 76.33°, higher than ours by 0.19°.

We wish to thank Professor Joel H. Hildebrand for suggestions on these procedures.

This research has been supported by the U. S. Atomic Energy Commission.

(3) G. D. Oliver, S. Blumkin and C. W. Cunningham, *ibid.*, **73**, 5722 (1951).

(4) D. Grafstein, *Anal. Chem.*, **26**, 523 (1954).

(5) R. D. Fowler, J. M. Hamilton, J. S. Kasper, C. E. Weker, W. B. Burford III, and H. C. Anderson, *Ind. Eng. Chem.*, **39**, 375 (1947).

THE SOLUBILITY AND PARTIAL MOLAL VOLUME OF IODINE IN PERFLUORO-*n*-HEPTANE

BY D. N. GLEW AND J. H. HILDEBRAND

Department of Chemistry and Chemical Engineering, University of California, Berkeley, California

Received November 1, 1955

The solubility of iodine in perfluoro-*n*-heptane has been redetermined with great care between -11.6 and 65° . Its mole fraction is given by the equation: $\log x_2 = -2,246.2/T + 3.7886$. At 25° , $x_2 = (1.799 \pm 0.001) \times 10^{-4}$. For the process I_2 solid to saturated solution, $\Delta H = 10,274$ cal./mole, and $\Delta S = 34.39$ cal./deg. mole. The partial molal volume of iodine in the nearly saturated solution is 100 ml./mole.

The purpose of the present work is to determine the solubility of iodine in *f-n*-heptane accurately over a large temperature range in order to obtain precise values of the thermodynamic functions for the dissolution of solid iodine in *f-n*-heptane.

The need for precise values for these thermodynamic functions is shown in the correlations given by Hildebrand and Glew,¹ where the dilute solutions of iodine in fluorocarbon solvents exhibit the largest deviations from ideality.

The determination of the partial molal volume of iodine in *f-n*-heptane, which is described in the second part of this work, is related to the solubility in an attempt to locate the seat of the deviations from ideality on the basis of volume effects.¹ The solubility of iodine in this solvent is so small that the determinations of both concentration and density had to be made with extraordinary precision. The procedures followed are given below in sufficient detail to establish confidence in the results.

Experimental

The Solubility of Iodine in Perfluoro-*n*-heptane.—The *f-n*-heptane is purified by the method described in detail by Glew and Reeves.² Iodine, twice sublimed, obtained from Baker and from Mallinckrodt, has been used indiscriminately and, showing no difference in solubility, has therefore been used without further purification.

Saturated solutions of iodine in *f-n*-heptane were prepared for all experiments by continuous stirring of the two phase mixture under thermostated conditions for periods of 20 to 60 hours, sometimes starting with unsaturated solvent and other times with solutions that had been saturated at a higher temperature. Replicate experiments showed no difference in the final iodine concentration after 20 hours of continuous stirring.

The continuously stirred saturator, shown in Fig. 1, embodies the principles described by Glew and Robertson³ in their two phase liquid-liquid saturator. The stirring shaft and vanes, mounted on Teflon bearings, is driven by a composite steel-copper armature sealed inside a glass casing at the upper end of the shaft. Constant temperature is maintained by the circulation of water from a large capacity thermostat through the outer jacket of the apparatus and the temperature is measured at the inlet and outlet with a platinum resistance thermometer. The vessel is insulated with glass wool and its temperature is maintained constant to $\pm 0.002^\circ$, with a maximum differential of inlet temperature above that of the outlet of $+0.011^\circ$ at 65° .

After the attainment of saturation the stirrer motor is temporarily stopped and samples are taken from the inner vessel *via* the bottom stopcock.

At temperatures between -10 and $+30^\circ$, saturated samples were run into six, calibrated, glass-stoppered, Beckman quartz cells, and the optical density measured at 25.00° on a Beckman D.U. spectrophotometer at 5200 \AA. , with a

slit width of 0.54 mm. using the hydrogen lamp. Each set of six cells was measured three times; a total of eighteen measurements for one set of readings. Further sets of readings were taken at ten-hour intervals to check the attainment of equilibrium. A final set of readings was taken on the blank cells containing the pure solvent, and the optical density of the dissolved iodine, calculated by difference, corrected to 1.000 cm. path. Optical densities of standard iodine solutions were measured at 25.00° in the same manner, and the iodine in weighed samples of the standard solutions titrated with $N/100$ sodium thiosulfate from a calibrated micro-buret. The calibration curve of optical density against mole fraction of iodine was constructed from the measurement of 234 optical densities and 26 independent titrations of 13 different standard solutions. The mole fraction of iodine in the saturated solution was determined, using the calibration curve.

At temperatures between 30 and 65° , samples of saturated iodine solutions, in duplicate, were withdrawn at ten-hour intervals from the saturator stirring vessel into long-necked glass-stoppered flasks, cooled, weighed and titrated directly with $N/100$ sodium thiosulfate solution.

Experimental Results.—In Table I are presented the experimental values for the solubility of solid iodine in *f-n*-heptane between -11.6 and 65.0° , where T is the absolute temperature in $^\circ\text{K.}$ ($0^\circ\text{C.} = 273.16^\circ\text{K.}$), and x_2 (obsd.) is the experimental saturation mole fraction of iodine. The final column gives x_2 (calcd.), which is the saturation mole fraction of iodine calculated from the equation

$$\log_{10} x_2 = -2,246.2/T + 3.7886 \quad (1)$$

using the experimental temperatures in the Table.

TABLE I
THE SOLUBILITY OF IODINE IN PERFLUORO-*n*-HEPTANE

T , $^\circ\text{K.}$	x_2 (obsd.) $\times 10^4$	x_2 (calcd.) $\times 10^4$	T , $^\circ\text{K.}$	x_2 (obsd.) $\times 10^4$	x_2 (calcd.) $\times 10^4$
261.59	0.1599	0.1592	298.16	...	1.799
263.06	.1776	.1778	303.10	2.370	2.387
268.03	.2535	.2560	308.19	3.146	3.165
273.13	.3599	.3670	313.17	4.145	4.132
278.01	.5078	.5118	318.15	5.360	5.350
282.98	.7154	.7096	323.10	6.890	6.864
288.11	.9929	.9827	328.17	8.679	8.791
293.10	1.360	1.334	333.26	11.19	11.18
298.04	1.826	1.786	338.19	13.90	14.02

Equation 1 has been calculated by the method of least squares from the experimental data. The theory of errors gives a standard error of $\pm 0.93\%$ for any single determination of x_2 (obsd.), and a standard error of ± 0.055 per cent. for x_2 (calcd.) at 298.16°K.

The partial molal heat of solution of iodine, from these data, is $10,274 \pm 5$ cal./mole, and the partial molal entropy is 34.39 cal./deg. mole.

(1) J. H. Hildebrand and D. N. Glew, *THIS JOURNAL*, **60**, 618 (1956).

(2) D. N. Glew and L. W. Reeves, *ibid.*, **60**, 615 (1956).

(3) D. N. Glew and R. E. Robertson, *ibid.*, **60**, in press (1956).

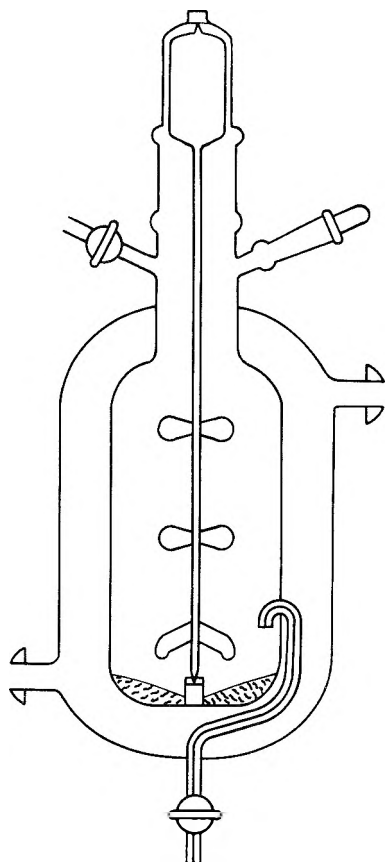


Fig. 1.—The saturator.

Experimental

Partial Molal Volume of Iodine in Perfluoro-*n*-heptane.—

The density of *n*-heptane and its iodine solutions was measured at 25° using a graduated double stem pyknometer, shown in Fig. 2.

The pyknometer is maintained at constant temperature, measured by a platinum resistance thermometer, in the interior of the double surface Pyrex vessel, through which water from a large thermostat is pumped. The interior of the Pyrex vessel is partly filled with water to provide good thermal contact between the thermometer and the pyknometer.

The pyknometer and stem graduations on the precision bore tubing are calibrated at 25.000° by weighing equilibrium conductivity water and measuring the heights of the two menisci against the stem graduations with a cathetometer. The volume is calculated from the density of water,⁴ allowing for the buoyancy of air. Eight independent weighings, of different quantities of water covering the whole range of the stem graduations, using calibrated weights established the pyknometer volume equation.

The density of the solvent and solution was measured in the same manner, using the same volume equation. Since *n*-heptane has a large coefficient of expansion, it was found more accurate to heat the pyknometer slowly from 24.998 to 25.002° and then cool slowly to 24.998°, taking corresponding sum of the two stem readings and temperature readings rather than to attempt to maintain temperatures for a long period. From the hysteresis curve obtained by plotting the stem readings against temperature the true temperature for each stem reading can be accurately estimated and a corresponding density value.

Table II shows the results obtained for a typical experiment, in this case, for an iodine solution in *n*-heptane containing a mole fraction $x_2 = 0.0001785$ of iodine.

The first two columns present corresponding temperatures and densities obtained from the

(4) N. E. Dorsey, "Properties of the Ordinary Water Substance." A.C.S. Monograph, Reinhold Publ. Corp., New York, N. Y., 1940.

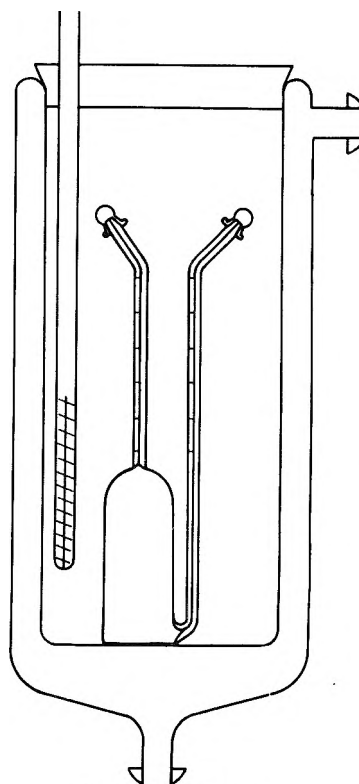


Fig. 2.—Pyknometer.

hysteresis curve. The final column gives the values of the density at 25.000°, calculated from the second column using the equation

$$D_{25} = D_t + 0.002765(t - 25) \quad (2)$$

obtained from the work of Oliver, Blumkin and Cunningham.⁵ The constancy of the values for the density at 25.000° serves to show the elimination of systematic temperature errors due to thermometer lag.

TABLE II

TEMPERATURE VARIATION OF DENSITY: IODINE SOLUTION

t (obsd.), °C.	D_t (obsd.), (g./ml.)	$D_{25.000}$ (cor.) (g./ml.)
25.0002	1.7201245	1.7201251
24.9998	1.7201253	1.7201248
24.9993	1.7201261	1.7201242
24.9990	1.7201268	1.7201240
24.9987	1.7201275	1.7201240
		1.7201244

The mole fraction of iodine in a saturated solution with *n*-heptane at 25° is small and the density change due to the presence is small; in order to eliminate systematic errors on the small density difference, two samples of *n*-heptane were purified and two series of experiments conducted on the pure liquids and their respective iodine solutions. In each series the density of the solvent, D_1 , was measured and the corresponding density, D_2 , of the iodine solution in that solvent: the iodine in solution was estimated by direct titration of

(5) G. D. Oliver, S. Blumkin and C. W. Cunningham, *J. Am. Chem. Soc.*, **73**, 5722 (1951).

weighed samples of solution with $N/100$ sodium thiosulfate.

Table III shows the density measurements obtained in the two series of experiments at 25.000°. The molecular weights are 388.069 and 253.820, and x_1 and x_2 are the mole fractions of perfluoro- n -heptane and iodine, respectively, in the solutions, the numbers in parentheses show the number of independent determinations made.

TABLE III
PARTIAL MOLAL VOLUME OF IODINE IN
PERFLUORO- n -HEPTANE AT 25°

	Series I	Series II
D_1 (g./ml.)	1.720059 (3)	1.720033 (2)
D_2 (g./ml.)	1.720124 (4)	1.720098 (2)
x_1	0.9998215	0.9998195
x_2	0.0001785 (4)	0.0001805 (2)
\bar{v}_2 (ml.)	99.8 ± 6.0	100.3 ± 2.6

\bar{v}_2 is the partial molal volume of iodine, calculated from the equation

$$\bar{v}_2 = \frac{x_1}{x_2} M_1 \frac{(D_1 - D_2)}{D_1 D_2} + \frac{M_2}{D_2}$$

which assumes that the partial molal volume of f - n -heptane in the solution is identical with its molal volume. Errors in \bar{v}_2 are assessed from the errors in $(D_1 - D_2)$, which in either series are due to weighing errors only.

This value of \bar{v}_2 , at practically $x_2 = 0$, is so amazingly greater than the (extrapolated) molal volume of the liquid, 59.0 cc., and of the solid, 51.4 cc., that L. W. Reeves, of our group, determined, as a check, the partial molal volume of bromine in the same solvent, where larger solubility yields easily measurable differences in density. He found, of course, a smaller but still large expansion, from 51.5 to 72 cc. This lends confidence in the value for iodine, $\bar{v}_2 - v_2^0 = 100 - 59 = 41$ cc. This will be reported in detail in a later paper.

The support of this work by the Atomic Energy Commission is gratefully acknowledged.

THE ENTROPY OF SOLUTION OF IODINE

BY J. H. HILDEBRAND AND D. N. GLEW

Department of Chemistry and Chemical Engineering, University of California, Berkeley, California

Received November 1, 1955

The entropy of solution of a solid can be determined from the change of solubility with temperature by the equation $\bar{S}_2 - S_2^s = R \left(\frac{\partial \ln a_2}{\partial \ln x_2} \right)_T \left(\frac{\partial \ln x_2}{\partial \ln T} \right)_{\text{sat}}$. A plot of $R(\partial \log x_2 / \partial \log T)_{\text{sat}}$ vs. $-\log x_2$ for iodine solutions at 25° shows all the points for violet regular solutions on a single straight line, and those for irregular solutions below it. This constitutes a sensitive test. The line is higher and steeper than the theoretical line for ideal solutions. The displacement is explained by three factors, a departure from Henry's law, the entropy of mixing at constant volume molecules of different size, and the entropy of expansion. The latter two are very large in the solution in n - f -heptane.

The senior author in 1952 showed¹ that the solubilities of solid iodine in a number of its violet solutions yield straight lines at mole fractions below about 0.1 when they are plotted as the logarithm of mole fraction, x_2 , vs. the logarithm of the absolute temperature, and he explained why this was to be expected in view of known trends in the enthalpies of fusion and dilution. Hildebrand and Scott² used the accurate values of $(\partial \ln x_2 / \partial \ln T)_{\text{sat}}$ yielded by aid of its linearity to calculate the entropy of transfer of solute from solid to saturated solution by the purely thermodynamic relation

$$\bar{S}_2 - S_2^s = R \left(\frac{\partial \ln a_2}{\partial \ln x_2} \right)_T \left(\frac{\partial \ln x_2}{\partial \ln T} \right)_{\text{sat}} \quad (1)$$

The values of $\partial \ln a_2 / \partial \ln x_2$ are unity for an ideal solution and approach unity with increasing dilution for regular solutions. The departure from unity can be adequately estimated for regular solutions by aid of the equation³

$$\ln a_2 = \ln x_2 + \phi_2^2 v_2 (\delta_2 - \delta_1)^2 / RT \quad (2)$$

The ϕ 's are volume fractions and the δ 's are solubility parameters.

The values in Table I for solutions of iodine at 25° are illustrative ($v_2 = 59.0$ cc.).

(1) J. H. Hildebrand, *J. Chem. Phys.*, **20**, 190 (1952).

(2) J. H. Hildebrand and R. L. Scott, *ibid.*, **20**, 1520 (1952).

(3) J. H. Hildebrand and R. L. Scott, "Solubility of Nonelectrolytes," Reinhold Publ. Corp., New York, N. Y., 1950.

TABLE I
IODINE SOLUTIONS AT 25°

	$100x_2$	v_1 , cc.	$\delta_2 - \delta_1$	$\left(\frac{\partial \ln a_2}{\partial \ln x_2} \right)_T$
CS ₂	5.58	60.6	4.1	0.81
CCl ₄	1.147	97.1	5.5	.96
C ₇ H ₁₆	0.679	147.5	6.7	.98
SiCl ₄	.499	115.3	6.5	.98
C ₇ F ₁₆	.018	225.0	8.4	.998

Table II gives values⁴ of $-\log x_2$ at 25° and of $R(d \log x_2) / (d \log T)$ for iodine in many solutions, both brown and violet. These are plotted in Fig. 1. The values for the latter quantity represent the slopes of the straight lines drawn through the points⁴ on a plot of $\log x_2$ vs. $\log T$. The sources of the experimental values are given in reference 3, except for the f -heptane solution, reported in the accompanying paper.

The accuracy with which $d \log x_2 / d \log T$ can be fixed depends, of course, upon the accuracy of the data and upon the range in temperature. Where both are adequate, the linearity of the relation is remarkable, as illustrated by agreement within successive temperature intervals, as shown in Table III, calculated from unsmoothed experimental points.

(4) J. H. Hildebrand, H. A. Benesi and L. M. Mower, *J. Am. Chem. Soc.*, **72**, 1017 (1950).

TABLE II
SOLUBILITY OF IODINE AT 25° AND ITS CHANGE WITH TEMPERATURE

	Solvent	$-\log x_2$	$R \frac{d \log x_2}{d \log T}$
1	<i>n</i> -C ₇ F ₁₆	3.745	34.4
2	(CH ₃) ₃ CC ₂ H ₅	2.328	23.6
3	SiCl ₄	2.302	23.8
4	<i>i</i> -C ₈ H ₁₈	2.270	23.3
5	<i>n</i> -C ₇ H ₁₆	2.168	23.1
6	cyclo-C ₆ H ₁₂	2.037	22.2
7	CCl ₄	1.940	21.9
8	<i>trans</i> -C ₂ H ₂ Cl ₂	1.849	20.7
9	<i>cis</i> -C ₂ H ₂ Cl ₂	1.841	20.9
10	1,1-C ₂ H ₄ Cl ₂	1.815	19.5
11	1,2-C ₂ H ₄ Cl ₂	1.658	19.5
12	TiCl ₄	1.687	20.7
13	CHCl ₃	1.642	20.3
14	CS ₂	1.253	18.8
15	C ₆ H ₆	1.319	16.3
16	<i>p</i> -C ₆ H ₄ (CH ₃) ₂	1.115	13.2
17	<i>s</i> -C ₆ H ₃ (CH ₃) ₃	0.930	11.9
18	1,2-C ₂ H ₄ Br ₂	1.107	15.9
19	C ₂ H ₅ OH	1.327	7.4
20	(C ₂ H ₅) ₂ O	1.047	7.0
21	Glycerol	2.55	16.7
22	H ₂ O	4.62	18.7
A	None	0	8.0
B	Ideal	0.565	10.6

TABLE III

Interval	$\Delta \log x_2 / \Delta \log T$ FOR I ₂		
	CS ₂	CCl ₄	<i>n</i> -C ₇ H ₁₆
0-25°	9.45	...	11.6
0-35°	...	11.08	...
25-35°	9.50	...	11.7
35-50°	...	11.00	11.2

The point for the solubility in C₇F₁₆ is so important for our purpose that it has been redetermined with great care, over a temperature range sufficient to permit the entropy of solution to be accurately fixed.⁵

Figure 1 reveals several interesting relations. First, the points for nearly all the pure violet solutions fall, within the limits of error, upon a straight line, while those for the red and brown solutions fall well below it. Such divergence evidently constitutes a sensitive test of non-conformity to the regular solution model, in agreement with the ultraviolet absorption spectra discovered by Benesi and Hildebrand⁶ of iodine in aromatic solvents. The points for the dichloroethanes and dichloroethylenes and for ethylene bromide are below the line by distances that exceed experimental uncertainty sufficiently to suggest the existence of complexes, therefore we investigated their spectra and found unmistakable evidence of interaction, which will be reported later.

The value of the ordinate when $\log x_2 = 0$ is the entropy of fusion of iodine at 25°. This was calculated by the appropriate thermodynamic equations from the measurements by Frederick and Hildebrand⁷ of the heat of fusion and the heat

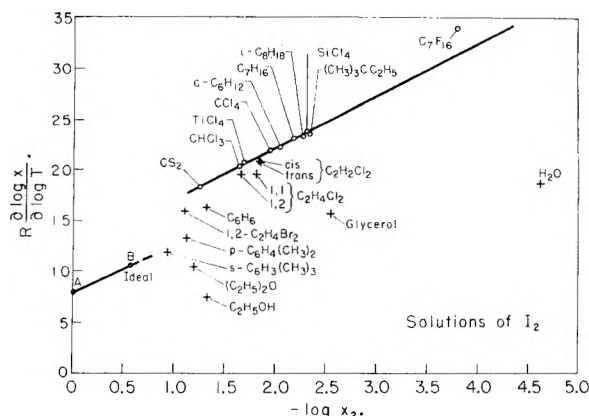


Fig. 1.—Iodine solutions at 25°.

capacities of solid and liquid iodine. Assuming that the constant heat capacity found for the liquid above the melting point persists down to 25°, one obtains for the entropy of fusion at that temperature $S_2^0 - S_2^s = 8.02$. The activity of liquid iodine at this temperature is 0.272, and this would be its mole fraction in an ideal solution. The value of $R(\partial \ln a_2^s / \partial \ln T)$ of an ideal solution is 10.61. Point A in Fig. 1 represents the value of $S_2^0 - S_2^s$ when $x_2 = 1.00$, and point B the value of $S_2 - S_2^0$, 10.6 for an ideal solution, for which $x_2 = 0.272$. The slope of the line, AB, corresponds to the entropy of dilution of an ideal solution, $-R \ln (x_2^1/x_2)$. It will be seen that the points for violet solutions lie on a line that is considerably higher and that has a somewhat greater slope.

There are three factors that may contribute to the difference between these two lines, apart from the uncertainty of the entropy of fusion. One is the departure from unity of the factor $\partial \ln a_2 / \partial \ln x_2$. Another arises from the unequal molal volumes of solvent and solute. The Flory-Huggins expression for the partial molal entropy involved in transferring liquid iodine to a solution in which its volume fraction is ϕ_2 is $-R[\ln \phi_2 + \phi_1(1 - v_2v_1^{-1})]$. This was derived, however, for an athermal solution with no volume changes. In a derivation recently reported⁸ an expression was first obtained in terms of free volumes, reducing to the above form if free volumes are set proportional to partial molal volumes and to molal volumes. The primary expression, if correct, should take care of expansion; because of uncertainty about free volumes we will assume that the above expression would give the entropy of mixing only at constant volume, and use an added term to care for expansion. The value of what we will call the uncorrected "F-H entropy" of iodine in *n*-heptane is 18.3 e.u. The "ideal" entropy for this dilution is 17.1 e.u. The entropy of this expansion may be calculated by aid of the equation $(\partial S / \partial v)_T = (\partial p / \partial T)_v$, giving $\Delta S(\text{expan.}) = (v_2 - v_2^0)(\partial p / \partial T)_v$. The expansion⁹ of 0.041 l. supposed to occur in 1250 l. of C₇F₁₆, is so small that the equation need not be integrated. The value of $\partial p / \partial T$ for C₇F₁₆ is 6.75 atm. deg.⁻¹ as directly measured by our group.⁹ If the $1/x_2$

(5) See accompanying paper, THIS JOURNAL, 60, 616 (1956).

(6) H. A. Benesi and J. H. Hildebrand, J. Am. Chem. Soc., 70, 2382 (1948); 71, 2703 (1949).

(7) K. J. Frederick and J. H. Hildebrand, *ibid.*, 60, 1436 (1938).

(8) J. H. Hildebrand, J. Chem. Phys., 18, 225 (1947).

(9) B. J. Alder, E. W. Haycock, J. H. Hildebrand, and H. Watts, J. Chem. Phys., 22, 1060 (1954).

moles of solvent are expanded by 41 cc. and the (liquid) I_2 then dissolved in it, the contribution of the expansion to the entropy would be 6.7 cal. deg.⁻¹. This agrees remarkably well with the value 6.9 calculated earlier by Hildebrand and Scott.² The sum of the entropy of fusion, expansion and dilution to $x_2 = 1.80 \times 10^{-4}$ is thus $8.0 + 6.7 + 18.3 = 33.0$ e.u. The experimental

value is 34.4 e.u. The difference, 1.4 e.u., must represent mainly the shortcoming of the simple F-H equation with respect to this system. We postpone a more detailed consideration of the matter pending completion of the study of the bromine-*i*-heptane system.

The support of the Atomic Energy Commission is gratefully acknowledged.

TRANSPORT NUMBER MEASUREMENTS IN PURE FUSED SALTS

BY H. BLOOM AND N. J. DOULL

Department of Chemistry, Auckland University College, Auckland, New Zealand

Received November 2, 1955

In all previous attempts to determine transport numbers in molten salts, the gravitational flow of melt in the reverse direction to that produced by the flow of electricity, has introduced large errors which have never been completely overcome by the insertion of narrow tubes or sintered disks between the anode and cathode compartments. In the present work, gravitational flow has been eliminated completely by the use of an accurately horizontal transport cell. The transport numbers of the chloride ion in molten lead chloride and cadmium chloride have been determined by measuring the movement of electrolyte in a capillary tube during the passage of a known quantity of electricity. The values of the measured transport number are $PbCl_2$, $t^- = 0.393 \pm 0.01$ (527–529°), $t^- = 0.382 \pm 0.01$ (602–608°); $CdCl_2$, $t^- = 0.340 \pm 0.007$ (602–608°). These values indicate that previous assumptions that these salts are predominantly anion conductors were incorrect. No evidence has been found for the presence of autocomplexes in these salts.

Comparison of the electrical conductivities of molten salts has led to the assumption that conduction in the molten alkali halides is predominantly cationic but the conduction process in the alkaline earths together with those of lead and cadmium is mainly anionic.^{1,2} To verify such assumptions determinations of transport numbers in pure fused salts are necessary.

For molten salts such measurements have not, in the past, yielded reliable results because, as Duke and Laity^{3,4} have pointed out, the transfer of electrolyte by the passage of current in a Hittorf type apparatus builds up a hydrostatic pressure which tends to nullify the electrolytic movement of the melt. Previous workers have attempted to counteract this gravitational flow by inserting a deterrent to such flow between the anode and cathode compartments. These devices, such as sintered glass disks or narrow capillary tubes, will slow down but do not prevent the gravitational movement of the melt.

Lorenz and Fausti⁵ attempted to determine the transport number of chloride ion in fused mixtures of lead chloride and potassium chloride. Two small porous cells immersed in the fused salt mixture formed the anode and cathode compartments, respectively. The measurements were carried out at about 800° and were inconclusive. Wirths⁶ used cells separated into three compartments by sintered disks for the investigation of lead chloride and added lead chloride containing radioactive lead (Th B) to the center compartment so as to permit radiochemical analysis. Temperature fluctuations and gravitational flow in the reverse

direction made the transport measurements inconclusive. Baimakov and Samusenko⁷ also used a Hittorf type apparatus for investigation of lead chloride but without success. Karpachev and Pal'guev⁸ used a similar method to investigate lead chloride but obtained results of poor reproducibility. Duke and Laity^{3,4} modified the usual Hittorf method. Their Pyrex glass transport cell consisted of two compartments separated by a sintered glass disk and joined above the disk by a capillary. Two lead pools at the bottom of the compartments formed the electrodes and the apparatus was filled so as to leave an air bubble in the capillary. To carry out a run, the air bubble was displaced by adding a weighed amount of powdered lead chloride to one compartment and electrolysis was carried out until the bubble returned to its original position, the quantity of electricity being measured. In this method the error due to gravitational flow of electrolyte in the opposite direction to that of electrolysis was not eliminated. This will be discussed below. There also have been attempts to investigate other salts.^{9,10}

The present research project was planned so as to eliminate errors due to gravitational flow of the melt in the direction opposite to that of the electrolysis.

Experimental

Materials.—These were all of analytical reagent purity.

Lead Chloride was prepared by precipitation from analytical reagent lead nitrate solution by analytical reagent hydrochloric acid. The product was filtered and evaporated to dryness several times with hydrochloric acid to remove any traces of nitrate.

- (1) E. Heymann and H. Bloom, *Nature*, **156**, 479 (1945).
- (2) H. Bloom and E. Heymann, *Proc. Roy. Soc. (London)*, **188A**, 392 (1947).
- (3) F. R. Duke and R. W. Laity, *J. Am. Chem. Soc.*, **76**, 4096 (1954).
- (4) F. R. Duke and R. W. Laity, *THIS JOURNAL*, **59**, 549 (1955).
- (5) R. Lorenz and G. Fausti, *Z. Elektrochem.*, **10**, 630 (1904).
- (6) G. Wirths, *ibid.*, **43**, 486 (1937).

- (7) Yu. V. Baimakov and S. P. Samusenko, *Trans. Leningrad Ind. Inst.* (1938), No. 1, Sect. Met. No. 1, 3–26.
- (8) S. Karpachev and S. Pal'guev, *Zhur. Fiz. Khim.*, **23**, 942 (1949).
- (9) K. E. Schwarz, *Z. Elektrochem.*, **47**, 144 (1941).
- (10) P. M. Aziz and F. E. W. Wetmore, *Canadian J. Chem.*, **30**, 779 (1952).

Cadmium Chloride was prepared by direct chlorination of molten cadmium, purity 99.99%, which was supplied by Electrolytic Zinc Co. of Australia.

Apparatus.—The transport cell was constructed of transparent silica. Pyrex was first tried but was abandoned because of deformation above 560° (553° is given as the annealing temperature of Pyrex¹¹). The cell consisted of two compartments (internal diameter 6 mm., length of each 1 cm.) separated by a sintered silica disk. Disks of various porosities from 2 (medium) to 4 (fine) were used in different runs without any systematic variation of results. Each compartment terminated in a capillary of length 10 cm. and bore 0.5 to 1.0 mm. These capillaries were calibrated and checked for uniformity by weighing with mercury inside. Tungsten wires of diameter 0.01 inch were introduced into the capillaries to carry the electrolysis current to the molten metal electrodes.

A transparent silica tube wound with nichrome V wire (8 turns per inch) formed the heating element. This element was mounted in an insulating case containing slits through which its contents could be viewed. By focusing a light source and cathetometer telescope on the boundary between molten salt and molten metal in the capillary, its movement during electrolysis could be measured. Temperature was measured by means of a chromel–alumel thermocouple in contact with the transport cell and a Leeds and Northrup type K2 potentiometer. Temperature was controlled by a variable voltage transformer and did not vary more than 0.5° during a run. The current source was carefully stabilized,¹² the current being measured by determination of potential drop across a standard resistance in the circuit, by means of the potentiometer.

The furnace was mounted so that it could be rotated in the vertical plane perpendicular to its axis. This allowed the transport cell to be filled in a vertical position, then rotated to a horizontal position to carry out the run.

Experimental Procedure.—To fill the transport cell, the empty cell with tungsten wires removed was attached at one end to a vacuum system and the cell was heated in the vertical furnace. Lead chloride melt was drawn into the bulk of the cell and then a small quantity of lead to form one of the electrodes. When the furnace was made horizontal the tungsten wires were introduced into the capillaries—one into the molten lead and the other into the lead chloride. The latter was made the cathode so that after a preliminary electrolysis this wire also became surrounded by molten lead. The current was then stopped and any movement of the boundary between lead and lead chloride noted. Levelling adjustments of the furnace were made until there was no gravitational movement of the boundary in 1 hour.

To carry out a determination of transport number, current was passed at 10 ma. and the rate of movement of the anolyte boundary measured over a time interval of 1–2 hours.

Results and Discussion

According to Duke and Laity^{3,4} the transport number of the chloride ion is equal to the fraction of an equivalent of salt transferred from catholyte to anolyte during the passage of one faraday of electricity. The transport number of the anion is thus given by the equation

$$t_- = \frac{2 \times 96500 Vd}{qM}$$

where

- V = increase in vol. of molten salt in the anode compartment
 q = no. of coulombs of electricity passed
 d = density of salt
 M = molecular weight of salt

Similar experiments were conducted to determine the anion transport number in cadmium chloride with molten cadmium electrodes.

(11) C. J. Phillips, "Glass—The Miracle Maker," Pitman, New York, 1941.

(12) M. Spiro and H. N. Parton, *Trans. Faraday Soc.*, **48**, 263 (1952).

	Temp. range, °C.	Transport no.
PbCl ₂	527–529	$t_- = 0.393 \pm 0.01$
	602–608	$t_- = 0.382 \pm 0.01$
CdCl ₂	602–608	$t_- = 0.340 \pm 0.007$

The determinations were not sufficiently accurate to decide whether there is a real variation of transport number with change of temperature.

It is clear however that the cations in molten PbCl₂ and CdCl₂ carry relatively more of the current than the anions. This is in agreement with the postulate by Bloom and Heymann² that the smaller ion will be expected to carry most of the current. These authors however further stated that PbCl₂ and CdCl₂ may be expected to be anion conductors because they are anion conductors in the solid state and the conductivity of molten lead and cadmium halides changes considerably with change of anion.

It can also be seen that autocomplex formation, involving the presence of lead and cadmium in the form of large complex anions, *e.g.*, PbCl₆⁴⁻, is ruled out by the results obtained. If autocomplexes were present in appreciable concentration the transport number of the cation would be very low or even negative.

Considering the relative magnitude of the t_+ values of PbCl₂ and CdCl₂ (where $t_+ = 1 - t_-$)

it can be seen that $\frac{t_+ \text{PbCl}_2}{t_+ \text{CdCl}_2} = 0.94$ which is approxi-

mately equal to $\frac{\Lambda_{\text{PbCl}_2}}{\Lambda_{\text{CdCl}_2}}$ at corresponding temperatures (10% in degrees absolute above the melting point²)— Λ refers to equivalent conductivity. This would be anticipated as we are comparing salts with common anion, hence the ratio of their conductances should be equal to the ratio of the cation mobilities.

The results for anion transport number in lead chloride do not agree with those obtained by Karpachev and Pal'guev or Duke and Laity, who obtained the value of $t_- = 0.75$. The latter authors criticized the work of Karpachev and Pal'guev even though their results agreed with those of the Russian workers. Duke and Laity's method does not overcome the problem of gravitational flow through the sintered disk in the opposite direction to that of electrolysis. These authors reduced the hydrostatic head causing this flow to very small values but in doing so they measured a correspondingly small movement of electrolyte. The net error due to gravitational flow therefore remains the same. To overcome the problem of gravitational flow Duke and Laity recommend the use of "ultrafine" disks—coarse disks did not give them any meaningful results. In the present work there is no gravitational flow as the apparatus was carefully levelled before each run, the porous disk being present merely to enable the detection of the movement of electrolyte relative to the bulk of the melt.

Other criticisms which apply to the experiments of Duke and Laity are as follows: (1) Pyrex glass at 565°, *i.e.*, slightly above its annealing temperature (553°) is likely to be slightly plastic and the relatively bulky apparatus may be subject to deformation at this temperature. (2) The temperature was "not too carefully controlled" which may

introduce errors due to thermal expansion both of the melt (if the apparatus is not perfectly symmetrical) and the air bubble. (3) The electrolysis currents used by Duke and Laity (up to 0.5 amp.) cause considerable local heating of the disk.

The present authors agree with Duke and Laity that the disk does not introduce errors due to electroosmosis. In the present investigation volt-

ages varying from 0.2 to 6 volts were applied across the transport cell without any systematic variation of the measured transport number.

The authors are pleased to acknowledge assistance from the University of New Zealand Research Fund for the purchase of the apparatus, and the many helpful discussions with N. E. Richards and J. Barton.

MEASUREMENT OF OPTICAL ABSORBANCY OF $\text{TiCl}_4(\text{g})$ IN THE ULTRAVIOLET REGION¹

BY DAVID M. MASON² AND STEPHEN P. VANGO

Jet Propulsion Laboratory, California Institute of Technology, Pasadena, Calif.

Received November 4, 1955

The optical absorbancy of gaseous TiCl_4 was measured at 25° at wave lengths from 240 to 360 $\text{m}\mu$. A maximum in absorbancy occurs at 280 $\text{m}\mu$ where the molar absorbancy index was found to be 7.29×10^3 liter/mole cm. The partial pressure of $\text{TiCl}_4(\text{g})$ in the equilibrium $2\text{TiCl}_3(\text{s}) \rightleftharpoons \text{TiCl}_4(\text{g}) + \text{TiCl}_2(\text{s})$ was measured by optical absorbancy and found to be about 1 mm. at 475°. By successively removing TiCl_4 and measuring the optical absorbancy of the system, solid solution of TiCl_2 in TiCl_3 was shown to be non-existent in this equilibrium.

I. Introduction

Few data are available on the absorption spec-

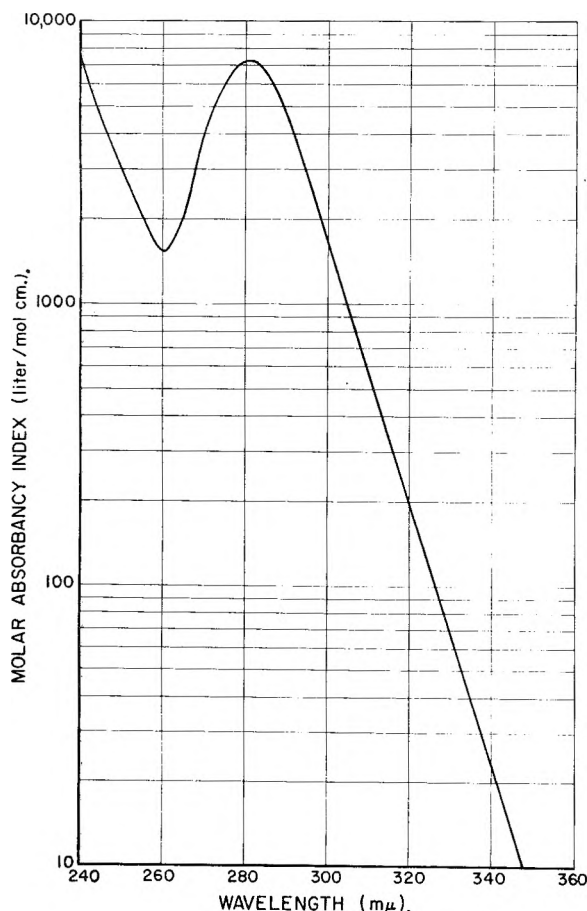


Fig. 1.—Optical absorbancy of $\text{TiCl}_4(\text{g})$.

(1) This paper presents the results of one phase of research carried out at the Jet Propulsion Laboratory, California Institute of Technology, sponsored by the Department of the Army, Ordnance Corps, and the Department of the Navy, Office of Naval Research, under Contract No. DA-04-495-ORD 18.

trum of gaseous TiCl_4 in the ultraviolet range.³ Such data were obtained to supplement kinetic and thermodynamic studies involving TiCl_4 , particularly the equilibrium of disproportionation of $\text{TiCl}_3(\text{s})$. In measurement of this equilibrium using the Knudsen effusion method,^{4,5} initially high partial pressures of $\text{TiCl}_4(\text{g})$ were obtained which leveled out at a lower value as the measurement progressed. This behavior suggested solid solution of $\text{TiCl}_2(\text{s})$ in $\text{TiCl}_3(\text{s})$ causing initially low activity of $\text{TiCl}_2(\text{s})$ and therefore high TiCl_4 pressure. This behavior was studied in an isochoric system using absorbancy to measure equilibrium pressures of TiCl_4 . The absorbancy of $\text{TiCl}_4(\text{g})$ was first measured as a function of wave length for use with these other physicochemical measurements.

II. Experimental

The absorbance measurements were made with a Beckman Model DU spectrophotometer using quartz cells either 1 cm. or 5 cm. in depth. A vertical quartz stem, which was bent over and sealed to a bulb, was attached to the cell. The bulb was kept in a constant-temperature liquid bath outside the spectrophotometer. This bulb was partially filled with $\text{TiCl}_4(\text{l})$ of 99.999% purity provided by the National Bureau of Standards. The TiCl_4 was frozen by immersing the bulb in liquid nitrogen, and the glass system was then evacuated and sealed. The cell temperature was maintained to within $\pm 0.1^\circ$ by controlling a special air bath surrounding the spectrophotometer cell holder. Most of the measurements were made with the cell at around 25°, although several measurements were made at 50° to check possible deviations from Beer's law. The concentration of $\text{TiCl}_4(\text{g})$ was varied by varying the temperature of the liquid TiCl_4 in the temperature range 0 to 8°. The molar absorbancy index was calculated from the measured absorbance together with vapor pressure data for TiCl_4 .⁶

(2) Department of Chemistry and Chemical Engineering, Stanford University, Stanford, California.

(3) Y. Hukumoto, *Sci. Repts. Tôhoku Imp. Univ.*, [I] **22**, 868 (1933).

(4) M. Farber and A. J. Darnell, to be published.

(5) G. E. MacWood and B. S. Sanderson III, "Disproportionation Equilibrium of Titanium Trichloride," Technical Report No. 4, Contract NR 037-024. Columbus, Ohio, Ohio State University Research Foundation, 1955.

(6) K. K. Kelley, "The Free Energies of Vaporization and Vapor Pressures of Inorganic Substance," Bureau of Mines, Bulletin No. 383, 1935.

III. Results and Discussion

Smoothed values of the molar absorptancy index of TiCl_4 vapor are shown as a function of wave length in Fig. 1 and Table I. A maximum in the absorptancy index is evident at 280 $m\mu$.

TABLE I

MOLAR ABSORPTANCY INDEX A_m OF TiCl_4 VAPOR			
Wave length (m μ)	A_m (l./mole cm.)	Wave length (m μ)	A_m (l./mole cm.)
240	7190	290	4970
250	2920	300	1880
260	1540	320	190
270	4100	340	32
280	7290	360	0

To check the possibility of solid solution of TiCl_2 (s) in TiCl_3 (s), high-purity TiCl_3 (s) prepared by the modified method of Schumb⁷ was sealed in an evacuated optical cell and the absorbance measured as a function of time at 100°. It was found that apparent equilibrium was attained in about 160 hours, at which time the partial pressure was about

(7) W. F. Krieve and D. M. Mason, to be published.

0.6 mm. This pressure is much greater than that indicated by effusion experiments of Farber and Darnell⁴ where an extrapolated pressure of less than a micron is indicated at this temperature. The possibility of solid solution causing this effect was tested by evacuating and re-establishing equilibrium several times, a lower partial pressure of TiCl_4 occurring after each evacuation. The equilibrium pressure in the cell was found to decrease linearly with the accumulated total number of moles of TiCl_4 (g) removed during the equilibrium measurements. This behavior is inconsistent with solid-solution formation where it would be expected that the equilibrium pressure would be inversely proportional to the number of moles of TiCl_4 formed. It thus appears that TiCl_4 (g) adsorbed on the TiCl_3 during its preparation accounts for the initially high TiCl_4 pressure and that solid solution between TiCl_3 (s) and TiCl_4 (s) does not occur to any measurable extent.

A measurement of the equilibrium partial pressure of TiCl_4 at 475° over TiCl_3 (s) with all adsorbed TiCl_4 first removed gives a value of about 0.7 mm. which agrees with the corresponding value of 0.4 mm. determined by the effusion method.⁴

ULTRACENTRIFUGAL CHARACTERIZATION BY DIRECT MEASUREMENT OF ACTIVITY. I. THEORETICAL

BY DAVID A. YPHANTIS¹ AND DAVID F. WAUGH²

Department of Biology, Massachusetts Institute of Technology, Cambridge, Massachusetts

Received November 7, 1955

Sedimentation or sedimentation and diffusion coefficients may be determined from Q , the ratio to the original concentration of the average concentration centripetal to a chosen separation position in the cell. When the separation position is in a plateau region of concentration, diffusion may be neglected. Simple equations then lead to sedimentation coefficients. If diffusion cannot be neglected, the treatment requires theoretical values of Q which are functions of the cell parameters (meniscus, base and separation position), $\tau = 2\omega^2st$ and $\sigma = \omega^2s/D$. Exact calculations of transient solute distributions for specific instances have been given previously.⁵ Greater flexibility with respect to cell parameters has been obtained through the development of suitable approximations. One of these assumes the cell to be rectangular and in a uniform field and gives the point by point distribution to within 0.03 for $\sigma = 0.467$ and values of Q to an average error of <0.01 for $\sigma = 0.467, 0.933$ and 1.399 (at 60,000 r.p.m. mol. wt. = 1000, 2000 and 3000). Two other rapid approximations have been developed which give values of Q : an exponential approximation useful for $\sigma \leq 0.467$ or for near equilibrium centrifugation times and a "diffusion deviation" approximation useful for initial and intermediate centrifugation times. The effects of sedimentation and diffusion during deceleration have been examined as well as the effects of dispersity.

We treat here the theoretical aspects of a technique by which physical information concerning an active principle may be obtained by ultracentrifugal studies of impure fractions. In addition to the information itself, there arise advantages in devising new fractionation procedures and in estimating maximum specific activity. It should be recognized that at early stages of purification, the relative concentration of the active material may preclude observations by any current physical technique; thus the technique employed should be based on assay of biological or chemical activity.

(1) (a) Taken in part from a dissertation presented by David A. Yphantis to the Faculty of the Department of Biology, the Massachusetts Institute of Technology, in partial fulfillment of the requirements for the degree of Doctor of Philosophy, May, 1955. (b) Currently a Fellow of the American Cancer Society at the Massachusetts Institute of Technology.

(2) Our appreciation is expressed to the Armour Laboratories and to the Research Division of Armour and Company, Chicago, for their support of this research.

In recent years an increasing number of biologically active molecules have been found to be of low molecular weight although in many instances even the most active early preparations appeared to be homogeneous populations of large molecules. The molecular weight range in which are found materials such as vitamin B₁₂, oxytocin, ACTH, cortisone, penicillin, etc. (*i.e.*, the range from 500–5000) has been particularly difficult to handle from the physico-chemical standpoint, even when pure preparations were available. At the start of the investigations discussed here there was clearly recognized a need for a technique which would handle, on the basis of biological activity or other assayable property, pure or impure systems of low or high molecular weight and, in addition, a technique which would operate at very low concentrations.

The basis of the technique, the physical aspects

of which are described in the following publication, lies in the fact that if, under known conditions of centrifugation, one can determine the average activity centripetal or centrifugal to a given plane of separation in the centrifuge cell, it is possible to determine the sedimentation coefficient, the diffusion coefficient and other physical information. Where the active principle has some unique chemical property it is possible to study the distribution of this property. The amount of information which can be obtained is essentially dependent on the accuracy of the chemical or biological assay.

Solute distributions may be divided into overlapping areas involving large and small molecules, the latter requiring a more extensive analysis. This differentiation is based on the fact that during ultracentrifugation, a high molecular weight substance exhibits a boundary. By virtue of relatively slow diffusion this boundary gives a distinct refractive index gradient maximum (schlieren peak) whose rate of motion is generally used to determine sedimentation coefficients. Centrifugal to this boundary there is a plateau region where concentration is independent of position. On the other hand, a low molecular weight solute exhibits no such boundary and the plateau region, although initially present, soon disappears as a result of rapid diffusion. Such low molecular weight substances generally have a reduced molecular weight, $M(1 - \bar{V}_\rho)$, below 3000. For proteinaceous materials this corresponds to molecular weights below 10,000.

High Molecular Weight Solutes.—For solutes of high molecular weight the concentrations centripetal (and centrifugal) to a chosen plane of separation (separation plate rest position, *i.e.*, r_p) can readily yield the sedimentation coefficients, provided the boundary does not overlap the separation plate rest position, *i.e.*, provided the separation plate rest position lies in the plateau region. Considerations of solute transport (see 3) show that under this condition $Q(t)$, the average fractional supernatant concentration at time t , is given by

$$Q(t) = \frac{\int_a^{r_p} c(r,t)r dr}{\int_a^{r_p} c_0 r dr} = \frac{r_p^2 - a^2 - r_p^2(1 - e^{-2\omega^2 st})}{r_p^2 - a^2} \quad (1)$$

where $c(r,t)$ is the concentration at r and t ; c_0 is the original concentration; a is the meniscus radius; ω is the angular velocity and s is the sedimentation coefficient. Setting $\lambda = r_p^2/r_p^2 - a^2$ and $\tau = 2\omega^2 st$ the effective centrifugation time, we have

$$Q = 1 - \lambda(1 - e^{-\tau}) \quad (2)$$

Equation 2 may be expanded into a series in τ . For $\lambda = 6$, a typical value, omission of terms of τ^3 or higher produces a maximum error of less than 0.005 in Q . Omitting such terms gives equation 3 which is used to determine sedimentation coefficients.

$$\frac{1 - Q}{\lambda} = \tau - \frac{\tau^2}{2} \quad (3)$$

The sedimentation that occurs during acceleration and deceleration often must be taken into account. If the motion of the boundary is ideal

(3) T. Svedberg and K. O. Pedersen, "The Ultracentrifuge," Clarendon Press, Oxford, 1940.

we note the angular velocity as a function of time and use

$$\tau = 2s \int_0^t \omega^2 dt \quad (4)$$

The procedure is then to determine τ from eq. 3 and then s by using this result and eq. 4. The s obtained will be that at the average temperature and average plateau concentration.

Low Molecular Weight Solutes.—If the sedimentation and diffusion coefficients are constant, the transient solute distributions may be obtained by solution of the general centrifuge differential equation (see 4, 5). The formal solution to the basic ultracentrifuge differential equation yields for the average fractional supernatant concentration, Q , the following

$$Q \equiv \left(\frac{\bar{c}}{c_0} \right)_{\text{supernatant}} = \frac{z_b - z_a e^{z_p} - e^{z_a}}{z_p - z_a e^{z_b} - e^{z_a}} + \frac{1}{z_p - z_a} \sum_{n=1}^{\infty} \beta_n \int_{z_a}^{z_b} M(\alpha_n, 1, z) dz e^{-(\alpha_n - 1)\tau} \quad (5)$$

where

$$z = \sigma \frac{r^2}{2} = \frac{\omega^2 s}{D} \frac{r^2}{2} = \frac{\omega^2 M(1 - \bar{V}_\rho)}{RT} \frac{r^2}{2};$$

$$\text{the } \beta_n \text{ are coefficients } \left(= \frac{\int_{z_a}^{z_b} e^{-\alpha_n} M(\alpha_n, 1, z) dz}{\int_{z_a}^{z_b} e^{-z} \langle M(\alpha_n, 1, z) \rangle^2 dz} \right)$$

dependent only on z_a and z_b (the values of z at the meniscus and base, respectively); $M(\alpha_n, 1, z)$ are the eigenfunctions of the solutions and are dependent only on z_a and z_b ; the α_n are the eigenvalues and depend only on z_a and z_b ; and $\tau = 2\omega^2 st$ is the effective centrifugation time. Thus, it is seen that the distributions depend only on the separation cell parameters (a , b and r_p), the effective reduced molecular weight $\sigma = \left(\frac{\omega^2 s}{D} = \frac{\omega^2 M(1 - \bar{V}_\rho)}{RT} \right)$

and the effective centrifugation time, τ .

Previously⁴ we have obtained exact solutions to the Lamm equation following the method of Archibald⁵ and with the aid of a differential analyzer. Three sets of s and D were used; these were calculated for molecular weights of 1000, 2000, and 3000 on the assumption of a specific model.⁶ In the text these molecular weights will be given in parentheses and for purposes of reference only since, as will be made apparent, experimental data will yield the values of s or s and D , without the requirement that the investigated molecules conform to an assumed model. In addition, particular values for the radii to the meniscus and cell base ($a = 6.067$ cm. and $b = 7.003$ cm.) and angular velocity ($\omega^2 = 3.919 \times 10^7$ sec.⁻²) were used. As will be shown, simple approximations have been developed which circumvent these physical restraints.

The eigenvalues and eigenfunctions for the exact solutions⁷ have been used in eq. 5 to obtain values of

(4) D. F. Waugh and D. A. Yphantis, *THIS JOURNAL*, **57**, 312 (1953).

(5) W. J. Archibald, *Ann. N. Y. Acad. Sci.*, **43**, 211 (1942).

(6) The model was that of a sphere hydrated 50% by volume. The partial specific volume of the solute was taken as 0.707.

(7) Tables of the eigenvalues and eigenfunctions are available on request.

Q for $r_p = 6.600$ cm. These are considered to be the exact values of Q to which will be compared other values obtained by approximations. Exact values of Q are given in column 3 of Table I; columns 1 and 2 give the centrifugation times and the values of τ , the latter being independent of an assumed model.

Figure 1 plots exact values of $1 - Q$ vs. τ for three values of $\sigma = \omega^2 s/D$ ($M = 1000, 2000$ and 3000) and for $\sigma = \infty$ ($D = 0$). It is apparent that for small τ , Q is dependent only on $\tau = 2\omega^2 st$ and is independent of D . As τ increases with centrifugation time, the effects of diffusion are apparent in the divergence of the other curves from that for $D = 0$.

Determination of Sedimentation Coefficients.—During the period of low effective centrifugation times when Q is essentially independent of D (Fig. 1), an experimental Q leads directly to a value of s . This is the basis of the procedures of Baldwin and others,⁸⁻¹⁰ for obtaining sedimentation coefficients from sedimentation patterns.

Since, for short centrifugation times, diffusion is not involved in determining Q one may apply eq. 3 and 4 to the direct evaluation of s . However, an accurate assay is essential, as s is roughly proportional to $1 - Q$. For example, if Q is 0.90, a 2% error in determining Q leads to a 20% error in the evaluation of s . Longer centrifugation times must therefore be anticipated where assay errors are significant.

As the size of the molecule decreases, deviations from the Q vs. τ plot for $D = 0$ become progressively larger. When prior information allows a minimum value or a range to be assigned to $\sigma = \omega^2 s/D$, the sedimentation coefficient may be obtained with greater accuracy for a given assay error. For example, let it be known that $\sigma \geq 0.467$ ($M \geq 1000$). The average of the curves of Q vs. τ for $\sigma = \infty$ and $\sigma = 0.467$ is constructed. Assay uncertainties of 2.3 and 10% then lead to uncertainties in s of 8 and 20%¹¹ when $Q \cong 0.68$ and 0.55, respectively. Similarly, if $\sigma \cong 0.933$ ($M = 2000$) an assay uncertainty of 22% for $Q \cong 0.35$ leads to an uncertainty in s of only 14%.

If σ is known, as for example for a synthetic material, the corresponding curve for Q vs. τ may be constructed and the error in s will then be that due to the assay alone. Other variations of these procedures are apparent.

Simultaneous Determination of s and D .—Where a precise assay for the solute is available, one may obtain unambiguously and without a need for assumptions, both the sedimentation and diffusion coefficients and hence, with a knowledge of the partial specific volume,¹² the molecular weight and frictional ratio.

(8) C. H. Li and K. O. Pedersen, *Arkiv. Kemi. Mineral. Geol.*, **1**, 533 (1950).

(9) H. Gutfreund and A. G. Ogston, *Biochem. J.*, **44**, 163 (1949).

(10) R. L. Baldwin, *ibid.*, **55**, 644 (1953).

(11) Considering independent random errors δ_1 and δ_2 as giving a total error of $\sqrt{\delta_1^2 + \delta_2^2}$.

(12) In principle \bar{V} can be determined by finding the solvent density at which neither sedimentation nor flotation occurs, as suggested by D. G. Sharp, D. Beard and J. W. Beard, *J. Biol. Chem.*, **182**, 279 (1950); J. W. McBain, *J. Am. Chem. Soc.*, **58**, 315 (1936); D. G. Sharp and J. W. Beard, *J. Biol. Chem.*, **185**, 247 (1950); H. K. Schach-

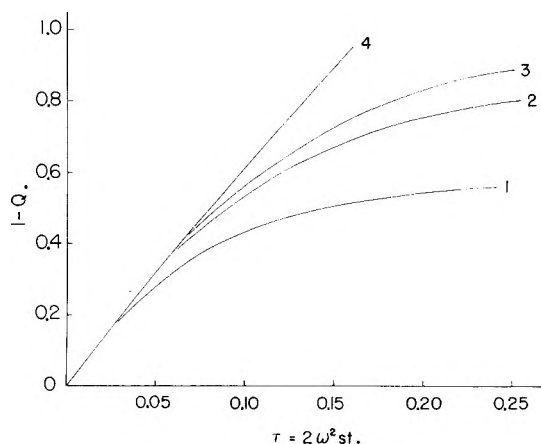


Fig. 1.—The change in average supernatant concentration, $1 - Q$, as a function of effective centrifugation time $\tau = 2\omega^2 st$ for four values of $\sigma = \omega^2 s/D$. For curve 1, $\sigma = 0.467$; for curve 2, $\sigma = 0.933$; for curve 3, $\sigma = 1.399$; and for curve 4, $\sigma = \infty$ ($D = 0$). Curves are obtained from exact solutions.

An examination of the formal solution of Lamm's equation (see 4, 5) shows that the concentration at any point in a cell having particular values of base and meniscus is determined solely by

$$z = \sigma \frac{r^2}{2} = \frac{\omega^2 s r^2}{D 2}$$

and $\tau = 2\omega^2 st$ and hence that the Q for a given r_p are determined solely by σ and τ .¹³ Beyond the initial, coincident phase, of the Q vs. τ plots shown in Fig. 1, each Q is related to an infinite number of paired values of σ and τ . If two (or more) values of Q are obtained for different times, t , such that at least one is beyond the initial, "no diffusion" stage considered above, then it should be possible to determine what particular values of s and σ (and hence D) give the observed values of Q . For example, for each experimental value of Q we tabulate a set of paired values of $\sigma = \omega^2 s/D$ and τ by using Fig. 1 (or Table I). The experimental ω and t allow us to convert these to values of D and s . Each experimental value of Q leads thus to a curve relating D to s . The point of intersection of these curves of D vs. s determines unique values for both. The situation is illustrated in Fig. 2 for the Q values of $\sigma = 0.933$ ($M = 2000$). The sedimentation coefficient is well defined but D not nearly so well unless the centrifugation time is prolonged. An assay with a 2% error in the determination of Q for a molecule with $s = 0.565 \times 10^{-13}$ sec. and $D = 2.37 \times 10^{-6}$ cm.² sec.⁻¹ gives, by the above method, the values for s and D listed in Table II. From this it may be seen that, theoretically, s can be determined in this case to within 0.02×10^{-13} sec. ($\sim 4\%$) and D to within 0.12×10^{-6} cm.² sec.⁻¹ ($\sim 5\%$). A similar analysis for a solute characterized by $s = 0.356 \times 10^{-13}$ sec. and $D = 2.99 \times 10^{-6}$ cm.² sec.⁻¹ yields, for a 2% assay error, an uncertainty of about 0.025×10^{-13} sec. in s ($\sim 7\%$) and 0.5×10^{-6} cm.² sec.⁻¹ in D ($\sim 17\%$).

man and M. A. Lauffer, *J. Am. Chem. Soc.*, **71**, 536 (1949); M. A. Lauffer, N. W. Taylor and C. C. Wunder, *Arch. Biochem. Biophys.*, **40**, 453 (1952); M. A. Lauffer and N. W. Taylor, *ibid.*, **42**, 102 (1953).

(13) Since the eigenvalues, α_n , and the eigenfunctions, $M(\alpha_n, 1, z)$ are eventually dependent only on z_n and z_b .

TABLE I
COMPARISON OF THE VALUES OF Q AS OBTAINED FROM THE
DIFFERENTIAL ANALYZER AND FROM THE VARIOUS APPROXIMATIONS

1 Time (hr.)	2 τ	3 Q Differential analyzer	4 Q Archibald's approx.	5 Q Exponential approx.	6 Q Rectangular approx.	7 Q Rectangular ^a approx.	8 Q diffusion dev.
$\sigma = \omega^2 s / D = 0.467 (M = 1000)$							
2	0.0201	0.874	0.874	0.854	0.877	0.868	0.871
4	.0402	.762	.762	.745	.770	.761	.766
5	.0502	.719	.716	.701	.725	.716	.721
8	.0804	.615	.610	.603	.622	.613	.619
12	.1205	.531	.528	.523	.538	.529	
∞	∞	.424	.424	.424	.433	.424	
$\sigma = \omega^2 s / D = 0.933 (M = 2000)$							
2	0.0319	0.789	0.766	0.744	0.804	0.797	0.797
4	.0638	.614	.593	.563	.626	.619	.624
5	.0797	.541	.521	.494	.552	.545	.553
8	.1275	.379	.364	.347	.387	.380	.393
12	.1913	.256	.247	.240	.263	.256	
∞	∞	.135	.135	.135	.142	.135	
$\sigma = \omega^2 s / D = 1.399 (M = 3000)$							
2	0.0418	0.735	0.673	0.635	0.742	0.739	0.735
4	.0835	.509	.460	.407	.511	.508	.509
5	.1044	.418	.376	.329	.419	.416	.424
8	.1670	.230	.204	.180	.231	.227	.244
12	.2506	.113	.101	.093	.115	.111	
∞	∞	.039	.039	.039	.042	.039	

^a Rectangular approximation with sectoral equilibrium values.

For plate positions near the meniscus the effect of diffusion becomes marked at higher values of Q and at lower centrifugation times. Although placing the plate so close to the meniscus allows s and D to be determined with somewhat shorter runs, the ultimate precision of determining s and D

by a given assay is relatively uninfluenced. From Fig. 1 it is apparent that, as molecules become larger, the diffusion deviations become smaller, making it increasingly difficult to determine s and D simultaneously. This can be overcome by operating at lower speeds.

Extensions and Simplification of the Solutions.—

As noted previously,⁴ the solutions for given cell parameters are determined solely by σ and τ . The differential analyzer solutions may be applied readily to molecular weights and sedimentation coefficients other than those used, simply by choosing values of ω and t for the new conditions so that σ and τ conform to the values employed in the calculations.

The exact solutions refer to a separation cell having $a = 6.067$ cm., $r_p = 6.600$ cm. and $b = 7.003$ cm. It is tedious to construct cells with exactly these parameters and since different values are required in general, we have examined approximations which readily yield solute distributions with sufficient accuracy.

Archibald's Approximation.—Archibald¹⁴ has developed approximations to the ultracentrifuge distribution for the case where $z_b - z_a \approx 1$. These have been found applicable to the present cases where $z_b - z_a$ ranges from 3 to 9.⁴ Numerical integration of these approximate distributions gave the values of Q listed in column 4 of Table I. Considerable computation however was involved in obtaining the data shown.

Exponential Approximation.—A simpler approximation to the values of Q has been examined. If

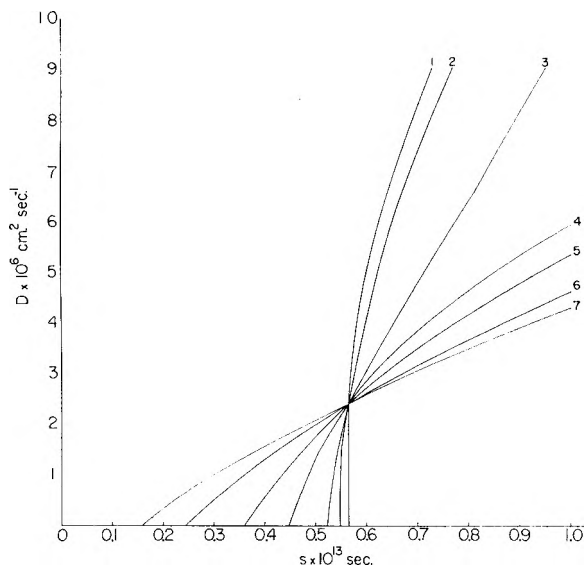


Fig. 2.—Simultaneous determination of s and D . A molecule having $s = 0.56 \times 10^{-13}$ sec. and $D = 2.37 \times 10^{-6}$ cm.² sec.⁻¹ was assumed. Values of Q were calculated for times of 2 hr. (curve 1), 4 hr. (curve 2), 5 hr. (curve 3), 8 hr. (curve 4), 12 hr. (curve 5), 20 hr. (curve 6), and 32 hr. (curve 7). In addition to the assumed values each Q can be accounted for by the series of paired s and D defined by the curves.

(14) W. J. Archibald, *J. Appl. Phys.*, **18**, 362 (1947).

the higher eigenfunctions are much less important than the first, then the following is approximately true

$$Q = Q(\tau = \infty) + \beta_1 \int_{z_a}^{z_p} M(\alpha_1, 1, z) dz e^{(\alpha_1 - 1)\tau} / (z_p - z_a) \tag{6}$$

where $Q(\tau = \infty)$ is given by the first term of eq. 5. Since $Q = 1$ at $t = 0$ the following approximation should also hold

$$Q \cong Q(\tau = \infty) + [1 + Q(\tau = \infty)]e^{(\alpha_1 - 1)\tau} \tag{7}$$

The values of Q thus calculated are compared with the exact solutions in column 5 of Table I. The α_1 were obtained by means of Archibald's approximation.^{14,4} It is seen that the error is largest when t is small and M is high. The errors are expected to decrease for σ less than 0.467, since the higher eigenfunctions become much less important with decreasing σ .

TABLE II

RANGE IN D AND s FOR A 2% ASSAY ERROR IN THE DETERMINATION OF Q FOR A MOLECULE OF ASSUMED $s = 0.565 \times 10^{-13}$, $D = 2.37 \times 10^{-6}$ CM.² SEC.⁻¹

Centrifugation time (hr.)		$D \times 10^6$ (cm. ² sec. ⁻¹)	$s \times 10^{13}$ (sec.)
Run 1	Run 2		
2	8	1.7-3.1	0.525-0.615
2	12	1.95-2.8	.525-.608
4	8	1.85-2.7	.530-.590
4	12	2.2-2.55	.545-.585
4	20	2.25-2.50	.545-.585
5	20	2.15-2.53	.545-.585

Rectangular Approximation.—The calculation of solute distributions in the sector shaped cell with a radially varying field is complicated. The process of computation can be simplified considerably by assuming a rectangular cell with a uniform field (rectangular approximation). Solutions for such a system have been given by Mason and Weaver¹⁶ in their treatment of the settling of spherical particles under gravity. Low molecular weight solute distributions have been calculated from suitable modification of these solutions of Mason and Weaver in which the diffusion and sedimentation coefficients have been introduced to characterize the particles. The modification leads to the result that

$$\frac{c}{c_0}(y, \tau) = \frac{e^{y/\alpha}}{\alpha(e^{1/\alpha} - 1)} + \frac{e^{y/2\alpha}}{2\alpha} \sum_{m=1}^{\infty} C_m(\tau) \{ \sin m\pi y + 2\pi m\alpha \cos m\pi y \} \tag{8}$$

$C_m(\tau)$ is given by

$$C_m(\tau) = \frac{16\alpha^2 \pi e^{-(\alpha m^2 \pi^2 + 1/4\alpha)\tau} m < 1 - (-1)^m e^{1/2\alpha}}{(1 + 4\pi^2 m^2 \alpha^2)^2} \tag{8a}$$

In equation 8 the symbols have the following significance

$$y = \frac{r - a}{b - a} \tag{8b}$$

$$\alpha = \frac{1}{\sigma \bar{r}(b - a)} = \frac{D}{\omega^2 \bar{r}(b - a)} = \frac{RT}{M(1 - \bar{v}\rho)} \frac{1}{\omega^2 r} \frac{1}{b - a} \tag{8c}$$

(15) M. Mason and W. Weaver, *Phys. Rev.*, **23**, 412 (1924).

and

$$\gamma = \frac{\bar{r}}{2(b - a)} \tag{8d}$$

Equation 8 has been evaluated for $\bar{r} = r_p = 6.600$ cm.¹⁶ using $s = 0.356 \times 10^{-13}$ sec. and $D = 2.989 \times 10^{-6}$ cm.² sec.⁻¹, as for the exact solutions ($M = 1000$). Values of $m = 1, 2$ and 3 were used. The results are compared with exact solutions in Figs. 3, 4 for times of 2 and 4 hours. The agreement is seen to be good. It should be pointed out that if the ratio of $b - a$ to \bar{r} is made smaller, the physical situation is closer to the rectangular system and that therefore this approximation should be more accurate.

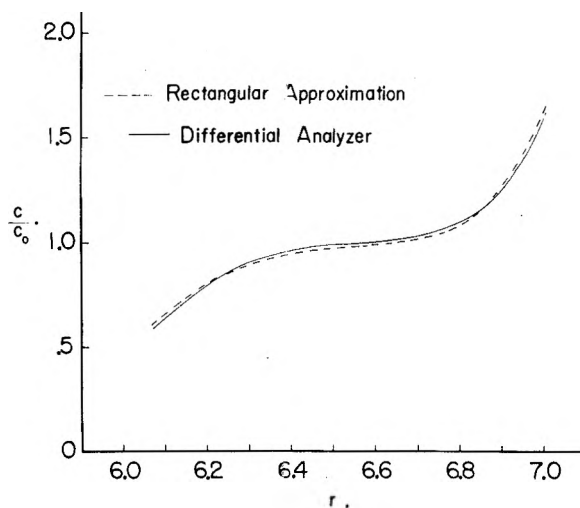


Fig. 3.—Solute distributions for $s = 0.356 \times 10^{-13}$ sec., $D = 2.989 \times 10^{-6}$ cm.² sec.⁻¹ and $t = 2$ hr.: solid line from exact solutions and dotted line from rectangular approximation.

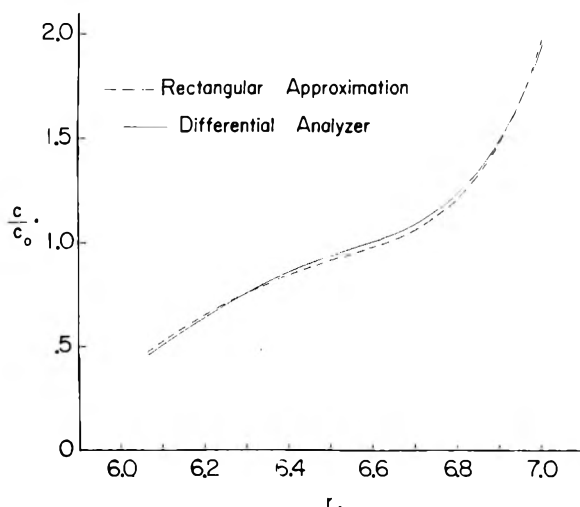


Fig. 4.—Solute distributions for $s = 0.356 \times 10^{-13}$ sec., $D = 2.989 \times 10^{-6}$ cm.² sec.⁻¹ and $t = 4$ hr.: solid line from exact solutions and dotted line from rectangular approximation.

(16) The average cell radius \bar{r} has been replaced by r_p for the rectangular approximations. This somewhat arbitrary procedure has been adopted because (a) generally \bar{r} will be so close to r_p that the maximum deviation of \bar{r} from a practical r_p is equivalent to a very small change in M (or σ) and (b) it is felt that for separation cell calculations the field to be used in these rectangular approximations should be that at r_p .

On examination, this approximation is seen to have the advantage of a somewhat easier computation than Archibald's approximation. Further, the expression for a distribution may be readily integrated to yield

$$Q(\tau) = \left(\frac{\bar{c}}{c_0}(\tau) \right)_{\text{supernatant}} = \frac{\int_0^{y_p} \frac{c}{c_0}(y, \tau) dy}{y_p} = \frac{1}{y_p} \left(\frac{e^{y_p/\alpha} - 1}{e^{1/\alpha} - 1} \right) + \frac{2\alpha}{y_p} \sum_{m=1}^{\infty} C_m(\tau) \sin m\pi y_p \quad (9)$$

Values of Q have been computed, using six terms ($m = 1-6$), for $\bar{r} = r_p = 6.60$ cm., $\sigma = 0.467$, 0.933, and 1.399 ($M = 1000$, 2000 and 3000) and various centrifugation times; these are compared with the exact solutions and with Archibald's approximations in column 6 of Table I. The rectangular approximations are seen to be reasonable and closer to the exact solutions than Archibald's approximations for the higher molecular weights.

The approximation to $Q(\tau)$ given by eq. 9 may be improved somewhat if the first term of eq. 9 is replaced by the first term of eq. 5. Then the equilibrium value used is not that of the rectangular constant field system, but rather that of the sectoral, radially varying field system. Values for Q thus obtained are tabulated in column 7 of Table I.

Diffusion Deviation Approximation to Q .—The curve for $D = 0$ in Fig. 1 shows Q as a function of τ in the absence of diffusion. The deviations from this line are due to diffusion and increase as τ increases and as σ decreases. The diffusion deviation is the difference at constant τ between the value of Q for $D = 0$ and the value of Q for a chosen σ . If the difference be divided by the change in supernatant concentration expected for $D = 0$, ($1 - Q_{D=0}$), there results the fractional diffusion deviation, Δ , the equation for which is

$$\Delta = \frac{Q(\tau)_D - Q(\tau)_{D=0}}{1 - Q(\tau)_{D=0}} = \frac{Q(\tau)_D - Q(\tau)_{D=0}}{\epsilon} \quad (10)$$

where for convenience, ϵ is set equal to $(1 - Q(\tau)_{D=0})$. A simple approximation to the fractional diffusion deviation now allows us to calculate values of Q .

The solutions for diffusion of a solute in a rectangular and a sector cell are closely the same for $Dt = 0.032$ cm.²,¹⁷ the rectangular and sectoral values for Q for high molecular weight solutes are likewise nearly the same over a considerable range of τ ¹⁷ and, as shown, the rectangular solutions closely approximate the differential analyzer solutions. Therefore, it is felt that the diffusion deviations calculated for the rectangular system will be very close to the diffusion deviations of the actual sectoral, varying field system.

In the rectangular system solutions are determined by α and $\gamma\tau$ (eq. 8), the values of which are dependent upon the cell parameters. For no diffusion in this system

$$Q_{D=0} = 1 - \epsilon = 1 - \frac{\gamma\tau}{y_p} \quad (11)$$

The diffusion deviation for the rectangular system has been obtained by subtracting corresponding

values of Q obtained from eq. 11 and 9. Figure 5 presents the results of calculations in which $a = 6.067$ cm., $b = 7.003$ cm., $\bar{r} = 6.600$ cm., and $y_p = 0.5$ and 0.6. Values of σ were 0.233, 0.467, 0.933 and 1.399 ($M = 500$, 1000, 2000 and 3000). Values of τ up to 0.0506, 0.0804, 0.1275 and 0.1670 were used, respectively. Fractional diffusion deviations are seen to be relatively insensitive to y_p in the range of y_p from 0.5 to 0.6 and to be proportional to ϵ beyond a certain minimum value in each case. These relationships allow us to add the diffusion deviation to the no diffusion values of Q (given for the sector case by $\epsilon = 1 - Q_{D=0} = \lambda < 1 - e^{-\tau}$) and thus obtain eq. 12.

$$Q_i = 1 - \epsilon \quad Q_i > 1 - B_i \quad (12a)$$

$$Q_i = 1 - \epsilon + K_i\epsilon(\epsilon - B_i) \quad Q_i < 1 - B_i \quad (12b)$$

Here K_i and B_i are the slopes and intercepts (ϵ -axis) of the lines given in Fig. 5. Table III gives values of K_i and B_i for lines corresponding to $r_p = 6.60$ cm. along with the corresponding values of α_i .

The last two columns of Table III record the values of M and σ_i for the particular values of a and b used in the exact solutions. If other cell parameters are employed, new values of σ_i are to be calculated using eq. 8c for each α_i . The values of Q obtained by this approximation are compared with those obtained from exact solutions in col. 8 of Table I. The approximation is useful up to the maximum values of ϵ shown in Fig. 5 and for $0.5 \leq y_p \leq 0.6$.

TABLE III

K_i AND B_i FOR VARIOUS $\alpha = \left(\frac{D}{\omega^2 s} \frac{1}{r_p(b-a)} \right)$

α_i	K_i	B_i	M^a	σ_i
0.694	1.145	0.058	500	0.233
.347	0.642	.132	1000	.467
.173	.420	.260	2000	.933
.116	.392	.380	3000	1.399

^a M corresponding to $a = 6.067$, $b = 7.003$, $\tau = 6.60$, $\omega^2 = 3.919 \times 10^7$ and a partial specific volume of 0.707.

Sedimentation and Diffusion of Low Molecular Weight Solutes During Deceleration.—A certain amount of time, of the order of 20 minutes, is required to decelerate the ultracentrifuge from full speed. During this time, the solute molecules will both sediment and diffuse. As an approximation, the effects of sedimentation and diffusion during deceleration have been assumed as completely independent. Under this assumption the sedimentation correction for both acceleration and deceleration is the same for both low and high molecular weight solutes, *i.e.*, τ , the effective sedimentation time, is taken as $2 \int \omega^2 s dt$, evaluated from the start of the run to the end and thus the effect on τ is essentially equivalent to running the ultracentrifuge a few minutes longer at full speed.

For a high molecular weight solute the problem of diffusion during deceleration is unimportant if the condition necessary to determine the sedimentation coefficient is adhered to, *i.e.*, if the diffusing solute boundary is sufficiently far from r_p , the separation plate rest position. In the case of low molecular weight solutes the effects of diffusion cannot be neglected *a priori*, rather a critical examination is essential.

(17) D. A. Yphantis, Ph.D. thesis, Massachusetts Institute of Technology, 1955.

Such an examination was carried out on the assumption that the ultracentrifuge cell was rectangular and was operated in a uniform acceleration field for the centrifugation times, after which the distributions were allowed to diffuse with no centrifugal field for various periods and the change in Q due to diffusion evaluated.¹⁷ This procedure allows a considerable simplification of the calculations, which should introduce a negligible error in view of the agreement between the solutions for sector and rectangular cells for combined sedimentation and diffusion and for diffusion alone.

For centrifugation times up to 8 hours the values of Q for $\sigma = 0.467$ ($M = 1000$) are not significantly altered by allowing the distribution to diffuse for times up to 20 minutes ($Dt \leq 0.0036$ cm.²). However, for longer centrifugation times diffusion becomes significant since the equilibrium distribution is changed by 0.02 in Q for a 20 minute diffusion time. For higher M it is expected that the effects of diffusion on Q during deceleration will likewise be very small for the transient curves, in part since D generally decreases with increasing M . Thus the effect of diffusion during a deceleration period of 20 minutes or less in duration may be neglected for transient runs of up to about 8 hours.

Polydisperse Solutes.—Only the two extreme cases of negligible diffusion and of the equilibrium distribution have been examined as the exact investigation of polydispersity in the intermediate cases appears quite complex. The case of negligible diffusion, which is realizable for high molecular weight solutes and for the initial stages of centrifugations involving low molecular weight solutes, can readily be treated through eq. 3 if the simplification is made of dropping the terms in τ with powers greater than unity. This simplification introduces only small errors since τ is practically always less than about 0.16. Equation 3 then reduces to

$$1 - Q = \lambda\tau = 2\lambda s \int_0^t \omega^2 dt \quad (13)$$

For a polydisperse system, where the original concentrations of the various species are given by $c_i(0)$ and where the supernatant concentrations after centrifugation for each species are given by $c_i(t)$, the average supernatant fractional concentration, $\bar{Q}(t)$, for all species is

$$\bar{Q}(t) = \frac{\sum_i c_i(t)}{\sum_i c_i(0)} \quad (14)$$

If the separation plate rest position is in the plateau region of all species, then

$$2\lambda \int_0^t \omega^2 dt \bar{s} = 1 - \bar{Q}(t) = \frac{\sum_i c_i(0) - c_i(t)}{\sum_i c_i(0)} = \frac{\sum_i c_i(0)(1 - Q_i)}{\sum_i c_i(0)} = 2\lambda \int_0^t \omega^2 dt \frac{\sum_i c_i(0)s_i}{\sum_i c_i(0)} \quad (15)$$

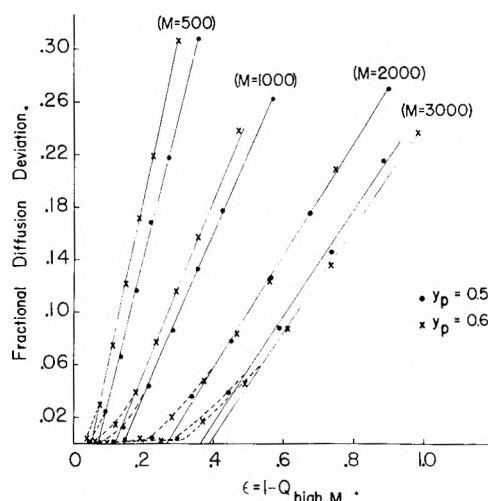


Fig. 5.—Fractional diffusion deviation, Δ , as a function of ϵ , the change in the average fractional supernatant concentration for $D = 0$. For details see text.

Therefore

$$\bar{s} = \frac{\sum_i c_i(0)s_i}{\sum_i c_i(0)} \quad (16)$$

Thus it is seen that the \bar{s} will depend on the type of assay for the concentration used in determining \bar{Q} . If such concentration determinations are performed on a weight basis, they yield the weight average sedimentation coefficient. If the concentration measurements indicate number concentrations, then the \bar{s} is the number average sedimentation coefficient, and so forth.

The approximate sedimentation coefficient distribution may be obtained by the use of a treatment such as that of Wattanabee, Stent and Schachman,¹⁸ where some of the solute boundaries are centrifuged beyond the separation position. The problem of paucidisperse systems has been treated by Svedberg and Pederson³ to obtain both the concentrations and sedimentation coefficients of the various species.

Polydisperse equilibrium distributions have also been examined.¹⁷ The average reduced molecular weight is an unusual type of average in which the lowest molecular weights are most effective in determining the average.

The treatment of the intermediate case for low molecular weight, typified for example by 5 to 12 hour runs, is quite complex. It may be reasonably inferred that the average sedimentation coefficient then obtained will be roughly the concentration average and that the molecular weight obtained will tend to be weighted toward the lower molecular weights, particularly as the time of the runs is increased. It is also expected that the employment of more than two runs to determine s and D will not yield a unique answer, but rather a range of values.

(18) I. Wattanabee, G. S. Stent and H. K. Schachman, *Biochem. Biophys. Acta*, **15**, 38 (1954).

ULTRACENTRIFUGAL CHARACTERIZATION BY DIRECT MEASUREMENT OF ACTIVITY. II. EXPERIMENTAL

BY DAVID A. YPHANTIS¹ AND DAVID F. WAUGH²

Department of Biology, Massachusetts Institute of Technology, Cambridge, Massachusetts

Received November 7, 1965

Details of construction and operation are given for a separation cell of new design. Separation is accomplished by a thin plastic plate whose rest position is determined by stops in the radial edges of the cell centerpiece. The plate is pushed centrifugally against the stops by U-shaped rubber strips. The dimensions of the plate are close to those of the centerpiece at the rest position. On acceleration, the plate compresses the strips and itself forms the effective cell base. The solute distribution is established undisturbed between the meniscus and this cell base. On deceleration the plate returns to its rest position and separates the cell contents into two fixed volumes. These volumes are removed separately for chemical, physical or biological assay. From the assays one may obtain Q , the average fraction of the original concentration remaining centripetal to the separation plate (supernatant). Values of Q may be interpreted in terms of sedimentation coefficients (s) alone (diffusion not important) or in terms of both sedimentation and diffusion coefficients (s and D) when diffusion is important in establishing the solute concentration in the supernatant. The effectiveness of this separation cell has been demonstrated in both static and operational tests. The results obtained include: values of s for bovine serum albumin at concentrations down to 0.01% ($s_{20,w} = 4.35 \pm 0.25 \times 10^{-13}$ sec.), values of both $s_{20,w}$ ($= 0.54 \times 10^{-13}$ sec.) and $D_{20,w}$ ($= 2.7 \times 10^{-6}$ cm.² sec.⁻¹) for vitamin B₁₂, values of s ($= 0.30 \pm 0.02 \times 10^{-13}$ sec.) for a synthetic pentapeptide in 95% ethanol at 25.6°. These values are in good agreement with comparison values. The separation cell has been used also to examine impure systems of biological origin.

Physico-chemical information concerning an active principle may be obtained by appropriate ultracentrifugal studies of pure or impure systems. The method devised requires first, procedures for predicting and interpreting transient solute distributions and, second, techniques for obtaining the required experimental data. The method depends upon the fact that after centrifugation the value of $Q = \bar{c}/c_0$, the ratio of the average concentration centripetal to a plane of separation in the centrifuge to the original concentration, may be interpreted in terms of a sedimentation coefficient, (s), or combined sedimentation and diffusion coefficients (s and D). The preceding publication³ considered theoretical aspects of the method. The present publication considers the construction of a suitable ultracentrifuge cell (separation cell) and certain experimental results.

The Separation Cell

Description and Construction.—The method requires that the contents of a cell be divided into two volumes. Previously, impure solutions of large molecules have been treated by the partition cell of Tiselius, Pedersen and Svedberg.⁴⁻⁸ The fixed partition, while functioning fairly well at high molecular weights and at high concentrations, introduces anomalies in solute distributions at low concentrations and with low molecular weights. With the former the density differences, which drive the solute through the partition, are very small and with low molecular weight solutes the partition presents an indefinite barrier to back-diffusion, thus rendering inapplicable theoretically calculated solute distributions.

It appeared preferable to devise a cell which fractionated its contents at the termination of a run. For this purpose a thin plastic plate is introduced. During acceleration this separation plate moves centrifugally and forms the effective cell base; on deceleration it returns to a predetermined rest position. By virtue of a close fit with the quartz discs and centerpiece walls the separation plate isolates two volumes. The travel of the separation plate is constrained by grooves and stops in the edges of the centerpiece; it is supported by two rubber strips which, at rest, hold the plate against the rest position stops. The sector shape of the cell makes possible this design: when the plate is centrifugal to its rest position there is a space on each side of it through which the solution can flow.

The separation cell requires only minor modification of the commercially available, standard, 12 mm., 4 degree, ultracentrifuge centerpieces. In order to guide the plate travel, each radial edge of the sectoral cavity is beveled at 45° to the cavity and side faces of the centerpiece (0.030" along each face) over its whole length except for a small region (a stop ~ 0.07 cm. long) near the center. The centripetal side of each stop is trimmed with a scalpel so that the transition from the beveled to the unbeveled part is gradual. The centrifugal sides are machined flat so that there is an abrupt transition from a beveled to an unbeveled part. These flats determine the plate rest position, therefore they must be machined at as closely the same radial position to each other as possible (< 0.0005"). It has been found necessary to smooth the beveled regions by means of a blunt needle, a process which eliminates too marks which can cause rough operation. The cells are beveled over almost the complete length of the sectoral edges, instead of just the centrifugal parts, so as to minimize distortions of solute distributions. Since the beveled surfaces are almost radial, the requirements of sectorality are satisfied, except for the small stop regions.

For convenience in loading and unloading the cells, the filling hole has been enlarged to 0.052" to accommodate larger hypodermic needles or polyethylene tubing. After the machining is complete, duralumin cells should be "clear anodized" to retard corrosion with aqueous solutions.

The separation mechanism consists of a thin, rigid plastic plate supported by two rubber strips. The separation plate may be made of a number of commercial plastics, of which Vinylite V has been employed most recently because of its ease of machining. The plate thickness used has been about 1/32". The shape of the plate is such as to conform to the modified centerpiece at the region of the stops. The width and length of the plate must be carefully adjusted to fit a particular centerpiece so as to assure not only a smooth and complete return on deceleration, but also a satisfactory seal between the separated volumes when at rest. The dimensions of each plate have been determined by trial and error and have been about 0.0004" smaller than the corresponding width of the compressed centerpiece at the stop position. The length has been similarly adjusted until the

(1) (a) Taken in part from a dissertation presented by David A. Yphantis to the Faculty of the Department of Biology, the Massachusetts Institute of Technology, in partial fulfillment of the requirements for the degree of Doctor of Philosophy, May, 1955. (b) Currently a Fellow of the American Cancer Society at the Massachusetts Institute of Technology.

(2) Our appreciation is expressed to the Armour Laboratories and to the Research Division of Armour and Company, Chicago, for their support of this research.

(3) D. Yphantis and D. F. Waugh, *This Journal*, **60**, 623 (1956).

(4) A. Tiselius, K. O. Pedersen and T. Svedberg, *Nature*, **140**, 848 (1937).

(5) T. Svedberg and K. O. Pedersen, "The Ultracentrifuge," Clarendon Press, Oxford, 1940.

(6) S. Gard and K. O. Pedersen, *Science*, **94**, 493 (1941).

(7) M. A. Lauffer, *J. Biol. Chem.*, **151**, 627 (1943).

(8) I. Wattanabee, G. S. Stent and H. K. Schachman, *Biochem. et Biophys. Acta*, **15**, 38 (1954).

plate was about 0.0007" less than the space between the quartz disks of the cell when fully tightened. The plates have been fitted to their centerpieces in a particular orientation, because of small deviations of available centerpieces from ideal shapes. The rubber strips are silicone rubber. Other types of rubber also have been used; for some applications, however, the silicone rubber has the advantage of a lower level of contamination, particularly after suitable extraction. Pieces of Silastic #250 or #152⁹ 1/32" thick were cut to a width of about 0.020" less than that of the plate and to a length of 0.5". Earlier versions of the separation cell used rectangular grooves in the cell edges for guiding the plate.

Operation.—The cleaned separation plate is oriented properly in the base of the cell sector and then brought against the stops. The clean rubber strips are bent into the shape of an U and inserted under (centrifugal to) the plate with the open ends of the U's pointing outwards. The remainder of the cell is assembled as usual. A weighed amount of solution is added to the cell by means of a #20 stainless steel hypodermic needle which is also used to depress the separation plate during injection. The cell is weighed against its balanced counter-weight before and after a run, the average cell loss being about 3 mg.

During the acceleration and deceleration, measurements of the speed (r.p.m.) are taken at frequent intervals, and the time at full speed noted. These data are used to calculate

$\int_0^t \omega^2 dt$. At full speed, the angular velocity is determined, at frequent intervals, by the use of the odometer and a calibrated stopwatch. A device based on thermal radiation exchange with the rotor base¹⁰ has been used to determine the rotor temperature at approximately 15-minute intervals. For long runs temperatures were maintained constant by opposing continuous refrigeration with a heater in the chamber.¹⁰

Deceleration is performed in an unusual manner, so as to avoid disturbing the solute distribution. If deceleration is performed with rapid braking only, it is often found that spurious peaks appear, particularly in non-aqueous systems. It is believed that these convective disturbances arise, at least in part, from the thermal affects of deceleration as well as possibly from rotor vibration. The slowest braking speed is employed until the rotor speed has dropped to about 0.7 of the full speed value; next the intermediate braking speed is used until 0.5 of the full speed has been reached; finally the rapid brake is applied until the separation plate just starts to return. At this point the slowest braking speed is used so that the plate moves slowly through the solute distribution. Photographic exposures are taken at about 7,000 r.p.m. and also after the plate has completely returned. With recent cells the separation plate is completely back to the rest position between 2,000 and 3,000 r.p.m.

The vacuum is released and the chamber opened before the rotor stops spinning (*i.e.*, at about 1,500 r.p.m.). The rotor is allowed to stop by itself and is then gently and quickly uncoupled and turned so that gravity acts in the centrifugal direction. In this orientation, a suitable jig is used to push the cell carefully and smoothly out of its hole with a plunger.

The supernatant is removed by means of a 1-cc. syringe to which is attached either a #22 stainless steel needle or a piece of polyethylene tubing. The solution is slowly and gently drawn up into the syringe as the needle is lowered down to one side of the separation plate. This procedure results in a fairly complete withdrawal of the supernatant, the amount of which is determined by weighing the cell. With some solutions an improvement can be had by siliconing the quartz windows and metal centerpiece. The contents of the syringe are mixed by drawing in an air bubble and tilting the syringe back and forth about ten times. Samples of the supernatant solution are removed after the solution is first mixed by depressing the separation plate a number of times with a clean dry syringe equipped with a #20 flat ended, stainless steel hypodermic needle. Then keeping the plate depressed, an aliquot is easily removed. If complete recovery is desired, the cell may be rinsed with solvent.

(9) Supplied through the courtesy of Dow-Corning Inc., Midland, Michigan.

(10) D. F. Waugh and D. A. Yphantis, *Rev. Sci. Instr.*, **23**, 609 (1952).

Determination of Cell Constants.—The determination of sedimentation coefficients for large and small molecules requires the value of $\lambda = r_p^2/r_s^2 - a^2$. For low molecular weights the simultaneous determination of sedimentation and diffusion coefficients requires, in addition, the radial distance to the cell base, b . The values of a , r_p and b required are those corresponding to operating conditions, namely, those at full speed. Determinations at full speed are complicated mainly by rotor expansion, solution compression, mechanical distortions of centerpiece and windows and probable optical distortions in the latter.

In order to avoid effects of photographic image spreading, short exposure times were used or measurements were made between points so as to cancel this effect. Rotor expansion has been examined by Kegeles and Gutter.¹¹ Between 0 and 60,000 r.p.m. the rotors used here expanded by approximately 0.04 cm. We have found also that the axis of rotation remains fixed and does not change with speed. The radii to the counterweight reference edges at any speed were taken as those directly measured at rest on the rotor and counterweight by micrometer plus the value of the rotor expansion for the particular rotor and speed employed in the runs. Thus, any values referred to the reference edge will be those of the expanded rotor.

Solution compression may be calculated readily: for a cell filled with water to a depth of 1.0 cm. it amounts to 0.6% of the total volume at 60,000 r.p.m. The calculated change in volume for the supernatant region alone (between 6.0 and 6.6 cm.) is but 0.3%. Additionally the decrease in average supernatant concentration on deceleration is partially compensated by the compression on acceleration. Thus the total effect should be less than 0.3% and accordingly has been ignored.

The meniscus shift relative to the counterweight edges observed in duralumin cells can be accounted for almost completely by solution compression. In plastic cells (Kell-F) the meniscus shift is larger, indicating some distortion. However, optical examinations of solute distributions and separation cell runs have frequently been made with test substances without any differences being observed. For this reason, distortion of plastic cell has been neglected. The meniscus radius, a , has been taken as that at low speed plus the value of the rotor expansion. This procedure avoids the complications due to compression and distortions and compensates for rotor expansion. The meniscus spreads at low speeds, but the centrifugal edge of the meniscus image is essentially independent of speed between 4–8,000 r.p.m.; hence the radius to this line is measured at low speed. This radius is too large, for at high speed the meniscus has an apparent thickness of 0.006 cm. Subtraction of 0.003 cm. should give the actual radius to the meniscus.

The plate rest position, r_p , is readily obtained from exposures at low speed (~ 2000 r.p.m.) when the separation plate is fully against the rest position stops. This procedure has been found adequate as the same results are obtained by other methods, *e.g.*, by supporting the separation plate mechanically with stronger pieces of rubber. To the value of r_p so obtained is added the increment due to rotor expansion.

The determination of the radius to the separation cell base presents a problem. The separation plate and the rubber strips are packed fairly tightly at operating speed with a small volume, ΔV , occupied by solution centrifugal to the top (centripetal) side of the separation plate. The value of b was approximated by measuring the radius to the top (centripetal) side of the separation plate at operating speed and adding to it the radius increment Δr that is geometrically equivalent to ΔV . A plot of meniscus position *vs.* solvent volume for a region below the plate rest position and in the absence of the separation cell parts is constructed. From this is obtained the total volume centrifugal to the position of the top of the separation plate. Subtraction of the volume of the cell parts yields ΔV . The values of the radius increment, Δr , for various cells ranged from 0.028 to 0.017 cm., a useful average being 0.02 cm.

Checks on Functioning. Static.—The effectiveness of the separation plate in preventing the mixing of the two separated volumes was checked. A concentrated methylene blue solution was placed in the assembled separation cell

(11) G. Kegeles and F. J. Gutter, *J. Am. Chem. Soc.*, **73**, 3770 (1951).

and the cell centrifuged a few minutes at low speed to pack the solution down. The solution above the plate was removed, the top compartment rinsed twice with distilled water and filled with about 0.2 ml. of distilled water. The separation cell was rotated twelve times each around the cylindrical and radial axes of the cell. The supernatant volume was found to contain methylene blue equivalent to 0.002 ml. of the subnatant. The procedure of putting the cell into the rotor, coupling the rotor to the ultracentrifuge, spinning the rotor by hand a few times, uncoupling and removing the cell from the rotor gave the same result.

Operational.—The effectiveness of the separation cell under actual operating conditions has been tested. An 0.5% bovine serum albumin solution (Armour lot #R370295, in phosphate buffer at pH 7.0 and $\Gamma/2 = 0.15$) was used. The volume of this aliquot was chosen so that the supernatant volume would be small, thus showing up prominently a small amount of flow past the separation plate or a mixing of the supernatant and subnatant solutions. The separation cell was then run in the ultracentrifuge at high speed until the serum albumin peak was ~ 1.5 mm. centrifugal to the plate rest position, thus ensuring that essentially all the serum albumin was past the separation plate rest position. Optical density measurements¹² on the removed supernatant and subnatant solutions revealed the equivalent of a flow of 0.002 ml. past the plate. Such flows would correspond to a maximum error of 0.01 in Q . Additionally, the sedimentation coefficients given in Table I would not be expected if significant mixing had occurred.

Disturbance of Distribution.—The effect of the separation plate stops on a high molecular weight solute distribution has been examined. A solution of bovine serum albumin (0.5% in phosphate buffer at pH 7.0 and $\Gamma/2 = 0.15$) was ultracentrifuged at 59,780 r.p.m. No disturbance was noted in the schlieren diagram before the sedimenting boundary reached τ_p . However, a very small disturbance of the peak was noted when the boundary was in the immediate neighborhood of τ_p . In a sample of lobster blood, very small disturbances at τ_p were noted before the major peak reached the same position.

The return of the separation plate through a peak produces no discernible disturbance in the schlieren pattern centripetal to τ_p . If the ultracentrifuge is speeded up again so that the plate descends, the peak reappears, albeit slightly distorted by the double passage of the separation plate through it. The stability of the peak undoubtedly is due to the marked stratification effected by the magnification of density differences by the centrifugal field.

Results

All runs were performed in a Spinco Model E ultracentrifuge at a full speed of 59,780 r.p.m. Temperatures were approximately that of the room and were not controlled with the exception of the B₁₂ runs. Sedimentation coefficients were reduced to standard conditions using the calculated (see 5) buffer densities and viscosities at the mean full speed temperature of the runs.

Bovine Serum Albumin.—Two series of runs at various concentrations were made with two types of separation cells to determine the reliability of the over-all procedure. Bovine serum albumin was chosen as the test substance since it is a relatively well characterized and well behaved protein.

The first series of runs (#1, 2 and 3 in Table I) were performed using a glyptal coated, metal centerpiece of an earlier design and crystallized bovine serum albumin, Armour control #123-165, dissolved in phosphate buffer at pH 6.5 and $\Gamma/2 = 0.15$. In the second series of runs, a metal centerpiece described under The Separation Cell was used with crystallized bovine serum albumin, Armour lot #R370295, in phosphate buffer at pH 7.0 and $\Gamma/2 = 0.15$. Sedimentation coefficients for com-

parison were calculated from the peak position, r_s , using a least squares treatment of $\ln r_s$ vs. t . In the case of run #3, the low concentration precluded reliable high speed measurements of peak positions. Therefore, in this run the sedimentation coefficient was calculated from the peak position at low speed and from the value of $\int_0^t \omega^2 dt$.

TABLE I

COMPARISON OF THE SEDIMENTATION COEFFICIENTS OF BOVINE SERUM ALBUMIN DETERMINED WITH THE SEPARATION CELL WITH THOSE OBTAINED FROM PEAK MOVEMENT

Run no.	Original concn. % w./v.	Separation cell $s_{20,w} \times 10^{13}$	Peak movement
1	0.5	4.45 \pm 0.11	4.31 \pm 0.04
2	.2	4.46 \pm .05	4.41 \pm .04
3	.05	4.43 \pm .07	4.41 \pm .07
4	.5	4.25 \pm .12	4.38 \pm .03
5	.5	4.42 \pm .04	4.44 \pm .01
6	.2	4.22 \pm .20	4.37 \pm .01
7	.012	4.6 \pm .2	
8	.010	4.1 \pm .24	

Supernatant, subnatant and original concentrations of serum albumin were determined in runs 1-6 from optical densities at 280 μ . A modified ninhydrin procedure¹³ was used to determine concentrations in runs 7 and 8, where optical densities were too low for reliable concentration determinations. Uncorrected sedimentation coefficients were calculated from the values of Q using eq. 3 and 4 of the preceding paper.³ The acceleration and deceleration corrections were equivalent to about ten minutes at full speed.

The reduced sedimentation coefficients obtained through the separation cell technique are compared with those obtained from peak movement in Table I. The original serum albumin concentrations indicated are approximate. The agreement between sedimentation coefficients as determined by the separation cell technique and as determined in the usual optical manner is seen from Table I to be quite good. Values for the sedimentation coefficients of bovine serum albumin at a concentration of 0.01% (100 γ /ml.) are also given in Table I. It is seen that these are not significantly different from the values obtained at the higher concentrations. Probably lower concentrations could also be used subject to assay reliability at low concentrations and to the possibility of concentration changes by solute adsorption.

Vitamin B₁₂.—Vitamin B₁₂ was chosen as a test substance because it has a known low molecular weight, is obtainable relatively pure and may be readily assayed by its strong absorption in the visible. Kel-F centerpieces were used, along with polystyrene plates and gum rubber strips. The B₁₂ was a crystalline Armour preparation (Lot #RR127303). Two solvents were used: aqueous 1.0% NaCl and 0.01 *N* HCl containing 1.0% NaCl. The separation cells were run for periods of two or five hours. Rotor temperatures at full speed were maintained at 22.0 \pm 0.7° during all runs. Acceleration and deceleration corrections were not measured. Concentrations

(12) Optical densities were measured with a Beckman model DU spectrophotometer, equipped with a photomultiplier and silica micro-cells.

(13) To be published.

were determined from the optical densities at the maximum near 360 $m\mu$.

The experimental values of Q for similar runs indicated a good reproducibility for the results at concentrations of 0.05% and above, even in the two different solvents. However, six runs at a B_{12} concentration of 0.003% showed a large variability. This could result from a variable adsorption or desorption of the B_{12} , as was indicated by the variation in recoveries.

The previous publication³ outlined a procedure for simultaneous determination of s and D . Any one experimental value of Q may be accounted for by a series of paired values of s and D . If two suitable values of Q are obtained (one must be beyond the plateau or "no diffusion" stage) then the intersection of the two s vs. D curves will define these quantities.

The separation cell used in the experiments with B_{12} did not have the same cell parameters as the exact solutions. The "diffusion deviation approximation"³ was therefore used to relate Q to s and D . This approximation is particularly useful since the calculations for a complete analysis require only a few minutes. These are carried out as follows.

The radii to the meniscus and separation plate rest position lead to a value of $\lambda = r_p^2/r_p^2 - a^2$. This in turn leads to paired values of ϵ and τ ($= 2\omega^2st$) by eq. 1

$$\epsilon = \lambda(1 - e^{-\tau}) \quad (1)$$

From the preceding publication we see that

$$Q_i = 1 - \epsilon \quad Q_i > 1 - B_i \quad (2a)$$

$$Q_i = 1 - \epsilon + K_i\epsilon(\epsilon - B_i) \quad Q_i < 1 - B_i \quad (2b)$$

where values of K_i and B_i corresponding to four values of α_i were given in Table III of reference 3. The α_i were given by

$$\alpha_i = \left(\frac{D}{\omega^2s}\right)_i \frac{1}{r_p(b-a)} \quad (3)$$

By employing eq. 1 and 2 we may construct for each α_i a curve relating Q_i to τ ($= \tau_i$). Each experimental value of Q is now used to determine a value of τ corresponding to each value of α_i . From these we obtain values of s and D using $\tau = 2\omega^2st$ and eq. 3. Thus each experimental Q leads to a curve relating s to D .

In Fig. 1, curve 1 gives the results of a five hour run performed on a 0.2% solution of B_{12} dissolved in 1.0% aqueous NaCl. Curve 2 was given by a five hour run on a 0.2% solution in 0.01 N HCl with 1.0% NaCl. Curves 3 and 4 represent the results of two 2-hour runs on 0.2% solutions in 1.0% aqueous NaCl. The common intersection of these runs yields the following approximate values for the uncorrected coefficients at 22° in 1.0% NaCl: $s = 0.55 \times 10^{-13}$ sec. and $D = 2.8 \times 10^{-6}$ cm.² sec.⁻¹.

The value for the partial specific volume of vitamin B_{12} of 0.66¹⁴ allows the reduction of the sedimentation coefficient to standard conditions. The diffusion coefficient was also corrected to standard conditions. The value of s was found to

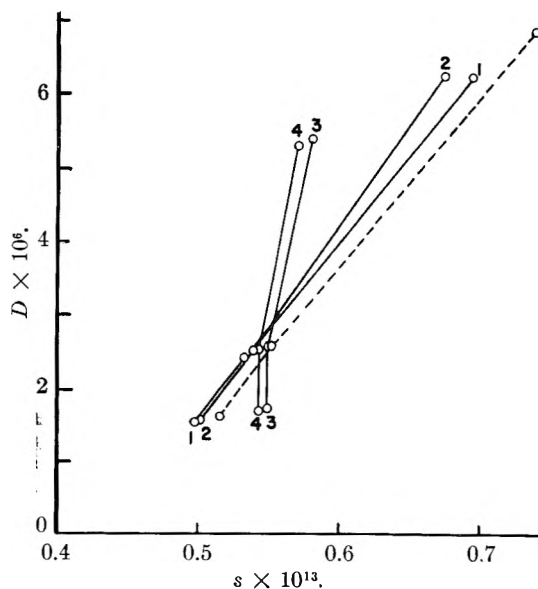


Fig. 1.—Simultaneous determination of s and D for vitamin B_{12} . Details are in text.

be 0.54×10^{-13} sec. and that of $D_{20,w}$ was 2.7×10^{-6} cm.² sec.⁻¹. These values yield, with the value of \bar{V} , a molecular weight of 1430 for B_{12} as compared to the formula weight of 1357. The reduced sedimentation coefficient of vitamin B_{12} has been determined carefully by Schachman¹⁴ with the aid of the synthetic boundary cell as 0.50×10^{-13} sec. in good agreement with the present values. The agreement, particularly for the value of M , is to a large extent fortuitous in view of the fact that an error of 0.03 in determining the value of Q given by the five hour runs ($Q \sim 0.6$) can change the calculated value of D (and hence that of M) by about 9% in this case. This can be seen readily from Fig. 1 where the dotted line refers to a Q that is 0.03 different from that of curve 2. This dotted curve represents the average of the results for two five-hour runs, each assayed twice, with a B_{12} concentration of 0.05% in 0.01 N HCl containing 1.0% NaCl.

Diphosphopyridine Nucleotide.—In most of the experiments on DPN, glyptal-coated centerpieces, Vinylite V separation plates and Silastic 152 (or 250) rubber strips were employed. The DPN examined was Sigma Cozymase "90," Lot #121-36, which was stored in the cold in a desiccator. The solvent used in the majority of runs was phosphate buffer at pH 6.5 and $\Gamma/2 = 0.15$. DPN concentrations were determined from optical density measurements at 259.5 $m\mu$.

Calculation of the sedimentation coefficients was performed, on the assumption of negligible diffusion, in the same manner as for high molecular weight solutes, using eq. 3 and 4 of reference 3. Since the molecular weight of DPN is ~ 660 , these experiments constitute an extreme test of this "no diffusion" approach. For purposes of reducing sedimentation coefficients to standard conditions the partial specific volume was taken as $\bar{V} = 0.63$ (the reduction was not very sensitive to \bar{V} since the buffer density was close to that of water at 20°).

(14) H. K. Schachman, private communication.

Sedimentation coefficients as determined by the separation cell technique for DPN at various concentrations are listed in Table II. A single run (#9) performed on 1% DPN dissolved in phosphate buffer at pH 7.0 and $\Gamma/2 = 0.15$ is also included. In addition, the results of two synthetic boundary cell¹⁵ runs for 1% DPN in pH 6.5 and $\Gamma/2 = 0.15$ phosphate buffer are tabulated for comparison. The recoveries from the separation cell as calculated from the volumes and concentrations are likewise listed in this table. These recoveries are seen to be quite reasonable, being within 2% of the amount added to the cell for original DPN concentrations of 0.05% and higher and within 4% for the lowest concentrations. The indicated deviations of all sedimentation coefficients are those resulting from the standard deviations of the measurements. In these separation cell runs Q was about 0.9, thus a 1% error in determining Q results in an error in s of about 10%. It can be seen from Table II that there is acceptable agreement between separation cell results at all concentrations and the synthetic boundary cell results. It appears that the separation cell will be useful at any concentration which can be adequately assayed. However, the B₁₂ runs at low concentrations (0.003%) showed large deviations. The B₁₂ runs differed from the DPN runs in a number of respects, one of which was in the use of gum rubber strips instead of Silastic strips. It is quite possible that there was a large absorption and desorption of the B₁₂ on the gum rubber and little of the DPN on the silicone rubber.

TABLE II

SEDIMENTATION COEFFICIENTS OF DPN OBTAINED WITH THE SEPARATION CELL AND THE SYNTHETIC BOUNDARY CELL

Run no.	Original concn. %, w./v.	Duration of run, hr.	Recoveries, %	$s_{20,w} \times 10^{13}$, sec.
1	1.0	1.1	98.8	0.460 ± 0.040
2	1.0	1.0	99.5	.417 ± .034
3	1.0	2.0	99.6	.413 ± .030
4	1.0	2.0	98.6	.404 ± .030
5	0.05	1.0	98.2	.524 ± .030
6	0.05	1.0	98.2	.495 ± .050
7	0.0044	1.0	104.0	.454 ± .050
8	0.005	1.0	103.5	.395 ± .045
9	1.0	1.2	100.7	.430 ± .027
Synthetic boundary cell @ 1%				{ .448 ± .013
				{ .459 ± .011

Synthetic Pentapeptide.—Dr. Murray Goodman of the Chemistry Department at M.I.T. has very kindly made available samples of a blocked synthetic pentapeptide: phthaloyl-*d*-phenylalanyl-*l*-prolyl-*l*-valyl- δ -carbobenzoxy-*l*-ornithyl-*l*-leucine ethyl ester. The samples have been estimated as over 99% pure. The pentapeptide is sparingly soluble in water but quite soluble in ethanol, which was used for the ultracentrifuge runs. In 95.5% ethanol it exhibits a particularly strong absorption maximum at 217.5 $m\mu$ and a weaker maximum at 295 $m\mu$. Since small amounts of impurities which

(15) E. G. Pickels, W. F. Harrington and H. K. Schachman, *Proc. Natl. Acad. Sci. U. S. A.*, **38**, 943 (1952).

absorbed at 217.5 $m\mu$ were present in the polyethylene gaskets and Silastic 250 plate supporting strips, these were extracted with ethanol. All runs were of two-hour duration except for SPP-1 which was of three-hour duration. Rotor temperatures were not controlled but were adjusted before running so that full speed temperatures would be about 25°. Sedimentation coefficients at the temperatures of the runs were calculated by means of eq. 3 and 4 of reference 3 on the assumption of negligible diffusion. For comparison a single run was performed using the synthetic boundary cell.¹⁵ The synthetic pentapeptide was run at a concentration of 1.0% in 95.5% ethanol, at a temperature of 25.6 ± 0.25°.

The separation cell results were corrected to 25.6° for viscosity¹⁶ alone to facilitate comparison with the synthetic boundary cell value. This procedure of using only the viscosity part of the correction is justifiable in this case (since the temperatures of the separation cell runs differed at most by 0.6° from that of the synthetic boundary cell run the partial specific volume and density part of the correction should be negligible).

The results are given in Table III. The original concentrations of the runs are listed in the second column. Recoveries, as calculated from the volumes and concentrations, are given in the third column. It is seen that the recoveries are acceptable. The uncorrected sedimentation coefficients are listed in the fourth column and the average full speed temperatures are given in the next column. The last column lists the sedimentation coefficients corrected to 25.6° for viscosity. Results are given for run SPP-5 as determined from (a) absorption at 217.5 $m\mu$ and (b) absorption at 295 $m\mu$. The last line gives the value of the sedimentation coefficient as determined by the synthetic boundary cell. It can be seen that the values for runs SPP-2,3,4,5 are all in good agreement with the sedimentation coefficient from the synthetic boundary cell run. The sedimentation coefficient determined in run SPP-1 is somewhat low, probably because deceleration was carried out too rapidly, as evidenced by the appearance of spurious peaks in the schlieren diagram.

TABLE III

SEDIMENTATION COEFFICIENTS OF SYNTHETIC PENTAPEPTIDE IN 95.5% ETHANOL

Run	Original concn. %, w./v.	Recovery, %	s	T_c , °C.	$s_{25.6}$
SPP-1 ^a	0.1	98.9	0.259 ± 0.019	25.4	0.261 ± 0.019
SPP-2	.1	100.0	.297 ± .013	25.2	.300 ± .013
SPP-3	.1	100.0	.303 ± .030	25.8	.302 ± .030
SPP-4	.1	99.4	.302 ± .025	25.4	.302 ± .025
SPP-5a	.5	100.5	.275 ± .020	25.0	.279 ± .020
b	.5	100.6	.293 ± .010	25.0	.297 ± .010
Synthetic boundary run at 1.0%: 25.6°					0.296 ± 0.009

^a Disturbance noted during deceleration.

Biological Applications.—Assays of concentrations are the only measurements required on the solutions obtained from the ultracentrifuge. Such

(16) Viscosity data interpolated from the "International Critical Tables."

assays can be performed on the basis of biological activity. Thus, even impure biological solutes may be physically characterized. One such substance, ACTH, was the main subject of the early phases of this investigation. Various preparations were examined, most of which were quite impure. In spite of the problems accompanying an imprecise assay, ACTH was shown at an early stage to be of low molecular weight.¹⁷ In the meantime, many improvements have been made in separation cell procedures and other solutes have been examined with much greater precision. By averaging the assay results of some twelve early runs the value of the sedimentation coefficient at 22° of the ACTH activity has been estimated as 0.6×10^{-13} sec. in 0.05 *N* HCl containing 1% NaCl. One may compare this with the value of 0.53×10^{-13} sec. obtained at 35° for pure preparations of corticotropin B by Brink, *et al.*¹⁸

Another biological system has been investigated by Lamy and Waugh.^{19,20} In preliminary experiments they found that citrate activation of prothrombin yields a series of fragments. The thrombin activity was identified with the component having an $s_{20,w}$ of 4.1×10^{-13} sec. Biological activation, on the other hand, yields a thrombin whose sedimentation coefficient is not markedly different from that of prothrombin ($s_{20,w} = 4.9 \times 10^{-13}$ sec.)

Fitzgerald and Waugh²¹ have used the separation cell to demonstrate that the activity of an apparently homogeneous heparin cofactor preparation does not reside with the main component of $s \sim 4 \times 10^{-13}$ sec. The activity was found to have an uncorrected sedimentation coefficient of $2.0 \pm 0.3 \times 10^{-13}$ sec. On concentration of the cofactor solutions, a component with $s \sim 2 \times 10^{-13}$ sec. was observed.

Discussion

The present separation cell technique has a number of advantages over the usual optical techniques. These advantages stem from the fact that sedimentation and diffusion coefficients are not necessarily obtained from the gross physical properties of the sample but rather from any assayable property of the system under study. Thus, not only may substances be examined at very low concen-

trations but also in impure states. This allows, for example, studies of the states of aggregation of biologically active moieties even in their native, unfractionated conditions. There are advantages also over the previous partition cells which employed a fixed perforated plate. In the present separation cell the solute distributions are established normally and are fractionated only at the termination of a run.

As has been outlined in the preceding communication and exemplified here, the separation cell can readily yield sedimentation coefficients for high molecular solutes. In addition, for low molecular weight solutes, the values of the diffusion coefficients are also accessible. Actually, diffusion coefficients of large molecules may be obtained by operating at suitably low speeds for long times.

The apparent mixing past the separation plate is equivalent to 0.002 ml. of the subnatant, which corresponds to 0.01 in *Q*. This is the maximum error in *Q* for a subnatant-supernatant exchange when the supernatant concentration is zero. Under the conditions used here the supernatant *Q* has been 0.4 to 0.9, consequently errors in *Q* should have been 0.008 to 0.001 at most. Actually mixing errors are expected to be less since in static tests for mixing it was difficult to wash the supernatant volume free of methylene blue. We may conclude that the mechanical operation of the separation cell is more than adequate. In addition, the results which have been obtained with test substances indicate satisfactory operation of the cell over a wide variety of experimental conditions. The assay error then becomes the limiting factor and experimental conditions should be sought so that the assay uncertainty is not a significant fraction of the solute transport, $1 - Q$. The experimental conditions to be sought are, of course, set largely by whether *s* alone or both *s* and *D* are to be determined. Ideally, for *s*, the angular velocity should be large enough so that an appropriate *Q* is obtained uninfluenced by diffusion. The lower limit of *s/D* which can be treated in this way is fixed by the assay uncertainty and the maximum realizable centrifugal field. The upper limit of *s/D* is mainly fixed by the lowest angular velocity at which the separation cell operates effectively.

Even though an adequate assay be available, adsorption of solute to cell components may be a limiting factor. Components have been chosen to minimize adsorption. However, at very low concentrations adsorption may become important. In this connection, concentrations of 0.01 to 0.005% have been used successfully.

(17) J. B. Lesh, J. D. Fisher, I. M. Bunding, J. J. Kocsis, L. J. Walaszek, W. F. White and E. E. Hays, *Science* **112**, 43 (1950).

(18) N. G. Brink, G. E. Boxer, V. C. Jelinek, F. A. Kuehl, Jr., J. W. Richter and K. Folkers, *J. Am. Chem. Soc.*, **75**, 1960 (1953).

(19) F. Lamy and D. F. Waugh, *Physiol. Rev.*, **34**, 722 (1954).

(20) F. Lamy, private communication.

(21) M. A. Fitzgerald and D. F. Waugh, *Arch. Biochem. Biophys.*, **58**, 431 (1955).

THE HEAT CAPACITY OF GASES AT LOW PRESSURE USING A WIRE-RIBBON METHOD

BY WILLIAM N. VANDERKOOI AND THOMAS DE VRIES

Contribution from the Department of Chemistry, Purdue University, Lafayette, Indiana

Received November 7, 1955

A wire-ribbon method was developed for determining the accommodation coefficients and heat capacities of gases in the micron of mercury pressure region, and equations for the power dissipations of the wire and ribbon were derived. The heat capacities at constant volume and 300°K. of CHF_3 , CClF_3 and CH_2CF_2 were found to be 10.23 ± 0.13 , 14.10 ± 0.38 and 16.83 ± 0.18 cal./mole/deg., respectively; and by comparison with spectroscopic data the barrier hindering the internal rotation of CH_2CF_2 was established to be 3370 cal./mole.

Since the heat capacity is the best function for checking vibrational assignments and estimating barrier heights resisting internal torsions, the wire-ribbon method, first proposed by Eucken and Krome¹ for the simultaneous determination of the thermal accommodation coefficient and heat capacity of gases, has been improved to provide an accurate method for measuring gaseous heat capacities at very low pressures. By measuring the heat capacity in the micron of mercury pressure region where gases behave ideally, the standard state heat capacity is obtained which can be compared directly with spectroscopic calculations without correcting for the non-ideality of the gas as usually must be done in comparing calorimetric and spectroscopic data.

Experimental

The rate at which a gas at low pressure conducts energy away from a heated surface is a function of the number of molecules striking the surface per second $nc/4$, the temperature difference between the surface and the gas ($T_s - T$), the heat capacity at constant volume, and the thermal accommodation coefficient which Knudsen² defined as

$$a = (T_1 - T)/(T_s - T)$$

where T is the temperature of gas molecules approaching the surface at T_s , and T_1 is that of the molecules leaving the surface. According to Knudsen² and Schafer³ the energy conducted away from the surface in the form of translational energy is proportional to 4/3 times the translational component of the heat capacity since the faster molecules strike the surface more frequently and thus conduct away more energy per second than the slow ones do, while the energy conducted away in the form of rotational and vibrational energy is directly proportional to their components of the heat capacity. From this and the relationships: $n/N = P/RT$, $\bar{c} = (8RT/\pi M)^{1/2}$, and $(1/3)C_{vt} = R/2$, a general equation for the power dissipation of a heated surface by gaseous molecular conduction is obtained directly

$$q = ka(C_v + 1/2R)(T_s - T)P(MT)^{-1/2} \quad (1)$$

where k includes the area of the surface, the constant terms and unit conversion factors. The total power dissipation of a heated wire or ribbon includes radiation and end losses; however, if the temperatures are maintained constant these terms drop out of the equation for the total power dissipation when it is differentiated with respect to pressure, provided that the experimental conditions are such that the end losses are not a function of pressure.

In this investigation a shiny platinum ribbon, 0.013×0.23 cm., was suspended along the axis of a 40 mm. diameter glass tube parallel to and 0.2 cm. from a platinum wire 0.007 cm. in diameter, both of which were about 15 cm. long. The cell containing the wire and ribbon was immersed in a thermostated bath which maintained a constant temperature of $25.00 \pm 0.02^\circ$. The resistances and power

dissipations of the wire and ribbon, which were heated by steady direct current from a rectifier-battery cascade system were determined by measuring the potential drops across them and across standard resistances in series with them with a potentiometer.

Since the resistances of the platinum wire and ribbon were proportional to temperature in the temperature range of this investigation, and since the pressure was assumed to be low enough to eliminate temperature gradients between the wire and ribbon and the cell wall, the power dissipation derivative for the ribbon is obtained directly from equation 1 in terms of the measured electrical quantities

$$d(I_R^2 R_R)/dP = K_R a_R (C_v + 1/2R)(R_R - R_R')(M)^{-1/2} \quad (2)$$

where R_R' is the resistance of the ribbon corresponding to the bath temperature, and the $T^{-1/2}$ has been included in the constant term K_R since the bath temperature was maintained constant. The power dissipation equation for the wire must include an additional term since energy is conducted by the gas molecules from the heated ribbon to the wire; and its magnitude is dependent on the geometry, the heat capacity of the gas, the temperature of the ribbon and the accommodation coefficient of the gas on both the wire and on the ribbon since there are two gas-surface energy transfer processes. (The quadratic nature of the accommodation coefficient in the interaction term is also attested to by Schafer and Riggert.⁴)

By replacing temperatures with resistances and including the bath temperature in the denominator in the constants we obtain the derivative for the power dissipation of the wire

$$d(I_W^2 R_W)/dP = K_W a_W (C_v + 1/2R)(R_W - R_W')(M)^{1/2} - K_{WR} a_W a_R (C_v + 1/2R)(R_R - R_R')(M)^{-1/2} \quad (3)$$

Two special cases of equation 3 are of interest; when the ribbon temperature equals the bath temperature the interaction term becomes zero which gives

$$d(I_W^2 R_W)/dP = K_W a_W (C_v + 1/2R)(R_W - R_W')(M)^{-1/2} \quad (4)$$

and when the wire temperature equals that of the bath, but the ribbon is heated, we obtain

$$d(I_W^2 R_W)/dP = -K_W a_W a_R (C_v + 1/2R)(R_R - R_R')(M)^{-1/2} \quad (5)$$

The power dissipation of the ribbon was determined at various pressures, measured with a McLeod gage and a cathetometer, and at a constant ribbon temperature of 36.0° to evaluate the derivative of equation 2; and that of the wire was determined with the ribbon at 36.0° and the wire at 26.0° , with the ribbon at 25.0° and the wire at 26.0° , and with the ribbon at 36.0° and the wire at 25.0° , at various pressures to evaluate the derivatives of equations 3, 4 and 5, respectively. By measuring the power dissipation of the wire and ribbon under these four conditions in the presence of one of the inert gases (for which $C_v = 2.9808$ cal./mole/deg.) and in the presence of another gas, the heat capacity at constant volume of the other gas, and its accommodation coefficients on the wire and on the ribbon relative to those of the inert gas are readily obtained by the simultaneous solution of equation 2 and any two of equations 3, 4 and 5.

(1) A. Eucken and H. Krome, *Z. physik. Chem.*, **B45**, 175 (1940).

(2) M. Knudsen, *Ann. Physik.*, **34**, 593 (1911).

(3) K. Schafer, *Fortschr. Chem. Forsch.*, **1**, 61 (1949).

(4) K. Schafer and K. H. Riggert, *Naturwissenschaften*, **40**, 219 (1953).

TABLE I
POWER DISSIPATION *versus* PRESSURE SLOPES FOR THE WIRE AND RIBBON

Gas	Pressure range, μ	Power dissipation derivatives in $\mu\text{watts}/\mu$				$R_w^a - R_w'$ ohms
		2	3	4	5	
A	0-6.9	536.11	-1.7053	3.2947	-4.9993	0.02289
He	0-12.1	609.98	+0.4229	3.3050	-2.7350	.01307
CHF ₃	0-5.3 (3)	1102.5	-3.2649	6.8739	-10.1900	.02211
CClF ₃	0-6.8 (2.5)	1221.7	-3.680	8.493	-11.107	.02236
CH ₂ CF ₃	0-3.5 (2)	1796.5	-7.499	11.500	-18.700	.02520

^a From the wire temperature at which the derivative of equation 3 is zero. ^b Conditions: 2, ribbon at 36.0°; 3, ribbon at 36.0°; wire at 26.0°; 4, ribbon at 25.0°; wire at 26.0°; 5, ribbon at 36.0°; wire at 25.0°.

Materials

Argon was purified by repeatedly condensing it with liquid nitrogen, evacuating, warming and recondensing it until a constant minimum pressure of 20.5 ± 0.5 cm. was obtained with the solid argon at the temperature of liquid nitrogen.

Helium.—A trace of condensable vapor was removed from the helium by passing it through a tube immersed in liquid nitrogen.

Trifluoromethane and Monochlorotrifluoromethane.—CHF₃ and CClF₃ were purified by fractional distillation in a Heli-Robot Low Temperature Fractional Analysis Apparatus made by Podbielniak, Inc. Middle fractions having boiling point ranges of less than 0.1° were collected in gas container bulbs.

1,1,1-Trifluoroethane.—A purified sample of CH₃CF₃ was obtained from Susi.⁵

Results

The slopes of the linear portions of power dissipation *versus* pressure graphs were evaluated using graphical and least squares methods and are listed in Table I in microwatts per micron, together with the pressure ranges over which measurements were made and the pressures (in parentheses) at which the curves began deviating from linearity. Also in Table I are given the values of $R_w - R_w'$ in equation 3 at which the derivative equals zero when the ribbon temperature is 36.0°, the ratios of which give the relative accommodation coefficient directly. In the cell used in this investigation to obtain the data given in Table I, the ribbon had a resistance of 0.83818 ohm at 25.0° and 0.86884 ohm at 36.0° and the wire 4.25083 ohms at 25.0° and 4.26598 ohms at 26.0°. At zero pressure the ribbon power dissipation was 2960 microwatts (μw), and the wire power dissipation was 28.9 μw , when the ribbon was at 36° and the wire at 26°, 31.9 μw , when the ribbon was at 25° and the wire at 26°, and -3.1 μw , when the ribbon was at 36° and the wire at 25°, which are due to conduction through their end supports and lead wires.

As can be seen from Fig. 1, which illustrates the power dissipations of the wire *versus* pressure in the presence of A and CHF₃ for the conditions of equations 3, 4 and 5 (the graph for the ribbon power dissipation is similar to that for the wire when the ribbon temperature is 25.0°), above a certain pressure the power dissipations deviate to the low side of linearity. The temperature of the molecules striking a surface corresponds to that of the gas at

a distance equal to 1.2 times the mean free path of the molecules according to Langmuir.⁶ When the mean free path becomes small enough the temperature of the gas at the above distance from the wire and ribbon is higher than 25.0° with the result that the temperature difference is smaller than 1.0 and 11.0° for the wire and ribbon, respectively, and hence the power dissipation is less

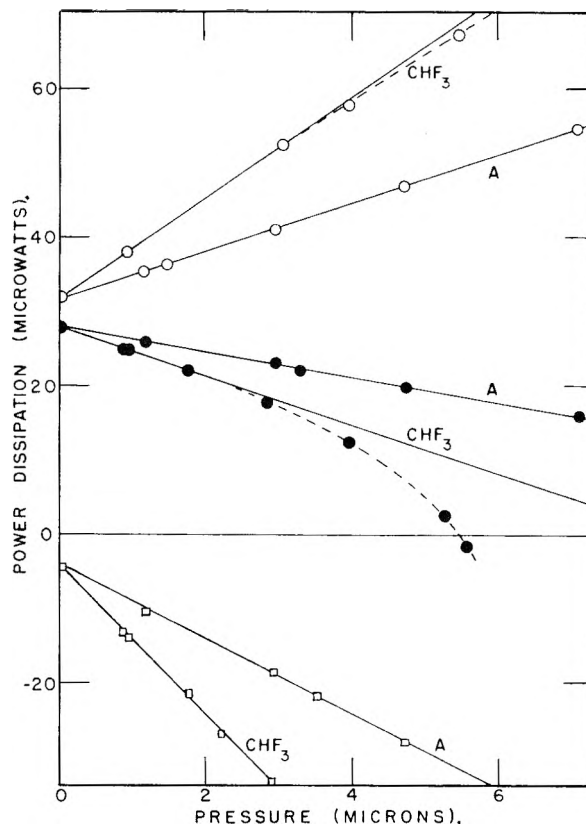


Fig. 1.—Power dissipation *versus* pressure at constant temperature for the wire in the presence of A and CHF₃: ●, ribbon at 36.0°, wire at 26.0°; ○, ribbon at 25.0°, wire at 26.0°; □, ribbon at 36.0°, wire at 25.0°.

than that required for linearity. When the mean free path is short there is an additional effect on the wire when the ribbon is heated; besides decreasing the power dissipation, the temperature of the wire at any given wire current is raised, as is apparent from the increasing elevation of wire resistance *versus* power dissipation lines at constant pressure above their point of intersection (from which the value of $R_w - R_w'$ is obtained in Table I) when the

(6) I. Langmuir, "Phenomena, Atoms and Molecules," Philosophical Library, New York, N. Y., 1950, p. 164.

(5) H. Susi, Chemistry Department, Purdue University.

pressure is raised above a certain value. This double action makes the power dissipation *versus* pressure curves for the wire when the ribbon is heated deviate very rapidly from linearity, as seen in Fig. 1, which provides a sensitive means for determining the pressure at which deviation begins.

Qualitatively, it can be seen from the results of this investigation that the pressure at which deviation from linearity begins decreases as the size of the molecules increases. It is probably reasonable to expect that at the pressures at which deviation begins, the mean free paths of the various gases are equal; in which case it would be possible to determine the mean free paths of gases by this method if a gas of known mean free path is used as a reference. From the mean free path at a known temperature and pressure the effective diameter of the molecules in the ideal gas state can be readily calculated.

For the inert gases used in this investigation the pressure *versus* power dissipation plots were linear over the entire range of pressure. Using the mean free path data given in the "Handbook of Chemistry and Physics,"⁷ at the highest pressure of 6.9 μ for argon the mean free path was 1.1 cm., while at helium's highest pressure of 12.1 μ its mean free path was 1.8 cm. Therefore, the value of the mean free path which corresponds to the beginning of deviation from linearity must be less than 1.1 cm.

Combining the data from the linear portions for argon with those for each of the other gases to eliminate the apparatus constants, and using various combinations of the relationships thus obtained, several values of the accommodation coefficients and heat capacities are obtained for each gas, the average values of which are listed in Tables II and III. The average deviation from

from the ribbon, hence it can be shown that the mean temperatures of the molecules striking the wire and ribbon under the conditions 2, 3, 4 and 5 of Table I, are 30.5, 26.4, 25.5 and 25.9°, the average of which corresponds to 300°K.

In Table II the average of the relative accommodation coefficients and the average of their values on the ribbon and on the wire are given together with the accommodation coefficients obtained by assuming that of CH_3CF_3 to be 1.0, and the values given by Amdur and Guildner⁸ and Eucken and Krome¹ for argon and helium on platinum. Table III contains the experimental heat capacities together with those calculated from spectroscopic data, exclusive of the contribution from the torsional degree of freedom, using the tables of Torkington⁹ for the vibrational contributions to the heat capacity. The average deviation from the mean, as indicated in Table III, ranged from 0.13 to 0.38. Gelles and Pitzer¹⁰ calculated 12.24 cal./mole/deg. for C_p at 300° for CHF_3 , and 16.22 cal./mole/deg. for CClF_3 . The latter value seemed high compared with the surrounding values in the table of Gelles and Pitzer and, therefore, it was recalculated from the data of Plyler and Benedict¹¹ giving 16.01 cal./mole/deg. Using the fundamental frequencies assigned by Pace¹² for ν_1 , ν_3 , ν_4 , ν_6 and those of Edgell and May¹³ for ν_2 and ν_5 we calculated a value of 10.25 cal./mole/deg. for C_p for CHF_3 . Thompson and Temple¹⁴ have calculated a value of 16.05 cal./mole/deg. for C_p of CClF_3 at 300°. The good agreement between the experimentally and spectroscopically determined heat capacities of these Freons indicates the accuracy of the wire-ribbon method.

The experimentally determined value of C_v for CH_3CF_3 at 300° is 16.83 cal./mole/deg. From the frequency assignments of Nielsen, Claassen and Smith,¹⁵ and from those of Thompson and Temple¹⁶ we calculated the heat capacity at constant volume for all the degrees of freedom except that of internal rotation to be 14.71 and 14.72 cal./mole/deg., respectively. The difference between these values and the experimental one is 2.115 cal./mole/deg. which is the contribution of restricted internal rotation to the heat capacity of CH_3CF_3 . Using this value together with molecular data evaluated from electron diffraction measurements by Brockway, Secrist and Lucht¹⁷ as reported by Nielsen, Claassen and Smith,¹⁵ and the tables of Pitzer and Gwinn¹⁸ we obtained 3370 cal./mole for the height of the

TABLE II
ACCOMMODATION COEFFICIENTS

Gas	a/a^A (av.)	a_R/a_R^A	a_W/a_W^A	a	Literature a	Ref.
A	1.00	1.00	1.00	0.907	0.925	8
					.91	1
He	0.4036	.368	8
					.41	1
CHF_3	0.979	0.972	0.980	.888	...	
CClF_3	0.976	0.976885	...	
CH_3CF_3	1.102	1.087	1.125	1.00	...	

TABLE III
HEAT CAPACITIES AT CONSTANT VOLUME AND 300°K.

Gas	Exptl. C_v , cal./mole/deg.	C_v Spectroscopic	
		(excl. of torsion)	Ref.
CHF_3	10.23 \pm 0.13	10.25	10, 12, 13
CClF_3	14.10 \pm 0.38	14.02	10, 11
		14.06	14
CH_3CF_3	16.83 \pm 0.18	14.71	15
		14.72	16

the mean of the individual values thus obtained was about 1% which means that the error in the average of the five to nine individual values is about 0.4%. From the geometry of the wire and ribbon, $1/6$ of the molecules striking the wire come

(7) "Handbook of Chemistry and Physics," Chemical Rubber Company, Cleveland, Ohio.

(8) I. Amdur and L. A. Guildner, Abstracts, Am. Chem. Soc. Meeting, Cincinnati, Ohio, 1955.

(9) P. Torkington, *J. Chem. Phys.*, **18**, 1373 (1950).

(10) E. Gelles and K. Pitzer, *J. Am. Chem. Soc.*, **75**, 5259 (1953).

(11) E. K. Plyler and W. S. Benedict, *J. Research, Natl. Bur. Standards*, **47**, 202 (1951).

(12) E. L. Pace, *J. Chem. Phys.*, **18**, 881 (1950).

(13) W. F. Edgell and C. May, *J. Chem. Phys.*, **21**, 1901 (1953).

(14) H. W. Thompson and R. B. Temple, *J. Chem. Soc.*, 1422 (1948).

(15) J. R. Nielsen, H. H. Claassen and D. C. Smith, *J. Chem. Phys.*, **18**, 1471 (1950).

(16) H. W. Thompson and R. B. Temple, *J. Chem. Soc.*, 1428 (1948).

(17) L. O. Brockway, J. H. Secrist, and C. M. Lucht, Abstracts, Am. Chem. Soc. Meeting, Buffalo, New York, 1942.

(18) K. S. Pitzer and W. D. Gwinn, *J. Chem. Phys.*, **10**, 428 (1942).

barrier hindering internal rotation in CH_3CF_3 . Since potential barriers are calculated from small differences between two experimental quantities, the possible error is always large, 200 cal./mole for a 0.02 cal./mole/deg. error in the torsional component of the heat capacity; and thus our value agrees well with those calculated by others: 3290 cal./mole by Nielsen, Claassen and Smith,¹⁵ 3450 cal./mole by Russell, Golding and Yost¹⁹ and 3250 cal./mole by Thompson and Temple.¹⁶

The results of this investigation have shown that

(19) H. Russell, D. R. V. Golding and D. M. Yost, *J. Am. Chem. Soc.*, **66**, 16 (1944).

the wire-ribbon method here described gives accurate heat capacity values which can be used directly with spectroscopic data to verify the assignments of fundamental vibrational frequencies and to estimate potential barriers hindering internal rotation.

Acknowledgments.—The authors wish to acknowledge the financial support of the Purdue Research Foundation and The Proctor and Gamble Company in the form of fellowships, and to thank H. Susi, Chemistry Department, Purdue University, for the purified sample of 1,1,1-trifluoroethane.

THE EXPLOSIVE OXIDATION OF DIBORANE

BY WALTER ROTH AND WALTER H. BAUER

Walker Laboratory, Rensselaer Polytechnic Institute, Troy, New York

Received November 11, 1955

Studies on the oxidation of diborane at the second pressure explosion limit have been extended. The effects of the addition of varying amounts of N_2 , He, A and H_2 to the stoichiometric mixture have been investigated. The results are shown to support a reaction mechanism involving bimolecular chain branching and trimolecular chain breaking. The gases, N_2 , He and A are shown to act as third bodies in excellent agreement with their behavior predicted by collision theory. The results of hydrogen addition indicate that the reaction $\text{BH}_3 + \text{B}_2\text{H}_6 \longrightarrow \text{B}_3\text{H}_7 + \text{H}_2$ occurs to a small extent, and that there is a competition between the reactions $\text{O} + \text{B}_2\text{H}_6 \longrightarrow \text{BH}_2\text{OH} + \text{BH}_3$ and $\text{O} + \text{H}_2 \longrightarrow \text{OH} + \text{H}$ for the removal of oxygen atoms.

The pressure^{1,2} and composition³ explosion limits have been studied for mixtures of diborane and oxygen. A mechanism for the reaction at the second pressure explosion limit was proposed.² This work represents an extension of the experimental studies at the second pressure explosion limit and provides additional support for the suggested mechanism.

The mechanism proposed² for the second pressure limit explosion involves bimolecular chain branching and trimolecular chain breaking reactions. Steady-state assumptions permitted the simplified limit expression

$$(M) = 2k_1/\Sigma k_{2,M} f_M \quad (a)$$

to be derived. Here (M) is the total concentration at the second limit and f_M are mole fractions. k_1 is the rate constant for the reaction



$k_{2,M}$ is the rate constant for the reaction



and is dependent on the nature of the third body, M. Equation (a) may be expanded and rearranged to give

$$f_{\text{B}_2\text{H}_6}/f_{\text{O}_2} + k_{2,\text{O}_2}/k_{2,\text{B}_2\text{H}_6} + k_{2,\text{M}}/k_{2,\text{B}_2\text{H}_6} + f_M/f_{\text{O}_2} = CT_2/f_{\text{O}_2} \exp(-\Delta E/RT_2) \quad (b)$$

M represents any third body except B_2H_6 or O_2 . $\Delta E = E_1 - E_2$, the difference between the activation energies of reactions (1) and (2). C is a constant and T_2 is the second limit temperature, both at constant pressure. This equation provides a

(1) F. P. Price, *J. Am. Chem. Soc.*, **72**, 5361 (1950).

(2) W. Roth and W. H. Bauer, "Fifth Symposium on Combustion," Reinhold Publ. Corp., New York, N. Y.

(3) A. J. Whatley and R. N. Pease, *J. Am. Chem. Soc.*, **76**, 1997 (1954).

means for testing the validity of the trimolecular chain breaking postulate. For example, the effect on the second limit explosion temperature of adding varying amounts of inert gases to a mixture whose $f_{\text{B}_2\text{H}_6}/f_{\text{O}_2}$ ratio remains constant permits a calculation of relative efficiencies of the inert constituents as third bodies in chain breaking. These efficiencies may then be compared with those calculated from collision theory.

Experimental

Nitrogen.—Matheson prepurified nitrogen (99.9% purity) was allowed to flow slowly through a series of two liquid nitrogen cooled traps and directly to a glass storage vessel. The initial storage pressure was about one atmosphere.

Helium.—Airco reagent helium in a 1-liter Pyrex break-seal vessel at one atm. was used without further purification. Mass spectrometric analysis by the manufacturer indicated the following impurities: oxygen, 0.001, nitrogen and/or carbon monoxide, 0.015, argon, 0.001, carbon dioxide, 0.001, and hydrocarbons, 0.005 mole per cent.

Argon.—Airco reagent argon in a 1-liter Pyrex break-seal vessel at one atm. was used without further purification. Mass spectrometric analysis by the manufacturer indicated the following impurities: hydrogen, 0.004, nitrogen and/or carbon monoxide, 0.004, oxygen, 0.002, and hydrocarbons, 0.005 mole per cent.

Hydrogen.—Matheson electrolytic hydrogen was passed through a De Oxo filter to remove oxygen and then through a series of two liquid nitrogen cooled traps and directly to a glass storage vessel. The initial storage pressure was one atm.

Diborane and oxygen were prepared and purified as previously described.²

Mixtures were prepared on a pressure basis. Detailed description of the apparatus and the heating method for determining explosion limits have been reported previously.² The only alteration in the procedure was in the method for cleaning vessels when the solid coating of reaction products became too heavy. Previously these had been treated with methyl alcohol, hot cleaning solution, distilled water and steam. In this work, it was found equally effective to flame the vessels during evacuation in order to remove coatings. Treatment of vessels in this manner caused a small shift in

the second limit for the pure stoichiometric mixture, $B_2H_6 + 3O_2$. Therefore, the effect of inert gas addition was determined by comparison with the result for $B_2H_6 + 3O_2$ in a flame treated vessel.

Explosion limit temperatures at constant pressure were compared rather than explosion limit pressures at constant temperature for reasons previously discussed.² The constant pressure chosen was 23 mm. It represented a point on the second limit for $B_2H_6 + 3O_2$ about midway between the first and third limits. Since only explosion limit temperatures at 23 mm. were significant, entire limit curves were not determined. Instead, linear interpolation of several points around 23 mm. was used to give the required value. In view of the steepness of the limits, linear interpolation could not have resulted in errors greater than $\pm 0.5^\circ$.

Results

Second limit explosion temperatures for stoichiometric mixtures of diborane-oxygen containing approximately 5, 10 and 20% of N_2 , He, A and H_2 were determined at a pressure of 23 mm. Results are given in Table I. Results for N_2 and He were

TABLE I

EFFECT OF ADDED GASES ON SECOND LIMIT EXPLOSION TEMPERATURE OF $B_2H_6 + 3O_2$

Gas added	Mole fraction added gas	Explosion temp. at 23 mm.
A	0	171
	0.058	165
	0.116	158
	0.214	161
H_2	0	171
	0.055	164
	0.101	160
	0.198	177

constant within experimental error. These gases could therefore be considered to have no significant effect on the second explosion limit. Argon and hydrogen, however, clearly exert a significant effect on the limit.

Discussion

The equivalence of behavior of He and N_2 indicates that they are equally effective as third

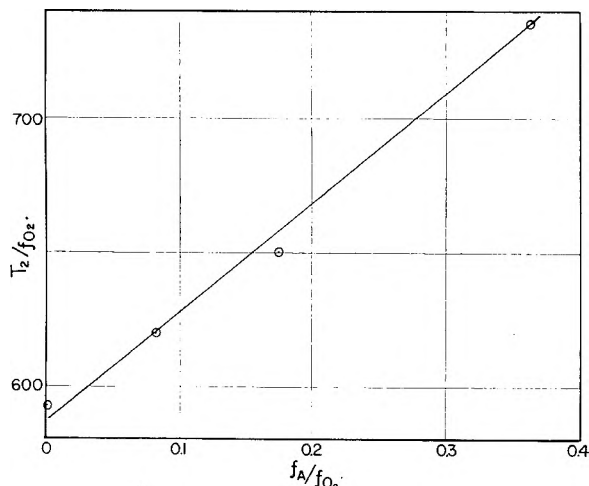


Fig. 1.—The effect of mixture composition on a function of the second explosion limit temperature at a pressure of 23 mm.

(4) R. C. Tolman, "Statistical Mechanics with Applications to Physics and Chemistry," A.S.C. Monograph, Chemical Catalog Co., New York, 1927, pp. 248, 327.

bodies in the chain breaking reaction,¹ *i.e.*, $k_{2,He}/k_{2,N_2} = 1$. It is interesting to compare this with the relative third body efficiencies calculated from collision theory. Thus, Tolman⁴ derived an expression for the termolecular collision frequency from which it can be shown that

$$\frac{Z_{He}}{Z_{N_2}} = \frac{\sigma_{23}^2(\mu_{12}^{-1/2} + \mu_{23}^{-1/2})}{\sigma_{24}^2(\mu_{12}^{-1/2} + \mu_{24}^{-1/2})} \quad (c)$$

Subscripts 1 and 2 refer to B_2H_6 and O_2 , respectively. Subscripts 3 and 4 refer to He and N_2 , respectively. σ is the mean of molecular diameters and μ is the reduced mass. Substitution of a range of molecular diameters calculated from viscosities and lists in several different tables and a molecular diameter for B_2H_6 estimated from its liquid density gives a range for Z_{He}/Z_{N_2} from 0.97 to 1.05. This is in agreement with the experimentally determined value of $k_{2,He}/k_{2,N_2}$.

Equation (b) may be applied to the results obtained from argon addition experiments. If E is assumed equal to zero and T_2/f_{O_2} is plotted against f_A/f_{O_2} , the straight line shown in Fig. 1 is obtained. Here, the slope, S , is equal to $C'(k_{2,A}/k_{2,B_2H_6})$ and the intercept, I , is equal to $C'[(f_{B_2H_6}/f_{O_2}) + (k_{2,O_2}/k_{2,B_2H_6})]$. Therefore

$$(k_{2,A}/k_{2,B_2H_6}) = (S/I)(f_{B_2H_6}/f_{O_2}) + (k_{2,O_2}/k_{2,B_2H_6})$$

It was found previously² that $E \leq 2$ kcal./mole. The assumption that it is equal to zero, however, does not significantly affect the ratio (S/I) . It also was shown previously that $(k_{2,O_2}/k_{2,B_2H_6}) \geq 1.50$. Therefore, since $(f_{B_2H_6}/f_{O_2})$ was always 0.33

$$k_{2,A}/k_{2,B_2H_6} \geq 1.83(S/I) \quad (d)$$

Using the method of least squares, the best straight line of Fig. 1 has a slope equal to 407 and an intercept equal to 586. Thus, $k_{2,A}/k_{2,B_2H_6} \geq 1.27$. A somewhat simpler treatment of the results from N_2 addition is possible since this had no significant effect on the second limit explosion temperature. If equation (b) is multiplied by f_{O_2} and then differentiated with respect to f_{O_2} and the condition $dT_2/df_{O_2} = 0$ applied, the equation

$$\frac{df_{B_2H_6}}{df_{O_2}} + \frac{k_{2,O_2}}{k_{2,B_2H_6}} + \frac{k_{2,N_2}}{k_{2,B_2H_6}} \times \frac{df_{N_2}}{df_{O_2}} = 0$$

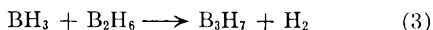
is obtained. Further, if the conditions $f_{B_2H_6} + f_{O_2} + f_{N_2} = 1$ and $f_{B_2H_6}/f_{O_2} = 1/3$ are applied, it is found that $k_{2,N_2}/k_{2,B_2H_6} \geq 1.38$. The minimum values $k_{2,A}/k_{2,B_2H_6} = 1.27$ and $k_{2,N_2}/k_{2,B_2H_6} = 1.38$ are for the condition $\Delta E = 0$. If these are compared, it is found that $k_{2,A}/k_{2,N_2} = 0.92$. This ratio is clearly independent of the actual value of ΔE . Application of equation (c) to this case gives a range of Z_A/Z_{N_2} from 0.88 to 0.92 in excellent agreement with the experimental value.

The agreement with collision theory constitutes strong evidence in favor of trimolecular chain breaking in the second limit explosive reaction of B_2H_6 and O_2 . The existence of a second pressure limit in branched chain explosions has necessitated the assumption that chain breaking reactions are of a higher molecularity than chain branching reactions.⁵ If the former are trimolecular, therefore, the latter must be bi- or unimolecular. Uni-

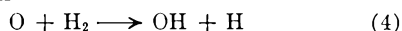
(5) B. Lewis and G. von Elbe, "Combustion, Flames and Explosions of Gases," Academic Press, New York, N. Y., 1951, p. 29-30.

molecular branching is inconceivable for the system under discussion in view of the pressures and the chemistry involved. Chain branching is thus probably bimolecular as was proposed.²

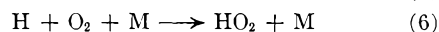
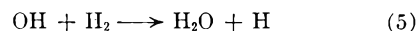
Addition of H₂ up to a mole fraction of 0.10 caused a decrease in explosion temperature. However, for a hydrogen mole fraction of 0.20, the explosion temperature increased. These results are explained by assuming that H₂ at relatively low concentration inhibits the reaction



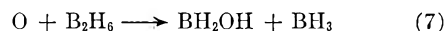
This reaction may normally remove the chain carrier, BH₃, to a small extent. Inhibition of reaction² would result in the observed decrease in explosion temperature. At higher H₂ concentration, oxygen atoms may be removed in the well known reaction



followed by



This would result in the increased explosion limit temperature which was observed when hydrogen concentration was increased sufficiently. It appears, therefore, that reaction (4) and



compete for the removal of O-atoms when the system contains hydrogen. Further, the validity of the foregoing would indicate that reaction (3) is not entirely negligible at the second explosion limit as was previously assumed. Indeed, the increasing importance of reaction (3) as the B₂H₆ concentration increases may explain the corresponding change in the slope of the second limit as (B₂H₆)/(O₂) is increased.²

A MODEL FOR CROSS-LINKED POLYELECTROLYTES¹

BY LEON LAZARE,^{2a} BENSON R. SUNDHEIM^{2b} AND HARRY P. GREGOR

Contribution from the Department of Chemistry of the Polytechnic Institute of Brooklyn, New York, and the Department of Chemistry, Washington Square College, New York University, New York

Received November 16, 1955

The swelling behavior of cross-linked polyelectrolytes is treated from the point of view of a non-ideal membrane equilibrium. In addition to osmotic effects and restraints provided by the cross-links, the effect of the charge of the network on the swelling equilibrium is taken into account. Numerical results are obtained for typical values of parameters of the system.

Introduction

Experimental studies of the swelling behavior of cross-linked polyelectrolytes such as ion-exchange resins immersed in salt solutions of varying concentrations indicate that these systems may be considered as a charged polymeric network and an internal solution consisting of interstitial water, counter-ions and diffusible electrolyte in equilibrium across a thermodynamic phase boundary with the ambient solution.³ The behavior is best described by plotting the swollen volume of one gram of dry resin, v_e , and the apparent mean (rational) activity coefficient, f_{\pm}^i , of the mobile ions in the internal solution as functions of the external electrolytic concentration. This apparent activity coefficient is obtained indirectly from concentration measurements, according to the following defined relationship, in which corrections arising from differences in standard states or osmotic pressure are omitted.⁴

$$f_{\pm}^i = \frac{(X_+^o X_-^o)^{1/2} v_e^o}{(X_+^i X_-^i)^{1/2}} \quad (1)$$

where X_+^i and X_-^i are the mole fractions of the cations and anions in the internal (i) solution,

(1) Based on a dissertation submitted by Leon Lazare in June, 1954, to the Graduate Faculty of the Polytechnic Institute of Brooklyn in partial fulfillment of the requirements for the degree of Doctor of Philosophy in Chemistry.

(2) (a) Chemical Construction Corporation, New York, N. Y. (b) New York University, New York, N. Y.

(3) H. P. Gregor, F. Gutoff and J. I. Bregman, *J. Colloid Sci.*, **6**, 245 (1951).

(4) f_{\pm}^i is a calcd. quantity, not strictly thermodynamic in nature.

including counter-ions, but not fixed charges, while $X_{\pm}^o = (X_+^o X_-^o)^{1/2}$ is the mole fraction of the ions in the ambient solution (^o).

The calculated relationships, which for any given resin differ somewhat for different salts, show the general behavior of Figs. 1a and 1b. The strong variation of f_{\pm}^i and its very low value for low external concentrations should be particularly noted. Deviations from ideality in the usual Debye-Hückel sense cannot account for this behavior.

Thermodynamic Treatment

For simplicity, it is assumed that the diffusible salt is a 1-1 electrolyte, that the ionized groups fixed to the polymeric network are univalent and that all mobile ions of the same sign are identical. We confine our analysis to that quantity of swollen

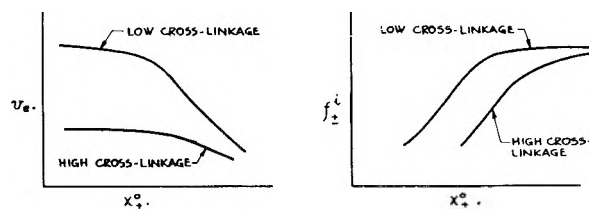


Fig. 1.—(a, left) Swelling and deswelling of ion exchange resins of high and low cross-linkage. Generalized curves based on data of Gregor, *et al.* (ref. 3). (b, right)—Mean internal activity coefficients of ions absorbed in ion exchange resins of high and low cross-linkage as functions of the salt activity in the external solution. Generalized curves based on data of Gregor, *et al.*

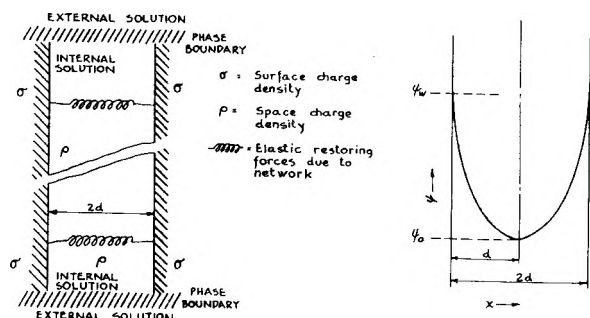


Fig. 2.—(a, left) Pictorial representation of model. (b, right) Variation of the potential ψ with distance.

polyelectrolyte containing one mole of fixed charges, N moles of diffusible electrolyte and a volume V of internal solution.

The procedure adopted is as follows: first, a general expression for the (Helmholtz) free energy of a resin phase is established from its principal contributions; second, a similar expression is given for the (external) solution phase; finally, a hypothetical, infinitesimal process is defined for the reversible transfer of electrolyte and other changes which may occur. Therefore, the Helmholtz free

Summing, we have

$$A^i = N_+^i(\mu_+^i)^i + N_-^i(\mu_-^i)^i + N_w^i(\mu_w^i)^i + A_c + A_D + A_e - P_s^i V^i + N_w^i RT \ln X_w^i + N_+^i RT \ln X_+^i + N_-^i RT \ln X_-^i \quad (2)$$

This communication is primarily concerned with the evaluation of the free energy of charging, A_c^i and the estimation of its relative importance in the distribution of mobile ions and in the swelling behavior.

The polyelectrolyte phase, so constructed, will later be equilibrated with the external aqueous phase containing the mobile ions. The Helmholtz free energy A^o of this phase may be expressed in an analogous manner as

$$A^o = N_+^o(\mu_+^o)^o + N_-^o(\mu_-^o)^o + N_w^o(\mu_w^o)^o - P_s^o V^o + N_w^o RT \ln X_w^o + (N_+^o + N_-^o) RT \ln X_{\pm}^o f_{\pm}^o \quad (3)$$

where $(\mu_+^o)^o$ and $(\mu_-^o)^o$ are the standard state chemical potentials of the ion species in the uncharged state; the contributions arising from the charging of the mobile species are taken into proper consideration by the use of the activity coefficient f_{\pm}^o .

To establish the fundamental equilibrium relationships between the internal and external phases, the conventional treatments for heterogeneous equilibrium must be modified to satisfy the assumed incompressibility of the mobile species. Thus, any infinitesimal process involving a change in volume dV must be accompanied by a change in either N , N_w or both. Similarly, a transfer of electrolyte dN must be accompanied by a change in volume or a change in N_w or both. Thus, we can consider V and N as the independent variables, and since $dV = dV^i = -dV^o$ and $dN = dN^i = -dN^o$ then

$$dA = \left[\left(\frac{\partial A^i}{\partial V} \right)_{N,T} - \left(\frac{\partial A^o}{\partial V} \right)_{N,T} \right] dV + \left[\left(\frac{\partial A^i}{\partial N} \right)_{V,T} - \left(\frac{\partial A^o}{\partial N} \right)_{V,T} \right] dN \quad (4)$$

Since V and N are independent variables, the criterion for equilibrium at constant temperature and total volume, namely, $dA = 0$, requires that the coefficients of dV and dN be identically zero, or

$$\left(\frac{\partial A^i}{\partial V} \right)_{N,T} = \left(\frac{\partial A^o}{\partial V} \right)_{N,T}; \quad \left(\frac{\partial A^i}{\partial N} \right)_{V,T} = \left(\frac{\partial A^o}{\partial N} \right)_{V,T} \quad (5a \text{ and } b)$$

It should be pointed out that N refers only to diffusible electrolyte, not to the solvent. Carrying out the differentiations

$$\left(\frac{\partial A^i}{\partial V} \right)_{N,T} = (\mu_w^i)^i \left(\frac{\partial N_w^i}{\partial V} \right)_{N,T} + \left(\frac{\partial A_D}{\partial V} \right)_T + \left(\frac{\partial A_e}{\partial V} \right)_T - P_s^i + RT \ln X_w^i \left(\frac{\partial N_w^i}{\partial V} \right)_{N,T} \quad (6)$$

and

$$\left(\frac{\partial A^o}{\partial V} \right)_{N,T} = (\mu_w^o)^o \left(\frac{\partial N_w^o}{\partial V} \right)_{N,T} - P_s^o + RT \ln X_w^o \left(\frac{\partial N_w^o}{\partial V} \right)_{N,T} \quad (7)$$

But

$$\left(\frac{\partial N_w^o}{\partial V} \right)_{N,T} = \left(\frac{\partial N_w^i}{\partial V} \right)_{N,T} = \frac{1}{v_w} \quad (8)$$

where v_w is the molar volume of water, and

$$(\mu_w^o)^o = (\mu_w^i)^i \quad (9)$$

energy of the resin phase is composed principally of the following contributions.

a. The standard state free energy of the water (subscript w) and of the mobile ions in a hypothetical uncharged state plus the standard state free energy (A_c) of the undeformed, uncharged polymer network

$$N_w^i(\mu_w^i)^i + N_+^i(\mu_+^i)^i + N_-^i(\mu_-^i)^i + A_c$$

b. The free energy of deformation of the uncharged polymer network to its final configuration, A_D

c. The free energy of mixing of the components

$$A_{\text{mix}}^i = N_w^i RT \ln X_w^i + N_+^i RT \ln X_+^i + N_-^i RT \ln X_-^i$$

The contribution to A_{mix}^i arising from the mixing of the polymer network with the internal solution is ignored in this treatment. Further comment is made in the discussion.

d. The free energy of adjustment of the hydrostatic pressure from the reference standard state to its final value, $-P_s^i V^i$.

e. The free energy of charging of all ionic species and the network, A_e .

Invoking equation 5a, we have

$$P_{OSM} + P_D + P_e + P_s^i - P_s^o = 0 \tag{10}$$

where

$$P_D = - \left(\frac{\partial A_D}{\partial V} \right)_{N,T}, P_e = - \left(\frac{\partial A_e}{\partial V} \right)_{N,T} \text{ and } P_{OSM} = \frac{RT}{v_w} \ln X_w^o / X_w^i$$

Noting that $P_s^i = P_s^o$

$$P_{OSM} + P_D + P_e = 0 \tag{11}$$

Similarly, A^i and A^o can be differentiated with respect to N

$$\left(\frac{\partial A^i}{\partial N} \right)_{v,T} = (\mu_+^o)^i + (\mu_-^o)^i + (\mu_w^o)^i \left(\frac{\partial N_w^i}{\partial N} \right)_{v,T} + \left(\frac{\partial A_e}{\partial N} \right)_{v,T} + RT \ln X_w^i \left(\frac{\partial N_w}{\partial N} \right)_{v,T}^i + RT \ln X_+^i + RT \ln X_-^i \tag{12}$$

and

$$\left(\frac{\partial A^o}{\partial N} \right)_{v,T} = (\mu_+^o)^o + (\mu_-^o)^o + (\mu_w^o)^o \left(\frac{\partial N_w^o}{\partial N} \right)_{v,T} + RT \ln X_w^o \left(\frac{\partial N_w}{\partial N} \right)_{v,T}^o + RT \ln (X^o_{\pm} f^o_{\pm})^2 \tag{13}$$

For the incompressible system under consideration

$$\left(\frac{\partial N_w^o}{\partial N} \right)_{v,T} = \left(\frac{\partial N_w^i}{\partial N} \right)_{v,T} = - \left(\frac{v_+ + v_-}{v_w} \right) \tag{14}$$

and assuming that the standard state chemical potentials for the ion species in the uncharged states are the same inside and out, we have from equation 5b the relationship

$$\mu_e + RT \ln \frac{X_+^i X_-^i}{(X^o_{\pm} f^o_{\pm})^2} + P_{OSM}(v_+ + v_-) = 0 \tag{15}$$

where

$$\mu_e = \left(\frac{\partial A_e}{\partial N} \right)_{v,T}$$

From the definition of f^i_{\pm} (equation 1)

$$\ln f^i_{\pm} = \frac{\mu_e}{2RT} + \frac{P_{OSM}(v_+ + v_-)}{2RT} \tag{16}$$

Description of the Model.—The interior of the resin is visualized as a pair or a series of pairs of interacting electrical double layers, maintained in mechanical equilibrium by elastic restoring forces. The charged planes, of surface charge density σ , represent the polymeric network and fixed charges; the planes are separated by a distance $2d$ and contain the internal solution between them. Since for a volume V of internal solution there corresponds one mole of fixed ionized groups, then

$$V\sigma/d = F \tag{17}$$

where F is the Faraday.

The elastic restoring force, or deformation pressure, P_D , due to the stretching of the cross-linked network, is taken as

$$P_D = - \frac{v_e - v_m}{v_m} Y \tag{18}$$

where v_e and v_m are the volumes of one gram of dry resin in the swollen and dry states, respectively, and Y is the linear elastic modulus. According to previous investigations⁵ in the field of polymeric networks, the elastic modulus is related to M_c , the average molecular weight of the network chain between cross-links, as

$$Y = \frac{3RT}{v_m M_c} \tag{19}$$

Furthermore, $v_e - v_m$ represents the volume of the internal solution corresponding to one gram of dry resin and is related to V according to the equation

$$v_e - v_m = c_E V \tag{20}$$

where c_E is the exchange capacity of one gram of dry resin. Substituting the above expressions for

(5) P. J. Flory and J. Rehner, *J. Chem. Phys.*, **11**, 512, 521 (1943).

Y and $v_e - v_m$ into equation 18, we obtain the relationship

$$P_D = - \frac{3c_E RT}{v_m^2 M_c} V \tag{21}$$

To describe the properties of the interplanar space, we assume that the space has a continuous charge density ρ and a fixed dielectric constant, D ; the electric potential ψ varies continuously throughout the field according to the Poisson equation

$$\nabla^2 \psi = - \frac{4\pi\rho}{D} \tag{22}$$

The local charge density is taken as the net charge due to the local ionic concentration; thus, for mobile ions having local concentrations n_+^i and n_-^i

$$\rho = (n_+^i - n_-^i)F \tag{23}$$

and

$$\frac{d^2\psi}{dx^2} = - \frac{4\pi F}{D} (n_+^i - n_-^i) \tag{24}$$

where x is the distance from the charge plane. In addition, it is assumed that n_+^i and n_-^i follow the Boltzmann distribution, *i.e.*

$$n_+^i = \eta_{\pm} \exp \left(- \frac{F\psi}{RT} \right) \tag{25}$$

$$n_-^i = \eta_{\pm} \exp \left(\frac{F\psi}{RT} \right) \tag{26}$$

where the constant η_{\pm} is defined by

$$\eta_+ = \frac{N}{\int \left[\exp \left(- \frac{F\psi}{RT} \right) \right] dV}$$

$$\eta_- = \frac{N + 1}{\int \left[\exp \left(\frac{F\psi}{RT} \right) \right] dV}$$

the zero point of ψ being so chosen that $\eta_+ = \eta_- = \eta_{\pm}$. Substituting these expressions into the Poisson equation leads to the Poisson-Boltzmann equation

$$\frac{d^2\psi}{dx^2} = \frac{8\pi F}{D} \eta_{\pm} \sinh\left(\frac{F\psi}{RT}\right) \tag{27}$$

or

$$\frac{d^2\phi}{d\xi^2} = \sinh \phi$$

where

$$\phi = \frac{F\psi}{RT}, \text{ and } \xi = \left[\frac{8\pi F^2}{DRT} \eta_{\pm}\right]^{1/2} x = \kappa x \tag{28}$$

The boundary conditions for this equation⁶ are

1. $\xi = 0, 2\kappa d; \phi = \phi_w, \psi = \psi_w$
2. $\xi = \kappa d; \phi = \phi_0, \psi = \psi_0, \frac{d\phi}{d\xi} = \frac{d\psi}{dx} = 0$ (29)

where w and o denote conditions at the wall and midpoint.

Mathematical Development

I. Extensive Properties.—The first integration of the Poisson-Boltzmann equation with substitu-

tion of the appropriate boundary conditions results in the equation

$$\frac{d\phi}{d\xi} = -(2 \cosh \phi - 2 \cosh \phi_0)^{1/2} \tag{30}$$

tion of the appropriate boundary conditions results in the equation

$$\operatorname{sn} v = \exp -\frac{\phi - \phi_0}{2}, m = \exp(-2\phi_0) \tag{31}$$

at

$$\xi = 0, 2\kappa d, \phi = \phi_w \text{ and } v = u$$

and at

$$\xi = \kappa d, \phi = \phi_0 \text{ and } v = \operatorname{sn}^{-1}(1) = K$$

where $\operatorname{sn} u = \exp -(\phi_w - \phi_0)/2$ and K is the complete elliptic integral of the first kind of parameter m .

By substitution

$$(2 \cosh \phi - 2 \cosh \phi_0)^{1/2} = \frac{dn v}{m^{1/4} \operatorname{tg} v} \tag{32}$$

but

$$\frac{d\phi}{d\xi} = -\frac{d}{d\xi} \ln(m^{1/4} \operatorname{sn}^2 v) = -\frac{2dn v}{\operatorname{tg} v} \frac{dv}{d\xi} \tag{33}$$

Hence

$$dv = \frac{d\xi}{2m^{1/4}} \tag{34}$$

Integrating between limits, we obtain

$$\kappa d = 2m^{1/4}(K - u) = 2m^{1/4}\mathfrak{F} \tag{35}$$

where \mathfrak{F} denotes $K - u$.

Other relationships are readily obtained, for example

$$\sigma = -\int_0^d \rho dx = \frac{D}{4\pi} \int_0^d \frac{d^2\psi}{dx^2} dx = -\frac{D}{4\pi} \left(\frac{d\psi}{dx}\right)_{x=0} = \frac{DRT}{4\pi F} \kappa \frac{dn u}{m^{1/4} \operatorname{tg} u} \tag{36}$$

Combining equations 17, 35 and 36 we find that

$$V\eta_{\pm} = m^{1/4} \mathfrak{F} \frac{\operatorname{tg} u}{dn u} \tag{37}$$

Further manipulation of the same three equations leads to the implicit relation

$$f_1 = V - \frac{DRT}{2\pi\sigma^2} \mathfrak{F} \frac{dn u}{\operatorname{tg} u} = 0 \tag{38}$$

The number of moles of diffusible electrolyte N is given as

$$N = \frac{V}{d} \eta_{\pm} \int_0^d \exp\left(-\frac{F\psi}{RT}\right) dx = \frac{V\eta_{\pm}}{\kappa d} \int_u^K 2m^{3/4} \operatorname{sn}^2 v dv \tag{39}$$

Substituting the expressions for $V\eta_{\pm}$ and κd , we have

$$N = \frac{\operatorname{tg} u}{dn u} \int_u^K m \operatorname{sn}^2 v dv \tag{40}$$

Integration leads to a second implicit relation

$$f_2 = N - \frac{\operatorname{tg} u}{dn u} (\mathfrak{F} - \epsilon) = 0 \tag{41}$$

where

$$\epsilon = \int_u^K dn^2 v dv = \frac{E}{K} (K - u) - Z(u) \tag{42}$$

E being the complete elliptic integral of the second kind of parameter m and $Z(u)$ the Jacobian zeta function of argument u and parameter m .

(6) See, e.g., E. J. W. Verwey and J. Th. G. Overbeek, "Theory of the Stability of Lyophobic Colloids," Elsevier Press, 1948, Chapter IV.

In addition to the quantities V and N , the free energy of charging, A_e , lends itself readily to calculation. This free energy consists of the reversible work of charging the surfaces and the mobile ions in the interplanar space. For convenience, the path at constant ψ_w is chosen

$$A_e = F\psi_w + \int_0^V \int_0^1 \rho(\lambda)\psi(\lambda) \frac{d\lambda}{\lambda} dV \quad (43)$$

λ being the degree of charging. By partial integration and substitution of boundary conditions,⁷ this equation reduces to

$$A_e = F\psi_w - 2RT\eta_{\pm} \int_0^V \int_0^{F/RT} \sinh\left(\frac{\lambda F\psi}{RT}\right) d\left(\frac{\lambda F\psi}{RT}\right) dV = \frac{D}{8\pi} \int_0^V \left(\frac{d\psi}{dx}\right)^2 dV \quad (44)$$

or

$$\frac{A_e}{RT} = \phi_w - 2V\eta_{\pm}(\cosh \phi_0 - 1) - \frac{2V\eta_{\pm}}{\kappa d} \int_0^{\kappa d} \left(\frac{d\phi}{d\xi}\right)^2 d\xi \quad (45)$$

But

$$\int_0^{\kappa d} \left(\frac{d\phi}{d\xi}\right)^2 d\xi = \int_{\phi_0}^{\phi_w} (2 \cosh \phi - 2 \cosh \phi_0)^{1/2} d\phi = 2 \int_{\phi_0}^{\phi_w} \frac{e^{-\phi} d\phi}{(2 \cosh \phi - 2 \cosh \phi_0)^{1/2}} + 2(2 \cosh \phi_w - 2 \cosh \phi_0)^{1/2} - 2\kappa d \cosh \phi_0 \quad (46)$$

Integrating and combining with the expression for N , we have on substituting back into equation 45

$$\frac{A_e}{RT} = \phi_w + 2V\eta_{\pm}(\cosh \phi_0 + 1) - \frac{4V\eta_{\pm}}{\kappa d} (2 \cosh \phi_w - 2 \cosh \phi_0)^{1/2} - 4N \quad (47)$$

Further substitutions result in the third implicit relation

$$f_3 = \frac{A_e}{RT} + \ln(m^{1/2}\text{sn}^2 u) - \frac{2\pi\sigma^2}{DRT} V \frac{\text{tg}^2 u}{\text{dn}^2 u} (1 + m^{1/2})^2 + 4N + 2 = 0 \quad (48)$$

II. Intensive Properties.—The three implicit relationships, f_1 , f_2 and f_3 , correlating m and u with the three thermodynamic variables, V , N and A_e , permit the evaluation of μ_e and P_e . Referring to equation 16 and neglecting the osmotic pressure effect on the activity of the ions, we note

$$\ln f^{i\pm} = \frac{1}{2RT} \left(\frac{\partial A_e}{\partial N}\right)_{T,V} \quad (49)$$

This partial derivative is obtained readily by applying the method of Jacobians to the three implicit functions, f_1 , f_2 and f_3

$$\begin{aligned} \ln f^{i\pm} &= -\frac{1}{2RT} \frac{J \begin{pmatrix} f_1, f_2, f_3 \\ N, m, u \end{pmatrix}}{J \begin{pmatrix} f_1, f_2, f_3 \\ A_e, m, u \end{pmatrix}} = -2 + \frac{J \begin{pmatrix} f_1, f_3 \\ m, u \end{pmatrix}}{2J \begin{pmatrix} f_1, f_2 \\ m, u \end{pmatrix}} \\ &= -2 + \frac{1}{2} \frac{\frac{\partial f_1}{\partial m} \frac{\partial f_3}{\partial u} - \frac{\partial f_1}{\partial u} \frac{\partial f_3}{\partial m}}{\frac{\partial f_1}{\partial m} \frac{\partial f_2}{\partial u} - \frac{\partial f_1}{\partial u} \frac{\partial f_2}{\partial m}} \end{aligned} \quad (50)$$

Similarly

$$\begin{aligned} P_e &= -\left(\frac{\partial A_e}{\partial V}\right)_{T,N} = \frac{J \begin{pmatrix} f_1, f_2, f_3 \\ V, m, u \end{pmatrix}}{J \begin{pmatrix} f_1, f_2, f_3 \\ A_e, m, u \end{pmatrix}} = -\frac{2\pi\sigma^2}{D} \frac{\text{tg}^2 u}{\text{dn}^2 u} (1 + m^{1/2})^2 + RT \frac{J \begin{pmatrix} f_2, f_3 \\ m, u \end{pmatrix}}{J \begin{pmatrix} f_1, f_2 \\ m, u \end{pmatrix}} \\ &= -\frac{2\pi\sigma^2}{D} \frac{\text{tg}^2 u}{\text{dn}^2 u} (1 + m^{1/2})^2 + RT \frac{\frac{\partial f_2}{\partial m} \frac{\partial f_3}{\partial u} - \frac{\partial f_2}{\partial u} \frac{\partial f_3}{\partial m}}{\frac{\partial f_1}{\partial m} \frac{\partial f_2}{\partial u} - \frac{\partial f_1}{\partial u} \frac{\partial f_2}{\partial m}} \end{aligned} \quad (51)$$

The evaluation of the six partial derivatives $\partial f_1/\partial u$, $\partial f_1/\partial m$, $\partial f_2/\partial u$, $\partial f_2/\partial m$, $\partial f_3/\partial u$, $\partial f_3/\partial m$ is straightforward but very lengthy and no attempt is made to show the evaluation here; however, substitution of the resulting expressions into equations 50 and 51 leads to the relationships

$$\ln f^{i\pm} = -2 - \frac{\left\{ (1 + m^{1/2})^2 \mathfrak{F} \left\{ \frac{\text{tg} u}{\text{dn} u} \left[\frac{1-m}{2} + 2m^{1/2} - \text{dn}^2 u \right] + \left(\text{tg}^2 u + \frac{1}{\text{dn}^2 u} \right) [\epsilon - (1 - m^{1/2})\mathfrak{F}] \right\} \right.}{\left. - \frac{\text{dn} u}{\text{tg} u} \left[\epsilon - \mathfrak{F} \left(\frac{1-m}{2} \right) \right] + \frac{1-m}{2} - \text{dn}^2 u \right\}} \frac{\text{dn}^2 u - 1 + \left(\text{tg}^2 u + \frac{1}{\text{dn}^2 u} \right) [(\mathfrak{F} - \epsilon)^2 - m\mathfrak{F}^2] - 2m \frac{\text{tg} u}{\text{dn} u} [\mathfrak{F} + \text{sn}^2 u (\mathfrak{F} - \epsilon)]}{\quad} \quad (52)$$

(7) E. J. W. Verwey and J. T. G. Overbeek, "Theory of the Stability of Lyophobic Colloids" (Chapter V).

and

$$P_e \frac{D}{\pi^2} = \frac{-2 \frac{\text{tg}^2 u}{\text{dn}^2 u} \left\{ (1 + m^{1/2})^2 [\epsilon - (1 - m^{1/2})\mathfrak{F}] \left\{ 2 \frac{\text{tg} u}{\text{dn} u} (1 - \text{dn}^2 u) + \left(\text{tg}^2 u + \frac{1}{\text{dn}^2 u} \right) [\epsilon - (1 - m^{1/2})\mathfrak{F}] \right\} \right.}{\left. + \frac{\text{tg} u}{\text{dn} u} (1 - m)^2 (F - \epsilon) - \frac{\text{dn} u}{\text{tg} u} [(1 + m)\epsilon - (1 - m)\mathfrak{F}] - 2m - 2m^{1/2}(1 - \text{dn}^2 u) \right\}}{\text{dn}^2 u - 1 + \left(\text{tg}^2 u + \frac{1}{\text{dn}^2 u} \right) [(\mathfrak{F} - \epsilon)^2 - m\mathfrak{F}^2] - 2m \frac{\text{tg} u}{\text{dn} u} [\mathfrak{F} + \text{sn}^2 u (\mathfrak{F} - \epsilon)]} \quad (53)$$

Other thermodynamic properties expressed in terms of m , u and the physical parameters D and σ are readily obtainable. From the definition of the activity coefficient (equation 1), we obtain the salt activity in the ambient solution

$$a^{\circ\pm} = x^{\circ\pm} f^{\circ\pm} = f^{\circ\pm} (X_+^i X_-^i)^{1/2} \sim v_w f^{\circ\pm} \frac{N}{V} \left(1 + \frac{1}{N} \right)^{1/2} \sim \frac{2\pi\sigma^2}{DRT} v_w \left\{ f^{\circ\pm} \frac{\text{tg}^2 u}{\text{dn}^2 u} \times \frac{\mathfrak{F} - \epsilon}{\mathfrak{F}} \left[1 + \frac{\text{dn} u}{\text{tg} u (\mathfrak{F} - \epsilon)} \right]^{1/2} \right\} \quad (54)$$

The osmotic pressure P_{osm} , is obtained as

$$P_{\text{osm}} = \frac{RT}{v_w} \ln \frac{X_w^o}{X_w^i} \sim \frac{RT}{v_w} [X_+^i + X_-^i \sim 2X^{\circ\pm}] - \frac{RT}{V} \left\{ 1 + 2N \left[1 - f^{\circ\pm} \left(1 + \frac{1}{N} \right)^{1/2} \right] \right\} \quad (55)$$

assuming $f_{\pm}^{\circ} = 1$, or

$$P_{\text{osm}} \times \frac{D}{\pi\sigma^2} \sim \frac{2\text{tg} u}{\text{dn} u} \left\{ 1 + 2(\mathfrak{F} - \epsilon) \frac{\text{tg} u}{\text{dn} u} \left[1 - f^{\circ\pm} \left(1 + \frac{\text{dn} u}{\text{tg} u (\mathfrak{F} - \epsilon)} \right)^{1/2} \right] \right\} \quad (56)$$

Combining equations 20 and 38 results in the following expression for $v_e - v_m$, the amount of swelling per gram of dry resin

$$v_e - v_m = c_E V = \frac{DRTc_E}{2\pi\sigma^2} \mathfrak{F} \frac{\text{dn} u}{\text{tg} u} \quad (57)$$

Substitution of this last equation into the expression for the deformation pressure (equation 21) gives

$$-P_D \times \frac{D}{\pi\sigma^2} = (P_e + P_{\text{osm}}) \frac{D}{\pi\sigma^2} = \frac{6c_E}{M_C} \left(\frac{DRT}{2\pi v_m \sigma^2} \right)^2 \mathfrak{F} \frac{\text{dn} u}{\text{tg} u} \quad (58)$$

Based on the above relationships, six functions of m and u are available which completely describe the behavior of the model

$$f_I(m, u) = \ln f^{\circ\pm} \quad (\text{see eq. 52})$$

$$f_{II}(m, u) = \frac{DRT}{\pi\sigma^2 v_w} a^{\circ\pm} \quad (\text{see eq. 54})$$

$$f_{III}(m, u) = (v_e - v_m) \frac{2\pi\sigma^2}{DRTc_E} \quad (\text{see eq. 57})$$

$$f_{IV}(m, u) = P_e \times \frac{D}{\pi\sigma^2} \quad (\text{see eq. 53})$$

$$f_V(m, u) = P_{\text{osm}} \times \frac{D}{\pi\sigma^2} \quad (\text{see eq. 56})$$

$$f_{VI}(m, u) = \frac{f_{IV} + f_V}{f_{III}} = \frac{6c_E}{M_C} \left(\frac{DRT}{2\pi v_m \sigma^2} \right)^2 \quad (\text{see eq. 57 and 58})$$

$f_{VI}(m, u)$ is completely fixed by physical parameters, some directly measurable as c_E , and v_m , and some assumed, but whose choice is founded on fairly sound bases. For the dielectric constant, D , we use the value for water. M_C can be indirectly estimated from the amount of cross-linking agent used in making the resin. On the other hand, σ , the effective surface charge density of the planes, is chosen solely on the basis of obtaining the fairest agreement with the experimental data. Having specified these parameters and consequently the quantity

$$\frac{6c_E}{M_C} \left(\frac{DRT}{2\pi v_m \sigma^2} \right)^2$$

the relationship between m and u is then established by f_{VI} . The other thermodynamic quantities are then computed from the correlated sets of values of m and u , substituted in the appropriate function.

Numerical Computations.—Complete grids for all six functions were computed for values of the parameter m , equal to 0.05, 0.10, 0.20, etc., up to and including 0.90, and corresponding values of the argument, u , starting with 0.10 and approaching K at intervals of 0.10. The numerical values of the elliptic functions $\text{sn} u$, $\text{cn} u$, $\text{dn} u$, as well as the Jacobian zeta function, $Z(u)$, were obtained directly from the tables of W. E. Milne-Thomson⁸ for values of m equal to 0.10 through 0.90, while values of these functions corresponding to m equal to 0.05 were obtained by interpolation.

Thus for any established value of

$$\frac{6c_E}{M_C} \left(\frac{DRT}{2\pi v_m \sigma^2} \right)^2$$

and m (or u), a set of Lagrangian interpolation coefficients were determined from values lifted from the grid for f_{VI} ; and, employing this set of coefficients, the corresponding values of the other five functions, as well as u (or m), were obtained directly by interpolating within the appropriate grid. For convenience, the interpolations were based on the logarithmic values to the base ten for f_{VI} , and f_{III} , and the arithmetic values of f_I , f_{II} , f_{VI} and f_V . The computation of the seven desired physical quantities $f^{\circ\pm}$, $a^{\circ\pm}$, $v_e - v_m$, P_e , P_{osm} , ψ_0 and ψ_w follows immediately, the last two being obtained from the relationships

$$\psi_0 = -\frac{RT}{F} \ln m^{1/2} \quad (59)$$

and

$$\psi_w = -\frac{RT}{F} \ln (m^{1/2} \text{sn}^2 u) \quad (60)$$

(8) W. E. Milne-Thomson, "Jacobian Elliptic Function Tables," Dover.

Complete curves were plotted from computed values of the above seven quantities based on five sets of physical parameters. These sets made use of these physical parameters, common to all: $D = 78.55$; $T = 298.16^\circ\text{K.}$; $c_E = 0.005$ equivalents per gram; $v_m = 0.80 \text{ cm.}^3$ per gram. The combinations of σ and M_c employed are shown in Table I.

TABLE I

Faradays/cm. ²	M_c	$\frac{6c_E}{M_c} \left(\frac{DRT}{2\pi v_m \sigma^2} \right)^2$
1.0×10^{-10}	1,000	6.4234
1.0×10^{-10}	3,000	2.1411
1.0×10^{-10}	10,000	0.64234
2.0×10^{-10}	1,000	.40146
2.0×10^{-10}	10,000	.040146

The values of M_c employed, namely, 1,000, 3,000 and 10,000, correspond roughly to the divinylbenzene sulfonated polystyrene resins DVB-17, DVB-6 and DVB-2, respectively.

Discussion of Results

The quantities f_{\pm}^i , $v_e - v_m$, P_e and P_{osm} , ψ_0 and ψ_w plotted as functions of the salt activity in the ambient solution are shown in Figs. 3, 4, 5 and 6. The marked dependence of f_{\pm}^i on the external salt concentration, the effects of higher cross-linking and the general shape of the curve show agreement with the experimental data; this is also true of the shape of the deswelling curve and the effect of cross-linkage.

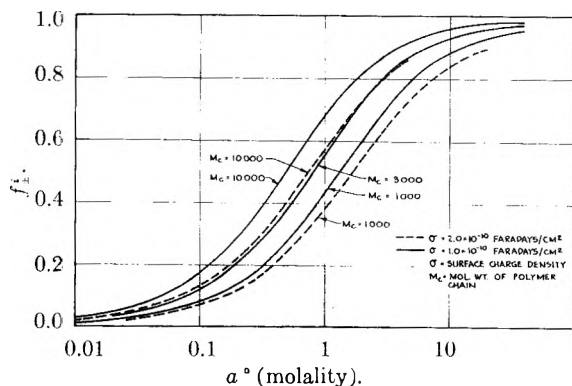


Fig. 3.—Internal mean activity coefficient (rational) of mobile ions in resin interior versus molality of the external solution.

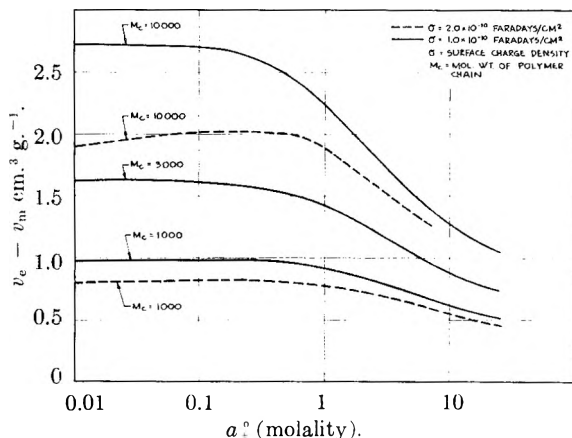


Fig. 4.—Total expansion per gram of dry resin versus molality of the external solution.

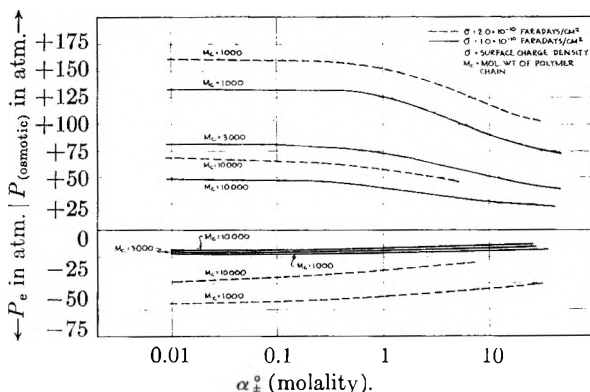


Fig. 5.—Electrical pressure and osmotic pressure versus molality of the external solution.

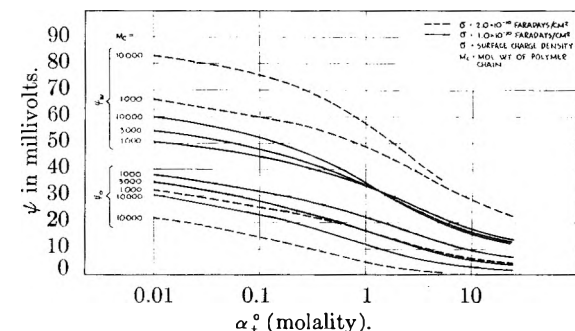


Fig. 6.—Wall and midpoint potentials in millivolts versus molality of the external solution.

The net sum of the electrical and osmotic pressure is always positive, indicating that, as in other proposed theories of polyelectrolytes and colloids, the effect of the electric double layer system is that of repulsion, countered in this case by the elastic restoring force, P_D . That the sign of P_e is negative is not necessarily in itself a contradiction, since the partial derivative $-(\partial A_e / \partial V)_{T,N}$ defines only a portion of the process, while the differentiation as performed by other investigators is generally a one-step operation.

Noteworthy are the relatively low values of ψ_0 and ψ_w which are sufficient to produce these marked effects on the internal activity coefficient; for example, for σ equal to 1.0×10^{-10} faraday per square centimeter, a value of ψ_w of sixty millivolts results in f_{\pm}^i being equal to 0.03. Thus the model is capable of accounting for quite radical effects of ionic binding without invoking extreme boundary conditions.

Discussion of Errors

Some consideration is directed to the magnitude of the errors introduced with the various assumptions throughout the development of the problem; in essence these are as follows.

1. Assuming that the salt activity coefficient in the external solution, f_{\pm}^o , is unity, and at the same time neglecting the effect on the internal activity coefficient f_{\pm}^i of the discreteness of the mobile ions (what may be called the local Debye-Hückel term).

2. Assuming that

$$\ln \frac{x_w^o}{x_w^i} = [X^+ + X^- - 2X^o_{\pm}]$$

The effect of these two assumptions on the osmotic pressure is small, since they tend to cancel each other.

3. Neglecting the osmotic pressure effect on f_{\pm}^i ; this presents an error tending to zero with higher electrolyte concentrations, and never exceeding ten per cent. in the dilute range.

4. Neglecting the mixing effects of the internal solution and the polymeric network, which would give rise to two important effects.

a. The activity coefficient of the water and the mobile ions would be multiplied by the factor

$$\exp \left\{ \frac{K}{2} \left(\frac{v_m}{v_e} \right)^2 + \ln \left(1 - \frac{v_m}{v_e} \right) + \frac{v_m}{v_e} \right\}$$

or

$$\exp \left\{ \left(\frac{v_m}{v_e} \right)^2 \left[\frac{K-1}{2} - \frac{1}{3} \frac{v_m}{v_e} - \frac{1}{4} \left(\frac{v_m}{v_e} \right)^2 \dots \right] \right\}$$

where K is the Van Laar dilution coefficient.

b. This factor applied to the activity of water in the internal solution increases the osmotic pressure by

$$- \frac{RT}{v_w} \left(\frac{v_m}{v_e} \right)^2 \left[\frac{K-1}{2} - \frac{1}{3} \frac{v_m}{v_e} - \frac{1}{4} \left(\frac{v_m}{v_e} \right)^2 \dots \right]$$

in addition to the secondary effects due to changes in the computed value of x_{\pm}^0 , resulting from the changes in f_{\pm}^i .

From a phenomenological viewpoint, it appears that the omission of the consideration of the network is justified. The Van Laar coefficient is not

known and from the experimental data of Gregor, Sundheim and Waxman,⁹ it appears that the net effect would be small.

Conclusions

A model has been developed which satisfactorily explains the generalized swelling behavior of cross-linked polyelectrolytes immersed and equilibrated with aqueous salt solutions, although no attempt is made to explain the specific action of the various salts. The application of the electrical double layer theory to represent the interior of the swollen resin appears to be valid, provided proper care is taken in choosing the normalization constant of the Boltzmann distribution expression, and including this "constant" when performing the various differentiations necessary in evaluating the electrical pressure and the internal activity coefficient. The internal activity coefficient and the swollen volume of one gram of dry resin, are computed as functions of the salt concentration in the ambient solution; the resulting curves are in agreement with the generalized curves taken from previously compiled experimental data.

Acknowledgments.—The authors are indebted to Mr. George Anick, who performed the tedious and lengthy numerical computations. This work was supported in part by the Office of Naval Research.

(9) H. P. Gregor, B. R. Sundheim and M. H. Waxman, *THIS JOURNAL*, **57**, 974 (1953).

REVERSIBLE ASSOCIATION OF CELLULOSE NITRATE IN ETHANOL¹

BY SEYMOUR NEWMAN,† WILLIAM R. KRIGBAUM AND DEWEY K. CARPENTER

Contribution from Allegany Ballistics Laboratory,² Hercules Powder Company, Cumberland, Md., and the Department of Chemistry, Duke University, Durham, N. C.

Received November 19, 1955

Cellulose nitrate in ethanol forms a thermally reversible gel on warming. Gelation is preceded by the growth of molecular aggregates, and the gel "melts" to a solution containing aggregates. These appear to be less ordered than the gel, but to be more compact than gelatin aggregates. Study of the gelation process reveals that the relative viscosity and the breadth of the molecular size distribution increase tremendously as the system proceeds toward gelation, in exact analogy with the behavior observed during the polymerization of polyfunctional units as the gel point is approached. The rate of gelation is very sensitive to temperature, closely resembling crystallization in this respect. There are presented osmotic pressure, light scattering and viscosity measurements for dilute solutions, and measurements of the equilibrium sorption of ethanol vapor by the polymer. The osmotic data yield $\Theta = 301\text{--}310^\circ\text{K}$. and $\psi_1 = -2$ to -4 for solutions of individual cellulose nitrate molecules in ethanol. Comparison of the theoretical liquid-liquid and crystal-liquid phase diagrams reveals that only the latter allows a representation of the observed concentration dependence of the gel "melting" temperature, thus confirming the supposition that the "cross-links" are crystallites.

Dilute solutions of cellulose nitrate in ethanol set to a gel on warming. The gel is slightly turbid and relatively elastic, superficially resembling gelatin-water gels to a remarkable degree. The modulus of the gel increases with increasing concentration, and also depends upon the molecular weight and the nitrogen content of the polymer. Once the gel has formed, the solvent may be replaced by a non-solvent with no external collapse of the structure. If ethanol is replaced by benzene

the rigidity increases, and because the refractive indices of benzene and cellulose nitrate are nearly the same, the turbidity diminishes markedly.

The formation of thermally reversible cellulose nitrate gels is not peculiar to ethanol, but has been observed in a variety of single solvent and mixed-solvent systems. We may cite as examples di-(1-methyl-3-propoxyhexyl)-succinate,³ acetone-chloroform, nitromethane-chloroform, etc. On cycling the temperature, these cellulose nitrate gels may be made to liquefy and reset, as do other thermally reversible gels (*e.g.*, gelatin in water,⁴

† Monsanto Chem. Co., Springfield, Mass.

(1) Presented at the Symposium on Thermodynamics of High Polymer Solutions, 128th meeting of the American Chemical Society, Minneapolis, Minnesota, Sept. 15, 1955.

(2) The Allegany Ballistics Laboratory is a facility owned by the U. S. Navy and operated by the Hercules Powder Company under Contract NOrd 10431.

(3) A. K. Doolittle, *Ind. Eng. Chem.*, **38**, 535 (1946).

(4) J. D. Ferry, Chapter I in "Advances in Protein Chemistry," Vol. IV, edited by M. L. Anson and J. T. Edsall, Academic Press, Inc., New York, N. Y., 1948.

poly-(vinyl chloride) in dioxane,⁵ and poly-(acrylonitrile) in dimethylformamide⁶). The formation of this type of gel is generally assumed to involve demixing as the solvent is made poorer, either by a change of temperature or by the addition of a non-solvent. It is not evident, however, whether the onset of gelation corresponds to thermodynamic conditions consistent with a liquid-liquid transition, a crystal-liquid transition, or to some other set of conditions. Experimental studies in this direction are largely non-existent, despite their obvious bearing on gel structure.

The work reported here is divided into two portions. In the first of these, the formation and properties of the cellulose nitrate aggregates and gels are examined and compared with those formed from other polymers. The effects of concentration, temperature and time on the state of aggregation are studied. The second part is concerned with a thermodynamic study of the cellulose nitrate-ethanol system, and with the inferences drawn therefrom concerning the formation and structure of the gel.

Experimental

Materials.—The major portion of the data was gathered on two cellulose nitrate fractions, IIA-3 and IIC-12 of about 12.6% nitrogen content, and on an unfractionated sample of 12.2% nitrogen content designated X-183. The fractions were prepared⁷ from the commercial cellulose nitrate by fractional precipitation from acetone solution, using hexane as the precipitant. The raw polymer was first separated into three broad fractions, each of which was further refractionated two times. Approximately twenty fractions, varying in molecular weight from 20,000 to 200,000, were obtained from each of the three original fractions.

Commercial U.S.P. anhydrous ethanol was further dried by refluxing with magnesium ethylate according to the procedure described by Fieser.⁸ Water analysis of the distilled alcohol by Karl Fischer titration disclosed less than 0.01% moisture. In subsequent manipulations precautions were taken to minimize the pick-up of moisture through exposure to the atmosphere.

Dissolution of cellulose nitrate in ethanol required severe cooling. Solutions were prepared in from one to three days by shaking the flasks immersed in Dry Ice-acetone mixtures. These were generally clear at low temperatures, and became slightly turbid on warming toward the temperatures at which gelation occurred. Solutions of fraction IIA-3 frequently retained a faint turbidity at all temperatures, indicating the presence of some insoluble material.

Viscosities.—Viscosity measurements were performed using Ubbelohde viscometers modified to exclude moisture. Two procedures were used for this purpose, depending on the temperature and the duration of the experiment. In the first of these, drying tubes were fitted to the open ends of the viscometer, while in the second the open ends were interconnected and completely closed off from the atmosphere. The latter system included a piston and bladder type air reservoir to allow movement of the polymer solution into the bulb of the viscometer, and to permit flow through the capillary without pressure differences developing in any part of the system.

Concentrations for the intrinsic viscosity determinations were chosen to yield relative viscosities of about 1.13 for the most dilute solutions. Extrapolation of η_{sp}/c and $(\ln \eta_{rel})/c$ was performed using the customary double plot: the best pair of lines having a common intercept and fulfilling the requirement $k' - k'' = 0.5$ was used.

(5) P. Doty, H. Wagner and S. Singer, *THIS JOURNAL*, **51**, 32 (1947).

(6) J. Bisschops, *J. Polymer Sci.*, **12**, 583 (1954); **17**, 89 (1955).

(7) We are indebted to Dr. P. Drechsel for supplying the polymer samples.

(8) L. F. Fieser, "Experiments in Organic Chemistry," D. C. Heath and Co., Boston, 1941.

Osmotic Pressure.—Osmotic measurements were carried out with Zimm osmometers immersed in a large bath regulated to better than 0.01°. The outer jacket of the osmometer was closed by a ground glass joint and mercury seal. In this manner the entire osmometer was isolated from the atmosphere. This modification was essential in view of the hygroscopicity of anhydrous ethanol, the low temperature employed, and the marked effect of water in inducing gelation.

Light Scattering.—The photometer has been described elsewhere.⁹ A cooling unit and thermostated jacket surrounding the cell permitted temperature control to within $\pm 0.1^\circ$ during a series of measurements. The incident light from a mercury AH-4 lamp was vertically polarized. A color filter transmitting 436 m μ was located between the scattering cell and the phototube, thus preventing any fluorescent light of other frequencies from reaching the detector. Purification of the solutions was accomplished by pressure filtration under anhydrous conditions.

Vapor Sorption.—A modified McBain-Bakr sorption balance¹⁰ was used to obtain the cellulose nitrate-ethanol sorption isotherm. The quartz spiral had a sensitivity of 0.8 mm./mg. Use of a traveling microscope allowed weight changes of 0.01 mg. to be detected. Pressures within the weighing chamber were measured to ± 0.5 mm. using a mercury manometer. The weighing chamber and vapor reservoir were located inside an air thermostat maintained to within $\pm 0.1^\circ$. To prevent condensation in the manometer and connecting tubes, these were placed in a separate chamber at a slightly higher temperature.

I. Aggregation Studies

Concentration Dependence of the Gelation and Aggregation Temperatures.—On cooling a cellulose nitrate-ethanol gel, liquefaction is observed to take place over a temperature range of a few degrees. Rate of cooling and previous thermal history influence the nature of the gel. However, the temperature of liquefaction does not represent the condition for the complete disappearance of aggregates; molecular clusters are still present below the "melt" temperature of the gel. In the neighborhood of this condition the system is thixotropic, and mechanical shaking or the shear field of a viscometer disrupts the gel structure. The highly associated solutions also exhibit a considerable degree of structural viscosity. Measurement of the gel "melt" temperatures were, therefore, necessarily crude.

The temperature of gel liquefaction was observed directly as the temperature at which the gel flows under its own weight. These temperatures are shown plotted against the volume fraction of polymer for cellulose nitrate sample X-183 (12.2% N) in Fig. 1, and are represented for fraction IIC-12 ($\langle M \rangle_n = 197,000$) by curve A in Fig. 2. Lack of material prevented an extensive investigation of fraction IIA-3 ($\langle M \rangle_n = 56,000$); however, as shown in the insert to Fig. 2, for $v_2 = 0.006$ and 0.012 the melting temperatures were 30 and 20°, respectively, to be compared with 8 and 3° for fraction IIC-12 at the same concentrations.

The temperature at which the last traces of aggregation disappear was determined both viscometrically and by light scattering. In the former procedure, the viscosity of the solution containing aggregates was measured as a function of temperature, starting at the gel "melt" temperature and cooling. The viscosity temperature relation for

(9) D. K. Carpenter and W. R. Krigbaum, *J. Chem. Phys.*, to be published.

(10) J. W. McBain and A. M. Bakr, *J. Am. Chem. Soc.*, **48**, 690 (1926).

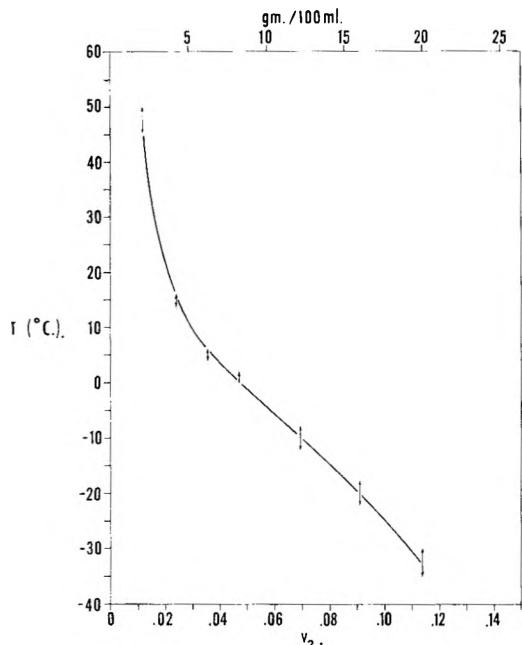


Fig. 1.—Visual "melting" or liquefaction temperatures for cellulose nitrate X-183 plotted against the volume fraction of polymer.

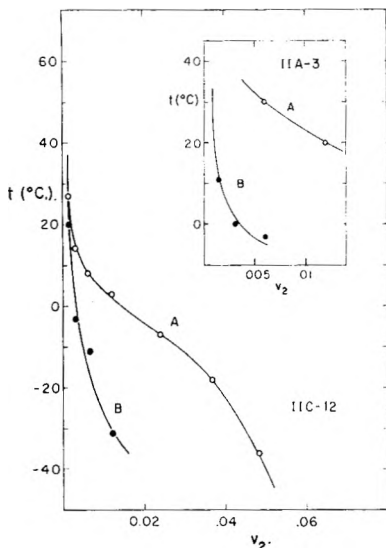


Fig. 2.—Visual "melting" temperature (curve A) and the temperature at which last aggregates disappear (curve B) for cellulose nitrate fraction IIC-12. The same data for fraction IIA-3 appear in the insert.

the same solution containing no aggregates also was established by first cooling the solution to completely dissolve all aggregates, followed by rapid measurement of the viscosity at higher temperatures. The latter curves were obtained for a wide range of temperatures, including those at which slow aggregation took place. This method is illustrated in Fig. 3, which shows the results obtained for a 0.25% ethanol solution of fraction IIC-12. The interaction of these two curves, representing the viscosity-temperature relations for the associated and non-associated states, was taken as the temperature at which the last traces of aggregation were detected viscometrically. These temperatures for IIC-12 are represented as a function of

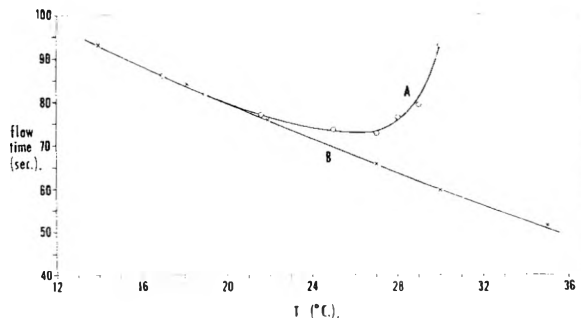


Fig. 3.—Flow time vs. temperature for a 0.25% solution of fraction IIC-12 in ethanol. Curve A was obtained by cooling, starting near the melt temperature of the gel, while curve B represents the same solution without aggregates.

composition by curve B of Fig. 2. The corresponding data for fraction IIA-3 appear in the insert to Fig. 2. The temperature-concentration relations for these two fractions do not coincide, but cross over. It is difficult to extend these relations to higher concentrations using the viscometric procedure.

The temperature at which aggregation occurs in a 0.25% solution of fraction IIC-12 was also investigated by light scattering. The solution was either chilled in a Dry Ice-acetone mixture for 20 minutes to remove aggregates, or heated at 45° for 15 minutes to form the gel. Measurements of the scattering intensities, i_{45} and i_{135} , were then made at the chosen temperature over a period of time. The observed i_{45}/i_{135} ratios appear in Fig. 4

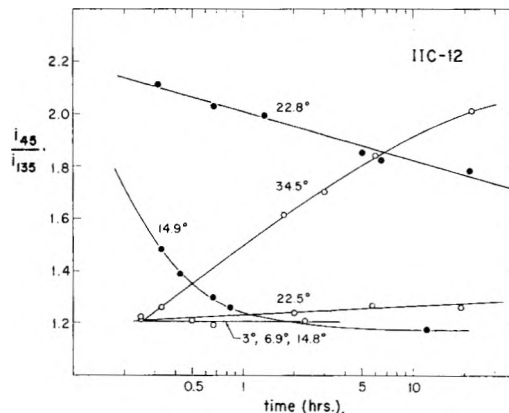


Fig. 4.— i_{45}/i_{135} ratios for a 0.25% solution of fraction IIC-12 shown plotted against time. The open circles represent aggregation; the filled circles represent dissociation of the aggregates.

plotted against time, using a logarithmic scale for convenience. Starting with a solution devoid of aggregation, no aggregates were detected at 14.8° or below, but at 22.5 and 34.5° aggregation could be observed. Starting with the gel, complete dissolution of the aggregates occurs at 14.9°, but at 22.8° some aggregation remains after 22 hours. Thus, we conclude that aggregates are stable in a solution of this concentration above 22°. This confirms the viscometric results shown in Fig. 3, which indicate that such a solution contains no aggregates at temperatures below 20°.

One difference should be noted in the procedures employed in these two types of measurements.

The solutions for viscometric studies were heated just to the gel "melt" temperature. Upon cooling, dissociation of the aggregates formed in this way was practically complete by the time thermal equilibrium was attained, since little further change was observed during the next several hours. On the other hand, the solutions used in the light scattering measurements were heated to a higher temperature to form the gel, and dissociation of these aggregates required a considerable period of time, as shown in Fig. 4. This suggests that the aggregation present in the gel state is characterized by a higher degree of order.

Rate of Aggregation.—It appears from Fig. 4 that the process of aggregation continues over long periods of time, even in the gel state. Moreover, the rate of this process is exceedingly temperature sensitive. Since the gel point should appear after a particular number of effective cross-links have been formed, the setting time of the gel should serve as a convenient measure of the aggregation rate. Setting times were measured by noting the minimum period required for a solution to gel to a condition when it ceased flowing under its own weight, or moved as a coherent bulk. In Fig. 5 are shown typical results, obtained with due caution to prevent mechanical disruption, for 1 and 2% solutions of fraction IIA-3. The setting time, t , is seen to be markedly dependent on the difference, ΔT , between the temperature of observation of setting and the temperature at which the gel liquefies on cooling. To a first approximation, t varies as $(\Delta T)^{-3}$ for both concentrations.

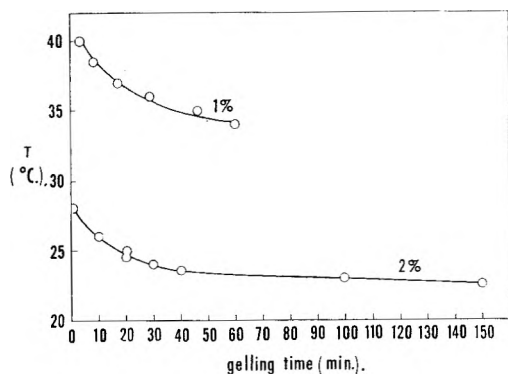


Fig. 5.—Setting time shown as a function of temperature for 1 and 2% solutions of fraction IIA-3.

A more detailed view is obtained by following the solution viscosity during the course of gelation. This was accomplished by first severely cooling the solution to remove all aggregates, then heating to a given temperature and measuring the flow time after some interval. Measurements were performed over a range of time intervals, but the solution was cooled before each measurement. Thus, the breakup of the gel in passing through the viscometer was not accumulated from one measurement to the next.

The dependence of η_{rel} on time at four temperatures in the range 10–15° is shown for a 1% solution of IIC-12 in Fig. 6. Each curve bears a similarity to the viscosity behavior during the polymerization of a polyfunctional monomer, as the extent of

reaction proceeds toward the gel point.¹¹ The isotherms can be superimposed by shifting the time scale for each. The marked temperature dependence of the growth rate is indicated by the fact that the time required for η_{rel} to increase by a given factor changes tenfold within this 5° temperature range. This family of curves exhibiting marked temperature dependence is strongly reminiscent of time effects observed¹² for crystallization isotherms. Thus, the isotherms of Fig. 6 suggest a similarity to both the formation of an infinite three-dimensional network, and to the crystallization of a polymer.

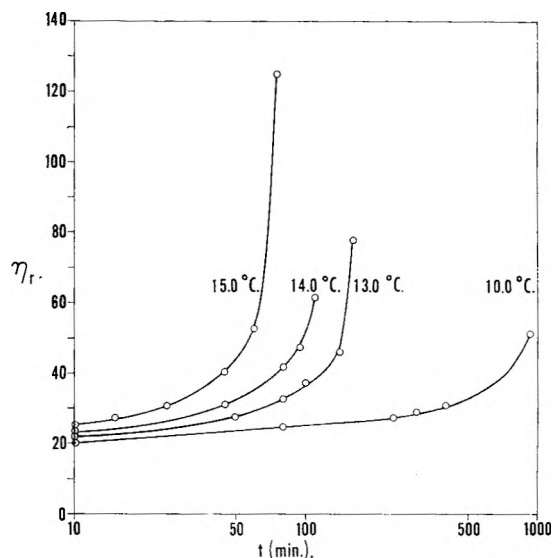


Fig. 6.—Relative viscosity vs. time during the gelation of a 1% solution of fraction IIC-12 at four temperatures.

Size and Shape of Aggregates.—The aggregates were investigated by light scattering measurements performed on the species existing at equilibrium in two stock solutions. These solutions contained 3.14×10^{-3} g./ml. from fraction IIC-12, and 4.45×10^{-3} g./ml. of fraction IIA-3, respectively, as determined at 30° by dry weight analysis. Measurements were made on IIC-12 at five temperatures covering the range 13.4–39.3°, and on IIA-3 at 29.4°. The equilibrium extent of aggregation was attained at each temperature by the following procedure. The solution was chilled with a Dry Ice-acetone mixture for several hours to remove aggregates, then heated at 40° for 20 hours and at 50° for one hour. The solution was then kept at the temperature of the measurement for at least 24 hours. Unfortunately, the solution of fraction IIA-3 turned yellow during the heating treatment.

For each temperature angular measurements over the range 45–135° were carried out on the stock solution conditioned as described above, and on three dilutions made with ethanol stored at the same temperature. This series of measurements could be performed in 40 minutes. The scattering power and dissymmetry of the most

(11) See P. J. Flory, "Principles of Polymer Chemistry," Cornell University Press, Ithaca, N. Y., 1953, p. 355.

(12) L. Mandelkern, F. A. Quinn, Jr., and P. J. Flory, *J. App. Phys.*, **25**, 830 (1954); L. Mandelkern, *ibid.*, **26**, 443 (1955).

dilute solutions did not begin to decrease until after approximately five hours. Furthermore, the data obtained for fraction IIA-3 by dilution were found to agree, within experimental error, with data obtained by concentrating the diluted solution by adding stock. Hence, we can safely assume that the aggregates formed were stable with respect to dilution during the time of the measurements.

We represent by I_v the reduced intensity in Rayleigh ratio units. A toluene solution of the Cornell polystyrene, for which $I_v(90) = 4.20 \times 10^{-4}$, was used as a reference standard. The data were treated by extrapolating c/I_v to zero angle by plotting against $\sin^2(\theta/2)$, as illustrated in Fig. 7.

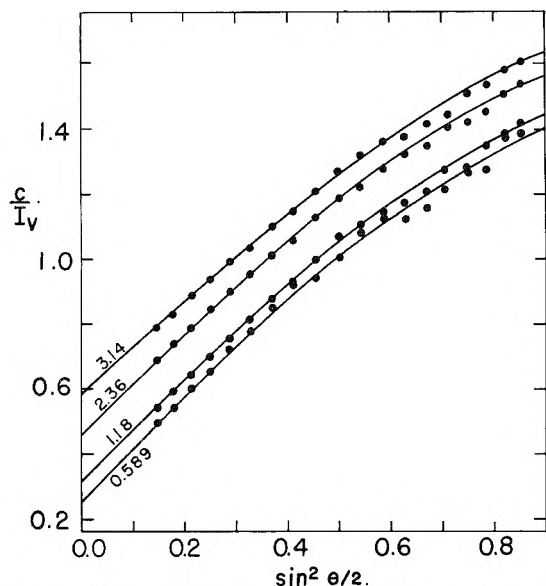


Fig. 7.—Values of c/I_v plotted against $\sin^2(\theta/2)$ for fraction IIC-12 in ethanol at 33.7° . The numbers beside the curves represent $10^3 \times$ concentration in g./ml.

The intercepts of these plots, $(c/I_v)_{\theta=0}$, were extrapolated to zero concentration as illustrated in Fig. 8. Weight-average molecular weights, $\langle M \rangle_w$,

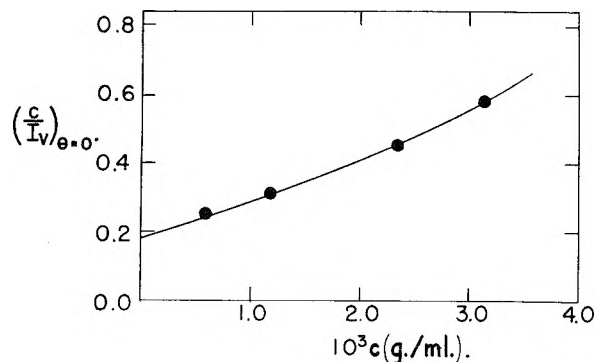


Fig. 8.—Values of $(c/I_v)_{\theta=0}$ plotted against concentration for fraction IIC-12 in ethanol at 33.7° .

were calculated from the intercepts, $(c/I_v)_{c=0, \theta=0}$, making use of the expression

$$\langle M \rangle_w = [K_v(c/I_v)_{c=0, \theta=0} (n_s/n_0)^2]^{-1} \quad (1)^{13}$$

(13) The term $(n_s/n_0)^2$ represents the n^2 refractive index correction, as derived by J. J. Hermans and S. Levinson, *J. Opt. Soc. Am.*, **41**, 460 (1951).

Here K_v is the usual constant, $(4\pi^2/N\lambda^4)n_0^2(dn/dc)^2$, and n_0 and n_s are the refractive indices of ethanol and toluene, respectively. No depolarization corrections were applied. The values of (dn/dc) appearing in Table I were calculated from a form of the Gladstone-Dale relationship

$$(dn/dc) = (n_1 - n_0)/d_1 \quad (2)$$

where n_1 and d_1 are the refractive index and density, respectively, of cellulose nitrate,¹⁴ and n_0 is the refractive index of ethanol.¹⁵

Values of the second virial coefficient, A_2 , in the expression

$$K_v(c/I_v)_{\theta=0} = 1/M + 2A_2c + \dots \quad (3)$$

were obtained by multiplying the initial slopes of the curves as illustrated in Fig. 8 by K_v . Values of the z -average RMS radius of gyration, $(\langle \bar{R}^2 \rangle_z)^{1/2}$, were deduced from the slopes and intercepts of $(c/I_v)_{c=0}$ plotted against $\sin^2(\theta/2)$.¹⁶ These results are collected in Table I. Values of $(\bar{R}^2)^{1/2}$ calculated by the "dissymmetry method,"¹⁷ assuming monodisperse random coils, are shown in parentheses in column six of Table I.

TABLE I
SIZE AND MOLECULAR WEIGHT OF AGGREGATES
Fraction IIC-12

T ($^\circ\text{C}.$)	dn/dc	$10^{-6} \langle M \rangle_w$	$\langle x \rangle_w$	$10^4 A_2^a$	$(\langle \bar{R}^2 \rangle_z)^{1/2b}$	$(\langle \bar{R}^2 \rangle_z)^{1/2}$	$\langle M \rangle_w /$ $(\langle \bar{R}^2 \rangle_z)^{3/2}$
13.4	0.090	0.366	1	3.47	368 (369)	7.3	
24.6	.092	6.35	17	0.42	962 (722)	7.1	
29.5	.092	8.88	24	.29	1010 (742)	8.6	
33.7	.093	14.9	41	.19	1100 (831)	11	
39.3	.094	19.7	54	.18	1270 (831)	9.6	

Fraction IIA-3

29.4	0.092	78.6	786	0.067	1770 (995)	14	
------	-------	------	-----	-------	------------	----	--

^a A_2 in $\text{cm}^3 \text{mole/g}^2$. ^b $(\langle \bar{R}^2 \rangle_z)^{1/2}$ in ångström units.

Figure 2 indicates that aggregation does not occur at temperatures below 20° for a solution of fraction IIC-12 having $v_2 = 0.0015$, corresponding to $c = 2.5 \times 10^{-3}$ g./ml. Hence, the value $\langle M \rangle_w = 366,000$ at 13.4° corresponds to individual chains. For the same fraction $\langle M \rangle_n = 197,000$ (*cf. seq.*). The $\langle M \rangle_w$ values shown in column three indicate that aggregation occurs to an increasing extent as the temperature rises. The weight-average degree of aggregation, $\langle x \rangle_w$, is given for the various temperatures in column four. Estimating $\langle M \rangle_w \cong 10^5$ for individual chains of fraction IIA-3, the extent of aggregation at 29.4° is seen to be much larger for this fraction, despite its lower $\langle M \rangle_n$ value, 56,000 (*cf. seq.*). Although Fig. 2 shows that aggregation sets in at a lower temperature for this fraction, and the initial concentration of the stock was greater, this result is still somewhat surprising. Since all solutions of this fraction exhibited a faint haze, a trace of high molecular weight impurity could have been responsible.

The downward curvature exhibited in Fig. 7 is

(14) Unpublished data, Hercules Powder Company, Allegheny Ballistics Laboratory.

(15) J. Timmermans, "Physico-Chemical Constants of Pure Organic Compounds," Elsevier Press, Inc., New York, 1950, p. 311.

(16) B. H. Zimm, *J. Chem. Phys.*, **16**, 1099 (1948).

(17) P. Doty and R. F. Steiner, *ibid.*, **18**, 1211 (1950).

characteristic of polydispersity,¹⁸ indicating that the size distribution in the aggregates is very broad. Using the disparity between the R values calculated by the zero angle extrapolation and by the "dissymmetry method" as a measure of polydispersity, one concludes from the entries in column six that the size distribution broadens as $\langle M \rangle_w$ increases. This behavior parallels that observed during the formation of an infinite network.¹⁹

Values of the quantity $\langle M \rangle_w / (\langle R^2 \rangle_z)^{3/2}$ found in column seven of Table I are very nearly constant. Interpreting this quantity as the density of a sphere, we conclude that the shape of the cellulose nitrate aggregates is that of a sphere with density increasing somewhat with size. Correction of M and R^2 to the same average would cause the densities to increase even more with M , since the size distribution broadens as M increases. Of the other convenient models, neither rods of constant diameter and density ($M \sim R$), nor random coils ($M \sim R^2$), fits the data. Thus, the shape of the cellulose nitrate aggregates appears to be significantly different from those of gelatin,²⁰ for which $M \sim R^2$.

II. Thermodynamic Studies

Osmotic Pressure.—Osmotic measurements were performed on the two cellulose nitrate fractions dissolved in ethanol and acetone with the aim of examining the effect of temperature on the second virial coefficient, A_2 , in the absence of aggregation. Hence, the ethanol solutions were stored at 0° prior to filling the osmometers, or the osmometers were filled at Dry Ice-acetone temperature. Measurements were also carried out on the equilibrium aggregates of fraction IIA-3 in ethanol at 30° for comparison.

Osmotic height (Δh) values were taken after a period of 24 hours, which was adequate for equilibrium to be established. At the higher temperatures the Δh values for the more concentrated ethanol solutions decreased slowly with time. This was shown to be due to the onset of aggregation, rather than to the adsorption of polymer upon the membrane,²¹ since the same behavior was exhibited by fresh membranes and by membranes which had been exposed to polymer solution for an extended time. A correction for this decrease was estimated by following Δh for several days. Fortunately $\langle M \rangle_n$ is relatively insensitive to the presence of a few large aggregates, although these may increase $\langle M \rangle_w$ enormously. The correction amounted to no more than 5% in any case.

The osmotic data for fraction IIA-3 in ethanol at five temperatures appear in Fig. 9. Table II summarizes the results obtained in the absence of aggregation. The $\langle M \rangle_n$ values for IIA-3 in ethanol found in column five are seen to increase slightly at higher temperatures, which may be attributed to the increased difficulty in accounting

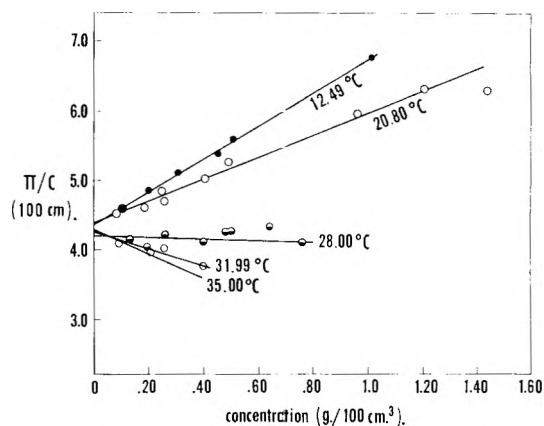


Fig. 9.— π/c ratios plotted against concentration for fraction IIA-3 in ethanol at five temperatures. Experimental points for 35° are omitted for purposes of clarity.

for aggregation at these temperatures. The molecular weights observed in ethanol stand in good agreement with that obtained in acetone, in which no association occurs. The fact that the molecular weights observed at all temperatures are essentially correct lends support to the A_2 values. It should be mentioned that use of the Δh values read after six days leads to π/c vs. c plots which exhibit negative curvature at the higher temperatures, and to molecular weights which vary considerably with temperature.

TABLE II

SUMMARY OF OSMOTIC PRESSURE DATA IN ETHANOL AND ACETONE

Fraction	Solvent	Temp., °C.	$10^{-2}(\pi/c)_{c=0}^a$	$\langle M \rangle_n$	$10^4 A_2$
IIA-3	Ethanol	12.49	4.38	55,400	10.1
		20.80	4.40	56,600	6.32
		28.00	4.20	60,600	-0.489
		31.99	4.22	61,600	-4.25
		35.00	4.18	62,600	-6.62
IIC-12	Ethanol	14.40	1.24	197,000	10.5

^a π in cm., c in g./cc.

Osmotic data were obtained for comparison on the equilibrium aggregates of IIA-3 in ethanol at 30°. For these measurements a stock solution was chilled to remove aggregation, then heated to 40° for 21 hours and 50° for 5 hours. The solution was subsequently cooled to 30° and maintained at this temperature for 19 hours to attain the equilibrium state of aggregation by dissociation. Three dilutions of this stock were prepared, exercising caution to maintain the temperature at 30°. Osmotic equilibrium was reached in 24 hours. After 276 hours Δh for the stock solution had increased only 3%; however, that for the most dilute solution had increased by 40%. The time dependence of Δh appeared to be linear, and the relatively short extrapolation back to zero time led to the Δh values shown in Table III.

We note that $\langle M \rangle_n$ for the aggregates of IIA-3 at 30° is not quite double that observed in the absence of aggregation (56,000), whereas the corresponding $\langle M \rangle_w$ value found in Table I

(18) H. Benoit, *J. Polymer Sci.*, **11**, 507 (1953); M. Goldstein, *J. Chem. Phys.*, **21**, 1255 (1953); H. Benoit, A. Holtzer and P. Doty, *THIS JOURNAL*, **58**, 635 (1954).

(19) See ref. 11, p. 383.

(20) H. Boedtker and P. Doty, *ibid.*, **58**, 968 (1954).

(21) S. Rothman, A. Schwehel and S. G. Weissberg, *J. Polymer Sci.*, **11**, 381 (1953).

TABLE III
OSMOTIC DATA FOR AGGREGATES OF IIA-3 IN ETHANOL
AT 30°

Concn. × 10 ³ , g./cm. ³	Δ <i>h</i> , cm.	10 ⁻² (π/ <i>c</i>)	< <i>M</i> > _n	10 ⁴ <i>A</i> ₂
(0.0)	...	(2.40)	107,000	2.8
1.294	0.420	2.50		
2.402	0.797	2.56		
3.511	1.190	2.65		
4.602	1.618	2.74		

has increased almost 800-fold. This demonstrates in a striking way the broadening of the molecular weight distribution as the gel state is approached.

The *A*₂ values for fraction IIA-3 appear plotted against the absolute temperature in Fig. 10.

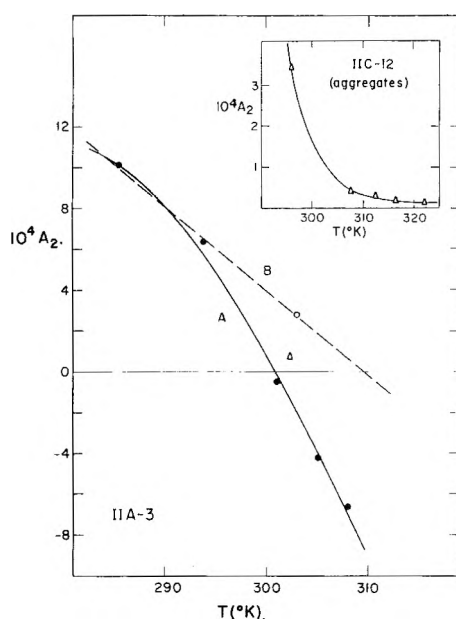


Fig. 10.—The temperature dependence of the second virial coefficient for IIA-3 in ethanol as determined osmotically for solutions ● and aggregates ○, and by light scattering for the aggregates Δ. The insert shows *A*₂ values for the aggregates of fraction IIC-12 in equilibrium at each temperature, as determined by light scattering.

According to the data on the chilled solutions, the Θ temperature (at which *A*₂ = 0) is 301°K. As given by the dilute solution treatment²²

$$A_2 = (\bar{v}^2/V_1)(1 - \Theta/T)\psi_1 F(X) \quad (4)$$

where \bar{v} and V_1 are the partial specific volume of polymer and the molar volume of the solvent, respectively, and $F(X)$ is a function whose value is unity at $T = \Theta$. If we neglect the variation of $F(X)$ with temperature, which would appear to be legitimate for chains having an extended unperturbed configuration (*cf. seq.*), then the temperature coefficient of *A*₂ in the vicinity of *A*₂ = 0 gives for the entropy parameter $\psi_1 = -4$. If, instead, we combine the data on the chilled solutions at 12.49 and 20.8° with that determined osmotically for the aggregates at 30°, then dashed line B of Fig. 10 yields $\Theta = 310^\circ\text{K.}$ and $\psi_1 = -2$.

(22) P. J. Flory, *J. Chem. Phys.*, **17**, 1347 (1949); P. J. Flory and W. R. Krigbaum, *ibid.*, **8**, 1086 (1950).

If the aggregation taking place in the chilled solutions of higher concentration were not completely accounted for, this would lower *A*₂ and result in an apparent Θ less than the true value. The same effect would be brought about by dissociation in the more dilute solutions of aggregates. These arguments favor the higher Θ value. On the other hand, the *A*₂ values for the aggregates of fraction IIC-12 determined by light scattering displayed the unexpected behavior shown in the insert to Fig. 10. At first *A*₂ decreases sharply with increasing temperature, but then levels off and remains slightly positive at the higher temperatures. Light scattering is, of course, more sensitive to the presence of a few large aggregates than is osmotic pressure. Since each point shown in the insert represents a different equilibrium aggregate size and density, and in that sense a different species, these data are not strictly susceptible to the usual thermodynamic analysis. Nevertheless, it is difficult to see that this offers an explanation for the anomalous behavior of *A*₂. Evidently one must be cautious about interpreting the data obtained for the aggregates, and particularly that provided by light scattering.

In conclusion, it appears that for cellulose nitrate molecules dissolved in ethanol, Θ is in the vicinity of 301–310°K., while ψ_1 is in the range –2 to –4. Three points are worth noting. This value for ψ_1 is an order of magnitude larger than the values 0.34 and 0.36 obtained²³ for the non-polar polymers polyisobutylene in benzene and polystyrene in cyclohexane, respectively. Secondly, the solvent becomes thermodynamically poorer at higher temperatures, therefore ψ_1 is negative. Finally, gelation occurs at temperatures below Θ corresponding to positive *A*₂ values, although the gelation temperature appears to exceed Θ at very low concentrations.

Intrinsic Viscosities.—The intrinsic viscosity data accumulated for the two cellulose nitrate fractions appear in Table IV.

TABLE IV
INTRINSIC VISCOSITIES

Fraction	Solvent	Temp., °C.	[η] ^a	<i>k</i> '
IIA-3	Acetone	25	1.52	0.48
		45	1.32	.54
	Ethanol	0	1.70	.55
		25	1.50	.49
		45	1.28	.41
IIC-12	Acetone	25	5.04	.40
		Ethanol	15	4.15
	Ethanol	25	(3.82) ^b	...
		30	3.65	.99

^a [η] in deciliters/g. ^b Interpolated value.

As in the osmotic studies, the solutions were cooled prior to measurement. Over the short intervals of time involved, no increase in the viscosity with time was noted for the low concentrations employed.

The molecular weight values calculated according to the relation for cellulose nitrate in acetone at

(23) W. R. Krigbaum and P. J. Flory, *J. Am. Chem. Soc.*, **75**, 5254 (1953); W. R. Krigbaum, *ibid.*, **76**, 3758 (1954).

25° ,²⁴ $[\eta] = 7.2 \times 10^{-3}$ D.P., were 58,000 for IIA-3 and 190,000 for IIC-12. These stand in good agreement with the $\langle M \rangle_n$ values found in Table II. The $[\eta]$ values for acetone and ethanol decrease with increasing temperature at comparable rates, and since Table II shows acetone to be a better solvent than ethanol at all temperatures investigated, this indicates that the decrease in $[\eta]$ is predominantly due to skeletal rather than osmotic effects. Thus, the temperature coefficient of $[\eta]$ for cellulose nitrate is large compared to that of vinyl polymers, and is in general agreement with that observed for cellulose tributyrates.²⁵ The cellulose nitrate chain is known^{26,27} to be relatively extended, so this behavior is not unexpected.

Vapor Sorption Measurements.—The equilibrium sorption of ethanol by cellulose nitrate was measured at two temperatures for a series of vapor pressures. The purpose of these measurements was to extend the range of the thermodynamic data obtained osmotically for dilute solutions. Films about 1 mil thick were cast from acetone solutions onto a clean mercury surface to minimize orientation effects. At 35° equilibrium was attained in one to three days, whereas three to five days were required at 25° . Successive determinations were made at increasing pressures. The data at $p/p_0 = 1$ were obtained by suspending the film over ethanol in a closed, evacuated vessel submerged in a water-bath. Weight take-up was determined by direct weighing. In view of the possibility of condensation of ethanol on the film, and the fact that the film was exposed to the atmosphere during weighing, the data obtained by the latter method are not completely reliable.

The weight of ethanol sorbed per gram of film is shown in Fig. 11 as a function of the relative vapor pressure. The maximum weight of ethanol sorbed at 25° is only of the order of 15%. This contrasts with the fact that cellulose nitrate dissolved in ethanol at lower temperatures will remain in solution at 25° without change, except for the formation of molecular aggregates.

The data were analyzed by expressing the relative vapor pressure in terms of the chemical potential of the solvent as given by the Flory-Huggins treatment^{28,29}

$$\ln(p/p_0) = \ln v_1 + v_2 + \chi_{12}v_2^2 \quad (5)$$

Values of χ_{12} calculated thereby from the smoothed sorption isotherms appear in Fig. 12. The χ_{12} values are quite concentration dependent, and decrease sharply as the volume fraction of ethanol approaches zero. The latter behavior parallels that of the cellulose nitrate-water system dis-

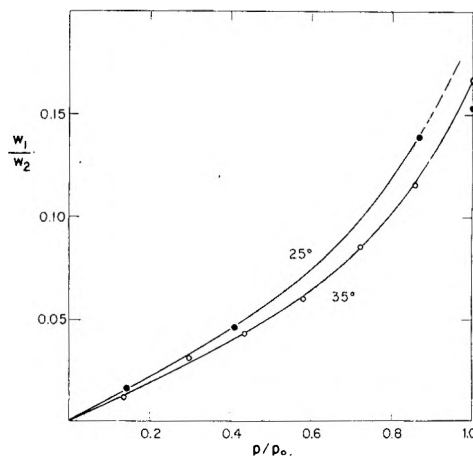


Fig. 11.—Weight of ethanol sorbed per gram of cellulose nitrate at 25° and 35° plotted against the relative vapor pressure of ethanol.

cussed in a previous paper.³⁰ For comparison, the osmotic measurements indicate that for $v_1 = 1$, $\chi_{12} = 0.5$ in the vicinity of $28-37^\circ$.

The interpretation of these χ_{12} values is subject to some doubt, inasmuch as equation 5 applies only to amorphous polymers. Since the temperatures involved are well below the melting range for these compositions, and the total sorption of ethanol is small, it is probably safe to assume that the degree of crystallinity remains constant throughout these measurements. The values of ψ_1 and Θ obtained assuming these parameters to be independent of temperature appear in the insert to Fig. 12.

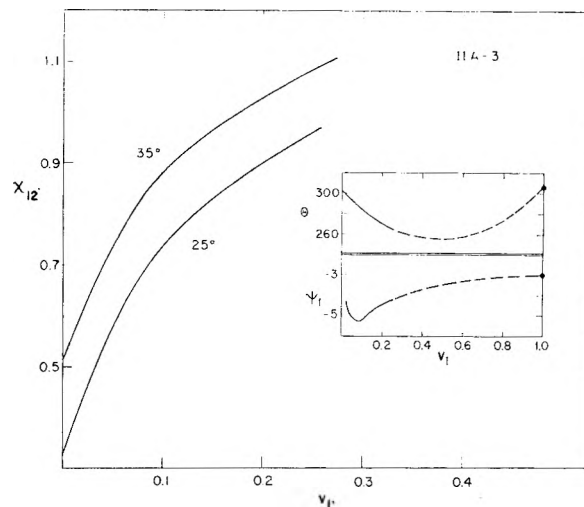


Fig. 12.— χ_{12} for cellulose nitrate (2) in ethanol (1) plotted against the volume fraction of ethanol. The insert shows the ψ_1 and Θ values for this system calculated as described in the text.

In order to gain further insight into the gelation process, the thermodynamic parameters obtained through the dilute solution measurements were utilized to construct the theoretical liquid-liquid and crystal-liquid phase diagrams for the dilute range. The former was calculated as described by Flory,³¹ making use of the values $\Theta = 301^\circ\text{K.}$

(30) S. Newman and W. R. Krigbaum, *J. Polymer Sci.*, **18**, 107 (1955).

(31) See ref. 11, p. 545.

(24) P. Doty and H. Spurlin, a chapter in "Cellulose and Cellulose Derivatives," edited by E. Ott and H. Spurlin, Revised Edition, Interscience Publishers, N. Y. (in preparation).

(25) L. Mandelkern and P. J. Flory, *J. Am. Chem. Soc.*, **74**, 2517 (1952).

(26) A. M. Holtzer, H. Benoit and P. Doty, *THIS JOURNAL*, **58**, 624 (1954).

(27) M. L. Hunt, S. Newman, H. A. Scheraga and P. J. Flory, paper presented before the Division of Polymer Chemistry at the 127th meeting of the American Chemical Society, Cincinnati, Ohio, April 4, 1955.

(28) P. J. Flory, *J. Chem. Phys.*, **10**, 51 (1942).

(29) M. L. Huggins, *Ann. N. Y. Acad. Sci.*, **43**, 1 (1942).

$\psi_1 = -4$ obtained osmotically in the absence of aggregates. The crystal-liquid curve was calculated according to the relation

$$T = \frac{1 + (RV_u/\Delta H_u V_1)\psi_1\theta v_1^2}{(1/T_0) + (RV_u/\Delta H_u V_1)[v_1 - (1/2 - \psi_1)v_1^2]} \quad (6)$$

where V_1 and V_u are the volumes of a solvent molecule and a polymer unit, respectively. From previous measurements³² we estimate for the melting point of this polymer $T_0 = 890^\circ\text{K.}$, and for the heat of fusion $\Delta H_u = 1400$ cal./unit. The θ and ψ_1 values for the concentration range $v_1 = 0.9$ to 1.0 were taken from the insert to Fig. 12.

These phase diagrams are compared with the melting point data for polymer X-183 and fractions IIA-3 and IIC-12 in Fig. 13. Evidently only the

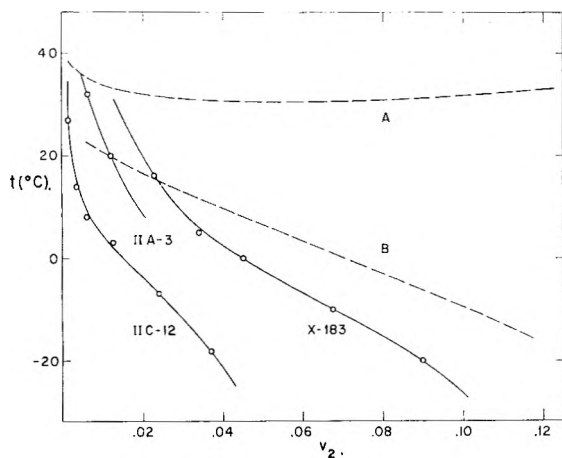


Fig. 13.—Theoretical liquid-liquid (dashed curve A) and crystal-liquid (dashed curve B) coexistence curves compared with the observed "melting" points for fractions IIC-12 and IIA-3 and polymer X-183.

crystal-liquid coexistence curve even approximates the observed concentration dependence. The numerical agreement is not too satisfactory, although a somewhat larger value of θ and a smaller ψ_1 would improve the agreement considerably. In fact, the "melting" curve for polymer X-183 could be reproduced fairly well by taking $\theta = 320^\circ\text{K.}$ and $\psi_1 = -1$ for the limiting values as $v_1 \rightarrow 1$. On the other hand, the lack of agreement may arise from a failure of the theoretical melting point expression at high dilutions. A similar paralleling of the temperature axis at high dilution, in contradiction to theoretical prediction, has been observed for polyethylene in xylene by Richards,³³ for gelatin in water by Ferry,⁴ and for poly-(N,N'-sebacoylpiperazine) in *o*-nitrotoluene by Flory, Mandelkern and Hall.³⁴ The latter authors suggest that a failure of the theoretical relationship may arise from the assumption that the polymer segments are uniformly distributed throughout the amorphous regions, whereas in dilute solutions the polymer concentration will be enhanced in the vicinity of the crystallines. A second possible source of error lies in the fact that the crystallites are in equilibrium with aggregates, rather than single molecules as assumed by theory.

(32) S. Newman, *J. Polymer Sci.*, **13**, 179 (1954).

(33) R. B. Richards, *Trans. Faraday Soc.*, **42**, 10 (1946).

(34) P. J. Flory, L. Mandelkern and H. Hall, *J. Am. Chem. Soc.*, **73**, 2532 (1951).

III. Conclusions

Studies of the gelation process reveal striking similarities to both the formation of an infinite network gel and to crystallization. The former is demonstrated by the prodigious increase in the relative viscosity and the extreme broadening of the molecular weight distribution as the gel point is approached. The gelation isotherms resemble crystallization in that the rate is strongly dependent on temperature. Further indication that the gel is crystalline is furnished by the fact that the calculated crystal-liquid coexistence curve at least approximates the observed concentration dependence of the gel "melt" temperature. Viscosity measurements indicate that the cellulose nitrate chains are relatively extended, and that their configuration is predominantly determined by skeletal rather than by osmotic effects. According to a recent paper by Flory,³⁵ the formation of crystalline regions at low polymer concentrations may be due in part to the stiffness of the cellulose nitrate chains.

The osmotic data in the absence of aggregation show that the entropy parameter ψ_1 is large and negative. This means that the solvent power changes rapidly with temperature, and that the solvent becomes poorer at higher temperatures. The gel forms as the solvent is made poorer; however gelation occurs before the condition for liquid-liquid separation is attained. The gel is formed through the growth of molecular aggregates and "melting" produces a solution of aggregates, rather than individual molecules in solution. At present there appears to be no theoretical basis for predicting the thermodynamic conditions corresponding to the formation of aggregates. The aggregates dissociate rather rapidly, in contrast to the slower "melting" of the gel, which suggests that they may have a less ordered structure than that of the gel. Light scattering indicates that the nitrocellulose aggregates behave approximately as spheres of uniform density, and are thus more compact than gelatin aggregates, which approximate the structure of a random coil.

A dilute solution of crystallizable polymer may undergo three transformations: it may exhibit liquid-liquid separation (with predominantly amorphous polymer in both phases), it may form a gel by crystallizing as a coherent bulk, or a predominantly crystalline phase may separate. The conditions leading to these three alternatives appear worthy of further study. At the present time one can only presume that the formation of a gel requires a certain balance between the rates of growth of aggregates (nucleation) and of crystal growth. How the factors of polymer structure and the polymer-solvent interaction influence this balance remains unanswered. Considerable progress has been made in understanding the kinetics of crystallization, both for bulk polymers and for polymer-diluent systems,¹² and these concepts have been applied qualitatively to gelation.⁶ It appears that further studies along these lines will result in a more penetrating insight into the phenomenon of gelation.

(35) P. J. Flory, Paper presented at the Symposium on Phase Equilibrium in Polymeric Systems, 128th meeting of the American Chemical Society, Minneapolis, Minnesota, September 14, 1955.

CRITICAL MICELLE CONCENTRATIONS OF POLYOXYETHYLATED NON-IONIC DETERGENTS¹

By LUN HSIAO, H. N. DUNNING AND P. B. LORENZ

Surface Chemistry Laboratory, Petroleum Experiment Station, Bureau of Mines, U. S. Dept. of the Interior, Bartlesville, Okla.

Received November 23, 1955

The critical micelle concentrations of non-ionic detergents composed of nonylphenol and various ethylene oxide chain lengths have been determined by the surface tension method. Critical micelle concentrations increase with ethylene oxide chain length and decrease with increasing electrolyte concentration. The effect of chain length on critical micelle concentration may be represented by the expression, $\ln(\text{CMC}) = 0.056R + k$, where CMC is expressed in molarity, R is the average number of ethylene oxide units in the chain, and k is a constant depending on the type and concentration of electrolyte. Comparison of the critical micelle concentration depressions with the lyotropic numbers of the anions indicates that these detergents form hydrophilic micelles that have associated weak positive charges.

Non-ionic detergents afford an unusual opportunity to study micelle formation. The hydrophilic portion of the non-ionic detergent molecule is generally larger than the hydrophobic part, while it is much smaller with ionic detergents. In addition, the absence of a distinct electric charge on the micelles formed by non-ionic detergents eliminates a factor that complicates the interpretation of data obtained with ionic micellar systems.² The critical micelle concentrations (CMC) of non-ionic detergent solutions may be expected to be lower than those of ionic detergents because there is little or no electrical force resisting aggregation of the non-ionic molecules.³

Detergents commonly are used in fresh water systems for household or industrial use. However, recent work has indicated that non-ionic detergents may be valuable additives to water injected into petroleum productive formations to increase the efficiency of petroleum production.⁴ This injected water and the water indigenous to these formations commonly are strongly saline. Therefore, the effects of detergent composition and of added electrolytes on the surface tensions and critical micelle concentrations of non-ionic detergent solutions were investigated.

Many methods have been used to measure CMC⁵; in fact, if almost any physical property of aqueous detergent solutions is plotted against concentration, the slope of the curve will change abruptly (Fig. 1) near the CMC,⁶ with slight differences depending on the property measured. The reported determinations of CMC were based on the measurement of surface tension. Although the validity of the surface tension method has been questioned,⁷ it is supported by theory⁸ and has been verified experimentally by comparison with methods based on color changes of

dyes,⁹ solubilization,¹⁰ and interfacial tension.¹¹

Materials and Methods

The detergents used were Igepals (condensate products of alkyl phenols with ethylene oxide) supplied by the General Aniline & Film Corp. The samples were mixtures of different molecular species varying in their ethylene oxide chain lengths. The major part of the investigation was conducted with four such detergents containing nonylphenol, and with averages of 10.5, 15, 20 and 30 units of ethylene oxide. These will be designated by NR-10.5, NR-15, NR-20 and NR-30, respectively. Three other detergents were used less extensively; two containing nonylphenol, with averages of 9.5 and 100 units of ethylene oxide (NR-9.5 and NR-100); and one containing octylphenol, with an average of 8.5 units of ethylene oxide (OR-8.5). These detergents are commercially available, except for NR-100. They contain 99% active ingredient, with water, salt,¹² and unreacted nonylphenol or ethylene oxide as possible impurities. Other chemicals used were analytical reagent grade.

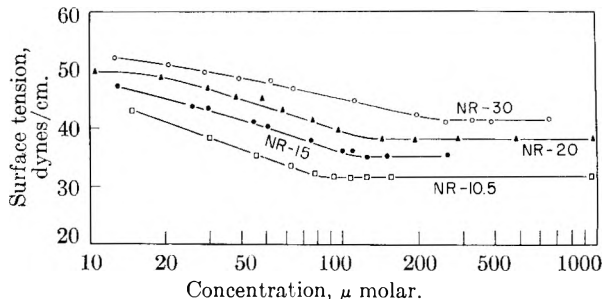


Fig. 1.—Surface tension-concentration curves of the Igepals.

Values of surface tension were determined by the du Nouy ring method at 25° as described elsewhere.¹³ Identical glass containers and solution volumes were used, and the container wall areas were kept at a minimum to reduce effects due to adsorption of detergents on the containers. Measurements were made at intervals of a few minutes until the values agreed within 0.1 dyne/cm. Usually three measurements were required to obtain constant values for the detergents in distilled water and the most dilute electrolyte solutions. In the presence of more concentrated electrolytes the second reading generally agreed with the first.^{14,15}

The curve of surface tension vs. $\log C$, where C is the detergent concentration, is linear within a certain concentration range, above which the surface tension remains

(1) Presented before the Division of Colloid Chemistry, 128th meeting of the American Chemical Society, Minneapolis, Minn., Sept. 15, 1955.

(2) L. M. Kushner and W. D. Hubbard, *THIS JOURNAL*, **58**, 1163 (1954).

(3) C. R. Bury and J. Browning, *Trans. Faraday Soc.*, **49**, 209 (1953).

(4) H. N. Dunning, H. J. Gustafson and R. T. Johansen, *Ind. Eng. Chem.*, **46**, 591 (1954).

(5) N. Sata and K. Tyuzyo, *Bull. Chem. Soc. Japan*, **26**, 177 (1953).

(6) J. Grindley and C. R. Bury, *J. Chem. Soc.*, 679 (1929).

(7) L. M. Kushner and W. D. Hubbard, *THIS JOURNAL*, **57**, 898 (1953).

(8) C. R. Bury, *Phil. Mag.*, **4**, 980 (1927).

(9) E. Ferroni and G. Giovagnoli, *Ann. Chim. Rome*, **43**, 259 (1953).

(10) K. Shinoda, *THIS JOURNAL*, **59**, 432 (1955).

(11) J. Powney and C. C. Addison, *Trans. Faraday Soc.*, **33**, 1243 (1937).

(12) The specific conductivities of a 1.5×10^{-3} molar solution of NR-10.5 and of distilled water used in these experiments were 2.1×10^{-6} and 0.9×10^{-6} mho/cm, respectively.

(13) L. Hsiao and H. N. Dunning, *THIS JOURNAL*, **59**, 362 (1955).

(14) Cf. E. J. Burcik, *J. Colloid Sci.*, **8**, 520 (1953).

(15) G. C. Nutting, F. H. Long and W. D. Harkins, *J. Am. Chem. Soc.*, **62**, 1496 (1940).

nearly constant as the concentration is increased. The concentration at which the two linear portions of the curve intersect (Fig. 1) was considered to represent the CMC value. The average uncertainty in determining CMC values graphically was about 10%.

Results

Surface Tension Curves.—Surface tension values of the Igepals in distilled water are plotted against the logarithm of the concentration in Fig. 1. The two linear portions of the curve typically are connected by a short curved section. There are indications of negative deviations from linearity at the lowest concentrations. The horizontal parts of the curves sometimes had a slight positive slope but the increase over the concentration range studied did not exceed 0.5 dyne/cm. This is barely significant, and probably results from the effects of mixtures of homologous compounds in the detergent samples.¹⁶

Area per Molecule.—In the curves of Fig. 1, the negative slopes reach a maximum at a very low concentration (about 10 μM) and remain constant as the CMC is approached. The surface excess can be calculated from Gibbs' adsorption equation, and if the constant slopes are assumed to represent a monomolecular layer, the area per molecule can also be evaluated. The results are shown in Table I.

TABLE I

SURFACE EXCESS AND MOLECULAR AREAS OF DETERGENTS

	Mole ratio ethylene oxide	CMC, μ molar	Surface excess, moles/cm. ²	Area per molecule, Å^2
Phenol				
Octyl	8.5	180-230	3.15	53
Nonyl	9.5	78-92	3.05	55
Nonyl	10.5	75-90	2.75	60
Nonyl	15	110-130	2.30	72
Nonyl	20	135-175	2.00	82
Nonyl	30	250-300	1.65	101
Nonyl	100	1000	0.95	173

The molecular area of NR-10.5 (60 Å^2) is in agreement with the value (55 Å^2) at the sand-solution interface, as determined by radiotracer and spectrophotometric methods.¹³ An indication of the precision of such measurements is obtained by comparing the present value with the previously reported value of 65 Å^2 .¹³ The molecular areas are considerably larger than the cross-sectional area of the benzene ring (25 Å^2)¹⁷ and increase with increasing ethylene oxide content. Evidently the ethylene oxide chain determines the areas occupied by the detergent molecules. It appears that the molecules at the surface are close-packed, with the alkyl-phenol part projecting outward.

CMC in Water.—The CMC values of the commercial detergents are of the order of 10^{-4} molar, in agreement with the results of other investigations on polyoxyethylated detergents. Gonick and McBain¹⁸ have reported a CMC of $9 \times 10^{-4} M$ for a similar detergent manufactured by another company. With aqueous solutions of polyoxy-

ethylene glycol alkyl ethers, the partial volume, viscosity and the solubilization of dye change abruptly suggesting micelle formation at a concentration of about 10^{-4} mole/liter.¹⁹ Figure 1 shows that the values of CMC and micellar surface tensions increase with increasing length of the ethylene oxide chain, when the alkyl phenol part of the molecule is kept the same. The rate of increase is given approximately by the expression

$$\ln(\text{CMC}) = 0.056R + 3.87 \quad (1)$$

where CMC is in micromolar units, and R represents the mole ratio of ethylene oxide to phenol. The positive coefficient of R means that the aggregation of the polar hydrophilic groups is accompanied by a positive change in free energy that varies directly with chain length. According to equation 1, an increase of 12 in the value of R approximately doubles the CMC value.

The CMC values of equimolar mixtures of NR-10.5 with NR-15 and with NR-30 were 95 and 130 μM , respectively. The corresponding values calculated from equation 1, assuming additivity on a molar basis, are 100 and 150 μM . These small deviations of experimental CMC from the calculated ones indicate that those species that are more surface active are also disproportionately effective in promoting micelle formation, and probably are relatively more abundant in the micelles than in the solution. This is a form of selective adsorption, such as was previously observed¹³ at the silica-solution interface.

The surface activity of ionic detergents usually has been studied by changing the length of the hydrophobic chain. These studies have shown^{11,20} that the CMC is generally doubled when the number of CH_2 groups is decreased by 1. This effect has been investigated briefly by measuring the CMC values of OR-8.5 and NR-9.5, which differ by one CH_2 unit in the hydrophobic chain, but are similar in hydrophobic-hydrophilic balance and cloud point. The CMC values were 210 and 90 μM , respectively. Therefore, as with ionic detergents, the CMC value was approximately doubled by decreasing the number of CH_2 groups in the hydrophobic chain by one.

Effect of Electrolyte.—Typical surface tension-concentration curves of NR-15 with and without added electrolyte are compared in Fig. 2. Electrolytes lower the surface tensions of Igepals below the CMC, and reduce CMC values, but do not affect micellar surface tension appreciably. Below the CMC, the surface tension curve of detergent in the salt solution has a slightly greater negative slope (indicating a stronger adsorption) than in water. The difference is small but statistically significant.

The effects of hydrophilicity (ethylene oxide-chain length) and added electrolyte on the CMC values of the detergents studied are summarized in Fig. 3. The R values are plotted against log CMC in distilled water and in 0.86 N NaCl solutions. The upper curve is a plot of equation 1. The curve with added electrolyte is a straight line

(19) R. Goto, T. Sugano and N. Koizuma, *J. Chem. Soc., Japan*, **75**, 73 (1954).

(20) W. D. Harkins, *J. Am. Chem. Soc.*, **69**, 1428 (1947).

(16) R. L. Mayhew and R. C. Hyatt, *J. Am. Oil Chem. Soc.*, **29**, No. 9, 357 (1952).

(17) N. K. Adam, W. A. Berry and H. A. Turner, *Proc. Roy. Soc. (London)*, **A117**, 532 (1928).

(18) E. Gonick and J. W. McBain, *J. Am. Chem. Soc.*, **69**, 334 (1947).

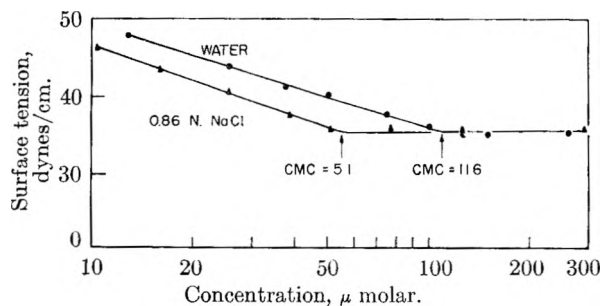


Fig. 2.—Surface tension-concentration curves of NR-15 in distilled water and 0.86 *N* NaCl.

paralleling the line described by this equation. Equation 1 can be written more generally

$$\ln(\text{CMC}) = 0.056R + k \quad (2)$$

in which k depends on the type and concentration of electrolyte but not on R .

Within the experimental uncertainty, the depression of CMC was proportional to salt concentration. This proportionality was not maintained at high salt concentrations when the depression became a substantial fraction of the original CMC value.

The specific effects of various added electrolytes (sodium salts) on the CMC values of NR-15 are presented in Fig. 4 which is a plot of CMC depression *versus* the lyotropic numbers of the anions. The effects of electrolytes on many colloidal properties may be represented by similar plots in which linear relationships are obtained.²¹ A linear relationship, within the limits of experimental error, is observed in this figure. The sulfate ion is omitted for ease of presentation. However, its effect is represented by an extension of the line established by the other ions. The linear relationship and the negative slope of the line indicate that the micelles are of a hydrophilic nature and have associated weak positive charges.

Discussion

The solubility of polyoxyethylated detergents is believed to be caused by hydrogen bonding between the oxygen atoms of the ethylene oxide chain and water molecules. When the hydrophilicity of the ethylene oxide chain is decreased by decreasing the chain length or by changing the solvent, the relative effect of the hydrocarbon chain and aggregative forces is increased, resulting in lower values of CMC. The detergents studied are more soluble in water than those of this series that are highest in surface activity. Therefore, decreases in hydrophilicity of the detergents also result in decreased surface tensions of their solutions.

An increase in R augments the total hydration of the molecule, and this increases the concentration at which attractions between the hydrocarbon chains can draw the molecules into micelles. On the other hand, the effect of added electrolytes is to decrease the hydration of the ethylene oxide chains,^{22,23} probably by breaking hydrogen bonds.²⁴

(21) A. Voet, *Chem. Revs.*, **20**, 169 (1937).

(22) H. L. Greenwald and G. L. Brown, *THIS JOURNAL*, **58**, 825 (1954).

(23) T. M. Doscher, G. E. Myers and D. C. Atkins, *J. Colloid Sci.*, **6**, 223 (1951).

(24) G. W. Stewart, *J. Chem. Phys.*, **11**, 72 (1943).

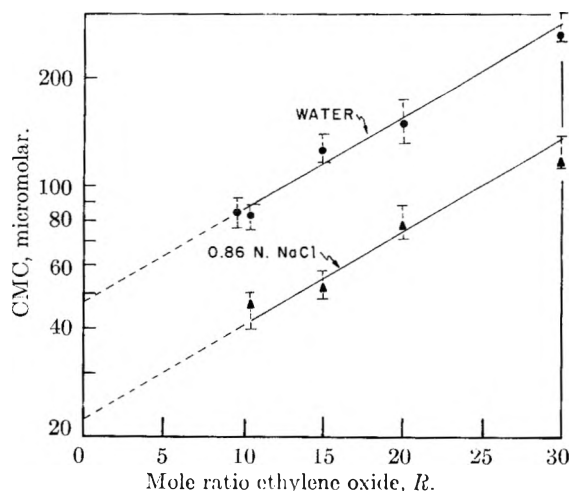


Fig. 3.—The effects of ethylene oxide contents and added electrolyte on CMC values.

If this is the reason for the lowering of CMC by salts, then Fig. 4 indicates that the effect is partially counteracted by the tendency of the counterions to become hydrated.

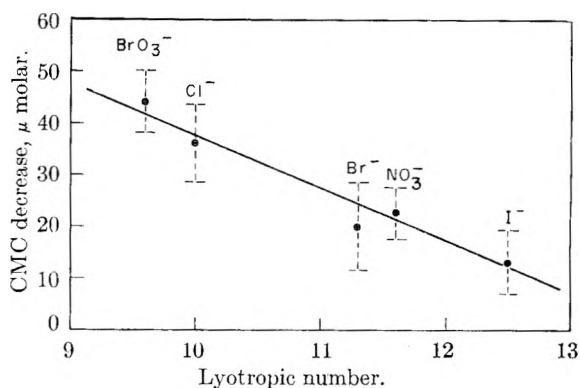


Fig. 4.—Specific effects of 0.5 *N* solutions of sodium salts on CMC values of NR-15 solutions.

The data indicate that, in micelle formation, 12 ethylene oxide units in the hydrophilic chain are equivalent to 1 methylene unit in the hydrophobic chain. This is in marked contrast to solubility phenomena, where an ethylene oxide unit is equivalent to one methylene unit.²⁵ The contrast is not surprising in view of the differences between the two phenomena. It would be expected that the increase in free energy caused by bringing one ethylene oxide group from the aqueous environment into the micelle surface still in contact with the aqueous phase would be much smaller in absolute value than the decrease in free energy caused by moving one CH_2 group from the aqueous phase into the interior of the micelle, almost eliminating the hydrocarbon-water interface.

The weak positive charges associated with the micelles of polyoxyethylated detergents may be caused by the formation of oxonium ions (resonant structures present only in small percentages). Such structures are known to exist in strong mineral acids, where oxonium salts are formed that largely decompose to the constituents on dilution

(25) M. N. Fineman, G. L. Brown and R. J. Myers, *THIS JOURNAL*, **56**, 963 (1952).

with water.²⁶ If the oxonium ion exists also in small quantities in water, acids should increase the ionic character of the detergents and bases should decrease it. Changes in the ionization of the detergents would be reflected in corresponding changes in CMC values. Hydroxide ions were very effective in decreasing the CMC of NR-15 (decrease in CMC = 69 at 0.5 *N*). This indicates a marked decrease in the charge on the micelles and supports the postulate that their weak positive charges are caused by oxonium ions. The acid and electrolyte effects nearly compensate each other in dilute acidic solutions. The CMC values of NR-15 in 0.86 *N* HCl and HNO₃ were 120 and 130 μ M, respectively. At higher concentrations the acid effect becomes predominant as the electrolyte effect levels off. The CMC values of NR-15 in 3.1 *N* HCl and HNO₃ were 150 and 290 μ M,

(26) G. A. Hill and L. Kelley, "Organic Chemistry," The Blakiston Co., Phila., Pa., 1943, p. 149.

respectively. These data show that the relative effectiveness of the chloride and nitrate ions are unchanged but that their actual effectiveness is superimposed on the effect of strong acids.

The results shown in Figs. 3 and 4 may be summarized by the two equations

$$\log (\text{CMC})_0 - \log (\text{CMC}) = D \quad (3)$$

$$\Delta (\text{CMC}) = (\text{CMC})_0 - \text{CMC} = (270 - 20N)C_s, \text{ for NR-15} \quad (4)$$

where $(\text{CMC})_0$ represents the value of CMC when $C_s = 0$, and C_s is the normality of the electrolyte and *N* is the lyotropic number of the anion. *D* is a parameter independent of *R*. By combining these two equations, it may be shown in general

$$\Delta (\text{CMC}) = C_s(270 - 20N)e^{0.056(\bar{r} - 15)}$$

from which the approximate CMC value (of a detergent based on nonylphenol) may be calculated at various values of *N*, *R* and C_s .

THERMAL DIFFUSION IN LIQUIDS;¹ THE EFFECT OF NON-IDEALITY AND ASSOCIATION

BY L. J. TICHACEK, W. S. KMAK AND H. G. DRICKAMER

Department of Chemistry and Chemical Engineering, University of Illinois, Urbana, Illinois

Received November 25, 1956

It is shown that the thermodynamics of irreversible processes, when appropriately applied to a system fixed in the laboratory, predicts that a thermal diffusion separation depends on the difference in the quantities Q_i^{**}/\bar{V}_i , where Q_i^{**} is the molal net heat of transport and \bar{V}_i is the partial molar volume. Q_i^{**} is related to the activation energy for motion by a physically logical argument and by a kinetic derivation. The results are applied to a series of binary solutions including one or more associated compounds. It is found that the activation energy for local expansion, $\Delta H_{1\pm}$, is probably the part transported in molecular diffusion. The introduction of the "partial molar activation energy" is shown to predict the correct concentration dependence in thermal diffusion. The role of X ($\partial\mu/\partial X$) in thermal diffusion is discussed.

In a recent paper² we have presented a theory of thermal diffusion in liquids which gives very good agreement with experiment for solutions which are ideal or only moderately non-ideal. The theory was, however, based on an abortive and artificial formulation for the "net heat of transport" of a molecule in a solution. It is our purpose here to show that essentially the same result can be obtained from the thermodynamics of irreversible processes by an appropriate transfer of coordinates from the center of mass to the laboratory system with no artificial assumptions necessary, or by a kinetic argument which is a generalization of that due to Prigogine, *et al.*³ We shall further show how the theory can be applied to associated and other non-ideal systems.

Thermodynamic Theory.—The development of this theory follows in principle that given by de Groot⁴; the chief differences are: (1) this treatment employs laboratory coordinates instead of center of mass coordinates, and (2) only constant

pressure systems are considered so that fluxes of pure heat and of enthalpy are simply related.

We define our phenomenological coefficients, L_{ik} , in a laboratory coordinate system by

$$\vec{J}_i = \sum_{k=1}^n L_{ik} \vec{X}_k \quad (1)$$

where \vec{X}_k is a force associated with component *k*, \vec{J}_i is the flux of component *i* in laboratory coordinates, and *n* is the total number of components in the system.

For an open system defined as an infinitesimal constant volume fixed in the laboratory coordinate system, the Gibbs equation yields

$$T \frac{\partial(s\rho)}{\partial t} = \frac{\partial(h\rho)}{\partial t} - \sum_k \mu_k \frac{\partial\rho_k}{\partial t} \quad (2)$$

where *s* and *h* are the total specific entropy and enthalpy, μ_k is the partial specific free energy of component *k*, ρ_k is the mass of component *k* per unit volume of system, and ρ is the total density of the system. We now represent the flux of enthalpy in

laboratory coordinates by \vec{J}_h and find that it is composed of two parts for systems at constant pressure

$$\vec{J}_h = \vec{J}_Q + \sum_{k=1}^n h_k \vec{J}_k \quad (3)$$

(1) This work was supported in part by the A.E.C.

(2) E. L. Dougherty and H. G. Drickamer, *THIS JOURNAL*, **59**, 443 (1955).

(3) I. Prigogine, L. de Broukere and R. Amand, *Physica*, **16**, 577, 851 (1950).

(4) S. R. de Groot, "The Thermodynamics of Irreversible Processes," Interscience Publishers, New York, N. Y., 1950.

where h_k is the partial specific enthalpy of component k and \vec{J}_Q can be described as the flux of *pure heat* (conducted energy); moreover, both the numerical value of \vec{J}_Q and the validity of equation 3 are found to be independent of the coordinate system chosen for expression of \vec{J}_h , \vec{J}_Q and \vec{J}_k . We now apply Gauss' theorem to the two time derivatives on the right side of equation 2; with the aid of equation 3 and appropriate rearrangement of terms we find that

$$T \frac{\partial(\rho_s)}{\partial t} = -T \operatorname{div} \left(\frac{\vec{J}_Q}{T} + \sum_k s_k \vec{J}_k \right) - \vec{J}_h \cdot \frac{\operatorname{grad} T}{T} - \sum_k \vec{J}_k \cdot T \operatorname{grad} \frac{\mu_k}{T} \quad (4)$$

where the relation $\mu_k = h_k - Ts_k$ has been used. The first term on the right embodies the entropy flux in the open system; the second and third terms, therefore, give the entropy generation within the system. Since the products of the fluxes and conjugated forces should be equal to the entropy generation, the forces are

$$\vec{X}_h = - \frac{\operatorname{grad} T}{T} \quad (5)$$

$$\vec{X}_k = - T \operatorname{grad} \frac{\mu_k}{T} \quad (6)$$

We notice that these forces are the same as those found in a center of mass coordinate system.

In the flux equations which are typified by equation 1, two types of relations must be found between the coefficients. The first set of relations is known as Onsager's relations; the second set of relations arises from the definition of our system as a fixed volume

$$\sum_{i=1}^n \nu_i \vec{J}_i = 0 = \sum_i \nu_i \sum_k L_{ik} \vec{X}_k \quad (7)$$

where ν_i is the partial specific volume of component i . We can thus conclude that

$$\sum_i \nu_i L_{ik} = 0 \quad (8)$$

We now pursue a development similar to that of de Groot by defining a Q_k to transform coefficients of the enthalpy flux-mass flux interaction

$$L_{ih} = \sum_{k=1}^n L_{ik} Q_k = \sum_{k=1}^n L_{ik} (Q_k^* + h_k) \quad (9)$$

The significance of Q_k and Q_k^* in this laboratory coordinate system will be discussed later.

The form of equations 1 and 9 has caused the definition of n different Q 's instead of $n - 1$ Q 's employed by de Groot. The information which we can obtain from the thermodynamics of irreversible processes is not altered by the manner of definition of Q ; however, if defined as in equation 9 it is simpler to introduce a physical interpretation for Q from outside the thermodynamic theory.

Now by a series of steps analogous to those used by de Groot, we find

$$\vec{J}_i = \sum_{k=1}^n L_{ik} \left[\frac{Q_k^*}{T} \operatorname{grad} T + \sum_{j=1}^{n-1} \frac{\partial \mu_k}{\partial C_j} \operatorname{grad} C_j \right] \quad (10)$$

where C_j is the concentration of component j . This relation can be applied to a binary system with the aid of equation 8 to give

$$\vec{J}_1 = - L_{11} \left[\frac{Q_1^*}{T} \operatorname{grad} T + \frac{\partial \mu_1}{\partial C_1} \operatorname{grad} C_1 \right] + L_{11} \frac{\nu_1}{\nu_2} \left[\frac{Q_2^*}{T} \operatorname{grad} T + \frac{\partial \mu_2}{\partial C_1} \operatorname{grad} C_1 \right] \quad (11)$$

Conversion of specific to molar quantities and the application of the Gibbs-Duhem equation gives for the steady-state condition

$$\left[\frac{Q_2^*}{\bar{V}_2} - \frac{Q_1^*}{\bar{V}_1} \right] \frac{\operatorname{grad} T}{T} = \left[\frac{1}{x_1 \bar{V}_1} + \frac{1}{x_2 \bar{V}_2} \right] x_1 \frac{\partial \mu_1}{\partial x_1} \operatorname{grad} x_1 \quad (12)$$

where \bar{V}_1 , \bar{V}_2 are the partial molar volumes of components 1 and 2; x_1 is the mole fraction of component 1; μ_1 is the molar chemical potential of component 1; and Q_1^* is now the product of Q_1^* and M_1 , the molecular weight of component 1. The definition of α , the thermal diffusion ratio, is commonly taken from the flux equation

$$\vec{J}_1 = - \rho_D \left[\operatorname{grad} x_1 - \frac{\alpha x_1 x_2}{T} \operatorname{grad} T \right] \quad (13)$$

The steady-state solution of equation 13 can be compared with equation 12 to find the value of α

$$\alpha = \frac{\bar{V}_1 \bar{V}_2}{\bar{V}_{x_1}} \frac{\partial \mu_1}{\partial x_1} \left[\frac{Q_2^*}{\bar{V}_2} - \frac{Q_1^*}{\bar{V}_1} \right] \quad (14)$$

where \bar{V} is the molar volume of the solution ($x_1 \bar{V}_1 + x_2 \bar{V}_2$). We now find the significance of Q_k^* in the following manner. We write

$$\vec{J}_h - \sum_k \vec{J}_k Q_k = L_{hh} \vec{X}_h + \sum_j L_{hj} \vec{X}_j - \sum_k Q_k \left[\sum_j L_{hj} \vec{X}_j + L_{kh} \vec{X}_h \right] \quad (15)$$

The definition of Q_k and Onsager's relations can be used to show that the sum of the terms involving \vec{X}_j is identically zero; the two terms involving \vec{X}_h are zero when there is no temperature gradient, so that the left side of (16) is then zero also. Thus

$$\vec{J}_h = \sum_k (Q_k^* + h_k) \vec{J}_k = \vec{J}_Q + \sum_k h_k \vec{J}_k \quad (16)$$

Now Q_1^* (eq. 14) is $M_1 Q_1^*$, and the significance of Q_1^* can be seen by a study of equation 16 in its various aspects. In particular, it can be seen that Q_1^* is the difference between the total enthalpy transported by one mole of *moving* molecules of type one in the solution and the average enthalpy of one mole of molecules of type one in the same mixture. It is clearly related to the activation energy for motion of type one molecules in this mixture. It is, in fact, that part of the activation energy which is transported with the moving molecule. A simple kinetic argument, given below, serves further to identify these quantities.

The same expression for α (equation 14) could be found directly from de Groot's result if one were

able to interpret his heat of transport, Q_{1m}^* . For the significance of Q_{1m}^* de Groot finds

$$\vec{J}_{qm} = \sum_{k=1}^{n-1} Q_{km}^* \vec{J}_{km} \quad (17)$$

where \vec{J}_{km} is the flux of component k in his center of mass system; a study of the properties of \vec{J}_{qm} shows that it is the flux of enthalpy in that center of mass system. A proper transformation between the two coördinate systems, plus the constraint given in the first quality of equation 8 shows that

$$Q_{1m}^* = \bar{H}_1 - \bar{H}_2 + \frac{\bar{V}_1 \bar{V}_2}{\bar{V}} \left[\frac{Q_2^*}{\bar{V}_2} - \frac{Q_1^*}{\bar{V}_1} \right] \quad (18)$$

where \bar{H}_1 is the partial molar enthalpy of component 1, the Q_1^* are used in equations 12 and 14, and Q_{1m}^* is the net molar heat of transport in the center of mass system. Substitution into the steady state solution of de Groot's flux equation yields equation 14.

Kinetic Theory.—Prigogine³ has written the flux of component one in a mixture of molecules of the same size as

$$\vec{J}_1 = \frac{a_j^0}{6} C_0 X_1(T_a) X_2(T_b) \exp \left[\frac{q_1}{R \left(T - \frac{\Delta T}{2} \right)} - \frac{q_2}{R \left(T + \frac{\Delta T}{2} \right)} - \frac{q_L}{RT} \right] \quad (19)$$

where

- X_1 = mole fraction component 1
- C_0 = total concentration of molecules
- q_1 = "localized" activation energy, *i.e.*, that part of the activation energy transported with component 1
- q_L = "non-localized" activation energy, *i.e.*, that part not transport with motion
- $T_a T_b$ = temperature one molecular jump apart
- $\Delta T = T_a - T_b$

The definition of the q 's used here is somewhat more general than that used by Prigogine, but this does not affect the form of the equation. Prigogine wrote a similar expression for the flux of component one in the opposite direction. He then equated those in steady state, expanded the exponentials, and obtained for α

$$\alpha = \frac{q_2 - q_1}{RT} \quad (20)$$

Rutherford and Drickamer⁵ showed that if the q 's are considered as free energies the corresponding expression for α is

$$\alpha = \frac{\left(q_2 - T \frac{\partial q_2}{\partial T} \right) - \left(q_1 - T \frac{\partial q_1}{\partial T} \right)}{RT} \quad (21)$$

We now propose for the flux in a system of molecules of different size the more general expression

$$\vec{J}_1 = \frac{a_j^0}{6} C_0 X_1(T_a) X_2(T_b) \frac{\bar{V}}{\bar{V}_1} \left[\exp \frac{-q_1}{R \left(T - \frac{\Delta T}{2} \right)} \right]^{V_2/V} \times \left[\exp \frac{-q_2}{R \left(T + \frac{\Delta T}{2} \right)} \right]^{V_1/V} \left[\exp \frac{-q_L}{RT} \right]^\varphi \quad (22)$$

where

- \bar{V}_i = partial molar volume of component i
- \bar{V} = average molar volume of system
- φ = function of \bar{V}_i and \bar{V} whose exact form is unimportant as the factor involving it will cancel out.

The other terms have their previous significance (eq. 22). The flux equation is written so that

$$\vec{J}_1 \bar{V}_1 + \vec{J}_2 \bar{V}_2 = 0 \quad (23)$$

$$\frac{d}{dt} (\vec{J}_1 \bar{V}_1) + \frac{d}{dt} (\vec{J}_2 \bar{V}_2) = 0 \quad (24)$$

as it must in a system fixed in the laboratory.

One can now write an analogous expression for the flux of component one in the opposite direction, equate the two for the steady state, and expand the exponentials as before. Then one obtains

$$\alpha = \frac{\bar{V}_1 \bar{V}_2}{\bar{V}} \left[\frac{q_2}{\bar{V}_2} - \frac{q_1}{\bar{V}_1} \right] \frac{1}{RT} \quad (25)$$

This is just like equation 14 obtained from the thermodynamic theory except that RT replaces $X(\partial\mu/\partial X)$ in the denominator as is understandable since no correction for solution non-ideality is included.

This kinetic development provides a further confirmation for our intuitively logical identification of the net heat of transport with the activation energy transported in molecular motion.

The Activation Energy Transported in Molecular Motion.—The best description of molecular motion of a component in a mixture would be obtained from measurements of "self-diffusion" of that component in the mixture as a function of temperature (and of pressure) using tagged molecules. Since these measurements are essentially non-existent, it is necessary to approximate those quantities in some way. A possible first approximation would be activation quantities derived from "self-diffusion" measurements on the pure components. These are also relatively scarce; however, according to Eyring's theory⁶ of molecular motion, the mechanisms of diffusion and of viscous flow are similar and the activation quantities for the two processes should be nearly the same. This has been shown to be true⁷ for a wide variety of substances, with one or two exceptions. In particular, for CCl_4 the diffusion activation enthalpy is 50% greater than the activation energy for viscous flow. In our discussion we shall use the activation quantities derived from viscosity coefficients of the pure components as the first approximation for the activation properties of the molecules in a mixture, except for CCl_4 where the values from diffusion will be used.

According to Eyring the viscosity coefficient can be written

$$\eta = \frac{h N_0}{V} \exp \left(\frac{\Delta F^\ddagger}{RT} \right) \quad (26)$$

where

- h = Planck's constant
- N_0 = avogadro's number
- V = molar volume
- ΔF^\ddagger = free energy of activation
- R = gas constant
- T = absolute temperature

(5) W. M. Rutherford and H. G. Drickamer, *J. Chem. Phys.*, **22**, 1157, 1284 (1954).

(6) S. Glasstone, K. L. Laidler and H. Eyring, "Theory of Rate Processes," McGraw-Hill Book Co., Inc., New York, N. Y., 1941.

(7) E. Fishman, *THIS JOURNAL*, **59**, 469 (1955).

Then

$$R \frac{\partial \ln \eta V}{\partial \frac{1}{T}} \Big|_p = \Delta H \ddagger \quad (27)$$

$$R \frac{\partial \ln \eta V}{\partial \frac{1}{T}} \Big|_v = \Delta H_j \ddagger = \Delta H \ddagger - T \left(\frac{\partial p}{\partial T} \right)_v \Delta V \ddagger \quad (28)$$

$$= \Delta H \ddagger - \Delta H_h \ddagger \quad (28a)$$

$$\frac{\partial \ln \eta V}{\partial p} \Big|_T - \frac{\Delta V \ddagger}{RT} \quad (29)$$

These quantities have been discussed in detail elsewhere^{2,6,8} although their exact significance is still not clear. $\Delta H \ddagger$ is the total activation enthalpy. It seems probable that $\Delta H_h \ddagger$ is the activation enthalpy associated with a localized expansion to permit motion, and $\Delta H_j \ddagger$ is the activation enthalpy associated with orientational effects. We are interested in the fraction of the activation enthalpy transported by the molecule when it moves. This could, of course, be $\Delta H_h \ddagger$, $\Delta H_j \ddagger$ or some fraction of each. For most non-associated liquids $\Delta H_h \ddagger$ is 65-75% of the total activation enthalpy at one atmosphere. For associated liquids $\Delta H_h \ddagger$ is only 20-40% of the total $\Delta H \ddagger$. It has been suggested that $\Delta H_j \ddagger$ is the measure of thermal diffusion separation, *i.e.*, that it is the quantity transported in motion. However, for non-associated systems it is an order of magnitude too small, and frequently fails to predict the correct sign.

Dougherty and Drickamer² predicted the correct sign and magnitude of α for a wide variety of non-associated mixtures using the total $\Delta H_0 \ddagger$ (the subscript 0 refers to a pure liquid) as the quantity transported. (It is now clear that the factor $1/2$ used on $\Delta H_0 \ddagger$ in that paper is necessary only because a factor of two is introduced spuriously earlier in the derivation, due to the definition used for the net heat of transport.) Since for all these systems $\Delta H_h \ddagger$ is the major part of $\Delta H_0 \ddagger$, and about the same fraction in each case, they do not provide an identification of the portion of the activation enthalpy transported in motion. For three systems involving alcohols the use of $\Delta H_0 \ddagger$ did not provide correct magnitudes. It will be shown later that if it is assumed that $\Delta H_h \ddagger$ is the enthalpy transported correct magnitudes can be predicted for all systems including associated liquids. This is rather surprising, and it is not at all clear intuitively why it is so.

Now in the above approximation, the concentration dependence of α appears to a limited extent in \bar{V}_1 , \bar{V}_2 and \bar{V} , and to a much greater extent in X_1 ($\partial \mu_1 / \partial X_1$). As will be discussed later, this latter quantity predicts trends with concentration correctly, but is not sufficient to give the entire con-

TABLE I

EXPERIMENTAL AND CALCULATED VALUES OF α^a

X_1	$X_1 \frac{\partial \mu_1}{\partial X_1}$ cal.	α_0^b	α_h^c	α_{exp}
Benzene (1)-Cyclohexane (2) at 40°				
0.20	540	0.09	0.17	0.58
.50	491	.10	.20	.40
.80	523	.10	.20	.10

Benzene (1)-Carbon Tetrachloride (2) at 40°				
0.20	599	1.27	1.15	1.37
.50	585	1.34	1.21	1.43
.80	598	1.34	1.21	1.48

Cyclohexane (1)-Carbon Tetrachloride (2) at 40°				
0.20	601	1.50	1.33	1.25
.50	592	1.48	1.31	1.27
.80	605	1.40	1.24	1.30

Benzene (1)-Methanol (2) at 40°				
0.20	261	8.6	0.15	-0.80
.50	127	13.8	.24	+0.15
.80	61	23.4	.41	+1.80

Carbon Tetrachloride (1)-Methanol (2) at 40°				
0.20	259	+6.1	-1.99	-3.0
.50	63	+19.5	-6.37	-4.9
.80	33	+29.9	-9.75	-2.8

<i>n</i> -Butyl Alcohol (1)-Carbon Disulfide (2) at 8° ^d				
0.20	Assume	-4.63	-0.64	-6.5
.50	<i>RT</i>	-4.05	-.56	0
.80		-3.59	-.50	+.25

Isobutyl alcohol (1)-Carbon Disulfide (2) at 8° ^d				
0.50	(<i>RT</i>)	-5.64	-0.92	-0.93

Ethanol (1)-Triethylamine (2) at 50°				
0.297	446	-7.0		-1.08
.444	440	-7.8		-1.19
.615	482	-8.2		-0.92
.706	528	-8.3		-1.22
.906	638	-8.2		-0.89
.956	640	-8.2		-0.67

Ethanol (1)-Diethylamine (2) at 50°				
0.430	745	-3.8		-1.11
.540	835	-3.6		-0.85
.683	930	-3.5		-0.48
.804	955	-3.8		-0.59
.909	805	-4.9		-0.88
.971	682	-6.0		-1.12

Water (1)-Diethylamine (2) at 49°				
0.388	400	-10		-1.64
.658	330	-24		-3.24
.794	258	-48		-2.71
.846	180	-65		-2.19
.931	180	-70		-1.52

Water (1)-Ethanol (2) at 25°				
0.145	486	-23.0	1.80	-0.50
.266	367	-29.5	2.02	-0.93
.582	239	-26.5	1.52	-1.47
.726	213	-12.5	0.64	-0.90
.884	377	-8.0	.42	+0.29

Water (1)-Methanol (2) at 40°				
0.200	558	-5.0	0.35	-0.46
.360	518	-7.0	.44	-0.93
.492	500	-9.0	.56	-0.54
.772	442	-9.5	.85	-0.44
.900	586	-8.4	.71	+0.62
.953	615	-8.0	.70	+1.17

^a α is positive when component (1) is enriched at the hot wall. ^b α_0 calculated using $\Delta H_0 \ddagger$ (activation enthalpy of pure components). ^c α_h calculated using $\Delta H_{h0} \ddagger$ (activation enthalpy for expansion of pure components). ^d From thermal diffusion data of E. L. Dougherty, Ph.D. Thesis, University of Illinois, 1955.

(8) A. Bondi, *J. Chem. Phys.*, **14**, 591 (1946); *Ann. N. Y. Acad. Sci.*, **53**, 805 (1951).

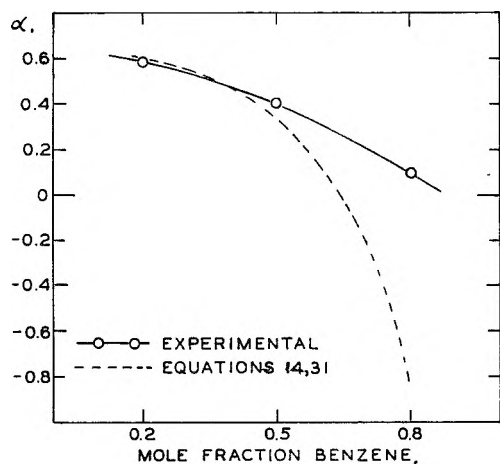


Fig. 1.—The concentration dependence of experimental and theoretical values for the thermal diffusion ratio of benzene-cyclohexane at 40°.

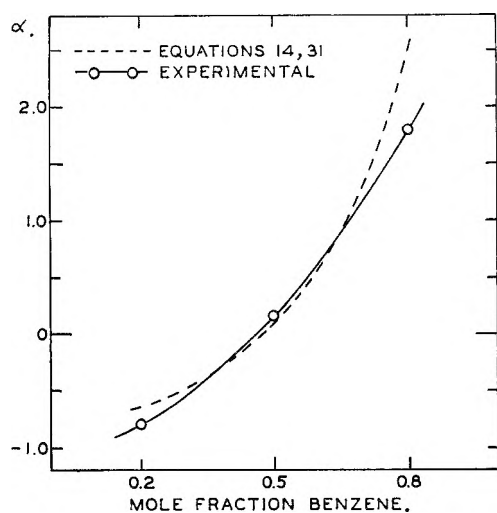


Fig. 2.—The concentration dependence of experimental and theoretical values for the thermal diffusion ratio of benzene-methanol at 40°.

centration effects in highly non-ideal (particularly associated) solutions. This is not surprising since the activation quantities wanted are those for the components in the mixture, and these could be very concentration dependent. It is clear that in reality the activation enthalpies of molecules in the mixture will not be simply related to those of the pure components, nor to the ΔH^\ddagger of the mixture. Nevertheless, it was decided to try, as a next approximation, a partial molar activation enthalpy $\overline{\Delta H}_1^\ddagger$ defined by the equation

$$\overline{\Delta H}^\ddagger_{\text{mix}} = \overline{\Delta H}_1^\ddagger X_1 + \overline{\Delta H}_2^\ddagger X_2 \quad (30)$$

These could then be evaluated from viscosity measurements as a function of temperature and composition. It would have been desirable to measure values of partial molar activation enthalpies for expansion, ΔH_h^\ddagger , but accurate measurements of viscosity as a function of pressure are not obtainable.

Results

The systems studied include benzene-cyclohexane, benzene-carbon tetrachloride, cyclohexane-carbon tetrachloride, benzene-methanol, carbon tetrachloride-methanol, *n*-butanol-carbon disul-

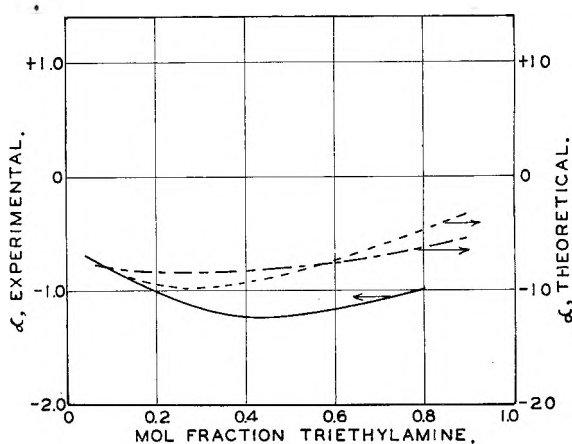


Fig. 3.—The concentration dependence of experimental and theoretical values for the thermal diffusion ratio of triethylamine-ethanol at 50°: —, experimental results; ----, theoretical values based on activation enthalpies of pure components; -·-·-, theoretical values based on partial molar activation enthalpies.

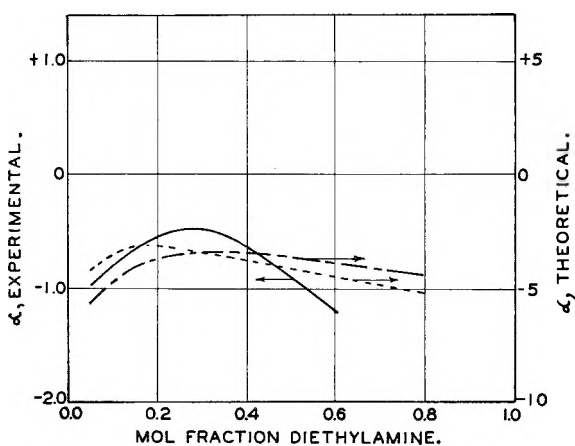


Fig. 4.—The concentration dependence of experimental and theoretical values for the thermal diffusion ratio of diethylamine-ethanol at 50°: —, experimental results; ----, theoretical values based on activation enthalpies of pure components; -·-·-, theoretical values based on partial molar activation enthalpies.

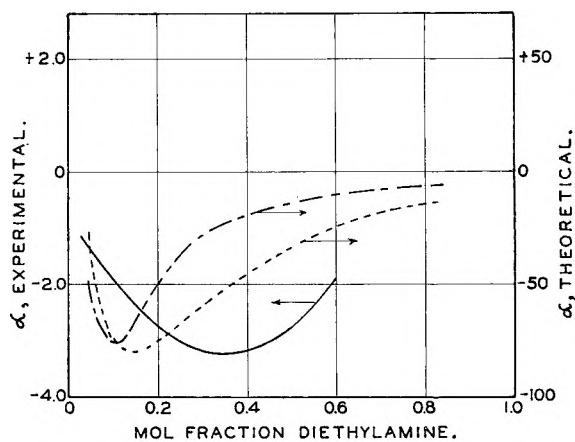


Fig. 5.—The concentration dependence of experimental and theoretical values for the thermal diffusion ratio of diethylamine-water at 49°: —, experimental results; ----, theoretical values based on activation enthalpies of pure component; -·-·-, theoretical values based on partial molar activation enthalpies.

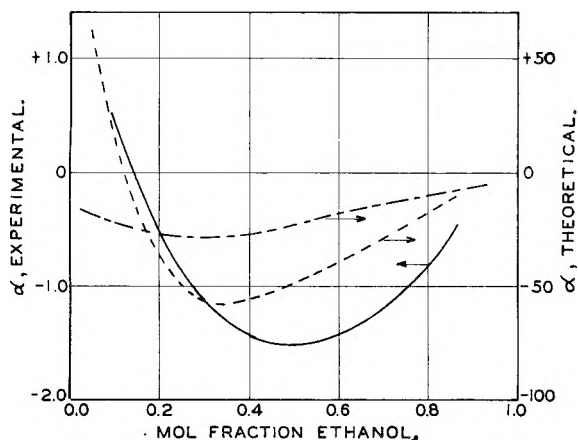


Fig. 6.—The concentration dependence of experimental and theoretical values for the thermal diffusion ratio of ethanol-water at 25°: —, experimental results; ----, theoretical values based on activation enthalpies of pure components; - · - · -, theoretical values based on partial molar activation enthalpies.

fide, isobutyl alcohol-carbon disulfide, triethylamine-ethanol, diethylamine-ethanol, diethylamine-water, ethanol-water, methanol-water.

These systems were selected because adequate thermodynamic data^{9,10} were available, permitting the evaluation of $X(\partial\mu/\partial X)$. The chemicals, which were reagent grade, were dried and redistilled or recrystallized. The thermal diffusion ratios were obtained in cells similar to those previously described^{2,9} calibrated as described there. The analyses were performed in a Zeiss interferometer with a 0.5 centimeter cell. The results are shown in Table I. Each point is the average of 2 to 6 runs with a deviation of not over $\pm 10\%$ for the extreme values of individual runs.¹¹

In column 3 are listed the values of α calculated using ΔH_0^\ddagger , the total activation energy for motion of the pure components. For non-associated mixtures the agreement is good, but gets poorer as the liquids become more associated. This corresponds to the results of Dougherty and Drickamer, who used a similar equation and ΔH_0^\ddagger to get good agreement for non-associated mixtures, but poor agreement for systems involving the alcohols.

In column 4 are listed the calculated α 's using ΔH_b^\ddagger , the activation energy of local expansion, of the pure components. These were calculated from the p - v - t data and viscosity data of Bridgman.¹² In every case the magnitude is nearly correct, but concentration effects are not very satisfactory. Almost all the concentration dependence in these calculated α 's comes from $X(\partial\mu/\partial X)$. The effect of this factor is discussed below.

Earlier, an approximation for the activation energy of a component in a mixture in terms of a

(9) G. Scatchard, S. E. Wood and J. M. Mochel, *THIS JOURNAL*, **43**, 119 (1939); *J. Am. Chem. Soc.*, **61**, 3206 (1939); **62**, 712 (1940); **68**, 1957, 1960 (1946).

(10) (a) A. G. Mitchell and W. F. K. Wynne-Jones, *Disc. Faraday Soc.*, No. 15, 161 (1953); (b) J. L. Copp and D. H. Everett, *ibid.*, No. 15, 174 (1953).

(11) R. L. Saxton, E. L. Dougherty and H. G. Drickamer, *J. Chem. Phys.*, **22**, 1166 (1954).

(12) P. W. Bridgman, *Proc. Amer. Acad. Arts Sci.*, **49**, 4 (1913); **61**, 57 (1926); **66**, 185 (1931).

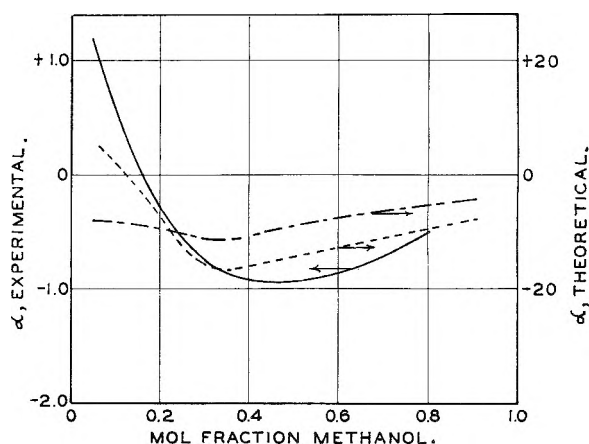


Fig. 7.—The concentration dependence of experimental and theoretical values for the thermal diffusion ratio of methanol-water at 40°: —, experimental results; ----, theoretical values based on activation enthalpies of pure components; - · - · -, theoretical values based on partial molar activation enthalpies.

“partial molar” activation energy was proposed. These were measured for systems not involving CCl_4 since for this compound it was necessary to use diffusion activation energies. Now, evidently it would be desirable to use partial molar $\overline{\Delta H_b^\ddagger}$. Since the necessary pressure measurements on the mixtures could not be made, it is unobtainable. However, for mixtures involving one or no associated compounds, one could assume $\overline{\Delta H_b^\ddagger}$ is a constant fraction of $\overline{\Delta H^\ddagger}$, i.e.

$$\overline{\Delta H_b^\ddagger} \cong \overline{\Delta H^\ddagger} \frac{\Delta H_{b0}^\ddagger}{\Delta H_0^\ddagger} \quad (31)$$

Figures 1 and 2 show the results of this calculation for benzene-cyclohexane and methanol-benzene. The agreement is remarkably good. For mixtures involving water particularly this approximation is certainly not valid. However, it is interesting to compare the values calculated from $\overline{\Delta H^\ddagger}$ with experiment. This is done in Figs. 3-7. The magnitudes are, of course, incorrect, but the concentration dependence, including a sign change, is predicted very well. The improvement over using ΔH_0^\ddagger for the pure component is marked. Considering the necessity of making rather crude approximations for results obtainable only from self-diffusion, the agreement with experiment is striking.

It is desirable here to say something about the role of $X(\partial\mu/\partial X)$. As can be seen from the graphs and calculations, this quantity alone does not give adequate concentration dependence. Nevertheless, as can be seen from Table I it differs by as much as a factor of ten from RT in some cases, and almost always corrects the concentration dependence more closely to experiment. Emery and Drickamer¹³ have also shown the importance of this term.

L. J. Tichacek would like to acknowledge financial assistance from a National Science Foundation Fellowship.

(13) A. H. Emery, Jr., and H. G. Drickamer, *J. Chem. Phys.*, **23**, 2252 (1955).

THE CATALYTIC OXIDATION OF ETHYLENE TO ETHYLENE OXIDE OVER SINGLE CRYSTALS OF SILVER

By J. T. KUMMER

The Dow Chemical Company, Midland, Mich.

Received November 25, 1965

The chemical efficiency of ethylene oxidation and to a lesser extent the absolute rate of reaction do not appear to depend on the type of crystal face used as the catalyst surface. Sulfur or halogen atoms on the surface of silver do increase the chemical efficiency of the reaction. The absolute rate of reaction per cm.² of surface and the energy of activation can be used to substantiate Twigg's proposed mechanism.

Twigg's^{1,2} work on the catalytic oxidation of ethylene has shown that the rate of oxidation of ethylene to carbon dioxide and water is proportional to the square of the concentration of chemisorbed oxygen atoms on the silver surface, which implies that a pair of oxygen atoms are involved, whereas the oxidation of an ethylene molecule to ethylene oxide involves only a single oxygen atom on the surface. Twigg's work leads one to the conclusion that the spatial separation of the chemisorbed oxygen atoms is important in determining the ratio of ethylene oxide to carbon dioxide in the reaction products. If this is so then it would be of interest to study the reaction using different crystallographic planes of silver as the catalytic surface for which the spatial separation of O atoms during reaction would be anticipated to be different on the different crystal faces. This paper describes some experiments in which single crystals of silver having different crystallographic surfaces have been used for the catalytic oxidation of ethylene. Contrary to expectations all of the crystals gave close to the same absolute rate of total oxidation per square centimeter of surface and the same relative amounts of ethylene oxide and carbon dioxide in the product. However, when the crystal surface is partially poisoned by sulfur or chlorine atoms, there is an increase in the ratio of ethylene oxide to carbon dioxide in the product together with a decrease in the total rate of reaction per square centimeter of surface.

Experimental

Catalyst Description.—Since commercial catalysts for the oxidation of ethylene to ethylene oxide have small silver surface areas (less than 2 m.² per gram of silver), it was thought that small flat sheets of silver would be sufficiently active so that the rate of oxidation of ethylene to the oxide could be conveniently measured. This is the case and a clean silver sheet 1.5 cm. wide and 10 cm. long will cause ~5 cc. of ethylene to react with oxygen during one hour at 210°. The surface must be free of sulfur and halogens. Separate experiments on the stability of the surface silver sulfide as a function of [H₂S]/[H₂] in the gas phase have shown that reduction of the silver sheet with hydrogen at temperatures greater than 450° is necessary in order to remove sulfur from the surface in a reasonable time. In the experiments described here a reduction temperature of 570° was used. Chlorine is more readily removed than sulfur. Fortunately the catalyst is not poisoned by oxygen, or water, or carbon dioxide, at reaction temperature. The 35 cm.² of silver surface of the sheet requires ~0.001 cc. S.T.P. of a gas with one sulfur atom per molecule in order to give each silver atom on the surface a sulfur atom. Since ~20 cc. S.T.P. of ethylene and ~30 cc. S.T.P. of oxygen are used per run, it can be seen that gases of com-

mercially available purity (<0.1 p.p.m. by vol. of H₂S will not poison the catalyst).

The polycrystalline silver sheet used for some experiments analyzed 0.02–0.03% Cu, 0.004–0.006% Fe, 0.005–0.01% Mg and 0.01–0.02% Si. It was ~0.004 in. thick and if it was reduced at 570° as received, it was not active as a catalyst. This inactivity is thought to be due to rejection of impurities to the surface as the silver grain size increased during reduction from 0.01 to 100 μ. In order for the polycrystalline sheet to be active it had to first be heated to 900° (this was done in air) and then the surface cleaned with dilute HNO₃. It could then be electropolished and after reduction used as a catalyst.

The $\frac{5}{8}$ " single crystal silver sphere was supplied by Dr. Henry Leidheiser of the Virginia Inst. for Scientific Research. The single crystal sheets were made from silver supplied by The Johnson Matthey & Co. Ltd. who give as an analysis 0.0003% Fe, 0.0002% Cu, 0.0001% Mg, 0.0001% Mn and 0.0001% Ca. They were grown in a graphite mold that had been treated with HF and HCl in an effort to remove impurities in the graphite. The single crystal sheets were 10 cm. long, 1.5 cm. wide and weighed ~30 grams. The metallic impurities were assumed to be in solid solution after reduction at 570°, and at the reaction temperature of 210° the rate of diffusion of these impurities to the surface is very low. Oxygen treatment of the silver catalyst at 210° after reduction does not change the catalyst activity but oxygen treatment at 575° lowers the catalyst activity.

The silver specimens used as catalysts were electropolished in a 5% potassium cyanide solution and washed with distilled water before use. Electron microscope pictures of surface replicas of the electropolished crystals show a smooth surface within the resolution of the microscope (~100 Å.).

Apparatus.—The apparatus used consisted of a vertical quartz reaction tube in which was hung the silver catalyst specimen. This vertical tube was placed over a trap and an all glass circulating pump. These three were connected in series so that the pump could circulate the gas over the silver catalyst through the trap and back over the catalyst again. A glass tube ran from the bottom of the trap through a stopcock to a vacuum system containing a manometer, gas buret, gas storage bulbs, McLeod gage and a mercury diffusion pump. A quartz to Pyrex graded seal was used to connect the quartz reaction vessel with the rest of the apparatus which was Pyrex. The fused quartz seal was used instead of a ground joint because Apiezon grease gradually poisoned the silver surface when the apparatus was left evacuated. It was thought that this poisoning was due to sulfur compounds in the stopcock grease of a higher vapor pressure than the rest of the grease (or sulfur compounds produced by the action of light on the grease) since a Dry Ice trap between the grease and the sample did not prevent poisoning. The Apiezon grease I. used contained 300–1000 p.p.m. of sulfur and the Apiezon hard wax W 3.5% sulfur. It was later found that a wax supplied by the Consolidated Engineering Co. for mass spectrograph use contained only ~7 p.p.m. of sulfur and can be used successfully as a joint seal in this apparatus. The trap in the circulating system was kept at the melting point of ethyl chloride (–138°) during an oxidation run. The temperature of the bath was measured by an ethylene vapor pressure thermometer (55 mm. C₂H₄ pressure at m.p.), and the catalyst system was protected at all times from mercury vapor by a Dry Ice trap.

In order to carry out an experiment, the silver sample was first reduced at 570° overnight with oxygen-free hydrogen

(1) G. H. Twigg, *Trans. Faraday Soc.*, **42**, 284 (1946).

(2) W. H. Langwell, *ibid.*, **42**, 290 (1946).

at 740 mm. pressure. The trap in the circulating system was kept in liquid nitrogen during reduction and the hydrogen was circulated by the all glass magnetic pump at ~ 120 cc. S.T.P. per min. After 24 hours the liquid nitrogen level was slowly lowered until ~ 1 " of the trap was left immersed and the rest was at room temperature. The circulation was stopped, the trap quickly warmed to room temperature, and then the system was evacuated for 5 to 10 min. A known amount of ethylene was added and ethyl chloride at its melting point was placed around the trap in the circulating system. This produced an ethylene pressure in the reaction system of 55 mm. which remained constant during the run since excess ethylene was added in order that a liquid ethylene phase would always be present in the trap. The gas buret bulbs were filled with a known amount of oxygen and at the start of the run the oxygen was admitted and the circulation pump started. The mercury was continually raised in the buret bulbs during the run as the oxygen was consumed in order to keep the total pressure constant at 165 mm. Consequently during the whole run, the partial pressure of both oxygen and ethylene remained constant at 110 and 55 mm., respectively, and the products, CO_2 , ethylene oxide and water were frozen out in the -138° trap (vapor pressure of CO_2 is 0.6 mm.). Since the circulation rate was high with respect to the reaction rate, the experiment was carried out at essentially zero conversion per pass and at constant partial pressure of reactants.

This technique eliminates the homogeneous oxidation of ethylene oxide which is of sufficient rate to be of concern in static experiments.³ The experiment was terminated by raising the furnace and replacing the ethyl chloride trap by liquid nitrogen. At the end of the run the product was analyzed in order to find the amount of oxygen and ethylene consumed and the amount of CO_2 , ethylene oxide and water produced. The oxygen was separated from the products and ethylene by a liquid nitrogen trap, the CO_2 from ethylene and the ethylene oxide by ascarite, and the ethylene from the ethylene oxide by the -138° trap. A small amount of the ethylene oxide ($\sim 5\%$) was lost to the ascarite during the analysis.

Results

A $5/8$ " single crystal sphere was electropolished and used for 4 days as a catalyst at 240° for the ethylene oxygen reaction. It was removed from the apparatus and examined by aid of a microscope. The surface appeared smooth all over the crystal and no evidence could be noted of preferential reaction at any crystal face.

A polycrystalline silver sheet $5/8$ " \times 4" \times 0.004" was placed in the apparatus. When the volume of oxygen left in the buret bulbs was plotted against time, very good straight lines were obtained indicating that the catalyst activity did not change during a run. Table I gives the material balances of the same runs. The energy of activation (Table II) found is lower than Twigg's² and higher than that found by Murray.⁴

The preparation of the polycrystalline surface used above was simple. In working with single crystals however one is faced with the difficulty of proving that the atomic surface plane is the same as the gross geometric surface plane. The literature states that silver crystals can undergo thermal etching at 500° in O_2 and expose the (111) face⁵; that electropolished surfaces are not atomically flat⁶ as prepared at room temperatures, and that the (110) plane of silver is not stable in a vacuum⁷ and

TABLE I

ETHYLENE-OXYGEN REACTION OVER A POLYCRYSTAL SILVER SHEET 34 CM.² AREA

O_2 pressure = 110 mm.; C_2H_4 pressure = 55 mm. during the run.

	Run 51 Temp., 185°			Run 52 Temp., 210°		
	Gas In	Gas vol. in cc. (S.T.P.) Out	Gas vol. in cc. (S.T.P.) Used	Gas In	Gas vol. in cc. (S.T.P.) Out	Gas vol. in cc. (S.T.P.) Used
O_2	38.31	23.17	15.14	36.73	15.91	20.82
C_2H_4	18.83	11.35	7.48	19.45	10.05	9.40
CO_2		8.87			13.05	
$\text{C}_2\text{H}_4\text{O}$		3.01			2.75	
H_2O		9.05			12.55	

Chemical efficiency = 40% to oxide; rate of O_2 consumption from graph (Fig. 2) = 2.73 cc./hr. S.T.P.; rate of C_2H_4 consumption 1.35 cc./hr.

Chemical efficiency = 30% to oxide; rate of O_2 consumption from graph (Fig. 3) = 11.31 cc./hr. S.T.P.; rate of C_2H_4 consumption 5.1 cc./hr.

Energy of activation for oxygen consumption 24,800 cal./mole.

Energy of activation for ethylene consumption 22,900 cal./mole.

rearranges to give other planes. In this work we have observed examples of surface changes due to mechanical strain. For example when a single crystal of silver, which was very slightly bent during mechanical polishing, was reduced at 570° an alteration of the surface took place. Photomicrographs of the surface show that the cube corners are protruding from the surface. Photomicrographs of the same crystal after reduction at 900° show that lines have appeared on the surface which mark the intersections of the (111) planes with the geometric surface. After this treatment the silver sheet was still a single crystal with the orientation of the surface plane 30° from (111), 24° from (110) and 8° from (311). Great care must be exercised in handling the long (10 cm. \times 1.5 cm. \times 0.15 cm.) silver crystals in order to avoid mechanical strains. No difficulty with this respect was encountered in working with the $5/8$ " single crystal sphere. The data in Table II for crystal No. 1 are for the single crystal described above with the cube corners of the cubic silver lattice protruding from the surface.

It became desirable at this point to determine the sensitivity of our silver catalyst to known poisons. By keeping the trap in the circulating system at -195° at all times except when evacuating for 5-10 min. after a reduction, and during an oxidation run, it is possible to avoid sulfur poisoning from the grease used for the only stopcock in the system. It is then possible to add known amounts of carbonyl sulfide before an oxidation run and to measure the rate and chemical efficiency as a function of the ratio of sulfur to silver atoms on the surface of the catalyst. Carbonyl sulfide is a good poisoning agent since it will react with silver to give silver sulfide and CO so that only a collision of the molecule with the correct energy is required to place a sulfur atom on the surface. Carbon dioxide containing 4% COS was measured in a McLeod gage and let into the evacuated tube containing the silver catalyst at 210° . In the absence of oxygen COS will not react with the mercury of the McLeod gage at room temperature. Figure 1 and Table III

(3) J. H. Burgoyne and P. K. Kapur, *Trans. Faraday Soc.*, **48**, 234 (1952).

(4) K. E. Murray, *Australian J. Sci. Research*, **3A**, 433 (1950).

(5) B. Chalmers, R. King and R. Shuttleworth, *Proc. Roy. Soc. (London)*, **A193**, 465 (1948).

(6) D. W. Pashly, *Proc. Phys. Soc. London*, **A64**, 1113 (1951).

(7) H. E. Farnsworth, private communication.

TABLE II

Run no.	Material	Total area, cm. ²	Temp. of run, C. ^o	Rate cc. S.T.P. of O ₂ consumed per hr.	Chemical efficiency, ^a %	Energy of activation for O ₂ consumption, cal./mole
48A	Crystal No. 1	34	210	11.21	31	25,100
48B	Crystal No. 1	34	185	2.71	40	
49A	Polycrystalline sheet	34	210	11.1		23,600
49B	Polycrystalline sheet	34	185	2.97		
50A	Polycrystalline sheet	34	210	9.97		22,400
50B	Polycrystalline sheet	34	185	2.86		
52	Polycrystalline sheet	34	210	11.31	30	24,800
51	Polycrystalline sheet	34	185	2.73	40	

^a Chemical efficiency is the per cent. of the ethylene consumed that goes to ethylene oxide.

show the results of COS poisoning of single crystal No. 4 of 36 cm.² area. The surface plane of this crystal made a dihedral angle of 3° with the (110) plane. This crystal was not mechanically polished before electropolishing in order to avoid any

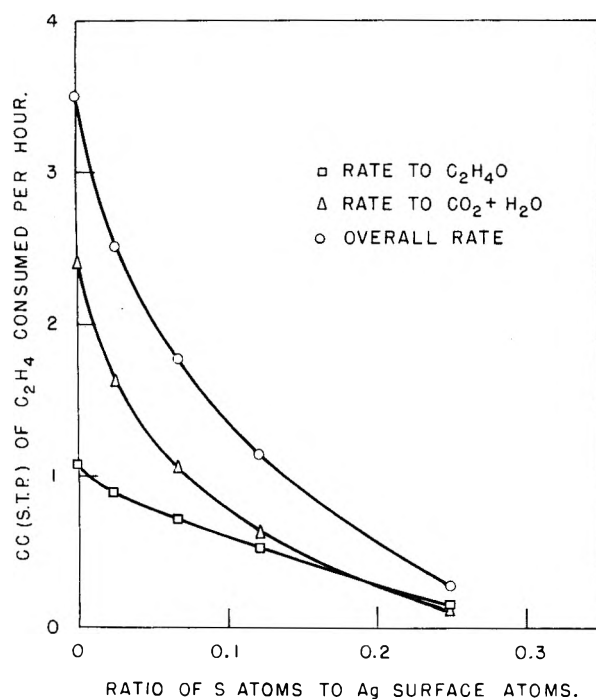


Fig. 1.—Sulfur poisoning of single crystal No. 4, 36.5 cm.² area, 210°.

strains that might produce surface changes. The area of the silver crystal (~36.5 cm.²) would require 0.00115 cc. S.T.P. of COS in order to supply

TABLE III

COS POISONING OF SINGLE CRYSTAL No. 4

[3° from (110)] of 36.5 cm.² total area; temperature, 210°; ethylene pressure, 55 mm. oxygen pressure 110 mm.

Cc. S.T.P. ^a of COS added	Ratio of S atoms to Ag surface atoms	Chem. eff. to C ₂ H ₄ O, %	Rate, cc. (S.T.P.) of C ₂ H ₄ consumed/hr.		
			Total	To CO ₂ and H ₂ O	To C ₂ H ₄ O
0	0	31	3.50	2.42	1.08
.029 × 10 ⁻³	.025	35	2.50	1.62	0.88
.078 × 10 ⁻³	.068	40	1.77	1.06	.71
.14 × 10 ⁻³	.122	46	1.13	0.61	.52
.29 × 10 ⁻³	.25	54	0.26	0.12	.14

^a The crystal was reduced overnight at 570° before each run.

one sulfur atom per silver atom of the surface. The sulfur may be present as a negative sulfur ion on the surface or as sulfate ions on the surface.

Attempts were made to poison the crystal surface with methyl chloride. The methyl chloride as a 4% constituent of CO₂ was added to the evacuated tube containing the silver catalyst at 210°, one cc. of oxygen was added and the mixture circulated over the catalyst for a known length of time (usually 20 min.). It was found that methyl chloride in the presence of oxygen at 210° did not react rapidly with the surface and that long times or large (relative to a surface monolayer) amounts of methyl chloride had to be added in order to poison the catalyst. The results are given in Table IV.

TABLE IV

POISONING OF SINGLE CRYSTAL No. 4 WITH METHYL CHLORIDE

Ethylene oxidation experiment carried out after poisoning. The conditions for the ethylene oxidation are: temperature, 210°; ethylene pressure, 55 mm.; oxygen pressure, 110 mm.

Cc. S.T.P. ^a of CH ₃ Cl added	CH ₃ Cl pretreatment conditions		Length of time of CH ₃ Cl pretreatment, min.	Rate, cc. of C ₂ H ₄ consumed/hr.	Chem. eff. of C ₂ H ₄ consumed
	Other gas present	Temp., °C.			
0.00018	No O ₂	210	~ 20	3.27	34
.00065	No O ₂	210	~ 20	3.51	33
.00076	H ₂	570	5	3.61	36
.00057	O ₂	210	20	3.51	35
.0032	O ₂	210	20	3.33	39
.0066	O ₂	210	20	2.63	47
.0094	O ₂	210	20	2.19	55
.012	O ₂	210	20	1.72	58
.016	O ₂	210	20	1.05	69
.016	O ₂	210	60	0.64	75
.016	O ₂	210	120	0.24	80

^a The crystal was reduced overnight at 570° before each run.

Experiments designed to poison single crystal No. 4 with HCl by treating the silver catalyst first with oxygen at 210° and then with HCl gave erratic results as can be seen by Table V. Amounts of HCl added in excess of that required for a monolayer poisoned the catalyst as would be expected but attempts to obtain quantitative data in the region below one monolayer failed to yield consistent results. It was known from experiments with a flow system for the oxidation of ethylene using commercial catalysts that HCl reacts very fast

with a silver surface covered with oxygen to poison the catalyst so that the single crystal should be poisoned by the HCl. The erratic results are thought to be due to the difficulty of admitting the small amounts of HCl to the catalyst without reacting with mercury or a trace of alkali from the glass, or to adsorption on the glass, and to the difficulties of reaction of this admitted HCl uniformly over the whole surface.

TABLE V

POISONING OF SINGLE CRYSTAL NO. 4 WITH HCl

After HCl poisoning, the ethylene oxidation was carried out at 210°, 55 mm. ethylene pressure, 110 mm. oxygen pressure.

HCl used, cc.	Pretreatment conditions ^a Temp., °C.	Gas present	Rate, cc. of C ₂ H ₄ consumed/hr.	Chemical efficiency, % of C ₂ H ₄ consumed that goes to oxide
12.8 × 10 ⁻³	210	Oxygen	0	—
6.8 × 10 ⁻³	210	Oxygen	0	—
2.27 × 10 ⁻³	210	Oxygen	0.008	(86)
0.95 × 10 ⁻³	210	Oxygen	0.81	68
0.55 × 10 ⁻³	210	Oxygen	2.42	34
0.47 × 10 ⁻³	210	Oxygen	1.94	41
0.40 × 10 ⁻³	210	Oxygen	2.98	38
0.26 × 10 ⁻³	210	Oxygen	2.6	53

^a Sample reduced at 570° before each run.

Table VI gives the data for the ethylene oxidation rate over single crystal surfaces with polycrystal data for comparison. The (111) surface was made by carefully machining the 5/8" single crystal sphere into an octahedron. The orientation of the faces was determined with X-rays before and after using as a catalyst and remained (111). As can be seen by the table there are no large differences in rate of oxidation over the faces employed, and even smaller differences in the chemical efficiencies.

TABLE VI

SINGLE CRYSTAL DATA FOR OXIDATION OF ETHYLENE

Temperature of reaction 210°, O₂ pressure 110 mm., C₂H₄ pressure 55 mm.

Specimen no.	Orientation of surface plane			Crystallographic plane closest to surface plane	Cc. of ethylene/hr./cm. per cm. ² to ethylene oxide	Cc. of ethylene/hr./cm. ² to CO ₂ and H ₂ O	Chemical efficiency, %
	Direction angles ^a of normal to surface plane						
3	35°	60°	72°	8° from (211)	0.017	0.028	37
4	48	42	90	3° from (110)	.028	.062	31
6	51	40	83	9° from (110)	.036	.072	33
Octahedron	54.7	54.7	54.7	0° from (111)	.015	.024	38
Polycrystal sheet045	.105	30

^a Coördinates chosen to coincide with cubic axes of silver crystal.

Discussion

If one believes that the atomic surface planes of the crystals given in Table VI are the same as their geometric planes during reaction, and for the crystals listed in Table VI we have no evidence to the contrary, then it is evident that the crystal face exposed is not of great importance in determining the rate and chemical efficiency of the ethylene oxidation. For other catalytic reactions⁸⁻¹⁰ a relation between reaction rate and the crystal face exposed has been observed.

(8) O. Beek, A. E. Smith and A. Wheeler, *Proc. Roy. Soc. (London)*, **177A**, 62 (1940).

(9) H. Leidheiser and A. T. Gwathmey, *J. Am. Chem. Soc.*, **70**, 1200 (1948).

(10) H. M. C. Sosnovsky, *J. Chem. Phys.*, **23**, 1486 (1955).

The poisoning experiments given here and elsewhere^{4,11,12} show that foreign atoms on the surface do change the rate of oxidation of ethylene and chemical efficiency to ethylene oxide. This can be interpreted in one of two ways. The foreign atoms may force a separation of the O atoms and as indicated by Twigg this will reduce the rate of carbon dioxide formation as the square of the surface O concentration and the rate of oxide formation as the first power of the O concentration. This is suggested by the shape of the curves in Fig. 1 if we assume the O concentration is 1 minus the S atom concentration. The other interpretation is that the S atoms deactivate the surface sites first that have the highest energy of binding of O atoms and that these sites produce more CO₂ and less ethylene oxide than the low energy sites.

As stated before, the rate of the ethylene oxygen reaction per square centimeter of silver surface is high. From the magnitude of this rate it can be shown that some reaction mechanisms are not feasible. The data are inconsistent with the mechanism of gas phase ethylene reacting with a silver surface covered with an adsorbed oxygen layer in which the amount of adsorbed oxygen does not increase with temperature. If the surface oxygen concentration does not increase with temperature, the observed energy of activation is equal to or less than the true energy of activation in this case. The rate of ethylene reaction calculated by collision theory using our experimental $E_A \leq 22900$ cal./mole (assuming the E resides in 2 square terms) is $\leq 8.3 \times 10^{11}$ molecules reacting per second per square centimeter at 210° and 55 mm. ethylene pressure whereas the experimentally observed number of ethylene molecules reacting per second per cm.² at 210° is 1.12×10^{15} . The discrepancy

of three orders of magnitude would indicate that the mechanism proposed above is not correct. If one assumes that the ethylene is physically adsorbed on top of a silver surface covered with an oxygen layer that does not increase with temperature one obtains the same result as above.

In order to calculate the rate correctly one must use a mechanism in which the true energy of activation for ethylene consumption is lower than the observed energy of activation. The only ways one can have the true E_A to be smaller than the observed E_A is for either or both the amount of adsorbed ethylene or oxygen to increase with temper-

(11) F. L. W. McKim and A. Canbron, *Canadian J. Research*, **27B**, 813 (1949).

(12) G. H. Law and H. C. Chitwood, British Patent 518823 (1940).

ature. Physically adsorbed ethylene or oxygen will decrease as the temperature is raised so we must be dealing with chemisorbed ethylene or oxygen. Ethylene appears not^{1,13} to be chemisorbed on silver so that the amount of chemisorbed oxygen must increase with temperature. This can happen

(13) We have been able to measure the exchange between C_2D_4 and H_2 over a polycrystal Ag sheet after reduction but the rate at 210° is considerably slower than the oxidation rate suggesting that ethylene chemisorbed to Ag plays no part in the oxidation reaction.

if the rate of oxygen adsorption is comparable with the rate of reaction and the energy of activation for oxygen adsorption is greater than the true E_A for the reaction. This mechanism is the one proposed by Twigg¹ from his kinetic measurements and in part confirmed by others.^{4,14,15}

(14) A. Orzechowski and K. E. MacCormack, *Canadian J. Chem.*, **32**, 388, 415 (1954).

(15) S. Z. Roginskii and L. Y. Margolis, *Doklady Akad. Nauk S.S.S.R.*, **89**, 515 (1953).

FLUOROCARBON SOLUTIONS AT LOW TEMPERATURES. I. THE LIQUID MIXTURES CF_4 - CHF_3 , CF_4 - CH_4 , CF_4 -Kr, CH_4 -Kr

BY N. THORP AND R. L. SCOTT

Contribution from the Department of Chemistry of the University of California, Los Angeles, California

Received November 26, 1955

The liquid-liquid binary systems, CHF_3 - CF_4 , CHF_3 - C_2F_6 , CF_4 - CH_4 , CF_4 -Kr and CH_4 -Kr, have been studied at low temperatures (105–140°K.). Fluoroform is completely miscible with perfluoroethane but forms two phases with perfluoromethane below a consolute temperature of 130.5°K. These results are in reasonable agreement with solubility parameter theory; the polar fluoroform has a much higher cohesive energy density than the fluorocarbons. The vapor pressures of methane-krypton, methane-perfluoromethane and krypton-perfluoromethane mixtures have been measured at temperatures near 110°K. The first system is nearly ideal, in agreement with the small difference in solubility parameters, but the latter two systems show abnormally large positive deviations from Raoult's law, much greater than can be explained easily. The anomalous deviations in the CH_4 - CF_4 mixture are analogous to those found previously in other fluorocarbon-hydrocarbon systems, but the similar behavior of the CF_4 -Kr system was completely unexpected.

Introduction

In recent years, considerable interest has been aroused by the unusual solvent properties of fluorocarbons and related fluorochemicals. In 1948 Scott¹ concluded that the unusually low mutual solubilities of fluorocarbons and standard organic solvents were a direct result of their low solubility parameters (5.7–6.0 cal.^{1/2}cm.^{-3/2}), and the experimental data then available^{1,2} seemed to be in good agreement with predictions.

In the last five years, however, several hydrocarbon-fluorocarbon solutions have been studied,^{3–9} and abnormally low mutual solubilities have been uniformly observed, in disagreement with the values predicted from the solubility parameters of hydrocarbons and fluorocarbons.¹⁰

As an explanation of this anomaly, Simons and Dunlap³ suggested an abnormally close interaction between the C-H groups of adjacent hydrocarbon molecules ("interpretation") which gives rise to greater heats of mixing than that calculated from the δ -values. On the other hand, Hildebrand¹¹ suggested that the solubility parameters of the hydrocarbons, normally calculated from their

energies of vaporization per ml., be empirically increased by about 0.6 unit in order to fit the data. These two suggestions have been shown to be mutually exclusive,¹² and neither seems very satisfactory for some systems.⁸

Simons and Dunlap^{3,13} included corrections in the theory of regular solutions to take into account volume changes which occur on mixing. This treatment has been extended by Reed¹⁴ to allow properly for differences in the ionization potential of the molecules; the harmonic mean of the two ionization potentials appears in the London formula for dispersion forces, but in the past has usually been approximated by the geometric mean. With this correction he was able to calculate partial molar free energies of mixing which were in accordance with the experimental values for the hydrocarbon but not the fluorocarbon in the systems studied by Simons and co-workers.^{3,5}

In continuation of a general program of research on fluorocarbon solutions, we have investigated the binary liquid systems of CHF_3 - CF_4 , CHF_3 - C_2F_6 , CF_4 - CH_4 , CF_4 -Kr and CH_4 -Kr at temperatures between 105–140°K. In general, our vapor pressure measurements give deviations from Raoult's law which are much greater than would be expected from the difference in solubility parameters.

Experimental

Perfluoromethane, perfluoroethane and fluoroform were obtained from the Jackson Laboratories of E. I. du Pont de Nemours and Company, Incorporated, and were further purified by repeated passage over activated charcoal held at solid CO_2 temperatures. Before being admitted to the storage bulbs, traces of air were removed by repeatedly freezing, pumping while frozen, and melting. Semi-quant-

(1) R. L. Scott, *J. Am. Chem. Soc.*, **70**, 4090 (1948).

(2) J. H. Hildebrand and D. R. F. Cochran, *ibid.*, **71**, 22 (1949).

(3) J. H. Simons and R. D. Dunlap, *J. Chem. Phys.*, **18**, 335 (1950).

(4) J. H. Hildebrand, B. B. Fisher and H. A. Benesi, *J. Am. Chem. Soc.*, **72**, 4348 (1950).

(5) J. H. Simons and J. W. Mausteller, *J. Chem. Phys.*, **20**, 1516 (1952).

(6) J. H. Simons and M. J. Linevsky, *J. Am. Chem. Soc.*, **74**, 4750 (1952).

(7) G. J. Rotariu, R. J. Hanrahan and R. E. Fruin, *ibid.*, **76**, 3752 (1954).

(8) R. L. Scott and E. P. McLaughlin, *ibid.*, **76**, 5276 (1954).

(9) J. A. Neff and B. Hickman, *THIS JOURNAL*, **59**, 42 (1955).

(10) J. H. Hildebrand and R. L. Scott, "Solubility of Non-electrolytes," 3rd Edition, Reinhold Publ. Corp., New York, N. Y., 1950.

(11) J. H. Hildebrand, *J. Chem. Phys.*, **18**, 1337 (1950).

(12) R. L. Scott, *J. Chem. Ed.*, **30**, 542 (1953).

(13) R. D. Dunlap, *J. Chem. Phys.*, **21**, 1293 (1953).

(14) T. M. Reed, III, *THIS JOURNAL*, **59**, 425 (1955).

tative mass spectra were taken of the purified products and they were found to contain less than 1% of impurities. Phillips Research Grade methane and Airco krypton were used directly.

Apparatus.—The general form of the apparatus, designed for use when only small quantities of gases are available, is shown diagrammatically in Figs. 1 and 2, the latter showing in greater detail the vapor pressure vessel and temperature control system.

The vapor pressure vessel has a volume of about 2 cc. and is closed by a click gage sensitive to a small pressure differential which is utilized to measure the total vapor pressures above the liquid mixture. This vessel is placed in a Dewar type container and is held at constant temperature by a bath of refluxing liquid. The boiling point is held constant by means of a solenoid operated valve, which admits liquid nitrogen to the cold finger whenever the pressure rises. Both the bath and the experimental mixture are stirred by means of magnetic stirring bars. The cold finger is filled with copper turnings to aid the heat transfer from the condensing vapors. By this arrangement it was possible to control the bath temperature to 0.2–0.3°K., below 112°K. by using methane, above 112°K., by using methane–propane mixtures.

Procedure.—A sample of gas was drawn from the storage bulbs into the Toepler pump, where its volume was measured, and then transferred to the vapor pressure vessel, where it was condensed. Small amounts of the second component were then added in a similar manner. The mole fraction composition of the liquid mixture was taken to be the ratio of the gas volumes, since the volume of the vapor pressure vessel was less than 1% of the volume of gases added.

To obtain mutual solubility data, the temperature of the bath was varied until two phases separated. This process was repeated several times until the unmixing temperature was determined to about 0.5°K.

Vapor pressure readings were taken after the mixture had been allowed to equilibrate for about five minutes. The pressure on the upper side of the click gage was varied until it operated. From the calibration of the gage, the vapor pressure of the mixture can be calculated with an estimated accuracy of about 1 mm.

Results

Table I gives some of the pertinent physical properties of the compounds studied.

TABLE I

SOME PHYSICAL PROPERTIES OF THE COMPOUNDS STUDIED					
	CF ₄	CHF ₃	CH ₄	Kr	C ₂ F ₆
M.p. (°K.)	89.5	113.0	91.7	115.9	173.1
B.p. (°K.)	145.1	189.0	111.7	119.9	197.9
Heat of vaporization, kcal./mole	3.01	4.23	1.95	2.16	3.86
Molal vol. at b.p. (cc.)	54.2	47.8	38.0	34.0	86.3
($\Delta E^v/V$) ^{1/2} = δ at b.p.	7.1	9.0	6.8	7.5	6.4
δ at 130°K., cal. ^{1/2} cm. ^{-3/2}	7.3	10.3	6.6	7.3	7.7
Electron polarizability $\times 10^{24}$, cm. ³	4.02	...	2.58	2.54	...
Ionization potential, e.v.	17.8	...	13.16	13.93	...

Figures 3, 4 or 5 show the measured total vapor pressures *versus* the mole fraction of one of the constituents in the mixture. The circles are the experimental points, and the full curves are those of the theoretical total vapor pressures, calculated by assuming that the concentration dependence of the excess free energies of mixing can be described by the equations of Scatchard.¹⁵

$$\Delta \bar{F}^E/RT = x_1 \ln \gamma_1 + x_2 \ln \gamma_2 = x_1 x_2 [\alpha + \beta(x_1 - x_2) + \epsilon(x_1 - x_2)^2 + \dots] \quad (1)$$

Considering the first two terms only, we obtain

(15) G. Scatchard, *Chem. Revs.*, **44**, 7 (1949).

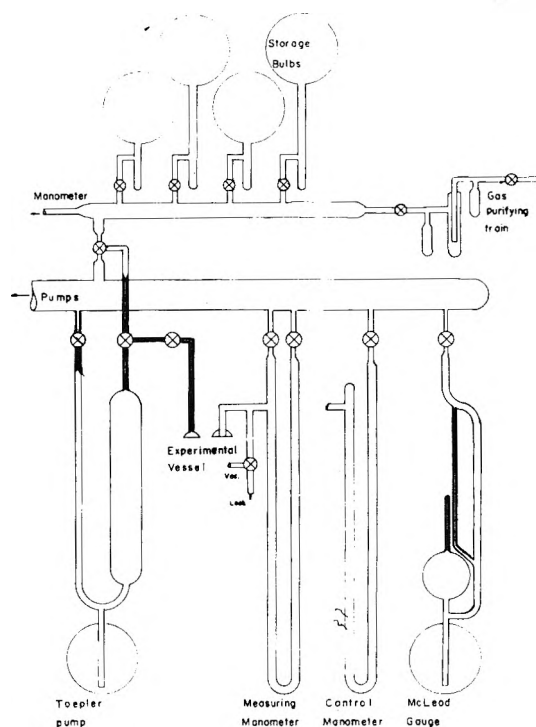


Fig. 1.

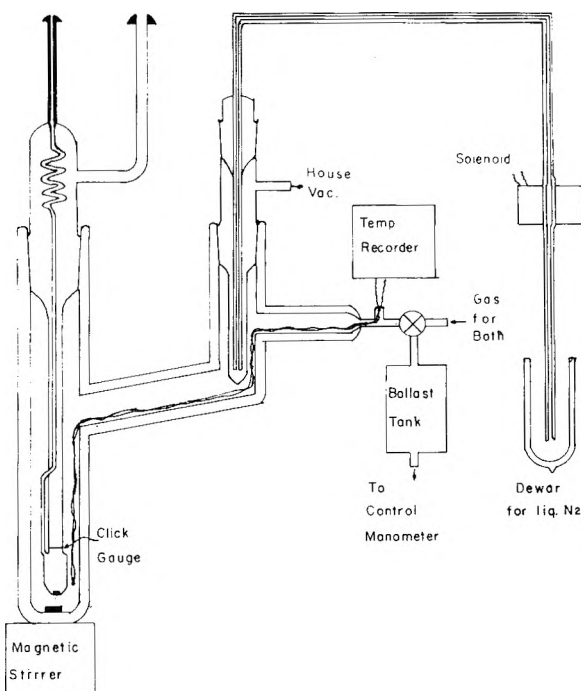


Fig. 2.—Experimental arrangement for measuring vapor pressures at low temperatures.

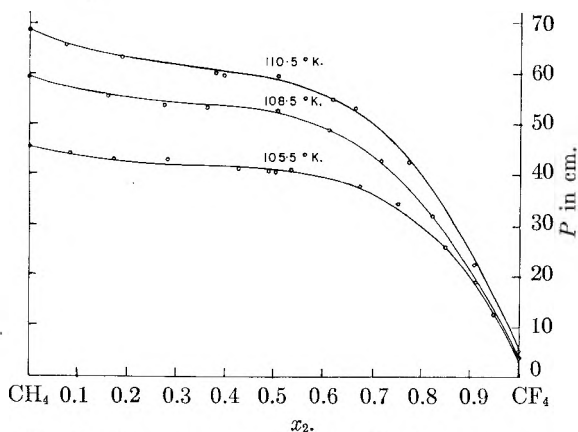
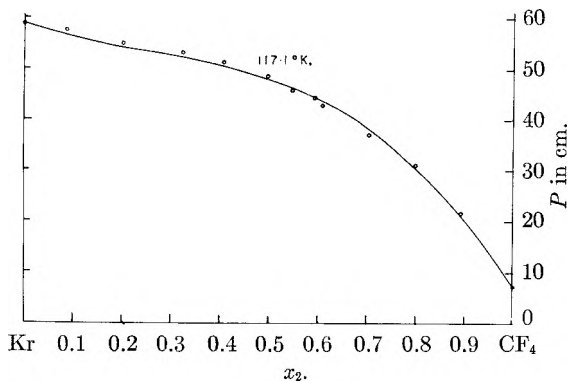
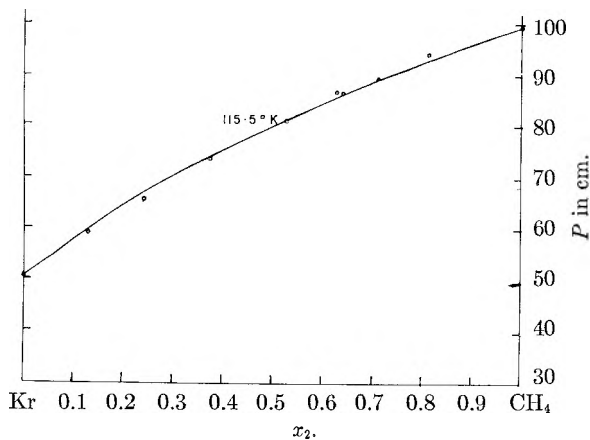
for the partial molal free energies of mixing

$$\frac{\Delta \bar{F}_1^E}{RT} = \ln \gamma_1 = x_2^2 [\alpha + \beta(3x_1 - x_2)] \quad (2a)$$

$$\frac{\Delta \bar{F}_2^E}{RT} = \ln \gamma_2 = x_1^2 [\alpha - \beta(3x_2 - x_1)] \quad (2b)$$

The total vapor pressure *P* of a two-component mixture may be expressed in terms of the vapor pressures of the pure components *p*₁⁰ and *p*₂⁰ as

$$P = p_1^0 a_1 + p_2^0 a_2 = p_1^0 r_1 \gamma_1 + p_2^0 r_2 \gamma_2 \quad (3)$$

Fig. 3.—Vapor pressures of CH₄-CF₄ mixtures.Fig. 4.—Vapor pressures of Kr-CF₄ mixtures.Fig. 5.—Vapor pressures of Kr-CH₄ mixtures.

Combining this equation with 2a and 2b we get

$$P = p_1^0 x_1 \exp x_2^2 [\alpha + \beta(3x_1 - x_2)] + \frac{p_2^0 x_2 \exp x_1^2 [\alpha - \beta(3x_2 - x_1)]}{x_1} \quad (4)$$

where a_1 and a_2 are activities, x_1 , x_2 mole fractions of components 1 and 2, respectively, and α and β are constants.

From the initial slopes of the total vapor pressure curve, a rough estimate of the value of the constants α and β was made. The final value of these constants was obtained by a method of least squares.¹⁶

From the second virial coefficient and the equations of Scatchard and Raymond¹⁷ corrections for

(16) J. A. Barker, *Austral. J. Chem.*, **6**, 207 (1953).

(17) G. Scatchard and C. L. Raymond, *J. Am. Chem. Soc.*, **60**, 1278 (1938).

the non-ideality of the vapor phase were made. These were found to have a negligible effect on the value of the constants α and β .

Table II gives the value of these constants for the systems CF₄-Kr, CH₄-Kr and CF₄-CH₄.

TABLE II
VALUES OF THE CONSTANTS α AND β BY THE METHOD OF LEAST SQUARES FOR THE THREE SYSTEMS CF₄-CH₄, CF₄-Kr, CH₄-Kr

$$\begin{aligned} \text{Equations } \ln \gamma_1 &= [\alpha + \beta(3x_1 - x_2)]x_2^2 \\ \ln \gamma_2 &= [\alpha - \beta(3x_2 - x_1)]x_1^2 \end{aligned}$$

System	Subscript 1 denotes	α	β
CH ₄ -CF ₄ at 110.5°K.	CH ₄	1.56	0.36
CH ₄ -CF ₄ at 108.5°K.	CH ₄	1.61	0.42
CH ₄ -CF ₄ at 105.5°K.	CH ₄	1.78	0.30
CF ₄ -Kr at 117.1°K.	Kr	1.21	0.32
CH ₄ -Kr at 115.5°K.	Kr	0.25	0.0

The solubility of a component of a solution of non-polar non-electrolytes may frequently be explained with the aid of the simple regular solution equation¹⁰

$$\Delta \bar{F}^E = (x_1 \bar{V}_1 + x_2 \bar{V}_2)(\delta_1 - \delta_2)^2 \phi_1 \phi_2 \quad (5)$$

where $\Delta \bar{F}^E$ is the excess free energy of mixing; x_1 , x_2 are mole fractions; ϕ_1 , ϕ_2 are volume fractions; \bar{V}_1 , \bar{V}_2 are molar volumes; δ_1 , δ_2 are the "solubility parameters" of the pure components and are the square roots of the energy of vaporization per ml. (*i.e.*, $\Delta E^v/V$)^{1/2}; the subscripts referring to components 1 and 2.

An alternative equation is obtained by using the Flory-Huggins entropy which attempts to correct for the difference in the molecular size of the two components

$$\Delta \bar{F}^E = RT[x_1 \ln(\phi_1/x_1) + x_2 \ln(\phi_2/x_2)] + (x_1 \bar{V}_1 + x_2 \bar{V}_2)(\delta_1 - \delta_2)^2 \phi_1 \phi_2 \quad (6)$$

where the symbols have the same meaning as equation 5.

TABLE III
 $\delta_1 - \delta_2$ DIFFERENCES FOR THE THREE SYSTEMS CF₄-CH₄, CF₄-Kr AND CH₄-Kr

System	δ_1^a	δ_2^a	Calcd. $ \delta_1 - \delta_2 $	Exptl. $\Delta \delta$ Eq. 5	Eq. 6
CF ₄ -CH ₄	7.6	6.8	0.8	2.9	2.6
CF ₄ -Kr	7.6	7.6	0.0	2.7	2.3
CH ₄ -Kr	6.8	7.6	0.8	1.3	1.1

^a Solubility parameters estimated at 110°K.

Table III gives the "thermodynamic" solubility parameters of the three substances, evaluated from the heats of vaporization and molar volumes of the pure components at 110°K. The difference of these δ 's is then compared with the "experimental" values obtained by fitting equations 5 and 6 to the experimental excess free energies.

Table IV gives the excess free energies of mixing at $x = 1/2$, for the systems studied, calculated from (a) the experimental value of the activity coefficient and (b, c) calculated from the "thermodynamic" δ values of the pure liquids, assuming (b) ideal entropy of mixing and (c) the Flory-Huggins entropy of mixing.

TABLE IV
EXCESS FREE ENERGIES OF MIXING,
CAL/MOLE AT $x_1 = x_2 = 1/2$

$\Delta \bar{F}^E$	CF ₄ -CH ₄	CF ₄ -Kr	CH ₄ -Kr
	at 110.5°K.	at 117.1°K.	at 115.5°K.
Obsd.	86	75	14
Calcd. from "thermodynamic" δ 's			
Eq. 5	7	0	6
Eq. 6	5	-5	6

Figure 6 shows the miscibility curve for CHF₃ and CF₄. The critical solution temperature is 130.5°K., and the critical mole fraction of CHF₃ is about 0.43 by the method of rectilinear diameters. The system CHF₃-C₂F₆ is miscible in all proportions.

The simplified expression for the critical solution temperature, T_c , is given by the regular solution theory¹⁰ as

$$4RT_c = (\bar{V}_1 + \bar{V}_2)(\delta_1 - \delta_2)^2 \quad (7)$$

where the \bar{V} 's and δ 's have the same meaning as in equations 5 and 6.

Discussion

The immiscibility of fluoroform and carbon tetrafluoride near the boiling point of the latter has been reported by Hadley and Bigelow.¹⁸ From the heats of vaporization at the boiling points,¹⁹ values at other temperatures were estimated by methods described elsewhere.¹⁰ With an accuracy of 0.1–0.2 δ unit, the solubility parameters of CF₄ and CHF₃ at 130°K. are 7.3 and 10.3 (cal./cm.³)^{1/2} respectively. The difference of these two is 3.0, and this compares favorably with a value of 3.3, derived from the experimental results and equation 7. Thus this system is in reasonable agreement with theoretical predictions. The great difference between CF₄ and CHF₃, as evidenced by the difference in solubility parameters, is also reflected in the large difference in the heats of vaporization and boiling points, in contrast with the great similarity in properties of CCl₄ and CHCl₃; an appealing explanation of the abnormal behavior of fluoroform lies in the possibility of hydrogen bonding.

C₂F₆ and CHF₃ do not form two phases. The estimated ($\delta_1 - \delta_2$) difference is 2.6 at 190°K. This gives T_c , by equation 7, about 110°K., well below the freezing point of C₂F₆. Therefore the miscibility of C₂F₆-CHF₃ mixtures is in agreement with theory.

The solubility parameters at 110°K. for CF₄, Kr and CH₄ are calculated as 7.6, 7.6 and 6.8, respectively, with an accuracy of 0.1–0.2 δ unit. The ($\delta_1 - \delta_2$) differences from these figures gives 0.0 for CF₄-Kr, 0.8 for CF₄-CH₄ and 0.8 for Kr-CH₄. The experimentally determined values for the same systems are 2.7, 2.9 and 1.3, respectively.

The difference between the calculated and observed excess free energy of mixing at $x_1 = x_2 = 1/2$, Table IV, is about 8 calories for CH₄-Kr mixtures, which is only 10% of a measure of thermal energies, $1/2 RT$. Small effects of this magnitude may be due to any number of minor causes, which

(18) E. H. Hadley and L. A. Bigelow, *ibid.*, **62**, 3302 (1940).

(19) "Selected Values of Chemical Thermodynamic Properties," United States Government Printing Office, Washington, D. C.

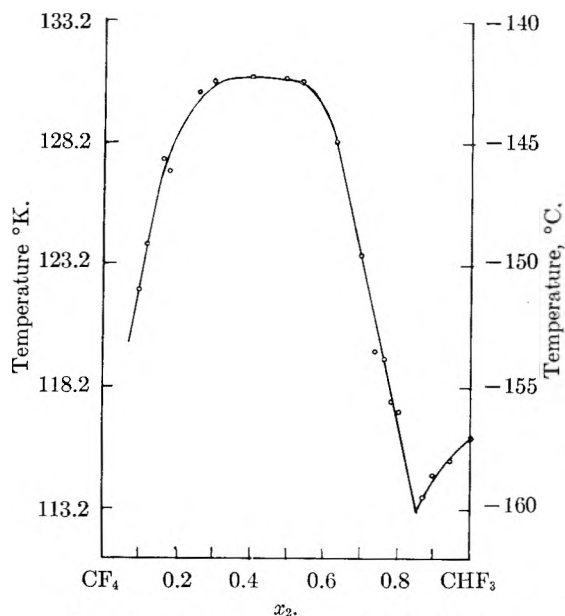


Fig. 6.—Immiscibility curve for CF₄-CHF₃.

are ignored in the derivative of the regular solution-solubility parameter equations. The experimental error in the measurement of excess free energy of mixing is certainly of this order. In this light, therefore, the CH₄-Kr system is unexceptional and in good agreement with theory.

However, this is not the case for the CH₄-CF₄ and Kr-CF₄ systems. Here $\Delta \bar{F}^E$ at $x = 1/2$ is approximately 86 cal./mole ($0.39RT$) at 110°K. and 75 cal./mole ($0.32RT$) at 117°K., respectively. Such a result was not unexpected for CH₄-CF₄ mixtures in view of anomalous behavior found by previous workers³⁻⁹ for fluorocarbon-hydrocarbon pairs. The large deviations from ideality found for Kr-CF₄ mixtures were not anticipated; solutions of fluorocarbons with liquids other than hydrocarbons have been found to conform well to solubility parameter theory.

Since the differences in molar volume of the various substances are not very large, use of the Flory-Huggins entropy of mixing does not alter the situation appreciably. Increasing the δ value of the hydrocarbon by about 0.6 unit, as suggested by Hildebrand,¹¹ only makes matters worse, for then the δ value of CH₄ almost equals that of both CF₄ and Kr.

No information is available on the volume changes of mixing for these systems, so we are unable to make the corrections of Simons and Dunlap.³ There is little agreement on the value of the ionization potential for CF₄, so it has not been possible to apply the corrections of Reed¹⁴ with any success.

Acknowledgment.—This work was supported by the Atomic Energy Commission under Project 13 of Contract AT(11-1)-34 with the University of California. We wish to thank the Jackson Laboratories of E. I. du Pont de Nemours and Company for their generous gift of the CF₄, CHF₃ and C₂F₆ used in these experiments, and Dr. B. B. Fisher for the construction of the major part of the apparatus.

SOLUBILITIES OF IODINE AND PHENANTHRENE IN HYDROFLUOROCARBONS

BY EDWARD P. McLAUGHLIN AND ROBERT L. SCOTT

Contribution from the Department of Chemistry of the University of California, Los Angeles, Calif.

Received November 26, 1955

1-Hydroperfluoroheptane and 1,8-dihydroperfluoroöctane were prepared and their vapor pressures over a range 25–50° were measured. Heats of vaporization, dipole moment, densities and refractive indices were determined at 25°. From these data, a solubility parameter of 6.3 was calculated for both liquids. The solubilities of iodine and phenanthrene in $C_7F_{15}H_2$ were measured at 25° and were found to be in reasonable agreement with the solubility parameters. The solubilities of these solutes in $C_7F_{15}H$ fit better with $\delta = 5.7$ for the solvent. Phenanthrene does not show in these solvents the anomalous solubility previously reported in fluorochemicals containing no hydrogen.

Introduction

The anomalous solvent properties of fluorocarbons which have become evident^{1–8} in the last five years have been considered in two recent papers from this Laboratory. One, by McLaughlin and Scott,⁶ showed that solutions of iodine and of stannic iodide in perfluorotri-*n*-butylamine and in perfluoro-*n*-propylpyran exhibit "normal" behavior (*i.e.*, in agreement with estimates based upon solubility parameters⁹), whereas the solubility of phenanthrene in these two solvents is much too low to be reconciled with theory. This anomaly parallels that found in hydrocarbon-fluorocarbon systems previously investigated.^{1–5} The other paper,⁸ by Thorp and Scott, has shown that these abnormally large deviations from ideality, in disagreement with the values predicted from solubility parameters, extend to fluorocarbon—rare gas liquid mixtures.

Fluorochemical solvents with one or two hydrogen atoms in known positions can now be prepared and in this paper we report investigations of the effect which substitution of hydrogen atoms into a fluorocarbon has upon solubility.

Experimental

Materials and Purification.—Baker and Adamson reagent grade iodine was further purified by resublimation and kept in a desiccator over Drierite.

Eastman Kodak White Label phenanthrene was purified according to the method of Bradley and Marsh,¹⁰ recrystallized ten times from ethanol and the fraction retained had m.p. 98°.

Through the kind cooperation of Dr. W. B. McCormack, a sample of 1,1,9-trihydroperfluorononanol was received from the E. I. du Pont de Nemours and Company, Inc. Following the method of Wolff,¹¹ the sample was oxidized to the acid by potassium permanganate in glacial acetic acid. The latter was neutralized with sodium hydroxide in methanol and decarboxylated in ethylene glycol according to the

procedure described by La Zerte,¹² *et al.*, to yield the product, 1,8-dihydroperfluoroöctane.

A research sample of perfluoroöctanoic acid, kindly donated by the Minnesota Mining and Manufacturing Company, was decarboxylated in the manner described by La Zerte,¹² *et al.*, to form the product, 1-hydroperfluoroheptane.

The perfluoro products cited above were redistilled in an 8 mm. \times 91 cm. helipak column (90 plates at total reflux) at a 20:1 take-off ratio. The fractions of 1,8-dihydroperfluoroöctane boiling from 134–135° and of 1-hydroperfluoroheptane boiling from 94–95° at 751 mm. were used in the investigation.

Apparatus and Procedures.—C. T. O'Konski's capacitance bridge apparatus¹³ was used to determine the dielectric constant of the pure liquid. The operating frequency was 10 kilocycles.

Standard pycnometric methods were employed in the density measurements.

Refractive indices were obtained with an Abbe refractometer equipped with special prisms and capable of measuring values in the range 1.2–1.5.

A static method was employed to measure vapor pressures of the fluorochemicals. The apparatus is shown in Fig. 1. The liquid was dried over P_2O_5 , introduced into flask A, and frozen by a liquid nitrogen bath. The entire system was then evacuated to pressures less than 10^{-5} mm. of mercury. Next, stopcock a was closed and the liquid degassed by several sequences of freezing, opening stopcock b, pumping off, closing stopcock b, and melting. Stopcock a was then opened and the liquid boiled gently under vacuum into bulb B where it was recondensed with liquid nitrogen. After closing stopcock a, mercury was placed in removable flask A and, with the liquid in bulb B frozen by a liquid nitrogen trap and stopcocks a and b open, the mercury was distilled into the sidarms c and d. Finally, stopcock a was closed, the apparatus was detached from the vacuum system and placed in a thermostat bath which was maintained to $\pm 0.01^\circ$. The measurements were made in the usual manner with a cathetometer to read the height of the mercury columns. The usual corrections were made.

Solubilities at $25.00 \pm 0.02^\circ$ of iodine and phenanthrene in the two fluorochemicals were determined using essentially the same apparatus and procedure as in the previous investigation.⁶ The solubilities of phenanthrene were calculated from the spectral absorption peak at 270 μ for which the extinction coefficients were found to be 1.20×10^3 and 1.21×10^4 l. mole⁻¹ cm.⁻¹ in $C_7F_{15}H$ and $C_8F_{16}H_2$, respectively.

Results

In a saturated solution, the activity of the solute is equal to the activity of the pure solid with which it is in equilibrium and is conventionally expressed as x_2^s , the mole fraction of solute in an ideal solution ($\gamma_2 = 1$). Thus, in a non-ideal solution, the activity coefficient, γ_2 , equals x_2^s/x_2 . Table I summarizes the solubility measurements and the calculated activity coefficients. The solubility of iodine in perfluoro-*n*-heptane measured by Hilde-

(1) J. H. Simons and R. D. Dunlap, *J. Chem. Phys.*, **18**, 335 (1950).
(2) J. H. Hildebrand, B. B. Fisher and H. A. Benesi, *J. Am. Chem. Soc.*, **72**, 4348 (1950).

(3) J. H. Simons and J. W. Mausteller, *J. Chem. Phys.*, **20**, 1516 (1952).

(4) J. H. Simons and M. J. Linevsky, *J. Am. Chem. Soc.*, **74**, 4750 (1952).

(5) G. J. Rotariu, R. J. Hanrahan and R. E. Fruin, *ibid.*, **76**, 3752 (1954).

(6) E. P. McLaughlin and R. L. Scott, *ibid.*, **76**, 5276 (1954).

(7) J. A. Neff and B. Hickman, *THIS JOURNAL*, **59**, 42 (1955).

(8) N. Thorp and R. L. Scott, *ibid.*, **60**, 670 (1956).

(9) Cf. J. H. Hildebrand and R. L. Scott, "Solubility of Non-Electrolytes," 3rd Ed., Reinhold Publ. Corp., New York, N. Y., 1950.

(10) G. Bradley and J. K. Marsh, *J. Chem. Soc.*, 650 (1933).

(11) N. E. Wolf, E. I. du Pont de Nemours and Co., Inc., private communication.

(12) J. D. La Zerte, L. J. Hals, T. S. Reid and G. H. Smith, *J. Am. Chem. Soc.*, **75**, 4525 (1953).

(13) C. T. O'Konski, *ibid.*, **73**, 5093 (1951).

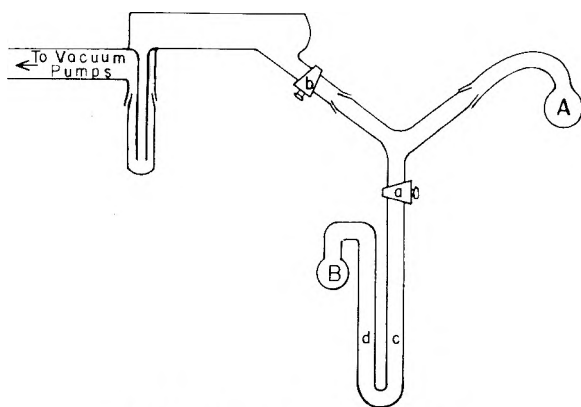


Fig. 1.—Vapor pressure apparatus.

brand, Benesi and Mower¹⁴ and the solubilities in *n*-hexane¹⁵ are also included for comparison.

The well-known equation applicable to components of a "regular" solution is⁹

$$\ln \gamma_2 = \bar{V}_2(\delta_1 - \delta_2)^2 \varphi_1^2 / RT \quad (1)$$

where γ_2 is the activity coefficient, \bar{V}_2 the molar volume of component 2, and φ_1 the volume fraction of component 1; the δ 's ("solubility parameters") are the square roots of the energies of vaporization per ml. of the pure components.

TABLE I
SOLUBILITIES AT 25.0°

Solute	Solvent	$\frac{\text{g. Solute}}{1000 \text{ g. Solvent}}$	Mole %	γ
I ₂	Ideal		25.8	1
	<i>n</i> -C ₆ H ₁₄	13.4	0.456	57
	C ₈ F ₁₆ H ₂	0.284	0.0451	572
		0.286		
	C ₇ F ₁₅ H	0.191	0.0278	928
C ₁₄ H ₁₀	<i>n</i> -C ₇ H ₁₆	0.119	0.0182	1400
	Ideal		22.1	1
	<i>n</i> -C ₆ H ₁₄	87	4.2	5
	C ₈ F ₁₆ H ₂	2.162	0.488	45
		2.165		
	C ₇ F ₁₅ H	0.781	0.160	138
		0.762		

Experimental measurement of the activity coefficients enables us to evaluate, by substitution of all known or fixed quantities into equation 1, an "empirical" δ_1 for the solvent. The results of such calculations for the two fluorochemicals treated here are shown in Table II; also included are the

TABLE II

SOLUBILITY PARAMETERS AT 25.0°

Solvent	Solute: I ₂ ; $\bar{V}_2 = 59$, $\delta = 14.1$			Solute: C ₁₄ H ₁₀ ; $\bar{V}_2 = 158$, $\delta = 9.8$		
	γ_2	$\delta_2 - \delta_1$	δ_1	γ_2	$(\delta_2 - \delta_1)$	δ_1
<i>n</i> -C ₆ H ₁₄	57	6.4	7.7	5	2.4	7.4
C ₈ F ₁₆ H ₂	572	7.9	6.2	45	3.8	6.0
C ₇ H ₁₅ H	928	8.3	5.8	138	4.3	5.5
(C ₄ H ₉) ₃ N	1120	8.4	5.7	757	5.0	4.8
C ₈ F ₁₆ O	1240	8.5	5.6	884	5.0	4.8
<i>n</i> -C ₇ F ₁₆	1400	8.5	5.6			

(14) J. H. Hildebrand, H. A. Benesi and L. M. Mower, *J. Am. Chem. Soc.*, **72**, 1017 (1950)

(15) J. H. Hildebrand, E. T. Ellefson and C. W. Beebe, *ibid.*, **39**, 2301 (1917).

values for *n*-C₆H₁₄, *n*-C₇F₁₆ and those determined previously⁶ for (C₄F₉)₃N and C₈F₁₆O.

The dipole moment of the pure liquid 1-hydroperfluoroheptane was evaluated by means of the Böttcher equation¹⁶

$$\mu = \left[\frac{9kT}{4\pi N} \times \frac{(\epsilon - n_\infty^2)(2\epsilon + n_\infty^2)}{\epsilon(n_\infty^2 + 2)^2} \right]^{1/2} \quad (2)$$

where μ is the dipole moment, k is the Boltzmann constant, ϵ is the dielectric constant of the pure liquid, N is the molecular number density, T is the absolute temperature, and n_∞ is the refractive index at infinite wave length. The values of μ obtained with equation 2 using n_D , the refractive index at the wave length of sodium light, instead of n_∞ are generally not less accurate than those obtained from dilute solutions with the usual extrapolation methods.¹⁶ The dipole moment obtained in this way is shown in Table III. The molar volume and refractive index, necessary for the calculation of μ , are also given in Table III both for 1-hydroperfluoroheptane and for 1,8-dihydroperfluoroheptane. Due to lack of sufficient quantity of the latter, its dipole moment was not obtained.

The logarithms of the vapor pressures, accurate to $\pm 0.5\%$, for both perfluoro compounds over a 25° temperature range are plotted in Fig. 2 against

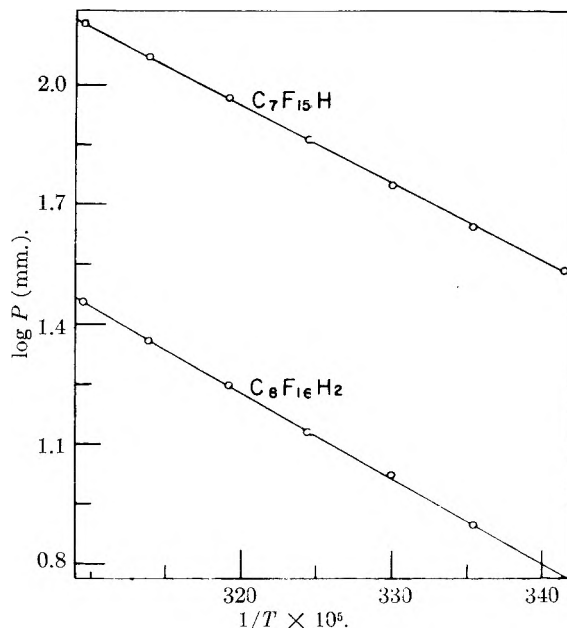


Fig. 2.—Hydrofluorocarbon vapor pressures.

$1/T$. Since the experimental points fell on straight lines and showed little or no change over the temperature range considered, the molar heats of vaporization, $\Delta\bar{H}^v$, at 25° were calculated using the integrated Clapeyron-Clausius equation. These values are given in Table III. With the assumption that at the low vapor pressures exerted by these fluorochemicals at 25° the vapor in equilibrium with the liquid is essentially ideal, we may evaluate δ by means of the equation⁹

$$\delta \cong \left(\frac{\Delta\bar{H}^v - RT}{\bar{V}} \right)^{1/2} \quad (3)$$

(16) C. J. F. Böttcher, "Theory of Electric Polarization," Elsevier Publishing Co., Amsterdam, Netherlands, 1952.

The "thermodynamic" δ values thus obtained are also shown in Table III.

TABLE III

THERMODYNAMIC CONSTANTS AT 25.0°

	\bar{V}_1 (cm. ³ mole ⁻¹)	n_D	$\Delta\bar{H}^v$ (kcal. mole ⁻¹)	δ_1 (cal. ^{1/2} cm. ^{-3/2})	ϵ dielec- tric con- stant	μ , dipole moment (Debyes)
C ₇ F ₁₅ H	215	1.2718	9.01	6.26	3.148	1.75
C ₂ F ₁₆ H ₂	229	1.2878	9.77	6.33		

Discussion

In order to determine whether solutions of phenanthrene in 1-hydroperfluoroheptane and 1,8-dihydroperfluoroöctane should be considered anomalous on the basis of regular solution theory, we may compare the empirical solubility parameter, δ_1 , of the solvent obtained, with the aid of equation 1, from the experimental measurements of phenanthrene solubility to that obtained from iodine solubility and from the heat of vaporization. In the case of 1,8-dihydroperfluoroöctane, δ_1 derived from iodine solubility is in good agreement with δ_1 derived from the heat of vaporization, 6.2 and 6.3, respectively. In the case of 1-hydroperfluoroheptane, δ_1 derived from the heat of vaporization is 6.3 while δ_1 derived from iodine solubility is 5.8. This discrepancy may be due to the dipole moment of the solvent which should reduce its mutual solubility with other components, but it is not clear why a similar effect should not be observed with the dihydro compound. Such an effect is not unusual. Chloroform which, like 1-hydroperfluoroheptane, in its solution with iodine, exhibits the violet color characteristic of regular solutions is a similar instance. However, presumably due to its dipole moment of 1.05 debyes, the solubility of chloroform with non-polar non-electrolytes can only be reconciled by an empirical δ -value of 9.0 instead of the "thermodynamic" value of 9.3.¹⁷

Experimental determination of phenanthrene solubility leads to a δ_1 value of 6.0 for C₈F₁₆H₂ and 5.5 for C₇H₁₅H. This is a discrepancy of 0.3 δ units in both cases and might be considered within the limits of error of the theory,¹⁶ whereas, in a previous investigation of solutions of phenanthrene in perfluoro solvents,⁶ a discrepancy of 0.8–0.9 units was noted. *Apparently the hydrocarbon-fluorocarbon anomaly largely disappears when there is any hydrogen in the fluorocarbon molecule!*

Reed¹⁸ has suggested that the ratio of the ionization potential of a fluorocarbon to that of a hydrocarbon is greater than 1.3. Consequently,

(17) J. H. Hildebrand, *Chem. Revs.*, **44**, 37 (1949).

(18) T. M. Reed, III, *This Journal*, **59**, 425 (1955).

the assumption in solubility parameter theory that the geometric mean may be substituted for the harmonic mean of the ionization potentials in computing the dispersion energy for 1–2 pairs, may be valid for hydrocarbon-fluorocarbon mixtures. If this suggestion is valid for all fluorocarbon-hydrocarbon mixtures, the reduction of the discrepancy in δ_1 from 0.9 to 0.3 unit may be due to the lowering of the ionization potential of the fluorocarbon by the introduction of hydrogen atoms into the molecule.

As an alternative explanation, we may consider the force fields of fluorocarbon molecules. Rowlinson¹⁹ has pointed out that the intermolecular forces, even in spherically symmetric perfluorocarbons, act through points well removed from the centers of the molecules. The abnormally low mutual solubility of hydrocarbon-fluorocarbon mixtures may be due to a pronounced difference in their force fields since the intermolecular forces of the hydrocarbons, whose polarizable electrons lie in the C–H bonds, probably much more closely approximate central forces. If this be the case, the introduction of hydrogen atoms into the fluorocarbon molecule may somehow disturb its force field so as to diminish this effect.

In any event, the results of this investigation, when coupled with previous data,^{1–3} suggest that grossly abnormal behavior in regular solutions is restricted to mixtures containing a perfluoro substance as one component and that the anomaly is due to some property specifically characteristic of perfluoro molecules; but it is far from clear why some fluorocarbon solutions (*e.g.*, those with I₂ and CCl₄) show no anomalies whatever.

Acknowledgments.—The major part of this research was supported by the Atomic Energy Commission under Project 13 of Contract AT(11-1)-34 with the University of California.

We wish to acknowledge the coöperation of Professor J. H. Hildebrand of the University of California at Berkeley in allowing one of us (E.P.M.) to work in his laboratory and utilize his equipment for the vapor pressure measurements and the coöperation of Professor C. T. O'Konski in allowing the utilization of his dielectric constant apparatus. We also wish to thank Dr. L. W. Reeves for his assistance in the design and construction of the vapor pressure apparatus.

We also wish to acknowledge the gift by the Minnesota Mining and Manufacturing Company and by the Organic Chemicals Division of E. I. du Pont de Nemours and Company of the raw materials for preparation of the hydrofluorocarbons.

(19) J. S. Rowlinson, *J. Chem. Phys.*, **20**, 337 (1952).

STRUCTURES OF SOME GERMANIDES OF FORMULA M_5Ge_3 ¹BY HANS NOWOTNY,² ALAN W. SEARCY AND J. E. ORR*Contribution from the Division of Mineral Technology, University of California, Berkeley, California**Received November 28, 1955*

The phase $NbGe_{0.67\pm 0.05}$ belongs to the $D8_8$ structure type. The phases $NbGe_{0.54\pm 0.06}$ and β - $TaGe_{0.5}$ are isostructural with Mo_5Si_3 . The phase α - $TaGe_{0.5}$ has the same structure as the high temperature Ta_5Si_3 phase. All the phases studied have the ideal composition M_5Ge_3 .

It is well-known that the germanides formed by transition metals are closely related to analogous silicides in respect to their compositions and structures.³ These relationships are to be expected from the fact that silicon and germanium belong to the same group of the periodic system and are of similar size.

Some of the most interesting silicides are those of the formula type " M_5Si_3 ."⁴ These silicides show exceptionally high melting points and have often a remarkable behavior with respect to stabilization by small metalloides, in particular by carbon and oxygen. The germanides Ti_5Ge_3 ⁵ and Mn_5Ge_3 ⁶ are known to be isostructural with the stabilized form ($D8_8$) of the analogous silicides.

In the present investigation structures of additional germanides with the M_5Ge_3 formula are described. The phase identified from composition studies as $NbGe_{0.67\pm 0.06}$ ⁷ was found to crystallize with the previously mentioned $D8_8$ structure. The phases identified as $NbGe_{0.54\pm 0.06}$ and β - $TaGe_{0.5}$ ⁸ have the same structure as the high-temperature tetragonal modification of Nb_5Si_3 ⁹ whose structure has been independently determined by different groups for Mo_5Si_3 and W_5Si_3 ¹⁰ and also for Cr_5Si_3 and Mo_5Ge_3 .¹¹

The structure of the phase identified as α - $TaGe_{0.5}$ was found to be the same as that of the low temperature tetragonal modification of Nb_5Si_3 ¹² and of the high temperature form of $TaSi_0.6$.¹³

The diffraction powder patterns were taken of samples whose preparations were described previously.^{7,8} Copper $K\alpha$ X-radiation ($\lambda_{\alpha_1} = 1.5405$; $\lambda_{\alpha_2} = 1.5443$) was used.

The Structure of $NbGe_{0.67}$.—Table I contains diffraction data for the first 20 indices, confirming the $D8_8$ -type. For the 6 Nb in (g) $x = 0.25$ and for the 6 Ge in (g) $x = 0.615$ were used. The lattice spacings are: $a = 7.71_8$ Å.; $c = 5.37_0$; and $c/a = 0.695_8$.

It should be noted that niobium used in preparing

these compounds contained approximately 0.4% carbon and probably some oxygen. It cannot yet be decided, therefore, whether the compound of this structure is stable in the absence of both carbon and oxygen. For a similar carbon-stabilized $D8_8$ phase formed by molybdenum and silicon, it has been shown that silicon substitutes for molybdenum in the 4-fold position only and that carbon substitutes for silicon in the ideal M_5Si_3 structure. In the present investigation, preparations in carbon crucibles yielded samples which showed decreases in lattice constants to be expected from the substitution of carbon for the larger germanium atoms. Samples containing NbC as well as the $D8_8$ -phase showed lattice constants: $a = 7.66$ and $c = 5.25$ Å. for the $D8_8$ -phase. These constants probably correspond to the maximum solubility of carbon.

TABLE I
STRUCTURE DATA FOR Nb_5Ge_3

(hkl)	$10^3 \sin^2 \theta$		Intensity	
	Calcd.	Obsd.	Calcd.	Obsd.
(100)	13.3	13.3	20.8	vw
(110)	39.9	...	0.1	..
(200)	53.0	53.3	27.3	w+
(111)	60.4	60.1	5.5	w
(002)	82.4	82.6	44.7	m
(210)	92.8	92.4	213.0	m-s
(102)	95.7	96.0	57.6	m
(211)	113.4	113.1	301.0	s
(300)	119.2	119.2	167.0	m-s
(112)	122.2	122.6	245.0	s
(202)	135.4	135.5	7.2	w-
(220)	159.0	159.0	1.1	vw
(310)	172.0	172.0	6.6	vw
(212)	175.2	...	0.0	..
(221)	179.2	180.0	13.7	w
(311)	192.6	192.9	24.6	m-
(302)	201.6	...	2.1	..
(400)	212.0	211.8	5.6	w-
(113)	225.3	...	0.5	..
(222)	241.4	241.7	73.0	m+

The close agreement of all these observations with those for the molybdenum-silicon-carbon system¹⁴ suggests that $NbGe_{0.67}$ should best be described as $Nb_6(Nb_{1-x}, Ge_x)_4(Ge_{1-y}, C_y)_6$.

The Structures of $NbGe_{0.54\pm 0.06}$ and β - $TaGe_{0.5}$.—Table II presents the structure data for the first 20 indices of $NbGe_{0.54\pm 0.06}$ and $TaGe_{0.5}$. For 8 Ge in (h) $x = 0.17$ and for 16 Nb or Ta in (k) $x = 0.074$ and $y = 0.277$ were chosen. These data confirm the structure as the same as that of the tetragonal

(14) H. Nowotny, E. Parthe, R. Kieffer and F. Benesovsky *Monatsh.*, **85**, 255 (1954).

(1) Work supported by the Office of Naval Research.
(2) Visiting Professor of Metallurgy, from: Department of Chemistry, Vienna Institute of Technology, Vienna, Austria.

(3) H. J. Wallbaum, *Naturwissenschaften*, **32**, 76 (1944).

(4) It should be noted that these phases whose structures have been interpreted in terms of the ideal formula M_5Si_3 have been observed in a wider composition range.

(5) P. Pietrokowsky and P. Duwez, *J. Metals*, **3**, 772 (1951).

(6) L. Castelliz, *Z. Metallkunde*, **46**, 198 (1955).

(7) J. H. Carpenter and A. W. Searcy, *J. Am. Chem. Soc.*, in press.

(8) J. M. Criscione, Ph.D. Thesis, Purdue University (1954).

(9) E. Parthe, H. Nowotny and H. Schmid, *Monatsh.*, in press.

(10) E. Aronsson, *Acta Chem. Scand.*, **9**, 137 (1955).

(11) C. H. Dauben, D. H. Templeton and C. E. Myers, *J. Am. Chem. Soc.*, in press, (1956).

(12) E. Parthe, H. Lux and H. Nowotny, *Monatsh.*, in press.

(13) L. Brewer, A. W. Searcy, D. H. Templeton and C. H. Dauben, *J. Amer. Ceram. Soc.*, **33**, 291 (1950).

TABLE II
 STRUCTURE DATA FOR β -Ta₅Ge₃ AND Nb₅Ge₃

(hkl)	β -“Ta ₅ Ge ₃ ”		Intensity		Nb ₅ Ge ₃		Intensity	
	Calcd.	Obsd.	Calcd.	Obsd.	Calcd.	Obsd.	Calcd.	Obsd.
(110)	11.9	...	1.7	..	11.54	...	0.0	..
(200)	23.7	...	2.9	..	23.1	...	1.0	..
(101)	28.1	...	0.0	..	28.2	...	0.0	..
(220)	47.4	47.8	8.3	vw	46.2	...	1.1	..
(211)	52.1	52.7	21.7	w	51.3	...	2.8	..
(310)	59.3	59.6	14.9	w	57.7	...	0.2	..
(002)	89.6	89.8	32.6	mw	89.6	89.4	11.0	m
(400)	94.9	94.7	21.6	w	92.3	91.4	6.6	vvw
(321)	99.5	99.3	79.5	ms	97.3	97.6	25.9	ms
(112)	101.5	101.8	7.3	w	101.1	...	1.1	..
(330)	106.7	106.8	7.4	w	103.5	103.9	3.7	w
(202)	113.3	113.1	53.7	m	112.7	111.9	25.6	s
(420)	118.6	118.4	70.7	m	115.4	115.2	27.3	s
(411)	123.2	122.8	135.7	s	120.4	120.4	48.6	vs
(222)	137.0	136.8	57.3	m	135.8	136.5	14.3	mw
(312)	149.8	...	0.4	..	147.3	148.5	0.1	vvw
(510)	154.2	...	0.2	..	150.0		0.2	
(431)	170.7	168.7	2.2	vw	166.4	...	0.0	..
(402)	184.5	183.7	2.1	vw	181.7	182.2	2.1	vw
(440)	189.8	...	0.7	..	184.0		0.6	

high-temperature modification of Nb₅Si₃ (space group D_{4h}¹⁸ or D_{2d}¹¹).

The lattice constants are for “Nb₅Ge₃” $a = 10.14_8$ Å.; $c = 5.15_2$ Å. and $c/a = 0.507_7$; and for β -“Ta₅Ge₃” $a = 10.01_0$ Å., $c = 5.15_0$ Å., $c/a = 0.514_5$.

Some of the niobium-germanium samples prepared in tungsten crucibles showed decreases of up to 1% in the c axis spacing of this phase due to dissolution of tungsten.

The Structure of α -TaGe_{0.5}.—The powder diagram of one low temperature (prepared below 1100°) tantalum germanide phase corresponds completely to that of the high temperature modification of Ta₅Si₃ and can be indexed on the basis of a tetragonal cell: $a = 6.59_9$ Å., $c = 12.01_0$ Å. and $c/a = 1.82_0$.

Reflections with $h + k + l$ odd and reflections ($0kl$) with both k and l odd are absent; these systematic absences are consistent with the space group D_{4h}¹⁸ with the following positions: 4 Ta in 4 (c), 16 Ta in 16 (1), 4 Ge in 4 (2) and 8 Ge in 8 (h). This arrangement suggests that α -TaGe_{0.5} is isostructural with Cr₅B₃.¹⁵ However, with the parameters proposed by Bertaut and Blum for 8 (h) it was impossible to obtain satisfactory agreement between observed and calculated intensities. Complete agreement between observed and calculated intensities could be obtained by decreasing the parameter in the 16-fold position from 0.166 to 0.160 and by changing the parameter of the germanium in the 8-fold position from $1/8$ to $3/8$. Table III contains the first 22 indices of the diagram. The ideal composition of this phase is therefore also Ta₅Ge₃ and the phase has the same structure as the corresponding silicide. Probably the boron parameter in Cr₅B₃ is also $3/8$ instead of $1/8$ since the new parameter places the boron atoms in larger

holes. It is obviously difficult to distinguish between the two positions experimentally because of the relatively small diffraction power of the boron atoms.

 TABLE III
 STRUCTURE DATA FOR α -Ta₅Ge₃

(hkl)	$10^3 \sin^2 \theta$		Intensity	
	Calcd.	Obsd.	Calcd.	Obsd.
(002)	16.5	...	1.4	..
(110)	27.3	...	0.0	..
(112)	43.8	43.9	7.5	vvw
(200)	54.6	...	1.1	..
(004)	65.8	...	4.2	..
(202)	71.1	72.1	19.2	m, d
(211)	72.4		45.6	
(114)	93.1	93.8	38.6	m
(213)	105.3	105.7	264.0	vs
(220)	109.2	109.3	19.2	m ^a
(204)	120.4	120.9	57.5	m
(222)	125.7	...	1.1	..
(310)	136.5	136.7	93.4	s
(006)	148.2	148.8	28.8	m
(312)	153.0	...	1.1	..
(215)	171.0	...	0.7	..
(224)	175.0	175.5	2.7	vw
(116)	175.5		2.1	
(321)	181.6	...	0.6	..
(314)	202.3	202.7	0.0	vw
(206)	202.8		2.5	
(323)	214.5	214.6	5.8	vw

^a Coincident with line of another phase.

Thus, phases of this type provide an additional example of the structural relationship between borides, silicides and germanides of transition metals. The relationships between the different structures of M₅Si₃ phases and the Ta₂Si-(Al₂Cu) type as well as the fluorite type already have been discussed.¹²

ELECTRODE POTENTIALS IN FUSED SYSTEMS. II. A STUDY OF THE AgCl-KCl SYSTEM¹

BY KURT H. STERN

Department of Chemistry, University of Arkansas, Fayetteville, Arkansas

Received December 10, 1955

The cell Ag|AgCl, KCl|Cl₂ has been studied over the complete concentration range from pure AgCl to pure KCl over the temperature range 500–900°. From mole fraction AgCl = 1 to 0.05 the cell behaves reversibly, for lower concentrations silver reacts spontaneously with potassium chloride. The kinetics of this reaction has been studied.

Introduction

The purpose of this series is the study of fused salt cells, especially those in which the concentration of common ions is low or zero, and to develop, if possible, an electrochemical method for following the kinetics of reactions between metals and molten salts.

In paper I of this series² the reaction between various metals and molten NaOH was studied. It was found there that, although potential changes in the cell M|NaOH|Au were related to the reactions the actual electrode reactions could not be determined. In the present paper results are presented for a cell in which the electrode reactions are unambiguous, Ag|AgCl, KCl|Cl₂.

In a series of papers on the thermodynamics of solutions of AgBr and various alkali bromides Hildebrand and Salstrom³ studied cells of the type Ag|AgBr, XBr|Br₂. Also, Salstrom⁴ studied the cell Ag|AgCl|Cl₂. The range of concentration investigated by these authors generally extended from pure silver halide to about 0.5 mole fraction. The softening point of the Pyrex glass used in these cells probably did not permit extension of the work to lower concentrations. In the present work the use of Vycor glass made it possible to work above 900°.

Experimental

The cells used were Vycor U-tubes of 15 mm. i.d. and 12 cm. high. Only the bottom of the cell was filled with electrolyte. Pyrex electrode holders for chlorine and silver electrodes fitted tightly into the openings of the cell. Chlorine electrodes were prepared by bubbling Mallinckrodt tank Cl₂ through concentrated H₂SO₄ and then, using Tygon tubing, through the hollow center of a spectrographic carbon rod. This allowed the gas to bubble through the melt rather than pass over it. Before settling on this arrangement the procedure of Salstrom⁴ was tried. Identical results were obtained but with the hollow electrode equilibrium was established more quickly, even without pretreatment of the electrodes under chlorine pressure. The silver electrodes were No. 10 B.&S. gage wire obtained from the American Platinum Works and were 99.99% pure. They were abraded and cleaned before every run. The silver chloride was variously Mallinckrodt Reagent Grade, prepared from pure silver wire, or recovered from previous runs. All samples were of comparable purity. The potassium chloride was C.P. grade.

The procedure used in making a run was as follows: The empty cell was placed in a well insulated furnace and

preheated above the melting point of the AgCl-KCl mixture to be used. Temperature was measured with a chromel-alumel thermocouple whose hot junction was placed in a nickel protection tube near the bend of the U-tube. Temperature could be measured, using a Wheelco potentiometer, and kept constant to ±1°. When the desired temperature had been reached the solid salt mixture, approximately weighed out for the composition desired, was placed in the tube and melted. The electrodes were immersed in the cell and chlorine flow started. Readings of temperature and e.m.f. (using a K-2 potentiometer) were taken until both were constant. The temperature was then changed and the procedure repeated. Runs were carried out as rapidly as possible to prevent changes in composition of the melt during the run. Points were randomized with respect to temperature. At the conclusion of the run the electrodes were removed, the cell cooled, and the melt removed for analysis by smashing the cell.

After it was found that steady potentials could not be measured in cells containing less than about 0.05 mole fraction AgCl the rate of reaction between silver and KCl was measured by two methods: (a) following the change of potential with time in a cell containing no AgCl initially, *i.e.*, Ag|KCl|Cl₂, and (b) periodically analyzing a molten KCl solution to which silver foil had been added. Both experiments were carried out at the same temperature, 890°, to facilitate comparison.

All analyses for silver were done gravimetrically by precipitating the silver as Ag₂S.

Results and Discussion

The temperature variation of the cell Ag|AgCl, KCl|Cl₂ for various mole fractions of AgCl is shown in Table I and Fig. 1.

TABLE I

ELECTRODE POTENTIALS OF THE CELL Ag AgCl, KCl Cl ₂							
Mole fraction AgCl	<i>t</i> (°C.)	<i>E</i> (volts)	Mole fraction AgCl	<i>t</i> (°C.)	<i>E</i> (volts)		
1.000	476	0.9079	0.1907	704	0.9847		
	507	.8972		810	.9737		
	511	.8922		914	.9620		
	534	.8878		.0982 ₁	740	1.0540	
	568	.8767			844	1.0470	
	572	.8755			978	1.0242	
	588	.8711		.0799 ₂	778	1.0730	
	628	.8556			816	1.0710	
	0.5909	568		.9158		862	1.0685
		600		.9082		872	1.0666
681		.8895		912	1.0626		
713		.8820	.0646 ₆	829	1.1154		
738		.8760		861	1.1127		
753		.8724		906	1.1103		
.4266		666	.9267				
		716	.9163				
	788	.8985					
	810	.8938					
	871	.8782					
	904	.8678					
	916	.8645					

(1) This research was supported by the United States Air Force through the Office of Scientific Research of the Air Research and Development Command.

(2) K. H. Stern and J. K. Carlton, *THIS JOURNAL*, **53**, 965 (1954).

(3) (a) E. J. Salstrom and J. H. Hildebrand, *J. Am. Chem. Soc.*, **52**, 4650 (1930); (b) E. J. Salstrom, *ibid.*, **53**, 1794 (1931); (c) *ibid.*, **53**, 3385 (1931); (d) *ibid.*, **54**, 4252 (1932); (e) J. H. Hildebrand and E. J. Salstrom, *ibid.*, **54**, 4257 (1932).

(4) E. J. Salstrom, *ibid.*, **55**, 2426 (1933).

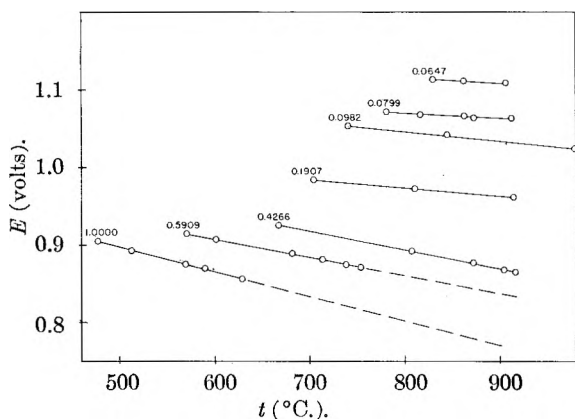


Fig. 1.—Electrode potentials of the cell $\text{Ag}|\text{AgCl}, \text{KCl}|\text{Cl}_2$ for various mole fractions of AgCl .

The curves are similar to those obtained by Salstrom and Hildebrand,³ *i.e.*, the temperature potential plot is linear and the temperature coefficient decreases with decreasing concentration of the silver salt. The data of Salstrom⁴ for the cell $\text{Ag}|\text{AgCl}|\text{Cl}_2$ give the same slope and the potentials differ by about 3 mv. This disagreement is outside experimental error, but could be accounted for if the temperature standards of the two studies differed by 10° . It would have been desirable to cover the same temperature range with all the cells, but as the freezing points of the solutions rise with increasing KCl concentration this was not possible. Also, when an attempt was made to run the cell $\text{Ag}|\text{AgCl}|\text{Cl}_2$ above 650° the plot became non-linear and the data irreproducible, possibly due to the decomposition AgCl , although this has not previously been reported.

The deviation of AgCl-KCl solutions from ideality was determined by plotting the function $\bar{F}_1 - \bar{F}_1^i$ against mole fraction of AgCl , where these functions are defined by Salstrom and Hildebrand,⁵ *i.e.*, $\bar{F}_1 = \Delta F_1 - \Delta F_1^0$, ΔF_1 and ΔF_1^0 are obtained from the measured potentials by the equation

$$\Delta F_1^0 = -23,060E^0 \text{ and } \bar{F}_1^i = RT \ln N_1$$

where N_1 is the mole fraction of AgCl . In order to calculate the isotherms of interest in this work it was necessary to obtain E^0 by straight-line extrapolation of data at lower temperatures. The 800 and 890° isotherms are shown in Fig. 2. For

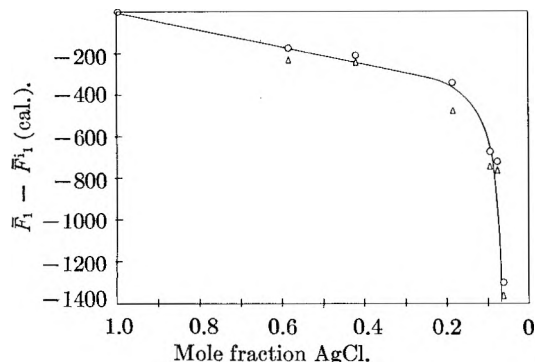


Fig. 2.—Thermodynamic difference function $\bar{F}_1 - \bar{F}_1^i$; O, 800° ; Δ , 890° .

(5) E. J. Salstrom and J. H. Hildebrand, *J. Am. Chem. Soc.*, **52**, 4641 (1930).

solutions from 1.0 to about 0.2 mole fraction AgCl the plot resembles that for the corresponding bromide system. The negative deviation from ideality was interpreted by Hildebrand and Salstrom^{3e} in terms of the loosening effect of the potassium ion on the silver-halogen bond.

Of particular interest in this work is the virtually vertical drop at about 0.08 mole fraction AgCl . It is in cells more dilute than this that steady potentials cannot be obtained. To test the hypothesis that cells in this range were irreversible because of the spontaneous reaction of silver with potassium chloride a time-potential curve was obtained for a cell initially free of AgCl , *i.e.*, $\text{Ag}|\text{KCl}|\text{Cl}_2$. This is shown in Fig. 3 for 890° . For a

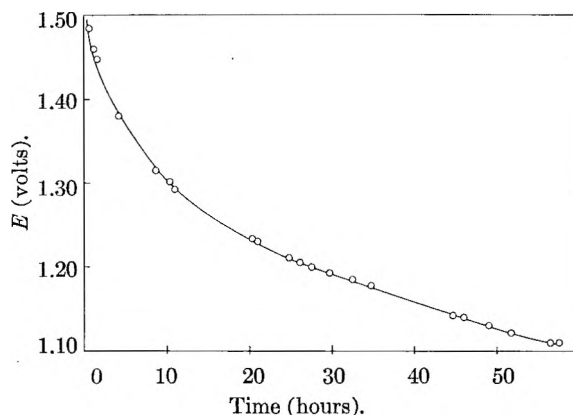


Fig. 3.—Time-potential curve for the cell $\text{Ag}|\text{KCl}|\text{Cl}_2$ at 890° .

considerable distance the plot is linear, indicating first-order kinetics. After about 52 hours the potential became nearly steady. Analysis of the solution gave 0.052 mole fraction silver, in addition to a small amount of silver which had dissolved as the metal. In order to follow the reaction independently of an e.m.f. cell several runs were made in which about 6 g. of silver foil was immersed in molten KCl at 890° and samples taken of the melt at various times for analysis. Although no exact reproducibility between runs could be obtained the concentration of silver never exceeded 0.08 mole fraction. Typical results are shown in Table II. Unfortunately it was not feasible to make runs for very much longer periods than 150 hours since Vycor becomes extremely brittle and fragile on prolonged exposure to KCl . Runs at lower temperatures were too slow to make measurements practical and higher temperature runs are limited by the melting point of silver. Thus activation energies could not be obtained. The data strongly suggest, however, that the reaction is inhibited by the accumulation of AgCl in the melt. Moreover, the limiting concentration lies close to 0.08 mole fraction, the same concentration at which the thermodynamic difference function (Fig. 2) drops toward minus infinity. In one experiment it was possible to preserve the cell referred to in Fig. 3 for about a week. After about 60 hours the change in potential became very slow, dropping to 1.044 volt after about 160 hours. The final concentration of AgCl was 0.0997 mole fraction.

TABLE II
KINETIC RUN FOR THE REACTION $\text{Ag} + \text{KCl}$ AT 890°

Time (hr.)	Mole fraction AgCl
57	0.0163
102	.0494
147	.0551

From the above results it seems reasonable to conclude that the cell $\text{Ag}|\text{AgCl}, \text{KCl}|\text{Cl}_2$ behaves reversibly for concentrations of common ion above 0.1 mole fraction, but is irreversible for lower concentrations. The correspondence of results obtained from kinetic runs on cells initially free of AgCl with those in which silver was allowed to react with KCl suggest that the same reaction occurs in both, *i.e.*, that of silver with KCl . The chlorine electrode, being in contact with constant chloride ion concentration in all the cells thus serves as reference electrode. Its potential remains con-

stant. It is difficult to escape the conclusion that the reaction proceeds by the reduction of potassium ion to the metal, $\text{Ag} + \text{KCl} \rightarrow \text{AgCl} + \text{K}$, although all attempts to isolate the metal have failed. This is not too surprising since the amounts involved are quite small, a few tenths of a gram over a period of several days. It is most likely that the metal would simply distill out since the system is well above the boiling point of potassium.

That the reaction is driven to the right by the distillation of potassium can also be shown by calculating E° from a recently published compilation of E° values for metal chlorides.⁶ At 800° E° is -2.61 volt.

A similar result has been obtained recently for the reaction between nickel and molten NaOH .⁷ In that case the reaction is driven by the distillation of metallic sodium.

(6) W. H. Hamer, M. S. Malmberg and B. Rubin, *J. Electrochem. Soc.*, **103**, 8 (1956).

(7) D. M. Mathews and R. F. Kruh, unpublished results.

NEGATIVE ION FORMATION IN HYDROGEN PEROXIDE AND WATER VAPOR. THE PERHYDROXIDE ION¹

By E. E. MUSCHLITZ, JR., AND T. L. BAILEY

College of Engineering, University of Florida, Gainesville, Florida

Received December 12, 1955

The negative ions formed by electron bombardment in water vapor and in a mixture of water and hydrogen peroxide vapors have been investigated in a mass spectrometer. The principal ions found with water vapor in the ion source are H^- , O^- and OH^- . With the addition of a small amount of hydrogen peroxide vapor, O_2^- and O_2H^- ions are also found at relatively high intensity. No H_2O_2^- (or $\text{O}^-\text{H}_2\text{O}$) ions were observed in either case. Data are presented to show that the OH^- ion is formed in a secondary collision between H^- and H_2O . Measurements of the total scattering cross-sections for 350 e.v. O_2^- and O_2H^- ions in oxygen have been made. It is shown from these measurements that the ions of mass 32 obtained by the electron bombardment of oxygen are the same as those obtained from the $\text{H}_2\text{O}-\text{H}_2\text{O}_2$ vapor. The utility of the scattering technique for the identification of gaseous ions is discussed.

Introduction

Investigations of the elastic and inelastic collisions of gaseous negative ions with neutral molecules are in progress in this Laboratory.² The interaction potential, as determined from measurements of elastic scattering, shows that a short range attractive force between H^- and O_2 exists and suggests that the perhydroxide ion, O_2H^- , is a stable entity. This ion has previously been reported in the early mass spectrometer work of von Dechend and Hammer (1911)³ who used mixtures of hydrogen and oxygen in a glow discharge ion source. However, they also reported H_2O_2^- . It is quite likely that the ions they observed were actually O_2^- and O_2H^- . The existence of the perhydroxide radical, O_2H , has recently been established by means of the mass spectrometer technique of Foner and Hudson.⁴ The electron affinity of the radical

has been calculated through the use of a cyclic process involving the dissociation energy of H_2O_2 and the heats of hydration of the H^+ and O_2H^- ions,⁵ and is found to be 70 kcal./mole. Both the negative ion and the radical are of considerable importance in the kinetics of oxygen reactions in solution. We have therefore investigated the negative ions produced by electron bombardment of water vapor and of a mixture of water and hydrogen peroxide vapors in a mass spectrometer. A similar investigation of the negative ions produced by electron bombardment of hydrocarbon gases has been reported previously.⁶

Experimental

A schematic diagram of the apparatus is shown in Fig. 1. Gas enters the ion source through the nozzle, N, which has a 0.5 mm. orifice. An electron beam originates at the directly-heated cathode, C, passes at an angle of 45 degrees through a slot in the anode, A, and intersects the jet of gas directly in front of the nozzle opening. Negative ions and some scattered electrons are drawn into the cylindrical focusing elements, FE, and are accelerated to the mass spectrometer, M. The spectrometer is a 90 degree, 6.50 cm. radius-of-curvature instrument with a relatively low resolution (± 0.4 A.M.U. for ions of mass 32). In the design of the instrument resolution is sacrificed for higher intensities

(1) This research is supported by the U. S. Office of Naval Research. Reproduction in whole or in part is permitted for any purpose of the United States Government.

(2) E. E. Muschlitz, Jr., *Phys. Rev.*, **95**, 635A (1954); E. E. Muschlitz, Jr., T. L. Bailey and J. H. Simons, *J. Chem. Phys.*, in press.

(3) G. Glockler and S. C. Lind, "The Electrochemistry of Gases and Other Dielectrics," John Wiley and Sons, Inc., New York, N. Y., 1939, p. 369.

(4) S. N. Foner and R. L. Hudson, *J. Chem. Phys.*, **21**, 1608L (1953).

(5) H. O. Pritchard, *Chem. Revs.*, **52**, 529 (1953).

(6) T. L. Bailey, J. M. McGuire and E. E. Muschlitz, Jr., *J. Chem. Phys.*, **22**, 2088L (1954).

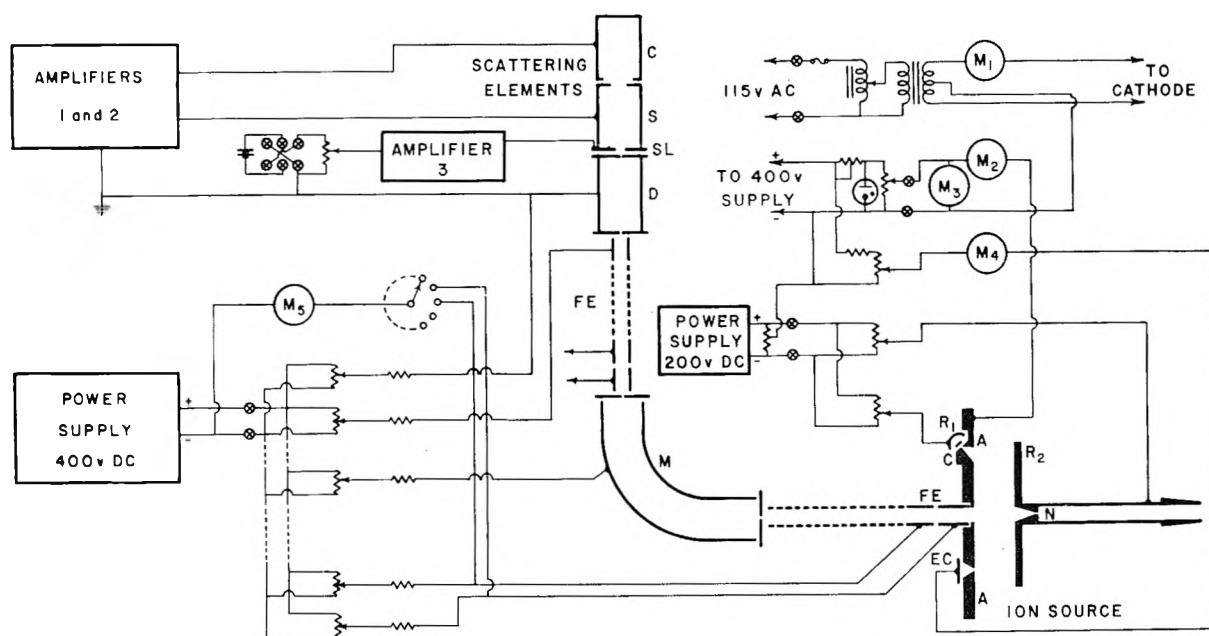


Fig. 1.—Negative ion apparatus (reproduced with the permission of the *J. Chem. Phys.*).

in the exit ion beam. The negative ion beam leaving the spectrometer is refocused and is defined by the cylinder, D. It then enters the scattering region, S, through a hole in the plate, SL. In the absence of gas in this region, the beam passes through S and is collected in the Faraday cage, C. Scattering measurements are made by introducing a gas into the scattering region through a capillary leak and measuring the ion currents to C, S, and SL. The gas pressures used (10^{-2} – 10^{-3} mm.) are adjusted so that one-third to one-half of the beam is collected on S. A differential pumping system consisting of four large mercury vapor pumps is employed to keep the pressure as low as possible in the spectrometer and focusing regions. Details of the construction and operation of the apparatus have been described elsewhere.²

Water vapor is introduced into the ion source through nozzle, N, from a bulb of degassed distilled water held at 0°. Hydrogen peroxide is introduced in the same manner from an aqueous solution also at 0°. Reagent grade 30% peroxide diluted with distilled water was used. An analysis made shortly before use gave 14.6% by weight.

The electron beam energy and anode current were kept constant throughout at 50 e.v. and 2.0 ma., respectively, and the ions passed through the magnetic field at 340 e.v. Ion masses were determined by a rotating-coil gaussmeter whose output e.m.f. was linear with the magnetic field. The average energies of the principal ions observed were determined by a retarding potential method and found to be the same within 1 e.v.

Results and Discussion

Water Vapor.—Relative intensities of the negative ions observed are shown in Table I. The principal ions observed are H^- , O^- and OH^- . The sensitivity of the current measurements is sufficient to detect readily masses 18 and 19 which arise from the O^{18} isotope. The H_2O^- ion, if present, and the OD^- ion would also contribute to the peak at mass 18. Masses 32 and 33 occur at very low intensity. Peaks at masses 35 and 37 occur but not at the proper intensity ratio for the chlorine isotopes. It is likely that another ion of mass 35 is present, possibly the hydrated ion $OH^- \cdot H_2O$. A peak at mass 34 ($H_2O_2^-$) was not observed; however, the measured current did not reach zero between 33 and 35. The peaks at masses 27 and 43 have not been identified.

TABLE I

NEGATIVE IONS FROM ELECTRON BOMBARDMENT OF WATER VAPOR

Mass	Ion	Intensity ^a	Remarks
1	H^-	1.2	
16	O^-	23	
17	OH^-	31	
18	$(O^{18})^-$	0.09	Shoulder on OH^-
19	$O^{18}H^-$.07	
27	?	.05	Unidentified
32	O_2^-	.05	
33	O_2H^-	.09	
34?	$O^- \cdot H_2O$ or $H_2O_2^-$?	.02	Minimum between 33 and 35
35	$(Cl^{35})^-$ or $OH^- \cdot H_2O$?	.06	
37	$(Cl^{37})^-$?	.006	
43	?	.30	Unidentified

^a $100 \sim 10^{-9}$ amp.

The question of the stability of the gaseous OH^- ion is an interesting one. Mann, Hustrulid and Tate did not observe it in their mass spectrometer investigation of both negative and positive ions formed by electron bombardment in water vapor.⁷ Branscomb and Smith found it to be the most abundant negative ion produced in a gaseous discharge in water vapor at 0.1 mm. pressure.⁸ An investigation was therefore made of the relative intensity of H^- , O^- and OH^- as a function of the ion-source nozzle backing pressure. These results are shown in Fig. 2. The flow of water vapor through the nozzle is hydrodynamic at all but the lowest pressures. At pressures below 0.5 mm. H^- is most abundant and OH^- just detectable. As the pressure is increased beyond 1 mm. the ion currents increase rapidly, particularly the OH^- current. Beyond 2 mm. the OH^- intensity becomes larger than the O^- and at 4.6 mm. the values given

(7) M. M. Mann, A. Hustrulid and J. T. Tate, *Phys. Rev.*, **58**, 340 (1940).

(8) L. M. Branscomb and S. J. Smith, *ibid.*, **98**, 1028 (1955).

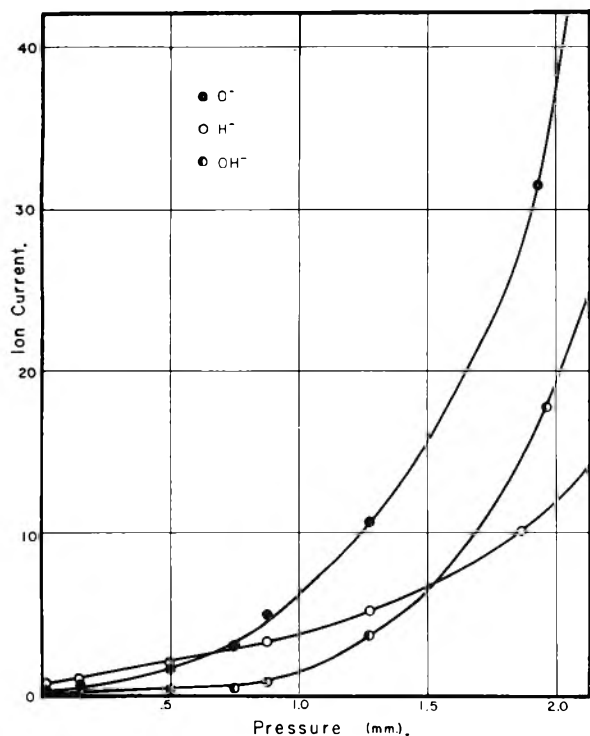
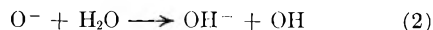


Fig. 2.—Intensities of negative ions obtained by electron bombardment of water vapor (ion current scale: $100 \sim 10^{-11}$ amp.).

in Table I are reached. It is evident that OH^- is not formed in a direct collision between an electron and H_2O , but that a secondary over-all process such as



or



takes place. The data indicate that the first reaction is primarily involved, since the sum of the H^- and OH^- intensities gives a curve which roughly parallels the O^- curve. Laidler has postulated these reactions in connection with the radiation chemistry of liquid water, and has given a theoretical discussion of the reasons for the low probability for the formation of OH^- in a primary collision.⁹ Mann, Hustrulid and Tate⁷ did not observe OH^- since the pressure used in their ion source was very low (about 10^{-4} mm.).

The Peroxide Ion.—Figure 3 shows a typical negative ion spectrum obtained using the hydrogen peroxide-water vapor mixture in the ion source. The spectrum was obtained by automatically sweeping the magnetic field at approximately 200 gauss/minute. At this speed, the effective resolution of the spectrometer is less than the theoretical resolution, due to the limited response time of the recorder. Figure 4 is a plot taken manually of the O_2^- and O_2H^- peaks showing the actual resolution obtained in this range.

The relative intensities of the principal ions obtained from pure water vapor and the $\text{H}_2\text{O}-\text{H}_2\text{O}_2$ vapor mixture are compared in Table II. The ion peaks at masses 32 and 33 increase by more than a factor of ten when a small amount of hydrogen per-

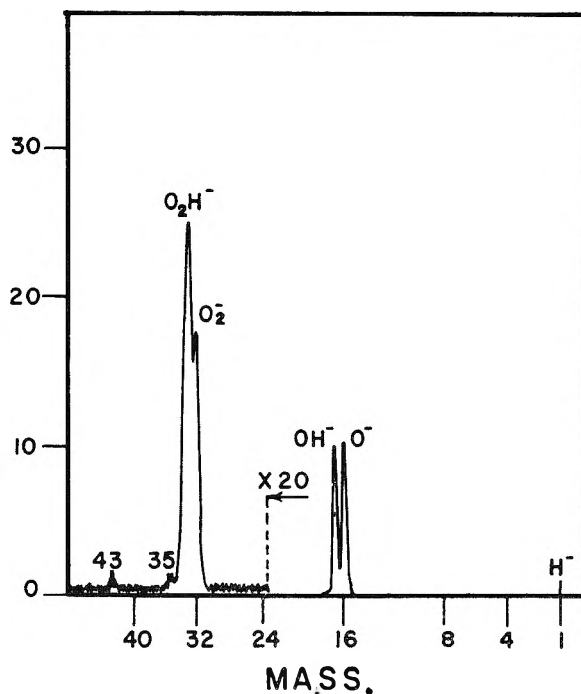


Fig. 3.—Negative ion mass spectrum for $\text{H}_2\text{O}-\text{H}_2\text{O}_2$ vapor.

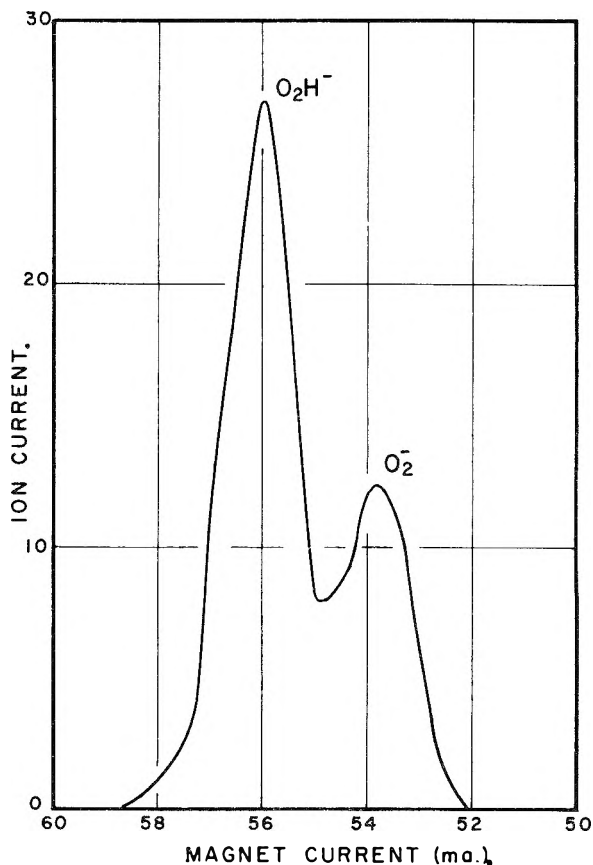


Fig. 4.— O_2^- and O_2H^- ion peaks.

oxide vapor is present. The total negative ion current obtained from the $\text{H}_2\text{O}-\text{H}_2\text{O}_2$ mixture is less than that obtained from water vapor alone. However, the total vapor pressure above the mixture at 0° , which may be estimated from the data of Gi-

(9) K. J. Laidler, *J. Chem. Phys.*, **22**, 1740 (1954).

guere and Maass¹⁰ as 4.2 mm., is appreciably less than the vapor pressure of pure water at 0° (4.6 mm.). It has been observed with the ion source used that the total negative ion intensity as well as the relative intensities of the various ions produced in water vapor vary markedly with the nozzle backing pressure (Fig. 2). At lower backing pressures the O⁻ intensity becomes larger than the OH⁻ intensity. No conclusion can be reached as to how much of the O⁻ and OH⁻ intensity arises from electron collisions with H₂O₂ molecules. It cannot be said with certainty, but it seems very likely that both O₂⁻ and O₂H⁻ are formed by direct electron collisions with H₂O₂. It would be hard to understand, otherwise, the relatively large intensities of these ions observed, particularly since the partial pressure of H₂O₂ above the aqueous solution is considerably less than the 0.031 mm. predicted by Raoult's Law.¹⁰

TABLE II

RELATIVE NEGATIVE ION INTENSITIES (100 ~10⁻⁹ AMP.)

Gas	H ⁻	O ⁻	OH ⁻	O ₂ ⁻	O ₂ H ⁻	Total	Backing pressure mm.
H ₂ O	1.2	23	31	0.05	0.09	55	4.6
H ₂ O-H ₂ O ₂	1.1	10	10	0.8	1.2	23	4.2 ^a

^a Partial backing *p* of H₂O₂ < 0.031 mm.

As an additional check on the identity of the O₂⁻ and O₂H⁻ ions, measurements of the total cross-sections for the scattering of the ions were made. These were compared with the cross-section for the scattering of O₂⁻ ions obtained using oxygen in the ion source. Electrolytic oxygen was used as the scattering gas. The cross-sections were obtained by the method of Simons and co-workers.¹¹ Currents to C, S and SL (Fig. 1) were measured both with and without gas in the scattering region. Cross-sections were calculated from the equation

$$\alpha_T (\text{cm.}^{-1}) = \frac{\ln R_0/R}{l(p - p_0)} \quad (3)$$

where $R = I_C / (I_C + I_S + I_{SL})$ measured at the pressure p , R_0 is the same ratio measured at the vacuum pressure p_0 , and l is the length of the scat-

(10) P. A. Giguere and O. Maass, *Can. J. Research*, **18B**, 181 (1940).

(11) J. H. Simons, C. M. Fontana, E. E. Muschlitz, Jr. and S. R. Jackson *J. Chem. Phys.*, **11**, 307 (1943).

tering region (3.723 cm.). Pressures were reduced to 0°. The cross-section, α_T , is related to the cross-section/molecule in cm.², S_T , by the equation

$$\alpha_T = NS_T \quad (4)$$

in which N is the number of gas molecules/cc. at 0° and 1 mm. pressure. The total cross-section is a measure of the sum of the elastic and inelastic scattering. The latter includes for negative ions such collision processes as electron detachment and electron exchange. The results of these measurements are shown in Table III. Since the cross-sections for the scattering of mass 32 ions obtained from oxygen and from the H₂O-H₂O₂ mixture are the same within the experimental error, it may be concluded that both ions are O₂⁻ and that both are in the same electronic state. The cross-section found for the scattering of O₂H⁻ ions is markedly different.

TABLE III

TOTAL SCATTERING CROSS-SECTIONS FOR NEGATIVE IONS IN OXYGEN

Ion	Energy (e.v.)	$p - p_0$ (mm.)	α_T (cm. ⁻¹)
O ₂ ⁻ from O ₂	339	2.724×10^{-3}	73.2 ± 1.0
O ₂ ⁻ from O ₂	339	2.792×10^{-3}	73.1 ± 1.0
O ₂ ⁻ from H ₂ O ₂ -H ₂ O	340	2.643×10^{-3}	74.3 ± 1.0
O ₂ H ⁻ from H ₂ O ₂ -H ₂ O	341	2.643×10^{-3}	63.2 ± 1.0

The scattering technique as used here for identification of gaseous ions is a useful one and should find many important applications. For example, the ions of mass 35 observed here (Fig. 2) could possibly be Cl⁻ if it were not for the fact that the ion of mass 37 occurred at only one tenth the intensity of mass 35. This could definitely be established by comparing the scattering of these ions with ions of mass 35 and 37 obtained from chlorine. H₂⁺ and D⁺ could be distinguished in the same fashion; in fact, the percentage of H₂⁺ in an unresolved peak containing both ions could be determined if the cross-sections for the scattering of pure beams of the ions are known.

Acknowledgment.—The authors wish to acknowledge helpful discussions of this research with Prof. J. H. Simons and Prof. L. B. Loeb.

ELUTION TIME AND RESOLUTION IN VAPOR CHROMATOGRAPHY¹

By A. K. WIEBE

Hercules Experiment Station, Hercules Powder Company, Wilmington, Delaware

Received December 14, 1955

Some of the variables associated with vapor phase chromatography have been studied to determine the conditions for minimum elution time and maximum resolution. The elution time is shown to vary inversely as the carrier gas flow rate, directly as the column length and exponentially with the reciprocal of the absolute temperature. An equation relating these variables to the free energy has been derived. Resolving power is improved with increase in column length and decrease in column temperature but passes through a maximum with increasing carrier gas flow rate. The improvement in resolution does not, however, appear to vary linearly with column length. The resolving power of a column appears to reach a point beyond which small improvements are obtained with comparatively large increases in elution time and with considerable dilution in the carrier gas (*i.e.*, zone spreading). A definition of column efficiency is suggested which relates the resolving power directly with the partition coefficients for all compounds and with the vapor pressures for classes of similar compound.

The theory of vapor phase chromatography has been shown to differ from that of liquid phase chromatography only in that the mobile phase is compressible.² This results in a velocity gradient down the length of the column which is proportional to the pressure drop necessary to sustain a reasonable carrier gas flow rate. However, theory derived for liquid phase systems can be applied to gas chromatography provided the necessary corrections for carrier gas compressibility are made.

The movement of a chromatographic zone in vapor-liquid partition systems has generally been described in terms of its retention volume,²⁻⁸ which may be defined as the volume of carrier gas that has emerged from the column from the time of administering a sample until the maximum concentration of its zone appears in the effluent. These retention volumes must be corrected for the pressure drop across the column and for the column temperature.⁸

The movement of a chromatographic zone may also be described by the relation⁹

$$K = \frac{V_m}{V_i} - 1 \quad (1)$$

where

K = equilibrium distribution of solute between the vapor and liquid phases

V_m = vol. of effluent that has passed through the column when the zone maximum appears in the effluent

V_i = interstitial vol. of the column, often referred to as the column vol.

In practice, the values of V_m/V_i are large compared with unity so that expression 1 can be written in the approximate form

$$K \doteq V_m/V_i \quad (2)$$

(1) Presented at the Delaware Chemical Symposium, Feb. 18, 1956, and at the Symposium on Vapor Phase Chromatography sponsored by the Division of Analytical Chemistry, ACS Meeting, Dallas, April 8-13, 1956.

(2) A. T. James and A. J. P. Martin, *Analysts*, **77**, 915 (1952).

(3) A. T. James and A. J. P. Martin, *Biochem. J. (London)*, **50**, 679 (1952).

(4) A. T. James, A. J. P. Martin and G. H. Smith, *ibid.*, **52**, 238 (1952).

(5) A. T. James, *ibid.*, **52**, 242 (1952).

(6) N. H. Ray, *J. Appl. Chem. (London)*, **4**, 21 (1954).

(7) A. T. James, *Chem. Process Eng.*, **36**, 95 (1955).

(8) A. B. Littlewood, C. S. G. Phillips and D. T. Price, *J. Chem. Soc.*, 1480 (1955).

(9) D. W. Simpson and R. M. Wheaton, *Chem. Eng. Progr.*, **50**, 45 (1954).

The above expression shows that the separation of two or more materials on a vapor-liquid partition column is proportional to the respective equilibrium constants. Furthermore, the equilibrium constant is equal to the ratio of two gas volumes which are affected to the same extent by the pressure differential across the column. Hence, no corrections need be applied for the variation of flow rate along the column as is the case with retention volumes.²

The theory of liquid phase chromatography and ion-exchange columns is generally developed around the concept of equilibrium stages¹⁰ which, in analogy with distillation, are termed theoretical plates. This concept leads to an expression of the form¹⁰

$$p = \frac{2K}{K+1} \left(\frac{V_m}{V_m - V_e} \right)^2 \quad (3)$$

where

p = no. of theoretical plates in the column

V_m = as previously defined

V_e = vol. of effluent that has passed through the column when a point on the elution curve has been reached where the solute concn. is 1/eth of the maximum

The application of equation 3 is shown for a typical elution curve in Fig. 1. Where K is large compared with unity, this equation may be written in the approximate form

$$p \doteq 2 \left(\frac{V_m}{\Delta V} \right)^2 \quad (4)$$

where $\Delta V = V_m - V_e$.

Apparatus.—The apparatus used was essentially similar to that described by Ray.⁶ Two column lengths were used. One consisted of a 4-ft. length of 8-mm. tubing (6-mm. bore) bent into a U; the other was made from an 8-ft. length of tubing bent into a W. The columns contained 45 in. and 85 in., respectively, of active packing composed of a mixture of size-graded Celite and dioctyl phthalate in the proportions of 0.45 g. of liquid to 1.0 g. of graded Celite. One end of the column was provided with a rubber serum bottle cap through which samples could be injected on to the column with a micrometer syringe. The column temperature was maintained constant by boiling liquids into a surrounding vapor jacket. Temperatures of 79, 100 and 121° were obtained with ethanol, water and methyl Cellosolve, respectively.

The carrier gas was oxygen-free nitrogen drawn from a cylinder through a diaphragm reducing valve to a 2-liter buffer vessel. The pressure in the buffer vessel was maintained constant with a cartesian manostat and was measured with a mercury manometer. The gas from the buffer vessel

(10) J. Beukenkamp, W. Rieman III, and S. Lindebaum, *Anal. Chem.*, **26**, 505 (1954).

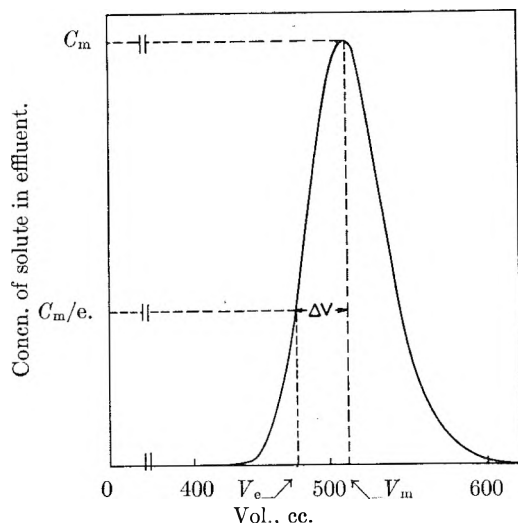


Fig. 1.—Elution of toluene with nitrogen at 100°; N₂ flow rate = 5.1 cc./min.; column volume = 22 cc.

passed through a rotameter into the reference side of a Gow-Mac thermal conductivity cell (modified as described by Kieselbach¹¹) and thence into one end of the column. The outlet of the column was connected to the sample side of the conductivity cell with copper tubing. The exit gas passed into the atmosphere.

The four 30-ohm filaments of the thermal conductivity cell were connected electrically to form the arms of a Wheatstone bridge. Before entering the chromatographic column, the carrier gas passed through the reference channel where it came in contact with the two reference filaments. The gas leaving the column flowed across the two sample filaments. Thus, all four filaments were exposed to carrier gas alone, except when a sample component was being eluted. During elution of a component, two of the filaments (in opposite arms of the bridge) were exposed to the mixture of carrier gas and the component leaving the column. This unbalanced the bridge. The resultant signal was fed into a 0-2.5 mv. Brown recording potentiometer which automatically plotted detector response versus time.

Results and Discussion

A known mixture composed of benzene, *n*-heptane, toluene, ethylbenzene and *p*-xylene was used throughout this work. The time required to effect a separation and the degree of separation obtained were studied as functions of carrier gas flow rate, column temperature and column length.

The time required for the appearance of the maximum in an elution curve at constant temperature is shown in Fig. 2 to vary inversely as the carrier gas flow rate. The elution time is also shown by curves 2 and 4 of Fig. 2 to vary directly as the column length. Similarly, the time required for the elution of a material at constant carrier gas flow rate and column length varies exponentially with the reciprocal of the absolute temperature as shown in Fig. 3. Hence, the elution time is described by an equation of the form

$$t_m = f\left(\frac{1}{F'}, l, \frac{1}{T}\right) \quad (5)$$

where

- t_m = elution time to the maximum in a zone
- F' = carrier gas flow rate
- l = column length
- T = absolute temperature

The nature of this relationship can be derived from the free energy (ΔF) equation

(11) R. Kieselbach, *Anal. Chem.*, **26**, 1317 (1954).

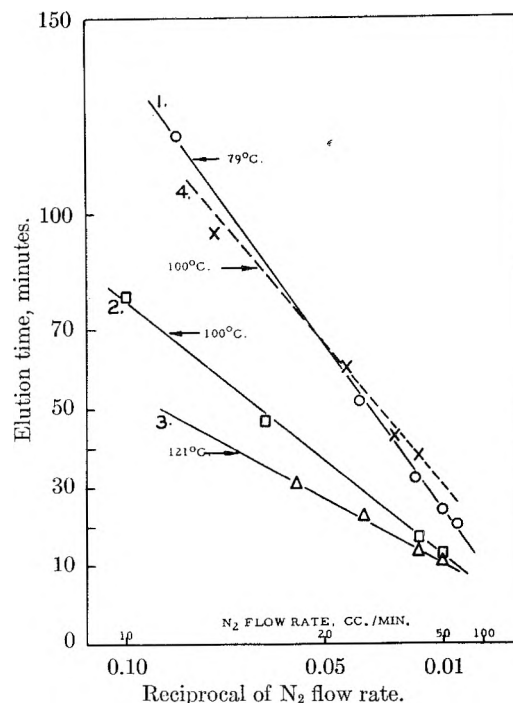


Fig. 2.—Elution time versus reciprocal of nitrogen flow rate for toluene; column length: curves 1, 2, and 3, 45 inches; curve 4, 85 inches.

$$\Delta F = RT \ln K \quad (6)$$

Since

$$K = \frac{V_m}{V_i} = \frac{\text{vol. to max. in zone}}{\text{column vol.}} \quad (2)$$

$$V_m = F' \times t_m$$

and $V_i = a_i l$ where a_i is the interstitial area of the column

$$K = \frac{F' t_m}{a_i l} \quad (7)$$

Substituting 7 into 6 and rearranging

$$t_m = \frac{a_i l}{F'} e^{-\Delta F/RT} \quad (8)$$

The column efficiency (*i.e.*, its ability to resolve the components of a complex mixture) is shown in

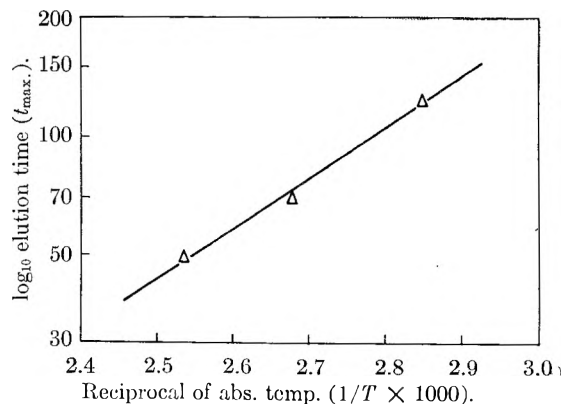


Fig. 3.—Effect of temperature on the movement of a chromatographic zone at constant flow rate.

terms of theoretical plates in Fig. 4 to pass through a maximum with increasing carrier gas flow rate. The poor column behavior at the lower flow rates

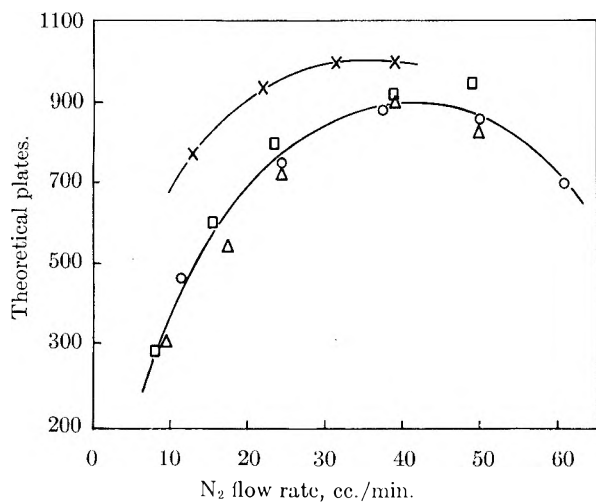


Fig. 4.—Column efficiency as a function of flow rate.

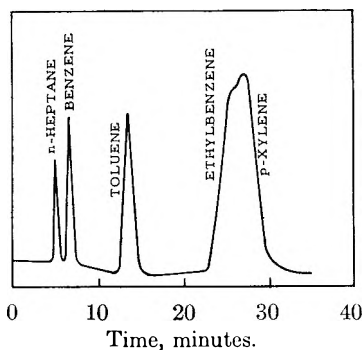
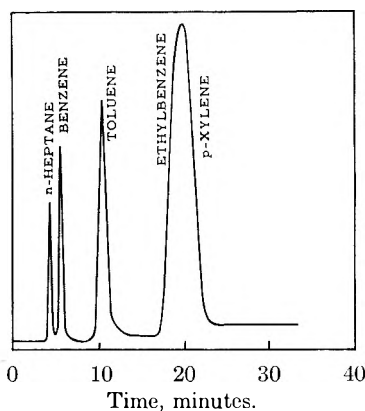
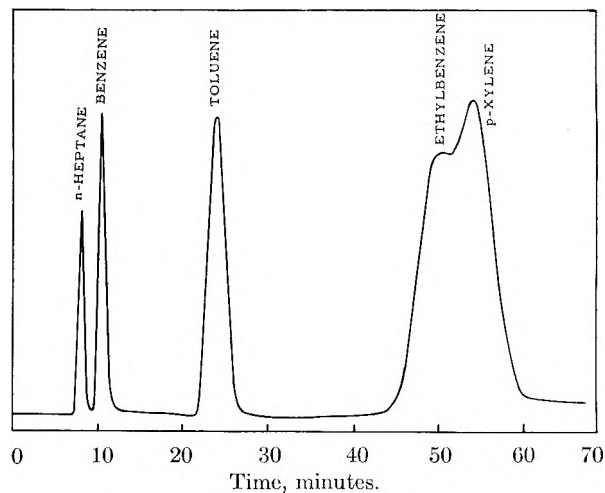
	Temp., °C.	Column length, in.
○	79	45
□	100	45
△	121	45
×	100	85

is probably due to back diffusion with a resultant broadening of the elution curves. At the higher flow rates, the solute probably does not reach an equilibrium distribution between the liquid and vapor phases. This would tend to cause spreading in the forward direction with a resultant zone broadening.

The column efficiency does not appear to be affected by temperature but increases with column length (Fig. 4). The efficiency, however, does not appear to be a linear function of column length. This is probably due, in part, to the fact that, as the column increases in length, so does the pressure drop across it. This results in a large velocity gradient so that as the length increases a progressively larger fraction of the column is operated at flow rates differing considerably from that required for maximum resolution. Hence, an indefinite increase in column efficiency does not appear to be possible by simply increasing the column length.

Vapor phase chromatograms of the known mixture are shown in Figs. 5, 6 and 7 for temperatures of 121, 100 and 79°, respectively. The most remarkable difference in the three chromatograms is the improved resolution of ethylbenzene and *p*-xylene with decrease in temperature. The column efficiency as determined by theoretical plate calculations based on the benzene, *n*-heptane and toluene zones is essentially constant for the three temperatures (Fig. 4). However, the degree of separation, as determined by the ratio of the *K* values, differed considerably for the various temperatures. These ratios for ethylbenzene and *p*-xylene at temperatures of 100 and 79° were 1.05 and 1.08, respectively. The resolution of ethylbenzene and *p*-xylene at 121° was too poor to make possible the determination of a *K* value ratio at this temperature.

The resolution obtained from any column is seen, from the foregoing, to vary in some manner with

Fig. 5.—Typical elution curves at 121°; N₂ flow rate = 50 cc./min.; column length = 45 inches.Fig. 6.—Typical elution curves at 100°; N₂ flow rate = 50 cc./min.; column length = 45 inches.Fig. 7.—Typical elution curves at 79°; N₂ flow rate = 50 cc./min.; column length = 45 inches.

the column length and carrier gas flow rate and with the reciprocal of the column temperature. For maximum resolution, the carrier gas flow rate must remain fixed as shown in Fig. 4. This figure also shows that improved resolution can be obtained by increasing the column length. However, the improvement is not linear whereas the time required for elution is linearly related to the length of the column. Improved resolution can also be obtained by decreasing the column temperature, but the time for elution is increased exponentially (Fig. 3). It would appear, therefore, that the resolving

power of a column soon reaches a point of diminishing returns beyond which small improvements in the column's ability to separate a mixture can be obtained only at a very great cost in time. Furthermore, increasing the column length tends to promote zone spreading and hence dilution in the carrier gas. This may be a limiting factor where minor constituents of a mixture are diluted below the sensing level of the detector.

Theoretical plate calculations, as applied to chromatography, do not appear to convey an immediate concept as to the resolving power of a column. However, a quantity that will convey directly the resolving power of a given column can be defined by the relation

$$E = 1 + \frac{V_{hw}}{V_m} \quad (9)$$

where

E = column efficiency or resolving power
 V_{hw} = vol. of effluent corresponding to the width of the elution zone at the half height (*i.e.*, the half width of the zone).

The threshold of resolution will exist between two elution zones when their peaks are separated by a distance equal to the half width of one of the zones. Thus, a given column will resolve, at least partially, all compounds whose equilibrium constants (K) differ by a factor greater than the column efficiency as defined by equation 9. This is illustrated by ethylbenzene and *p*-xylene in Figs. 6 and 7. The column efficiency as calculated on the benzene, *n*-heptane and toluene curves was 1.07. The ratio of the K values for ethylbenzene and *p*-xylene in Figs. 6 and 7 is 1.05 and 1.08, respectively. The two compounds are not resolved in Fig. 6 but are partially resolved in Fig. 7.

Ratios of the equilibrium constants (K) for the various components of the known mixture at 100° are compared with the ratios of their vapor pressures at the same temperature in Tables I and II. These results show that the degree of separation of the aromatic compounds, as signified by their K value ratios, follows the corresponding ratios of the

TABLE I
RATIOS OF VAPOR PRESSURES FOR THE COMPONENTS OF THE KNOWN MIXTURE (100°)

	Benzene	<i>n</i> -Heptane	Toluene	Ethylbenzene
<i>n</i> -Heptane	1.79
Toluene	2.44	1.37
Ethylbenzene	4.42	2.47	1.82	...
<i>p</i> -Xylene	5.00	2.80	2.06	1.14

TABLE II
RATIOS OF K VALUES FOR THE COMPONENTS OF THE KNOWN MIXTURE (100°)

	Benzene	<i>n</i> -Heptane	Toluene	Ethylbenzene
<i>n</i> -Heptane	1.3
Toluene	2.0	2.6
Ethylbenzene	3.9	4.5	1.9	..
<i>p</i> -Xylene	4.0	5.2	2.1	1.1

vapor pressures quite closely, especially for the substituted aromatics. The behavior of *n*-heptane, however, differs greatly from that of the aromatics. Hence, compounds of a similar nature will probably be separated by a column having an efficiency (as defined by equation 9) which is numerically less than the ratio of their vapor pressures. Furthermore, the temperature at which the ratio of the vapor pressures of two materials is sufficiently great for resolution can be determined from vapor pressure curves. Thus, a simple determination of column efficiency together with a table of vapor pressure *versus* temperature will make it possible to predict the compounds that can be resolved and the temperatures most likely to give good separation.

The above scheme refers to compounds of a similar nature. For compounds differing in structure (*e.g.*, aromatic and aliphatic), separations can often be made, even when the vapor pressures are identical, by selecting an appropriate partitioning medium. Partition coefficients (*i.e.*, K values) rather than vapor pressures must be used for predicting the medium most likely to give an adequate separation in a reasonable time.

THE OXIDATION OF GRAPHITIZED CARBON BLACK¹

By W. R. SMITH AND M. H. POLLEY

*Research and Development Laboratory, Godfrey L. Cabot, Inc.
Cambridge, Massachusetts**Received December 14, 1955*

The oxidation of Fine Thermal carbon black at 600° increases its surface area about sixfold. This increase is not accompanied by a corresponding decrease in particle diameter and hence must be interpreted as development of porosity. A sample of Fine Thermal black graphitized at 2700° does not develop porosity when similarly oxidized. The slight area increase obtained on oxidation of the graphitized sample is related to decrease in particle diameter. These results may be interpreted as preferential attack of oxygen on a heterogeneous surface in the first case, and random attack on a uniform surface in the second. A true chemical process has been used to confirm the nature of the carbon black surface previously predicted by physical methods.

Partially graphitized carbon blacks prepared in this Laboratory have been used as adsorbents in a number of investigations concerned with the role of surface activity in absorption.^{2,3} Graphitized Fine Thermal blacks⁴ have been of most recent interest because of the remarkable uniformity of their surface.³ These blacks, graphitized⁵ at 2700°, have been shown³ to provide stepwise isotherms for the adsorption of argon, krypton and nitrogen at -195° rather than the smooth sigmoid type characteristic of ungraphitized blacks. While similar results have been observed with Graphon [Spheron 6 (2700°)], they are much more striking in the case of the graphitized Fine Thermal blacks. These experiments offer excellent confirmation of the theories of Hill⁷ and of Halsey⁸ and, following their theories, indicate that the surface of this adsorbent is extremely uniform with regard to distribution of energy sites. It occurred to us that further confirmation of this uniformity, as well as an insight into the development of carbon black porosity, might be obtained by studying the high temperature oxidation of graphitized thermal blacks.

Non-graphitized carbon blacks display a surface heterogeneity with regard to distribution of energy sites. This has been established both from the character of the adsorption isotherms as well as from heats of adsorption measurements.^{2a} When a

standard carbon black is treated with air or oxygen at temperatures of from 300–650° a sixfold increase in area, as measured by nitrogen adsorption, may be noted without appreciable reduction in particle diameter. This development of porosity upon air oxidation has long been recognized.^{9,10} It is interpreted as arising from preferential attack of the oxygen at high energy sites on the carbon surface. These sites may be associated with the edge atoms of the quasi-graphitic parallel layer groups composing the particle. Long and Sykes¹¹ have claimed that these edge atoms are more susceptible to chemical attack than are the atoms in the center of the basal plane. Since it has also been established that high energy sites are destroyed on high temperature (2700–3000°) graphitization,^{3a} then preferred sites for oxygen attack must either be removed or greatly diminished in number. If the surface of the graphitized carbon particle is as uniform as has been suggested, then oxygen attack should occur uniformly over the surface, and the area increase on oxidation should be proportional to the decrease in particle diameter without development of porosity. The present paper presents data confirming these observations.

Experimental

The Fine Thermal carbon black used in the present study was taken from commercial production. This grade of carbon black is prepared by thermal decomposition of natural gas diluted with flue gas consisting chiefly of hydrogen. The decomposition occurs in large preheated checker brick filled retorts at about 1100°.

Samples of Fine Thermal black were graphitized to varying degrees by heating in an inert atmosphere at temperatures of from 1000 to 2700°. A 40 kw. input Ajax-Northrup converter was used for the heat source. This converter is a spark-gap unit utilizing 18 to 36 kc. at 4400 volts across the induction coil. Details of the "graphitizing" procedure have been reported in an earlier publication.¹² Oxidation of the carbon black was carried out by weighing samples into a 7 × 1 cm. platinum combustion boat placed in the center of an electric combustion furnace heated to the desired temperature. The flow of air over the sample was by natural draft, achieved by leaving the door of the furnace ajar by about 1 cm. Temperature was measured with a chromel-alumel thermocouple located in the center of the furnace about 3 inches over the carbon sample. After 15 minutes, the sample was removed and cooled in a desiccator. The per cent. of carbon burned away was determined from loss in weight of the sample. The rate of ox-

(1) Presented before the Division of Colloid Chemistry at the Meeting of the American Chemical Society, held in Minneapolis, Minnesota, September, 1955.

(2) (a) R. A. Beebe, J. Biscoe, W. R. Smith and C. B. Wendell, *J. Am. Chem. Soc.*, **69**, 95 (1947); (b) R. A. Beebe and D. M. Young, *THIS JOURNAL*, **58**, 93 (1954); (c) L. G. Joyner and P. H. Emmett, *J. Am. Chem. Soc.*, **70**, 2353 (1948); (d) J. Mooi, C. Pierce and R. N. Smith, *THIS JOURNAL*, **57**, 52 (1953).

(3) (a) C. H. Amberg, W. B. Spencer and R. A. Beebe, *Can. J. Chem.*, **33**, 305 (1955); (b) M. H. Polley, W. D. Schaeffer and W. R. Smith, *THIS JOURNAL*, **57**, 469 (1953); (c) S. Ross and W. Winkler, Based on Thesis presented by W. Winkler in partial fulfillment of the requirements for the degree of Doctor of Philosophy to the Department of Chemical Engineering, Rensselaer Polytechnic Institute, June 1955. (d) J. Singleton and G. D. Halsey, *THIS JOURNAL*, **58**, 330, 1011 (1954).

(4) Fine Thermal carbon blacks are designated as FT blacks in rubber technology. They are semi-reinforcing in rubber. Representative commercial grades are P-33 and Sterling FT.

(5) In the past, it has been the habit to refer to increase in parallel layer group dimensions as increasing "degree of graphitization." As Warren has pointed out,⁶ there is considerable ambiguity associated with this designation, since it appears that growth of these crystallites to a value of L_n of the order of 100 Å. occurs prior to any significant ordering of the layers into the graphite configuration.

(6) C. Houska and B. E. Warren, *J. Appl. Phys.*, **25**, 1503 (1954).

(7) T. L. Hill, *J. Chem. Phys.*, **15**, 767 (1947).

(8) (a) G. D. Halsey, Jr., *J. Am. Chem. Soc.*, **73**, 2693 (1951); (b) G. D. Halsey, Jr., *ibid.*, **74**, 1082 (1952).

(9) W. R. Smith, F. S. Thornhill and R. I. Bray, *Ind. Eng. Chem.*, **33**, 1303 (1941).

(10) P. H. Emmett and M. Cines, *THIS JOURNAL*, **51**, 1329 (1947).

(11) F. J. Long and K. W. Sykes, *Proc. Roy. Soc. (London)*, **A193**, 377 (1948).

(12) W. D. Schaeffer, W. R. Smith and M. H. Polley, *Ind. Eng. Chem.*, **45**, 1721 (1953).

ation decreased with increasing degree of graphitization of the carbon black. In order to produce the desired degree of oxidation in the 15-minute interval, the temperature of the furnace was increased. Approximately 600° sufficed for oxidizing the original FT black, while about 800–900° was required to produce a corresponding weight loss for the highly graphitized samples. The per cent. weight loss on oxidation of the various samples at increasing temperatures is summarized in Fig. 1.

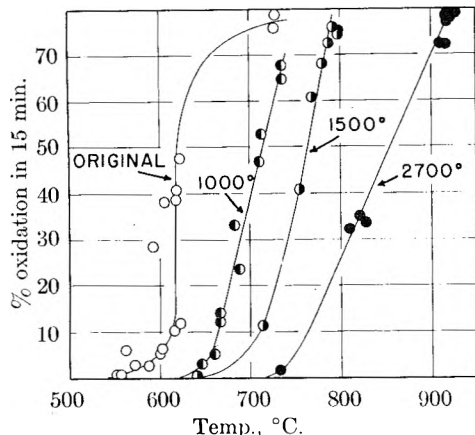


Fig. 1.—The oxidation of Sterling FT (original), Sterling FT (1000°), Sterling FT (1500°) and Sterling FT (2700°).

Surface areas were calculated both from adsorption isotherms of nitrogen at -195° and from particle size measurements obtained with the RCA-EMU electron microscope.

Results and Discussion

Pertinent particle size, surface area and X-ray diffraction data for the Fine Thermal black, both original and heat treated at 1000, 1500 and 2700°, are reported in Table I. The nitrogen surface

TABLE I
PROPERTIES OF THE STERLING FT SERIES

Treatment temp., °C.	Electron microscope		Nitrogen surface area, m. ² /g.	Parallel layer group dimensions ^c	
	d_A , Å	Calcd. area, m. ² /g.		L_a , Å	L_c , Å
None	2094	15.4	14.5	27.6	16.8
1000	2018	10.0	13.1	37.5	17.5
1500	1984	16.2	12.9	62.0	38.6
2700	1940	16.6	12.5	132	88

^a d_A = surface average diameter = $\Sigma nd^3/\Sigma nd^2$. ^b E. M. surface area = $(6 \times 10^4)/(1.86 \times d_A)$ m.²/g. ^c L_a = dimension along parallel plane; L_c = dimension perpendicular to layer normal. See ref. 6, and also B. E. Warren "Proceedings of 2nd Bi-Annual Carbon Conference, University of Buffalo, June 10, 1955" (in press).

areas of the samples agree sufficiently well with that calculated from the surface average diameter, as measured by the electron microscope, to indicate that the particles are essentially non-porous. There is a decrease in nitrogen surface area with increasing temperature of heat treatment, due perhaps to some degree of particle sintering. The area, as measured by the electron microscope, appears to increase slightly. However, with increasing degree of graphitization, the departure of particle shape from spherical to rather regular polyhedra becomes marked. This not only increases the difficulty in measuring the particle but it also introduces uncertainty in the computed area since the expression employed is derived for a system of spheres. This may account for the

somewhat larger electron microscope values for the area over those calculated from nitrogen adsorption. However, these variations are not of major significance in the present studies since changes due to porosity will be several times larger.

In the last two columns of Table I are dimensions of the parallel layer groups or quasi-graphitic crystallites within the particle.¹² Attention is called to the remarkable increase in the dimensions of these crystallites with increasing temperature of heat treatment. It is our opinion that the unusual surface uniformity of the 2700° material arises from the dimensions of the crystallites composing the particle. The stepwise isotherm characteristic of this uniform surface is shown in Fig. 2. The smooth sigmoid isotherm obtained for the original Fine Thermal black prior to graphitization is included for comparison. Isotherms for the 1000 and 1500° heat treated samples we found to be intermediate between those of the original and 2700° material.

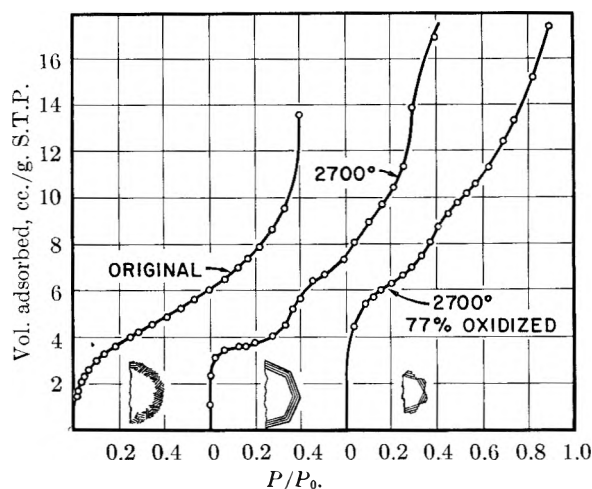


Fig. 2.—Argon isotherms at -195° on Sterling FT (original), Sterling FT (2700°), and Sterling FT (2700°) oxidized 77% with suggested configurations of the surface.

The effect of oxygen attack on the surface area of the carbon blacks described in Table I is evident from data of Fig. 3. The original Fine Thermal black undergoes an area increase, as measured by nitrogen adsorption, of about 63.5 m.²/g. when some 39% of the black has been burned away. In contrast, the area of the 2700° sample increases only 4 m.²/g. for the same weight loss. Particle size data and areas, as computed from electron microscope measurements of the oxidized carbon blacks are presented in Table II. Electron microscope measurements show that oxidation does produce some decrease in particle diameter. For example, when 39% of the original FT black was burned away the diameter is reduced about 320 Å. This reduction in particle size would account for an increase of only 2.8 m.²/g. It is quite evident that the increase of 63.5 m.²/g. found by nitrogen adsorption must be accounted for principally in the development of an internal porosity, arising from preferential attack of oxygen at certain sites on the carbon black surface. Close examination of the electron micrographs of this oxidized material re-

veals some degree of surface roughness suggestive of porosity.¹³ However, the nature of oxygen attack after the Fine Thermal black has been graphitized at 2700° is quite different. In this case, there is no development of porosity. The small increase in nitrogen area after oxidation, as shown in Table II, is in agreement with that anticipated on the basis of the decrease in particle diameter as measured in the electron microscope. From purely geometric considerations, assuming uniform removal of carbon from the particle surface, it is possible to calculate the diameter decrease from weight loss of the sample. The areas so calculated are shown in the last column of Table II and in the dotted curve of Fig. 3. The calculated values and the areas measured by nitrogen adsorption are in good agreement for the FT (2700°) sample, demonstrating that the oxidation has occurred uniformly over the surface.

TABLE II

PROPERTIES OF THE STERLING FT SERIES AFTER OXIDATION

Sample	Oxidation	Electron microscope		Nitrogen surface area, m. ² /g.	Area calcd. from wt. loss, m. ² /g.
		Diameter, Å.	Surface area, m. ² /g.		
Original FT	None	2094	15.4	14.5	—
Original FT	6	1950	16.6	48.8	14.8
Original FT	39	1771	18.2	78.0	17.1
FT (2700°)	77	1155	27.9	20.2	20.5

It is interesting to note in Fig. 2 that after oxidation of the 2700° graphitized material, the steps originally observed in the argon isotherm become less pronounced.

These data appear to confirm our original opinion that oxygen attack on standard carbon black occurs preferentially at specific high energy sites on the surface. These sites may be edge carbon atoms in the layer lattice. Upon heat treatment at 2700°, the number of edge sites is greatly reduced. For the Fine Thermal blacks studied here, the X-ray diffraction data quoted in Table I reveal an increase of about fivefold in the size of the parallel layer groups. This growth occurs presumably at the expense of the smaller and less-ordered crystallites within the particle. Since the size of the carbon black particle as revealed by the electron microscope does not change significantly upon graphitization, it is obvious that the surface of the particle must become more uniform with regard to the crystal faces exposed.

Recent experimental evidence from dark-field electron microscopy indicates that the surface of the 2700° material is composed primarily of oriented 002 planes. Dark-field electron micrographs of the FT (2700°) sample show well-defined diffraction images at the surface of the graphitized carbon particles. They do not occur symmetrically around the particle circumference as they would if the parallel layer groups were randomly oriented

(13) Electron micrographs have been omitted from this publication since they do not reproduce clearly on the stock presently used in THIS JOURNAL. The authors will be happy to supply prints upon request.

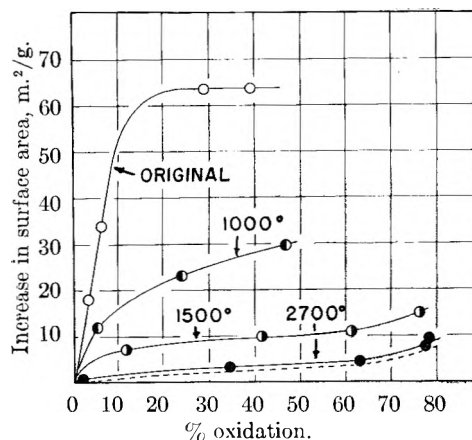


Fig. 3.—Change in surface area with increasing oxidation on the Sterling FT series. The dotted line is the calculated area assuming uniform particle diameter decrease.

at the surface. They occur only on edges facing toward or away from the aperture. This means that the crystallites are oriented so that diffractions from these two sides are directed through the dark-field aperture, while diffractions from the other sides are lost against the dark-field mask. Since electron diffraction diagrams of the 2700° material indicate that most of the diffracted intensity is in the 002 reflection, we have concluded that the great preponderance of crystal images seen in dark field are from the 002 reflection of crystallites oriented parallel to the carbon surface.

Electron micrographs of the FT black graphitized at 2700° reveal a striking change from the spherical particles of the original material to regular polyhedra with sharply defined faces. These faces are most evident if the black is dispersed and embedded in polybutyl methacrylate prior to examination. Microtome sections¹⁴ examined under the electron microscope clearly reveal quite uniform faces on the graphitized black surface. The area of the majority of these faces is between 1 and 2 × 10⁶ square Ångström units. Since the average diameter of the particles measured is about 1600 Å, there are of the order of 40 of these faces per particle. The first atoms or molecules adsorbed may orient preferentially along the intersection of these faces. However, since this "edge" area is comparatively small, it will be filled rapidly, and subsequent adsorption will then be random on what is, in essence, a surface composed of a single crystal face.

Perhaps the most interesting conclusion to be drawn from the present study is that from evaluations of the nature of a surface by physical adsorption it has been possible to predict and confirm its behavior toward a true chemical process.

Acknowledgments.—The authors wish to acknowledge the assistance of Mrs. M. M. Chappuis for the electron micrographs and Mr. A. F. Cosman for the adsorption measurements. We are also indebted to Professor B. E. Warren for providing X-ray diffraction data.

(14) M. M. Chappuis, M. H. Polley, and R. A. Schulz, *Rubber World*, **130**, 507 (1954).

ELECTROLYTIC INTERACTION OF NYLON WITH AQUEOUS SOLUTIONS OF HYDROCHLORIC ACID

BY F. T. WALL AND A. BERESNIEWICZ

Noyes Chemical Laboratory, University of Illinois, Urbana, Illinois

Received December 19, 1955

The absorption of hydrochloric acid by nylon fibers has been studied as a function of acid concentration. It is found that the initial stages of absorption qualitatively follow theoretical expectations based on a model involving interaction of HCl with the polymer end groups. If the nylon has an excess of amino over carboxyl end groups, then the absorption of HCl takes place in two stages which can be described more or less quantitatively by thermodynamic considerations. In the presence of concentrated hydrochloric acid solutions, nylon is found to absorb more HCl than would be expected from the number of amino groups present. This excess absorption is attributed to interaction with amide linkages. From the temperature coefficients of the various absorptions, heats of absorption are calculated for each of the stages.

Introduction

The interaction of natural and synthetic fibers with acids and bases has been a subject of extensive study by many groups of workers. Most attention thus far has been given to the absorption of acids on wool. Steinhardt and co-workers¹⁻³ measured very accurately the absorption of HCl and of KOH on wool as a function of pH. In order to explain the experimental data they proposed that the interaction of ions with the solid fiber is simply based on the mass action law. Somewhat later Gilbert and Rideal⁴ treated theoretically the interaction of wool with hydrochloric acid. In deriving their titration equations, Gilbert and Rideal made use of the statistical mechanical expression derived by Fowler and Guggenheim⁵ for the case of absorption of neutral molecules on definite sites of an absorbent. They recognized the important role of the fiber potential, since their equations pertain to the absorption of ions and not of neutral molecules. A different approach to this problem was used by Peters and Speakman⁶ who considered the activity of hydrogen ions in the solution internal to the wool. On the basis of thermodynamic considerations they derived an expression for the pH of the imbibed solution and were able to interpret quantitatively the earlier data obtained by Steinhardt and Harris.¹

Nylon is a synthetic polymer which has a certain number of acid and basic end groups, and for this reason the absorption of acids and bases on it should follow a pattern similar to that of wool. The first qualitative study of absorption of acids on nylon was made by Elöd and Schachowsky in 1942⁷ and thereafter by several other investigators.⁸⁻¹⁴ Rem-

ington and Gladding¹⁵ were first to interpret quantitatively the absorption of acid dyes on nylon applying slightly modified equations of Gilbert and Rideal. More recently Wall and Swoboda,¹⁶ using thermodynamic methods, extended the theory of Gilbert and Rideal to the absorption of both acids and bases on fibers with unequal number of acid and basic end groups. In a study of absorption of sodium hydroxide on nylon having roughly twice as many carboxyl as amino end groups, Wall and co-workers^{16,17} have confirmed the applicability of their theory to this special case.

Actually the amide groups of nylon can also display acid or basic character, depending on the pH of the surrounding medium. For this reason nylon can be regarded as a doubly amphoteric substance capable of binding acids and bases not only on its end groups but also on the amide groups. The basic character of the amide groups of nylon seems to be reasonably well established^{8,12,18} although it has not yet been subjected to a quantitative study.

In the study reported here the absorption of hydrochloric acid on nylon having an excess of amino end groups, and on nylon having an excess of carboxyl end groups, has been studied at several different temperatures. An empirical titration equation is arrived at for the case of absorption of HCl on nylon having a very large excess of basic end groups. A comparison of the absorption of hydrochloric acid on nylon and on wool is made.

Theory

Let A_0 and B_0 be the number of carboxyl and amino end groups, respectively, expressed in equivalents per gram of dry nylon. The absorption of HCl on the end groups of nylon having $B_0 > A_0$ is expected to proceed in two stages. First the acid will react with the more basic amino end groups, and after those are virtually gone, it will add to the zwitterions which are equal in number to A_0 . The treatment of Wall and Swoboda leading to titration equations for both stages of absorption of the acid will be summarized here.

The first reaction to occur when nylon with an excess of amino end groups is suspended in a dilute solution of hydrochloric acid is

(15) W. R. Remington and E. K. Gladding, *J. Am. Chem. Soc.*, **72**, 2553 (1950).

(16) F. T. Wall and T. J. Swoboda, *THIS JOURNAL*, **56**, 50 (1952).

(17) F. T. Wall and P. M. Saxton, *ibid.*, **57**, 370 (1953).

(18) M. Harris and A. M. Snooke, *Bur. Standards J. Research*, **26**, 289 (1941).

(1) J. Steinhardt and M. Harris, *Bur. Standards J. Research*, **24**, 335 (1940).

(2) J. Steinhardt, C. H. Fugitt and M. Harris, *ibid.*, **25**, 519 (1940).

(3) J. Steinhardt, C. H. Fugitt and M. Harris, *ibid.*, **28**, 201 (1942).

(4) G. A. Gilbert and E. K. Rideal, *Proc. Roy. Soc. (London)* **A182**, 335 (1944).

(5) R. H. Fowler and E. A. Guggenheim, "Statistical Thermodynamics," Cambridge University Press, 1939.

(6) L. Peters and J. B. Speakman, *J. Soc. Dyers Colourists*, **65**, 63 (1949).

(7) E. Elöd and T. Schachowsky, *Melliand Textilber*, **23**, 437 (1942).

(8) R. H. Peters, *J. Soc. Dyers Colourists*, **61**, 95 (1945).

(9) J. Boulton, *ibid.*, **62**, 65 (1946).

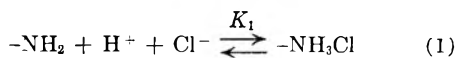
(10) P. W. Carlene, A. S. Fern and T. Vickerstaff, *ibid.*, **63**, 388 (1947).

(11) E. Elöd and H. G. Fröhlich, *Melliand Textilber*, **30**, 103 (1949).

(12) E. Elöd and H. G. Fröhlich, *ibid.*, **30**, 239 (1949).

(13) F. C. McGrew and A. K. Schneider, *J. Am. Chem. Soc.*, **72**, 2547 (1950).

(14) G. T. Douglas, *Am. Dyestuff Repr.*, **40**, 122 (1951).



The excess of NH_2 over the COOH groups is $B_0 - A_0$; therefore, at any point of the titration, the concentration of free amino groups is given by

$$[\text{NH}_2] = B_0 - A_0 - [\text{NH}_3\text{Cl}] \quad (2)$$

The expression for the equilibrium constant K_1 in terms of measurable quantities is

$$K_1 = \exp(-\Delta F_1^\circ/RT) =$$

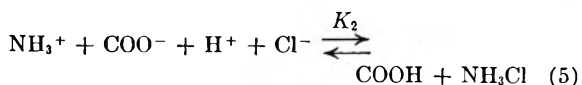
$$\frac{[\text{NH}_3\text{Cl}]}{\{B_0 - A_0 - [\text{NH}_3\text{Cl}]\} [\text{H}^+] [\text{Cl}^-]} \quad (3)$$

in which ΔF_1° is the standard free energy change of reaction (1). If the absorption of the acid takes place from solutions of pure hydrochloric acid, eq. 3 can be written in a form

$$-\frac{\Delta F_1^\circ}{2.3RT} = 2 \text{pH} + \log \frac{[\text{NH}_3\text{Cl}]}{\{B_0 - A_0 - [\text{NH}_3\text{Cl}]\}} = 2 \text{pH} + \log \rho \quad (4)$$

Equation 4 can be tested graphically since it predicts a straight line of slope equal to -2 when $\log \rho$, where $\rho = [\text{NH}_3\text{Cl}]/(B_0 - A_0 - [\text{NH}_3\text{Cl}])$, is plotted against pH . On the other hand, when the absorption of HCl on nylon takes place from solutions which are maintained at a constant chloride ion concentration, such a plot should then yield a straight line of slope equal to -1 . Actually, we shall see later that, at least when B_0 is very much larger than A_0 , this prediction is not confirmed experimentally.

After all free amino end groups have been converted to the alkyl ammonium ions, the acid will add to the zwitterions as



Assuming that at the beginning of this reaction $[\text{COO}^-] = A_0$, and that the electrical neutrality of the fiber is preserved, we can write

$$[\text{COO}^-] = [\text{NH}_3^+] = B_0 - [\text{NH}_3\text{Cl}] \quad (6)$$

$$[\text{COOH}] = [\text{NH}_3\text{Cl}] - (B_0 - A_0) \quad (7)$$

The expression for K_2 in terms of experimentally measurable quantities becomes

$$K_2 = \exp(-\Delta F_2^\circ/RT) = \frac{[\text{NH}_3\text{Cl}]\{[\text{NH}_3\text{Cl}] - (B_0 - A_0)\}}{\{B_0 - [\text{NH}_3\text{Cl}]\}^2 [\text{H}^+] [\text{Cl}^-]} \quad (8)$$

in which ΔF_2° is the standard free energy change accompanying reaction (5).

In the case of nylon with $A_0 > B_0$, reaction (1) will not occur and only reaction (5) is to be expected when nylon is immersed into a dilute solution of HCl ; in the latter case the expression for K_2 remains the same, but, of course, the quantity $B_0 - A_0$ is negative.

The titration equation for the second stage of absorption of HCl from solutions to which no KCl has been added is obtained from eq. 8 as

$$-\frac{\Delta F_2^\circ}{2.3RT} = 2 \text{pH} + \log \frac{[\text{NH}_3\text{Cl}]\{[\text{NH}_3\text{Cl}] - (B_0 - A_0)\}}{\{B_0 - [\text{NH}_3\text{Cl}]\}^2} = 2 \text{pH} + \log \pi \quad (9)$$

The correctness of this equation may be asserted graphically by plotting $\log \pi$ against pH , where $\pi =$

$$\frac{[\text{NH}_3\text{Cl}]\{[\text{NH}_3\text{Cl}] - (B_0 - A_0)\}}{\{B_0 - [\text{NH}_3\text{Cl}]\}^2}.$$

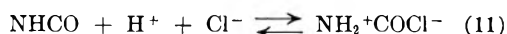
The value of K_2 can easily be determined from eq. 8, rewritten in the form

$$\beta = \sqrt{\frac{[\text{NH}_3\text{Cl}]\{[\text{NH}_3\text{Cl}] - (B_0 - A_0)\}}{[\text{H}^+]^2}} = \frac{\sqrt{K_2} B_0 - \sqrt{K_2} [\text{NH}_3\text{Cl}]}{\sqrt{K_2} B_0 - \sqrt{K_2} [\text{NH}_3\text{Cl}]} \quad (10)$$

By plotting β against $[\text{NH}_3\text{Cl}]$ a straight line should result with an intercept equal to B_0 and a slope of $-\sqrt{K_2}$.

Interaction of HCl with Amide Groups.—The amount of HCl bound on the end groups of nylon increases steadily with the concentration of acid in the equilibrium solution until it reaches a constant value between about pH 2.7 and pH 1.7. This plateau represents the amount of available amino end groups for addition of HCl . For still lower pH values the absorption of the acid on nylon increases again, with the amide groups presumably acting as base sites. There seems to be good evidence that the acid forms ionic linkages with the amide groups of nylon, instead of being merely dissolved in the imbibed solution.^{8,12,18}

The addition of HCl to the amide groups can be represented by



The equilibrium constant of this reaction may be expressed by

$$K_3 = \frac{[\text{NH}_2^+\text{COCl}^-]}{[\text{NHCO}][\text{H}^+][\text{Cl}^-]} = \frac{\{[\text{HCl}]_n - B_0\}}{\{A_m - [\text{HCl}]_n + B_0\} (N\gamma_\pm)^2} \quad (12)$$

where $[\text{HCl}]_n$ is the number of equivalents of HCl bound on one gram of nylon, A_m is the number of amide groups in one gram of the polymer free to react with HCl and $N\gamma_\pm$ is the mean activity of HCl in the equilibrium solution. K_3 cannot be evaluated because the exact value of A_m is not known. An estimate of it could be obtained graphically by applying a Langmuir type isotherm to the process of addition of HCl to the amide groups. However, the data obtained in the course of this work do not cover the range of higher acid concentrations and therefore do not warrant our drawing any conclusions as to the maximum available amide groups for reaction with HCl .

The heat associated with reaction (11) can be calculated without knowledge of K_3 if the temperature dependence of the absorption isotherm in this region is known. Taking logarithms of both sides of eq. 12 and differentiating with respect to temperature we obtain

$$\frac{d \log K_3}{dT} = \frac{d}{dT} \log \frac{\{[\text{HCl}]_n - B_0\}}{\{A_m - [\text{HCl}]_n + B_0\}} + \frac{d}{dT} 2 \text{pH} \quad (13)$$

Assuming that A_m does not change with temperature and keeping $[\text{HCl}]_n$ constant, eq. 13 reduces to

$$\frac{d \log K_3}{dT} = 2 \frac{d}{dT} \text{pH} \quad (14)$$

Making use of the van't Hoff equation we can ob-

tain an expression for the change in heat accompanying reaction (11).

$$\Delta H_3^\circ = \frac{4.6RT_1T_2\Delta pH}{T_1 - T_2} \quad (15)$$

where ΔpH is the change in the pH of the titration curve necessary to maintain the same amount of HCl absorbed on the amide groups of nylon when the temperature is changed from T_1 to T_2 .

The absorption of HCl on the amide groups of nylon can be represented by Freundlich's absorption isotherm

$$\{[HCl]_a - B_0\} = k(N\gamma_\pm)^n \quad (16)$$

The constants k and n can be evaluated from a logarithmic plot of eq. 16.

The heats associated with the first two stages of absorption of HCl on nylon can be obtained by using the van't Hoff equation, provided the values of K_1 and K_2 are known at several different temperatures. This assumes, of course, that ΔH_1° and ΔH_2° are constant in the temperature intervals considered. The heats can also be calculated by means of equations analogous to eq. 15.

Experimental

The absorption of hydrochloric acid on three kinds of nylon was measured at several temperatures at many different concentrations of the acid. The first stage of absorption was studied on a 10 filament, 101 denier, undrawn nylon fiber, referred to as nylon I, which had $A_0 = 27 \times 10^{-6}$ and $B_0 = 142 \times 10^{-6}$ equivalents per gram. Nylon II, which was used for the study of the second stage of absorption consisted of undrawn fiber of 13 filament, 125 denier, with $A_0 = 73 \times 10^{-6}$ and $B_0 = 42 \times 10^{-6}$ equivalents per gram. Finally, a 60 mesh granular nylon III, $A_0 = 31 \times 10^{-6}$ and $B_0 = 130 \times 10^{-6}$, was used for the study of the interaction of amide groups with hydrochloric acid. The number of end groups was determined in this Laboratory by the method of Waltz and Taylor.¹⁹

Prior to equilibrating the nylon with acid, the fibers were cut into 3 inch long pieces and washed at first with distilled water and then with ether. The ether was removed from the polymer by keeping it for at least 10 hours under vacuum and then by washing it again with water, usually for another 24 hours, until no more odor of the ether could be noticed in the washwater.

The procedure for making a set of measurements was as follows. First the nylon was equilibrated with atmospheric moisture and then one to two gram samples were weighed out into 4-ounce polyethylene bottles. Samples of the same nylon were dried for 10 hours at 100° in order to determine the moisture absorbed from air. To prevent any contamination with carbon dioxide, the air was replaced by nitrogen in those reactors to which the most dilute solutions of hydrochloric acid were added. Measured amounts of hydrochloric acid of known concentration, usually 100 ml., were added to the reactors which were then capped air-tight and kept in a water-bath which maintained a constant temperature to within 0.05°. The reactors were shaken every 24 hours and after 10 to 14 days the concentrations of the equilibrium solutions were determined.

The reagents, HCl solutions of different concentrations, were prepared from 1.000 N and from 0.100 N "Acculute" solutions by dilution with conductivity water. The exact concentrations were determined by titrating with standard NaOH solutions against phenolphthalein. The concentrations below 0.001 N were determined by volumetric dilution of the more concentrated solutions of known normalities. Solutions to which KCl was added were prepared in the following way. Reagent grade KCl was dried first at 150° for 24 hours. Then precalculated amounts of the salt were weighed and two sets of HCl solutions of different concentrations were made up, one being 0.2 N and the other 1.0 N with respect to the chloride ion.

The concentrations of the equilibrium solutions in the range between 0.4 and 0.004 N were determined by direct titration with standard NaOH solutions against phenolphthalein. The standard solutions were stored in polyethylene bottles connected directly to automatic burets. For most titrations, which were always performed at least in duplicate, the volume of the standard acid used ranged between 30 to 50 ml.

The equilibrium solutions in the range of concentrations between 0.003 and 0.00006 N were titrated conductometrically with standard 0.01 N and 0.005 N sodium hydroxide solutions. Fifty- or 100-ml. samples of the equilibrium solutions were used for one titration. The amount of standard reagent, which was admitted portionwise to the conductance cell from a microburet, rarely exceeded 10 ml. The conductance in the course of a titration was followed using a modified Wheatstone bridge, operated at a frequency of 1000 cycles. The conductances were multiplied by the relative increase in volume of the solution being titrated, so as to correct for the dilution taking place.

The concentrations of the most dilute solutions, and of solutions to which KCl was added, were determined by measuring the pH with a model G Beckman pH Meter using a #290 glass electrode and a saturated calomel electrode, #270. Up to pH 5, experimentally determined corrections for the potassium ions were applied. All measurements were carried out under an atmosphere of nitrogen to protect the solutions from carbon dioxide in the air.

The amount of acid combined with one gram of nylon was calculated by the equation

$$[HCl]_a = \frac{V_i N_i - V_e N_e}{W} \quad (17)$$

in which V_i , N_i , V_e and N_e are the volume in liters and concentration in equivalents of the initial and equilibrium solutions, respectively, and W is the weight of nylon. V_e is smaller than V_i by the volume of solution imbibed in nylon. This difference has been neglected in calculating the amount of the acid absorbed on nylons I and II, since in the case of those nylons we were primarily interested in the absorption isotherms at relatively low concentrations. In calculating the absorption of HCl on the amide groups, which takes place at higher concentrations of the acid, the amount of solution imbibed in nylon had to be known. The dependence of swelling of nylon III on the pH of the equilibrium solution has not been determined in this laboratory. Instead, the data of Elöd and Fröhlich,¹¹ who worked with a nylon of practically the same molecular weight as nylon III, were used.

Results and Conclusions

The first stage of absorption of hydrochloric acid on nylon I was studied at three different temperatures: 14.0, 34.7 and 50.0°. In Fig. 1 the amounts of hydrochloric acid absorbed on one gram of nylon, designated by $[HCl]_a$, are plotted against the pH values of the corresponding equilibrium solutions. The plateaus in the absorption isotherms indicate that all available amino end groups, designated by B_a , have already undergone reaction with protons at about pH 2.7. B_a is smaller than B_0 , apparently because of the presence of certain regions which are inaccessible to penetration by aqueous hydrochloric acid. If this assumption is true, then the regions accessible to hydrochloric acid represent 84% of the total volume. Therefore, the amount of the available carboxyl end groups, A_a , is only 84% of A_0 . In all calculations reported in this section the values A_a and B_a instead of A_0 and B_0 were used.

The experimental data and results calculated therefrom are represented graphically in the accompanying figures. In analyzing the results, it was necessary to secure values of the mean activity coefficient of HCl at different concentrations and temperatures; these were obtained from the

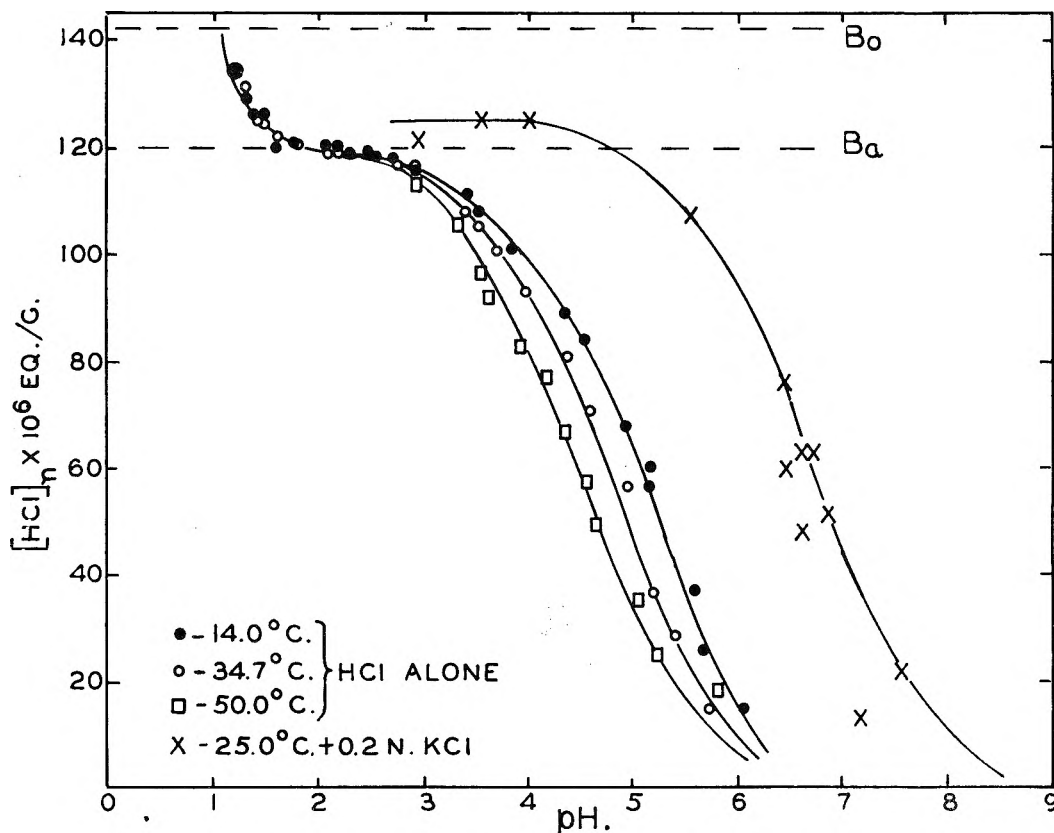


Fig. 1.—Absorption of HCl at different temperatures on nylon I.

“Physical Chemistry of Electrolytic Solutions” by Harned and Owen.²⁰

When $\log \rho$ is plotted vs. pH (Fig. 2), it is observed that the slope of the line is -1 instead of -2

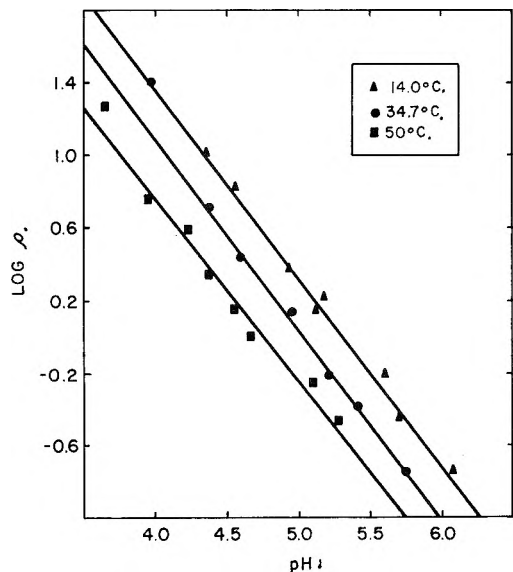


Fig. 2.—Plot of $\log \rho$ vs. pH at different temperatures. as predicted theoretically according to eq. 4. Although some dubious explanations can be offered for this behavior, we have no really good way to account for the results. However the empirical result makes it appear that $1/[H^+]$ is linearly de-

pendent upon $[NH_2]/[NH_3Cl]$ which is the same as $\{B_0 - A_0 - [NH_3Cl]\}/[NH_3Cl]$. This further suggests that $[NH_3Cl]/[H^+]$ is a linear function of $[NH_3Cl]$, viz.

$$\frac{[NH_3Cl]}{[H^+]} = \sqrt{K_1^*} (B_0 - A_0) - \sqrt{K_1^*} [NH_3Cl] \quad (18)$$

where K_1^* is a modified empirical “equilibrium” constant.

The values of K_1^* at the three temperatures were obtained graphically by plotting w ($= [NH_3Cl]/[H^+]$) against $[NH_3Cl]$. Figure 3 indicates that

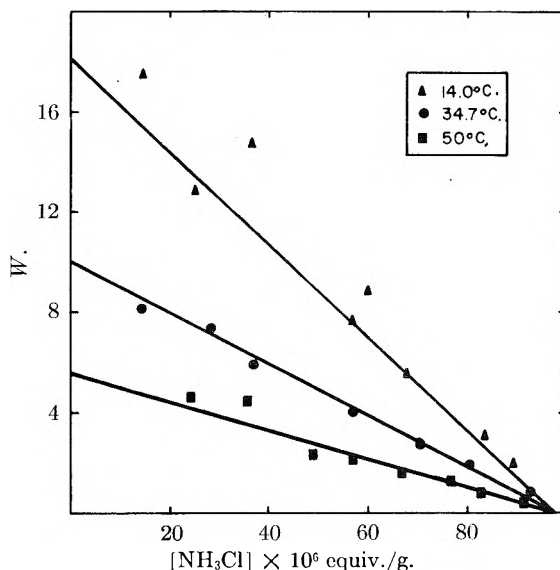


Fig. 3.—Graphical determination of K_1^* .

(20) H. S. Harned and B. B. Owen, “The Physical Chemistry of Electrolytic Solutions,” Reinhold Publ. Corp., New York, N. Y., 1939.

the points in such a plot do determine straight lines, even though they are somewhat scattered at higher values of w . This scatter is caused by the extreme difficulty in accurate determination of the hydrogen ion concentration in the pH range between 5 and 6. It is significant, however, that all three lines have a common intercept at 97×10^{-6} , which is in a very good agreement with the expected value, since $B_a - A_a = 96.4 \times 10^{-6}$.

Actually eq. 18 is empirical and it is somewhat surprising that it applies so well to the experimental data which could not be analyzed, as originally expected, in terms of eq. 3 and 4. Thus, the values of K_1 computed by eq. 3 are not constant but steadily increase with increasing pH of the equilibrium solutions.

The heat accompanying the first stage of absorption of hydrochloric acid was computed by an equation identical in form to eq. 15. As can be seen in Fig. 2 a plot of $\log \rho$ against pH gives a set of three parallel lines corresponding to the three temperatures at which the reaction was studied. The abscissa displacement of any two lines corresponding to T_1 and T_2 is the value of ΔpH to be used to calculate ΔH_1° . Assuming that ΔH_1° is temperature independent between 14 and 50° , its numerical value has been found to be -13.5 ± 0.5 kcal.

TABLE I
VALUES OF K_1^* , ΔF_1° , ΔH_1° AND ΔS_1° FOR THE FIRST STAGE OF ABSORPTION OF HYDROCHLORIC ACID ON NYLON

Temp., °C.	K_1^* $\times 10^{-9}$	ΔF_1° (kcal.)	ΔH_1° (kcal.)	ΔS_1° (e.u.)
14.0	31	-13.8		
34.7	9.4	-13.8	-13.5 ± 0.5	0
50	2.1	-13.9		

The standard free energy computed from values of K_1^* has been found to be quite independent of temperature. Its numerical value is equal, within the experimental error, to that of ΔH_1° ; therefore

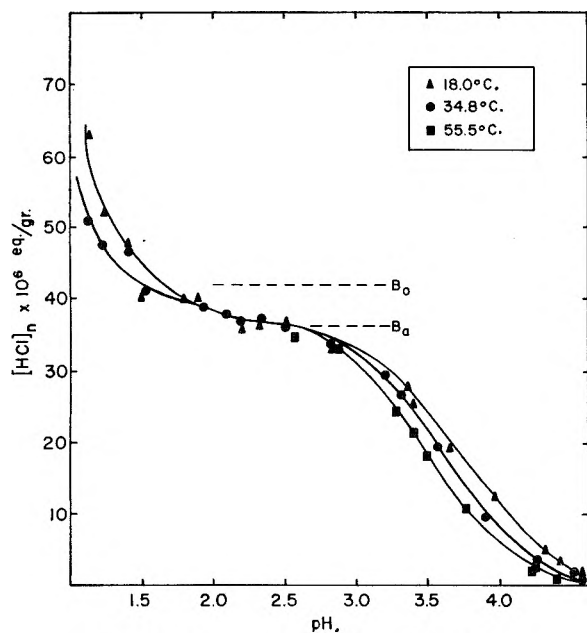


Fig. 4.—Absorption of HCl on nylon II.

the change in entropy is assumed to be zero, or at any rate too small to be calculated. A summary of results pertaining to the first stage of absorption is given in Table I.

The second stage of absorption of HCl was studied on nylon II at 18.0, 34.8 and at 55.5° . It can be seen from the plateaus in the absorption isotherms, represented in Fig. 4, that B_a is only 87% of B_0 . For this reason the value of A_a equal to $0.87 A_0$ has been used in the subsequent calculations. The plot reproduced in Fig. 5 confirms the validity of eq. 9, since there is a perfect agreement between the experimental points and the drawn line which has the theoretical slope of -2 . The same titration equation applies just as well to the second stage of absorption of the acid on nylon having $B_a > A_0$. This can be also seen in Fig. 5, where eq. 9 is tested using data obtained with nylon I at 14.0° .

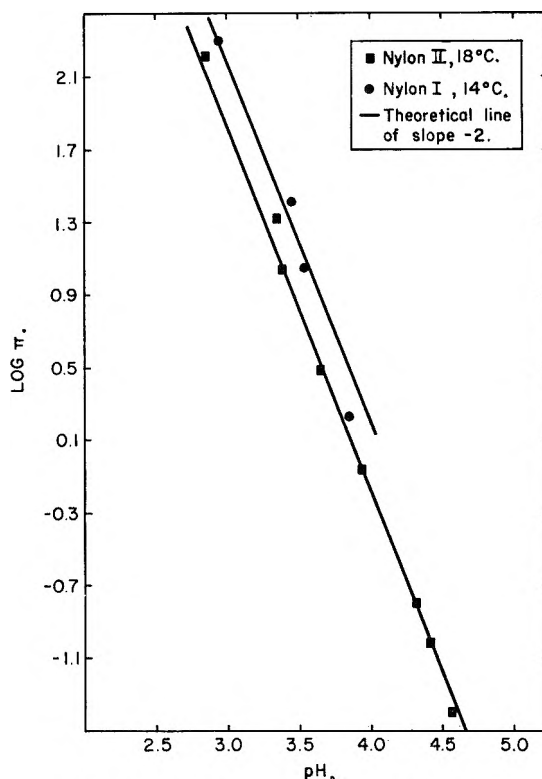


Fig. 5.—Plot of $\log \pi$ vs. pH for nylon I and II.

The values of K_2 were determined graphically, as suggested by eq. 10. It can be seen in Fig. 6 that the points determine reasonably straight lines with a common intercept at 37×10^{-6} equiv./g. The abscissa intercept of the line corresponding to 55.5° is greater than the expected value of B_a . This can be explained if it is assumed that some hydrolysis of the amide linkages took place at this relatively high temperature. The dotted line in Fig. 6 represents the plot of eq. 10 corresponding to 55.5° with the imposed restriction that its abscissa intercept be the same as of the other two lines. The value of K_2 at 55.5° has been obtained from the slope of this line.

The heat associated with reaction (5) has been determined by means of the van't Hoff equation. The plot of $\log K_2$ vs. $1/T$ gives, as expected, a

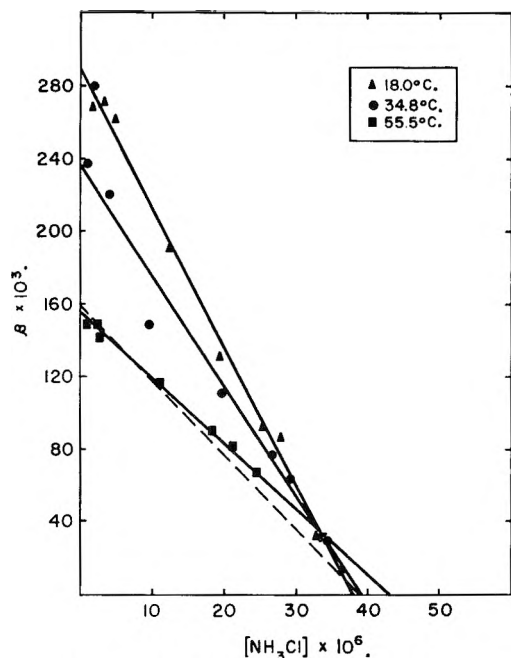


Fig. 6.—Graphical determination of K_2 .

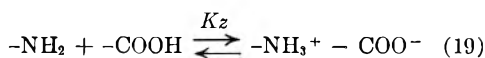
straight line, whose slope is $-\Delta H_2^\circ/(2.3RT)$. A summary of significant quantities relating to the second stage of absorption appears in Table II.

TABLE II

VALUES OF K_2 , ΔF_2° , ΔH_2° AND ΔS_2° FOR THE SECOND STAGE OF ABSORPTION OF HCl ON NYLON

Temp., °C.	$K_2 \times 10^{-7}$	ΔF_2° (kcal.)	ΔH_2° (kcal.)	ΔS_2° (e.u.)
18.0	6.2	-10.4		
34.8	3.7	-10.7	-6.4	13.7
55.5	1.7	-10.9		

Subtracting eq. 5 from eq. 1 we obtain the expression for the mutual ionization of the end groups in nylon.



The values of K_z at different temperatures are given below

Temp., °C.	18.0	34.7	50
$K_z = K_1^*/K_2$	360	250	100

It is apparent that the tendency of zwitterions to form decreases with increasing temperature. Wall and Saxton,²¹ who studied the absorption of NaOH on nylon, found that at 25°, K_2 equals 280, which is in very good agreement with the present results.

Due to interaction of the amide groups with the acid, the amount of HCl absorbed on nylon exceeds the value of B_a at lower pH values of the equilibrium solutions. It is extremely difficult to determine the effect of temperature on the interaction of HCl with the amide groups. This effect is small and at higher concentrations of the acid the error in determining $[\text{HCl}]_n$ is relatively large. The most accurate work in this region of concentrations has been done using nylon III; therefore these data are used in the interpretation of results, which are only of qualitative significance.

(21) F. T. Wall and P. M. Saxton, *THIS JOURNAL*, **58**, 83 (1954).

It is seen in Fig. 4 and Fig. 7 that at a given pH the amount of HCl bound on the amide groups increases with decreasing temperature. This indicates qualitatively that the reaction of the amide groups with HCl is exothermic. The approximate value of the heat accompanying this reaction, calculated by eq. 15, seems to lie between -2 and -3 kcal.

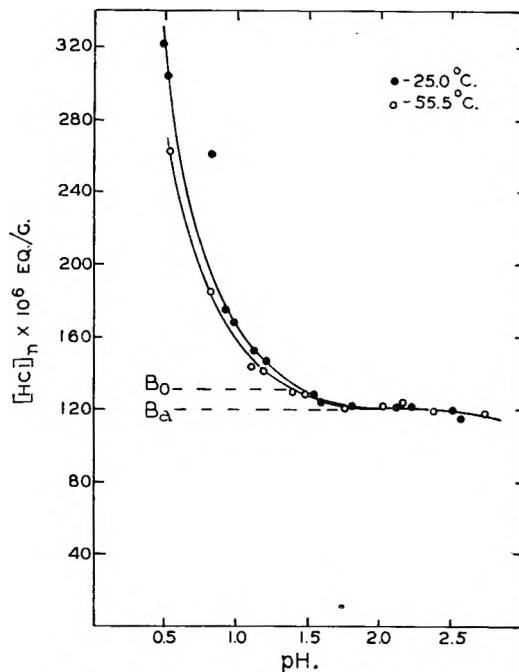


Fig. 7.—Absorption of HCl by amide linkage.

The constants k and n of the Freundlich isotherm, eq. 16, have been determined graphically, as shown in Fig. 8. The value of k is 7.7×10^{-4} at both

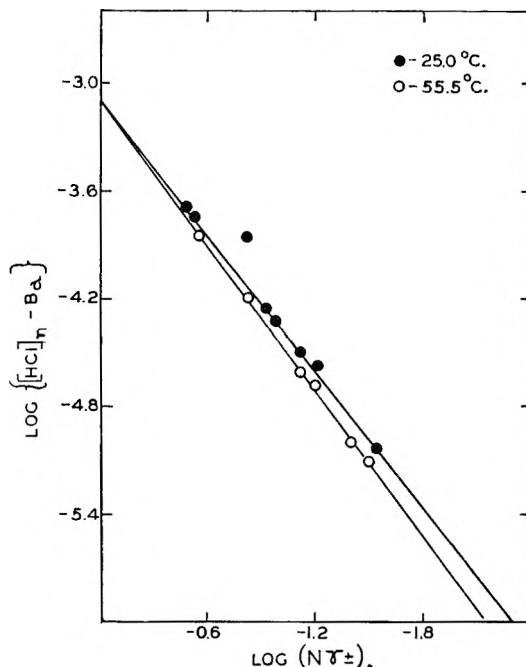


Fig. 8.—Graphical evaluation of constants in the Freundlich's adsorption isotherm.

temperatures, and the values of n are -1.34 and -1.15 at 25.0 and 55.5° , respectively.

The addition of KCl to solutions of hydrochloric acid enhances very markedly the absorption of the acid on nylon, as can be seen in Fig. 1. The absorption of HCl on nylon I from solutions of a constant ionic strength of 0.2 has been interpreted in view of eq. 4 and correct log-log slopes are obtained. (It

will be recalled that the theory failed when ionic strength and $[Cl^-]$ were not kept constant.) When $\log \rho$ is plotted *versus* pH , a straight line is obtained with a slope equal to -1 as predicted by eq. 4. Data on the effect of the addition of KCl appear in Table III. The absorption of HCl in the presence of $1.0 N$ KCl has also been studied, but the data are too scattered to be graphically analyzed.

In conclusion, we shall compare the interaction of nylon and HCl with that of wool and HCl. Steinhart and co-workers² found that the absorption of HCl on wool is practically temperature independent in the range between 25 and 50° . This is clearly not the case with nylon. The carboxyl end groups of wool keratin are markedly stronger acids than the carboxyl end groups of nylon. This conclusion is based on the fact that the mid-point of the acid absorption isotherm on wool is at pH 2.1 , whereas the mid-point for the second stage of absorption of HCl on nylon is at pH 3.6 .

Steinhart and Harris¹ found that the data obtained at a constant ionic strength show a different functional relationship between the amount of acid bound on wool and pH . In this respect the titration of wool resembles that of nylon, the only difference being that the data obtained with wool can be explained quantitatively in terms of the internal pH theory,⁶ whereas this theory cannot be applied in explaining the data obtained with nylon.

TABLE III

ABSORPTION ON HCl IN NYLON I AT 25.0° IN THE PRESENCE OF $0.2 N$ KCl

$[HCl]_n$ $\times 10^6$	pH	$(N\gamma_{\pm})$ $\times 10^{-7}$	$\frac{[NH_4Cl]}{[N\gamma_{\pm}]}$	$\log \rho$
121	2.97			
125	3.58			
125	4.04			
107	5.58			
76	6.48	3.31	230	0.56
63	6.62	2.40	263	.27
63	6.64	2.29	276	.27
51	6.87	1.35	377	.05
59 ^a	6.47	3.39	174	.19
48 ^a	6.63	2.34	205	.00
22	7.57	0.27	820	-.53
13 ^a	7.18	0.66	213	-.81

^a The pH values corresponding to these points are too low, as can be seen in Fig. 1.

THE THERMOLUMINESCENCE OF DOLOMITE AND CALCITE

BY D. R. LEWIS

Publication No. 74, Shell Development Company, Exploration and Production Research Division, Houston, Texas

Received December 27, 1955

The thermoluminescence glow curves of calcium carbonate as the mineral calcite and of calcium-magnesium double carbonate as the mineral dolomite have characteristic peaks resulting from groupings of energy levels in the crystals which can be populated with metastable electrons by exposure of the minerals to cobalt-60 γ -radiation. In geochemical environments in which the mineral composition grades from calcite to dolomite, the ratio of the peak heights from the glow curves varies regularly with the composition. Dolomite can also be distinguished from mixtures of the single compounds, calcite and magnesite, by the characteristic glow-curve peak heights and the temperatures at which they occur.

Introduction

The thermoluminescence of calcite and of limestones of unspecified dolomite content has been qualitatively observed by visual means for many years.¹⁻³

Recently some thermoluminescence glow curves of limestones have been published.⁴⁻⁶ There has, however, been no attempt to relate the reported variations in thermoluminescence to the chemical or mineralogical composition of the limestones. There has been a specific need to compare the glow curves of the minerals calcite, $CaCO_3$, and magnesite, $MgCO_3$, with that of the double carbonate dolomite, $CaMg(CO_3)_2$, to determine if these data could

aid in the interpretation of limestone glow curves. The glow-curve structure is greatly influenced by any trace impurities and by defect structure of the crystals which make up the minerals.^{7,8} Variations of thermoluminescence between calcite and dolomite may reflect both the differences in lattice structure and the distribution of impurity atoms which can be accommodated in the different lattices. Therefore, the elucidation of their thermoluminescence behavior should ultimately contribute to the geochemistry of the carbonate minerals and their accessory elements. Moreover, the proposed application of the glow curves of the carbonate minerals for geological age determination in sedimentary rocks⁹ will also require cognizance of any effect of chemical composition on glow curves.

The chemical conditions necessary for the forma-

(1) S. Hata, *Sci. Papers Inst. Phys. Chem. Research (Japan)*, **20**, 163 (1933).

(2) A. Kohler and H. Leitmeier, *Z. Krist.*, **87**, 146 (1934).

(3) M. A. Northrop and O. I. Lee, *J. Opt. Soc. Amer.*, **30**, 206 (1940).

(4) F. Daniels, C. A. Boyd and D. F. Saunders, *Science*, **117**, 343 (1953).

(5) J. M. Parks, Jr., *Bull. AAPG*, **37**, 125 (1953).

(6) D. F. Saunders, *ibid.*, **37**, 114 (1953).

(7) F. E. Williams, *This Journal*, **57**, 780 (1953).

(8) R. H. Bube, *ibid.*, **57**, 785 (1953).

(9) E. J. Zeller, Paper 34, Division of Physical and Inorganic Chemistry, 128th National Meeting of the American Chemical Society, Minneapolis, September 12, 1955.

tion of dolomite in nature are still not well understood. The development of dolomite, however, is frequently associated with the development of porosity in the limestone, which suggests a recrystallization process in which the porosity may result from solution of a volume of the limestone which is not subsequently filled with crystals. Since dolomite has not yet been synthesized in the laboratory except at elevated temperatures and pressures¹⁰ which have not necessarily existed in the sedimentary rocks in which dolomite occurs, only natural mineral samples can be studied.

Experimental

To investigate the effects of variations in chemical composition on the glow curves of calcite and dolomite, an outcrop section was selected which was known to provide a broad gradation in composition from pure calcite to pure dolomite with a range of intermediate compositions.^{11,12} Samples were taken at regular intervals from the calcite to the dolomite side of the bed in the Honeycut Bend section and were numbered consecutively in the order in which they were collected. Fresh samples were then ground to pass a 100-mesh sieve and after thorough blending were used in this form for subsequent analysis. The amounts of total carbonate and of calcite and dolomite were determined by differential thermal analysis with the method of Rowland and Beck.¹³

The glow curves were all made at a constant rate of temperature rise of 1° per second. The light intensity was measured with a 1P21 photomultiplier tube. The block diagram of the apparatus is shown in Fig. 1. As shown in this figure, the sample is heated by electric current supplied by a magnetic amplifier. As its temperature is raised, the sample emits light which reaches a photomultiplier tube whose output current varies linearly with the amount of light striking it. This output current is converted into a convenient voltage for measurement by an adjustable resistance in the sensitivity selector and is fed into one channel of a strip chart recorder where it causes a deflection proportional to the light intensity from the sample at that time. The other channel of the two-pen recorder is connected directly to a chromel-alumel thermocouple and records the temperature of the sample. Since the photomultiplier tube sensitivity varies greatly with small changes in the high voltage, it is necessary to provide a regulated power source for the high-voltage supply to achieve the necessary stability.

The program-controller unit indicated in the lower right-hand block of Fig. 1 generates a voltage as a function of time which corresponds to the desired thermocouple voltage function of time necessary to provide a uniform heating rate of the sample. The actual thermocouple voltage from the heater unit is continuously compared with the desired program voltage, and the error signal is used in a feedback loop to control the instantaneous power which the magnetic amplifier is supplying to the heater. With this type of program controller, the rate of temperature rise is extremely constant in the range 25 to 500° through which these samples were heated.

Before each glow curve is measured the sensitivity of the equipment to light is determined in arbitrary units by the deflection produced by a reference light source with a surface brightness of approximately five microlamberts.¹⁴ The units in which light intensity is reported are the same for all samples but are completely arbitrary.

(10) F. M. Van Tuyl, *Iowa Geological Survey*, **25**, 251 (1914).

(11) P. E. Coud and V. E. Barnes, *University of Texas Publication No. 4621*, bed 84, p. 326, 1946.

(12) The assistance of Prof. Carl W. Beck, Geology Department, University of Indiana in collecting these samples is gratefully acknowledged.

(13) R. A. Rowland and C. W. Beck, *Am. Mineral.*, **37**, 76 (1952).

(14) These units are supplied by the United States Radium Company, New York City, as phosphors which luminesce under β -ray excitation. The sources used in this work are activated by strontium-90 and constructed in the form of a disc one centimeter in diameter sealed in a cylinder of Lucite to duplicate the configuration of the glowing sample with respect to the photomultiplier tube.

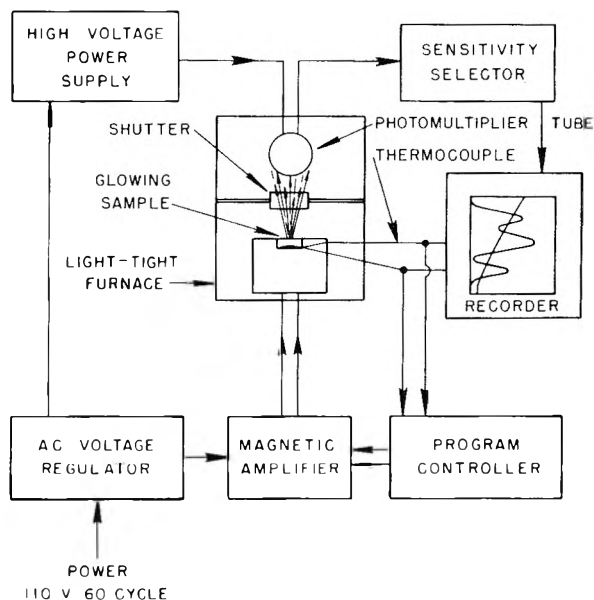


Fig. 1.—Block diagram showing the interrelation of the various sections of the thermoluminescence equipment.

All glow curves were made with 50-mg. ground samples. The natural glow curves were obtained by heating the ground samples without any additional treatment. For irradiation the samples were placed in a cylindrical cobalt-60 source of approximately ten curies total activity. The source, sealed in an aluminum cylinder, is of the same general type as that described by Saunders, Morehead and Daniels¹⁵ except that the cobalt metal is in the form of a wire spiral rather than a loose powder; the activity thus remains uniform along the walls of the cylinder. The irradiation volume is approximately 3 inches by 3/4 inch. The dose rate at the geometrical center measured by means of ferrous sulfate dosimetry¹⁶ is approximately 8500 roentgens per hour. Samples to be γ -activated were placed in the source in an aluminum loading canister and were irradiated at room temperature for 16 hours. Immediately after removal from the source the samples were stored in a Dewar flask filled with Dry Ice from which each was removed as it was needed for making the glow curve.

Experimental Results

The composition of the samples in terms of total carbonate and calcite and dolomite percentages of total carbonate is given in Table I.

Figures 2 and 3 present the glow curves of each sample with and without prior sample irradiation. Those samples which have been irradiated are given the suffix “-1” in the figures. After γ -irradiation both the calcites and dolomites exhibit three well-resolved light intensity maxima. The lowest temperature peak (at approximately 120°), relative to the other peaks, is much larger in the calcite than in the dolomite. This relation between the relative peak heights and the mineralogical composition of the samples is shown in Fig. 4.

This regular variation in the logarithm of the ratio of the glow-curve peak heights implies a systematic dependence on the mineralogy. This does not necessarily imply that the thermoluminescence depends primarily on the composition of the crystalline matrix since there may be systematic variations in the impurity ions with composition of the crystal. From the data available on these samples,

(15) D. F. Saunders, F. F. Morehead, Jr., and F. Daniels, *J. Am. Chem. Soc.*, **75**, 3096 (1953).

(16) J. Weiss, *Nucleonics*, **10**, No. 7, 28 (1952).

maximum intensity, however, was much less than 1% of any of the irradiated calcite or dolomite samples. Additional magnesite samples from Styria, Austria, and from Luning, Nevada, have given the same generally very low level of thermoluminescence. It is concluded from this that the contribution of magnesite to the thermoluminescence would be negligible in the presence of the calcite or dolomite in these samples.

Discussion

The glow curves of the Honeycut Bend calcite and dolomite samples after γ -irradiation show a systematic variation in the ratio of the peaks at 120 and 240° with composition. There is some evidence that the peak at approximately 240° is associated with lattice defects rather than impurity ions.¹⁷ There are not definitive data which permit the assignment of the peak at 120° either to impurity or to defect trapping centers. The largest change in magnitude with structure is in the peak at 120°. Accordingly, the question is still unresolved

(17) J. Handin, D. V. Higgs, D. R. Lewis and P. K. Weyl, presented at the New Orleans Meeting of the Geological Society of America, November, 1955.

whether the basis for the observed change in peak ratios with mineral composition is primarily due to the change in the gross crystal composition or due to some characteristic assemblage of trace impurities which may be accommodated in the calcite lattice but more efficiently excluded from the dolomite lattice as it is formed.

Conclusions

The principal conclusions which can be based on the experimental results reported in this paper are the following.

(1) The ratio of the glow-curve peaks at approximately 120° and at 240° of the Honeycut Bend limestone after irradiation with cobalt-60 γ -rays can be simply related to the mineralogical composition.

(2) The glow curves of unirradiated dolomite from the Honeycut Bend produce only a single peak at approximately 310° while those samples with 15% or more calcite produce recognizable peaks at 240 and 310°.

(3) The contribution to the glow curve of any free magnesite which might be present in these limestones is negligible.

NOTES

KINETICS OF THE REACTION BETWEEN NEPTUNIUM(IV) AND NEPTUNIUM(VI) IN A MIXED SOLVENT¹

BY DONALD COHEN, E. S. AMIS,² J. C. SULLIVAN AND J. C. HINDMAN

Chemistry Division, Argonne National Laboratory, Lemont, Illinois

Received October 31, 1956

In an endeavor to further elucidate the mechanism of the kinetics of the reaction between Np(IV) and Np(VI) ions in solution³ an attempt was made to study the reaction in a medium with a dielectric constant other than that of water.

Experimental

The preparation of the reagents and the experimental techniques have been described previously.³ In spite of the thermodynamic stability of neptunium ions in molar perchloric acid the presence of organic material greatly reduces the stability of the ions. Dowex-50 had been found to reduce Np(VI).⁴ A good deal of difficulty was found in obtaining a suitable solvent which would neither oxidize or reduce the neptunium ions.

Earlier it had been demonstrated that ethylene glycol, when purified, did not reduce Np(VI).⁵ Additional spectrophotometric investigations indicated Np(IV) and Np(V)

were stable with respect to oxidation or reduction in the alcohol, for the period of the experiment which was measured in minutes. However, over longer periods of time (hours) some oxidation of the Np(IV) occurred in the glycol solutions. It was not feasible to follow the progress of the reaction by use of the Np(IV) band at 724 m μ due to the marked alterations of the spectrum occurring in the glycol solutions. The drastic change in the absorption spectra of the Np(IV) when ethylene glycol-aqueous perchloric acid is used as the solvent is shown in Fig. 1 by comparison with the spectra in aqueous perchloric acid.⁶

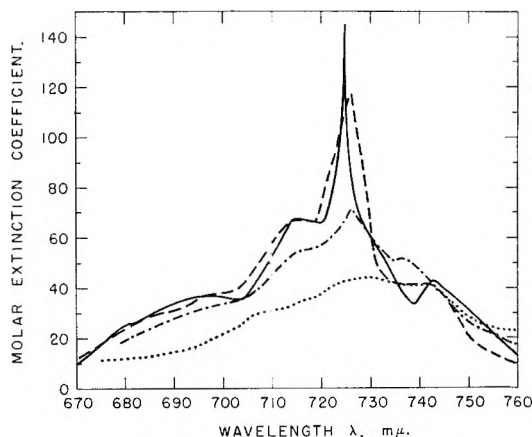


Fig. 1.—The effect of ethylene glycol on the absorption spectrum of neptunium(IV), $[Np(IV)] \approx 6 \times 10^{-3} M$, $t = 25^\circ$: —, 1 M HClO₄; ---, 1 M HClO₄, 1.23 M ethylene glycol; - · - ·, 1 M HClO₄, 5.74 M ethylene glycol; · · · ·, 1 M HClO₄, 12.1 M ethylene glycol.

(1) Work performed under the auspices of the U. S. Atomic Energy Commission.

(2) Resident Research Associate from the University of Arkansas.

(3) J. C. Hindman, J. C. Sullivan and D. Cohen, *J. Am. Chem. Soc.*, **76**, 3278 (1954).

(4) J. C. Sullivan, D. Cohen and J. C. Hindman, *ibid.*, **77**, 6203 (1955).

(5) Donald Cohen, J. C. Sullivan, E. S. Amis and J. C. Hindman, *ibid.*, **78**, 1543 (1956).

(6) R. Sjöblom and J. C. Hindman, *ibid.*, **73**, 1744 (1951).

As was to be expected, the change in the electric field surrounding the ion due to change in solvent composition was minimal for the Np(V) due to the domination by the axially symmetrical field arising from the oxygenated cation.⁷ Therefore after the preparation of a suitable calibration curve, the reaction was followed by observing the increase in the 983 m μ peak characteristic of Np(V).

Results and Discussion

The data obtained were analyzed using the method of initial slopes. From the results we have the following approximate rate law in 12.1 *M* ethylene glycol

$$\frac{d[\text{Np(V)}]}{dt} = k[\text{Np(IV)}]^{1/2}[\text{Np(VI)}][\text{H}^+]^{-2} \quad (1)$$

Figure 2 is a graphic presentation of the data in terms of equation 1. In 12.1 *M* ethylene glycol,

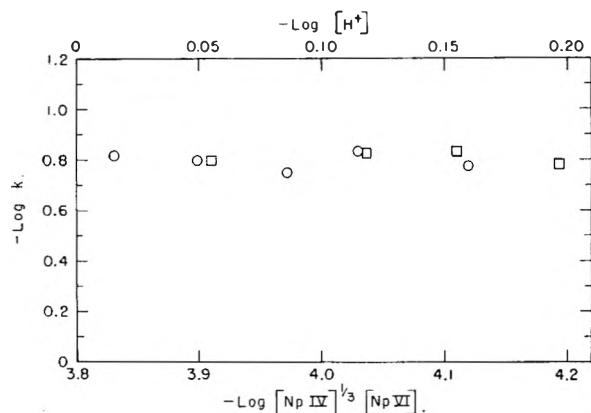


Fig. 2.—Effect of metal and hydrogen ion variation on the rate: O, $\log k$ vs. $\log [\text{Np(IV)}]^{1/2}[\text{Np(VI)}]$; □, $\log k$ vs. $\log [\text{H}^+]$.

k was found to be 0.158 ± 0.009 mole^{5/3} l.^{-3/2} sec.⁻¹ at 25.0°. For purposes of comparison, the previously determined rate law in molar perchloric acid is given by

$$\frac{d[\text{Np(V)}]}{dt} = k[\text{Np(IV)}][\text{Np(VI)}][\text{H}^+]^{-2} \quad (2)$$

The variation of the rate as a function of ethylene glycol is graphically demonstrated in Fig. 3. It is obvious that ethylene glycol is present in the acti-

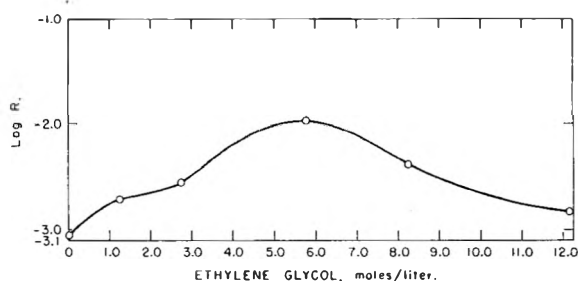


Fig. 3.—The effect of ethylene glycol on the rate of the reaction: $[\text{HClO}_4] = 0.9 M$; $[\text{Np(IV)}] = 1.33 \times 10^{-3} M$; $[\text{Np(VI)}] = 1.15 \times 10^{-3} M$, $t = 25^\circ$.

ivated complex. This is consistent with the observed changes in the absorption spectrum of the Np(IV). The fact that ethylene glycol is involved in the reaction precludes the possibility of determining the effect of change of the macroscopic dielectric constant of the medium on the reaction in any simple matter.

(7) J. C. Eisenstein and M. H. L. Pryce, *Proc. Roy. Soc. (London)*, **229A**, 20 (1955).

THE ADSORPTION OF DEUTERIUM BY A PLATINUM CATALYST

By G. C. BOND¹

Frick Chemical Laboratory, Princeton University, Princeton, N. J.

Received July 15, 1955

In the course of other work, it became of interest to determine the ability of a platinum catalyst to retain deuterium after considerable periods of pumping at different temperatures; 0.50 g. of platinum-pumice catalyst² containing 0.025 g. of metal was placed in a static reactor of 45-cc. volume, and reduced *in situ* for 1 hour at 200°, after which it was evaluated for 2 hours.

The following standard procedure was then employed. A further amount of deuterium (60–80 mm.) was introduced into the reactor at 200°, and after 5 minutes the temperature was adjusted to the required value, if other than 200°. The deuterium was then pumped out, the pumping being continued for varying periods; the final pressure was invariably less than 10^{-5} mm. A measured pressure of hydrogen was then introduced, and after 15 minutes a sample was withdrawn and its deuterium content measured reproducibly to $\pm 0.1\%$ or better on a mass spectrometer. From the known hydrogen pressure and its deuterium content, the volume of exchangeable deuterium held by the catalyst was determined. Separate experiments at 0° showed that increasing the time allowed for the exchange from 15 to 30 minutes did not further increase the deuterium content. Variation of the pumping time, both at 0 and 200°, showed that the volume of exchangeable deuterium fell to a minimum after 1 hour, and did not further decrease; the 1 hour period was used in all later experiments. After each experiment, the hydrogen was evacuated and the catalyst treated with deuterium for 1 hour at 200° before starting the next cycle of operations.

Table I shows how the volume of exchangeable deuterium varies with temperature. Since this volume increases with temperature, it cannot be equivalent to the total deuterium chemisorbed on the metal surface, since the chemisorption process is always exothermic and its extent would therefore decrease with increasing temperature. It seemed possible that an endothermic occlusion or solution process was being observed, although the volumes found were four to five powers of ten greater than the known solubility of hydrogen in annealed platinum.³ However, the physical form of a metal greatly affects its occluding capacity.⁴

TABLE I

EFFECT OF PUMPING TEMPERATURE ON THE VOLUME OF EXCHANGEABLE DEUTERIUM

Pumping temp., °C.	200	95	0	−78
Vol., cc. S.T.P.	0.112	0.035	0.022	0.004

However further experiments showed that the phenomenon was not simple occlusion or solution. If after the initial procedure the reactor was cooled to 0° and pumped, and then again heated to 200°, the volume of deuterium detected was approximately the same as if the pumping had been carried out at the higher temperature. Subsequent experiments confirmed this finding, and normal behavior was found in intervening runs

(1) Department of Chemistry, The University, Hull, England.
 (2) G. C. Bond and J. Turkevich, *Trans. Faraday Soc.*, **49**, 281 (1953).
 (3) A. Sieverts and E. Jurisch, *Ber.*, **44**, 2394 (1912).
 (4) D. P. Smith, "Hydrogen in Metals," University of Chicago Press, Chicago, 1947.

using the usual procedure. Some results are given in Table II.

TABLE II

EFFECT OF PUMPING AT 0° FOLLOWED BY HEATING TO 200°

	Vol. of exchangeable deuterium, cc. S.T.P.
(i) pumped at 0° and heated to 200°	0.169
(ii) pumped at 0°	0.025
(iii) pumped at 0° and heated to 200°	0.141

It is evident that the amount of deuterium which is exchangeable at 0° is less than the total adsorbed deuterium remaining after pumping, since a larger amount is again made available on heating to 200°. The following interpretation of these results is tentatively advanced: it is likely that the volume of exchangeable deuterium at 200° is approximately equivalent to the total volume remaining adsorbed after pumping. At temperatures of 95° and less (and perhaps at somewhat higher temperatures) there must therefore be a considerable amount of deuterium adsorbed so strongly that it will not exchange with hydrogen. If after the addition of the hydrogen the surface were energetically homogeneous (that is, if all atoms were equally strongly adsorbed), complete exchange of all the adsorbed deuterium would be expected; these results therefore suggest an energetically inhomogeneous surface. The volumes adsorbed after pumping both at 200 and at 0° are about the same (see Tables I and II), and the fraction of the total adsorbed deuterium which is exchangeable rises exponentially with temperature, indicating that the exchange of the strongly held deuterium is an activated process.

I am indebted to Professor John Turkevich for his interest in this work, to Princeton University for the award of a post-doctoral Fellowship, and to the referee for his guidance in matters of terminology. The deuterium was provided by the Stewart Oxygen Company.

THE CORRECTION OF STOKES' LAWS OF FRICTION FOR PARTICLES OF MOLECULAR SIZE

BY A. SPERNOL¹

Received November 10, 1955

The laws of Stokes for the friction on moving particles in liquids $\alpha_{St} = 6\pi\mu r$ (translation) and $\alpha_{St} = 8\pi\mu r^3$ (rotation) are neither experimentally nor theoretically² valid when the particles are of molecular size. The true friction on molecules and other small particles can, however, be evaluated from the extensive experimental data available, in particular from diffusion coefficients D using Einstein's formula $\alpha_{exp} = kT/D$, from ionic mobilities u using the formula $\alpha_{exp} = \text{const.}/u$, and from dielectric relaxation times t using Debye's

(1) Isotopenlabor der Medizinischen Forschungsanstalt in der Max-Planck-Gesellschaft, Göttingen.

(2) The hydrodynamic assumptions from which the laws are derived not being valid in this case.

formula $\alpha_{exp} = 2kTt$. In this way an empirical correction factor $f = \alpha_{exp}/\alpha_{St}$ ("microfriction factor") can be determined for Stokes' laws.³

The investigation of the experimental data on the subject⁴ revealed the necessity of distinguishing between two correction effects. The first is a purely geometrical effect, depending only on the size of the particles both of the solute and solvent. The analysis, applied only to solutions in which all the intermolecular forces are approximately equal and the molecules are nearly spherical, gives an empirical geometrical correction factor (Fig. 1) f_0 for translation represented simply by the formula

$$f_0 = (1 + r_L^2/r^2)^{-1} \quad (1)$$

when $r/r_L \geq 0.7$ or by $f_0 = 0$, $1 + 0.4r/r_L$ in the neighborhood of $r/r_L = 1$ (r = radius of solute particles, r_L of solvent particles). The accuracy of these formulas for such solutions is estimated to be about 10%.

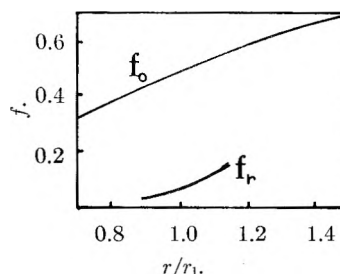


Fig. 1.—Microfriction factors f_0 for translation (formula 1) and f_r for rotation, the latter calculated from empirical relaxation constants.⁵

Due to the scarcity of experimental data and to the size of the corrections involved, a simple and sufficiently accurate formula for the geometrical correction of Stokes' law of rotation has not yet been determined, although the same effects occur as in translation (Fig. 1).

The second effect not included in Stokes' laws is a close dependence of the friction on the intermolecular forces in the solution. The friction increases with increasing interaction between the moving particles and their surroundings.⁶ If the stronger local force centers are saturated by suitable solvation or association, this increase of friction may be determined quantitatively in terms of the increase of the effective size of the particles owing to solvation or association and *vice versa*. As in this case the forces between the effectively moving solvates or associates and the solvent particles become about equal to those between the solvent particles themselves, the correction factor (1)—with appropriate values of r —should be

(3) The particle radii necessary for the evaluation of f and f_0 can be determined within 10% accuracy from the mole volume V according to $r = (3\beta V/4\pi N_L)^{1/3}$ with a space filling β of about 0.7.³

(4) A. Spornol and K. Wirtz, *Z. Natf.*, **8a**, 522 (1953), and there further references.

(5) D. H. Whiffen, *Trans. Faraday Soc.*, **46**, 124 (1950).

(6) For example, in the diffusion of chlorobenzene in benzene, the value $f = \alpha_{exp}/\alpha_{St}$ increases continuously with the number of partial moments (induction forces) from 0.43 for *o*-dichlorobenzene to 0.65 for hexachlorobenzene; similarly in the diffusion of trihalogenmethane in benzene, f increases with the polarizability (dispersion forces) from 0.46 for chloroform to 0.56 for bromoform and 0.65 for iodoform, the ratio r/r_L remaining approximately constant.

valid for these solvates or associates. It is thus possible to determine from experimental values of diffusion, etc., and formula (1) the enlarged radii of the particles, and hence the solvation numbers or association factors.

The analysis of the known experimental data on the principles outlined above⁷ yields many interesting results, of which only the most important will be indicated here. Diffusion measurements on iodine in solution show that the effective size of the diffusing particles is greater in brown solutions (corresponding to an association of I_4 - I_6) than in violet solutions (I_2 - I_3). (It is impossible to determine here whether this enlargement is due to solvation or association.) From measurements of the diffusion of mannite in water an inner and an outer hydration layer must be assumed. The inner layer consists of about 10 water molecules, and is practically temperature independent in the measured interval 0-70°, the outer layer diminishes rapidly with increasing temperature from about 8 water molecules at 0° to 0 molecules at about 30°. Ionic hydration numbers can be determined exactly from ionic mobilities (Table I). From the temperature dependence of the mobilities of slightly hydrated ions, one can determine from (1) the temperature dependence of the radii of the (associated) solvent molecules and hence the temperature

(7) A. Spagnol 1952, unpublished, and there further references.

dependence of the degree of association. All results are in good agreement with other methods.

TABLE I

HYDRATION NUMBERS H FOR THE ELEMENTARY IONS IN WATER AT 25° CALCULATED FROM EMPIRICAL IONIC MOBILITIES ACCORDING TO FORMULA 1

Ion	$r_{\text{cryst}} \times 10^{-8},^a$ cm.	f	$r_H,^b$ Å.	f_0	H^c	H^d (Ulich)
Li ⁺	0.78	3.02	3.26	0.72	7	5
Na ⁺	0.98	1.87	2.60	.70	3-4	3.5
K ⁺	1.33	0.94	2.32	.56	2-3	2
NH ₄ ⁺	1.43	.86	2.28	.54	2	
Rb ⁺	1.49	.80	2.26	.53	2	2
Cs ⁺	1.65	.72	2.23	.51	1-2	
Cl ⁻	1.81	.66	2.26	.53	1-2	2
Br ⁻	1.96	.59	2.27	.52	1	1.5
I ⁻	2.20	.54	2.26	.53	0	0.5
ClO ₄ ⁻	2.38	.57	2.38	.57	0	
Mg ⁺⁺	0.78	4.00	3.45	.90	9.5	9
Ca ⁺⁺	1.06	2.90	3.41	.90	9	8
Sr ⁺⁺	1.27	2.36	3.36	.89	8.5	
Ba ⁺⁺	1.43	2.03	3.26	.88	7.5	7.5

^a These radii calculated from ionic distances in crystals give the values $f = \alpha_{\text{exp}}/\alpha_{\text{st}} = 0.815v/ur$ (v = valency, u = ionic mobility in $\text{cm}^2 \text{ ohm}^{-1} \text{ mole}^{-1}$, r in cm.). ^b These radii give the values $f_0 = 0.815v/ur_H$ according to (1) ($r_L = 2.9 \text{ Å.}$ for the associated water). ^c Calculated from $H = (r_H^3 - r_{\text{cryst}}^3)/r_L^3$ ($r_L = 1.8 \text{ Å.}$ for the hydration water). ^d Calculated by Ulich from ionic entropies.

Just Released

New 1955 Edition

**American Chemical Society
Directory of Graduate Research**

**Faculties, Publications and
Doctoral Theses in
Departments of Chemistry and
Chemical Engineering at
United States Universities**

INCLUDES:

- All institutions which offer Ph.D. in chemistry or chemical engineering
- Instructional staff of each institution
- Research undertaken at each institution for past two years
- Alphabetical *index* of over 2,000 individual faculty members and their affiliation as well as alphabetical *index* of 151 schools

The only U. S. Directory of its kind, the ACS Directory of Graduate Research (2nd edition) prepared by the ACS Committee on Professional Training now includes all schools and departments (with the exception of data from one department received too late for inclusion) concerned primarily with chemistry or chemical engineering, known to offer the Ph.D. degree.

The Directory is an excellent indication not only of research of the last two years at these institutions but also of research done prior to that time. Each faculty member reports publications for 1954-55; where these have not totalled 10 papers, important articles prior to 1954 are reported. This volume fully describes the breadth of research interest of each member of the instructional staff.

Because of new indexing system, access to information is straightforward and easy—the work of a moment to find the listing you need. Invaluable to anyone interested in academic or industrial scientific research and to those responsible for counseling students about graduate research.

Paper bound.....446 pages.....\$2.50

Order from

Special Publications Department
American Chemical Society
1155—16th St., N. W.
Washington 6, D. C.

Engineer or Chemist

CERAMICS

Develop High Temperature
Materials for Nuclear Flight

General Electric is now vitally committed in the area of nuclear powered aircraft. Even though General Electric has an unexcelled complex of test facilities, equipment and scientific personnel, much remains to be done. This qualified senior engineer will find our small congenial project-group just the right medium in which he can make a lasting contribution to the development of improved materials. For in truth, professional achievement is best fostered in an atmosphere of face to face stimulation. This, as much as anything else, is what you get at GE.

At least 8 to 10 years experience is required, involving non-metallic inorganic materials for use at high temperatures. (If directly related, time spent in obtaining an advanced degree may be considered part of this experience.) Applicant must be a graduate physical chemist, metallurgical engineer, or ceramic engineer, preferably with PhD or equivalent.

Publication of research results in the appropriate classified or open literature is encouraged.

OPENINGS IN CINCINNATI, OHIO
AND IDAHO FALLS, IDAHO

*Address Replies, stating salary requirements,
to location you prefer:*

W. J. Kelly
P. O. Box 132
Cincinnati, O.

L. A. Munther
P. O. Box 535
Idaho Falls, Idaho

GENERAL  ELECTRIC

Number 4 in
Advances In Chemistry Series

edited by the staff of
Industrial and Engineering Chemistry

SEARCHING THE CHEMICAL LITERATURE

Covers market research methods, usefulness of trade literature, patent search techniques, and 21 other topics.

171 pages plus index
paper bound—\$2.00 per copy

order from:

Special Publications Department
American Chemical Society
1155 Sixteenth Street, N.W.
Washington 6, D. C.

Literature Resources for Chemical Process Industries

Designed To Help Both The *New* And
The *Experienced* Searcher Of Literature Find What He Wants

Discusses various information sources with 13 articles on market research, 7 on resins and plastics, 6 on textile chemistry, 10 on the food industry, 10 on petroleum, and 13 on general topics, plus 34 pages of index.

order from:

Special Publications Department
American Chemical Society
1155 Sixteenth Street, N.W.
Washington 6, D.C.

Number 10 in
Advances in Chemistry Series

edited by the staff of
Industrial and Engineering Chemistry

582 pages—paper bound—\$6.50 per copy